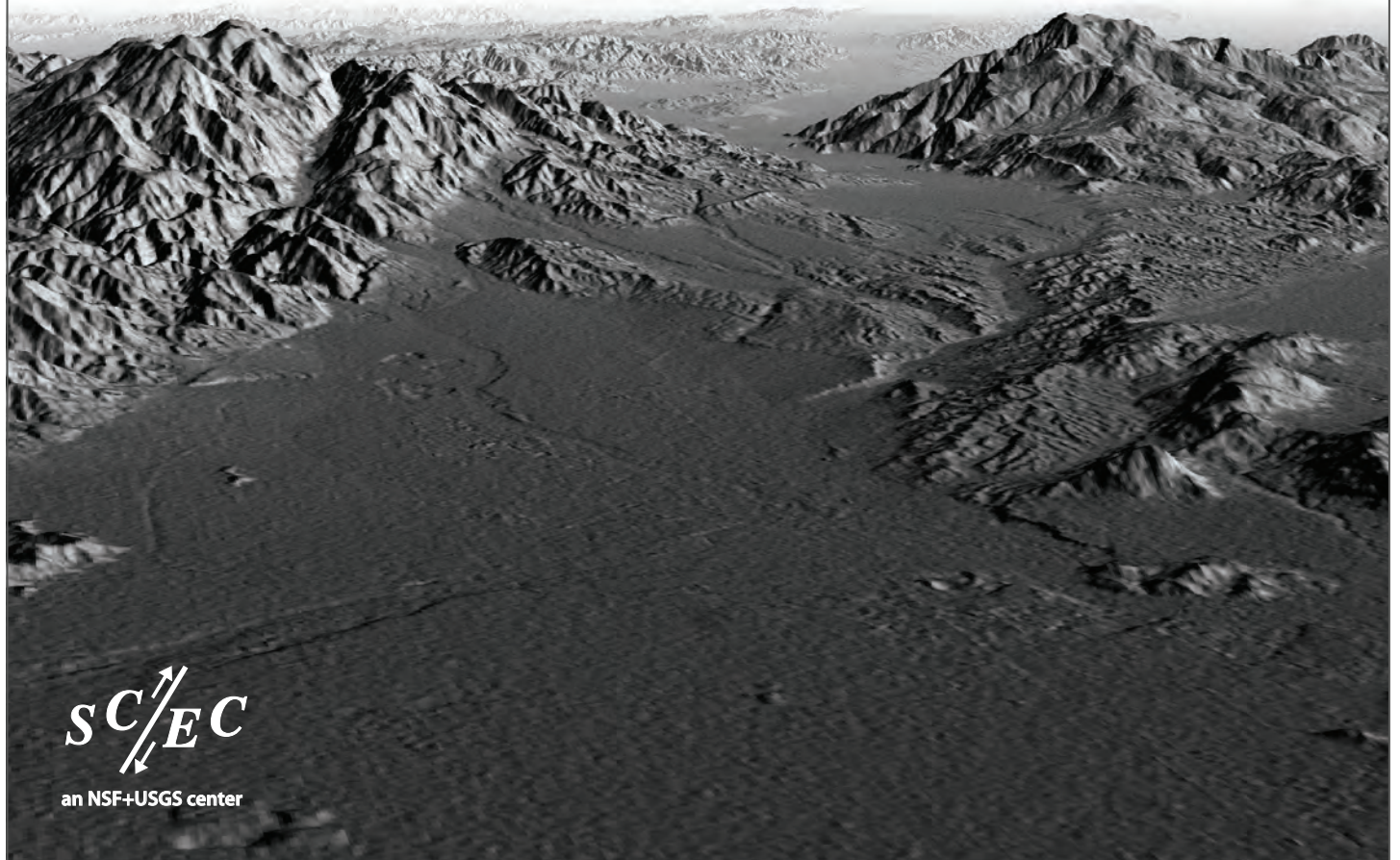


2009 Southern California Earthquake Center Annual Meeting



SC/EC
an NSF+USGS center

Proceedings and Abstracts, Volume XIX
September 12-16, 2009

SCEC ORGANIZATION

Center Director, *Tom Jordan*

Deputy Director, *Greg Beroza*

Associate Director for Administration, *John McRaney*

Associate Director for Communication, Education, and Outreach, *Mark Benthien*

Associate Director for Information Technology,
Phil Maechling

Special Projects and Events Coordinator, *Tran Huynh*

Research Contracts and Grants Coordinator,
Karen Young

Administrative Assistant, *Deborah Gornley*

Education Programs Manager, *Bob de Groot*

Digital Products Manager, *John Marquis*

Research Programmers, *Maria Liukis, Scott Callaghan, Kevin Milner, Patrick Small*

Systems Administrator, *John Yu*

SCEC BOARD OF DIRECTORS

Tom Jordan, *Chair, USC*

Lisa Grant-Ludwig, *Vice-Chair, UCI*

Ralph Archuleta, *UCSB*

Peter Bird, *UCLA*

David Bowman, *CSUF*

Tom Brocher, *USGS Menlo*

Emily Brodsky, *UCSC*

Jim Brune, *UNR*

Steve Day, *SDSU*

James Dieterich, *UCR*

Yuri Fialko, *UCSD*

Tom Herring, *MIT*

Ken Hudnut, *USGS Pasadena*

Nadia Lapusta, *CalTech*

Jim Rice, *Harvard*

Paul Segall, *Stanford*

Bruce Shaw, *Columbia*

Rob Wesson, *USGS Golden*

SCEC ADVISORY COUNCIL

Mary Lou Zoback, *Chair, Risk Management Solutions*

Gail Atkinson, *Carlton University*

Lloyd Cluff, *Pacific Gas and Electric*

John Filson, *Scientist Emeritus, U.S. Geological Survey*

Jeffrey Freymuller, *University of Alaska*

Jim Goltz, *CalEMA*

Patti Guatteri, *Swiss Reinsurance*

Anne Meltzer, *Lehigh University*

Denis Mileti, *California Seismic Safety Commission*

Kate Miller, *University of Texas at El Paso*

Steve Mahin, *Pacific Earthquake Engineering Research Center*

John Rudnicki, *Northwestern University*

SCEC PLANNING COMMITTEE

Chair, *Greg Beroza*

Seismology, *Egill Hauksson, Elizabeth Cochran*

Tectonic Geodesy, *Jessica Moraleda, Rowena Lohman*

Earthquake Geology, *Mike Oskin, James Dolan*

Unified Structural Representation, *John Shaw, Kim Olsen*

Fault and Rupture Mechanics, *Judith Chester, Ruth Harris*

Crustal Deformation Modeling, *Liz Hearn, Kaj Johnson*

Lithospheric Architecture and Dynamics, *Paul Davis, Thorsten Becker*

Earthquake Forecasting and Predictability, *Terry Tullis, Jeanne Hardebeck*

Ground Motion Prediction, *Brad Aagaard, Rob Graves*

Seismic Hazard and Risk Analysis, *Paul Somerville, Nicolas Luco*

Southern San Andreas Fault Evaluation, *Tom Rockwell, Kate Scharer*

Working Group on California Earthquake Probabilities, *Ned Field*

Collaboratory for the study of Earthquake Predictability, *Tom Jordan, Danijel Schorlemmer*

Extreme Ground Motion, *Tom Hanks*

Community Modeling Environment, *Phil Maechling*

Table of Contents

SCEC ANNUAL MEETING PROGRAM	1
Workshop Descriptions and Agendas	5
STATE OF SCEC, 2009	21
Welcome to the 2009 Annual Meeting!	21
Goals of the Meeting	21
Highlights of SCEC Achievements	22
Organization and Leadership	24
Center Budget and Project Funding	27
Communication, Education, and Outreach	28
SCEC4 Planning Process	29
REPORT OF THE ADVISORY COUNCIL	31
Introduction	31
Some General Impressions	31
Evaluation of the CEO Program	32
Feedback on CSEP	34
Advice on Initiatives in Earthquake Simulation and Ground Motion Prediction	35
Other Feedback	36
SCEC4 Planning	38
Final Comments	39
SCEC COMMUNICATION, EDUCATION, AND OUTREACH	40
Introduction	40
Public Outreach Activities	40
Education Program	45
RESEARCH ACCOMPLISHMENTS	50
A. Disciplinary Activities	50
1. Seismology	50
2. Tectonic Geodesy	68
3. Earthquake Geology	72
B. Focus Group Activities	78
1. Unified Structural Representation	78
2. Fault and Rupture Mechanics	84
3. Crustal Deformation Modeling	90
4. Lithospheric Architecture and Dynamics	95
6. Ground Motion Prediction	106
7. Seismic Hazard and Risk Analysis	120
C. Special Projects	129
1. Southern San Andreas Fault Evaluation	129
2. Collaboratory for the Study of Earthquake Predictability	131
3. Extreme Ground Motion	136
4. Community Modeling Environment	140
DRAFT 2010 SCIENCE PLAN	160

Table of Contents

I. Introduction	160
II. Guidelines for Proposal Submission	160
III. SCEC Organization	161
IV. Proposal Categories	162
V. Evaluation Process and Criteria	163
VI. Coordination of Research Between SCEC and USGS-EHRP	164
VII. SCEC3 Science Priority Objectives	165
VII-A. Disciplinary Activities	167
1. Seismology	167
2. Tectonic Geodesy	168
3. Earthquake Geology	169
VII-B. Interdisciplinary Focus Areas.....	170
1. Unified Structural Representation (USR)	171
2. Fault and Rupture Mechanics (FARM).....	171
3. Crustal Deformation Modeling (CDM)	172
4. Lithospheric Architecture and Dynamics (LAD)	173
5. Earthquake Forecasting and Predictability (EFP)	174
6. Ground Motion Prediction (GMP)	175
7. Seismic Hazard and Risk Analysis (SHRA)	175
VIII. Special Projects and Initiatives	177
1. Southern San Andreas Fault Evaluation (SoSAFE).....	177
2. Working Group on California Earthquake Probabilities (WGCEP)	178
3. Next Generation Attenuation Project, Hybrid Phase (NGA-H).....	179
4. End-to-End Simulation.....	179
5. Collaboratory for the Study of Earthquake Predictability (CSEP).....	179
6. National Partnerships through EarthScope	180
7. Extreme Ground Motion Project (ExGM).....	180
8. Petascale Cyberfacility for Physics-Based Seismic Hazard Analysis (PetaSHA)	180
9. Advancement of Cyberinfrastructure Careers through Earthquake System Science (ACCESS).....	181
IX. SCEC Communication, Education, and Outreach.....	181
Appendix: SCEC3 Long-Term Research Goals	182
Basic Research Problems	182
1. Earthquake Source Physics	183
2. Fault System Dynamics	183
3. Earthquake Forecasting and Predictability	184
4. Ground Motion Prediction	185
SCEC ANNUAL MEETING ABSTRACTS	186
Plenary Presentations.....	186
Group 1. Poster Abstracts.....	189
Communication, Education, and Outreach (CEO).....	189
Community Modeling Environment (CME).....	195
Ground Motion Prediction (GMP)	205
Seismic Hazard and Risk Analysis (SHRA)	205
Earthquake Forecasting and Predictability (EFP)	226
Seismology	233
Earthquake Geology	251
Southern San Andreas Fault Evaluation (SoSAFE).....	251
Group 2. Poster Abstracts.....	260

Table of Contents

Unified Structural Representation (USR).....260
Lithospheric Architecture and Dynamics (LAD).....269
Crustal Deformation Modeling (CDM).....269
Tectonic Geodesy.....282
Fault Rupture and Mechanics (FARM).....296
MEETING PARTICIPANTS.....333
GROUP 1 POSTER MAP.....336
GROUP 2 POSTER MAP.....337

SCEC Annual Meeting Program

SATURDAY, SEPTEMBER 12, 2009

- 10:00 – 17:00 Workshop on Dynamic Weakening Mechanisms (*pages 5-6*)
13:00 – 17:00 Workshop on Transient Anomalous Strain Detection (*pages 7-8*)

18:30 – 20:00 Dinner (*Poolside*)

SUNDAY, SEPTEMBER 13, 2009

- 07:00 – 08:00 Breakfast (*Poolside*)

08:00 – 11:59 Workshop on Dynamic Weakening Mechanisms (*pages 5-6*)
08:00 – 11:59 Workshop on Transient Anomalous Strain Detection (*pages 7-8*)
08:00 – 15:00 Student Field Trip to the San Gorgonio Pass (*page 12-19*)
08:00 – 17:00 Source Inversion Validation Workshop (*pages 9-10*)
13:00 – 17:30 Southern San Andreas Fault Evaluation Workshop (*page 11*)
13:30 – 17:30 Science Educator Workshop (*Palm Canyon Room*)

16:30 – 18:30 Poster Session Set-Up (*Plaza Ballroom*)

18:00 Annual Meeting Ice-Breaker / Welcome Reception (*Poolside*)

18:30 SCEC Advisory Council Meeting (*Boardroom*)
20:00 – 22:30 Poster Session I - Group 1 Posters (*Plaza Ballroom*)

MONDAY, SEPTEMBER 14, 2009

- 07:00 – 08:00 Breakfast (*Poolside*)

Annual Meeting Session I (*Horizon Ballroom*)

- 08:00 Welcome and State of the Center (*T. Jordan*)
08:30 Report from NSF (*G. Anderson*)
08:40 Report from USGS (*M. Blanpied, E. Lemersal*)
08:50 Communication, Education, & Outreach Highlights (*M. Benthien*)
09:10 SCEC Science Accomplishments (*G. Beroza*)

10:10 Break

Annual Meeting Session II (*Horizon Ballroom*)

- 10:40 Introduction to the SCEC4 Proposal Process
(*T. Jordan, N. Lapusta, G. Beroza*)
- 11:00 **Plenary Talk:** Deciphering tectonic tremor beneath the San Andreas fault near Parkfield: Repeating events, migration, and possible deep slip preceding the 2004 M 6.0 earthquake (*D. Shelly*)
- 11:30 **Science Discussion:** What data are most needed to understand the processes of active faulting, and which are the most promising for discovering new earthquake phenomena?
(Moderator: *G. Beroza* | Reporter: *M. Oskin*)
- 13:00 Lunch (*Poolside*)
- 14:30 – 16:00 Poster Session II - Group 1 Posters (*Plaza Ballroom*)

Annual Meeting Session III (*Horizon Ballroom*)

- 16:00 **Plenary Talk:** Bridging the gap between seismology and engineering: avenues for collaborative research (*C. Goulet*)
- 16:30 **Science Discussion:** How can earthquake scientists most effectively work with earthquake engineers to reduce earthquake risk?
(Moderator: *S. Krishnan* | Reporter: *R. Graves*)
- 18:00 Adjourn
- 19:15 SCEC Recognition Banquet (*Horizon Ballroom*)
- 20:30 – 23:00 Poster Session III - Group 1 Posters (*Plaza Ballroom*)

TUESDAY, SEPTEMBER 15, 2009

- 07:00 – 08:00 Poster Turn-Over (*Plaza Ballroom*)
- 07:00 – 08:00 Breakfast (*Poolside*)

Annual Meeting Session IV (*Horizon Ballroom*)

- 08:00 **Plenary Talk:** Fault lubrication during earthquakes (*G. Di Toro*)
- 08:30 **Science Discussion:** What field and laboratory observations are most crucial for validating models of stress evolution and rupture dynamics?
(Moderator: *J. Chester* | Reporter: *N. Lapusta*)
- 10:00 Break

TUESDAY, SEPTEMBER 15, 2009

Annual Meeting Session V (*Horizon Ballroom*)

- 10:30 **Plenary Talk:** Magnitude-frequency statistics on a single fault: Does Gutenberg-Richter scaling apply? (*M. Page*)
- 11:00 **Science Discussion:** How can progress best be made in understanding the predictability of earthquake ruptures?
(Moderator: *N. Field* | Reporter: *J. Hardebeck*)
- 12:30 Lunch (*Poolside*)
- 12:30 SCEC Advisory Council Meeting, Executive Session (*Boardroom*)
- 13:30 – 15:30 Salton Trough Seismic Project Group Meeting (*Palm Canyon Room*)
- 14:00 – 15:30 Poster Session IV - Group 2 Posters (*Plaza Ballroom*)

Annual Meeting Session VI (*Horizon Ballroom*)

- 15:30 **Plenary Talk:** Seismic tomography and imaging of the southern California crust (*C. Tape*)
- 16:00 **Science Discussion:** What innovations in theoretical and numerical modeling are needed to understand fault-system dynamics, forecast earthquake occurrence, and predict earthquake effects?
(Moderator: *B. Aagaard* | Reporter: *T. Becker*)
- 17:30 2010 Science Collaboration and Planning
- 18:00 Adjourn
- 19:00 Dinner (*Poolside*)
- 20:00 – 22:30 Poster Session V - Group 2 Posters (*Plaza Ballroom*)
- 20:00 – 22:00 SCEC Advisory Council Meeting, Executive Session (*Boardroom*)

WEDNESDAY, SEPTEMBER 16, 2009

07:00 – 08:00 Remove Posters (*Plaza Ballroom*)

07:00 – 08:00 Breakfast (*Poolside*)

Annual Meeting Session VII (*Horizon Ballroom*)

08:00 **Plenary Talk:** Long- and short-term operational earthquake forecasting in Italy: the case of the April 6, 2009, L'Aquila earthquake (*W. Marzocchi*)

08:30 **Science Discussion:** How should SCEC participate in national and international partnerships to promote earthquake system science? (Moderator: *R. Lohman* | Reporter: *J. Shaw*)

10:00 Report from the SCEC Advisory Council (*M.L. Zoback*)

10:30-12:00 SCEC4 Planning and Wrap-Up Session (*including reports from Session Themes Discussion, input from the SCEC Board Committee on Fundamental Problems in Earthquake Science, and forward planning for SCEC4 Proposal*)

12:00 Adjourn

12:00 – 14:00 SCEC Board Working Lunch Meeting (*Boardroom*)

12:00 – 14:00 SCEC Planning Committee Working Lunch Meeting (*Palm Canyon Room*)

Workshop Descriptions and Agendas

DYNAMIC WEAKENING MECHANISMS WORKSHOP

Conveners: Eric Dunham and Judi Chester

Over the past several years there has been a surge of research on dynamic weakening mechanisms, i.e., processes by which fault strength is dramatically reduced during coseismic slip. Dynamic weakening offers a possible resolution of a number of outstanding issues in fault and rupture mechanics, including the heat flow paradox, the low stresses inferred to be acting on major faults, and why ruptures take the form of narrow slip pulses. A variety of weakening mechanisms have been proposed, including flash heating of asperity contacts, thermal pressurization of pore fluid, macroscopic melting, and thermal decomposition weakening. At this workshop, speakers will provide an overview of 1) the latest high velocity friction experiments; 2) theoretical predictions of fault strength as a function of slip rate, normal stress, and other variables; 3) consequences of dynamic weakening in spontaneous rupture models; and 4) field constraints. The objective of the workshop is to foster discussion between experimentalists, modelers, and geologists in order to determine which weakening mechanisms are active in natural earthquakes and how they influence rupture behavior.

SATURDAY, SEPTEMBER 12, 2009 — *Horizon Ballroom I*

Introductions and Overview

- 10:00 – 10:10 Introduction (*E. Dunham and J. Chester*)
10:10 – 10:40 Overview of Dynamic Weakening Mechanisms (*J. Rice*)

Session I: High Velocity Experiments and Understanding Weakening Mechanisms

- 10:40 – 11:10 (*D. Goldsby*)
11:10 – 11:40 (*V. Prakash*)
11:40 – 12:10 (*K. Brown*)
12:15 – 13:45 Lunch
13:45 – 14:15 (*Z. Reches*)
14:15 – 14:45 (*H. Kitajima*)
14:45 – 15:30 Session I Discussion
15:30 – 15:45 Break

Session II: Interpreting Observations and Integrating Dynamic Weakening into Rupture Models

- 15:45 – 16:15 (*A. Rempel*)
16:15 – 16:45 (*H. Noda*)
16:45 – 17:00 Wrap-Up Discussion
18:30 – 20:00 Dinner

SUNDAY, SEPTEMBER 13, 2009 — *Horizon Ballroom I*

Session II: Continued

08:00 – 08:30 (E. Brodsky)
08:30 – 09:00 (G. Di Toro)
09:00 – 09:30 (N. Beeler)
09:30 – 09:45 Break
09:45 – 10:15 (J. Andrews)
10:15 – 11:30 Session II Discussion

Moving Forward – What earthquake physics science priorities should SCEC4 pursue?

11:30 – 11:59 Wrap-Up Discussion (E. Dunham and J. Chester)

WORKSHOP ON TRANSIENT ANOMALOUS STRAIN DETECTION

Conveners: Rowena Lohman and Jessica Murray-Moraleda

The Transient Detection Test Exercise is a project in support of one of SCEC III's main science objectives, to "develop a geodetic network processing system that will detect anomalous strain transients." Fulfilling this objective is a high priority for SCEC and will fill a major need of the geodetic community. A means for systematically searching geodetic data for transient signals has obvious applications for network operations, hazard monitoring, and event response, and may lead to identification of events that would otherwise go (or have gone) unnoticed.

As part of the test exercise datasets are distributed to participants who then apply their detection methodology and report back on any transient signals they find in the test data. Phase I of the exercise ran from January 15 to March 15, 2009; the test data and results are posted at <http://groups.google.com/group/SCECtransient>. Phase II of the test exercise has begun with the distribution of test data June 16, 2009. Both Phase I and II have used synthetic GPS datasets, but we plan to expand this to include real data and other data types in future phases.

The goal of the workshop will be to assess what we have learned to-date and directions on which to focus as the project moves forward. Presentations and discussion in the first half of the workshop will cover the methodologies under development by different groups, characteristics of the Phase I and Phase II test datasets, modifications to the testing procedure based on Phase I results, and release of the results from Phase II testing. In the second half of the workshop participants will address issues relating to the next phase of the project, including whether the next test phase should involve real data, what modifications to the metrics for comparing results will be required by real data, what features could be added to synthetic datasets to enable testing of specific functionality, which types of approaches may be best able to distinguish tectonic vs. non-tectonic spatially-coherent transient signals, and what additional data types should we involve. In addition, we will establish a timeline for these activities and identify objectives for beyond Phase III.

All interested individuals are encouraged to attend, regardless of whether they have participated in the test exercise up to this stage.

SATURDAY, SEPTEMBER 12, 2009 — *Plaza Ballroom AB*

13:00 – 13:20 Introduction and Organization of Test Exercise (*J. Murray-Moraleda*)

13:20 – 15:00 Methodologies and Test Results Using Real and/or Synthetic Data

(J. Langbein)

(K.H. Ji, T. Herring)

(P. Segall, Z. Liu, J. Murray-Moraleda)

(S. Kedar)

(J. McGuire)

15:00 – 15:20 Break

Workshop on Transient Anomalous Strain Detection | **Agenda**

- 15:20 – 17:00 Methodologies and Test Results Using Real and/or Synthetic Data
(continued)
(*K. Johnson*)
(*B. Lipovsky*)
(*W. Holt*)
(*M. Simons*)
- 18:30 – 20:00 Dinner

SUNDAY, SEPTEMBER 13, 2009 — *Plaza Ballroom AB*

- 07:00 – 08:00 Dinner
- 08:00 – 09:00 Methodologies and Test Results Using Real and/or Synthetic Data
(continued)
(*I. Zaliapin*)
(*F. Ohya*)
- 09:00 – 09:20 Phases I and II Test Data (*D. Agnew*)
- 09:20 – 10:00 Phases I and II Results (*R. Lohman*)
- 10:00 – 10:15 Break
- 10:15 – 11:00 Discussion Session for Phase I and II (What we have learned, synthetic
and/or real data: modifications, metrics for comparisons)
- 11:00 – 11:59 Beyond Phase III (Further testing using synthetic data, timeline for
ingesting real data, implementation of monitoring systems)

SOURCE INVERSION VALIDATION WORKSHOP

Conveners: P. Martin Mai, Morgan Page, Danijel Schorlemmer

Detailed knowledge about the kinematics of the earthquake source process is critical for inferring rupture dynamics, for building source models for ground-motion simulation, and for studying earthquake mechanics in general. However, source-inversion results for past events exhibit large intra-event variability for models developed by different research teams for the same earthquake. Also, the reliability, resolution, and robustness of the inversion strategies and the obtained rupture models have not received their due attention.

This workshop is a follow-up on two workshops in the past year during which the Source Inversion Validation (SIV) project for earthquake rupture imaging was discussed. We thus particularly invite researchers working in earthquake source inversion and statistical analysts interested in developing a "testing platforms" for the SIV-project. The first part of this workshop will be dedicated to invited lectures. This will be followed by presentations and discussions on the first "testing models", and in particular results from initial Green's function testing. The second part of the workshop will feature presentations and discussions on the infrastructure and implementation of the testing center. Future funding for participating groups will also be discussed. We hope for many dedicated scientists who will devote time and energy into the SIV-project, but we also invite users of source-rupture models and those genuinely interested in earthquake source inversion.

SUNDAY, SEPTEMBER 13, 2008 — *Horizon Ballroom II*

PART A: Methods

- 08:00 Introduction and Review of SIV Activities (*M. Mai, M. Page*)
- 08:15 Uncertainty Assessment in Source Inversions (*R. Archuleta*)
- 08:45 Bayesian Inference of Kinematic Rupture Parameters (*D. Monelli*)
- 09:15 Kinematic Inversion of Physically Plausible Earthquake Source Models Obtained from Dynamic Rupture Simulations (*O. Konca*)
- 09:45 Break
- 10:15 Resolution of Source Inversion Problems and the Use of Inhomogeneous and Multi-Scale Source Models (*T. Uchide*)
- 10:45 What Did We Learn From the Exercise of the SIV Blind Test I? (*G. Shao*)
- 11:15 – 12:00 OPEN DISCUSSION ON METHODS
- 12:00 – 13:30 Lunch

PART B: SIV Implementation

- 13:30 CSEP: Experience with a Scientific Testing Center (*D. Schorlemmer*)
- 13:45 Implementational Aspects of CSEP (*M. Liukis, D. Schorlemmer*)
- 14:15 – 15:00 OPEN DISCUSSION ON IMPLEMENTATION OF SIV
- 15:00 – 15:30 Break

OPEN SESSION: Planning the Next Steps

15:30 - 17:00 Expectations for the Forward-Modeling Problems

- Point-Source Green's Function
- Finite-Fault with Known (and Simple) Inhomogeneous Rupture

Expectations for Inverting for a Simple, But Inhomogeneous Rupture

Workshop in March 2010

- Date, Location, and Duration
- Source of Future Funding
- Commitment to Participation of the Modeling Groups

17:00 Adjourn

SOUTHERN SAN ANDREAS FAULT EVALUATION WORKSHOP

Conveners: Tom Rockwell and Kate Scharer

The Southern San Andreas Fault Evaluation (SoSAFE) project is in the final (3rd) year of its initial phase (affectionately referred to as Phase 1). SoSAFE has made significant progress in its first three years towards better defining slip rates and earthquake history of southern San Andreas fault system for the last 2000 years.

This workshop will focus on two primary aspects: 1) summarizing the highlights of SoSAFE for phase 1 in preparation of writing a summary report for the project; and 2) discussing the future direction of the southern San Andreas initiative, potential funding sources in addition to SCEC and the USGS, and discussion of exciting new directions of research. For each group funded by SoSAFE in the past three years, we request a 12-minute presentation with your best stuff, along with a written summary of your group's work. The initial three years of SoSAFE have been funded primarily by the USGS Multi-Hazards Demonstration Project. As with other workshops tied to the annual meeting, travel and accommodations are covered under the individual PI grants.

SUNDAY, SEPTEMBER 13, 2009 — *Horizon Ballroom 1*

13:00 Brief History of SoSAFE (*T. Rockwell, L. Jones*)

Fault Projects: North to South, East to West

13:10 Summary of Carrizo Plan Paleoseismology and Mapping (*S. Ackiz*)

13:30 Paleoseismic Results from Frazier Mountain (*K. Scharer*)

13:50 Slip rates from the San Bernardino Segment (*S. McGill*)

14:10 Summary of Biskra Palms Slip Rates (*W. Behr*)

14:30 Summary of Southernmost San Andreas Fault Work (*P. Williams*)

14:50 Break

15:10 New Slip Rate Estimates Along the Northern San Jacinto Fault
(*N. Onderdonk*)

15:30 Summary of Slip History, Southern San Jacinto Fault (*K. Le*)

15:50 Slip and Timing for the Past Six Events, Imperial Fault (*A. Meltzner*)

Modeling Studies

16:10 Integration of Site Data into Rupture Histories (*R. Weldon*)

16:30 Discussion of Future Goals

17:30 Adjourn

A STUDENT-ONLY FIELD TRIP: THE ENIGMATIC SAN GORGONIO PASS

Trip Leader: Doug Yule

SUNDAY, SEPTEMBER 13, 2009 — *Depart from Hilton Palms Springs Lobby at 08:00.*

The largest discontinuity along the 1100-km length of the San Andreas fault occurs in the San Gorgonio Pass region. The structural complexity presents a formidable challenge to forecasting the source characteristics of the fault system there. A primary objective of this field trip is to introduce student participants to some of the world-class geologic features on display and inspires questions and new directions for research. For those so inspired, a short overview article by Yule (2009) (and articles referenced therein) may be a good place to start learning more about the Pass region.

Mileages for this field trip begin at the intersection of Indian Canyon Drive and Tahquitz McCallum Way, a short distance to the west of the Hilton Palm Springs Resort, site of the 2009 SCEC Annual Meeting.

Directions to Stop 1. Drive 7.0 mi north on Indian Canyon Drive to Dillon Road and turn left (west). Drive 3.0 mi to Worsely Road and turn right (north). Drive 0.75 mi to Stop 1. Park vehicles on the right shoulder of Worsely Road.

While driving to Stop 1. Indian Canyon Drive intersects the Garnet Hill fault ~5 mi north of the starting point for this trip. The fault trace is mapped at the base of Hill, immediately to the northeast of this location. Located in the center of a broad alluvial plain, Garnet Hill's occurrence can be explained by oblique slip (dextral-reverse slip) at a left stepover along the trace of the Garnet Hill fault (Figure 1). Other compressive steps in the fault trace occur to the northwest at Hugo Hill and East Whitewater Hill located to the east and west of the Hwy 62/Interstate 10 interchange, respectively. Indian Canyon Drive also crosses the Coachella Valley Banning fault ~6 mi north of the starting point. Buildings on both sides of the road are constructed directly on the fault trace here (pre Alquist-Priolo Act?). The Coachella Valley Banning fault also intersects Dillon Road ~0.75 mi to the west of Indian Canyon Drive. To the north of Dillon Road here, a south-facing scarp is evident where the fault has truncated an alluvial fan remnant. A similar-looking fan remnant occurs ~2 km along strike to the northwest, near Stop 1, and may represent the displacement across the Coachella Valley Banning fault since fan abandonment.

Stop 1. Coachella Valley Banning fault. Geomorphic expression of the fault here suggests pure, or nearly pure, strike slip motion. Shutter ridges occur to the east of the parking area. Here, a narrow, elongate gully marks the fault and separates shutter ridges on either side of the fault. Walk east ~150 m to the top of these ridges for a view of the southern alluvial fan fragment that may match with the northern fragment along Dillon Road ~ 2 km to the east. On a clear day, Garnet Hill (and the trace of the Garnet Hill fault) is visible ~5 km to the southeast.

The epicenter of the 1986 ML 5.9 North Palm Springs earthquake is located ~7.5 km to the north of Stop 1 (Figure 1). The rupture is interpreted to have occurred along a plane oriented ~N70°W, 45°NE, with a first-motion rake of 180°, indicating pure strike-slip faulting (Jones et al., 1986). First motion solutions for aftershocks indicate predominantly oblique motion (dextral reverse). Surface cracks were observed along the trace of the

Agenda | Student Field Trip to San Gorgonio Pass

Coachella Valley Banning fault from Devers Hill to Whitewater Canyon; cracks were also observed in the fault scarp of the Garnet Hill fault at the mouth of Whitewater Canyon (Sharp et al., 1986). Displacements across cracks were determined to be legible.

Directions to Stop 2. Continue north on Worsely Road for 0.4 mi to the intersection with Painted Hills Rd. Make a hard left turn (now heading SW) and drive 0.25 mi to intersection with Old Morongo Rd. Bear left at intersection and drive 3.25 mi bearing generally SW to intersection with Whitewater Cutoff. Follow Whitewater Cutoff 0.65 mi across the Whitewater River to intersection with Whitewater Canyon Road. Turn right (north) and drive 1.45 mi to Stop 2. Park on shoulder of road and walk to where one has a good view of canyon exposures to the west.

While driving to Stop 2. The Coachella Valley Banning fault follows the base of the hills to the north. About halfway to Whitewater Canyon, the road passes north of East Whitewater Hill, a hill located at a left stepover of the Garnet Hill fault (Figure 1). Descending into Whitewater Canyon, roadcut exposures show a well-developed, orange-weathering soil beneath the upland surface; also note the coarse alluvial gravel that comprises the outcrop beneath the soil. Note the south-facing scarp of the Garnet Hill fault to the north of the road and to the west of Whitewater River (Matti et al., 1985). Buildings are constructed at the base of this scarp.

Stop 2. Coachella Valley Banning fault at Whitewater Canyon (Figures 1 and 2). Vegetation in Whitewater Canyon marks the surface trace of the Coachella Valley Banning fault. The fault is also exposed in a large side canyon to the west of the parking area. Here the fault juxtaposes a Cretaceous-Precambrian granite and gneiss complex on the north against Pleistocene alluvial gravels on the south. Where exposed, the fault dips 45° N in the south-facing slopes of the side canyon. Time permitting one may walk into the side canyon to view the fault and its geomorphic expression of small ridges cutting parallel to contour, across the south-facing slopes of the side canyon.

Directions to Stop 3. Return to intersection of Whitewater Canyon Road and Whitewater Cutoff. Turn right (west) and drive 0.15 mi to I-10 onramp. Enter Interstate 10 and drive 2.55 mi to exit for Haugen Lehman Way. Exit and follow off ramp for 0.2 mi (it passes beneath an overpass and then doubles back). Turn left (north) onto Haugen Lehman Way. Drive 0.7 mi to intersection with Cottonwood Dr. Turn right (NW) and drive 0.8 mi to end of pavement, continue uphill 0.5 mi on dirt road to parking area and Stop 3.

While driving to Stop 3. The large hill to the north, known as West Whitewater Hill, exposes fluvial deposits of the Cabezon Formation and is capped with a deep-red soil, indicative of $\geq 100,000$ yrs of exposure. The surface has an anticlinal shape. Moderate dips in underlying deposits define this anticlinal warp as well. The deposits appear more deformed than the surface, so the anticline was growing during, as well as after, deposition of the sediments (Yule and Sieh, 2003). Northwest-trending faults cut the deposits and the old surface.

The provenance of Cabezon gravels exposed at West Whitewater Hill indicates a source from the north of the Mission Creek fault, by way of an ancestral Whitewater River (Allen, 1957; Matti et al., 1985, 1992; Matti and Morton, 1993). Paleocurrent indicators in the gravels led Matti et al. (1985, 1992) and Matti and Morton (1993) to propose about 2-3

km of dextral slip across the Coachella Valley Banning fault since the gravels were deposited.

The Garnet Hill fault bounds the southern flank of West Whitewater Hill and has two traces, one along the flank of the steep southern slope of the anticline, and another in the young alluvium farther south (Matti et al., 1992, Matti and Morton, 1993, Morton et al., 1987). There is geomorphic evidence that slip on these faults is a combination of dextral and reverse slip, and by the rule of V's, the trace geometry of the northern fault indicates a steep to moderate dip northward.

Stop 3. Cottonwood Canyon. A major change in the style of active faulting occurs at Cottonwood Canyon (Figures 1 and 2). To the east, shutter ridges in gravel as well as channels cut into bedrock show dextral offset along the Coachella Valley Banning fault. Active strike-slip motion on the Coachella Valley Banning fault diminishes toward the west where it appears to end as an active strike-slip fault at Cottonwood Canyon (Yule and Sieh, 2003).

To the west, thrust faults dominate the neotectonic landscape. The active and inactive thrusts include the San Gorgonio Pass thrust and Banning fault systems, respectively. We will explore the evidence for this style of faulting at this stop. Here, several old alluvial surfaces along the mountain front project well above neighboring active alluvial fans (see Figure 11 in Yule and Sieh, 2003). For example, a few hundred meters south of the mountain front a broad active channel separates an old alluvial surface into two remnant terraces. Young alluvium laps onto both remnants except for the western flank of the western remnant that has been eroded. The southeastern edges of both terrace remnants are also eroded, but that erosion occurred in response to uplift of the terraces along a NE-SW-striking, NW-dipping thrust.

Small thrust scarps also occur in young alluvium to the north of the terrace remnants, at the foot of the range. Exposed in the hill above these scarps, granite and gneiss overlie older alluvium along a low-angle, south-dipping contact. This contact is interpreted to be a thrust fault that is no longer active as slip has stepped southward to the thrusts described above.

A large rotational landslide obscures the geologic relationships of the slopes immediately west of Cottonwood Canyon (Morton et al., 1987; Yule and Sieh, 2003). The headscarp and lateral margins of this slide are readily apparent and leave no doubt that the feature is of non-tectonic origin. A small sector on the western flank of the slide failed in 1993.

Directions to Stop 4. Return to I-10. From the onramp, enter I-10 freeway and drive 4.9 mi to Cabezon exit. Drive 0.15 mi to stop sign at end of off ramp and turn left (west) onto frontage road. Drive 1.9 mi to a roundabout intersection and continue west on frontage road for 1.3 mi to Fields Rd. Turn right and proceed to entrance gate to Morongo Band of Mission Indians Reservation. Note: permission to access tribal lands can be obtained beforehand from the Tribe's Environmental Office. Once inside the gate make an immediate right turn onto Martin Road. Drive 1.0 mi to end of pavement and bear left (NE) onto dirt road heading into Millard Canyon. Drive 0.65 mi to intersection with small dirt road and park (Stop 4a). If time permits, continue north 0.75 mi to a four-way, dirt intersection and park (Stop 4b).

While driving to Stop 4. As one approaches the 27-story Casino Morongo and Hotel, look to the north and notice a scarp that cuts at a high angle across the mouth of Millard Canyon. This base of this scarp marks the surface trace of the San Gorgonio Pass thrust. We will visit this feature at Stop 4a. The scarp at Millard Canyon continues southwest

Agenda | Student Field Trip to San Gorgonio Pass

where it almost intersects Interstate 10 (Figures 1 and 2). Here, cutting through the parking lots behind a large factory-outlet shopping mall, the fault trace bends northwest toward the mountain front along a series of strike-slip tear faults (Yule and Sieh, 2003). After entering the Morongo Reservation, look to the south while driving east on Martin Road and notice that the alluvial surface projects above the outlet mall. This surface has been uplifted in the hanging wall of the San Gorgonio Pass thrust.

Stop 4a. Millard Canyon, San Gorgonio Pass thrust scarp. A fluvial terrace riser is evident ~150 m east of the parking area. Climb the riser and walk southeast to the highest point on the scarp, a height of 12.5 m above the base of the scarp. Walk down the scarp and notice that the slope gradually gets steeper and reaches its maximum steepness at the base of the scarp. This steeping down the slope defines an asymmetric fold and suggests that little, if any, diffusion has occurred across the scarp. Shortening at the surface may be accommodated entirely by folding above a blind thrust. If the thrust has reached the surface here it must have a slip vector of ~S40°E parallel to a small fluvial terrace riser that can be followed from the hanging wall block to the footwall block with no lateral offset (see Fig. 6 in Yule and Sieh, 2003).

Walk east from the high scarp and climb down another fluvial terrace riser onto a much younger alluvial surface. Look for a 1.5 m scarp on this lower surface to the east of a dirt road. The west wall of the modern arroyo exposes gravel and sand layers cut by a 24° north-dipping thrust.

Ages of the high and low scarps are poorly constrained. Detrital charcoal from gravel layers beneath the lower surface yield an age of 2850-3600 radiocarbon years (J.C. Tinsley and J.C. Matti in Matti et al., 1992a, p. 26). The poor degree of soil development on the upper surface suggests that it is no older than latest Pleistocene in age. The preliminary age data from these surfaces constrain uplift and north-south shortening each to be >1-2 mm/yr over the past 10,000 yrs or so.

Stop 4b. Millard Canyon, Banning fault scarp. Much of the Banning fault in San Gorgonio Pass is inactive. However, a 3-km-long segment of the northern strand is active. About 100 m to the north of the parking area, a 5-m-high scarp and a 2.5-m-high scarp occur in older and younger alluvial surfaces. The fluvial terrace riser between these two surfaces appears to be offset right-laterally ~4.5 m (Figure 8, Yule and Sieh, 2003). Thus the dextral offset across the fault appears to be ~80% greater than the vertical component.

To the east, this active portion of the Banning fault also offsets the late Pleistocene Heights fanglomerate several hundred meters. On the eastern wall of the canyon, the fault trace rises from the canyon floor at a dip of ~45° N and juxtaposes crystalline rocks over the fanglomerate. Farther up the canyon wall the fault flattens to a nearly horizontal dip and overrides the surface of the Heights fanglomerate. Exposures in the canyon wall reveal a buttress unconformity between the fanglomerate and an older eastern wall of the canyon. The base of the buttress unconformity is offset obliquely across the Banning fault with a strike-slip: dip-slip ratio of ~2.5:1, greater than that derived from the younger scar on the valley floor (Yule and Sieh, 2003). Nonetheless, both observations show that strike-slip offset exceeds dip-slip offset on this active section of the Banning fault.

Directions to Stop 5. Return to the Reservation's entrance gate at the intersection of Fields and Martin Roads. Proceed (north) on Fields Road 1.0 mi to Morongo Road and turn left (west). Drive 0.35 mi west to Potrero Road and turn right (north). Drive 0.65 mi to Foothill Road; continue north through the intersection and a metal gate. Drive 2.75 mi uphill along a graded dirt road to a fork in the road at the foot of a small hill. Park and

walk to the top of the hill (Stop 5a). If time permits drive on the right fork and continue uphill 0.35 mi to a 'T' intersection. Turn left (west) and drive 1.25 mi to fork in road and park (Stop 5b, a walking tour along a 500 m segment of the fault).

While driving to Stop 5. Note several 'bumps' in Fields Road that step up on the north. A large house is constructed adjacent to the third and largest of these steps. Each step represents a fault trace of the San Gorgonio Pass thrust system. These structures are interpreted as tear faults that connect thrust faults west of Potrero Canyon with those of Millard Canyon (Matti et al., 1985, 1992a; Matti and Morton, 1993; Yule and Sieh, 2003).

A fluvial terrace riser occurs immediately west of the intersection with Morongo Road. The higher, oldest surface is an isolated erosional remnant that shows an east-west striking scarp, parallel to and north of Morongo Road. Potrero Road crosses this structure provides a profile view of the broad asymmetric fold exposed in the west wall of the modern arroyo. This structure is slightly larger, but similar in style, to the scarp observed at Stop 4a.

The subtle expression of a scarp along the Gandy Ranch fault (Allen, 1957) occurs ~1 km north of the mouth of Potrero Canyon. The scarp is defined by a slight steepening of the alluvial fan surface from north to south immediately north of the modern arroyo.

Stop 5a. Burro Flats overview. Stop 5a is located on top of a low east-west ridge. This ridge is underlain by granite and gneiss and capped by a veneer of coarse alluvium. A marshy area occurs at the base of the hill to the north where groundwater ponds against the bedrock contact. A small up-on-the-south scarp cuts obliquely across the alluvial fan to the north of the marsh. East-trending, down-on-the-south faults occur at the base of the mountains to the north. These east-trending faults comprise the Cox Ranch fault zone, a discontinuous set of inferred normal slip faults in the hanging wall of the San Gorgonio Pass thrust (Yule and Sieh, 2003). The Cox Ranch fault zone can be traced east to the Cottonwood and Whitewater Canyon areas where it appears to merge with the Coachella Valley Banning fault. To the west, the San Bernardino San Andreas fault occurs as a series of right-stepping fault segments. The road to stop 5b runs parallel to the fault. Burro Flats is therefore a fault-bounded, intermontane basin.

On a clear day, this vantage point provides a spectacular view of San Jacinto Peak (elev. 3,270 m). Also to the south, the mouth of Potrero Canyon frames the 27-story Casino Morongo Hotel located in the footwall of the San Gorgonio Pass thrust system.

Stop 5b. Burro Flats trench site. The parking area is located at right-stepover along the San Bernardino San Andreas fault. Walk northwest along the fault trace ~250 m to where the fault branches into two strands at the southeastern edge of another right stepover. Here, in an middle Holocene alluvial fan cut by the fault, a three-dimensional trench excavation was undertaken to explore for buried channels and other features to try and constrain the slip across the fault (Orozco, 2004). A wedge of sand and silt was discovered on both sides of the fault. The wedge tip provided a crude piercing line that indicates 30 ± 15 m of dextral offset has occurred across the fault since deposition of the sand and silt. Detrital charcoal grains constrain the age of the sand/gravel at ~3,800 yrs BP. The slip rate for the San Bernardino San Andreas fault here is 4-12 mm/yr (Orozco, 2004). Further excavation here may help to better constrain the dextral offset and provide a more precise slip rate.

Farther to the northwest, the fault zone broadens to form a 100-m-wide stepover basin. Here the fault enters a marsh that is partially buried by a very young alluvial fan. Interlayered peat and alluvium, in combination with active deformation of the stepover

Agenda | Student Field Trip to San Gorgonio Pass

basin, make this an ideal paleoseismic site. A series of 10 trenches excavated at this site expose evidence for at least nine paleoearthquakes that span the last 2,000 yrs. The most recent rupture deformed peat layers that contain European-introduced pollen and therefore must post-date ~1750 A.D. This most recent event probably represents the 1812 earthquake known from sites 50 to 150 km to the northwest. The penultimate event is constrained to have occurred between 1670 and 1730 A.D. and may correlate with a large earthquake ~300 yrs ago that is known from the paleoseismic record in regions both to the northwest and southeast. In fact, the timing of five paleoearthquakes at this site overlap with the timing of ruptures at sites in both the Mojave and Coachella Valley regions. However, the overlap in age data of 50-100 years cannot rule out competing scenarios. On the one hand, one very large (M 7.9) quake may have ruptured a >300 km length of the fault from the Salton Sea to the Mojave Desert. On the other hand, two or more large (M 7.4) quakes may have ruptured the same length of the fault over a span of 50 to 100 yrs, perhaps with the structural complexity of San Gorgonio Pass acting as a barrier to thoroughgoing rupture. The former scenario has been adopted over the latter for use in preparing the ShakeOut Exercise.

End of Trip.

Acknowledgements

The author of this field guide would like to acknowledge the work of a team of USGS scientists led by Jonathan Matti and Douglas Morton whose work has contributed immeasurably to our understanding of the geologic evolution of the San Gorgonio Pass region. Though not a co-author on this field guide, Jonathan Matti has volunteered to help lead this trip and the expertise he brings will help to ensure that this will be a superior field trip.

References Cited

- Allen, C.R., 1957, San Andreas fault zone in San Gorgonio Pass, southern California: Geological Society of America Bulletin, v. 68, p. 315-350.
- Matti, J.C., and Morton, D.M., 1993, Paleogeographic evolution of the San Andreas fault in southern California: A reconstruction based on a new cross-fault correlation, in Powell, R.E., Weldon, R.E., II, and Matti, J.C., eds., The San Andreas fault system: Displacement, palinspastic reconstruction, and geologic evolution: Geological Society of America Memoir 178, p. 107-159.
- Matti, J., Morton, D., and Cox, B., 1992, The San Andreas fault system in the vicinity of the central Transverse Ranges province, southern California, U.S. Geological Survey Open-File Report 92-354, 40 p.
- Matti, J.C., Morton, D.M., and Cox, B.F., 1985, Distribution and geologic relations of fault systems in the vicinity of the central Transverse Ranges, southern California: U.S. Geological Survey Open-File Report 85-365, 23 p.
- Morton D., Matti, J., and Tinsley, J., 1987, Banning fault, Cottonwood Canyon, San Gorgonio Pass, southern California, in Cordilleran Section of the Geological Society of America Centennial Field Guide, ed. M. Hill, p. 191-192.
- Orozco, A., 2004, Offset of a mid-Holocene alluvial fan near Banning, CA: Constraints on the slip rate of the San Bernardino strand of the San Andreas fault, California State University Northridge M.S. thesis, 58 p.
- Jones, L.M., Hutton, K.L., Given, D.D., and Allen, C., 1986, The North Palm Springs, California, earthquake sequence of July 1986, Bulletin of the Seismological Society of America, v. 76, p. 1830-1837.

- Sharp, R.V., Rymer, M.J., and Morton, D.M., 1986, Trace-fractures on the Banning fault created in association with the 1986 North Palm Springs earthquake, *Bulletin of the Seismological Society of America*, v. 76, p. 1837-1843.
- Yule, D., 2009, The enigmatic San Gorgonio Pass, *Geology*, v. 37, p. 191-192.
- Yule, D., and Sieh, K., 2003, Complexities of the San Andreas fault near San Gorgonio Pass: Implications for large earthquakes: *Journal of Geophysical Research*, v. 108, no. B11, ETG 9-1-9-23, doi: 10.1029/2001JB000451.

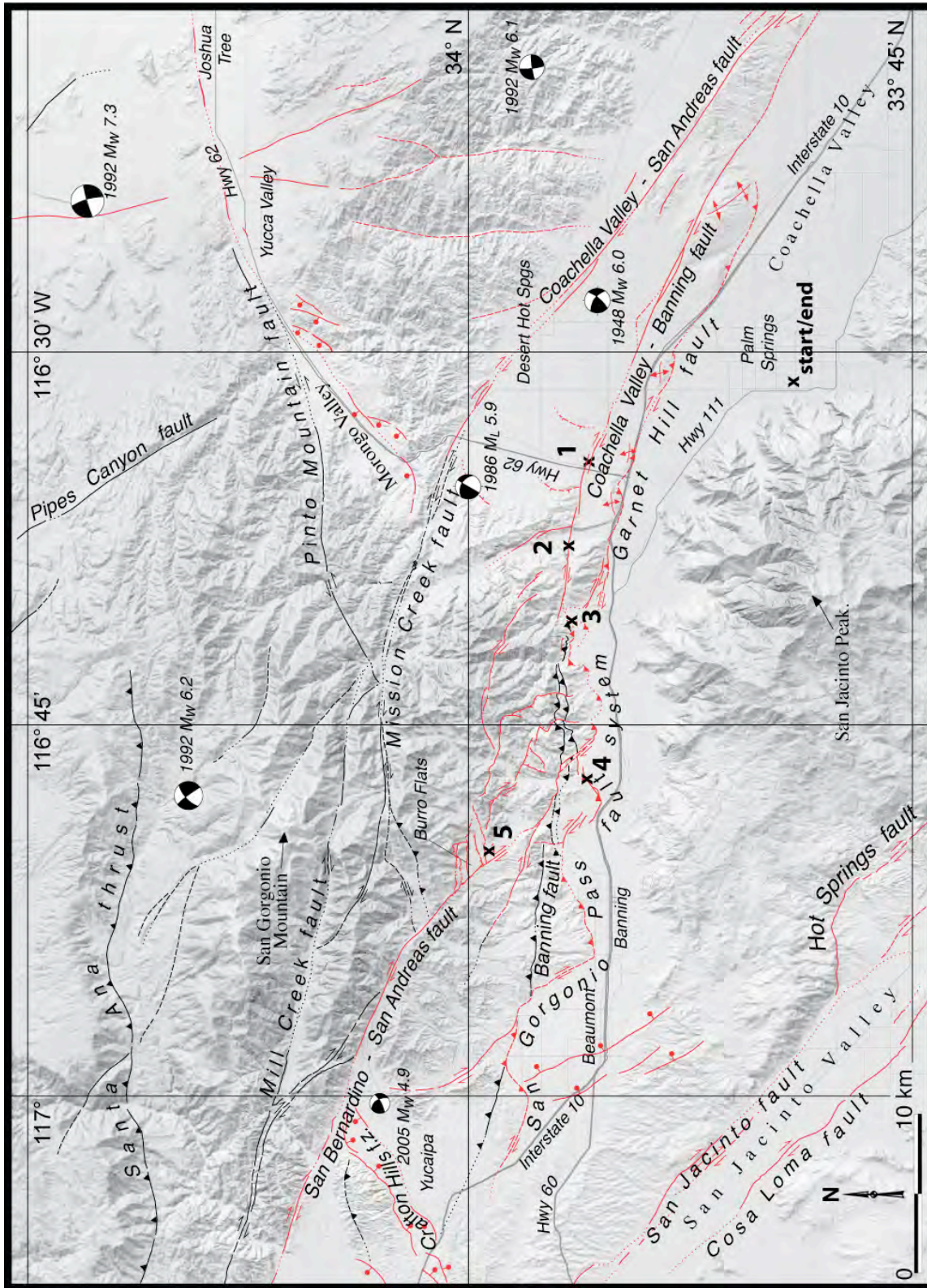


Figure 1. (modified from Figure 1 of Yule, 2009). Field trip stops 1-5 located by "x's". Shaded-relief topographic map of San Gorgonio Pass (SGP) region. Traces of active faults shown in red, inactive faults shown in black. Mapping from Allen (1957), Matti et al. (1985), and Yule and Sieh (2003). Beach-balls show epicenters of moderate earthquakes to strike the region since 1948.

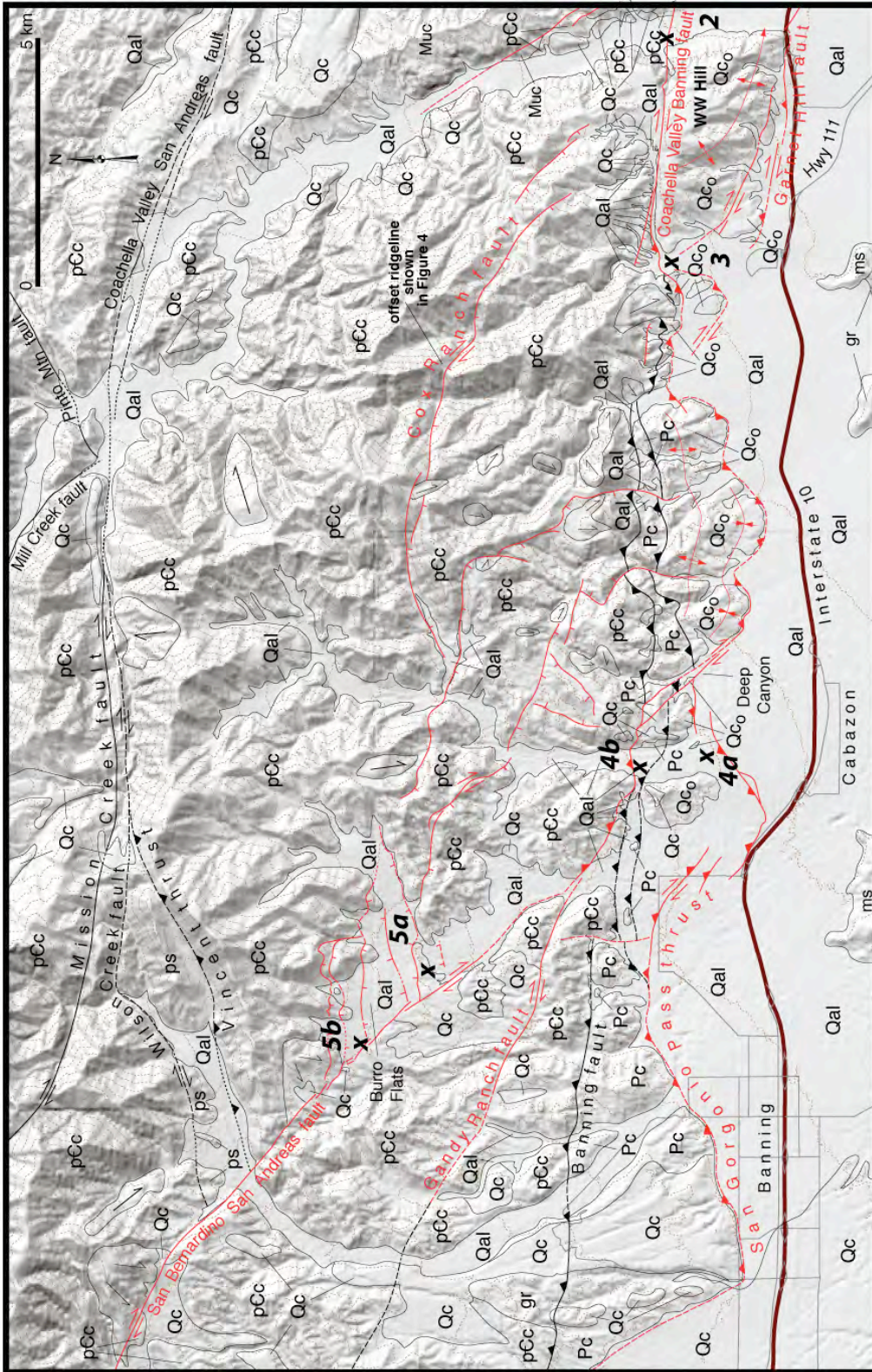


Figure 2. (modified Figure 3a of Yule and Sieh, 2003). Field trip stops 2-5 located by "x's". Generalized geologic map of the central San Gorgonio Pass region. Active and Late Pleistocene structures are shown in red and black, respectively. Rock units: Qal, Holocene alluvium; Qc, early Pleistocene and late Pleistocene alluvium; Qco, moderately deformed late Pleistocene alluvium, including but not limited to the Cabazon Formation; Pc, strongly deformed Pliocene nonmarine deposits; Muc, upper Miocene nonmarine deposits; gr, Mesozoic granitic rocks; ms, metasedimentary rocks; pCc, undivided Cretaceous to Precambrian igneous and metamorphic complex. Topographic contour interval = 100 m. Base map is shaded relief of a composite DEM. Geology modified from Allen, 1957; Matti et al., 1985, 1992; Matti and Morton, 1993.

State of SCEC, 2009

Thomas H. Jordan

SCEC Director

Welcome to the 2009 Annual Meeting!

This is SCEC's 19th Annual Meeting and the third community-wide gathering under the five-year SCEC3 program. The agenda features some very interesting presentations by keynote speakers, discussion sessions on major issues, many outstanding science posters, and a variety of IT demonstrations, education & outreach activities, and social gatherings. Four workshops and a student field trip are scheduled on the weekend before the meeting, and it will be followed by a special review of SCEC's Communication, Education & Outreach (CEO) program.

The week's activities will bring together one of the largest collaborations in geoscience (Figure 1): 466 people have pre-registered so far (compared to 453 last year), and 270 poster abstracts have been submitted—the most ever. This will be the first annual meeting for 121 of this year's pre-registrants, so we will welcome many new faces!

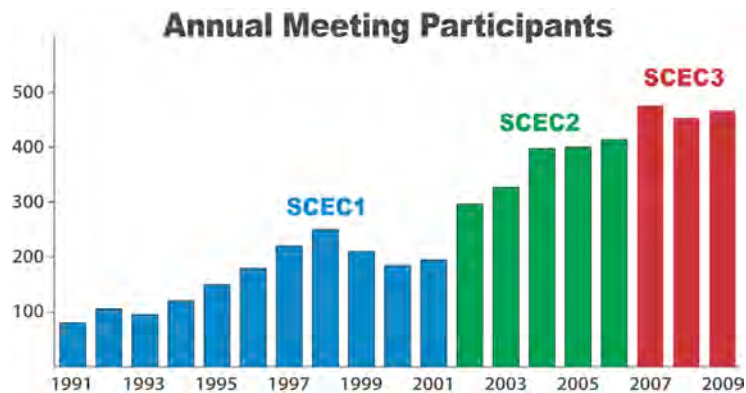


Figure 1. Registrants at SCEC Annual Meetings, 1991-2009. Number for 2009 (466) is pre-registrants.

Goals of the Meeting

Our annual meetings are designed to achieve three goals: to share scientific results and plans in poster sessions, at the meals, and around the pool; to mark our progress toward the priority objectives of the SCEC3 science plan given in Table 1; and to incorporate your ideas for new research into the annual planning process. A draft of the 2010 Science Plan, prepared by Deputy Director Greg Beroza and the Planning Committee, is included in this meeting volume.

A special goal of this year's meeting is to look beyond our annual cycle toward SCEC4, the next five-year phase of the Center's program. The SCEC4 planning process began at a leadership retreat in early June and will culminate with the submission of the SCEC4 proposal to the National Science Foundation (NSF) and the U.S. Geological Survey (USGS) on March 1, 2010. I will describe some

aspects of the SCEC4 planning process and how it relates to the meeting activities at the end of this report.

Table 1. Priority Science Objectives for SCEC3

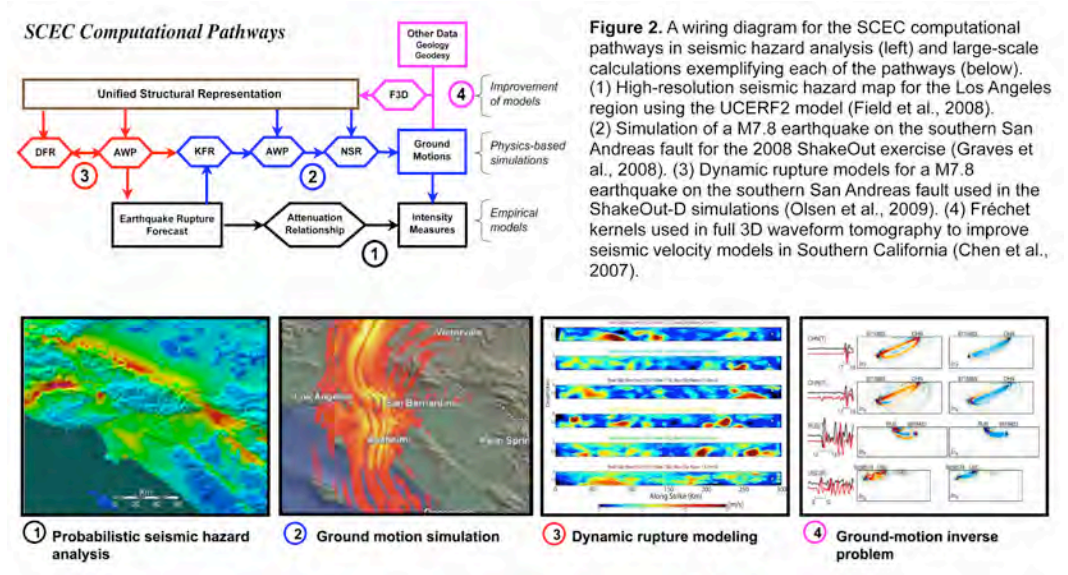
-
1. Improve the unified structural representation and employ it to develop system-level models for earth-quake forecasting and ground motion prediction
 2. Develop an extended earthquake rupture forecast to drive physics-based SHA
 3. Define slip rate and earthquake history of southern San Andreas fault system for last 2000 years
 4. Investigate implications of geodetic/geologic rate discrepancies
 5. Develop a system-level deformation and stress-evolution model
 6. Map seismicity and source parameters in relation to known faults
 7. Develop a geodetic network processing system that will detect anomalous strain transients
 8. Test of scientific prediction hypotheses against reference models to understand the physical basis of earthquake predictability
 9. Determine the origin and evolution of on- and off-fault damage as a function of depth
 10. Test hypotheses for dynamic fault weakening
 11. Assess predictability of rupture extent and direction on major faults
 12. Describe heterogeneities in the stress, strain, geometry, and material properties of fault zones and understand their origin and interactions by modeling ruptures and rupture sequences
 13. Predict broadband ground motions for a comprehensive set of large scenario earthquakes
 14. Develop kinematic rupture representations consistent with dynamic rupture models
 15. Investigate bounds on the upper limit of ground motion
 16. Develop high-frequency simulation methods and investigate the upper frequency limit of deterministic ground motion predictions
 17. Validate earthquake simulations and verify simulation methodologies
 18. Collaborate with earthquake engineers to develop rupture-to-rafters simulation capability for physics-based risk analysis
 19. Prepare for post-earthquake response.
-

Highlights of SCEC Achievements

Greg and the PC have put together an impressive report (included in the meeting volume) on the research projects supported by SCEC in 2009. It demonstrates substantial progress towards the SCEC3 objectives listed in Table 1. Greg will highlight the research results in his plenary address on Monday morning. The poster presentations at the Annual Meeting will provide a forum for more detailed discussions and interchange of ideas. In this section, I'll mention just a few of the many accomplishments achieved by the SCEC special projects.

Under two large grants from NSF's Earth Sciences Division and Office of Cyberinfrastructure, the Community Modeling Environment (CME) collaboration, comprising computer scientists as well as geoscientists, has been developing a petascale cyberfacility for seismic hazard analysis, dubbed PetaSHA. The PetaSHA computational platforms, managed by Phil Maechling, the SCEC Associate Director for Information Technology, are rapidly evolving towards petascale capability. During this past year, the CME was allocated over 30 million service units on NSF and DOE supercomputers, and it delivered major advances in earthquake system science (Figure 2). A broadband simulation of a M7.8 earthquake on the San Andreas fault, computed by Rob Graves

and colleagues on the TeraShake platform, provided the scenario for the Great Southern California ShakeOut in November, 2008, the largest earthquake disaster drill in U.S. history. A series of dynamic rupture simulations computed by SDSU and SDSC scientists further elucidated the ground motions expected from San Andreas earthquakes of this type, as well as their variability. Kinematic and dynamic rupture simulations are underway for a number of other interesting earthquake scenarios in Southern California as part of CME’s “Big Ten” project. Capabilities for full-3D tomography, first demonstrated by the USC group in 2006, are now being applied to the inversion of regional waveform data on the Tera3D platform. Physics-based probabilistic seismic hazard analysis has been implemented on the CyberShake platform, and the first physics-based hazard maps, completed this summer, are showing how source directivity, rupture complexity, and basin effects control strong ground motions throughout the Los Angeles region.



The first time-dependent, uniform California earthquake rupture forecast (UCERF2), released in April, 2008, was developed on, and is being delivered to end-users via, the OpenSHA computational platform. OpenSHA, created by Ned Field and colleagues, is rapidly becoming the software of choice for seismic hazard calculations worldwide, including the Global Earthquake Model (GEM) now being constructed by a large international consortium. Ned chaired the 2007 Working Group on California Earthquake Probabilities that produced UCERF2; this very successful partnership among SCEC, the USGS, and the California Geological Survey (CGS) was co-sponsored by the California Earthquake Authority (CEA). In June, the CEA Governing Board approved major funding for UCERF3, which will incorporate short-term as well as long-term forecasting techniques. The new WGCEP—again a USGS-CGS-SCEC partnership chaired by Ned—will be formally launched in January, 2010. Several informal discussions at the Annual Meeting will focus on the scientific challenges of the new UCERF3 project.

The Collaboratory for the Study of Earthquake Predictability (CSEP), which became operational in September, 2007, has expanded into an international cyberinfrastructure for conducting and evaluating earthquake forecasting models. Through the efforts of Danijel Schorlemmer and his colleagues, testing centers have been established at USC (Los Angeles), GNS (Wellington), ERI (Tokyo), and ETH (Zürich). CSEP is now running earthquake forecasting experiments in California, New Zealand, Japan, the western Pacific, and (as of August 1) Italy.

The results from these large collaborations and several others, including the Southern San Andreas Fault Evaluation (SoSAFE) and Extreme Ground Motions projects will be presented at the meeting.

Organization and Leadership

SCEC is an institution-based center, governed by a Board of Directors, who represent its members. The membership currently stands at 16 core institutions and 53 participating institutions (Table 2). SCEC currently involves more than 650 scientists and other experts in active SCEC projects. A key measure of the size of the SCEC community—registrants at our Annual Meetings—is shown for the entire history of the Center in Figure 1.

Table 2. SCEC Institutions (September 1, 2009)

Core Institutions (16)	Participation Institutions (53)
California Institute of Technology Columbia University Harvard University Massachusetts Institute of Technology San Diego State University Stanford University U.S. Geological Survey, Golden U.S. Geological Survey, Menlo Park U.S. Geological Survey, Pasadena University of California, Los Angeles University of California, Riverside University of California, San Diego University of California, Santa Barbara University of California, Santa Cruz University of Nevada, Reno University of Southern California (lead)	Appalachian State University; Arizona State University; Berkeley Geochron Center; Boston University; Brown University; Cal-Poly, Pomona; Cal-State, Long Beach; Cal-State, Fullerton; Cal-State, Northridge; Cal-State, San Bernardino; California Geological Survey; Carnegie Mellon University; Case Western Reserve University; CICESE (Mexico); Cornell University; Disaster Prevention Research Institute, Kyoto University (Japan); ETH (Switzerland); Georgia Tech; Institute of Earth Sciences of Academia Sinica (Taiwan); Earthquake Research Institute, University of Tokyo (Japan); Indiana University; Institute of Geological and Nuclear Sciences (New Zealand); Jet Propulsion Laboratory; Los Alamos National Laboratory; Lawrence Livermore National Laboratory; National Taiwan University (Taiwan); National Central University (Taiwan); Ohio State University; Oregon State University; Pennsylvania State University; Princeton University; Purdue University; Texas A&M University; University of Arizona; UC, Berkeley; UC, Davis; UC, Irvine; University of British Columbia (Canada); University of Cincinnati; University of Colorado; University of Massachusetts; University of Miami; University of Missouri-Columbia; University of Oklahoma; University of Oregon; University of Texas-El Paso; University of Utah; University of Western Ontario (Canada); University of Wisconsin; University of Wyoming; URS Corporation; Utah State University; Woods Hole Oceanographic Institution

Board of Directors. Under the SCEC3 by-laws, each core institution appoints one member to the Board of Directors, and two at-large members are elected by the Board from the participating institutions. The Board is chaired by the Center Director, who also serves as the USC representative; the Vice-Chair is Lisa Grant Ludwig. During the past year, Tom Brocher replaced Bill Ellsworth as the Board member from USGS Menlo Park, and Ken Hudnut replaced Sue Hough as the Board member from USGS Pasadena. The complete Board of Directors is listed on page ii of the meeting volume.

Advisory Council. The Center’s external Advisory Council (AC), chaired by Dr. Mary Lou Zoback, is charged with developing an overview of SCEC operations and advising the Director and the Board. Since the inception of SCEC in 1991, the AC has played a major role in maintaining the vitality of the organization and helping its leadership chart new directions. A verbatim copy of the AC’s 2008 report follows my report in the meeting volume.

We thank Dr. Jack Moehle, who is rotating off the AC this year, and we welcome Drs. Jim Goltz and Steve Mahin as new AC members.

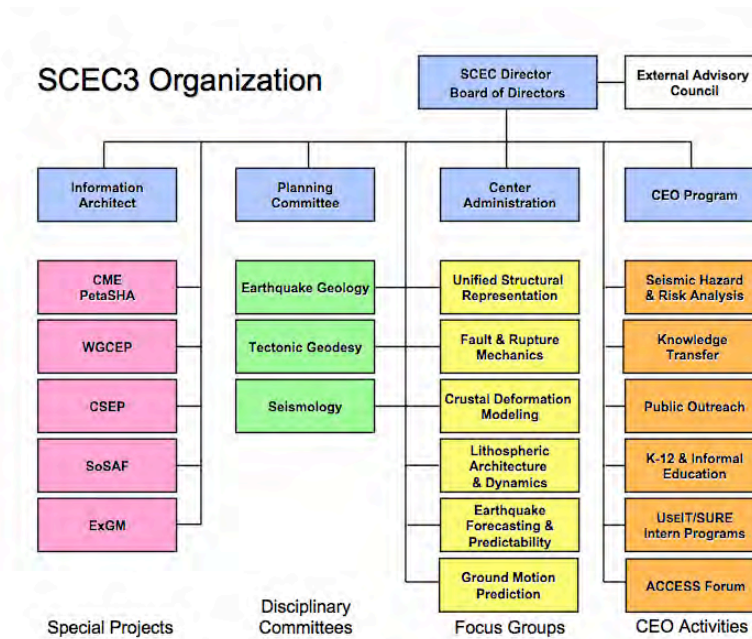


Figure 3. The SCEC3 organization chart, showing the disciplinary committees (green), focus groups (yellow), special projects (pink), CEO activities (orange), management offices (blue), and the external advisory council (white).

Working Groups. The SCEC organization comprises a number of disciplinary committees, focus groups, and special project teams (Figure 3). These working groups have been the engines of its success. The discussions organized by the working-group leaders at the Annual Meeting have provided critical input to the SCEC planning process.

The Center supports disciplinary science through three standing committees in Seismology, Tectonic Geodesy, and Earthquake Geology (green boxes of Figure 3). They are responsible for disciplinary activities relevant to the SCEC Science Plan, and they make recommendations to the Planning Committee regarding the support of disciplinary research and infrastructure.

SCEC coordinates earthquake system science through five interdisciplinary focus groups (yellow boxes): Unified Structural Representation (USR), Fault & Rupture Mechanics (FARM), Crustal Deformation Modeling (CDM), Lithospheric Architecture & Dynamics (LAD), Earthquake Forecasting & Predictability (EFP), and Ground Motion Prediction (GMP).

A sixth interdisciplinary focus group on Seismic Hazard & Risk Analysis (SHRA) manages the “implementation interface” as part of SCEC Communication, Education & Outreach (CEO) program (orange box). In particular, SHRA coordinates research partnerships with earthquake

engineering organizations in end-to-end simulation and other aspects of risk analysis and mitigation.

Table 3. SCEC3 Working Group Leadership

Disciplinary Committees	
Geology	Mike Oskin*
	James Dolan
Seismology	Egill Hauksson*
	Elizabeth Cochran
Geodesy	Jessica Murray-Moraleda*
	Rowena Lohman
Focus Groups	
Structural Representation	John Shaw*
	Kim Olsen
Fault & Rupture Mechanics	Judi Chester*
	Ruth Harris
Crustal Deformation Modeling	Liz Hearn*
	Kaj Johnson
Lithospheric Architecture & Dynamics	Paul Davis*
	Thorsten Becker
Earthquake Forecasting & Predictability	Terry Tullis*
	Jeanne Hardebeck
Ground Motion Prediction	Brad Aagaard*
	Rob Graves
Seismic Hazard & Risk Analysis	Paul Somerville*
	Nico Luco
Special Project Groups	
Community Modeling Environment	Phil Maechling*
WG on Calif. Earthquake Probabilities	Ned Field*
Collaboratory for Study of Equake Predictability	Tom Jordan
	Danijel Schorlemmer*
Southern San Andreas Fault Project	Tom Rockwell*
	Kate Scharer
Extreme Ground Motion	Tom Hanks*

* *Planning Committee members*

Planning Committee. The SCEC Planning Committee (PC) is chaired by the SCEC Deputy Director, Greg Beroza, and comprises the leaders of the SCEC science working groups—disciplinary committees, focus groups, and special project groups—who together with their co-leaders guide SCEC’s research program (Table 3). According to our by-laws, this mid-point of SCEC3 is the time to rotate the PC membership, and we are fortunate that some of our emerging new leaders have agreed to join. At this Annual Meeting, we will welcome Elizabeth Cochran as Seismology co-leader, Kim Olsen as USR co-leader, Kaj Johnson as CDM co-leader, Thorsten Becker as LAD co-leader, Jeanne Hardebeck as EFP co-leader, Brad Aagaard as GMP leader, Kate Scharer as SoSAFE co-leader, and Tom Rockwell as SoSAFE leader. We will also take the opportunity to thank those exceptional scientists they will replace, all of whom have led so well:

Report | SCEC Director

Jamie Steidl, Jeroen Tromp, Tom Parsons, Gene Humphreys, Bernard Minster, Steve Day, and Ken Hudnut.

The PC has the responsibility for formulating the Center's science plan, conducting proposal reviews, and recommending projects to the Board for SCEC support. Its members will play key roles in formulating the SCEC4 proposal. Therefore, I urge you to use the opportunity of the Annual Meeting to communicate your thoughts about future research plans to them.

Center Budget and Project Funding

In April, 2009, SCEC received an \$800K supplement to its NSF budget, which increased its NSF base funding to \$3,500K. Combined with \$1,100K from the U.S. Geological Survey, the total base funding now stands at \$4,600K. In addition, the Center received \$240K from the USGS Multi-Hazards Demonstration Project for SoSAFE, \$90K from Pacific Gas & Electric Company for the broadband platform, and \$37K rolled over from the 2008 Director's reserve. Exclusive CME, CSEP, ExGM, and CEO special projects, SCEC's total core funding was \$4,967K.

The base budget approved by the Board of Directors for this year allocated \$3,490K for science activities managed by the SCEC Planning Committee; \$475K (including \$25K for intern programs) for communication, education, and outreach activities, managed by the CEO Associate Director, Mark Benthien; \$215K for information technology, managed by Associate Director for Information Technology, Phil Maechling; \$332K for administration and \$225K for meetings, managed by the Associate Director for Administration, John McRaney; and \$130K for the Director's reserve account. As directed by NSF, \$100K of the supplemental funding for this year is being expended for an external review of the CEO program.

Structuring of the SCEC program for 2009 began with the working-group discussions at our last Annual Meeting in September, 2008. An RFP was issued in October, 2008, and 176 proposals (including collaborative proposals) requesting a total of \$5,632K were submitted in November, 2008. All proposals were independently reviewed by the Director and Deputy Director. Each proposal was also independently reviewed by the leaders and/or co-leaders of three relevant focus groups or disciplinary committees. (Reviewers were required to recuse themselves when they had a conflict of interest.) The Planning Committee met on January 22-23, 2009, and spent two days discussing every proposal. The objective was to formulate a coherent, budget-balanced science program consistent with SCEC's basic mission, short-term objectives, long-term goals, and institutional composition. Proposals were evaluated according to the following criteria:

- a. Scientific merit of the proposed research.
- b. Competence and performance of the investigators, especially in regard to past SCEC-sponsored research.
- c. Priority of the proposed project for short-term SCEC objectives.
- d. Promise of the proposed project for contributing to long-term SCEC goals.
- e. Commitment of the P.I. and institution to the SCEC mission.
- f. Value of the proposed research relative to its cost.
- g. The need to achieve a balanced budget while maintaining a reasonable level of scientific continuity given the very limited Center funding.

The recommendations of the PC were reviewed by the SCEC Board of Directors at a meeting on February 8-9, 2009. The Board voted unanimously to accept the PC's recommendations, pending a

final review of the program by the Center Director, which was completed in April, 2009 following notification of the supplemental funding from NSF.

Communication, Education, and Outreach

Through its CEO Program, SCEC offers a wide range of student research experiences, web-based education tools, classroom curricula, museum displays, public information brochures, online newsletters, workshops, and technical publications. Highlights of CEO activities for the past year are reported in the meeting volume by the Associate Director for CEO, Mark Benthien, who will present an oral summary on Monday morning.

SCEC has led the development of the Earthquake Country Alliance (ECA), an umbrella organization that includes earthquake scientists and engineers, preparedness experts, response and recovery officials, news media representatives, community leaders, and education specialists. The ECA has become our primary framework for developing partnerships, products, and services for the general public. SCEC maintains the ECA web portal (www.earthquakecountry.info), which provides multimedia information about living in earthquake country, answers to frequently asked questions, and descriptions of other resources and services provided by ECA members.

A major focus of the ECA and the SCEC/CEO programs during the past year has been the organization of, and follow-up to, the Great Southern California ShakeOut, which was held in mid-November, 2008. As you know, ShakeOut was a tremendous success, thanks to the able leadership of Lucy Jones and the resources provided USGS Multi-Hazard Demonstration Project. ShakeOut has really changed the way organizations are approaching the problems of earthquake preparedness, not just here in the U.S., but worldwide (check out the "New Zealand Great West Coast Shakeout" at www.shakeout.org.nz). The SCEC staff, led by Mark Benthien, really put a huge effort into supporting ShakeOut, and the Annual Meeting will be an appropriate time to thank them for contributing to its success.

Owing to increased cooperation across California fostered by ShakeOut, the 1906 San Francisco Earthquake Centennial, and other events aimed at increasing community resiliency to earthquakes, the ECA has been broadened into a statewide organization with a number of regional chapters (see Mark's report for a more complete description). We look forward to working with our partners around the state in future preparedness activities, including a statewide ShakeOut exercise on October 15, 2009, and annually thereafter. I would like to encourage California members of the SCEC community to register for the ShakeOut (at www.shakeout.org) and to encourage their institutions to join USC and others that are already registered.

SCEC CEO staff continues to work with museums and other informal education venues to develop content and programs for earthquake education and to distribute SCEC resources, such as the extensive set of publications that has grown out of *Putting Down Roots in Earthquake Country*. In 2008, SCEC organized a group of museums and other locations interested in earthquake education into a network of *Earthquake Education and Public Information Centers* (Earthquake EPIcenters), which now involves 27 venues distributed around Southern California and the Bay Area.

SCEC is very active in the earth science education community, participating in organizations such as the National Association of Geoscience Teachers, The Coalition for Earth System Education, and local and national science educator organizations (e.g. NSTA). An example of a successful project was a partnership with EarthScope in hosting a San Andreas fault workshop for park and museum interpreters in April, 2009.

Bob de Groot is now skillfully leading SCEC's Office for Experiential Learning and Career Development. His office manages three SCEC intern programs: Summer Undergraduate Research

Experiences (SURE), Undergraduate Studies in Earthquake Information Technology (USEIT), and Advancement of Cyberinfrastructure Careers through Earthquake System Science (ACCESS). The ELCA office promotes diversity in the scientific workforce and the professional development of early-career scientists (Figure 4). As someone very involved in these intern programs, I really enjoy seeing the students grapple with the tough but engaging problems of cutting-edge earthquake science. For example, the “grand challenge” for this year’s USEIT program was to *deliver SCEC-VDO images and animations of faults and earthquake sequences to SCEC, the Earthquake Country Alliance, and other virtual organizations via a content management system that captures the metadata and guides the user*. Many of the summer interns will be presenting their work at this meeting, and I hope you’ll have the opportunity to check out their posters and demos.



Figure 4. This “Brady Bunch” picture shows the students from around the country who participated in the 2009 USEIT summer program at USC. It includes 4 ACCESS-U interns and one SURE intern who worked with the 18 UseIT interns on this year’s “grand challenge” project. Many will be attending the Annual Meeting to present posters, demos, and animations, as well as a film about the 2009 USEIT program.

SCEC4 Planning Process

The Center operates under cooperative agreements with NSF and the USGS. The current agreement (SCEC3) expires on January 31, 2012. We will apply for a new five-year agreement by submitting a proposal to these agencies on March 1, 2010. The proposal will be peer reviewed, and a special panel will be convened for a site review on June 22-24, 2010. If all goes according to plan, NSF and the USGS will inform us of their decision in the Fall of 2010, perhaps by the time of the next SCEC Annual Meeting (September 12-15, 2010).

The SCEC Board of Directors and Planning Committee will be very active in proposal process. The PC will summarize the SCEC3 accomplishments, with emphasis on our progress toward the objectives in Table 1, and they will work with the BoD to lay out the SCEC4 science plan. I have

appointed a special BoD Committee on Fundamental Problems in Earthquake Science, chaired by Nadia Lapusta, to think broadly about our future research objectives, including the basic scientific hypotheses that will be proposed for testing in the proposed science plan.

I am hoping that all members of the SCEC community will contribute to this process. At this meeting, we have organized special discussion sessions around six key questions related to future SCEC research:

- What field and laboratory observations are most crucial for validating models of stress evolution and rupture dynamics?
- What data are most needed to understand the processes of active faulting, and which are the most promising for discovering new earthquake phenomena?
- How can progress best be made in understanding the predictability of earthquake ruptures?
- What innovations in theoretical and numerical modeling are needed to understand fault-system dynamics, forecast earthquake occurrence, and predict earthquake effects?
- How can earthquake scientists most effectively work with earthquake engineers to reduce earthquake risk?
- How should SCEC participate in national and international partnerships to promote earthquake system science?

I encourage you to participate vigorously in these discussions and other aspects of the SCEC4 planning process. The SCEC leadership is keen to get your input, and Greg and I would welcome personal communications, written or oral, about any suggestions regarding the SCEC4 proposal.

The SCEC/CEO program is an important—and very successful—component of the Center's activities, distinguished by its national leadership in earthquake preparedness, its exceptional student intern curriculum, and its close coordination of technology transfer with the SCEC research program. As part of the SCEC4 proposal process, an external panel will conduct a review of the CEO program in Palm Springs, immediately following the Annual Meeting. As input to this review process, an extensive report documenting CEO activities has been prepared by a team of outside consultants with experience in education and outreach. The review panel's assessment will be transmitted to the SCEC Advisory Council for comment in December. If you would like to provide your own input to this process, please contact Mary Lou Zoback, the AC chair, or another AC member during or after the meeting.

As SCEC Director, I want to express my thanks to all of you for your attendance at the Annual Meeting and your sustained commitment to the collaboration. And I'd especially like to thank Tran Huynh, the SCEC Special Projects and Events Coordinator, for her hard work and exceptional skill in organizing this meeting and arranging its many moving parts. Please do not hesitate to contact me, Tran, or other members of the SCEC staff if you have questions or comments about our meeting activities or future plans. Now please enjoy Palm Springs!

Report of the Advisory Council

Southern California Earthquake Center

September 2008 Meeting

Introduction

The Advisory Council (AC) of the Southern California Earthquake Center (SCEC) met during the 2008 SCEC Annual Meeting, held in Palm Springs, California, during 7-10 September 2008. The principal meeting of the Advisory Council was during the evening of 9 September; an earlier session was held prior to the start of the Annual Meeting on 7 September to outline areas of focus. The Council chair summarized the principal Council findings and recommendations in an oral report delivered during the closing session of the Annual Meeting on the morning of 10 September.

On 5 September the SCEC Director circulated to the Advisory Council a report summarizing how SCEC had responded to Advisory Council recommendations from the previous year and raised a number of new and continuing issues warranting Council attention. Those issues included:

- a formal evaluation of the Center's Communication, Education, and Outreach (CEO) Program
- feedback on the Collaboratory for the Study of Earthquake Predictability (CSEP), particularly on engaging NASA in a workshop and on sustainable funding
- advice on initiatives in large-scale earthquake simulation and ground motion prediction
- documenting SCEC3 earthquake system science accomplishments
- leadership development within SCEC
- the SCEC4 planning process

After a few general remarks below, we discuss the issues raised by the Director in his 5 September mailing; we also comment on a number of recurring topics and make several recommendations on some additional issues raised by the AC at this meeting. At our September 7 evening meeting with SCEC leadership, John McRaney raised concerns about the need to develop sustainable funding for the continually expanding Annual Meeting. Unfortunately, the Advisory Council did not have time to discuss this topic, but we would welcome any relevant data and suggestions related to the funding for the Annual Meeting prior to next year's meeting and we would be glad to comment.

Some General Impressions

First of all, this has been a banner year for SCEC with the release of two major products – and congratulations are in order. In April of 2008 the Uniform California Earthquake Rupture Forecast, the first-ever, statewide time-dependent assessment of earthquake likelihood was released. This report was requested and partially funded by the California Earthquake Authority. This project, a collaboration of SCEC, the U.S. Geological Survey (USGS), and the California Geological Survey (Working Group on California Earthquake Probabilities), under the superb leadership of Ned Field, USGS, involved more than 100 earthquake scientists who participated in workshops, contributed data, and assisted in its review.

In June of 2008, SCEC and the USGS released the ShakeOut Earthquake Scenario, a USGS Open-File report. This 400-page publication of the initial results of a large cooperative project, led

masterfully by Lucy Jones (USGS), examined the implications of a major earthquake in southern California. Its results will be used as the basis of an emergency response and preparedness exercise, the Great Southern California ShakeOut, in November 2008. Members of the southern California community from firefighters to utility operators will use the ShakeOut Scenario to plan and execute this exercise. The resulting community input and feedback will then be utilized to refine the assessment of the physical, social and economic consequences of a major earthquake in southern California and will lead to a formal publication in early 2009.

Since members of the Advisory Council are not also members of SCEC, the Annual Meeting provides an important opportunity for Council members to assess the community's annual progress on the Center's goals and programs. The 2008 meeting and associated workshops proved again to be impressive demonstrations of the energy and enthusiasm of the SCEC community. The 139 registrants who were attending their first SCEC Annual Meeting (30% of the 460+ total registrants), including many students and interns, provided heartening evidence of the center's growing participation and its compelling mission. The Advisory Council particularly applauds SCEC's continually strengthening of partnerships with the earthquake engineering community. It is heartening to see their ranks grow at each meeting.

The Advisory Council also lauds the entire SCEC membership for its persistently selfless spirit which produced the landmark reports mentioned above, and which continues to enable considerable progress in developing communal, system-level models that are advancing the goals of both fundamental and applied earthquake science. The structure of the 2008 meeting allowed for ample discussion of issues, lively interactions at the many poster presentations of new science, and was punctuated by a series of well-chosen overview talks, most featuring early-career scientists who exemplify the new generation of SCEC leaders.

Finally, the Advisory Council would like to acknowledge the tremendous effort in the past year by Tran Huynh, SCEC's Project Planning Coordinator. Special thanks to Tran for her always cheerful and indefatigable assistance in producing the UCERF report and for organizing this year's Annual Meeting, both of which came off flawlessly.

Before moving to our recommendations on specific topics, the Advisory Council noted several issues for the leadership to be mindful of:

- We urge SCEC3 to maintain focus and avoid getting spread too thin
- With the SCEC3 goals in mind, we endorse strong and active efforts to move the SCEC community towards progress in goals not yet realized
- We also urge SCEC to begin now to explore new, creative funding opportunities for this highly visible and highly successful regionally-focused program—perhaps considering some kind of industrial associates program or seeking funding from utilities and other infrastructure ownership groups.

Evaluation of the CEO Program

In his 2007 and 2008 requests of the Advisory Council to provide guidance on evaluating SCEC's CEO program, the Director posed the following specific questions:

- Are the basic elements of the CEO program – formal and informal education, public outreach, knowledge transfer – in appropriate balance?
- Is there any “right now” advice that might enhance the prospects for ShakeOut success?
- What is the best way to capitalize on the connections and “bounce” from the ShakeOut exercise—after involving close to 5 million Southern Californians—what should be next? Could you please comment on SCEC's plan to convene a 1-2 day workshop in January or

February of 2009 to leverage gains of the ShakeOut exercise. and develop a strategy for next 2-3 years.

- Is SCEC's premier effort in public outreach appropriately organized through the Earthquake Country Alliance? In particular, is the current organization of the Earthquake Country Alliance appropriate for outreach to the full spectrum of non-governmental organizations (NGOs)?
- Would it be appropriate and feasible for a member or members of the AC to lead a formal review of the CEO program?
- Regarding a research program within CEO that was proposed by the Advisory Council in 2007 – which aspects of CEO might be worthy targets for proposals submitted to NSF/SBE Directorate or other funding organizations, including foundations, and what partnerships would be most effective in extending SCEC expertise in the social science?

As noted in last year's report, the Advisory Council knows of no other organization that has accomplished more in the area of communication, education, and outreach, nor done so as effectively and as informed by knowledge from the social and behavioral sciences, than SCEC. Existing CEO activities have focused on what works best to motivate people to prepare and mitigate for events that they really don't believe will actually happen, and, if they did, they think will affect others and not themselves. The Earthquake Country Alliance has functioned extremely successfully in bringing together a diverse group of stakeholders, well outside of the traditional earth science academic environment.

The Advisory Council would like to particularly acknowledge Mark Benthien for his exemplary and visionary leadership of this program, and to thank the members of his staff, each of which are functioning at an extraordinarily high level. The visibility and success of the Shakeout event, with several months remaining to the exercise, are really unparalleled.

Regarding the request for "right now" advice that might enhance the prospects for ShakeOut success, the Advisory Council reported at the Annual Meeting that just as the SCEC community is asking southern Californian residents, utility operators, business community and government officials to modify their behavior as part of the ShakeOut exercise, we strongly encouraged the SCEC scientific community embrace the exercise and do the same. It is an excellent opportunity for the focus groups to design and practice well-coordinated post-quake response plans and to involve their institutions as well.

Specific Recommendations for CEO program review

Following up on the Advisory Council's 2007 recommendations for a formal review of the scope and impact of the CEO program, SCEC leadership requested specific input and advice for this review. The desire to define future directions for CEO, and to take advantage of and build upon ShakeOut's success, makes a review especially timely.

The Advisory Council recommends a two phase review:

- A **Phase 1 review** to evaluate the impact and effectiveness of the SCEC's outreach and education program to date. This review should fulfill the evaluation requirements of SCEC's two principal funders, the USGS and NSF and should:
 - Produce a report that will serve as an important supporting document for the SCEC4 proposal
 - Be informed by examples of previous NSF or USGS reviews and the expected elements, if available
 - Be based on CEO staff presentations, as well as overviews, summaries and data compiled by the CEO staff

- Be carried out by an independent external panel, populated in consultation with the two primary funding agencies
- A **Phase 2 review** that would be much more forward-looking, focused on exploring new CEO activities and directions and the means to sustain and expand the program funding. This review should:
 - Be informed by a range of disciplines, including
 - Social and behavioral science
 - Marketing and advertising
 - Public health
 - Identify new opportunities and directions for SCEC CEO, including specific plans and follow-up activities to leverage and build on the success of the ShakeOut.
 - Include a component based on CEO staff presentations, as well as overviews, summaries and data compiled by the CEO staff.
 - Be carried out by an interdisciplinary external review panel consisting of specialists in the above fields, not all members of which need to have specific earthquake hazard experience or background. One or more of the Advisory Council members may be involved in the phase 2 review panel, serving as a liaison to the panel and/or in helping SCEC select the panel members
 - Recommend possible additional social and behavioral research activities and programs focused on building on and extending the impact of SCEC's CEO program. These could be carried out by SCEC CEO alone or in partnership with others.
 - One example of such a research program could address the daunting challenge of motivating and empowering underserved communities to take preparedness and mitigation actions when they lack the financial resources to address everyday needs. A network of NGOs in southern California already serves these communities daily and is trusted by them (e.g. Meals on Wheels, Senior Day Health programs, etc.). Research could involve inventorying existing NGOs in southern California and the communities they serve and evaluating the capacity of the NGOs (and the resources they would need) to take a more substantive role in earthquake preparedness and post earthquake response. This research could help determine if the Earthquake Country Alliance's organization (or some other) is the most effective means to engage these NGOs.
 - Provide advice on potential non-earth science funding sources for both new CEO research programs as well the overall CEO program.

In preparation for the Phase 2 review, the Advisory Council endorses SCEC's CEO Office's plan to convene a workshop to investigate post-ShakeOut activities and spinoffs and develop a strategy for the CEO office over the next 2-3 years. This workshop should proceed very soon after the ShakeOut exercise in November, before the momentum is lost. The proposed January or February 2009 timeframe seems ideal.

Feedback on CSEP

The Collaboratory for the Study of Earthquake Predictability is in a stage of rapid development. As a SCEC special project in its third year of support from the Keck Foundation, but must also be looking to the future, in 2010, when the Keck one-time funding runs out.

In his 5 September letter to the Advisory Council, the SCEC Director asked:

- Given the tricky problems in dealing with space-based earthquake prediction, should SCEC plan a joint workshop with NASA on earthquake predictability? If yes, how might it be configured?

- Does the AC believe that involvement in CSEP would be attractive to the private sector, and that pursuing their financial and other commitment would be worthwhile?

It is the Advisory Council's view that CSEP's approach to earthquake predictability is appropriately rigorous and a direction likely to engender broad community support—as evidenced by the continued expansion to other geographic areas. We applaud CSEP for its tremendous progress in the past year, in both meeting software release milestones and firming up international participation.

The success of CSEP (and its prospects for sustainable funding) will depend, largely, on whether there are interesting outcomes to the collaboratory's activities—will all prediction methodologies fail rigorous tests or will at least one algorithm shows promise? It is unlikely that another year or two of operation will be sufficient to decide this question.

With regard to developing future funding for CSEP, the Advisory Council recommends that:

- The primary focus for CSEP in the coming year should be domestic, getting the U.S.-based program and product delivery in order, as this will be a requirement in seeking any U.S. government funding.
- CSEP should continue to monitor scientific progress in earthquake prediction in other countries; however, it should avoid the appearance of validation or confirmation of earthquake predictions in foreign countries. Entanglement in issues involving public safety in foreign countries could be a huge distraction of personnel and resources.
- Private industry funding could be explored in a workshop involving potential users from the insurance/reinsurance industry and soliciting input on which products and timeframes would be of most interest to this community.

With regard to a possible joint workshop with NASA:

- As part of its recommended focus on domestic prediction issues, the Advisory Council endorses a joint SCEC-NASA workshop to explore potential guidelines for engaging space-based earthquake forecasting techniques in CSEP's rigorous and independent testing environment. Many of the space-based prediction techniques have involved retrospective predictions and identification of precursory anomalies after an earthquake occurred. We recommend that the workshop have a very sharp focus around the issue of developing guidelines defining "baselines" for datasets other than seismicity and an objective set of rules for prospective prediction (analogous to the seismicity algorithms).

Advice on Initiatives in Earthquake Simulation and Ground Motion Prediction

Another special project area within SCEC that is now undergoing rapid growth is large-scale earthquake simulation and ground motion prediction. It is the view of the Advisory Council that physics-based simulations and coupled hazard assessments represent a valuable integration of much of the knowledge and new understanding gained from SCEC's earthquake system science approach. These simulations are gaining more acceptance in the engineering design community, particularly as an important alternative to the use of a limited set of 'real' earthquake recordings and as a means to explore ground motions expected at a site for various scenarios and conditions. The simulations are also being used as a means to provide theoretical confirmation and physical insights into the commonly-used empirical ground-motion prediction equations that form the backbone of probabilistic seismic hazard analysis. We agree that this remains a critical direction for SCEC.

The Advisory Council recommends:

- A strong focus on understanding those aspects of ground motion prediction that have significant engineering impact

- A strong connection between simulation and empirical validation with existing data – what aspects of simulation-based predictions can be validated with ground-motion data, and what aspects are currently untestable? Are there alternative ways to test such aspects?
- Less emphasis on exploring computational challenges--such as whether deterministic modeling can be extended from 1 to 3 Hz- expending a great deal of effort on the computational challenges of extending deterministic simulations from 1 to 3 Hz does not seem warranted because:
 - This will only bring a modest increase to the frequency range available via deterministic simulation, with a large frequency range of engineering interest remaining above the 3 Hz limit;
 - Existing methodologies of joining deterministic to stochastic simulations above the deterministic frequency limit will still continue to be required (and appear to be a sound and useful approach). The exploration of the computational challenges in marginally extending the frequency range of deterministic simulations, while technologically interesting, could thus expend considerable resources with little payback in practical terms.
- Work more closely with the Fault and Rupture Mechanics focus group and attempt to include or evaluate some of the more elaborate physical modeling they are developing. For example, how much complexity of fault geometry is needed to accurately simulate strong ground motions for engineering applications? Does off-fault damage affect strong ground motions, and if so how should it be included?
- Considering a code validation effort, similar to CSEP and conducted jointly with leaders in the earthquake engineering community, that could be critical in establishing user acceptance of simulated ground motions as input to engineering designs.
- Comprehensive documentation of the sensitivity of simulation-based ground motions to the input parameters (and their interactions), with investigation of the extent to which each input parameter can be determined and constrained by data.

The final recommendation stems from comments made at the 2008 Annual Meeting by Rob Graves (URS Corp). He reported that in his analysis of ShakeOut simulations he found the rather disturbing result that just a 15% change in average rupture speed can change the peak ground motions by factors of 2 to 3. He then asked if these results were realistic and if the seismological community could confidently specify median values and uncertainties for rupture speed and other key parameters influencing ground motion. The AC found these statements particularly significant, as should the SCEC community. They point to the need for a continued focus on understanding the sensitivity of simulations to input source conditions, particularly as the interest in using such techniques in engineering practice continues to widen.

Other Feedback

Leadership Development within SCEC

The Advisory Council was extremely impressed with the diversity and youth within the SCEC community and particularly within the new membership on the Planning Committee. Rotation within this leadership group is healthy, and provides more opportunities for young scientists to have a chance to lead. We urge SCEC senior leadership to remain diligent to the need for mentoring and development to guarantee the success of these young scientists, many of whom are in their first real scientific leadership role.

The Advisory Council was pleased to hear that a succession plan is in place for Tom Jordan's stated desire to step down from SCEC leadership in 2010. The vision, energy and savvy Tom has brought to SCEC will be a difficult act to follow and while there appears to be an excellent succession plan in place, perhaps there should be some backup plan as well.

The Vital Role of SCEC Workshops and Increasing Awareness of Their Outcomes

It is the intent of the Advisory Council to continue to provide advice on new scientific opportunities and potential partnerships on an ongoing basis. The Advisory Council regularly provides feedback to SCEC leadership on their performance and encourages SCEC members to voice their views on leadership issues either during the Annual Meeting or privately to Advisory Council members. It is the current sense of the Advisory Council that the senior leadership of SCEC is doing an outstanding job, and that the many individuals now leading committees and focus groups constitute a broadly diverse, extremely able, and committed group.

SCEC is filling a tremendous need for the community by facilitating easy-to-convene topical workshops in a very short time frame—as evidenced by the requests for many more such workshops in the coming year. The Advisory Council noted that while many SCEC members were aware of recent workshops in a related area, in general they were not very aware of the workshop outcomes if they did not personally attend.

The Advisory Council recommends:

- Continued SCEC-wide promotion of workshop opportunities, this part of the process seems to be working well.
- Workshop conveners be required to prepare a brief summary for posting on the SCEC website shortly (within 30 days?) after the workshop, with email notification to the SCEC community containing a link to the summary.

Evaluating SCEC Progress and Publishing SCEC Accomplishments

The Advisory Council was pleased to learn last year that the SCEC Planning Committee will be tracking progress toward the achievement of Center objectives. We look forward in the coming year to receiving synthesis of the results of this tracking and the status of progress on the various goals.

Documenting the accomplishments of the earthquake system science done by the SCEC community is challenging—both in determining the appropriate medium for such interdisciplinary work and in capturing the full impact of the contributions. Despite these challenges, the Advisory Council continues to believe that creating a monograph of synthesis papers covering topical and disciplinary contributions by SCEC will be a critical part of the Center’s legacy, not just within the earth sciences—but in the broader scientific community.

The Advisory Council strongly recommends that:

- SCEC begin soon to produce an accomplishment document for SCEC3. We believe that the synthesis required to produce such a document will be essential to the SCEC4 planning—and such a report will be an important supporting document for the SCEC4 proposal.
- Venues and formats outside of traditional publication medium should be explored—however, independent and stringent peer review must be assured.

Science Planning Discussions at the Annual Meeting

At this year’s Annual Meeting, various members of the Advisory Council observed a wide variability in format and level of interaction in the individual Focus Group’s science planning session. This variability took many different forms:

- How much previous science was presented
- How the discussion was facilitated, and in particular, how much the Group Leaders spoke versus audience participation

- Uneven success in engaging younger SCEC members in the discussions, we wonder if it might be helpful to encourage some kind of caucus by the grad students possibly lead by a very recent PhD.
- And a logistical issue, attempts at discussion focused on small type, ponderous sentences shown in PowerPoint were generally not as successful as short key bullet items put up to stimulate discussion

The Advisory Council recommends that the Planning Committee work harder in the future to stimulate more interactive discussion engaging a broad segment of the audience.

SCEC4 Planning

SCEC3 will mark 20 years of investment in a focused attack on a complex scientific problem with a unique interdisciplinary, system-level approach. Both the funders and the broader Earth Science community will expect products and deliverables commensurate with such an investment. Now, halfway through SCEC3, it is time to refocus on achieving SCEC3 goals with a sense of urgency, rather than slipping into a feeling of complacency that SCEC could go on forever

SCEC4 presents an exciting opportunity to build upon a number of major scientific products and contributions of SCEC3 as well as the huge outreach and preparedness success of ShakeOut. A compelling case for SCEC4 must be based on demonstrating the impact of SCEC's interdisciplinary approach focused on building system-level community models – a demonstration that these models and new understanding are changing the way earthquake scientists and engineers solve problems and approach their research.

The Shakeout exercise is an outstanding example of a "wall to wall" activity within SCEC, grounded in science that is likely to change the behavior of both residents and government officials in southern California. We believe that this work should be thoroughly documented as a national exemplar of interdisciplinary research.

Creating the earthquake rupture scenario for ShakeOut required drawing a line in the sand, and using the best understanding at the time. However, new data and understanding (largely as a result of the Southern San Andreas Fault Evaluation Project) have already raised important scientific questions about the validity of the selected rupture scenario—is one 7.8 earthquake more likely than 3 events in a short time period, e.g., a M7.4, M7.2, and a M7.3 in 10 years? Is 13 m peak slip likely, or do the new LIDAR data suggest smaller offsets per event? Also, the most appropriate rupture velocity and even the sense of directivity remain unconstrained.

Both the ShakeOut scenario and the Uniform California Earthquake Rupture Forecast exercises demonstrated the value of having to make judgments based on the best available information at the time. Both identified significant gaps where future research is required and focused attention on the key parameters that influence results.

The Advisory Council recommends a strong emphasis on synthesis and completing planned predictive models/platforms before the end of SCEC3, even with incomplete knowledge. In doing so, the researchers will learn what critical data or observations are needed and which parameters actually have little effect on model outputs—defining future research. This focus on synthesis will enable SCEC to write a strong accomplishment document as well as a strong SCEC4 proposal.

The Advisory Council also urges SCEC to think broadly about how to both measure and improve the impact of the Center's efforts. We recommend you begin immediately to develop a process to document impact in both scientific and outreach arenas. Finally, we (continue to) recommend that you initiate a speakers program to further disseminate the results of the earthquake system-science approach.

Final Comments

It is the current sense of the Advisory Council that the researchers and senior leadership of SCEC is doing an outstanding job, and the many individuals now leading committees and focus groups constitute a broadly diverse, extremely able, and committed group. The Advisory Council applauds SCEC's continued role in catalyzing and supporting related projects such as the new NSF Margins/EarthScope Salton Trough seismic experiment. Support for these kinds of activities are essential to growing the community of scientists who are engaged in earthquake science and to leverage the knowledge and understanding developed in SCEC.

The Advisory Council is pleased to continue to provide assistance to SCEC in its efforts to formulate and accomplish the center's major goals. At any time the Council welcomes comments, criticism, and advice from the seismological community, including individuals and groups both inside and outside SCEC membership, on how best to provide that assistance.

One cautionary comment falling into the category of being a victim of one's own success—we heard from some participants that it is becoming increasingly hard to maintain the intimacy and level of participation as the number of Annual Meeting participants gets larger. As noted above, we felt that the discussion in some of the science planning sessions was somewhat tentative or inhibited by the large number of people. We have no specific suggestions about how or whether the meeting size should possibly be constrained, but it is an important aspect to consider if SCEC continues to grow.

Finally, the Advisory Council welcomes new members John Filson and Anne Meltzer and looks forward to working with SCEC leadership assist in SCEC4 planning and to help ensure that the products and progress of the center in the SCEC3 era continue to be commensurate with agency and community investment.

SCEC Advisory Council

Mary Lou Zoback, Risk Management Solutions-RMS (Chair)*
Gail Atkinson, Carleton University*
Lloyd S. Cluff, Pacific Gas and Electric Company
John Filson, USGS (Retired)*
Jeffrey T. Freymueller, University of Alaska*
Mariagiovanna Guatteri, Swiss Reinsurance America Corporation
Anne Meltzer, Lehigh University
Dennis Miletti, University of Colorado, Boulder*
Kate C. Miller, University of Texas at El Paso
Jack P. Moehle, Pacific Earthquake Engineering Research Center (PEER)**
Chris Rojahn, Applied Technology Council
John Rudnicki, Northwestern University*
Ellis M. Stanley, Sr., City of Los Angeles Emergency Preparedness Department

*Attended at least part of the 2008 Annual Meeting and Advisory Council sessions

** Represented by Yousef Bozorgnia, PEER

SCEC Communication, Education, and Outreach

Mark Benthien

CEO Director for SCEC

Introduction

The SCEC Communication, Education, and Outreach (CEO) program has four long-term goals:

- A. Coordinate productive interactions among a diverse community of SCEC scientists and with partners in science, engineering, risk management, government, business, and education;
- B. Increase earthquake knowledge and science literacy at all educational levels, including students and the general public;
- C. Improve earthquake hazard and risk assessments; and
- D. Promote earthquake preparedness, mitigation, and planning for response and recovery.

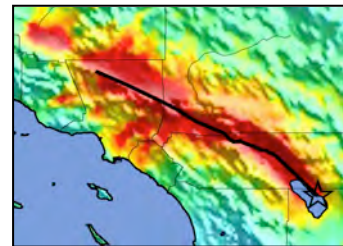
These goals are pursued through activities organized within four CEO focus areas: *Research Partnerships* coordinated within the SCEC Seismic Hazard & Risk Analysis focus group; *Knowledge Transfer* activities with practicing professionals, government officials, scientists and engineers; *Public Outreach* activities and products for the general public, civic and preparedness groups, and the news media; *Education* programs and resources for students, educators, and learners of all ages, including the Experiential Learning and Career Advancement office which coordinates undergraduate and graduate internships and support for early career scientists. Many activities span more than one CEO focus area.

Partnerships are key to achieving SCEC's mission, research objectives, and outreach goals. These partners include other science organizations (e.g. IRIS, EarthScope, and UNAVCO), engineering organizations (e.g. PEER, CUREE, and EERI), education organizations (e.g. Los Angeles County Unified School District, Southern California County Offices of Education, museums, and the National Association of Geoscience Teachers), and public service / risk management organizations (e.g. California Office of Emergency Services, the California Earthquake Authority, FEMA, and the American Red Cross).

The following are highlights of SCEC's Public Outreach and Education activities in the last year.

Public Outreach Activities

Great (Southern & Statewide) California ShakeOut. A major focus of the CEO program in 2008 and 2009 has been organizing the inaugural ShakeOut drill for Southern California on November 13, 2008, and the first statewide ShakeOut drill planned for October 15, 2009. The purpose of the Shakeout is to motivate all Californians to practice how to protect ourselves during earthquakes ("Drop, Cover, and Hold On"), and to get prepared at work, school, and home.



2008 Southern California ShakeOut. In 2008, over 5.4 million participants (which exceeded the initial goal of 5 million people) registered to participate at www.ShakeOut.org, hosted and maintained by SCEC. Individuals, families, businesses, schools, and organizations joined firefighters and other emergency responders (involved in the statewide “Golden Guardian” exercise the same week) in the United States’ largest-ever earthquake preparedness activity. Registered participants received information on how to plan their drill, connect with other participants, and encourage a dialogue with others about earthquake preparedness. This was an unprecedented opportunity to educate the public.

The 2008 ShakeOut was based on a potential 7.8 magnitude earthquake on the southernmost San Andreas Fault. In the past this size of earthquake has occurred on that section of the fault every 150 years on average, yet the last was over 300 years ago! Dr. Lucy Jones (USGS) led a group of over 300 scientists, engineers, and others to study the likely consequences of this enormous earthquake in great detail. Many SCEC scientists have been involved including those who produced the ShakeOut Simulation. The final simulation used in analysis of losses was by Rob Graves (URS), and the visualization was by Geoff Ely (USC).

In addition to the ShakeOut drill, the City of Los Angeles and the Earthquakes and Megacities Initiative (of which SCEC CEO director Mark Benthien is the Los Angeles liaison) hosted an International Earthquake Conference November 12-14, bringing together over 45 international experts to discuss policy, planning, and preparedness with U.S. counterparts. More information is at www.iec.lacity.org. On Friday, November 14, the Art Center College of Design presented the “Get Ready Rally” at the new Nokia LA Live in downtown Los Angeles to engage the public in earthquake preparedness. Southern Californians were invited to celebrate the success of the Drill and share their experiences. The event included food, entertainment, and vendors.

Organizers and participants of the 2008 ShakeOut included Southern California Earthquake Center, U.S. Geological Survey, California Office of Emergency Services, City of Los Angeles, Caltech, Art Center College of Design, University of Southern California, State Farm, California Earthquake Authority, the California Seismic Safety Commission, American Red Cross, and businesses, schools and governments (in Riverside, San Bernardino, Orange, Los Angeles, San Diego, Imperial, Kern, Santa Barbara, and Ventura Counties), and *many other members of the Earthquake Country Alliance (ECA)*.

2009 Great California ShakeOut. Immediately following the 2008 ShakeOut (initially conceived as a “once-in-a-lifetime” event), participants began asking for the date of the 2009 ShakeOut. After significant discussion among ECA partners and state agencies, the decision was made to organize an annual, statewide Shakeout drill to occur on the third Thursday of October (October 15 in 2009). This date is ideal for our school partners and follows National Preparedness Month in September, which provides significant exposure prior to the drill.

Expanding statewide has been much more complicated than simply deleting the word “Southern” from all materials and webpages. The 2008 ShakeOut was based on a single earthquake scenario, which does not apply to the entire state. Thus, 11 “ShakeOut Information Areas” (see map, next page) were created, based on earthquake hazards, geography, media markets, and other factors, to provide local hazard information for participants throughout California. The redesigned ShakeOut.org website contains a description of each area’s earthquake hazard and ShakeOut registration statistics down to the county level. Resources from the 2008 ShakeOut are being updated for a statewide audience, or “generalized” to be useful for any drill (anywhere and anytime).



In addition, expanding statewide required considerable partnership development with state agencies and regional alliances. As described below, the Earthquake Country Alliance, which has also expanded statewide, is the primary organization behind the ShakeOut, connecting four regional alliances. The group works together to coordinate messaging, develop resources, and recruit participation.



As of September 4, 2009, over 4.3 million participants people have been registered throughout the state. Many of the 2008 participants have registered again, along with new participants from 53 of California's 58 counties (thus far).

SCEC has also created and hosts the website for "New Zealand Great West Coast Shakeout" (www.shakeout.org.nz), planned for September 18, 2009. Twenty percent of the region's 30,000 residents are participating, and expansion of the drill nationwide in coming years is being considered. Similarly, SCEC is consulting with the Central U.S. Earthquake Consortia to support a ShakeOut drill in 2011 or 2012 to commemorate the bicentennial of the New Madrid earthquakes.

Putting Down Roots in Earthquake Country. In 1995 SCEC, the USGS, and a large group of partners led by Lucy Jones (USGS) developed and distributed 2 million copies of a 32-page color handbook on earthquake science, mitigation and preparedness. Funding was primarily from the National Science Foundation and USGS. The booklet was distributed through libraries, preparedness partners, cities, companies, and directly to individuals through SCEC.

The creation of the Earthquake Country Alliance in 2003 was concurrent with the desire to update *Putting Down Roots* in advance of the 10th anniversary of the Northridge earthquake. The process brought the ECA together to develop consensus messaging and notably introduced the "Seven Steps to Earthquake Safety," which has become a standard approach to organizing earthquake preparedness messaging. Since 2004, the booklet has undergone five additional revisions and printings, the latest of which was finalized in October, 2008, and included the ShakeOut Scenario and an overview of the Uniform California Earthquake Rupture Forecast study led by SCEC.

Putting Down Roots has been widely distributed through newspaper inserts, museums, schools, at events organized by SCEC and ECA partners, and via an online order form. Over 2.3 million copies have been distributed since 2004, and an additional 1.25 million copies in Spanish have been distributed. Printing and distribution of the booklet was made possible by generous support of the California Earthquake Authority and additional funding from the Federal Emergency Management Agency (FEMA), and the USGS. The handbook is available at www.earthquakecountry.info/roots as an online version and downloadable PDF, and printed copies can be ordered for free through an online request form.



Putting Down Roots is the principal SCEC framework for providing earthquake science, mitigation, and preparedness information to the public. The "Roots" framework extends beyond the distribution of a printed brochure and the online version. For example, the Birch Aquarium in San

Diego developed an earthquake exhibit that featured a “Seven Steps” display, similar to SCEC’s “ShakeZone” exhibit at the Fingerprints Children’s Museum in Hemet, CA. The Emergency Survival Program (managed by LA County) based its 2006 and 2009 campaigns around the “Seven Steps.” Many other adaptations of *Roots* and *Seven Steps* content have been developed by ECA and other partners.

The new version of *Putting Down Roots* was designed to allow other regions to adopt and adapt its structure to create additional versions. The first is a Greater San Francisco Bay Area version produced by a partnership led by the USGS with SCEC, local and state emergency managers, the Red Cross and many other organizations. Over 2.3 million copies have been printed, many distributed in newspapers, with funding from the California Earthquake Authority, USGS, FEMA, Red Cross, OES, CGS, and several others). In addition, a new booklet, *Protecting Your Family From Earthquakes– The Seven Steps to Earthquake Safety*, was produced in 2006 as part of the *Putting Down Roots* series, in two versions - English and Spanish in one booklet, and English, Chinese, Korean, and Vietnamese in another booklet. All Bay Area booklets can also be accessed from www.earthquakecountry.info/roots. All printings of the Bay Area version to date have been coordinated through SCEC.



Two other versions were produced over the last year, and can be downloaded from the *Roots* website:

- E. The Utah Seismic Safety Commission in 2008 produced the first version of *Putting Down Roots* outside of California, and discussion for a Central United States version has been moving forward (though slowly).
- F. *Living on Shaky Ground*, an update to the well-known earthquake booklet for California’s North Coast, now including the Seven Steps to Earthquake Safety, has been in development for several years and is subtitled “Part of the *Putting Down Roots in Earthquake Country* Series.”



Finally, SCEC and ECA partners have developed a new supplement to *Putting Down Roots*, titled *The Seven Steps to an Earthquake Resilient Business*, an exciting new 16-page guide for businesses to develop comprehensive earthquake plans, printed in Fall, 2008. This booklet is the first non-regional publication, created as a supplement to all *Putting Down Roots* or other materials that include the *Seven Steps to Earthquake Safety*. It can be also downloaded and ordered from www.earthquakecountry.info/roots.

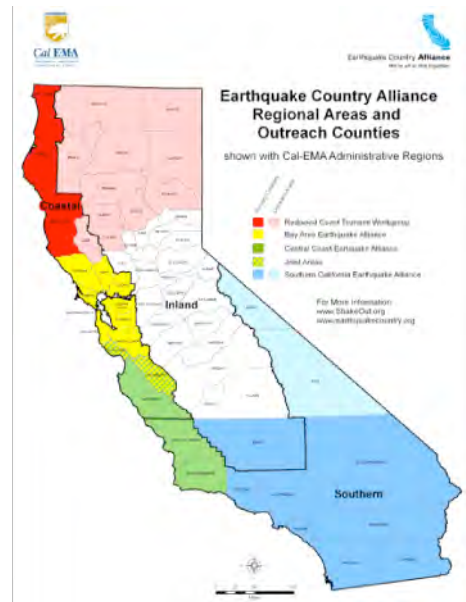
Earthquake Country Alliance. To coordinate activities for the 10-year anniversary of the Northridge Earthquake in January 2004 (and beyond), SCEC led the development of the "Earthquake Country Alliance" (ECA) beginning in summer 2003. This group was organized to present common messages, to share or promote existing resources, and to develop new activities and products. The ECA includes earthquake scientists and engineers, preparedness experts, response and recovery officials, news media representatives, community leaders, and education specialists. The mission of the ECA is to foster a culture of earthquake and tsunami readiness in California.

In 2006, the ECA launched the *Dare to Prepare* Campaign, to promote earthquake awareness and preparedness and to mark the 150th anniversary of the January 9, 1857, Ft. Tejon earthquake on the

San Andreas Fault. With a strategy of getting southern Californians to “talk about our faults,” the campaign acknowledged that “Shift Happens,” and if you “Secure Your Space” you can protect yourself, your family, and your property. A new website (www.daretoprepare.org) was created, along with public events throughout the region (presentations, preparedness fairs, etc.) and a comprehensive media campaign with television, radio, and print promotion, public service announcements, on-air interviews and much more. A new Spanish-language website, www.terremotos.org, was also created and is hosted by SCEC.

The Earthquake Country Alliance is now the primary SCEC mechanism for maintaining partnerships and developing new products and services for the general public. Following the success of developing and implementing the 2008 Great Southern California, the ECA has now been expanded into a statewide organization and currently includes regional stakeholder alliances in southern California, the central coast, Bay Area, and north coast (see map). The statewide ECA, including state agencies, is currently planning the Great California ShakeOut, an annual statewide event in October.

SCEC developed and maintains the ECA website (www.earthquakecountry.info), which provides multimedia information about living in earthquake country, answers to frequently asked questions, and descriptions of other resources and services that ECA members provide. The site is set up separately from the main SCEC web pages (though has attribution to SCEC) so that all members of the ECA see the site as their own and are willing to provide content. The site features the online version of *Putting Down Roots* and special information pages that all groups can promote, such as a special page about the “10.5” miniseries and a page about the “Triangle of Life” controversy (see assessments below). The site is being completely redesigned in fall of 2009 to complement the new design of the *ShakeOut.org* website.



Media Relations. SCEC engages local, regional and national media organizations (print, radio and television) to jointly educate and inform the public about earthquake-related issues. The goal has been to communicate clear, consistent messages to the public—both to educate and inform, and to minimize misunderstandings or the perpetuation of myths. In 2008, SCEC coordinated the major release of the Uniform California Earthquake Rupture Forecast, which involved a two-location press conference (with scientists at USC and at USGS in Menlo Park, with streaming video between the locations), a comprehensive website (www.scec.org/ucerf), a new USGS fact sheet, and other resources. SCEC CEO encourages scientists who are interested in conducting interviews with media reporters and writers to take advantage of short courses designed and taught by public information professionals.

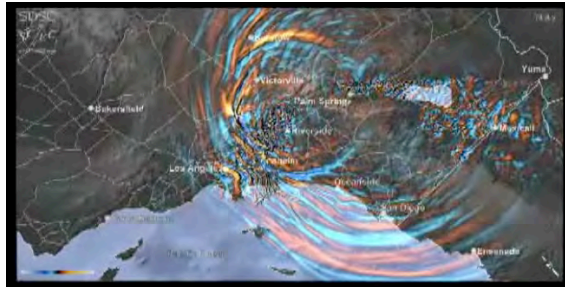
Earthquake Country - Los Angeles. This video was produced by Dr. Pat Abbott of SDSU as the second in his “Written in Stone” series. The video tells the story of how the mountains and valleys of the Los Angeles area formed, including the important role of earthquakes. The video features aerial photography, stunning computer animations, and interviews with well-known experts. The video features 3D fault animations produced by SCEC interns from the Undergraduate Studies in

Earthquake Information Technology (USEIT) Program. In addition to conducting several focus groups with teachers and preparedness experts, where the video was evaluated, SCEC has developed curricular kits for school and community groups to accompany the video, and has added captions in both English and Spanish. These kits have been duplicated in large quantities with funding from the California Earthquake Authority.

Emergency Survival Program. SCEC serves on the Coordinating Council of the Los Angeles County-led Emergency Survival Program, with emergency managers from all southern California counties, many large cities, the American Red Cross, and Southern California Edison. The primary role of the program is to develop a series of public information materials including monthly Focus Sheets, newsletter articles, and public service announcements related to a yearly theme. In 2006 and 2009 the program focused on earthquakes, with seven of the monthly focus sheets based on the “seven steps to earthquake safety” in *Putting Down Roots in Earthquake Country*. SCEC provided the Spanish version of the seven steps text, and coordinated the translation of the five other monthly focus sheets for 2006.

Use of SCEC Community Modeling Environment (CME) Products. Many SCEC CME products are being used in public presentations, webpages (*scec.org*, *earthquakecountry.info*, etc.), printed publications such as *Putting Down Roots in Earthquake Country* (English and Spanish), our “Earthquake Country – Los Angeles” DVD and in other venues to communicate earthquake hazards and encourage preparedness. These products, including the SCEC TeraShake and ShakeOut simulations, Puente Hills earthquake simulation, and Community Fault Model, have also had extensive media coverage through press briefings, reporters attending the SCEC Annual Meeting, and television documentaries, and have been used frequently as background imagery in

many news stories. The visualizations were featured extensively in the National Geographic Channel documentary “Killer Quake,” which presented SCEC TeraShake and Puente Hills animations, along with fault movies produced using SCEC’s Virtual Display of Objects (SCEC-VDO) software. In June 2009 the Department of Energy honored the most advanced visualization to date of a magnitude 7.8 earthquake on the southern San Andreas Fault as one of this year’s best scientific visualizations at the Scientific Discovery through Advanced Computing Conference. The new visualization was created by Amit Chourasia at the San Diego Supercomputer Center in collaboration with SCEC scientists Kim Olsen, Steven Day, Luis Dalguer, Yifeng Cui, Jing Zhu, David Okaya, Phil Maechling and Tom Jordan. The visualizations are featured at <http://www.wired.com/wiredscience/2009/08/visualizations/>.



Education Program

SCEC and its expanding network of education partners are committed to fostering increasing earthquake knowledge and science literacy at all grade levels and in a variety of educational environments.

The SCEC Education program uses the research literature (science education, learning psychology, sociology, etc.) and evaluation methodology to:

- G. Develop new materials and products (e.g. lesson plans, evaluation instruments, websites) where needed.

- H. Collaborate with partner organizations to enhance existing materials or products to meet the needs for SCEC’s Earthquake Program mission.
- I. Utilize and promote existing materials that coincide with or complement SCEC’s earthquake K-12 Education Program mission.
- J. Provide innovative experiential learning opportunities to undergraduate and graduate students during the summer and year-round.

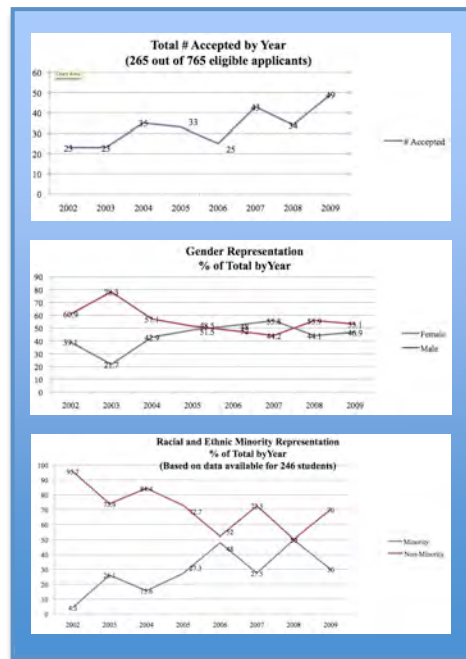
SCEC Education programs include three internship programs, facilitated activities at museum exhibits, earthquake education workshops, public earthquake talks, and activities at conferences such as the National Science Teachers Association. SCEC Education programs and products are implemented in a variety of educational environments- any place, situation, or context where the transmission of knowledge to learners is taking place.

SCEC Experiential Learning and Career Advancement programs. Since 1994, SCEC has provided 338 internships to undergraduate and graduate students, with 265 internships since 2002 (charts included here are for 2002-2009 only). SCEC offers two summer internship programs (SCEC/SURE and SCEC/USEIT) and a year-round program for both undergraduate and graduate students (ACCESS). These programs are the principal framework for undergraduate student participation in SCEC, and have common goals of increasing diversity and retention. In addition to their research projects, participants come together several times during their internship for orientations, field trips, and to present posters at the SCEC Annual meeting. Students apply for both programs at www.scec.org/internships.

The SCEC Summer Undergraduate Research Experience (SCEC/SURE) has supported 172 students to work one-on-one as student interns with SCEC scientists since 1994 (100 since 2002). SCEC/SURE has supported students working on numerous projects in earthquake science, including the history of earthquakes on faults, risk mitigation, seismic velocity modeling, science education, and earthquake engineering.

The SCEC Undergraduate Studies in Earthquake Information Technology (SCEC/USEIT) program, unites undergraduates from across the country in an NSF REU Site at USC. SCEC/USEIT interns interact in a team-oriented research environment with some of the nation’s most distinguished geoscience and computer science researchers. Since 2002, 145 students have participated. Research activities are structured around “Grand Challenges” in earthquake information technology. Each summer the interns build upon the foundation laid by previous intern classes to design and engineer increasingly sophisticated visualization tools.

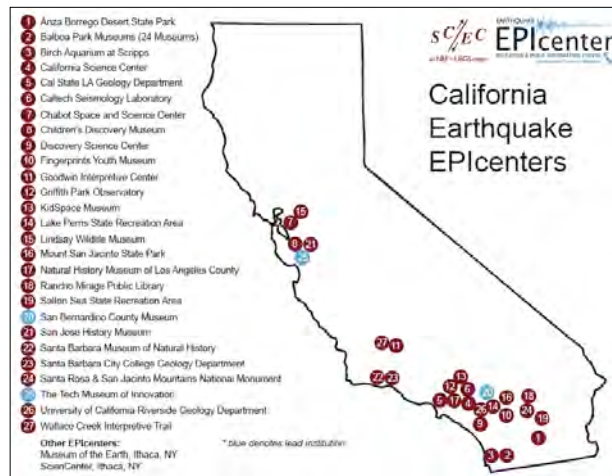
Our USEIT and CME experience has identified a “weak link” in cyberinfrastructure (CI)-related career pathways: the transition from discipline-oriented undergraduate degree programs to problem-oriented graduate studies in earthquake system science. We address this educational linkage problem through a CI-TEAM implementation project entitled the *Advancement of Cyberinfrastructure Careers through Earthquake System Science* (ACCESS). The objective of the ACCESS project is to provide a diverse group of students with research experiences in earthquake



system science that will advance their careers and encourage their creative participation in cyberinfrastructure development. Its overarching goal is to prepare a diverse, CI-savvy workforce for solving the fundamental problems of system science. Undergraduate (ACCESS-U) internships support CI-related research in the SCEC Collaboratory by undergraduate students working toward senior theses or other research enhancements of the bachelor's degree. Graduate (ACCESS-G) internships support up to one year of CI-related research in the SCEC Collaboratory by graduate students working toward a master's thesis. 20 ACCESS internships have been awarded.

Earthquake Exhibits and Museum Partnerships. Recognizing the key role that museums have in engaging communities not often reached by schools, SCEC facilitates a network of museums and other locations interested in providing earthquake education programming. These organizations also serve as a distribution point for SCEC resources such as *Roots*. SCEC has worked with some of these partners for many years, and in summer 2008 they have been organized as Earthquake Education and Public Information Centers (Earthquake EPIcenters). The concept emerged during the planning of the 2008 Great Southern California ShakeOut, and the need to organize museums for the ShakeOut has evolved into a year-round interaction with the ShakeOut being the culminating community event for the year. The ShakeOut has provided a basis for institutions to share resources and expertise

EPIcenters share a commitment to demonstrating and encouraging earthquake preparedness. They help coordinate Earthquake Country Alliance activities in their county or region (including the ShakeOut), lead presentations or organize events in their communities, or in other ways demonstrate leadership in earthquake education and risk reduction. EPIcenters are found in a variety of public meeting places such as museums, science centers, libraries, and universities.



SCEC's first major project in the development of a free choice learning venue was the *Wallace Creek Interpretive Trail*. In partnership with the Bureau of Land Management (BLM), SCEC designed an interpretive trail along a particularly spectacular and accessible 2 km long stretch of the San Andreas Fault near Wallace Creek. Wallace Creek is located on the Carrizo Plain, a 3-4 hour drive north from Los Angeles. The trail opened in January 2001. The area is replete with the classic landforms produced by strike-slip faults: shutter ridges, sag ponds, simple offset stream channels, mole tracks and scarps. SCEC created the infrastructure and interpretive materials (durable signage, brochure content, and a website at www.scec.org/wallacecreek with additional information and directions to the trail). BLM has agreed to maintain the site and print the brochure into the foreseeable future. In 2009-2010, the website will undergo major revision to include new images created by using Light Detection and Ranging (LIDAR) techniques. A SCEC intern is creating a suite of activities to accompany the LIDAR images.

The *ShakeZone Earthquake Exhibit* at Fingerprints Youth Museum in Hemet, CA was developed originally in 2001 and was redesigned in 2006. The current version of the exhibit is based on SCEC's *Putting Down Roots in Earthquake Country* handbook. Major partners involved in the exhibit

redesign included Scripps Institution of Oceanography and Birch Aquarium at Scripps. With funding from the United Way and other donors ShakeZone will be expanded in 2010 to include a section on Earthquake Engineering.

In 2006 SCEC has embarked on a long-term collaboration with the San Bernardino County Museum (SBCM) in Redlands, California. SCEC participated in the development and implementation of *Living on the Edge Exhibit*. This exhibit explains and highlights natural hazards in San Bernardino County (e.g. fire, floods, and earthquakes). SCEC provided resources in the development phase of the project and continues to supply the exhibit with copies of *Putting Down Roots in Earthquake Country*.

As a result of the successful collaboration on *Living on the Edge*, SCEC was asked to participate in the development of SBCM's *Hall of Geological Wonders*. To be completed in 2010, the Hall is a major expansion of this important cultural attraction in the Inland Empire. One of the main objectives of the Hall is to teach about the region from a geologic perspective. The museum is devoting a large space to the story of Southern California's landscape, its evolution and dynamic nature. SCEC has played an ongoing advisory role, provided resources for the development of the earthquake sections of the exhibit, and will have an ongoing role in the implementation of educational programming

The most recent debut of a SCEC earthquake display is the *Earthquake Information Center* at California State University, Los Angeles (CSULA). This exhibit, created in partnership with the geology department at CSULA, features two computer screens showing recent worldwide and local earthquakes. Located in the lobby of the Physical Science Building this exhibit also displays the seven steps to earthquake safety and components of a basic earthquake disaster supply kit. Many hundreds of students pass by the exhibit every day on their way to science classes.

K-12 Education Partnerships and Activities

Partnerships with Science Education Advocacy Groups and Organizations with Similar Missions. SCEC is an active participant in the broader earth science education community including participation in organizations such as the National Association of Geoscience Teachers, the Coalition for Earth System Education, and local and national science educator organizations (e.g. NSTA). Improvement in the teaching and learning about earthquakes hinges on improvement in earth science education in general. Hence, SCEC contributes to the community through participation on outreach committees wherever possible, co-hosting meetings or workshops, and building long-term partnerships. An example of a current project is a partnership with EarthScope to host a San Andreas Fault workshop for park and museum interpreters that will be held in Spring 2009.

Teacher Workshops. SCEC offers teachers 2-3 professional development workshops each year. The workshops provide connections between developers of earthquake education resources and those who use these resources in the classroom. The workshops include content and pedagogical instruction, ties to national and state science education standards, and materials teachers can take back to their classrooms Workshops are offered concurrent with SCEC meetings, at National Science Teachers Association annual meetings, and at the University of Southern California. In 2003 SCEC began a partnership with the Scripps Institution of Oceanography Visualization Center to develop teacher workshops. Facilities at the Visualization Center include a wall-sized curved panorama screen (over 10m wide).



Sally Ride Science Festivals. Attended by over 1000 middle school age girls (grades 5–8) at each venue, Sally Ride Science Festivals offer a festive day of activities, lectures, and social activities emphasizing careers in science and engineering. Since 2003, SCEC has presented workshops for adults and students and participated in the Festival’s “street fair,” a popular venue for hands-on materials and science activities. At the street fair SCEC demonstrates key concepts of earthquake science and provides copies of *Putting Down Roots in Earthquake Country*. The workshops, presented by female members of the SCEC community share the excitement and the many career opportunities in the Earth sciences.

National Science Teachers Association and California Science Teachers Association. Earthquake concepts are found in national and state standards documents. For example, earthquake related content comprises the bulk of the six grade earth science curriculum in California. SCEC participates in national and statewide science educator conferences to promote innovative earthquake education and communicate earthquake science and preparedness to teachers in all states.

Development of Educational Products

Earthquake Country - Los Angeles Video Kit. The video, produced by Dr. Pat Abbott of SDSU, tells the story of how the mountains and valleys of the Los Angeles area formed, and the important role of earthquakes. The video features aerial photography, stunning computer animations (some produced by SCEC’s USEIT interns), and interviews with well-known experts. SCEC developed an educator kit for school and community groups, available online and provided at SCEC’s teacher workshops.

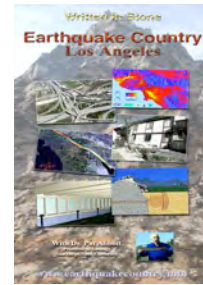


Plate Tectonics Kit. This new teaching tool was created to make plate tectonics activities more accessible for science educators and their students. SCEC developed a user-friendly version of the *This Dynamic Earth* map, which is used by many educators in a jigsaw-puzzle activity to learn about plate tectonics, hot spots, and other topics. At SCEC’s teacher workshops, educators often suggested that lines showing the location of plate boundary on the back of the maps would make it easier for them to correctly cut the map, so SCEC designed a new (two-sided) map and developed an educator kit.

Use of SCEC Community Modeling Environment (CME) Products in K-12 Education. SCEC has included CME animations in its teacher education workshops since 2002 with the initial visualization of the Community Fault Model (CFM), and through 2008 with the latest TeraShake and ShakeOut animations. SCEC’s “Earthquake Country – Los Angeles” DVD and *Putting Down Roots handbook* are used by teachers throughout Southern California, and both feature CME products. A compilation of CFM visualizations have also distributed on a CD at teacher conferences such as the NSTA annual meeting.



Research Accomplishments

Southern California Earthquake Center

2009 Draft Annual Report

This section summarizes the main research accomplishments and research-related activities during 2008 and the early months of 2009. The research reported here was funded by SCEC with 2008 research funds. While the presentation is organized sequentially by disciplinary committees, focus groups, and special project working groups, it is important to note that most SCEC activities are crosscutting and could be presented under multiple focus groups.

A. Disciplinary Activities

The following reports summarize recent progress in the three main infrastructural activities and the discipline-oriented research, *Seismology*, *Geodesy*, and *Geology*.

1. Seismology

Four projects were funded in the Seismology Infrastructure focus group in 2008-09. These were the Southern California Earthquake Data Center, the Borehole Seismometer Network, the Portable Broadband Instrument Center, and a Caltech/UCSD collaboration assembling earthquake catalogs and measuring earthquake properties and structure. In addition, several innovative projects were funded as part of the seismology research effort.

a. Southern California Earthquake Data Center (SCEDC)

Major 2008-09 Accomplishments:

1. Continued our key data-acquisition and archiving functions by maintaining and updating the primary online, near real-time searchable archive of seismological data for southern California. Added 88,246 station-days of continuous data and parametric and waveform data for 13,291 local events and 274 teleseismic earthquakes.
2. The SCEDC has upgraded both its database servers in both hardware and database version and they are now used fully in production. One is a database cluster composing of 3 Dell nodes. The other is an IBM server that was awarded to the SCEDC through an IBM-Caltech grant. This upgrade has allowed significant performance improvements to the users of catalog search applications and STP, especially in continuous waveform searches.
3. The SCEDC has replaced its single web server with two IBM x3650 web servers. This will allow greater redundancy and ability to handle higher loads that are expected with heightened public interest from a significant event.
4. In response to user recommendations at the SCEDC town-hall meeting, the SCEDC began continuous archiving of all EH and SH channels as of Jan 1, 2008. This is a significant increase spatial coverage of the continuous archive – from 328 stations in 2007 to 374 stations in 2008.

Report | SCEC Research Accomplishments

5. In an effort with the SCSN, timing on the entire SCSN catalog is now complete. Events from 1932 to present are now all available through STP or the catalog search pages on www.data.scec.org.
6. The SCEDC continues to make improvements Station Information System (SIS) with the Southern California Seismic Network (SCSN). Station fieldwork is entered by field technicians in SIS through a web interface, any changes to the station response are then automatically distributed to the data center databases and a dataless SEED volume is produced. The response changes are also made available to SCSN Real Time processes. All updates made by a field technician in the SIS are now available to users of SCEDC within 24 hours. Some developments in 2008-09 include a user interface called 'Channel Manager' which allows users to edit station response data for single channel epochs as well as batch updates. This kept the SCSN metadata current when SCSN renamed the HL channels of 170 stations to HN in compliance with SEED channel naming convention.
7. The SCEDC hosted a mirror site to the SCEC Earthquake Response Content Management System (ERCMS) for the November 2008 ShakeOut. The SCEDC will continue to host this mirror site for SCEC.
8. The SCEDC expanded the ANSS XML straw man and developed a schema for distributing seismic station metadata. The SCEDC has been a leader in XML formats, having previously developed an event and parametric information schema for the distribution of catalog data. The SCEDC released version 1.0 of the StationXML schema for sharing station metadata. StationXML has been accepted by the CISN and opened to review from the ANSS. The SCEDC is a leader in XML development, having previously developed an event and parametric information schema for the distribution of catalog data. StationXML and our other schemas are available at <http://www.data.scec.org/xml/station/> and <http://www.data.scec.org/xml/>.
9. The SCEDC will continue to serve out fault data to the SCEC WGCEP group. Contribution to the SCEC Community.

The Data Center is a central resource of SCEC and continues to be an integral part of the Center. In 2008-09, the SCEDC continued to contribute to the SCEC scientific community by providing online access to a stable and permanent archive of seismic waveforms and earthquake parametric data. The seismological data archive held at the SCEDC has contributed significantly to the publication of many scientific papers pertinent to the region, most of which have SCEC publication numbers. The Caltech/USGS catalog archived by the SCEDC is the most complete archive of seismic data for any region in the United States.

The SCEDC has allowed the data to be distributed to a much broader community of scientists, engineers, technologists, and educators than was previously feasible. The electronic distribution of data allows researchers in the worldwide scientific community to analyze the seismic data collected and archived in southern California and contribute their results to the SCEC effort.

The archive at the SCEDC currently has the following holdings:

- Caltech/USGS catalog of over 631,854 earthquakes spanning 1932-present.
- 12.92 terabytes of continuous and triggered waveforms (Figure 1).
- 15.2 million phase picks.
- 70.1 million triggered waveform segments.

- Nearly 8 years of continuous broadband recording of representing more than 470,880 station-day records, accumulating at ~50,000 station-days per year (for the current 166-station network).
- 30.4 million amplitudes available for electronic distribution.
- Triggered data for more than 9,475 significant teleseismic events.

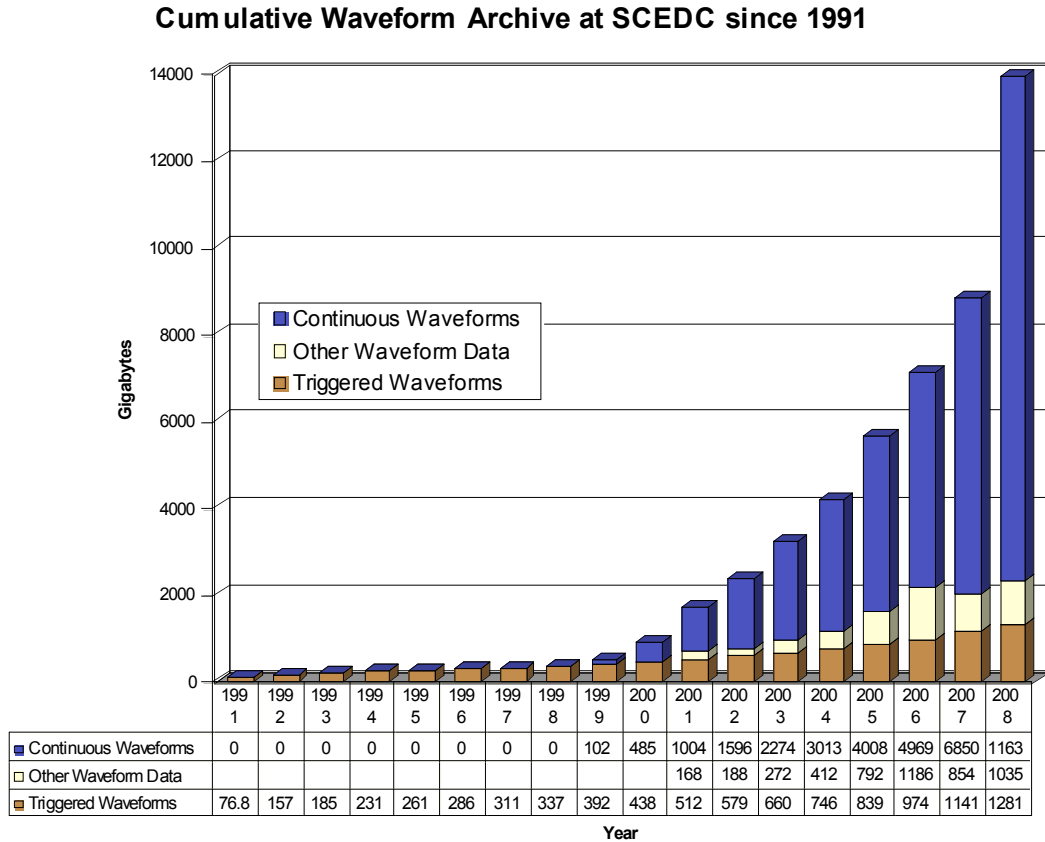


Figure 1. The SCEDC waveform archive.

b. 2008-09 SCEC Borehole Instrumentation Program Activity

One of the main accomplishments of the SCEC borehole instrumentation program has been the high degree of collaboration and cost sharing between multiple agencies and institutions that operate networks and collect and archive seismic data. The goal of the SCEC borehole instrumentation program, from its inception in SCEC 1, has been to facilitate the deployment of borehole observation stations in southern California (Figure 2).

The philosophy behind the SCEC borehole instrumentation program was that all data should be integrated with the existing network infrastructure for real-time transmission, processing, and archival. This provides all researchers with equal access to the data as soon as it's made available from the network operators. In addition, the borehole data is being used by the network for earthquake locations. In 2008-09 multiple researchers have started using the borehole data in southern California to look for evidence of non-volcanic tremor signals. Access to this data through the SCEDC made this possible.

Southern California Borehole Instrumentation

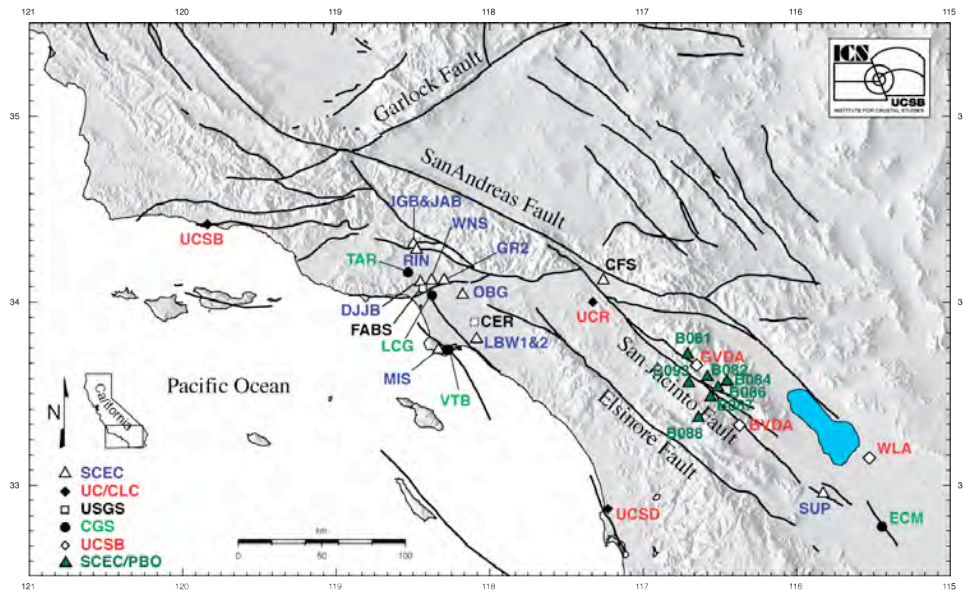


Figure 2. The Borehole instrumentation network in the Southern California region.

Other accomplishments for 2008-09 include:

1. SCEC collaboration with NEES program

- Software development using the Matlab toolbox interface to the Antelope real-time data processing at UCSB.
- Routine processing of borehole data to provide signal to noise quality factors on event-by-event basis.
- Calculation of spectra and routine spectral source parameter estimation using Matlab curve fitting toolbox.
- Development of web-based data dissemination tool for providing event based data in multiple formats from the SCEC borehole stations.

2. Collaborative upgrade of the communication link on Superstition Mountain (SUP) site.

- WiLan 11 Mbps radios at the superstition mountain site were replaced with Trango 45 Mbps radios to support the increased data communications from this SCEC borehole station that also servers as a repeater station. This repeater serves as a communication link to many stations in the PBO network, and the NEES facility in the Imperial Valley.

3. General maintenance of the SCEC borehole instrumentation infrastructure.

- Replacement of datalogger at the WNS site. The GPS engine had failed on the existing datalogger causing the data to be incorrectly time stamped. Swapping out the datalogger (using a working replacement provided by CISEN) fixed the timing issue.
- Repair and critter abatement at the LBW site. Data quality began to degrade at this station and the culprit was rodent infestation. Cables for power, GPS, and sensors had to be repaired or replaced. Improvements to overall security of the site and protection for the cables were made.
- Restoration of the communications at the JAB site. Data telemetry was restored when the failed UPS was removed, and power returned to the WiLan radio.

- General quality control of all the existing borehole stations using the NEES@UCSB software data processing systems to pull data from the real-time systems at Caltech and UNAVCO to provide assistance with troubleshooting problem stations.

c. 2008-09 SCEC Portable Broadband Instrument Center Activities

2008-09 ShakeOut: Integration of PBIC and IRIS real-time stations to CISM. The data from the PBIC stations can be integrated directly into the network processing at Caltech/USGS in Pasadena. In 2008-09, as part of the ShakeOut exercise, the SCEC real-time equipment was deployed along with equipment delivered from IRIS PASSCAL. A total of 12 stations were deployed, with a single station located in Indio right along the SoSAF and an array of 11 stations deployed in a fault-crossing configuration on the SoSAF at Whitewater Canyon (Figures 3-5).

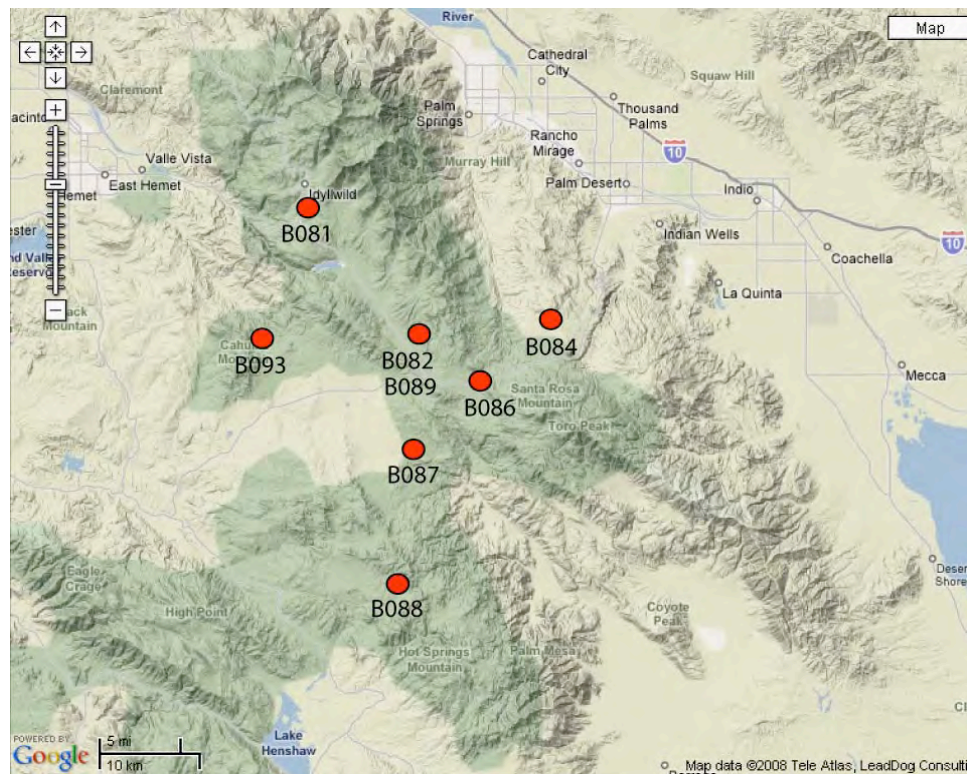


Figure 3. Joint SCEC/PBIC and IRIS/PASSCAL RAMP deployment for the 2008 ShakeOut exercise. Station IND1 located in Indio and WWC0 the center station of the fault-crossing array at Whitewater Canyon shown on Google Earth along with 1-week of seismicity.

This deployment is testing the ability to quickly integrate newly deployed portable stations into the routing data processing at the regional network level. Normally new stations come on line over the course weeks to sometimes months, as the station is prepared both in the field and at the network level with the collection of metadata into the station information system and the network systems configuration. Given a significant earthquake, the speed at which we can integrate new stations is important, and pushing the integration of new stations down to 24 hours is a significant challenge. The ShakeOut exercise using the SCEC and IRIS RAMP equipment tested the capabilities at the

network level in southern California and this exercise will improve our ability to respond quickly in the next significant event.



Figure 4. Joint SCEC/PASSCAL ShakeOut deployment in 2008. Installation of the SCEC PBIC real-time equipment at the [Left] Indio site with SCEC researcher Yong-gang Li shown for scale, and WWC0 center station [Right] at Whitewater Canyon.

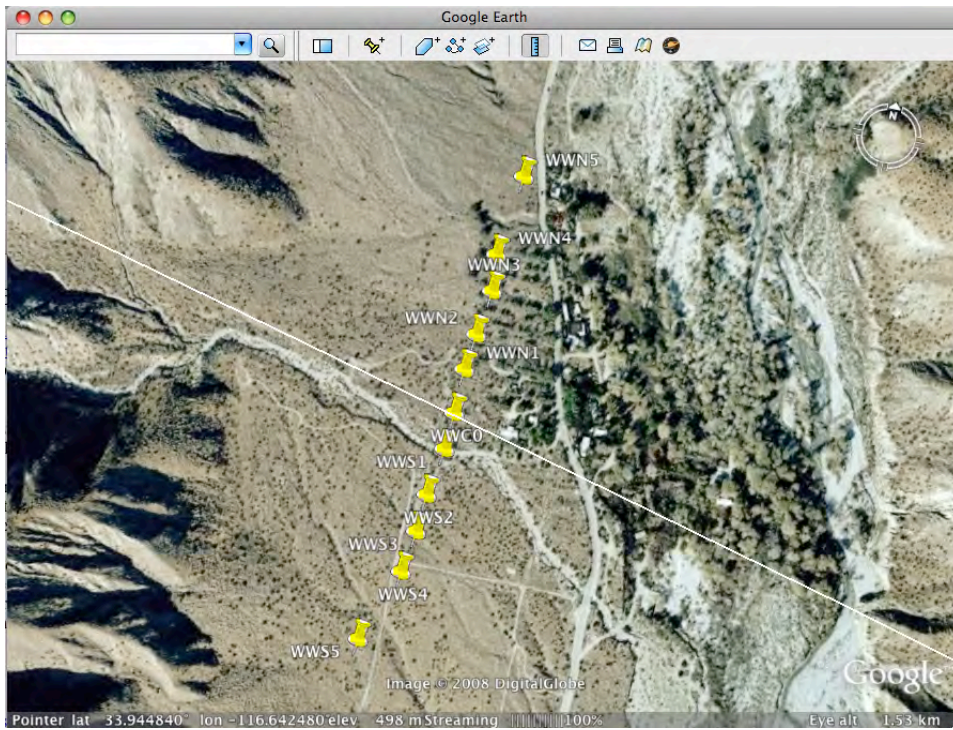


Figure 5. ShakeOut 2008 Whitewater Canyon fault-crossing array with the SoSAF approximate location shown as a white line running perpendicular to the array.

d. Superstition Hills Fault Project Support

One of the important aspects of the PBIC is the involvement of undergraduate students in field deployments, and post processing of the data as it comes back from the field. This year continued this involvement with two geology and one geophysics undergraduate majors participating in these activities through the Superstition Hills Fault monitoring project. This experiment ended in 2008, with the students being involved with the decommissioning of the stations and the data processing and archival procedures.

This experiment was the testing ground for the two new PBIC stations that have real-time capabilities. The deployment of these real-time stations in this rather remote location and harsh environment was a great success for the PBIC. Data was transmitted in real-time to the Caltech/USGS regional network monitoring, and was used help improve the location of earthquakes in this seismically active region. The use of 6-channel real-time stations also provides the three-component strong-motion channels for use in shake map production in the event a significant earthquake strikes the region and the weak-motion channels go off scale. The use of this modern equipment provided the project PI with instant access to the data with no post processing, and is now already available to the entire research community via the usual data dissemination tools from the SCEC data center!

Database and Web page updates. The newest PBIC equipment has been added to the PBIC online inventory database and is now tracked there as it comes into and goes out from the lab space at UCSB. The main website page as well as the “locals only” student assistant pages are being updated on a regular basis now. The latter being pages that the students use to document and provide tutorials on PBIC maintenance tasks, and data processing procedures.

Satellite Phone testing. The PBIC equipment now includes a Satellite phone (purchased with matching funds from UCSB) for communications after a significant event, when cell towers may be unavailable and wireless networks are over capacity. The UCSB phone was tested as part of the ShakeOut response planning, and the number is now listed on the SCEC response wiki.

e. Application of Waveform Cross-Correlation and Other Methods to Refine Southern California Earthquake Data

Earthquake focal mechanisms are a key constraint on fault orientations and the state of stress in the crust. However, moment tensor solutions based on synthetic seismograms can be computed only for earthquakes of $M \sim 3.5$ or greater because of signal-to-noise limitations. Thus focal mechanisms for the vast majority of earthquakes recorded in southern California are computed from high-frequency P phase data. Traditional methods, such as the FPFIT program [Reasenber and Oppenheimer, 1985], use P polarity information alone. Results of Jeanne Hardebeck [Hardebeck and Shearer, 2002, 2003] have shown that focal mechanisms computed from P polarities typically have large uncertainties due to gaps in the focal sphere coverage; however, improved results are possible, even from small numbers of stations, when S/P amplitude information is also used. Adding S/P ratios needs to be done carefully because S/P amplitude ratios can vary significantly, both at local and regional distances [e.g. Kennett, 1993]. Julian and Fougler [1996] developed a method to use amplitude ratios as inequality constraints, thus making it possible to use ratios as additional polarity observations. Using a different approach, Tan and Helmberger [2007] have shown that short-period P amplitudes can be used to determine focal mechanisms, and are particularly effective when empirical amplitude correction terms are computed for individual stations.

Shearer and Hauksson have done a preliminary comparison of three methods for determining focal mechanisms: 1) Tan and Helmberger [2007] using both first motion polarities and P-wave amplitudes (Ying Tan kindly provided their results); 2) Hardebeck and Shearer [2002] polarity only; and 3) Hardebeck and Shearer [2002] polarity and S/P amplitude ratios. Figure 6 compares the three methods (TH07, HS_pol, and HS_amp) for the 2003 Big Bear sequence. Generally, there is reasonable agreement among the methods. The biggest discrepancies are TH07 events such as 13936380, 13936812, and 13939520, which deviate from the prevailing strike-slip trend.

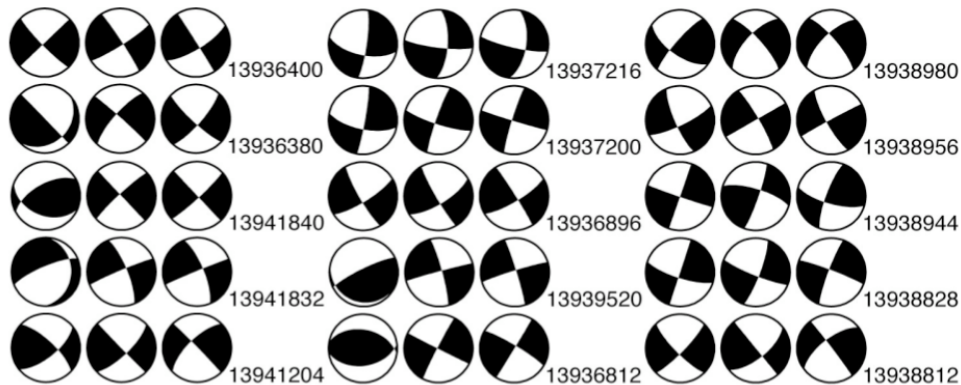


Figure 6. *P* velocity perturbations in the new 3-D crustal velocity model (Lin et al., 2007). The black contour lines enclose the well-resolved parts of the model. The best resolution is between about 3 and 10 km depth where ray coverage is best.

Ground Motion Prediction Using the Ambient Seismic Field. Under this grant Beroza et al. have developed the capability to use the ambient seismic field, sometimes referred to as ambient noise, to predict ground motion in earthquakes. Despite the complex and apparent random nature of the ambient field, it has a weak coherence that can be extracted even in the presence of multiple scattering. In particular, the correlation of diffuse wavefields recorded at two receivers can be used to extract the impulse response (i.e., the Green’s function) for an impulsive excitation at one receiver, as recorded at the other. Figure 7 from Ma et al. [2008] compared all three components of the ambient-noise Green’s functions at station FMP with theoretical, finite-element Green’s functions calculated by applying a smooth vertical force with Gaussian time dependence at station ADO for SCEC CVM 4.0 and CVM-H5.2 community velocity models. The fit is limited primarily by our imperfect and incomplete knowledge of crustal structure.

They have used the ambient field to document basin amplification for seismic stations in the Los Angeles basin. We use 31 days of non-overlapping 2-hour segments recorded during January 2007 and calculate the impulse response of the unaltered seismograms between all three components of velocity. We stack using coherence weighting to reduce the effect of incoherent data on the results, and use the closest station to the coast to deconvolve, since it is closest to the predominant microseism source. Prieto and Beroza [2008] compared the response to a horizontal impulse, using station BBR as a virtual earthquake source, at seismic stations across metropolitan Los Angeles with seismograms of the February 10, 2001 (Mw 4.63) Big Bear earthquake, which is within 4 km horizontally and 10 km vertically of station BBR. The horizontal impulse is applied in the fault normal direction, following the earthquake mechanism given by Graves [2008], who independently modeled ground motions.

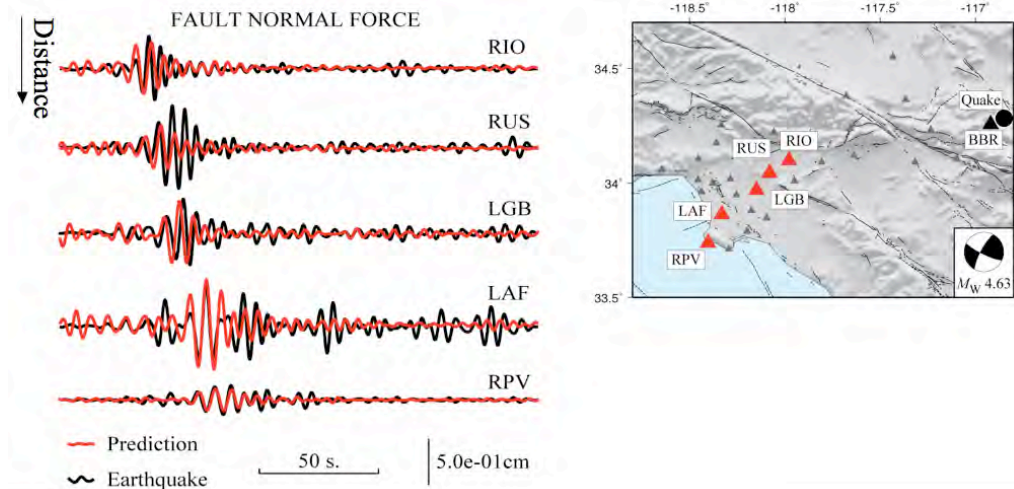


Figure 7. Ambient-noise Green's functions (red) at 4-10s period for 5 stations in the Los Angeles basin and seismic station BBR, compared to ground motions from the 2001 Big Bear earthquake (black), located near station BBR. Both the duration and relative amplitudes of ground motions across the Los Angeles Basin are recovered from ambient-noise observations.

Taken together, these techniques form the kernel of an important new capability for SCEC. Ambient-noise Green's functions can be used both for direct ground motion prediction, and to improve and test velocity models.

f. Seismic Documentation of Fault Cores and Damage Zones on the San Andreas Fault from Fault-Zone Guided Waves

In their previous study at Parkfield, San Andreas and the Calico fault in Eastern Mojave Desert, Li et al. used the fault-zone trapped waves (FZTWs) generated by explosions and microearthquakes and recorded at the dense linear seismic arrays to characterize the near-fault crustal properties, including the fault-zone rock damage magnitude and extent, and healing process from measurements of seismic velocity changes caused by the mainshock. The damage magnitude and extent on the SAF inferred by FZTWs [Li et al., 2004, 2006] have been confirmed by the SAFOD mainhole drilling and logs. The progression of coseismic damage and postseismic healing observed at the Parkfield SAF is consistent with those observed at rupture zones of the Landers and Hector Mine earthquakes [Li et al., 2006, 2007]. These results indicate that the greater damage was inflicted and thus greater healing is observed in regions with larger slip in the mainshock.

Li et al continued their efforts to determine the on- and off-fault damage at the San Andreas fault, Parkfield and the Calico fault using fault-zone guided waves. They used the FZTWs data recorded at the seismograph installed in the SAFOD mainhole at ~3 km depth where the borehole passed the SAF. The data include three-component waveforms from ~350 aftershocks of the 2004 M6 Parkfield earthquake. Many of aftershocks occurred at depths of 5 to 10 km so that the data allow us to constrain damage on the deep portion of the fault zone with higher resolution than those recorded at the surface array. They studied the heterogeneities in geometry and material property of fault zones to further understand the origin and mechanisms of fault damage and healing and their implications for stress heterogeneity and seismic hazard over the earthquake cycle. They also studied the contribution of on-fault damage to the total earthquake energy budget and the relationship between the damage magnitude and the absolute local stress level and stress drop.

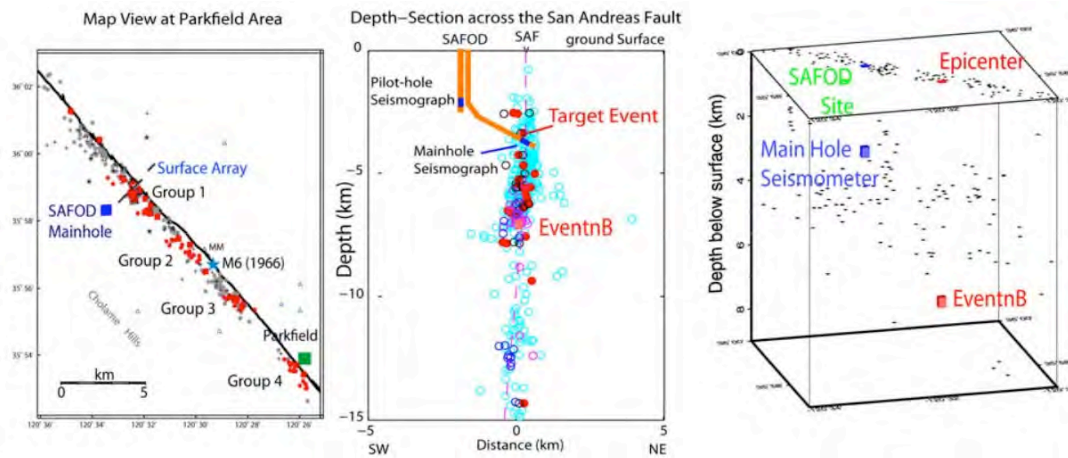


Figure 8. Left: Map view shows locations of ~350 aftershocks (circles) of the 2004 M6 Parkfield earthquake recorded at SAFOD borehole seismographs during December of 2004 and afterwards. Red circle denotes aftershocks in 4 groups at different epicentral distances to SAFOD site. The fault-zone trapped waves generated by these aftershocks are used in this study. The data recorded at the surface array (solid line across the fault) deployed in 2003 have been used in Appendix I. Middle: The vertical section across the SAF fault strike show locations of ~350 aftershocks (circles) recorded at SAFOD main-hole and pilot-hole seismographs. The fault-zone trapped waves generated by aftershocks in 4 groups denoted by red, black, pink and blue, respectively, are prominent in the SAFOD main-hole seismograms but not clear in the pilot-hole seismograms. Right: The 3-D view of locations of aftershocks (black dots) of the 2004 M6 Parkfield earthquake recorded at the SAFOD Main Hole seismograph (blue box). The red box denotes an example event which waveforms show the large secondary phases identified here as fault zone guided waves (see Fig. 2d in Appendix I). Waveforms recorded at the surface array for the target event and recorded at the SAFOD main-hole seismograph for Event B are shown in Fig. 2c of Appendix I.

In December 2004 a seismograph was installed in the SAFOD mainhole at ~3 km depth, where the highly fractured, low velocity zone of the SAF was found in the SAFOD drilling and well logs [Hickman et al., 2005]. A string of seismographs worked in the 1.2-km-deep pilot hole at the same time. The borehole seismographs recorded ~350 aftershocks of the 2004 M6 Parkfield earthquake. Locations of these aftershocks are shown in Figure 8. They have systematically examined the data recorded at the SAFOD borehole seismographs for the aftershocks in 4 groups with epicentral distances from the array: 1-2 km, 4-5 km, 8-10 km and 14-16 km, respectively (Figure 8).

g. Seismic and Geodetic Evidence For Extensive, Long-Lived Fault Damage Zones

During earthquakes slip is often localized on preexisting faults, but it is not well understood how the structure of crustal faults may contribute to slip localization and energetics. Accumulating evidence suggests that the crust along active faults suffers macroscopic strain and damage during large quakes [Fialko et al., 2002; Vidale and Li, 2003; Li et al., 1998; Ben-Zion et al., 2003].

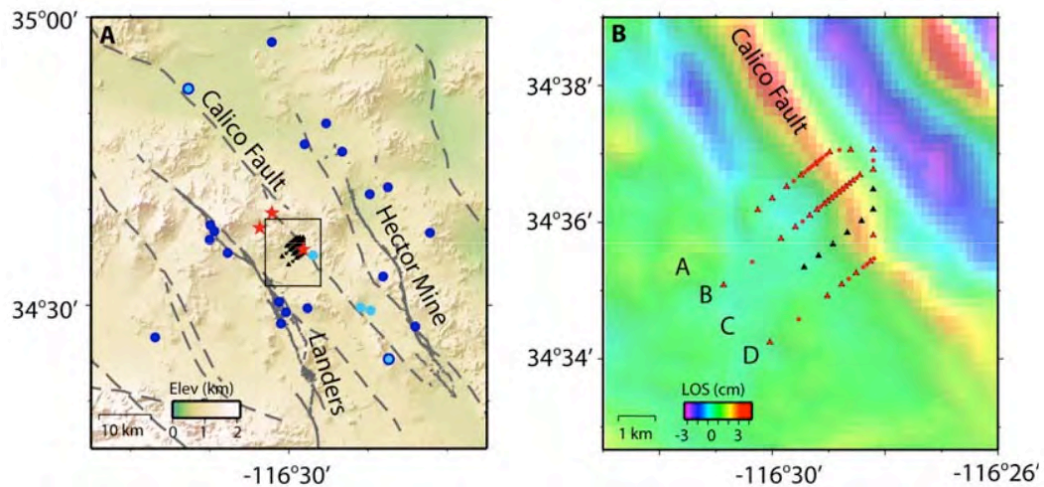


Figure 9. (A) Shaded relief map of Mojave region. Faults shown by dashed gray lines. Landers and Hector Mine ruptures are solid gray lines. Circles indicate local earthquakes used in the fault zone trapped wave and travel-time analyses, respectively. Light blue circles were used in both analyses. Red stars denote shots. Black triangles and circles show seismic stations. Gray square outlines the region in Figure 9B. (B) High-pass-filtered coseismic interferogram from the Hector Mine earthquake that spans the time period from 13 January 1999–20 October 1999 (after Fialko et al., [2002]). Colors denote changes in the line of sight (LOS) displacements. Black triangles and red circles are intermediate-period and short-period seismic stations.

Seismic and geodetic data from the Calico fault in the eastern California shear zone reveal a wide zone of reduced seismic velocities and effective elastic moduli (Figure 9). Using seismic travel times, trapped waves, and inSAR observations, Cochran et al. document seismic velocities reduced by 40 - 50% and shear moduli reduced by 65% compared to wallrock in a 1.5-km- wide zone along the Calico fault. Observed velocity reductions likely represent cumulative mechanical damage from past earthquake ruptures. No large earthquake has broken the Calico fault historically, implying that fault damage persists for hundreds or perhaps thousands of years. These findings indicate that faults can affect rock properties at substantial distances from primary fault slip surfaces, and throughout much of the seismogenic zone, a result with implications for the portion of energy expended during rupture to drive cracking and yielding of rock and development of fault systems.

h. Maintenance and Further Products for the Online-Database of Finite-Source Rupture Models

Since the launching of the Internet-accessible database of finite-source rupture models (<http://www.seismo.ethz.ch/srcmod>) summer 2007, Mai et al. have received very positive feedback on the quality and accessibility of the source-model data. With “data quality” we refer to the representation of the available rupture-model information in form of MATLAB-based data structures and in form of comprehensive ascii-files. In terms of “accessibility”, individual rupture-model data can be easily reviewed online (and downloaded), or the entire database can be retrieved as an easy-to-use MATLAB-structure (which seems to be the preferred choice for most users). However, despite this initial positive feedback, we received a number of constructive suggestions for improving and expanding the database. Many of these suggestions were implemented in the SCEC funding period 2008-09.

i. Interaction and Predictability of Small Earthquakes at Parkfield

How stress perturbations influence earthquake recurrence is of fundamental importance to understanding of the earthquake cycle. The large population of repeating earthquakes on the San Andreas fault at Parkfield provides a unique opportunity to examine the response of the repeating events to the occurrence of moderate earthquakes.

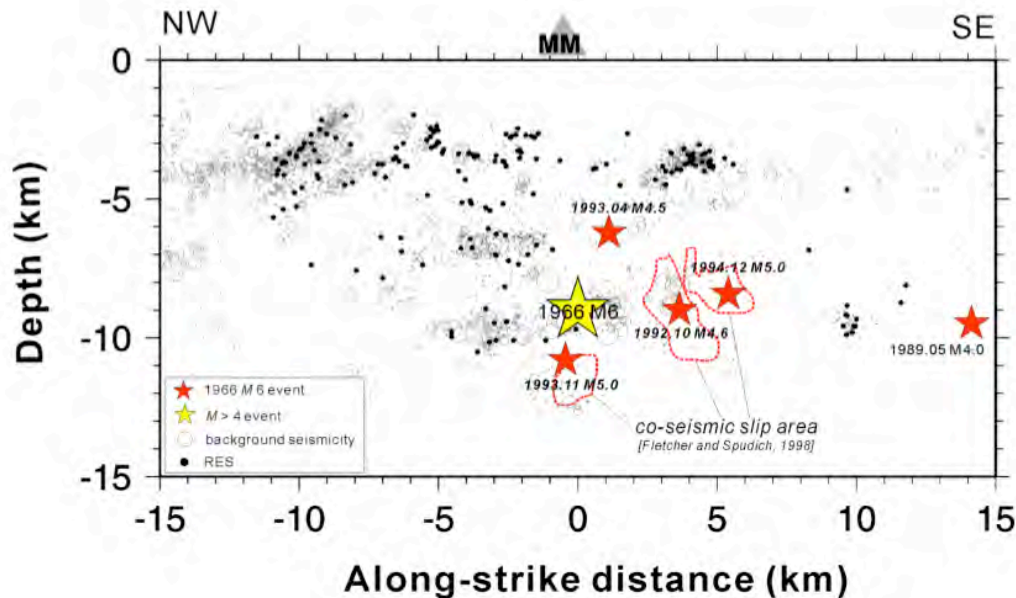


Figure 10. Along fault depth section showing 187 repeating earthquake sequences (1987-1998, black dots) and background seismicity. Catalog data are available at <http://www.ncedc.org/hrsn/hrsn.archive.html>. 1966 M 6 hypocenter is indicated by a yellow star. M 4-5 earthquakes that occurred in the period of 1987-1998 are denoted by red stars. Slip models of the $M \geq 4.6$ events that occurred in October 1992, November 1993, and December 1994 by Fletcher and Spudich [1998] are outlined by red dashed lines.

Using 187 $M -0.4 \sim 1.7$ repeating earthquake sequences from the High Resolution Seismic Network catalog, Burgmann et al. find that the time to recurrence of repeating events subsequent to nearby $M 4-5$ earthquakes is shortened, suggesting triggering by major events. The triggering effect is found to be most evident within a distance of ~ 5 km, corresponding to static coseismic stress changes of $> 6 - 266$ kPa, and decays with distance (Figure 10). They also find coherently reduced recurrence intervals from 1993 to 1998. This enduring recurrence acceleration over several years reflects accelerated fault slip and thus loading rates during the early 1990s.

j. The Source and Significance of High-Frequency Bursts Observed on Strong Motion Records from the Chi-Chi Taiwan and Parkfield California Earthquakes

High-pass filtering (>20 Hz) of acceleration records from the 1999 Chi-Chi Taiwan and 2004 Parkfield, California earthquakes reveal a series of bursts that occur only during strong shaking. Initially interpreted as originating from asperity failure on the Chelungpu fault, bursts observed during the Chi-Chi earthquake were subsequently determined to be a local effect within about 1 km of the seismic stations. Similar bursts were observed at UPSAR during the Parkfield earthquake

and were constrained to originate less than 20 m from the instruments. Such small shallow events cannot result from the triggered release of stored elastic energy because rate-and- state friction rules out stick-slip instability on small, shallow patches. Sammis et al. infer that the bursts are not triggered, but are driven by simultaneous shear and tensile stresses near the surface during the strong motion. At 2 Hz, SV to P wave mode conversion at the free surface produces tensile stresses to depths of 70 m. Where standard triggering releases stored elastic energy and adds to the incident wavefield, this new driving mechanism takes energy out of the 2 Hz strong motion and reradiates it at high frequencies. It is thus an attenuation mechanism, which we estimate can contribute 3% to the net attenuation in the very shallow crust [Fischer et al., 2009].

k. Near real-time determination of earthquake sources for post-earthquake response

This past year Shaw et al. initiated a new project to develop an automated system for determining, immediately following an earthquake in southern California, what fault or faults likely generated the event. This effort employs the SCEC Community Fault Model (CFM) [Plesch et al., 2007] and CISEN/SCSN real-time earthquake information. The system takes real-time earthquake information and calculates distances between the hypocenters and faults represented in the CFM. This data is used in combination with other criteria, such as the event magnitude and preliminary focal mechanism solution (including both event type and nodal plane orientations), to assign probabilities of association with various faults in the CFM. In the first year of this project, Shaw et al. have defined and implemented the approach for automatically calculating the proximity of earthquakes to triangulated surface representations of faults in the CFM, and are now in the process of refining an algorithm that will combine this information with other fault and earthquake attributes to assign probabilities of association (Figure 11). In the next phase of the project, we will set up a prototype system using a training dataset of southern California earthquakes.

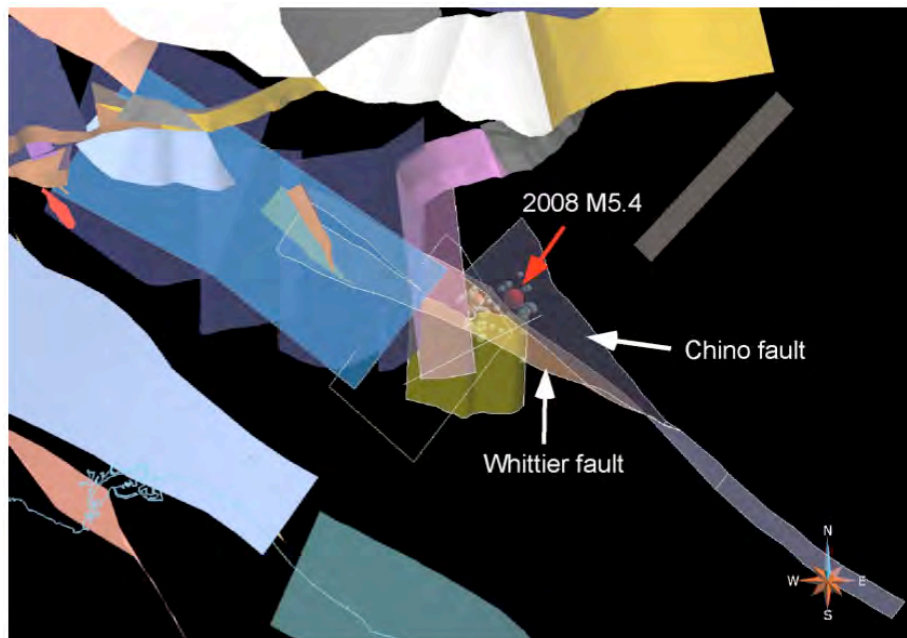


Figure 11. View of the CFM with the mainshock and aftershocks of the 2008 Chino Hills (M 5.4) earthquake. The earthquake occurred at a complex juncture of the Chino, Whittier, and several other faults, illustrating the complexity of defining the causative fault(s) for such events.

I. Modeling Short-Period Seismograms

Helmberger et al. report on a detailed test of a recently developed technique, CAPloc, in recovering source parameters from a few stations against results from a large broadband network in Southern California.

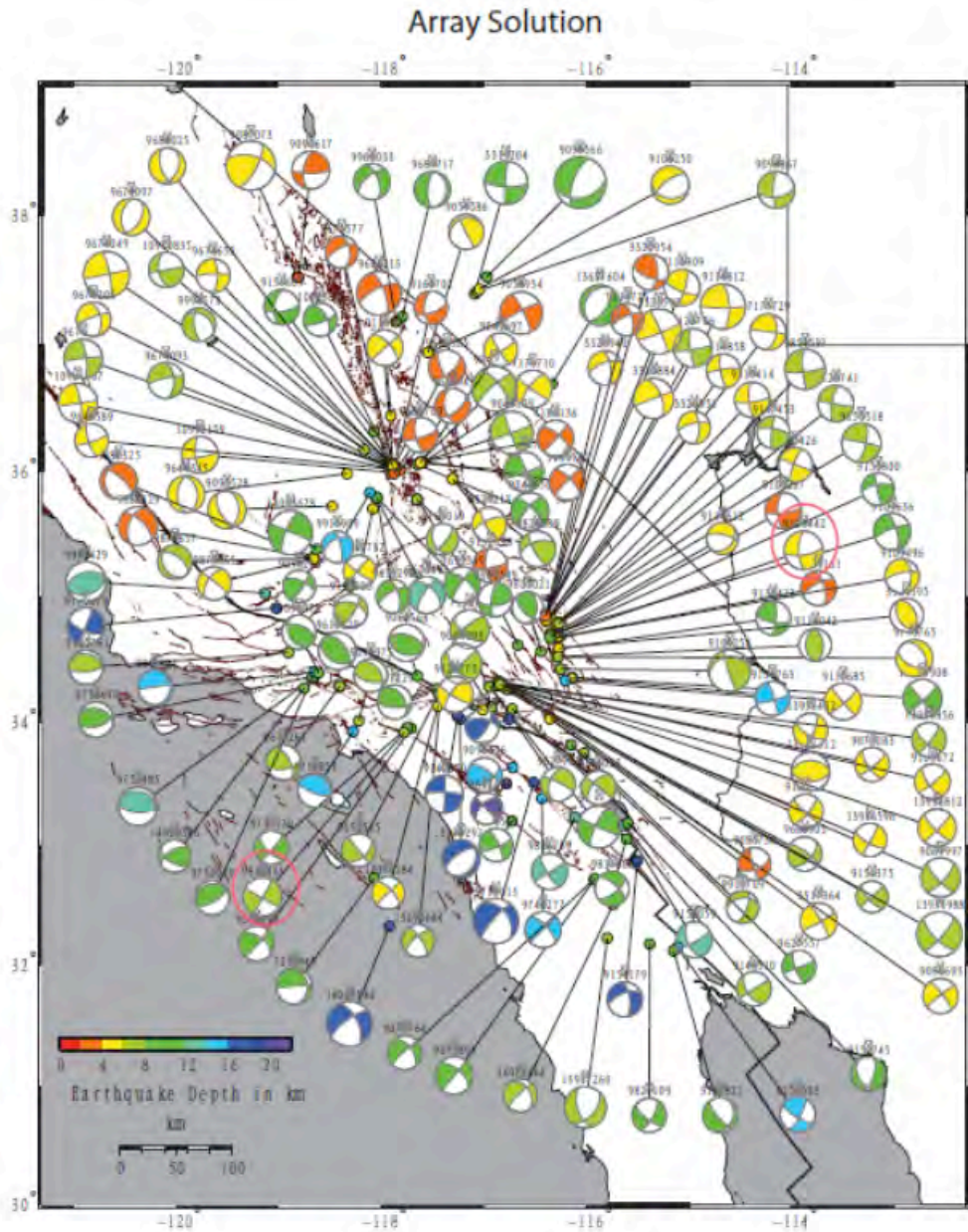


Figure 12. Source parameters of 160 Southern California events estimated by the CAP method with source parameters are shown. Source depths are indicated by color, ranging from 3 to 20 km.

The method uses a library of 1D Green's functions, which are broken into segments and matched to waveform observations with adjustable timing shifts. These shifts can be established by calibration against a distribution of well-located earthquakes and assembled in tomographic images for predicting various phase-delays. Synthetics generated from 2D cross-sections through these models indicates that 1D synthetic waveforms are sufficient in modeling but simply shifted in time for most hard- rock sites. This simplification allows the source inversion for both mechanism and location to easily obtain by grid search (Figure 12). We test one-station mechanisms for 160 events against the array for both PAS and GSC, which have data since 1960. While individual solutions work well for mechanism (about 80%), joint solutions using these two stations produce more robust results. Inverting for both mechanism and location also works well except for complex paths crossing deep basins and along mountain ridges [Tan *et al.*, 2009].

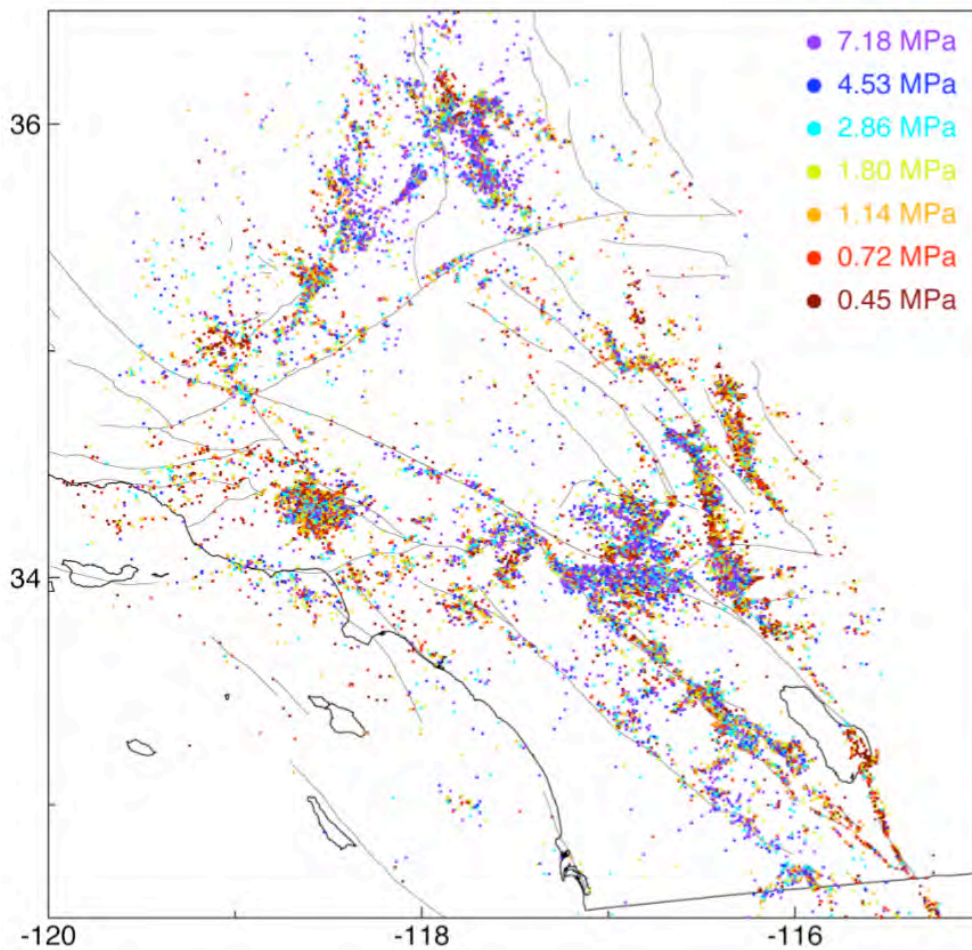


Figure 13. Estimated Brune-type stress drops for over 65,000 southern California earthquakes from 1989 to 2001. Results are colored in equal increments of $\log \Delta\sigma$.

m. Analysis of Coda Waves in Southern California for Earthquake Source Properties

In earlier SCEC work, Shearer et al. computed and saved P , S , and noise spectra from over 2 million seismograms from 1984 to 2003 using a multitaper method applied to a 1.28 s signal window and a pre-arrival noise window. Next, they stacked the P spectra to isolate source, receiver, and propagation path contributions to the spectra (Figure 13). The advantage of the method is that it identifies and removes anomalies that are specific to certain sources or receivers. This is an important step because individual spectra tend to be noisy and irregular in shape and difficult to fit robustly with theoretical models. However, by stacking thousands of spectra it is possible to obtain much more consistent results [Shearer et al., 2006].

Shearer et al also analyzed Mogi doughnut behavior preceding small earthquakes in southern California. Earthquakes cluster strongly in time and space, but it is not yet clear how much of this clustering can be explained as triggering from previous events (such as occurs for aftershock sequences following large earthquakes) and how much the clustering may reflect underlying physical processes (such as apparently drive many earthquake swarms, e.g., Hainzl, [2004], Vidale and Shearer, [2006]). Seismologists have long studied the seismicity preceding big earthquakes to see if any distinctive precursory patterns could be identified. In some cases, a period of low earthquake activity or quiescence is observed for years in the vicinity of the eventual rupture zone of large earthquakes, surrounded by a region of continuing or increasing activity [Kanamori, 1981]. This seismicity pattern has been given the name “Mogi doughnut” (e.g., Mogi [1969]), with the doughnut hole representing the low seismicity rate around the impending hypocenter. However, analyses of large earthquake catalogs to evaluate the reliability of quiescence in predicting earthquakes have yielded mixed results [Habermann, 1988; Reasenber and Matthews, 1988]. At shorter time scales of days to hours, some earthquakes are preceded by foreshock sequences near their hypocenters, but no distinctive properties in these sequences have yet been identified that would distinguish them from the many observations of earthquake clusters that do not lead to large earthquakes.



Figure 14. (Left) students working to conceal the location of seismometer and solar panels using tumbleweeds. (Right) A sizeable hole dug for one of the sensors deployed along the array.

n. Seismology Rapid Response Test During the SoSAFE Shakeout

With the funding provided by SCEC, Cochran, Steidl, Li, and others tested the procedure for requesting instruments for a RAMP array, deploying seismometers with both on-site and telemetry data collection and integrating the data into the Southern California part of the project we also coordinated the deseismic RAMP equipment from two sources, a undergraduates to deploy seismometers (Figure 14).

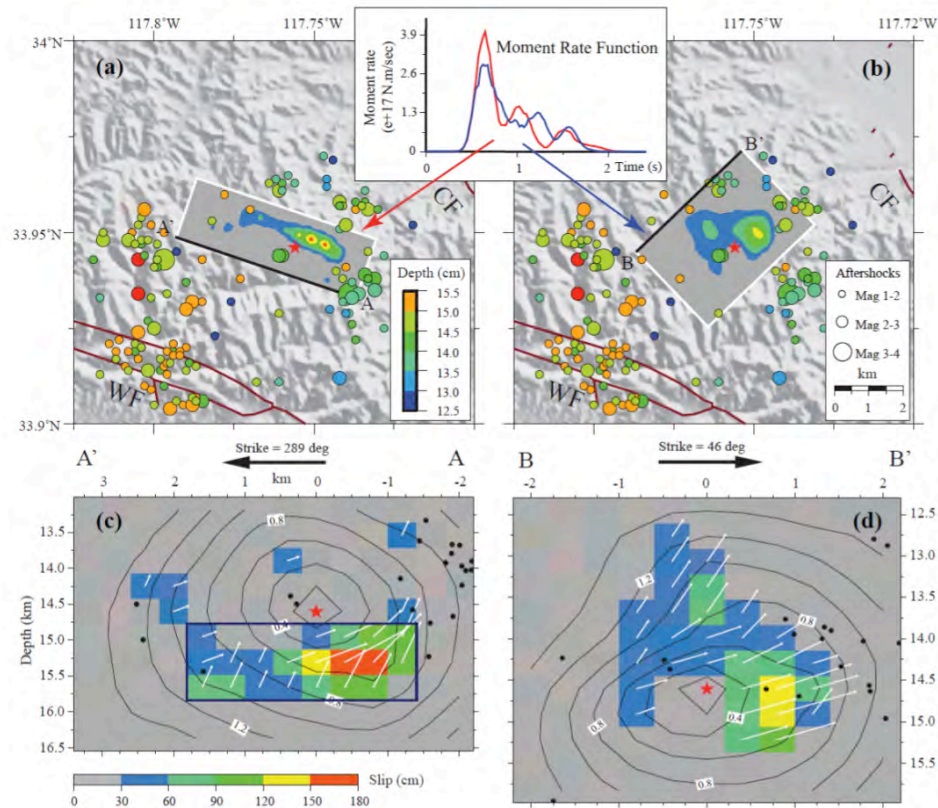


Figure 15. Comparison of inverted finite fault models based on two nodal planes (Table 1). (a) Surface projection of the Model I (white box) superimposed on the shaded relief. The red star indicates the epicenter of the mainshock. Black line A-A' indicates the top edge of the fault plane. Circles represent relocated aftershocks [Hauksson et al., 2008] during the first month, with filled color denoting their hypocenter depth, and the radius indicating their magnitudes. WF-Whittier Fault; CF-Chino Fault. (b) Same as (a) but for Model II (c) Vertical cross-section of slip distribution of Model I. The black arrow indicates the fault strike and the red star denotes the hypocenter location. For each subfault, the color shows its dislocation amplitude and the arrow indicates the motion direction of the hanging wall relative to the footwall. The high slip region was outlined by a blue box. Black contours show the rupture initiation time in an interval of 0.2 s. Black dots denote the selected aftershocks located within 1 km of the fault plane (d) Similar to (c) but for Model II. Inserted figure compares the moment rate functions of Model I (red line) and Model II (blue line).

o. Finite fault parameterization of intermediate and large earthquakes in Southern California

The quick finite-fault algorithm, which is currently used to monitor the global large earthquakes, is being modified by Ji et al. to routinely study finite fault parameters of the mediate and large earthquakes in Southern California using the CISN real-time dataset. Since this technique has already been demonstrated for the study of large earthquakes, during 2008-09 our research focused on the feasible data process and inverse schedules for the study of the moderate earthquakes. To study the moderate earthquake, we need use the higher frequency seismic waveforms, which is very sensitive to the 3D earth structure. *Tan and Helmberger* [2007] pointed out that the high frequency P waveforms (0.5-2Hz) recorded at LA basin could be modeled using 1D Green's functions after adding path-dependent time shifts and multiplying amplitude amplification factors (AAFs). They defined the AAFs as the amplitude ratios between records of a calibration event and the corresponding 1D synthetics, and found that the AAFs are relatively stable and mechanism independent [*Tan and Helmberger*, 2007]. However, a good calibration event may not always be available. So we have attempted to define them using state-of- art 3D SCEC-CVM models. The 2008 Chino Hills earthquake was used as the test event [Shao et al., 2009] (Figure 15).

p. References

- Ben-Zion, Y., Peng, Z., Okaya, D., Seeber, L., Armbruster, J. G., Ozer, N., Michael, A. J., Baris, S., Aktar, M., A shallow fault-zone structure illuminated by trapped waves in the Karadere-Duzce branch of the North Anatolian Fault, western Turkey: *Geophysical Journal International*, **152**, p. 699–717, doi: 10.1046/j.1365-246X.2003.01870.x, 2003.
- Ellsworth, W. L., and P. E. Malin, A first observation of fault guided PSV-waves at SAFOD and its implications for fault characteristics, *EOS, Transactions, and American Geophysics Union*, **87**, T23E-02, p154, 2006.
- Fialko, Y., Sandwell, D., Agnew, D., Simons, M., Shearer, P., Minster, B., Deformation on nearby faults induced by the 1999 Hector Mine earthquake: *Science*, **297**, p. 1858–1862, doi: 10.1126/science.1074671, 2002.
- Fischer, A. D. and C. G. Sammis, Dynamic driving of small shallow events during strong motion, *Bull. Seismol. Soc. Am.*, **99**; 1720-1729; DOI: 10.1785/0120080293, 2009.
- Fletcher, J. B., and P. Spudich, Rupture characteristics of the three *M* 4.7 (1992-1994). Parkfield earthquakes, *J. Geophys. Res.*, **103**, 835-854, 1998.
- Habermann, R. E., Precursory seismic quiescence: past, present and future, *Pure Appl. Geophys.* **126**, 279 – 318, 1998.
- Hainzl, S., Seismicity patterns of earthquake swarms due to fluid intrusion and stress triggering, *Geophys. J. Int.* **159**, 1090–1096, 2004.
- Hardebeck, J.L. and P.M. Shearer, A new method for determining first-motion focal mechanisms, *Bull. Seismol. Soc. Am*, **92**, 2264–2276, 2002.
- Hardebeck, J.L. and P.M. Shearer, Using S/P amplitude ratios to constrain the focal mechanisms of small earthquakes, *Bull. Seismol. Soc. Am.*, **93**, 2434–2444, 2003.
- Hauksson E., K. Felzer, D. Given, M. Given, S. Hough, K. Hutton, H. Kanamori, V. Sevilgen, S. Wei, and A. Yong, Preliminary Report on the 29 July 2008 Mw5.4 Chino Hills, Eastern Los Angeles Basin, California, Earthquake Sequence, *Seismo. Res. Letters*, **79**, p. 855- 868, 2008
- Hickman, S. H., M. D. Zoback, and W. L. Ellsworth, Structure and Composition of the San Andreas fault zone at Parkfield: Initial results from SAFOD Phase 1 and 2, *EOS, Transactions, and American Geophysics Union*, **83**, No.47, p237, 2005.
- Julian, B. R., and G. R. Fougler, Earthquake Mechanisms from Linear-Programming Inversion of Seismic-Wave Amplitude Ratios, *Bull. Seism. Soc. Am.*, **86**, No. 4, pp. 972–980, 1996.
- Kanamori, H., The nature of seismicity patterns before large earthquakes, in *Earthquake Prediction, An International Review* (ed. Simpson, D. and Richards, P.) (American Geophysical Union, Washington, 1981), pp. 1–19, 1981.

- Kennett, B. L. N., The distance dependence of regional phase discriminants, *Bull. Seism. Soc. Am.*, **83**, No. 4, pp. 1155–1166, 1993.
- Li, Y.-G., Vidale, J.E., Aki, K., Xu, F., and Burdette, T., Evidence of shallow fault zone strengthening after the 1992 M7.5 Landers, California, earthquake: *Science*, **279**, p. 217–219, doi: 10.1126, 1998.
- Li, Y.-G. and P. Malin, San Andreas Fault damage at SAFOD viewed with fault-guided waves, *Geophys. Res. Lett.*, **35**, L08304. Doi:xx/2007GL032924, 2007.
- Li, Y. G., E. S. Cochran, and J. E. Vidale, Low-velocity damaged structure on the San Andreas Fault at seismogenic depths near the SAFOD drilling site, Parkfield, CA from fault-zone trapped waves, *EOS, Transactions, and AGU*, **85**, No. 47, F1313, 2004b.
- Li, Y.-G., Chen, P., Cochran, E.S., Vidale, J.E., and Burdette, T., Seismic evidence for rock damage and healing on the San Andreas Fault associated with the 2004 M 6.0 Parkfield earthquake: *Bull. Seism. Soc. Am.*, **96**, p. S349–S363, doi: 10.1785/0120050803, 2006.
- Lin, G., P. Shearer, and E. Hauksson, A Search for Temporal Variations in Station Terms in Southern California from 1984 to 2002, *Bull. Seismol. Soc. Am.*, **98**, 2118 – 2132, 2008.
- Ma, S., G.A. Prieto, and G. C. Beroza, Testing Community Velocity Models for Southern California Using the Ambient Seismic Field, *Bull. Seismol. Soc. Am.*, **98**, 2694– 2714, DOI: 10.1785/0120080947, 2008.
- Mogi, K., Some features of recent seismic activity in and near Japan (2): Activity before and after great earthquakes, *Bull. Earthquake Res. Inst. Univ. of Tokyo* **47**, 395–417, 1969.
- Plesch, A., J. H. Shaw, C. Benson, W. A. Bryant, S. Carena, M. Cooke, J. Dolan, G. Fuis, E. Gath, L. Grant, E. Hauksson, and others, Community Fault Model (CFM) for Southern California, *Bull. Seismol. Soc. Am.*, **97**, 1793-1802, 2007.
- Prieto, G. A., and G. C. Beroza, Earthquake Ground Motion Prediction Using the Ambient Seismic Field, *Geophys. Res. Lett.*, **35**, L14304, doi:10.1029/2008GL034428, 2008.
- Reasenber, P. and Matthews, M., Precursory seismic quiescence: A preliminary assessment of the hypothesis, *Pure Appl. Geophys.* **126**, 373–406, 1988.
- Reasenber, P., and D. Oppenheimer, FPFIT, FPLOT, and FPPAGE: FORTRAN computer programs for calculating and displaying earthquake fault-plane solutions, *U.S. Geol. Surv. Open-File Rept.*, 85-739, 1985
- Shao, Guangfu, C. Ji and E. Hauksson, Rupture process and dynamic implications of the July 29, 2008 Mw 5.4 Chino Hills, California Earthquake, *BSSA*, 2009. (submitted)
- Shearer, P. M., G. A. Prieto, and E. Hauksson, Comprehensive analysis of earthquake source spectra in southern California, *J. Geophys. Res.*, **111**, B06303, doi:10.1029/2005JB003979, 2006.
- Tan, Y., and D. Helmberger, A new method for determining small earthquake source parameters using short-period P waves, *Bull. Seismol. Soc. Am.*, **97**, 1176–1195, doi: 10.1785/0120060251, 2007.
- Tan, Ying and Don Helmberger, Rupture Characteristics of Small Earthquakes; 2003 Big Bear Sequence, *Bull. Seismol. Soc. Am.*, 2009 (submitted).
- Vidale, J.E., and Li, Y.-G., Damage to the shallow Landers fault from the nearby Hector Mine earthquake, *Nature*, **421**, p. 524–526, doi: 10.1038/nature01354, 2003.
- Vidale, J. E., and P. M. Shearer, A survey of 71 earthquake bursts across southern California: Exploring the role of pore fluid pressure fluctuations and aseismic slip as drivers, *J. Geophys. Res.*, **111**, B05312, doi:10.1029/2005JB004034, 2006.

2. Tectonic Geodesy

In 2008-09, geodetic activities within SCEC focused on a range of activities that were highlighted in the RFP, including the acquisition of new GPS and strainmeter data, modeling of fault slip rates, and the use of multiple data types to estimate interseismic velocity fields. Areas in the RFP that received less attention include the use of high-rate GPS data, and the assessment of use of combined data sets in interpretation of tectonic or non-tectonic signals. continued as chair and co-chair of Tectonic Geodesy.

a. Transient detection and investigation of underlying processes and implications

In the summer of 2008, the leaders of the Tectonic Geodesy working group (Jessica Murray-Moraleda and Rowena Lohman) held a 2-day workshop on transient detection, which recommended a blind test exercise using synthetic data to identify promising detection approaches. This spring Phase I of the blind test transient detection exercise was completed and Phase II, with ~ 11 participating groups, is currently underway. There will be a 2-day workshop immediately before the 2009 SCEC meeting to summarize the results and discuss the timeline for tests using real data.

b. Modeling of geodetic data for slip rates, strain rates, and stress evolution

Efforts to invert geodetic data this year fell into two main categories – placing constraints on fault slip rates (and exploring the implications of geologic/geodetic rate discrepancies), and estimates of the spatial distribution of stress or strain rates across Southern California (linked to earthquake productivity and seismic hazard). Fault slip rate studies were generally divided into block models and field studies.

Johnson found that block models using an elastic layer overlying viscoelastic asthenosphere (uniform or layered), can result in differences in inferred slip rate of the order that are observed between geodetic and geologic estimates. He found that the predicted rates (Figure 16) are higher for models that include a layered viscoelastic space than for those with a uniform, high viscosity layer beneath the elastic crust. A test for the distribution of fault creep on the San Andreas reproduced the known creeping sections in the Salton trough and Parkfield. This year, Meade adapted his block models to include more realistic rectangular dislocations over most of Southern California (from CMM-R), with complicated triangulated geometries (500 elements) from CFM for the Puente Hills Thrust. In cases where the CMM-R representation included intersecting faults (which could not be included in the block model approach), they used the fault deemed most likely to have the fastest slip rate.

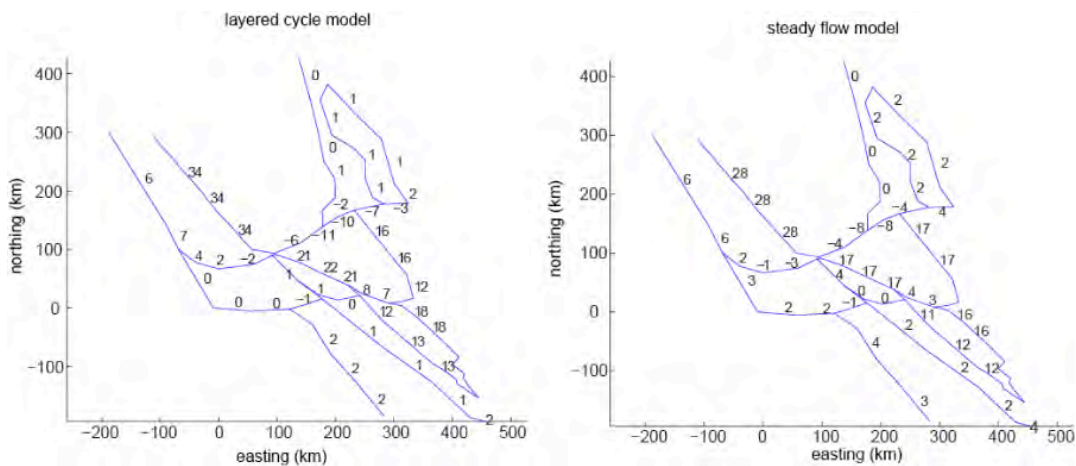


Figure 16. Slip rate estimates for a layered and homogeneous (steady flow) lower crust. Right-lateral rates are positive, left-lateral rates are negative.

Smith-Konter and Sandwell continued development of a model of the San Andreas Fault system that ingests historic and paleoseismic data and estimates the stress field due to coseismic, postseismic and interseismic loading. This year they explored uncertainties in their stress rate estimate due to variations in slip rates, locking depths, frictional coefficients, slip history, and mantle viscosity. Ward examined the use of geodetic data in seismic hazard estimation, either independently (stand-alone approach) to determine moment rate and earthquake rate from estimates of strain rate, or in combination with fault systems and earthquake simulators (combined approach). Part of the stand-alone approach involves the use of a virtual “scoop” of the Earth, with the base of the scoop tiled with slipping dislocations constrained by geodetic observations. This allows forward modeling of strain fields both at the surface and along arbitrary faults, and facilitates integration with earthquake simulator efforts (the ALLCAL simulator in this work).

c. Refine interseismic crustal motion maps - particularly vertical motion

Efforts in this category included attempts to merge SCIGN and Plate Boundary Observatory GPS products. Herring and King reported on three activities: Merging non-PBO data from SCIGN into the routine PBO processing, inclusion of the effects of the Landers and Hector Mine earthquakes into Southern California GPS time series, and their participation in the SCEC-sponsored transient signal detection activity. They find that sites in their merged data show similar weighted rms scatter, at least within the uncertainty due to differences in the length of processing for the different families of sites. The merged results are made available through the REASON project (reason.scign.org). Hreinsdottir and Bennett also include the processing of PBO and SCIGN data using an absolute phase-center model, with a focus on the vertical rate and data since 1994. They have completed processing of all of the PBO stations and have completed 70% of the SCIGN stations. They check for offsets at the times of equipment changes and earthquakes and perform first-order evaluations of time series quality.

Work on refining crustal motion maps included the use of both GPS and InSAR observations, with some discussion of whether the results were consistent with one another. Fialko and collaborators continued work on improvements to InSAR time series analysis using their stacking algorithm. Their method focuses on the suppression of the contribution from individual noisy imagery to the secular rate, where “noisy” is defined as scenes that tend to result in interferograms with a large norm. They compare their results to independent time series methods along a profile across the southern San Andreas Fault and get good agreement. They focus on high-gradient profiles across the Blackwater fault in particular, using data from two overlapping tracks that have different viewing angles. The steep gradient would be interpreted as corresponding to a very shallow (3-5km) locking depth if the entire LOS signal came from horizontal motion. However, they find that a compliant zone 2-3km wide along the fault might be responding to coseismic strain from the Hector Mine and Landers earthquakes, resulting in vertical deformation that contributes to the LOS signal.

Funning, Jin, Houlie and Burgmann estimate the effects of tropospheric water vapor on SAR interferograms and GPS within the Los Angeles Basin. They explore three approaches to assess or mitigate the effects of atmospheric noise, using estimates from surface-based meteorological stations, families of SAR interferograms, and dense networks of GPS sites. They observed tropospheric delays that vary by up to 10 cm at individual GPS sites, with the magnitude of the total delay depending on thickness of the troposphere at each site. The use of collocated weather data suggests shifts of a similar magnitude. InSAR observations made using two sets of scenes each spanning 70 days, but that are separated by only 28 minutes, show that significant variability exists even over timescales where we would not expect to see surface deformation due to the

extraction/injection of subsurface fluids, suggesting that atmospheric models must be generated at time intervals that are dense at the timescale of atmospheric phenomena.

Fay and Bennett focused on determining and modeling the vertical GPS velocity field, within a swath extending from south of the Sierra Nevada northeast to the Walker Lane Belt in Nevada. They are particularly interested in the constraints that are placed on buoyancy, rheology and lithospheric stress state. They constrain vertical velocity of 11 sites relative to the average of 5 sites in the Yucca Mountain region, and find rates of ± 0.5 mm/year with 0.2-0.3 mm/yr precision. They explore several viscoelastic structures and model relaxation due to the 1872 Owens Valley and 1952 Kern County earthquakes, finding that lateral viscosity variations or a more complete catalog of earthquakes may be needed to explain the observations.

d. Data collection

Efforts to collect new data or to improve existing catalogs are related to better estimates of interseismic motion, preparations for the next big earthquake and detection and interpretation of transient strain events. SCEC continued support of the strainmeters at Pinon Flat observatory (PFO), which consists of three laser strainmeters and two long-base tiltmeters. This year, the PI's reported on comparisons between PFO strainmeters and other instruments in Southern California, including those at Durmid Hill and the EarthScope instrumentation (Figure 17). Comparisons between a Plate Boundary Observatory borehole strainmeter installed at PFO with the laser strainmeters show that the latter are more stable at periods longer than a week or two. Data accessibility has been improved significantly through the archiving of all data at the NCEDC, with older data available on request. Standard upgrades and maintenance were performed, including the reconstruction of the long-base tiltmeters, which were damaged by lightning.

McGill, Bennett and Spinler resurveyed 18 (including 3 new) sites in the San Bernardino Mountains – a key region near the junction of several major faults that is poorly-constrained by continuous geodetic sites, and important for understanding deformation in this tectonically complex area. All data are being archived through the SCEC data center by Duncan Agnew. The work was primarily completed by undergraduate students and SCEC interns. They also explored modeling of data from SCEC Crustal Motion Map 3 with slip rates for the San Bernardino and San Geronio pass sections of the San Andreas. New observations from their survey are plotted, but not included in the analysis pending assessment of reference frame issues.

Lipovsky, Funning & Miller attempted to resurvey 35 sites in the San Jacinto/Anza region, of which 21 were successfully resurveyed. Previous surveys of these sites range from 1990 to 2009. Rinex files from all the surveys are freely available on their website.

Sandwell and graduate student Brendan Crowell performed rapid static GPS surveys of the region south of the Salton Sea. The surveys included at least three occupations of ~50 densely spaced monuments associated with the Imperial fault and Brawley seismic zone, and the establishment of new, easily located, monument types along irrigation culverts in two locations. All data is being archived at SOPAC. The real-time accuracy had the side benefit of facilitating the identification of some monuments, which were often buried in regions that were resurfaced frequently by farming equipment or road crews.

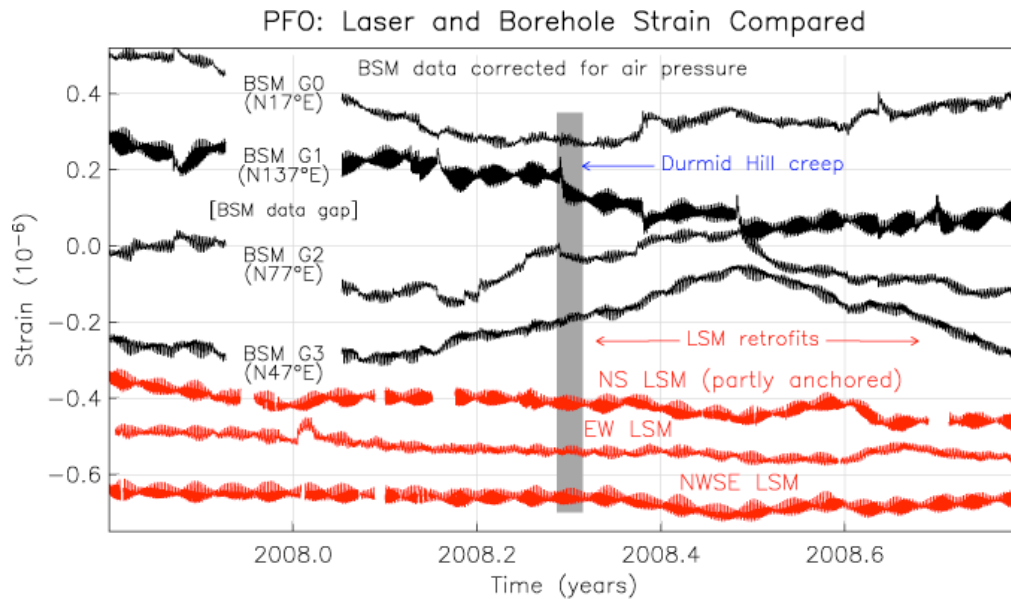


Figure 17. Comparison of most recent PBO borehole strainmeter data (black) and laser strainmeter data (red), both located at Pinon Flat. No signal is observed during the time period where localized aseismic deformation was observed at Durmid Hill.

e. References

- Fay, N. P., R. A. Bennett, and S. Hreinsdóttir, Contemporary vertical velocity of the central Basin and Range and uplift of the southern Sierra Nevada, *Geophys. Res. Lett.*, **35**, 2008.
- Houlié, N., G. J. Funning and R. Bürgmann, Application of a GPS-derived troposphere model to an InSAR study of San Gabriel Valley deformation, *Geophys. J. Int.*, submitted, 2008.
- Meade, B. J., and B. H. Hager, Block models of crustal motion in southern California constrained by GPS measurements, *J. Geophys. Res.*, **110**, B03403, doi:10.1029/2004JB003209, 2005.
- Meade, B. J., and J. P. Loveless, Block modeling with multiple fault network geometries and a linear elastic coupling estimator in spherical coordinates, *Geophys. J. Int.*, submitted.
- Wei, M., D. Sandwell and Y. Fialko, A Silent M4.8 slip event of October 3-6, 2006, on the Superstition Hills fault, Southern California, *J. Geophys. Res.*, (in press).

3. Earthquake Geology

The SCEC geology disciplinary group coordinates diverse field-based investigations of the Southern California natural laboratory. The majority of Geology research accomplishments in SCEC3 fall under two categories, (1) focused studies of the southern San Andreas and San Jacinto faults in coordination with the SoSAFE (Southern San Andreas Fault Evaluation) special project, and (2) studies of other portions of the southern California fault network toward better understanding fault system behavior. Geology also continues efforts to characterize outstanding seismic hazards to the urban region, and supports field observations related to various focus-group activities. In support to these efforts the Geology group coordinates geochronology infrastructure resources that are shared among various SCEC-sponsored projects.

a. Southern San Andreas Fault Evaluation (SoSAFE)

By focusing the efforts of the geology community, the SoSAFE special project has blossomed into the centerpiece of SCEC3 geology research. The primary objective of the SoSAFE is to develop a comprehensive 2000-yr event history for the main plate boundary structures (San Andreas and San Jacinto faults). As a result of this project several critical data gaps have been filled and exciting new developments have unfolded.

The foremost SoSAFE research target was to develop a paleoseismic site in the northern Big Bend of the San Andreas fault. Information here is desperately needed for correlation of event records from the Carrizo Plain to the central Transverse Ranges [Biasi and Weldon, 2009]. Land-access, drought conditions, and special project funding all aligned to enable new, deeper investigations at the Frasier Park site to begin filling this critical data gap [Scharer et al., 2007]. Work at this site is now externally supported by the NSF tectonics program. The other paleoseismic focus of the SoSAFE project has been in the Coachella Valley – the only portion of the San Andreas fault that has not ruptured historically [Philisobian et al., 2007] and is presumably overdue. The northern San Jacinto fault remains a target of interest for paleoseismology because of the potential trade-off of activity with the nearby San Andreas fault [Bennett et al., 2004; McGill et al., 2008; Le et al., 2008]. SoSAFE-supported efforts to locate a suitable site for investigation are ongoing [Onderdonk, 2008].

The other objective of the SoSAFE special project is to gather new slip-rate and slip-per event data. A highlight is the exciting result from Zielke and Arrowsmith [2008] that numerous, subtle 5m offsets are present along the Carrizo Plain section of the San Andreas fault. These offsets are about half the ~10 m slip attributed to the 1857 Fort Tejon earthquake by Sieh [1978]. This new result agrees well with new paleoseismic recurrence from the Bidart fan paleoseismic site [Akciz et al., 2009]. The net impact of these findings is that great earthquakes on the southern San Andreas fault are about twice as frequent as previously thought. Slip-rate studies within the Big Bend and south have focused on longer time-scales that integrate earthquake behavior. One of these sites, near Palmdale, promises to resolve a long-standing debate on the rate of slip (25 vs. 35 mm/yr) of the San Andreas through the Transverse Ranges (Sgriccia and Weldon, research in progress). Several studies address the long-term slip-rates and trade-off inactivity between the southernmost San Andreas fault and the San Jacinto fault. These include an intensive study of slip-rate and epistemic uncertainty of rate calculations from the Biskra Palms site on the San Andreas [Behr et al., 2008; Fletcher et al., 2007], thorough documentation of slip-rates showing a gradient in activity on the San Bernardino segment San Andreas north of San Geronio Pass [McGill et al., 2008], and a multi-site investigation of slip rates and their potential temporal variation on the southern San Jacinto fault [Le et al., 2008; Janecke, 2008]. Much of this slip-rate work is ongoing, but the preliminary results so far suggest that slip on the southernmost San Andreas system involves complex spatial and temporal trade-offs in activity. Results from SoSAFE funding are detailed in the “special projects” section of the annual report.

b. Fault System Behavior

The second major emphasis of the Geology group has been to characterize patterns in fault system behavior that could significantly affect earthquake hazards. This effort specifically addresses earthquake clustering and its potential relationship to temporal variation in fault loading rates. The eastern California shear zone and the conjugate Garlock fault offer the most compelling examples of clustered earthquake behavior and its potential relation to anomalously elevated fault loading [Peltzer et al., 2001; Dawson et al., 2003; Oskin and Iriondo, 2004; Dolan et al., 2007; Oskin et al., 2008; McGill et al., 2009]. As a test of the clustering hypothesis SCEC3 sponsored a paleoseismic study of one of the dextral faults of the shear zone: the Calico fault. Because this fault slips at a rate

~2x its neighbors [Oskin et al., 2007, 2008], it was expected that its earthquake record would show clusters of events during periods of regional earthquake activity documented by Rockwell et al. [2000]. This expectation was confirmed by Ganev et al. (in preparation) who found a cluster of two earthquakes ~5-6 ka (Figure 18), during the penultimate regional cluster documented by Rockwell et al. [2000].

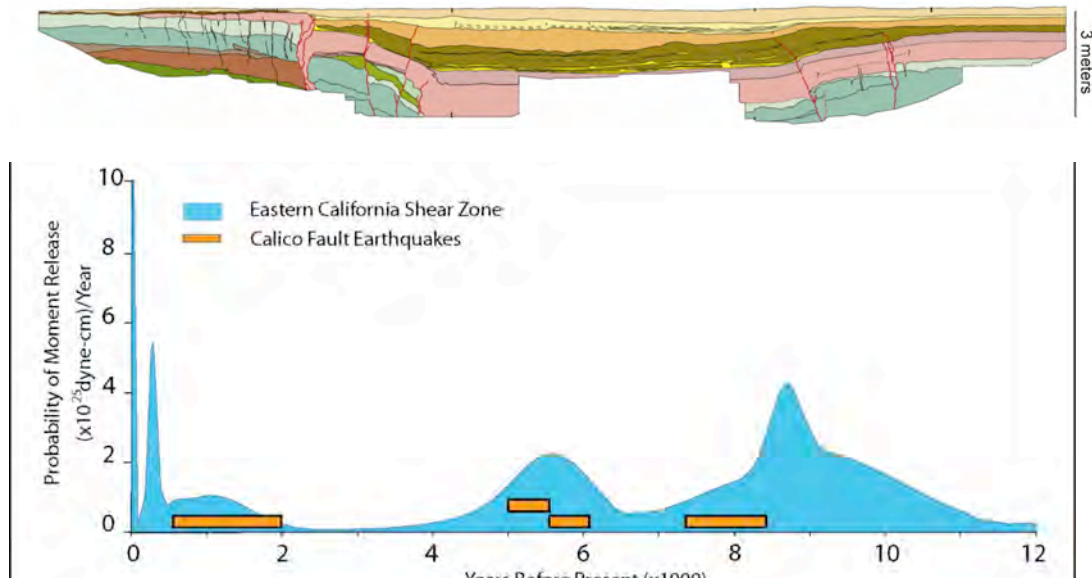


Figure 18. (A) Log of exposure of the Calico fault near Newberry Springs, California. Thickening of units and cross-cutting relationships indicate four event horizons in this exposure. (B) Plot of event ages from the Calico fault against aggregate event probability for the Eastern California Shear Zone from Rockwell et al. [2000]. Calico fault earthquakes fall within regional cluster time periods. Two events are found to lie within the penultimate cluster at 5-6 ka, consistent with the hypothesis that multi-event clusters on the Calico fault contribute to its faster longer-term slip rate than other shear-zone faults. Data from Plamen Ganev, James Dolan, and Mike Oskin.

The multi-site slip-rate study of the San Jacinto fault by Le et al. [in review; 2008] tackles the problem of what processes may drive variations in fault slip-rate over time. By exploiting the multi-stranded nature of the southern San Jacinto fault, she shows that slip-rates may have coherently varied across this system. Because these strands are separated by >5 km throughout the seismogenic zone, their coherent behavior is likely driven by changes in strain rate on a shared ductile shear zone at depth. Work is currently underway to confirm the ages of offset features from multiple techniques in order to rule out systematic errors. Another approach to study of fault system behavior is to examine the repeatability of earthquake ruptures at a site. The Imperial fault is a rare well-documented example that ruptured twice in historic time. In their SCEC3 study, Meltzner and Rockwell [2008] showed that these historic events were anomalously low slip. Their detailed 3-D paleoseismic investigations indicate that larger earthquake slips are more common on the Imperial fault. The significant (factor of ~2) variability in slip per event at this site undermines the characteristic earthquake/slip patch model that is often assumed in the course of seismic hazard estimation.

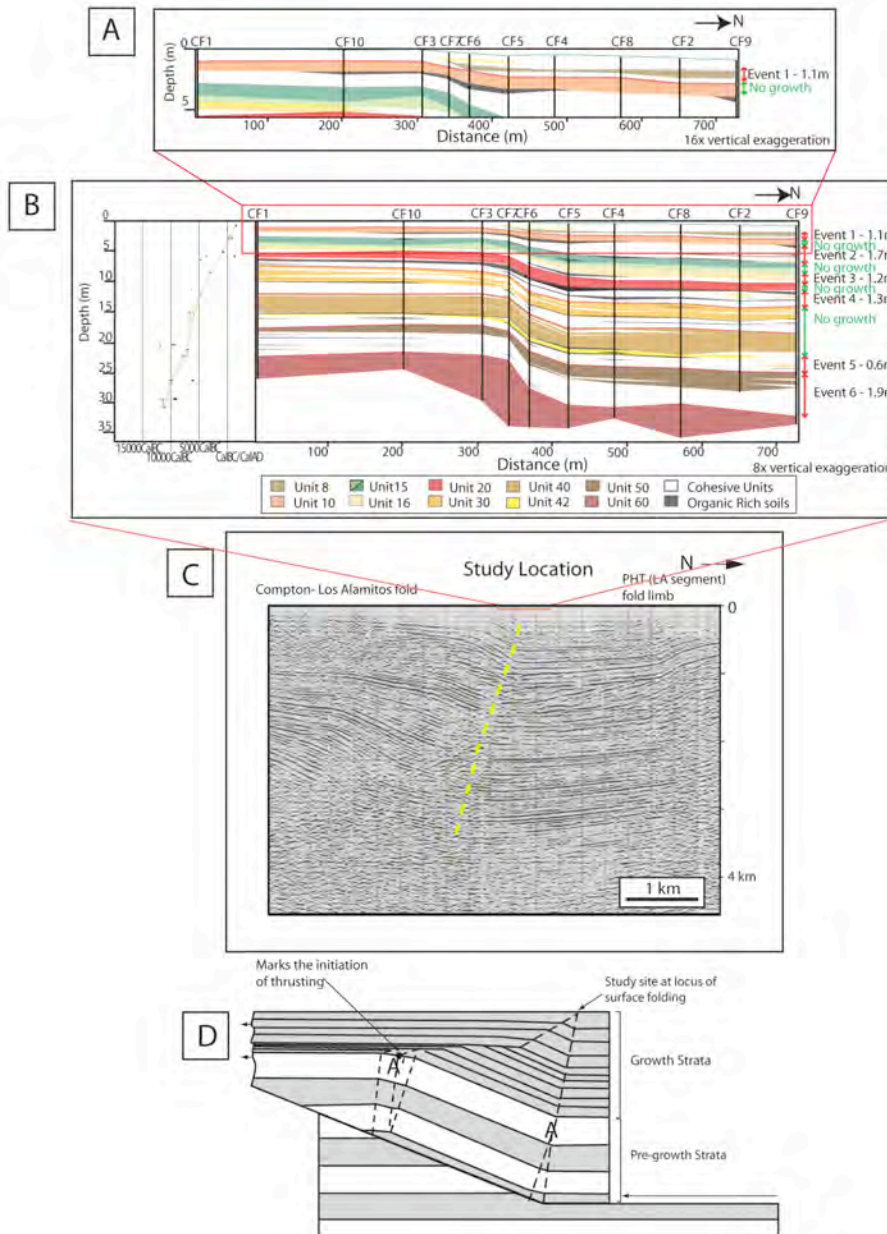


Figure 19. (A) Borehole results from the Stanford Avenue transect. Cross section of major stratigraphic units (16x vertical exaggeration) showing details of the most recent uplift event (Event 1). Vertical lines are boreholes. Green horizontal line is the ground surface. (B) Cross section of major stratigraphic units (8x vertical exaggeration). Colors denote sedimentary units. Thin red lines mark tops of major sand and gravel units. Double-headed red arrows along the side of the figure show stratigraphic range of sedimentary thickening across the transect, with uplift in each event shown in red to the right of each arrow. Double-headed green arrows show intervals of no sedimentary growth. Red box indicates location of cross-section in A. (C) Seismic reflection data across the Los Angeles central trough showing folding associated with Compton Thrust and Puente Hills Thrust. (D) Kinematic model for folding of the hanging wall of the Compton Thrust as it is buried by basin deposits. Data from Lorraine Leon and James Dolan.

c. Blind Thrust Faults

Though Geology's emphasis has shifted away from hazard estimation to process-based studies, SCEC3 continues to sponsor research of major blind-thrust earthquake sources in the urban region. Documentation of activity of blind thrust systems beneath central Los Angeles continues with borehole studies of the Compton thrust, once declared inactive [Mueller, 1997]. More recent data collection clearly shows evidence of activity from thickening of strata across fold hingelines [Dooling et al., 2008]. Work is also in progress to recover a high-precision record of coseismic folding and earthquake timing from a trench investigation of folding above the Puente Hills thrust (Figure 19). Another SCEC3 study targets the Ventura anticline, one of the fastest-moving shortening structures in California. Here work is in progress by T. Rockwell to date emergent beach terraces that record at least four several-meter-high coseismic uplift events in the late Holocene. The magnitude of coseismic uplift on both the central Los Angeles and Ventura folds both suggest that large ($M \sim 7$) blind-thrust earthquakes are likely.

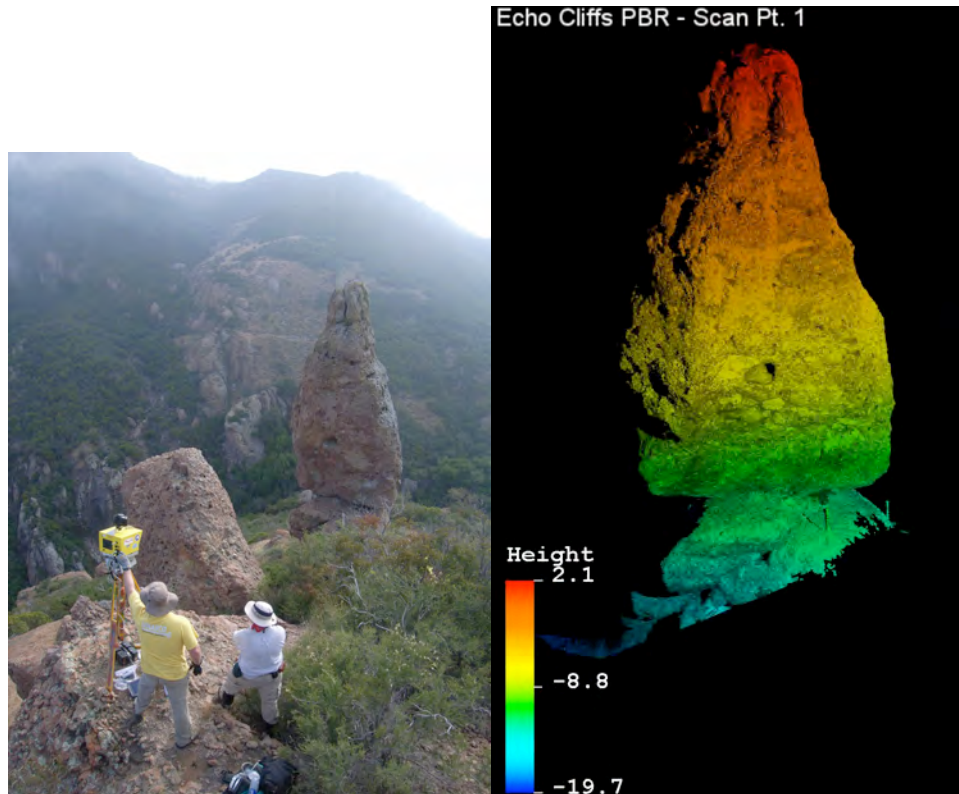


Figure 20. (A) Photograph of precariously balanced rock (PBR) 'Echo Cliffs' and survey team using ground-based LIDAR to image rock geometry (David Haddad, Arizona State University and David Phillips, UNAVCO). (B) LIDAR scan produced in part A, color coded by height above the base of the PBR. This data will be used to more precisely quantify the stability of the PBR during earthquake shaking. Photo and LIDAR image from Ken Hudnut.

d. Shared Geochronology Infrastructure

The shared geochronology infrastructure program represents an important innovation that has greatly enhanced the quality of SCEC3 Geology results. In short, more dates lead to better

constraints on earthquake time series and slip rates. By pooling resources under established partnerships (expanded under SCEC3), SCEC efficiently allocates resources and exposes the research community to new techniques/collaborations. SCEC Geology was able to quickly re-allocate geochronology among the various San Andreas trenching studies as needs arose. The collaborations developed under the geochronology program also led to new innovations, such as developing applications of surface-exposure dating to precarious rocks (Figure 20) that are important for constraining extreme ground motions [Rood et al., 2008] and an intensive effort to date the Lake Cahuilla shorelines [Verdugo and Rockwell, 2008] to develop a system-level record of earthquake activity from the high slip-rate faults that traverse the Salton Trough.

e. References

- Akciz, S. O., L. Grant Ludwig, and J. R. Arrowsmith, Revised dates of large earthquakes along the Carrizo section of the San Andreas Fault, California, since A.D. 1310 \pm 30, *J. Geophys. Res.*, **114**, B01313, doi:10.1029/2007JB005285, 2009.
- Behr W., Rood, D., Fletcher, K., Guzman, N., Finkel, R., Hanks, T., Hudnut, K., Kendrick, K., Platt, J., Sharp, W., Weldon, R., Yule, D., Uncertainties in slip rate estimates for the Mission Creek strand of the southern San Andreas fault at Biskra Palms Oasis, 2008 SCEC annual meeting proceedings, 2008.
- Bennett, R. A., Friedrich, Anke, M., Furlong, Kevin P, Codependent histories of the San Andreas and San Jacinto fault zones from inversion of fault displacement rates: *Geology*, **32**, p. 961-964, 2004.
- Biasi, G., and Weldon, R., San Andreas Fault rupture scenarios from multiple paleoseismic records; stringing pearls, *Bull. Seismol. Soc. Am.*, **99**(2A):471-498, 2009.
- Dawson, T., McGill, S.F., and Rockwell, T.K., Irregular recurrence of paleoearthquakes along the central Garlock fault near El Paso Peaks, California, *J. Geophys. Res.*, **108**, p. DOI: 10.1029/2001JB001744, 2003.
- Dolan, J.F., Bowman, D.D., and Sammis, C.G., Long-range and long-term fault interactions in southern California: *Geology*, **35**, p. 855–858, 2007.
- Dooling, P., Leon, L., Dolan, J., Shaw, J., Pratt, T., and Martinez, A.. New Late Pleistocene and Holocene slip rates on the southern segment of the Compton blind thrust fault, Lakewood, California, 2008 SCEC Annual Meeting Proceedings, 2008.
- Fletcher, K., Sharp, W., Kendrick, K., Behr, W., and Hudnut, K., U-series ages for the Biskra Palms alluvial fan and their implications for long-term slip-rate of the Coachella Valley segment of the San Andreas fault, southern California: Geological Society of America 2007 Annual Meeting, 2007.
- Janecke, S., High geologic slip rates since early Pleistocene initiation of the San Jacinto and San Felipe fault zones in the San Andreas fault system, southern California, USA., 2008 SCEC Annual Meeting Proceedings, 2008.
- Le, K., Oskin, M., Rockwell, T., and Owen, L., Spatial and temporal slip-rate variability on the San Jacinto fault, 2008 SCEC Annual Meeting Proceedings, 2008.
- McGill, S., Weldon, R., and Owen, L., Preliminary slip rates along the San Bernardino strand of the San Andreas fault, 2008 SCEC Annual Meeting Proceedings, 2008.
- McGill, S., Wells, S., Fortner, S., Kuzma, H., and McGill, J., Slip rate of the western Garlock fault, at Clark Wash, near Lone Tree Canyon, Mojave Desert, California, *Geol. Soc. Am. Bull.*, **121**, p. 536-554, 2009.
- Meltzner, A., and Rockwell, T., Late Holocene slip on the Imperial fault, Mesquite basin, Imperial Valley, California, 2008 SCEC Annual Meeting Proceedings, 2008.
- Mueller, K., Recency of folding along the Compton-Los Alamitos trend: Implications for seismic risk in the Los Angeles basin, *EOS Transactions of the American Geophysical Union*, **78**, p. F702, 1997.
- Onderdonk, N., Determining fault offsets and slip rates on the Claremont strand of the San Jacinto fault zone, 2008 SCEC Annual Meeting Proceedings, 2008.
- Oskin, M., and Iriondo, A., Large-magnitude transient strain accumulation on the Blackwater fault, Eastern California Shear Zone, *Geology*, **32**, p. 313-316, 2004.

- Oskin, M.E., Perg, L.A., Blumentritt, D., Mukhopadhyay, S., and Iriondo, A., Slip rate of the Calico fault: Implications for geologic versus geodetic discrepancy in the Eastern California shear zone, *J. Geophys. Res.*, **112**, p. doi:10.1029/2006JB004451, 2007.
- Oskin, M., Perg, L., Shelef, E., Strane, M., Gurney, E., Singer, B., and Zhang, X., Elevated shear-zone loading rate during an earthquake cluster in eastern California, *Geology*, **36**, no. 6, p. 507-510, 2008.
- Peltzer, G., Crampé, F., Hensley, S., and Rosen, P., Transient strain accumulation and fault interaction in the Eastern California Shear Zone, *Geology*, **29**, p. 975-978, 2001.
- Philibosian, B., T. Fumal, R. Weldon, K. Kendrick, K. Scharer, S. Bemis, R. Burgette, and B. Wisely, Paleoseismology of the San Andreas fault at Coachella, California, 2007 SCEC Annual Meeting Proceedings, 2007.
- Rockwell, T.K., Lindvall, S., Herzberg, M., Murbach, D., Dawson, T., and Berger, G., Paleoseismology of the Johnson Valley, Kickapoo, and Homestead Valley faults: Clustering of earthquakes in the Eastern California Shear Zone, *Bull. Seismol. Soc. Am.*, **90**, 1200-1236, doi: 10.1785/0119990023, 2000.
- Rood, D. H., J. Brune, K. Kendrick, M. D. Purvance, R. Anooshehpour, L. Grant-Ludwig and G. Balco, How Do We Date a PBR?: Testing Geomorphic Models Using Surface Exposure Dating and Numerical Methods, 2008 SCEC Annual Meeting Proceedings, 2008.
- Scharer, K., Weldon, R., Dawson, T., Sickler, R., Sheridan, H., McGinnis, K., Gerard, T., Weldon, C., and Hunt, S., Evidence for 4-5 earthquakes at the Frazier Mountain paleoseismic site since A.D. 1400, 2007 SCEC annual meeting proceedings, 2007.
- Sieh, Kerry, Slip along the San Andreas Fault associated with the great 1857 earthquake, *Bull. Seismol. Soc. Am.*, **68**, No. 4, 1421-1448, 1978.
- Verdugo, D., and Rockwell. T., A new late Holocene lacustrine chronology for ancient lake Cahuilla, Salton Sea, Imperial County, CA: Towards basin-wide correlation of earthquake chronologies, 2008 SCEC Annual Meeting Proceedings, 2008.
- Zielke, O., and Arrowsmith, R., Slip along the San Andreas fault associated with the great 1857 earthquake between Cholame and Pine Mountain from "B4" LIDAR high resolution topographic data, 2008 SCEC Annual Meeting Proceedings, 2008.

B. Focus Group Activities

Within the new SCEC structure, the focus groups are responsible for coordinating interdisciplinary activities in six major areas of research: *unified structural representation, fault and rupture mechanic, crustal deformation modeling, lithospheric architecture and dynamics, earthquake forecasting and predictability, ground motion prediction, and seismic hazard and risk analysis*. The following reports summarize the year's activities in each of these areas.

1. Unified Structural Representation

The Unified Structural Representation (USR) Focus Area develops digital models of crust and upper mantle structure in southern California for use in a wide range of SCEC science, including strong ground motion prediction, earthquake hazards assessment, and fault systems analysis. These efforts include the development of Community Velocity Models (CVM & CVM-H) and Community Fault Models (CFM & CFM-R), which together comprise the USR. The Focus Area also supports the evaluation and improvement of these models. For the CVM/CVM-H, this often involves the comparisons of recorded seismograms with synthetic waveforms generated by numerical ground motions simulations.

This past year's efforts have been focused on:

1. Improving the Community Velocity Model (CVM-H v. 5.7), by development of independent Vp and Vs models, and the inclusion of updated regional basin models,

tomographic models, teleseismic surface wave models, and a bedrock geotechnical layer;

2. Evaluating the CVM and CVM-H models by comparisons of the recorded seismograms with synthetics, including those for the 2008 Mw5.4 Chino Hills earthquake;
3. The development of new, 3D adjoint tomographic models based on CVM-H that offer significant improvements to the crustal wave speed structure;
4. Developing a statewide Community Fault Model, through partnerships with the U.S. and California Geological Surveys, and improving fault representations in the CFM using new relocated earthquake catalogs.

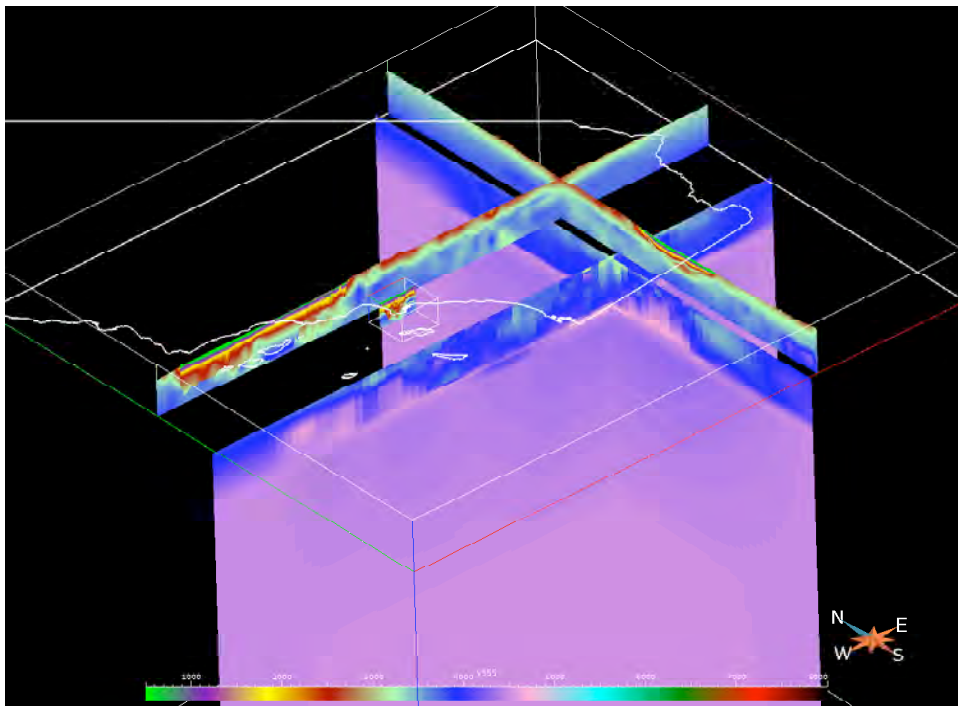


Figure 21. Perspective view of CVM-H 5.5, which includes basin structures embedded in a tomographic model that extends to 35 km depth, which is underlain by a teleseismic surface wave model that extends to a depth of 300km. Vs is shown.

a. Community Velocity Models (CVM, CVM-H)

This past year's efforts involved a series of improvements to the community velocity model (CVM-H) [Plesch et al., 2008; Süß and Shaw, 2003], to better facilitate its use in strong ground motion prediction and seismic hazards assessments. The community velocity models consist of basin descriptions, including structural representations of basin shapes and sediment velocity parameterizations, embedded in regional tomographic models. Enhancements to the community velocity model were implemented in new model versions (CVM-H 5.5, 5.7) released at the 2008 annual meeting and in January 2009, respectively (Figure 21). Model improvements included:

1. New V_p , V_s , and density parameterizations within the Santa Maria basin and Salton Trough;

2. Incorporation of updated Vp and Vs tomographic models (Hauksson, 2000) that extend to a depth of 35 km. These new models were developed by Egill Hauksson at Caltech using the sedimentary basin structures included in the current CVM-H;
3. Addition of a new upper mantle teleseismic and surface wave model that extends to a depth of 300 km. This new model was developed by Toshiro Tanimoto at UCSB using Hauksson's tomographic model as a starting point;
4. Implementation of a new bedrock geotechnical layer (GTL) based on the depth-velocity relations of *Boore and Joyner* [1997]. In this implementation, we used the empirical velocity gradient to scale upwards from the base of the GTL (top of basement), resulting in gradual vertical velocity gradients and lateral variations in velocities at the surface.

In addition, we made a series of enhancements to the structure of the CVM-H and the code that delivers the model. Most significantly, the CVM-H now consists of separate Vp and Vs models, whereas previous model versions consisted of only Vp with Vs and density specified by fixed relations with Vp. We chose to develop separate Vp and Vs models to more faithfully represent data that independently constrain these properties and the nature of the upper mantle models. In addition, we updated the C-code that delivers the CVM-H. These code enhancements were designed to enhance the precision of the model output, and facilitate better the construction of computational meshes and grids used for numerical wave propagation simulations.

b. Evaluating the Community Velocity Models (CVM, CVM-H)

Efforts within SCEC have been initiated to develop an algorithm to systematically examine the goodness-of-fit (GOF) between two sets of broadband ground motion time series (Mayhew and Olsen, 2009). The method includes a set of user-weighted metrics such as peak ground motions, response spectrum, the Fourier spectrum, cross correlation, energy release measures, and inelastic elastic displacement ratios. The GOF algorithm was initially used to evaluate the accuracy of the CVM-H and CVM-S, using synthetics and observed data for the 2008, Mw 5.4 Chino Hills, CA, earthquake. The two CVMs generate similar (and high) levels of goodness-of-fit for this event (see Figure 22). However, at selected sites, one of the CVMs tends to generate a slightly better fit to data than the other; i.e., CVM-S is better at STS and KIK, and CVM-H is better at CHN and LFP. Such comparisons, which have engineering significance, will be improved upon using additional stations, events and bandwidths in the future.

It is also interesting to note that the two CVMs generate some of the best fit to data in a banded area circling the epicenter counter-clockwise from the southeast to the northwest. This result is important, as this area of good fit includes the critical wave-guide corridor (San Bernardino-Chino-San Gabriel basin, CVM-S slightly better than CVM-H), where simulations of large northwestward earthquake rupture scenarios of the southern San Andreas fault (M7.7 TeraShake; M7.8 ShakeOut) produced unexpectedly large ground motions. The favorable long-period fits for Chino Hills include the Whittier Narrows area (e.g., station RUS), where the largest wave-guide amplification was found in the TeraShake and ShakeOut scenarios, as well as the Los Angeles basin. Other areas, such as the southern Los Angeles area (Orange County - Irvine) produce less favorable long-period GOF values and may suggest that improvement of the crustal structure in the SCEC CVM-S (V4.0) is needed here.

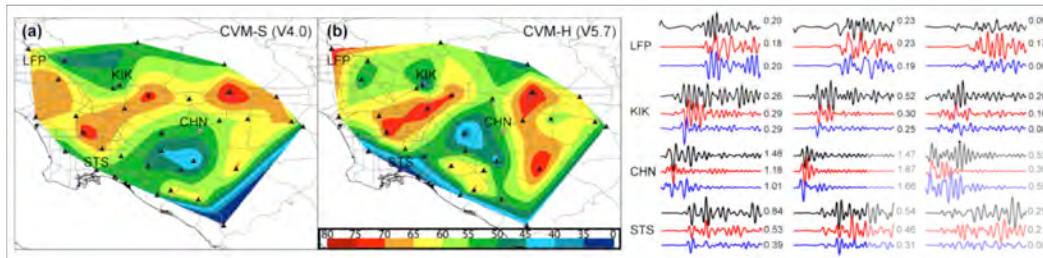


Figure 22. Maps of goodness-of-fit (perfect fit=100) at 0.1-0.5 Hz for synthetics relative to data from the 2008 Mw 5.4 Chino Hills, CA, earthquake. Simulations use (a) CVM-S4.0 and (b) CVM-H5.7. Seismogram comparisons show the E, N, and Z components of the recorded data (black traces), CVM-S synthetics (red traces), and CVM-H synthetics (blue traces) for selected stations, normalized by peak ground velocities (number labels, cm/s).

Additional comparisons of CVM-H and CVM-S were carried out by Robert Graves (unpublished reports, June 2009). As compared to CVM-S, a simulation of long-period (<0.5 Hz) ground motion for the ShakeOut V1.1.0 scenario (Figure 23) in CVM-H generated long-period ground motions (a) generally stronger in the near-field (b) significantly weaker in the LA basin, particularly along the Whittier-Narrows channel, (c) stronger in the Fillmore/Santa Clarita area, (d) stronger in the NW model area, and (e) stronger in the offshore area west of San Diego and Ventura/Santa Barbara. Another difference in ground motion patterns for the two models is a very strong and localized 'bright spot' at the intersection of the Garlock and San Andreas faults (PGV>800 cm/s). These differences in ground motions are clearly related to differences in the two CVMs. Future works should analyze the causes of these differences, and use observational data (e.g., as demonstrated in Figure 22) to estimate the accuracy of the two CVMs in the areas generating large differences in scenario ground motions.

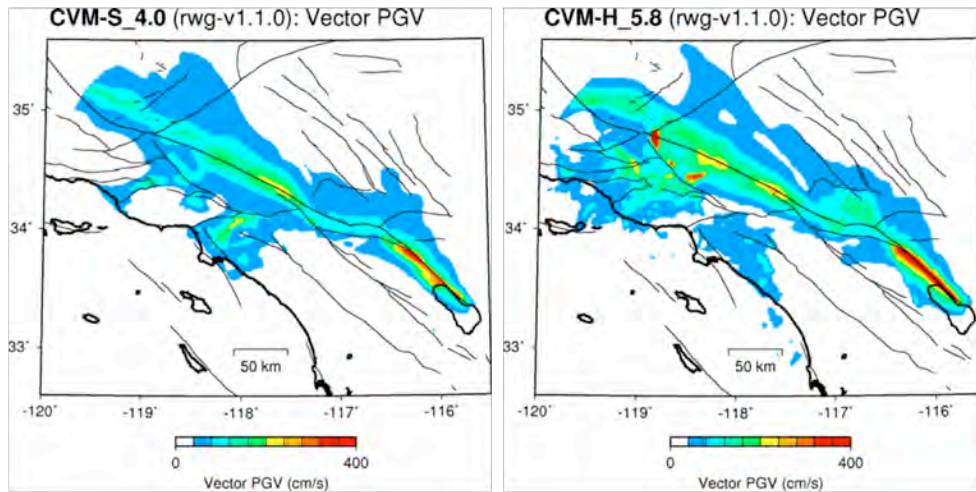


Figure 23. Maps of PGVs for a simulation of the ShakeOut V1.1.0 scenario in (left) CVM-S and (right) CVM-H.

c. Developing the Next Generation CVM

The USR Focus Area also supports the development and implementation of promising new approaches for improving 3D structural representations in future iterations of the community models. Previous efforts have focused on the development of new 3D waveform tomography models of southern California using scattering integral [Chen et al., 2007] and adjoint tomographic [Tromp et al., 2006] methods. Chen et al. [2007] employed this approach to develop the first fully 3D waveform inversion model of the Los Angeles basin, using the SCEC CVM 3.0 [Magistrale et al., 2001] as a starting model. This past year, efforts have focused on developing a 3D waveform tomographic model of southern California using adjoint methods and spectral element (SEM) wave propagation simulations [Tape et al., 2009] (Figure 24).

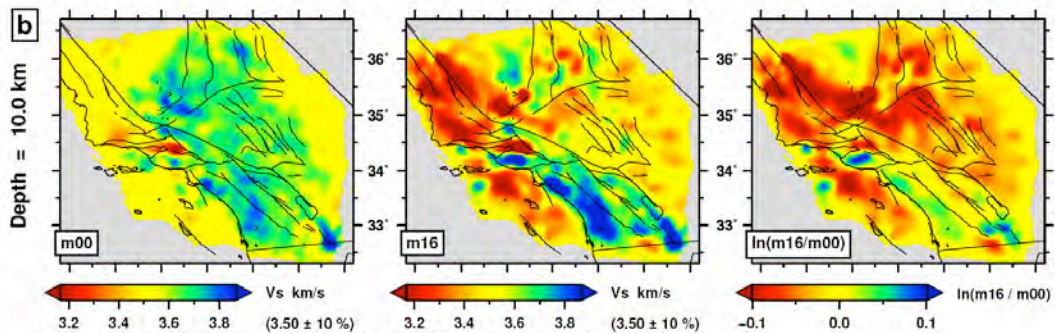


Figure 24. Horizontal sections of Vs adjoint tomographic model: Left, starting model (CVM-H); Center, adjoint model after 16 iterations; Right, model differences (after Tape et al., 2008; 2009).

The new model used an early version of the CVM-H as a starting point, and involved 16 iterations seeking to minimize the differences between simulated and recorded seismograms. This process involved 6800 wavefield simulations and nearly 1 million CPU hours, and yielded a revised crustal model with strong lateral velocity heterogeneity that illuminates a number of major tectonic features. The new model incorporates local changes in wave speeds of up to 30% relative to the background travel-time tomography models in the CVM-H, and clearly highlights key basin structures that were not represented in the original model, such as the San Joaquin basin. The primary goal for the USR Focus Area in 2009 will be to implement this revised velocity parameterization directly into a new version of the CVM-H. This will involve embedding the latest basin structures in the new adjoint tomography model, which will overlie the Moho surface and the underlying teleseismic/surface wave model. Subsequent testing of the model will establish the improvements it offers in simulating strong ground motions for southern California earthquakes.

d. Community Fault Model (CFM)

In partnership with the U.S. and California Geological Surveys, the USR Focus Area has continued efforts to develop a statewide fault model, consisting of the CFM in southern California [Plesch et al., 2007] and new representations of faults in northern California. This process included a SCEC-sponsored workshop in 2008, to review a preliminary statewide model and plan a course for its improvements. Following careful review of each of the preliminary fault representations, the working group agreed that geologic models of the greater San Francisco Bay area, developed largely by the U.S.G.S. (Menlo Park), should serve as the basis for representation in that area of

northern California in a statewide CFM (e.g., Brocher et al. [2005]). Moreover, priorities were established for making improvements to fault representations in other areas of the state. These updates are currently being implemented by the working group with the goal of releasing an initial statewide CFM at the 2009 annual meeting. Ultimately, this new model will help improve our assessment of seismic hazards in California, and contribute directly to fault systems modeling activities within SCEC. In a related effort, the CFM in southern California is being systematically re-evaluated using new re-located earthquake catalogs developed by SCEC [Hauksson and Shearer, 2005; Shearer et al., 2005]. These new catalogs provide significantly improved resolution of many faults, and are being used to refine interpolated fault patches for many of the representations in the CFM [Nicholson et al., 2008]. These updates will also be incorporated in a new release of the CFM.

e. References

- Brocher, T.M., R.C. Jachens, R. W. Graymer, C. W. Wentworth, B. Aagaard, and R. W. Simpson, A new community 3D seismic velocity model for the San Francisco bay Area: USGS Bay Area Velocity Model 05.00, SCEC Annual Meeting, Proceedings and Abstracts, Volume XV, p. 110, 2005.
- Chen, P., L. Zhao, Li, T. H. Jordan, Full 3D tomography for the crustal structure of the Los Angeles region, *Bull. Seismol. Soc. Am.*, **97**, no.4, 1094-1120, 2007.
- Hauksson, E. and P. Shearer, Southern California Hypocenter Relocation with Waveform Cross-Correlation: Part 1: Results Using the Double-Difference Method, *Bull. Seismol. Soc. Am.*, **95**, 896-903, 2005.
- Magistrale, H., S. Day, R. W. Clayton, and R. Graves, The SCEC Southern California Reference Three-Dimensional Seismic Velocity Model Version 2: *Bull. Seismol. Soc. Am.*, **90**, no. 6B, p. S65-S76, 2001.
- Mayhew, J.E., and K.B. Olsen, Goodness-of-fit criteria for broadband synthetic seismograms, with application to the 2008 Mw5.4 Chino Hills, CA, earthquake, to be submitted to *Bull. Seis. Soc. Am.*, 2009.
- Nicholson, C., E. Hauksson, A. Plesch, G. Lin, and P. Shearer, Resolving 3D fault geometry at depth along active strike-slip faults: simple or complex?, 2008 SCEC Annual Meeting, Palm Springs, CA, 2008.
- Plesch, A., John H. Shaw, Christine Benson, William A. Bryant, Sara Carena, Michele Cooke, James Dolan, Gary Fuis, Eldon Gath, Lisa Grant, Egill Hauksson, Thomas Jordan, Marc Kamerling, Mark Legg, Scott Lindvall, Harold Magistrale, Craig Nicholson, Nathan Niemi, Michael Oskin, Sue Perry, George Planansky, Thomas Rockwell, Peter Shearer, Christopher Sorlien, M. Peter Süss, John Suppe, Jerry Treiman, and Robert Yeats, Community Fault Model (CFM) for Southern California, *Bull. Seismol. Soc. Am.*, **97**, no. 6, 2007.
- Shearer, P., E. Hauksson, and G. Lin, Southern California hypocenter relocation with waveform cross correlation: Part 2. Results using source-specific station terms and cluster analysis, *Bull. Seismol. Soc. Am.*, **95**, 904-915, doi: 10.1785/0120040168, 2005.
- Süss, M. P., and J. H. Shaw, P-wave seismic velocity structure derived from sonic logs and industry reflection data in the Los Angeles basin, California, *J. Geophys. Res.*, **108**/B3, 2003.
- Tape, C., Q. Liu, A. Maggi, and J. Tromp, Strong southern California crustal heterogeneity revealed by adjoint tomography, 2008 SCEC Annual Meeting, Palm Springs, CA, 2008.
- Tape, C., Q. Liu, A. Maggi, and J. Tromp, Adjoint tomography of southern California, *Science*, (in press), 2009.

2. Fault and Rupture Mechanics

The primary mission of the Fault and Rupture Mechanics focus group is to develop physics-based models of the nucleation, propagation, and arrest of dynamic earthquake rupture. We specifically target research that addresses this mission through field, laboratory, and modeling efforts directed at characterizing and understanding the influence of material properties, geometric irregularities, and heterogeneities in stress and strain over multiple length and time scales, and that contributes to our understanding of earthquakes in the Southern California fault system.

FARM studies aim to:

- Determine the properties of fault cores and damage zones and their variability with depth and along strike, including the width and particle composition of actively shearing zones, extent, origin and significance, of on- and off-fault damage, and poroelastic properties.
- Determine the relative contribution of on- and off-fault damage to the total earthquake energy budget, and the absolute levels of local and average stress.
- Investigate the relative importance of different dynamic weakening and fault healing mechanisms, and the slip and/or time scales over which these mechanisms operate.
- Characterize the probability and possible signatures of preferred earthquake rupture direction.
- Develop realistic descriptions of heterogeneity in fault geometry, properties, stresses, and strains, and tractable ways to incorporate heterogeneity in numerical models.
- Understand the influence of small-scale processes on larger-scale fault dynamics.
- Evaluate the relative importance of fault structure, material properties, and prior seismic and aseismic slip to earthquake dynamics, in particular, to rupture initiation, propagation, and arrest, and the resulting ground motions.

FARM encompasses a broad range of basic research aimed at illuminating physical processes of faulting and earthquake rupture mechanics. In 2008-09 research accomplishments included new findings by investigators working on earthquake and faulting problems in field, laboratory and computational settings. Over the past year important progress was made by FARM scientists on a number of fronts, much of this took place through a series of workshops. These workshops are a showcase of our collaborative efforts.

a. Dynamic Fault Parameters

On March 11, 2008, the SCEC-sponsored "Workshop on Dynamic Fault Parameters: What Do We Know, and Where Do We Go?" was held in Pomona, California. The workshop was lead-convened by David Oglesby. 43 people participated. Now that there are extensive computational capabilities for numerically simulating dynamic rupture, the theme of this workshop was how to decide which parameters are appropriate to use in the simulations, so as to best predict earthquake rupture physics and ground motions. Results from the March workshop included a compilation of what is known and guidance about what needs to be done next. Among the consensus views, is that confining pressure is approximately lithostatic to hydrostatic, and that the San Andreas fault likely corresponds to a "strong crust, weak fault" model. For friction, it appears that many mechanisms may lead to slow sliding at high slip rates, and that thermal effects may be particularly important. The bulk of slip appears to occur predominantly in the middle of the seismogenic zone; however, it was emphasize that kinematic seismic inversions determine the velocity of an apparent rupture front that is radiating seismic energy, but this does not necessarily correspond to the rupture velocity in spontaneous rupture models; The resolution of kinematic inversions may be event and data specific; Off-fault damage is an energy sink and it reduces rupture velocity.

An important outcome of the March workshop was a compiled list of future needs. From the observational perspective these included good near-source data, in situ temporally-strategic observations at depth across active faults, and a better understanding of shallow crustal rheology. From the modeling perspective, these included a recommendation that fault friction simulations explore mechanisms other than slip-weakening, including standard rate/state behavior at slow slip speeds and additional weakening mechanisms at fast slip speeds, such as those that involve thermal and chemical effects. The final recommendation, as with the other SCEC workshops this year, was that this is just a beginning and that the conversation should continue.

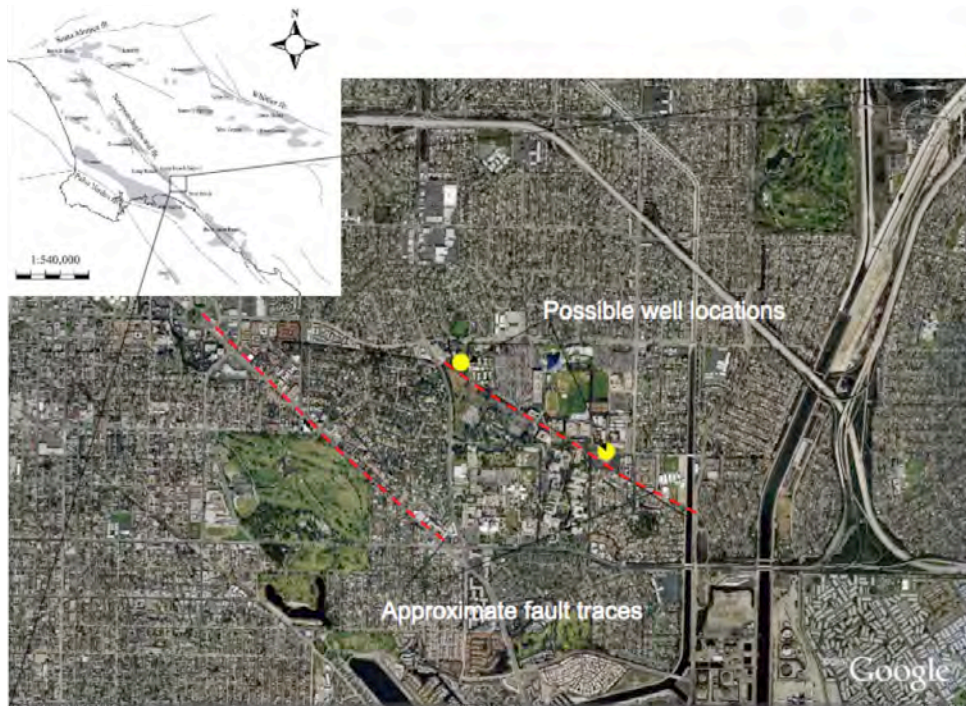


Figure 25. Possible locations of a well for drilling deep into the Newport Inglewood fault. Dashed lines are approximate locations of the Newport-Inglewood fault zone.

b. Newport-Inglewood Fault Zone Drilling

On May 9, 2008 more than 19 scientists participated in a SCEC workshop co-convened with California State University Long Beach and Signal Hill Petroleum. The topic was the Newport-Inglewood Fault Zone Corehole Project. The Newport-Inglewood fault zone produced the damaging 1933 Long Beach earthquake, and it currently cuts through one of the most densely populated areas in southern California, including major societal infrastructure. Critical questions remain about the structure of this fault zone, especially at depth, where most of the seismic energy is released in earthquakes.

The workshop, led on the SCEC front by Ralph Archuleta, presented information about an opportunity (Figure 25) to examine the Newport-Inglewood fault zone fault at depth, especially near the northern end of the 1933 rupture. Signal Hill Petroleum (SHP) is planning a 3D seismic survey, with analysis to be completed in a year. SHP then plans to drill a 3 km hole that would penetrate the fault zone at one or two depths, and collect intact core of the fault zone and its

surrounding environment. In addition, there is an opportunity to collect ground motion data by instrumenting the drill hole after the drilling and coring are completed. This will allow for studies of how amplification occurs as seismic waves emerge from bedrock into softer sediments. The SCEC coordinator for this project is Ralph Archuleta.

c. Structure and Formation of Fault Zones

From June 11-12, 2008, approximately 35 scientists participated in the SCEC sponsored workshop 'The Structure and Formation of Fault Zones and their Role in Earthquake Mechanics'. Charlie Sammis was the lead organizer. Invited presenters covered topics including field, laboratory, and computational simulations of fault zones. Themes involved off-fault damage, fault geometry, and the evolution of fault zones. Particular emphases in the discussion sessions included whether or not fault zones record information about recent earthquakes, including size, rupture velocity and direction, and, if fault zone structure affects the dynamics of individual earthquake ruptures.

d. 3D Dynamic Rupture Modeling

The November 17, 2008 '2008 SCEC 3D Rupture Dynamic Code Workshop' led by Ruth Harris included approximately 34 participants, and was convened by SCEC on the Cal Poly Pomona campus. The theme of this meeting had close ties with the SCEC/USGS/DOE Extreme Ground Motions project, and one goal of the ExGM-related part of the project has been to test that other codes can reproduce results presented by Andrews, Hanks, and Whitney [2007] for elastic simulations of dynamic rupture and ground motions at Yucca Mountain. For the first time in the code-comparison exercise, the benchmark assignments tested 2D, in addition to the usual 3D simulations, and this was the first time that the benchmarks moved from vertical strike-slip faulting to simulated rupture on dipping faults (Figure 26). At this meeting the participants also viewed comparisons of results for rate-state friction benchmarks on a vertical strike-slip fault in a wholespace and in a halfspace (to date most rate-state modelers work with vertical rather than dipping faults).

During part of the dynamic rupture code meeting the participants learned about new results from spontaneous rupture simulations that include off-fault yielding, and participated in related discussions about whether or not critical benchmarks in the future, especially those related to Yucca Mountain, should include off-fault non-elastic yielding. Information about the benchmarks and participants in the SCEC code comparison exercise can be found at the SCEC Code website <http://scecddata.usc.edu/cvws/>. General information about this SCEC collaboration can also be found Harris *et al.* [2009].

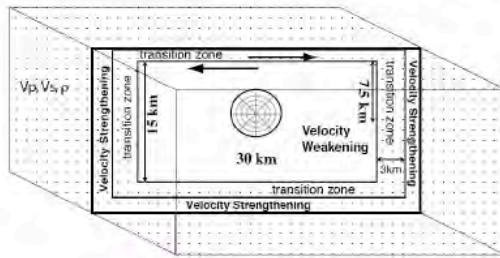
The October-November 2008 benchmarks

Slip-weakening

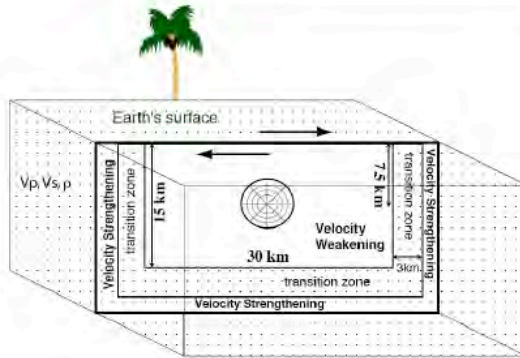


TPV10 and 11
Normal faulting on a dipping fault set in a half-space

Rate-State Friction using a slip law with strong rate-weakening



TPV103
Strike-slip faulting on a vertical fault set in a whole-space



TPV104
Strike-slip faulting on a vertical fault set in a half-space

Figure 21. The benchmarks discussed at the November workshop involved slip-weakening on a dipping fault and rate-state friction on a vertical strike-slip fault.

e. Rapid Response Drilling

From November 17-19, 2008, 44 scientists participated in a three-day SCEC co-sponsored workshop on 'Rapid Response Drilling, Past, Present, and Future', in Tokyo, Japan. Other co-sponsors included the International Continental Scientific Drilling Program, UC Santa Cruz, and the University of Kyoto. The talks presented examples of previous work on drilling after large earthquakes, and general information about fault zone drilling in general. Discussion during the

meeting presented tradeoffs between rapid drilling and the option of satisfying a diverse range of scientific goals.

Among the topics of discussion were collecting temperature measurements to assess the friction during a large earthquake, obtaining direct stress measurements to assess the magnitudes of stresses on faults, and procuring observations about fault healing mechanisms (Figure 27). A major challenge presented for all of these proposals is that previous drilling studies have found it difficult to find the most recent or most active slip surface. It was recommended that this challenge be confronted with a multi-disciplinary approach involving real-time gas monitoring, core analysis and borehole logs, and continuous coring with high recovery near the suspected slip zones. The SCEC coordinator for this project is Emily Brodsky.

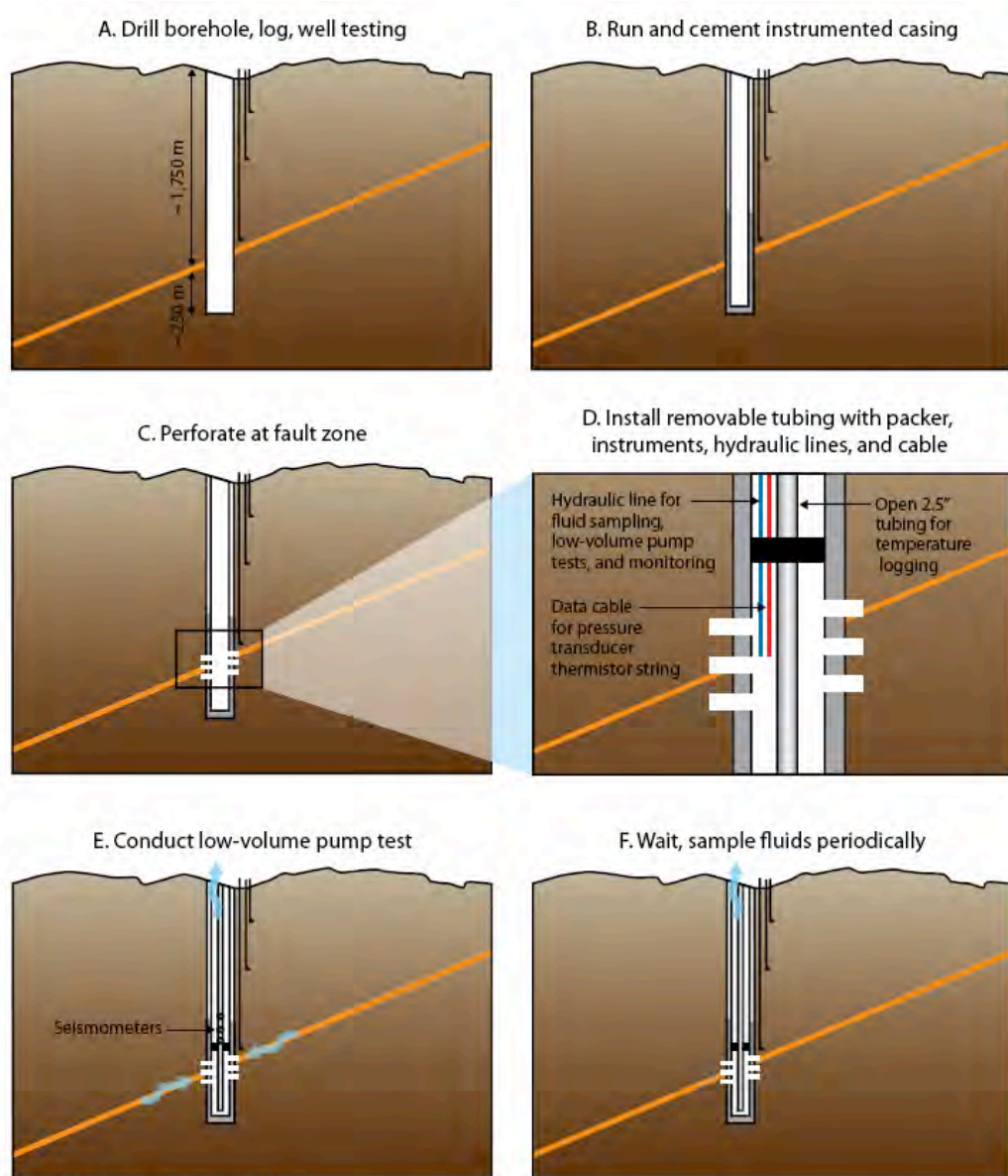


Figure 27. Schematic of a rapid drilling plan.

f. Effects of Rheology/Complex Fault Geometry

In addition to the 2008 workshops, much was learned by SCEC PT's about the effects of fault geometry and rheology on dynamic rupture, ground motions, and sequences of earthquakes. These were mainly elastic studies, but it was also recognized that off-fault behavior that is not elastic likely occurs, for example Dmowska and colleagues numerically showed the effects on ground motions of fault branching, in conjunction with off-fault yielding (Figure 28). Observations and measurements by Dor and colleagues (Figure 29) examined particle contents for off-fault materials, and a number of other FARMers observed, simulated and inferred the interactions between dynamic rupture on a fault and the medium surrounding the fault, providing a more comprehensive picture of fault zone behavior than has occurred in previous years.

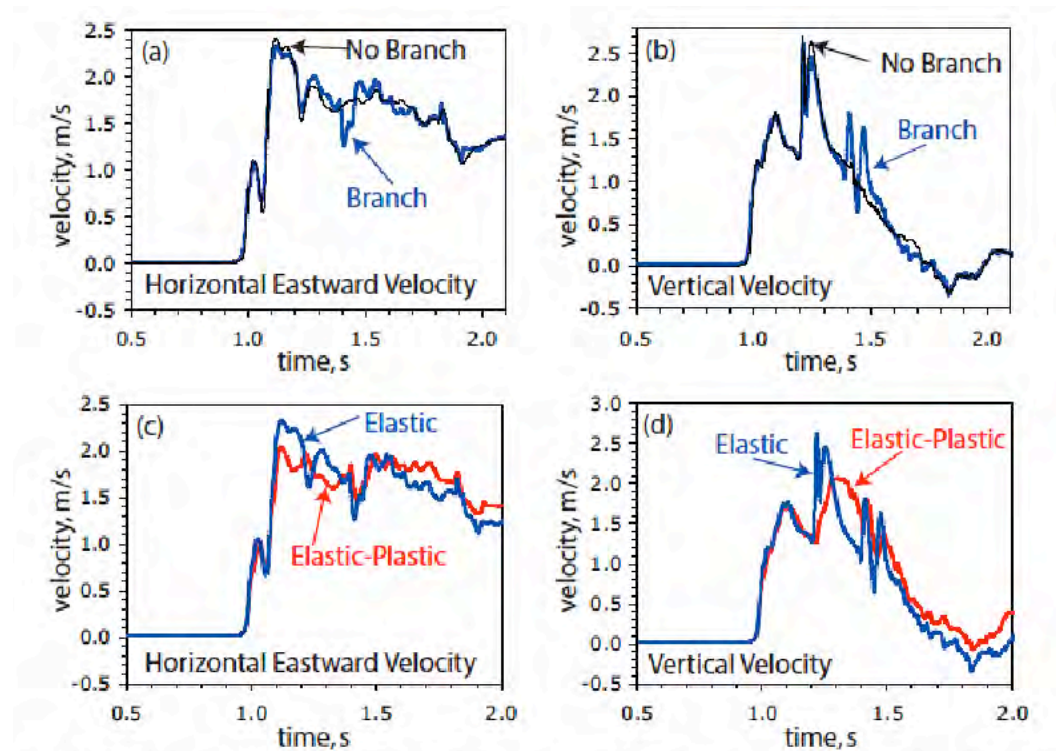


Figure 28. Effects of branch activation (a-b) and elastic-plastic off-fault material response (c-d) on vertical and horizontal ground velocities at the proposed repository site (1 km east of Solitario Canyon Fault, 200 m below the free surface) during supershear rupture of the SCF. Fault geometries that do and do not have a branch in the fault geometry of a dipping normal fault produce different ground motions. There is also a difference in the ground motions if off-fault yielding is included (red curves).

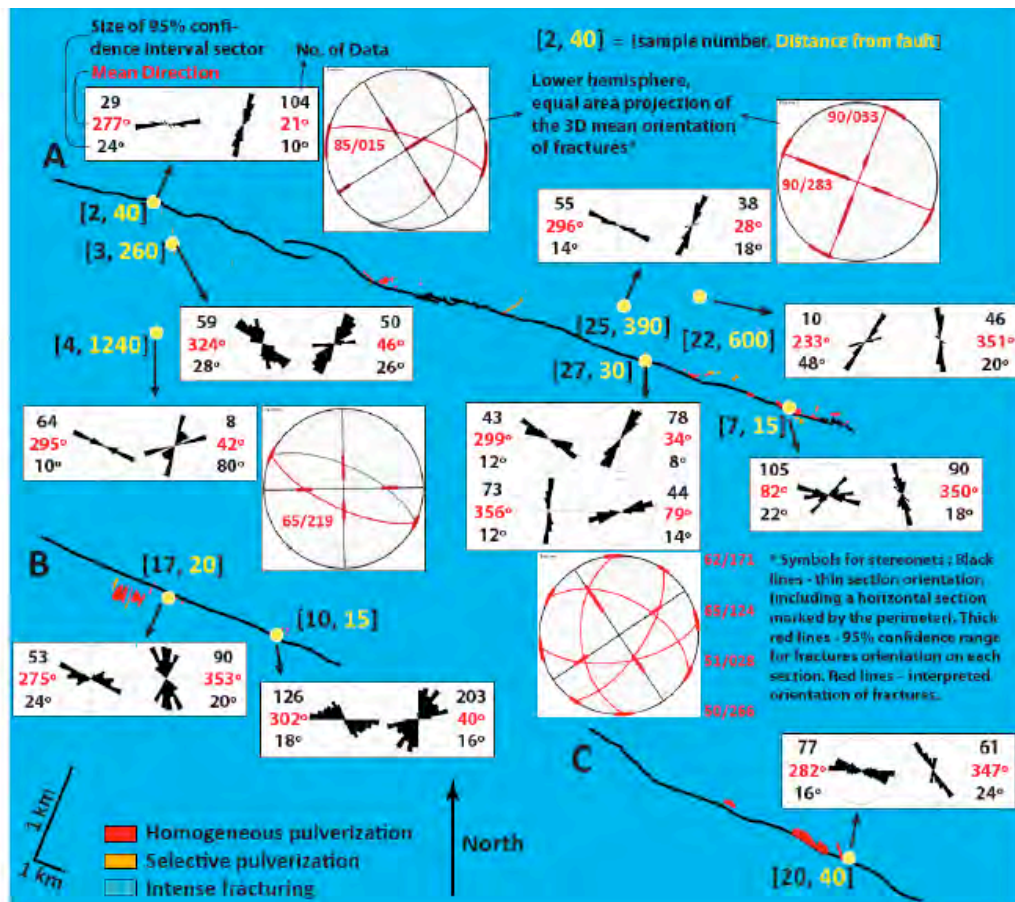


Figure 29. Analysis of data from pulverized rock samples collected along 3 different sections (A,B,C) of the San Andreas fault.

g. References

- Andrews, D. J., T. C. Hanks, and J. W. Whitney, Bull. Seismol. Soc. Am., 97, 1771-1792; DOI: 10.1785/0120070014, 2007.
- Harris, R., M. Barall, R. Archuleta, E. Dunham, B. Aagaard, J. P. Ampuero, H. Bhat, V. Cruz-Atienza, L. Dalguer, P. Dawson, S. Day, B. Duan, G. Ely, Y. Kaneko, Y. Kase, N. Lapusta, Y. Liu, S. Ma, D. Oglesby, K. Olsen, A. Pitarka, S. Song, E. Templeton, The SCEC/USGS Dynamic Earthquake-Rupture Code Verification Exercise, *Seismol. Res. Lett.*, 80, 2009.

3. Crustal Deformation Modeling

The SCEC Crustal Deformation Modeling (CDM) group conducts research on deformation associated with fault systems over time scales ranging from minutes to thousands of years, using mathematical models. The ultimate goal of our research is to understand spatial and temporal variations of stresses and stressing rates in the southern California crust, so this information can be incorporated into physics-based probabilistic seismic hazard assessment.

In the 2007 RFP, we emphasized numerical deformation models based on SCEC USR data products (the community seismic velocity model CVM-H; and the community fault models, CFM and/or CFM-R). We also sought studies assessing the level of detail required to adequately model stress

evolution in the southern California crust, given available constraints. Progress on CFM-based models is accelerating, and we have begun to identify processes that may safely be excluded from system-wide stress transfer models.

a. Incorporating the SCEC CFM and CVM-H into Fault System Models

This past year, Charles Williams developed a model of southern California lithosphere incorporating 55 faults from the SCEC CFM and elastic properties computed from seismic velocity and density data in the SCEC CVM-H. This model incorporates viscoelastic earthquake cycles for all 55 faults, and is “spun up” to a state wherein modeled velocities have become insensitive to the initial stress conditions. Spinning up the model requires modeling many earthquake cycles for the fault with the longest recurrence interval (tens of thousands of years). Preliminary results illustrate the extensive influence of viscoelastic mantle and lower crust relaxation on the surface velocity field. Models with Newtonian or Kelvin-Voigt viscoelastic mantle and lower crust yield results that differ dramatically from each other and from elastic models. Suites of models are being run with plausible viscoelastic rheologies to assess which are consistent with the GPS velocity field: given slip rates, recurrence intervals, and penultimate event timing for the most important (high slip rate) faults. Currently, these fault parameters are based on UCERF 2. Implementation of power-law rheology and afterslip (not funded by SCEC) and new southern California models incorporating these rheologies are planned.

Kaj Johnson is doing something similar, using a combined boundary element + semi-analytical approach he has used to model active fault systems in several parts of the world. His preliminary models are based on the SCEC CFM, and incorporate both afterslip (at constant stress) and viscoelastic relaxation. He models various viscosity structures, including one based on his models of postseismic deformation in the Mojave region, thus taking the first step toward requiring a single lithosphere model to explain deformation over a variety of time scales. Like Williams’ models, Johnson’s models show that viscoelastic mantle relaxation contributes a significant, long-wavelength term to the interseismic GPS velocity field (Figure 30). This perturbation is sufficient to complicate efforts to invert GPS velocities for slip and locking rate with elastic models. However, it may be essentially stationary, except shortly after a large earthquake. Johnson has also inverted for interseismic creep rates (and level of uncertainty for these estimates) along the San Andreas Fault, taking into account simultaneous surface velocity contributions due to slip on all modeled southern California faults.

As Johnson and Williams continue to focus on a suite of realistic rheologies and lithosphere structures, we will soon have our answer to the question, do we really have to spin up all of our southern California stress transfer models to calculate stress accumulation on active faults over the next few decades? If a wide range of reasonable models gives somewhat stationary velocity contributions from viscoelastic relaxation of the mantle, for example, we may be able to just correct the GPS velocity field and carry on with elastic stress transfer modeling (e.g. Smith-Konter and Sandwell [2009]) for first-order solutions. For models incorporating stress-driven fault creep, viscoelastic relaxation, and other processes to address stress evolution between earthquakes, it may be sufficient to apply a traction-free boundary condition at the mantle asthenosphere. This could reduce computation time and increase the number of models we can run, leading to better estimates of poorly known fault parameters and stress transfer.

Brendan Meade (Harvard) has continued his work refining and improving kinematic block models of southern California. For the first time, his models of the region incorporate fault geometries from the SCEC CFM-R, and for the Puente Hills thrust fault, the CFM. Much of his work in 2008-09 has involved coming up with a reliable method to get the CFM into a format suitable for block modeling; this was a large enough task

to merit a publication [Meade and Loveless, submitted, 2009]. The results of his modeling study (including slip rates for all CFM faults) will be described in a paper to be submitted this summer (2009).

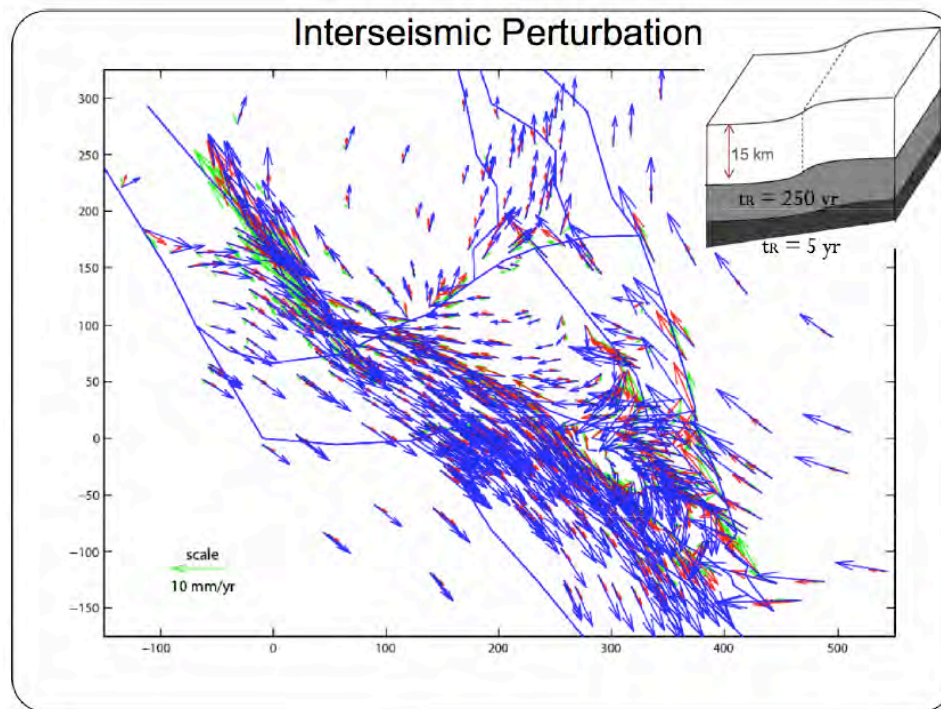


Figure 30. Interseismic velocity field perturbation relative to an elastic model, midway through an 1857-SAF earthquake cycle, due to viscoelastic relaxation (from Kaj Johnson). Indicated Maxwell times yield the velocity field perturbation shown with blue arrows. This model suggests significant viscoelastic contributions to the velocity field from relaxation of the mantle.

b. Models of Smaller, Geometrically Complex Regions

Brad Hager (MIT), his senior PhD student Jiangning Lu, Charles Williams, and Carl Gable (Los Alamos), have developed detailed elastic finite element meshes of the Ventura Basin region. Two sets of models, incorporating the CFM and CFM-R faults in this region, were developed, and heterogeneous elastic properties were assigned based on seismic velocities and densities from the CVM-H. The elastic models show that the CFM-R is not adequate for representing faults in this region, suggesting that the CFM (with its triangulated surfaces) should be used in models of areas with closely-spaced, geometrically complex faults. Hager's group also quantified the dramatic effect of elastic heterogeneity on deformation in the Ventura Basin. Modeled displacements differ from those predicted by a uniform elastic model by 30 to 100%.

Michele Cooke (U. Mass.) continues to investigate the kinematics of the San Geronio Pass and the LA Basin, using 3D elastic boundary element models. These models incorporate SCEC CFM fault geometries, constrained principally with uplift and fault slip rates. One goal of the San Geronio

Pass work has been to actually refine SCEC CFM fault geometries at depth in this area, as well as estimating slip and stress accumulation rates [Dair and Cooke, 2009].

c. Other Crustal Deformation Modeling

Noah Fay (Arizona) and Thorsten Becker (USC) are using ABAQUS develop visco-plastic, dynamic FE models of the southern California lithosphere. Their models address fault loading and crustal stressing over the long term, without EQ cycles. They are not based on the SCEC CFM as they assume a simplified fault geometry and use plastic elements, rather than surfaces, to represent faults. Traction from mantle convection models, buoyancy forces from estimates of gravitational potential energy variations, and velocity boundary conditions drive the deformation, and fault strength is varied to fit fault slip rates and GPS surface velocities. Figure 31 shows how variations in fault strength control patterns of surface velocities and crustal stresses. This modeling is distinct from most other CDM group efforts because it offers estimates of absolute stresses in the upper crust. Aside from the effort of Hearn and Fialko [2009], which addresses only the shallowest crust in a small region, this is unique.

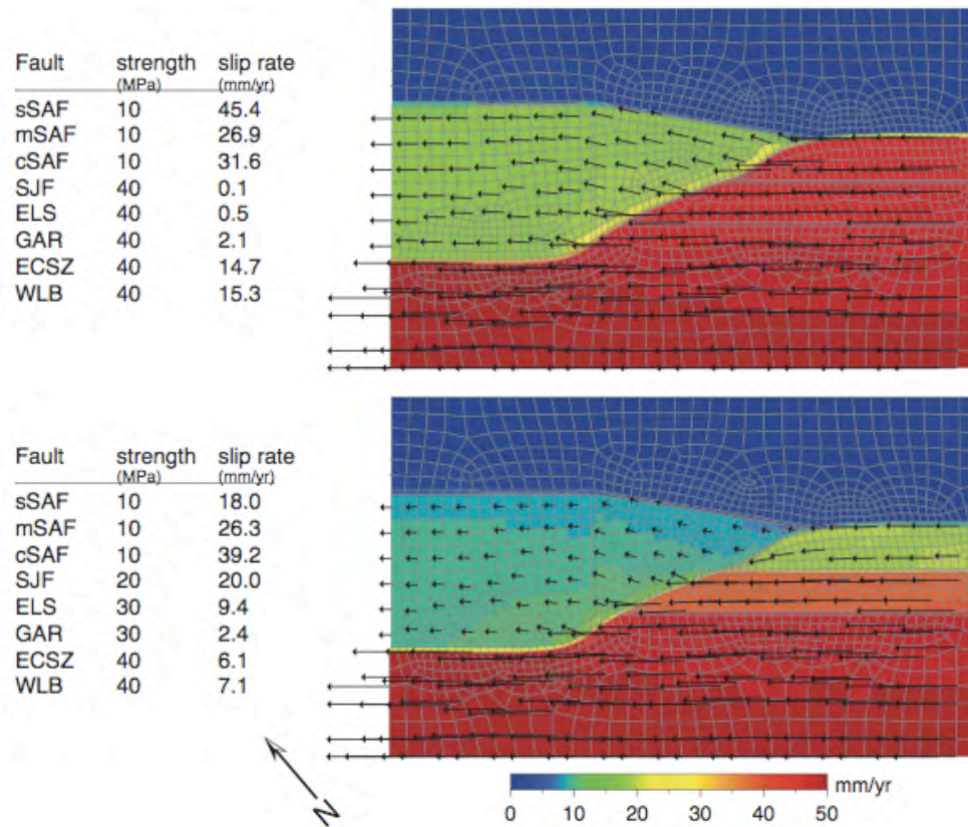


Figure 31. Results from Noah Fay and Thorsten Becker’s lithosphere deformation models, showing how fault strength affects time-averaged surface velocities and slip rates. These models are not based on the SCEC CFM and do not explicitly include earthquakes, but they may provide valuable insights on the absolute strength of faults.

Another newly updated modeling study based on a simplified (non-CFM) representation of faults by Bridget Smith-Konter (U. Texas El Paso) addresses stress accumulation over a long history of

paleoseismically-constrained SAFZ earthquakes [Smith-Konter and Sandwell, 2009]. Estimates of stress accumulation over past few thousand years are provided, as well as analyses of model sensitivity to uncertainties in fault slip rates and other parameters. Figure 32 shows how these stress accumulation rates, which are estimated with purely elastic models, differ from an estimate based on a model incorporating viscoelastic relaxation [Freed, 2007]. SCEC-supported viscoelastic earthquake cycle modeling (described above), together with improved surface velocity constraints near the SAF should address the extent to which viscoelastic relaxation of the lower crust and upper mantle affect stress accumulation estimates. Smith-Konter also points out that uncertainties in the length extent of large earthquakes (such as the 1857 SAF earthquake) could map to very large uncertainties in integrated stress accumulation along other SAF segments (because of differences in coseismic stress transfer).

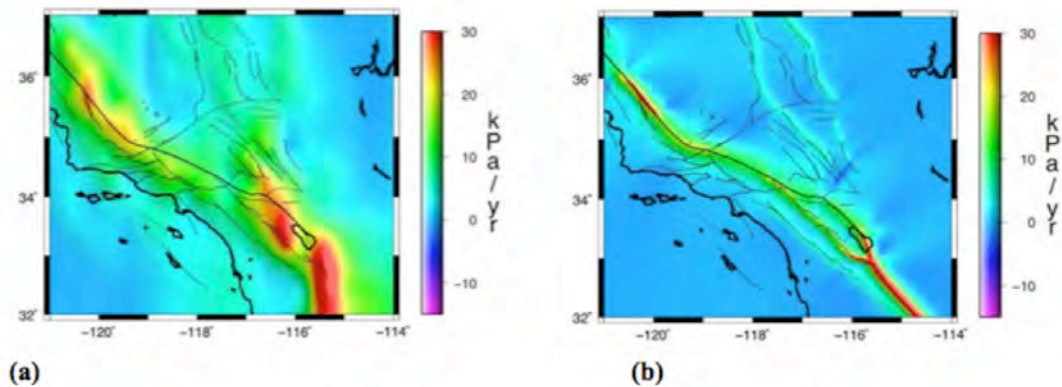


Figure 32. Stress accumulation rates for models with (left) and without (right) viscoelastic mantle relaxation (from Freed, 2007 and Bridget Smith-Konter, respectively; figure supplied by Bridget Smith-Konter). The model with viscoelastic relaxation at depth introduces a longer wavelength component to the stressing rate patterns. Better resolution of the GPS velocity field near faults, and more earthquake cycle modeling (with realistic rheologies and heterogeneities that are consistent with observed postseismic deformation) may help resolve which representation of stressing rates is closer to the truth.

d. Fault System and Damage Evolution

Modeling by Elizabeth Hearn's PhD student Yaron Finzi (UBC), in coordination with Yehuda Ben-Zion (USC), addresses whether damage evolution could significantly influence static stress transfer among southern California faults. Away from faults, modeled damage levels are low (except in the top few tens of meters): damage rapidly localizes to narrow zones, which appear to simplify geometrically as time progresses. Modeled fault damage zones are narrow at depth (in agreement with seismic and geologic observations) and may be treated as frictional surfaces. At depths of less than about 5 km and at extensional stepovers and bends, a highly softened damaged zone with essentially unchanging elastic properties is also present, and may locally affect stress transfer [Hearn and Fialko, 2009] and perhaps rupture propagation. These zones, also imaged with seismic methods, InSAR (e.g. Cochran et al., [2009]) and LIDAR [Wechsler et al., 2009], are up to 2 km wide at the surface along fault segments, and may be even wider at stepovers. These permanently softened zones achieve essentially steady dimensions and damage levels early in Finzi's simulations, and evolution of damage levels (and hence elastic properties) over earthquake-cycle

time scales is minor. This work suggests that implementation of a brittle damage rheology in the upper crust is not needed for modeling static stress transfer among southern California faults.

e. NMCDEF Workshop

The CDM group continues to partner with the NSF and the Computational Infrastructure for Geodynamics (CIG) to sponsor the annual Numerical Modeling of Crustal Deformation and Faulting (NMCDEF) workshop at the Colorado School of Mines in Golden, Colorado. This well-attended workshop (now capped at 60 participants) includes tutorial sessions for meshing and finite-element modeling codes, as well as opportunities to provide feedback on CIG code development and participate in online benchmarking exercises. Presentations on topics such as experimental and theoretical constraints on lithosphere and fault zone rheologies have become more frequent in recent years. This meeting provides valuable hands-on training for graduate students and postdoctoral fellows, as well as a unique opportunity to solve modeling difficulties by brainstorming with like-minded researchers.

f. References

- Cochran, E. S., Y.-G. Li, P. M. Shearer, S. Barbot, Y. Fialko, and J. E. Vidale Seismic and geodetic evidence for extensive, long-lived fault damage zones, *Geology*, 37, 315-318, 2009.
- Dair, L., and Cooke, M.L., San Andreas fault geometry through the San Geronio Pass, California, *Geology*, 37, 119-122, doi: 10.1130/G25101A.1, 2009.
- Finzi, Y., E. H. Hearn, Y. Ben-Zion and V. Lyakhovsky, Structural properties and deformation patterns of evolving strike-slip faults: numerical simulations incorporating damage rheology, *Pure Appl. Geophys.*, 166, DOI: 10.1007/s00024-009-0522-1, 2009.
- Freed, A. M., S. T. Ali, and R. Bürgmann (2007), *Geophys. J. Inter.*, 169, 1164-1179.
- Hearn, E. H., and Y. Fialko, Can compliant fault zones be used to measure absolute stresses in the upper crust?, *J. Geophys. Res.*, 114, B04403, doi:10.1029/2008JB005901, 2009.
- Smith-Konter, B., and D. T. Sandwell. Stress evolution of the San Andreas fault system: Recurrence interval versus locking depth, *Geophys. Res. Lett.*, 36, L13304, doi:10.1029/2009GL037235, 2009.
- Meade, B. and J. Loveless (2009), *Geophys. J. Int.*, (submitted).
- Wechsler, N., T. K. Rockwell and Y. Ben-Zion, Analysis of rock damage asymmetry from geomorphic signals along the trifurcation area of the San Jacinto Fault, *Geomorphology*, doi: 10.1016/j.geomorph.2009.06.007, 2009.

4. Lithospheric Architecture and Dynamics

a. P/S Structure

Gene Humphreys' group has presented new P and S wave tomographic images based on finite frequency inversions (Figure 33). The travel times at a given station were corrected for crustal effects by ray tracing through the SCEC Harvard community velocity model (CVM and Thurber's crustal model, discussed below). The resulting images of mantle velocity variations exhibit high velocities under the southern Great Valley, and an east-west feature under the Transverse Ranges that extends to depths of 265 km. Both structures are attributed to dynamically important downwellings. Low velocities beneath the Salton Trough extend down to only ~180 km, and are especially pronounced in the S wave model.

Thurber developed a new crustal P and S crustal wavespeed model using the adaptive-mesh double-difference method, that incorporates data from the LARSE I and II profiles, as well as

earthquake data. Significant differences are seen with the present version of the CVM in the upper 6 km. Methods of verification and updating of that model need to be developed (Figure 34).

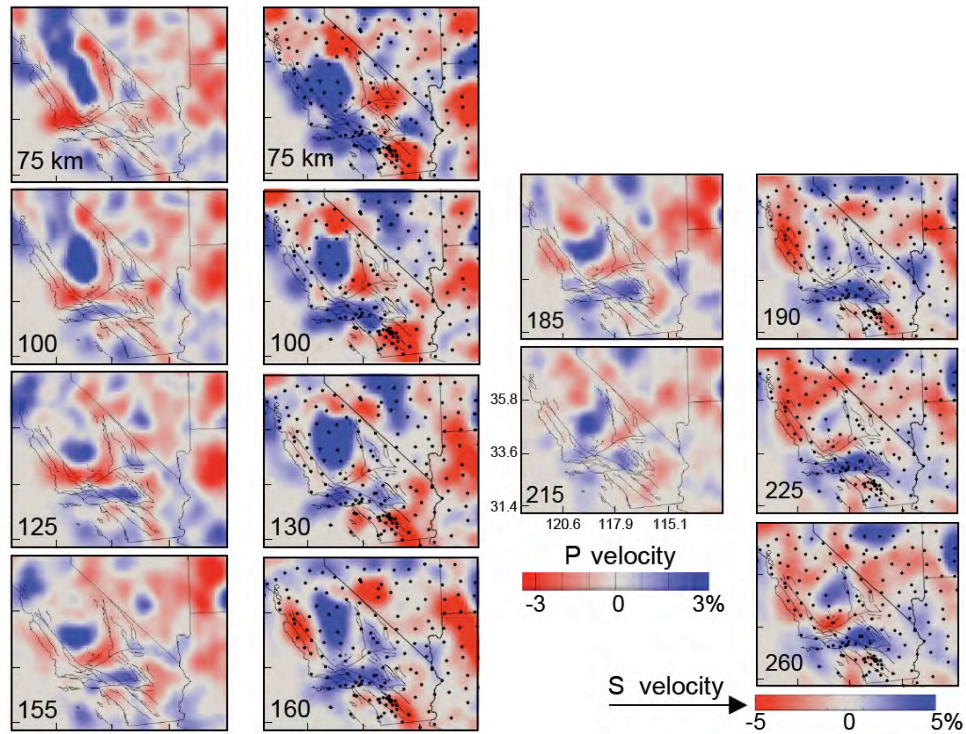


Figure 33. Finite frequency P and S velocity model cross sections at depth (km).

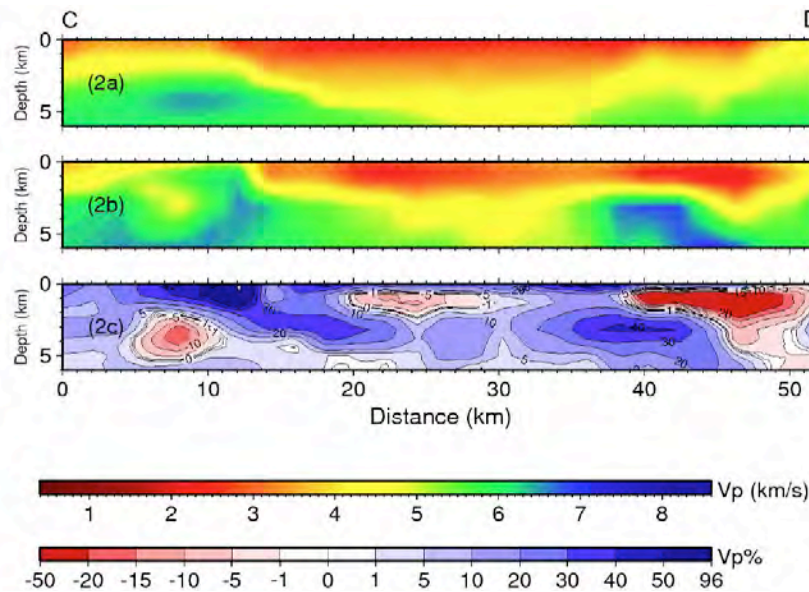


Figure 34. New crustal P-wave velocity model [Thurber, 2008] along the LARSE II line (though Malibu) based on double difference tomography and incorporating LARSE data. The three rows of panel shows (top) the starting CVM-H model, (middle) new model, and (bottom) the velocity perturbation of the new model relative to CVM-H. Significant differences from the CVM are apparent.

b. Anisotropy

The SKS splitting map has been updated and extended to include central and northern California stations (Figure 35). North of the Transverse Ranges splitting directions are parallel to the absolute plate motions of the Pacific and North American plates making a rapid transition near the San Andreas Fault (SAF), but south of the Big Bend they remain more parallel to the North American plate and do not make the transition to Pacific plate motion. Figure 36 shows southern California splitting values, corrected for splitting in the upper 100 km as determined by surface waves [Prindle et al., 2002], with absolute North American plate motion vectors plotted on top. The degree of parallelism is so close that in many cases the underlying splitting vector is obscured. A tendency towards Pacific plate motion is seen in west-southern California, but for most stations west of the SAF including those in the Peninsular Ranges, nominally on the Pacific plate, the directions are parallel to the North American plate motion.

This puzzling behavior was recognized by Silver and Holt [2002] in which they proposed that a west directed flow in the mantle, possibly connected to the sinking Farallon plate, was needed to explain the difference. However the expected transition to Pacific plate motion west of the SAF does occur further north. Perhaps mantle flow related to the deeper structures found from tomography, if those structures are attached and moving with the North American plate could provide the explanation. Also Figure 36 shows that while directions are mostly parallel to NA plate motion values of splitting can be quite varied at nearby stations. Whether this is due to noisy data or associated with small scale motions in the mantle needs to be investigated.

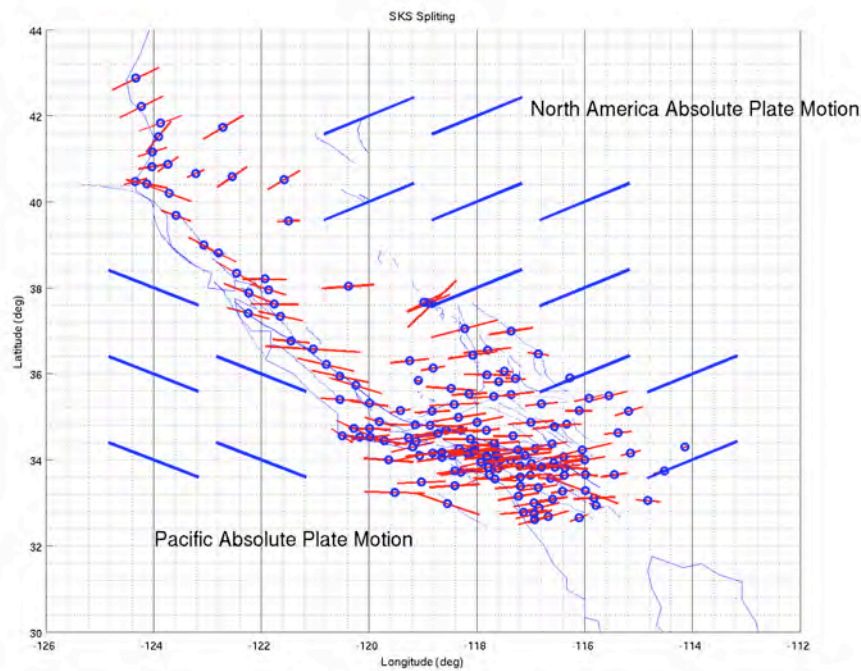


Figure 35. SKS splitting in southern California west of the San Andreas Faults splitting is more aligned with North American than Pacific plate motion. Perhaps movement of the deeper structures in the mantle shown in Figure 33 are affecting the asthenospheric flow as the North American plate moves WSW.

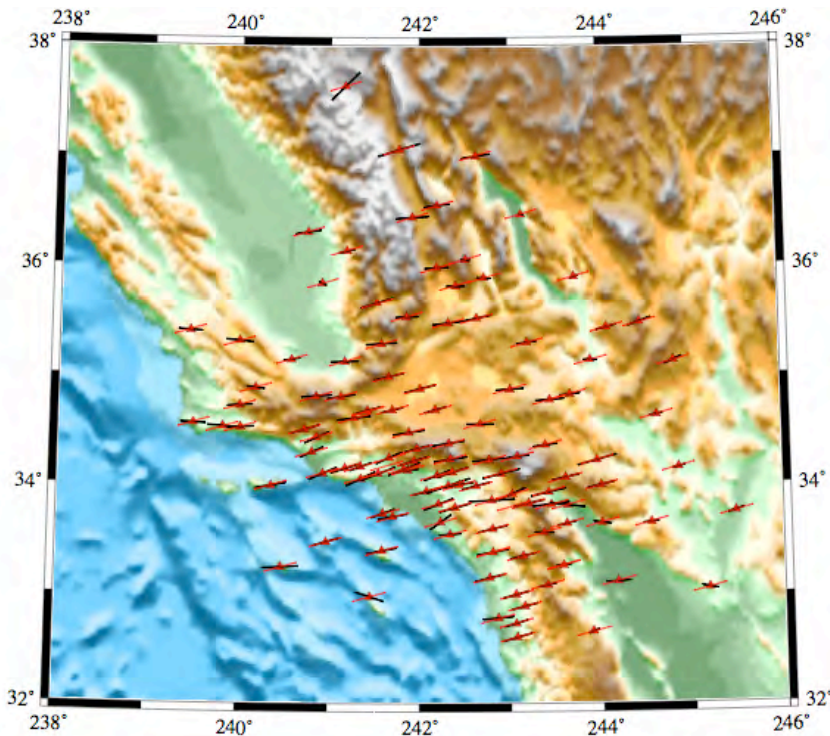


Figure 36. SKS splitting and Apparent plate motion. Black lines give SKS splitting directions. Red lines are North American absolute plate motion relative to the stationary mantle hot-spot reference frame. The disagreement with Pacific plate motion (NW) west of the SAF, suggests that asthenospheric flow does not follow plate motion in Southern California, but may in northern and central California (Figure 35).

Zandt is examining receiver functions RF in order to obtain seismic properties of the lower crust including anisotropy. A large negative polarity contrast with depth is seen in the middle crust beneath the LARSE 1 line, that ran across the San Gabriel Mountains through Azusa, followed by a positive contrast associated with the Moho (Figure 37). Converted RF phases at the Moho have tangential energy. Both these observations are explained as due to the lower crust being composed of under-plated schist related to relative motion of the Farallon and North American plates (Figure 38).

Estimates of lower crustal anisotropy show that, while anisotropic, it is too small a region and too low an anisotropy to explain SKS splitting. Similarly various estimates (Surface waves, splitting from local earthquakes) of upper crustal anisotropy show that splitting is of order 0.1 s again not a significant part of the splitting signal.

In summary anisotropy in southern California can be separated into at least 4 layers (1) the upper crust with about 0.1 sec splitting with fast axis north-south, possibly associated with cracks and structures related to N_S compressive stresses, (2) lower crust with a similar splitting value oriented NE associated with underplaying of schists such as Catalina etc., at the time of subduction, (3) Mantle lithosphere with variable fast directions, but a coherent pattern in the Big Bend region aligned with structures caused by the transpression and (4) deeper asthenospheric values that amount to 1.5 s splitting and for most of the State are aligned with absolute plate

motion, but in southern California is at a large angle to Pacific plate motion, for reasons we do not completely understand. A version of the CVM could be developed that includes anisotropy.

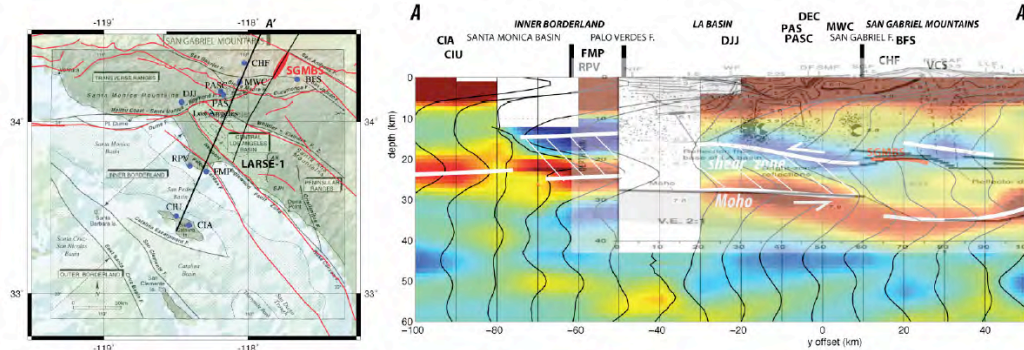


Figure 37. Moho variation (red) lies beneath an anisotropic low velocity layer (blue) in the lower.

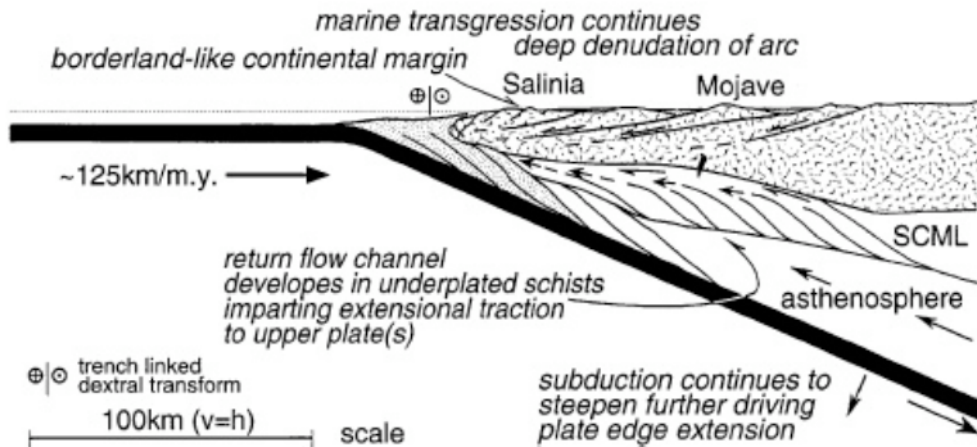


Figure 38. Interpretation of lower crustal anisotropy based on Saleeby model. Underplated schist associated with relative motion of the Farallon slab and NA plate develops a fabric that can explain tangential energy in receiver functions.

c. Viscosity of the Lower Crust and Mantle

Fay and Bennett have used vertical motion of long-term, low-noise GPS time series to constrain the viscosity of the lower crust/upper mantle. After taking into account vertical uplift from glacial rebound they model expected vertical motions from major past earthquakes (Owens Valley, Kern County,) to infer viscosity structure (Figure 39). Their preferred model is one where the lower crust has higher viscosity than the mantle e.g. (1021 Pa-s versus 1020 Pa-s). However no single layered model fits all data, and lateral variations in viscosity, or effects from more recent events may need to be taken into account. Similar 2-layer viscosities are assumed by Johnson. They use lower crustal and uppermost mantle viscosity of 1020-1021 Pa-s with mantle viscosity of about 1018-5x1018 Pa-s.

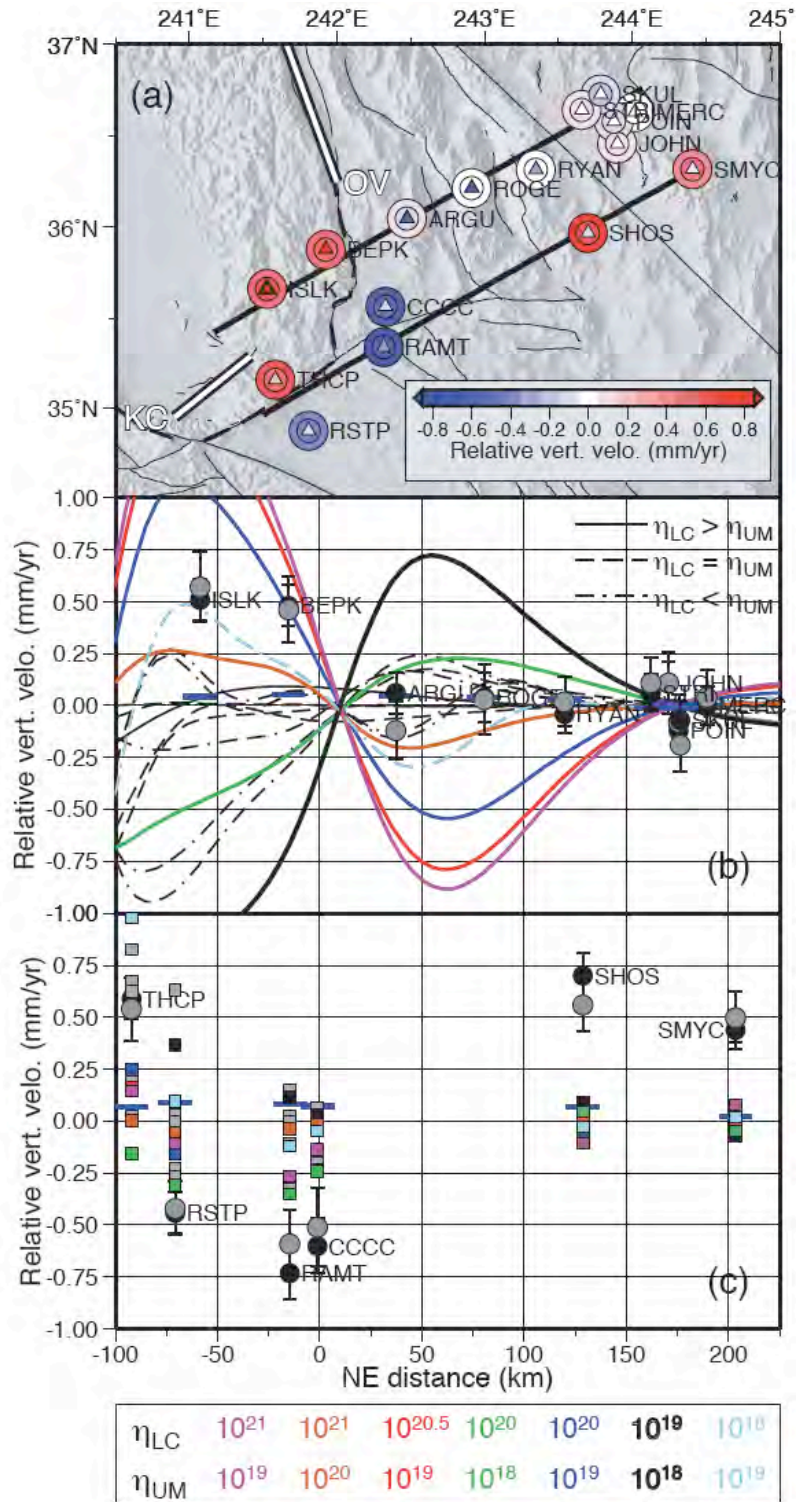


Figure 39. Post-earthquake (Owens Valley and Kern County) vertical motions compared with modeled values based on assumed viscosities of the Lower Crust (LC) and Upper Mantle.

d. Dynamic Models of Lithospheric Deformation

Becker’s group is developing finite element models (SMOG3D) to understand driving forces, fault strength and rheology. They model curved faults with large off-fault strain similar to that observed geodetically (Figs 40 and 41) and the interaction of the San Andreas, San Jacinto (SJF) and Elsinore (ELS) faults and conclude that if only fault strength is varied to accommodate the geodetically observed distribution of slip-rates, the strength of the ELS must be larger than that of the SJF, which must be larger than that of the SAF Indio by at least a factor of 3 and 2, respectively. The results show that the models can be used to test several suggested forces acting upon southern California faults include in crustal as well as mantle tractions.

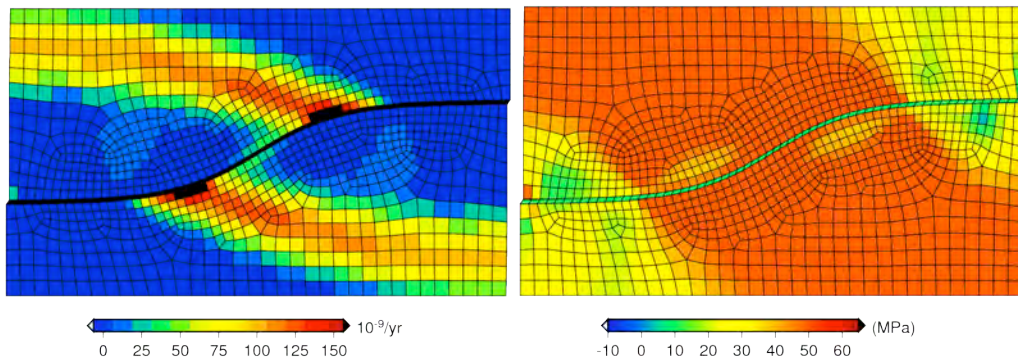


Figure 40. Finite element model used to describe stress and strain in southern California. Left panel shows square root of the second (shear) invariant of the strain tensor at 5 km depth. Color scale emphasizes off-fault strain (nano-strain/yr). Shear strain is off scale in the fault zone and would otherwise dominate the plot. Right panel shows square root of the second invariant of the stress tensor at 5 km depth.

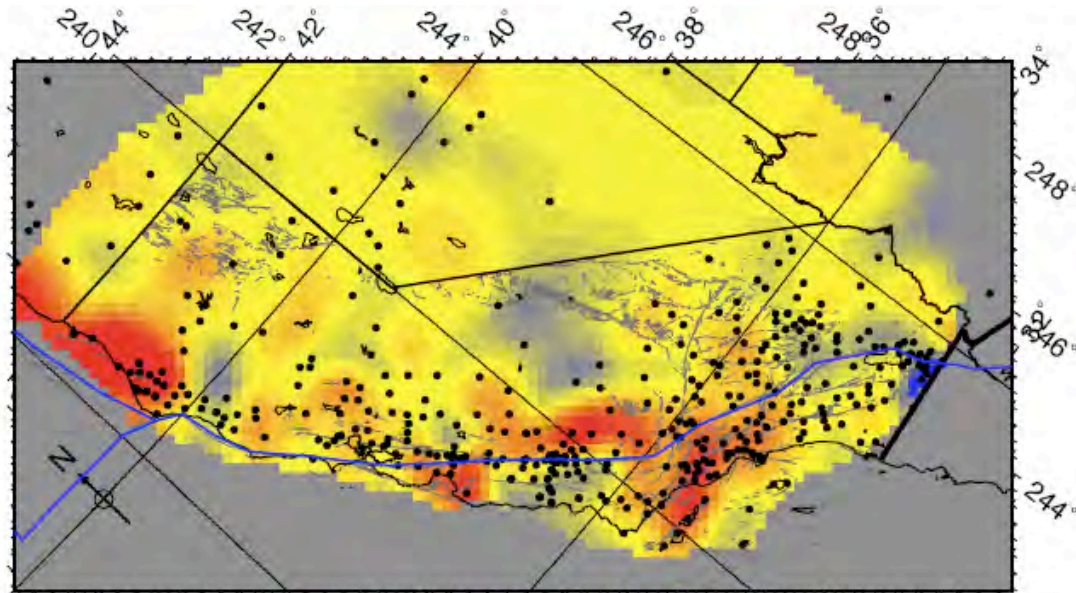


Figure 41. Dilatational strain inferred from high-quality GPS sites against which models are tested.

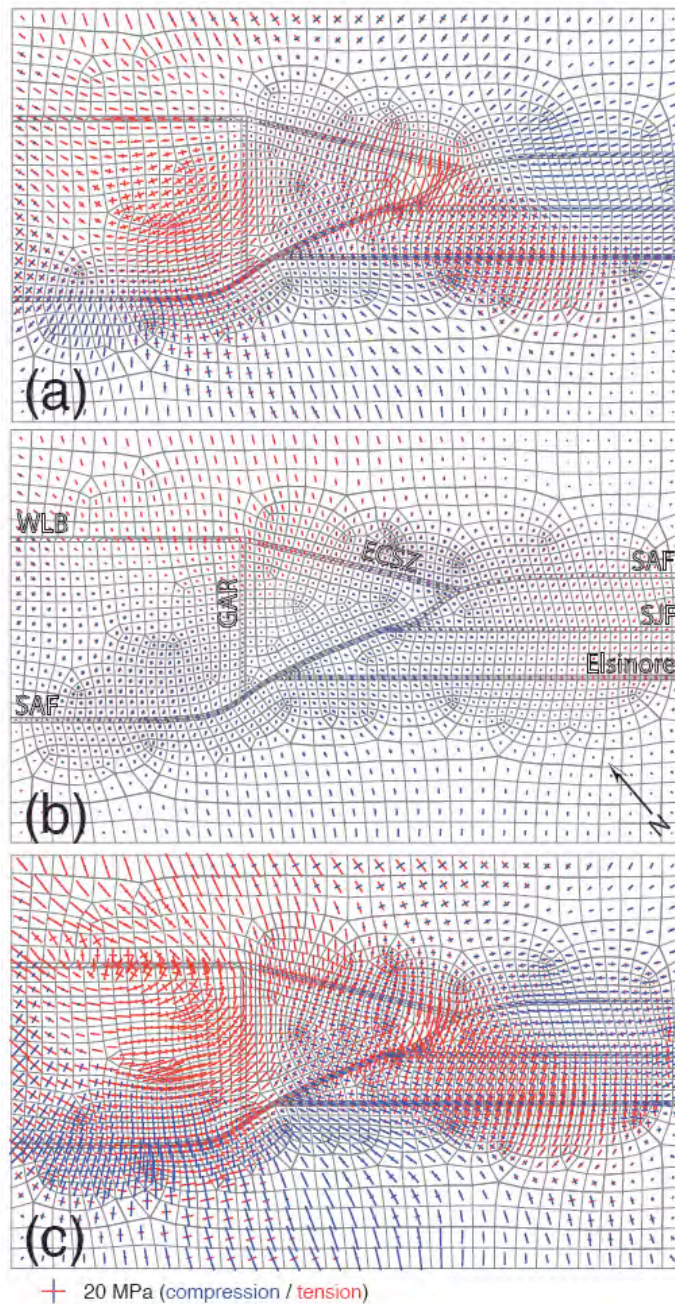


Figure 42. Estimated stress field, from body forces associated with topography, Moho variation and mantle loads inferred from tomography. Horizontal deviatoric principal stress field at 7.5 km depth caused by buoyancy heterogeneity. Blue bars indicate compression, red indicate tension. (a) Stress field caused by lateral variation in crustal thickness. Moho depth taken from receiver function studies [Zhu and Kanamori, 2000; Yan and Clayton, 2007] (b) Stress field caused by anomalous upper mantle density structure and tractions caused by density driven upper mantle flow [Fay et al., 2008]. SAF, San Andreas fault trace. (c) Total stress field ($c = a + b$) caused by crustal and upper mantle density variations. In the vicinity of the eastern and central Transverse Ranges the stress field is dominantly N-S compression and E-W tension.

Becker and coworkers are also characterizing stress based on relative plate motion traction, mantle flow, including that driven by body forces associated with topographic and crustal thickness variations. They find that tractions proportional to excess elevation and excess Moho depth result in tensional stress in the vicinity of the Transverse Ranges. The largest magnitude of this stress is of ~10-20 MPa in the east where the crust appears in isostatic equilibrium. Traction on the crust derived from upper mantle flow driven by upper mantle density [Fay et al., 2008] produce compression throughout the Transverse Ranges, and tension in the southern Walker Lane Belt and Salton Trough area. Principal stress magnitudes are of order 5 MPa (Figure 42b). These stresses are known only to within a multiplicative constant that maps upper mantle seismic anomalies to density anomalies [Fay et al., 2008], and for the case shown here are smaller than the stresses caused by topography (Fig. 42a) by a factor of 2 or more.

They vary fault strengths to compare with the geodetic strain field and 'tentatively' conclude that a non-uniform distribution of fault strengths, possibly a consequence of differing fault maturity and offset, is required to produce the compressional stress to counter the tensional stress produced by the Transverse Ranges. They suggest it is necessary to consider the entire (simplified) fault system because the kinematics and stress at any one point is nonlinear and dependent on the material properties at that point and everywhere else in the system, the objectives of their continuing research. The variation of absolute stress for comparison with seismicity and stress drops is an outstanding SCEC goal. It will be important to compare this approach with the more comprehensive upper crustal model of the Hager group that incorporates the CFM, CBM and USR.

e. References

- Fay, N. P., R. A. Bennett, J. C. Spinler and E. D. Humphreys, Small-scale Upper Mantle Convection and Crustal Dynamics in Southern California, *Geochem. Geophys. Geosyst.*, **9**, Q08006, doi:10.1029/2008GC001988, 2008.
- Prindle Sheldrake, K., C. Marcinkovich, and T. Tanimoto, Regional Wavefield reconstruction for teleseismic P-waves and Surface waves, *Geophys. Res. Lett.*, **29**, 391-394, 2002.
- Silver, P. G., and W. E. Holt, The mantle flow field beneath western North America, *Science*, **295**, 1054-1057, DOI: 10.1126/science.1066878, 2002.
- Yan, Z., and R. W. Clayton, Regional mapping of the crustal structure in southern California from receiver functions, *J. Geophys. Res.*, **112**, B05311, doi:10.1029/2006JB004622, 2007.
- Zhu, L. and H. Kanamori, Moho Depth Variation in Southern California from Teleseismic Receiver Functions, *J. Geophys. Res.* **105**, 2969-2980, 2000

5. Earthquake Forecasting and Predictability

The Earthquake Forecasting and Predictability (EFP) focus group coordinates two types of research projects. The first type encourages the development of earthquake prediction methods to the point that they can be moved to testing within the framework of the Center for the Study of Earthquake Predictability (CSEP). The other type of research project encouraged by EFP are those that are far from being ready for testing within the CSEP framework, but that aim to obtain fundamental knowledge of earthquake behavior that may be relevant for forecasting earthquakes.

Several proposals supported the CSEP testing centers and implementation of CSEP tests. Gerstenberger's "CSEP Forecast Test Methodology: Development and Participation" supported travel for collaboration and meeting participation for the New Zealand testing center. Wiemer's "Travel funds for CSEP integration & development" provided similar support for the testing center in Zurich. Jordan's "Alarm-based Evaluation of Earthquake Forecasts" supported the development

of appropriate statistical tests for alarm-based earthquake forecasts. Schoenberg's "Spontaneous and triggered earthquakes in diverse tectonic zones of the globe" leads to submission to CSEP of both long-term and short-term global earthquake forecasts based on earthquake branching models and estimates of tectonic deformation (Figure 43).

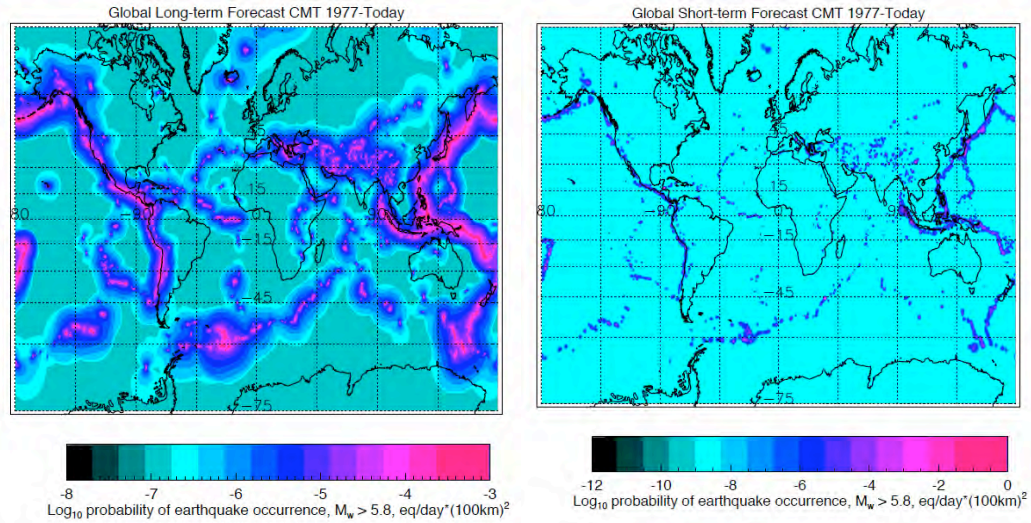


Figure 43. Long-term and short-term global earthquake forecasts. (Left) Global earthquake long-term potential based on smoothed seismicity. Earthquakes ($M_w \geq 5.8$) from the CMT catalog since 1977 are used. Earthquake occurrence is modeled by a time-independent (Poisson) process. Colors show the long-term probability of earthquake occurrence. (Right) Global earthquake short-term potential based on smoothed seismicity. Earthquakes ($M_w > 5.8$) from the CMT catalog since 1977 are used. Earthquake occurrence is modeled by a temporal process controlled by Omori's law type dependence. Colors show the long-term probability of earthquake occurrence.

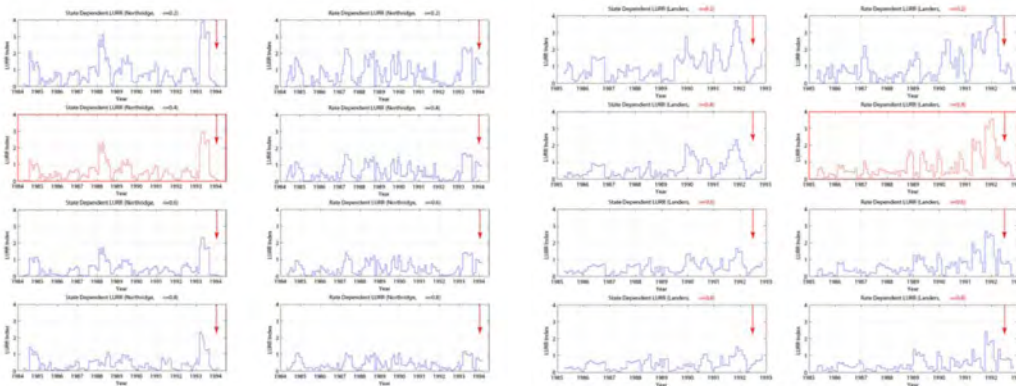


Figure 44. Retrospective test of the Load/Unload Response Ratio (LURR) method for intermediate-term earthquake forecasting, for the Northridge (left) and Landers (right) earthquakes. The triggering criterion is either "stress state" or "stress rate", and the Coulomb friction coefficient $\mu = 0.2, 0.4, 0.6, \text{ or } 0.8$. Significant LURR "anomalies" appeared a few months before the mainshock for some of the test runs but not the others.

Shen's "Improvement and earthquake predictability test of the load response ratio method" carried out retrospective tests of the Load/Unload Response Ratio (LURR) method for intermediate-term earthquake forecasting, based on the rate and state of Coulomb stress changes induced by earth tides. This proposed method of earthquake prediction introduced by scientists in China has received much favorable attention there, although some studies by US scientists have brought those results into question. The retrospective tests had positive results for earthquakes in California, although different events required different friction parameters, and some earthquakes had a larger signal related to stress magnitude while others had a larger signal related to stress change (Figure 44). The method did not work for the 2008 M7.9 Wenchuan earthquake in China. The real test will come when this method is moved into the CSEP environment, where the method will be subjected to prospective testing with fixed parameters.

Other work placed observational constraints on physical models of earthquake occurrence. Bürgmann's "Interaction and Predictability of Small Earthquakes at Parkfield" found that the recurrence time of repeating events at Parkfield shortened after nearby larger earthquakes, placing constraints on the stress magnitude necessary for triggering. Brodsky's "Triggerability: A tool to connect aftershocks and long-range triggering" studied evidence for dynamic triggering of aftershocks by demonstrating a continuous relationship between peak dynamic stress and triggering rate in the near and far field. Zaliapin's "Modeling seismic moment rate in San Andreas Fault -- Great Basin system: Combination of seismological and geodetic approaches" reconciled apparent differences in moment rate from seismicity and geodetic information, through detailed geodetic velocity and strain rate analysis and statistical modeling of seismic moment rate. These topics were addressed in a debate at the SCEC annual meeting in September, 2008.

The multi-disciplinary nature of EFP led to support of geological studies, including support of SoSAFE-related projects. Scharer's "Slip per event at the Frazier Mountain paleoseismic site" better constrained the earthquake and slip history of the San Andreas fault near Ft. Tejon. Rockwell's "SoSAFE: Confirming and Extending the Event Record at Hog Lake, San Jacinto Fault" was postponed until the summer of 2009. Stirling's "Age of precariously balanced rocks at near fault sites in New Zealand: Reduction of age uncertainties" found that precariously balanced rocks in temperate environments New Zealand may have reached their precarious state much more quickly than precarious rocks in desert environments. Additionally, in support of SoSAFE, Cochran's "Seismology Rapid Response Test During the SoSAF Shakeout" tested how rapidly portable seismometers could be deployed after a southern San Andreas event.

Earthquake Simulators

Several investigators have conducted research using Earthquake Simulators, including Ward's "ALLCAL -- An Earthquake Simulator for All of California", Tullis's "Quasi-Dynamic Parallel Numerical Modeling of Earthquake Interactions Over a Wide Magnitude Range Using Rate and State Friction and Fast Multipoles", and Dieterich's "Physics-Based Simulation of Earthquake Occurrence in Fault Systems". These simulators are numerical models aimed at generating catalogs of simulated earthquakes over a variety of spatial and temporal scales. The aim of these studies is to gain some understanding of the behavior of real earthquakes by studying the behavior of simulated earthquakes. For example, one line of inquiry is to see if patterns of simulated seismicity in space and time occur that might also be discovered in real seismicity. If so, forecasting future earthquakes might be done by recognizing ongoing patterns in past and current seismicity.

The "SCEC Earthquake Simulators Workshop 2" was held in June 2008. At this workshop, participants compared the results of their simulators for two benchmark problems outlined at the previous workshop, and discussed possibilities for future benchmark tests.

6. Ground Motion Prediction

The primary goal of the Ground Motion Prediction focus group is to develop and implement physics-based simulation methodologies that can predict earthquake strong motion waveforms over the frequency range 0-10 Hz. At frequencies less than 1 Hz, the methodologies should deterministically predict the amplitude, phase and waveform of earthquake ground motions using fully three-dimensional representations of the ground structure, as well as dynamic or dynamically-compatible kinematic representations of fault rupture. At higher frequencies (1-10 Hz), the methodologies should predict the main character of the amplitude, phase and waveform of the motions using a combination of deterministic and stochastic representations of fault rupture and wave propagation.

Source characterization plays a vital role in ground motion prediction and significant progress has been made in the development of more realistic implementations of dynamic and dynamically-compatible kinematic representations of fault rupture within ground motion simulations. Verification (comparison against theoretical predictions) and validation (comparison against observations) of the simulation methodologies continues to be an important component of this focus group with the goal being to develop robust and transparent simulation capabilities that incorporate consistent and accurate representations of the earthquake source and three-dimensional velocity structure. The products of the Ground Motion Prediction group are designed to have direct application to seismic hazard analysis, both in terms of characterizing expected ground motion levels in future earthquakes, and in terms of directly interfacing with earthquake engineers in the analysis of built structures. Activities in these areas are highlighted by the projects described below.

a. Ground Motion Simulations and Model Validation

Precariously Balanced Rocks. (*Purvance, Anooshehpour, Brune, and Jordan*). Recent work has developed refined fragility estimates of precariously balanced rocks (PBRs) in the San Bernardino region to test if their existence is consistent with current seismic hazard models. Figure 45 indicates the locations of PBRs chosen for this analysis. These include PBRs at sites very close to the Cleghorn and North Frontal Thrust Faults (sites SW at Silverwood Lakes and GV at Grass Valley) along with sites near to the San Jacinto Valley section of the San Jacinto Fault and between the San Jacinto and San Andreas Faults (sites SJ). Pictures of the PBRs at these sites are also presented with targets affixed, which are utilized for accurate shape determination via photogrammetry. These PBRs have all be field tested via forced tilting tests as outlined in Purvance et al. [2008] in an effort to more accurately delineate their fragilities. Rood et al. [2008] presents the only residence time study of PBRs in this region, indicating initial residence time estimates of 23-28 ka for Grass Valley PBR pedestals and 50 ka for one PBR. Thus there is evidence that the Grass Valley PBRs have resided in their current positions for many earthquake cycles.

The estimated PBR fragility models have been exposed to suites of ground motions produced by ensembles of earthquakes taken from the UCERF 2, along with the GMPE of Abrahamson and Silva [1997] and the NGA relation of Campbell and Bozorgnia [2008]. Monte Carlo simulations have been undertaken using the recurrence intervals and maximum magnitudes of events, sampling the GMPE for the magnitude/ distance pairs. Since the PBR overturning fragilities depend on both the high- and lower-frequency ground motion amplitudes, PGA and spectral acceleration at 1 Hz have been used to estimate the overturning probabilities. Figure 45 presents the overturning probabilities for each PBR when exposed to the UCERF 2 where the ground motions have been estimated based on the CB08 and AS97 GMPE.

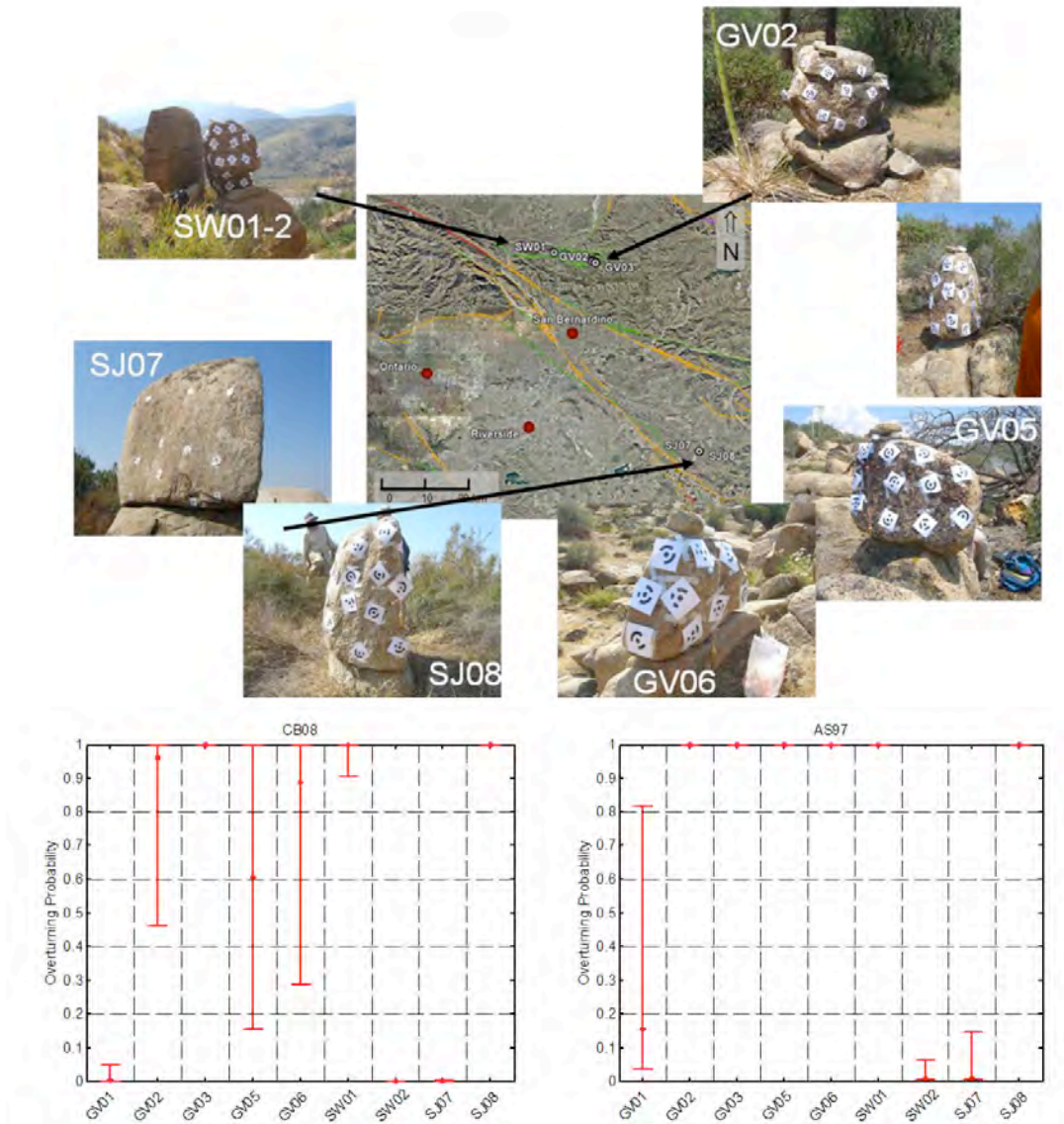


Figure 45. Top panel shows PBRs investigated in the vicinity of San Bernardino. The SW and GV sites lie very close to the Cleghorn, North Frontal Thrust, and San Andreas Faults while the SJ (San Jacinto) PBRs are very close to the San Jacinto Fault (within ~ 5 km). Bottom panels show PBR overturning probabilities assuming 10,000 year residence times when exposed to the UCERF 2 (Field et al. 2008) earthquake rupture forecast. Results for the Campbell and Bozorgnia [2008] and Abrahamson and Silva [1997] GMPE are shown.

The ground motions are assumed to be statistically independent from earthquake to earthquake in these analyses and 10,000 year residence times have been assumed ubiquitously. The AS97 GMPE produces significantly higher rates of overturning when compared with the CB08. However, in both cases, a number of the PBRs should have overturned with high probability if exposed to the earthquakes represented by the UCERF 2. These results suggest that either the recurrence intervals of some earthquakes as indicated in the UCERF 2 are unrealistically short or that the Campbell and

Bozorgnia [2008] GMPE predicts unrealistically large ground motions amplitudes in the near field of large earthquakes. Moreover, further constraints on ground motion levels from PBRs may soon be available (Figure 46).



Figure 46. The Echo Cliffs precariously balanced rock (see discussion in the Geology section) in the western Santa Monica Mountains. stands at just over 14 meters in height, and has a 3 to 4 second oscillatory period, corresponding to that of a 30 to 40 story building. This rock withstood ground motions during the 1994 Northridge earthquake estimated to have been 0.2 g (PGA) and 12 cm/sec (PGV) at this site. This rock, discovered in March 2009, may provide constraints on future ground motion simulations, especially for long-period shaking that is relevant for tall buildings in the Los Angeles area. Dylan Rood (LLNL & UCSB) and David Haddad (ASU) provide scale (from Hudnut et al., 2009 SCEC Annual Meeting abstract).

Ambient Noise Analyses. (Beroza, Ma and Prieto). Beroza, Ma and Prieto have developed the capability to use the ambient seismic field to predict ground motion. Despite the complex nature of the ambient field, it has a weak coherence that can be extracted even in the presence of multiple scattering. In particular, the correlation of diffuse wavefields recorded at two receivers can be used to extract the impulse response (i.e., the Green's function) for an impulsive excitation at one

receiver, as recorded at the other. The top panel of Figure 47 from Ma et al. [2008] compares all three components of the ambient-noise Green's functions at station FMP with theoretical, finite-element Green's functions calculated by applying a smooth vertical force with Gaussian time dependence at station ADO for SCEC CVM 4.0 and CVM-H5.2 community velocity models. The fit is limited primarily by our imperfect and incomplete knowledge of crustal structure.

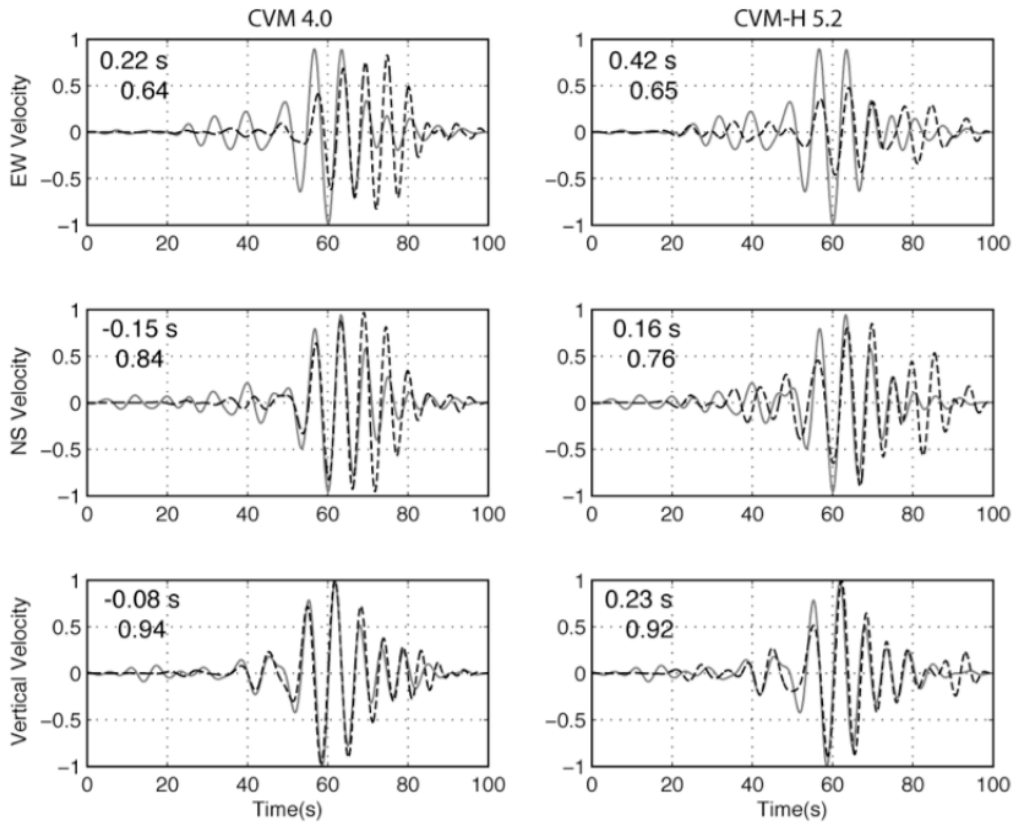


Figure 47. Top panel shows comparison of ambient field (gray) and synthetics (black dashed) at FMP for a vertical force at ADO filtered between 0.1 and 0.2 Hz. Time lag and correlation coefficient are shown in upper left.

They have also used the ambient field to document basin amplification for seismic stations in the Los Angeles basin. Figure 48 [Prieto and Beroza, 2008] compares the response to a horizontal impulse, using station BBR as a virtual earthquake source, at seismic stations across metropolitan Los Angeles with seismograms of the February 10, 2001 (Mw 4.6) Big Bear earthquake, which is within 4 km horizontally and 10 km vertically of station BBR. The horizontal impulse is applied in the fault normal direction, following the earthquake mechanism given by Graves (2008), who independently modeled ground motions. Both the duration and relative amplitudes of ground motions across the Los Angeles Basin are recovered from ambient-noise observations.

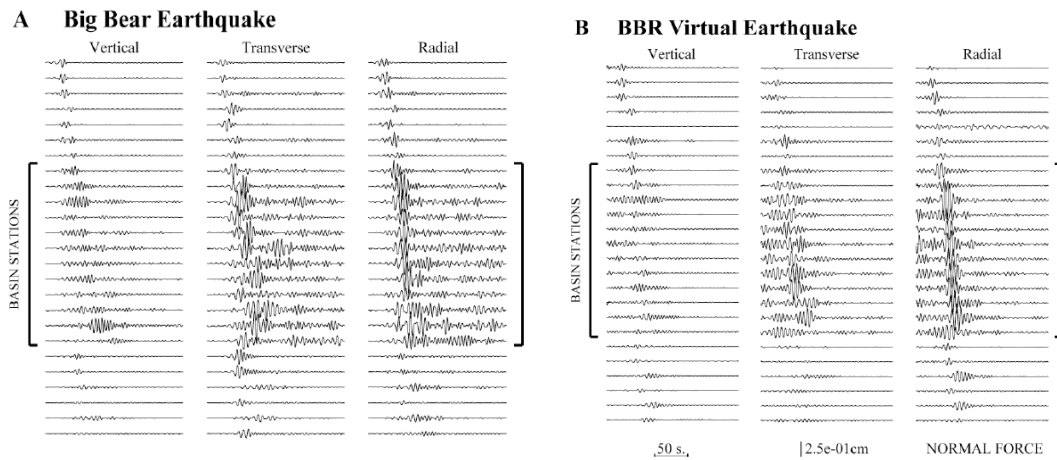


Figure 48. A) Earthquake record section of ground displacements for sites around the Los Angeles Basin. Records are plotted roughly with increased epicentral distance. The large brackets indicate basin sites. B) Same as A but for impulse response records for a horizontal force for station BBR. Note the amplification in the Los Angeles basin for both the impulse response as well as the earthquake records.

Parametric Correlations in Kinematic Ruptures. (*Archuleta and Schmedes*). Liu et al [2006] have proposed a hybrid low/high frequency method for the prediction of broadband ground-motion time histories that utilizes correlation of the kinematic source parameters as suggested by previous models of dynamic faulting. For any point on the fault the choice of the source parameters is based on statistical distributions. The method computes 1D and 3D synthetics for a given station using a standard representation theorem that convolves the spatial varying slip rate function on the fault with the computed Greens functions of the medium between the fault and the station and integrates this combination over the fault. To produce more accurate high-frequency amplitudes and durations, we correct the 1D synthetics using a randomized, frequency dependent perturbation of azimuth, dip, and rake. To correct the 1D synthetics for local site response and nonlinear soil effects we use a nonlinear propagation code and a generic velocity structure appropriate for the site. Finally, we combined the low frequencies from the 3D calculation with the high frequencies from the 1D calculation using a wavelet-based approach at a specified cross over frequency.

Current work is aimed at the refinement of the method using dynamic modeling. The focus here is on the spatial interdependency of the kinematic parameters. Spatial correlation coefficients have been computed for different parameter pairs and 315 spontaneous rupture models, including three dynamic Shakeout ruptures computed by Luis Dalguer [2008, pers. Comm.]. Selected histograms are shown in Figure 49. The first important result is contained in the first row, which shows the correlation of final slip with the ratio of rupture velocity over shear wave velocity. The distribution is centered on 0, hence for most ruptures there is no correlation between these two parameters. Therefore, for a given slip distribution on the fault there are many fundamentally different spatial distributions of rupture velocity possible, which translates into great variability in the possible ground motion. This result argues against using slip as a controlling parameter for rupture velocity. If a positive correlation between slip and rupture velocity is assumed, areas of large slip are sampled in a shorter time (faster rupture), which yields strong peaks in the ground motion. Hence, if such a correlation is wrongly assumed one might over-predict ground motion.

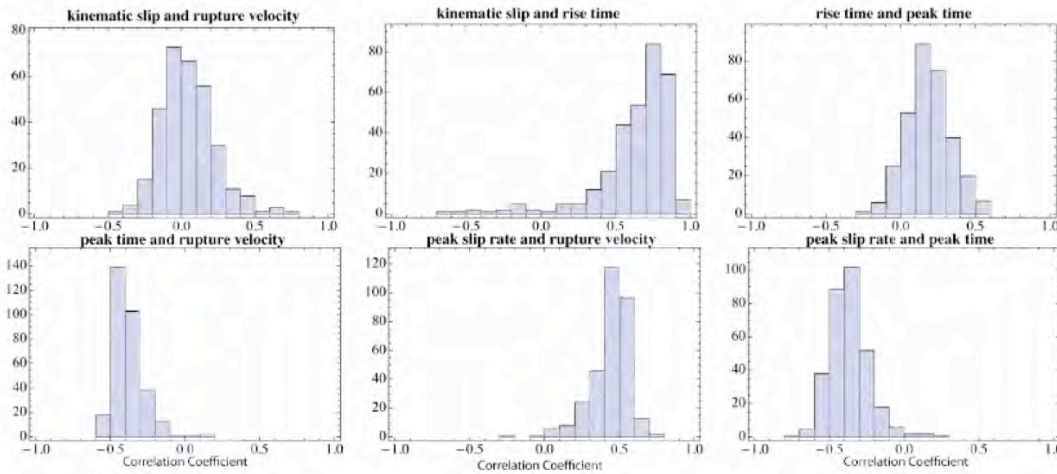


Figure 49. Histograms of computed spatial correlation coefficients for 315 ruptures and different parameter pairs. This result indicates that there is no correlation between slip and rupture velocity.

Validation of Synthetic Ground Motions. (Bazzurro, Tothong, Shome, Park, and Gupta). This study focuses on the statistical comparison of the characteristics of ground motion intensity measures at a given site derived from numerical simulations, ground motion prediction equations (GMPEs) and observed records. The analysis utilizes both elastic and inelastic response quantities. The simulations analyzed for this project were generated in 2005 and are for the 1989 Loma Prieta earthquake and a scenario based on the 1906 San Francisco earthquake [Aagaard et al., 2008a and 2008b].

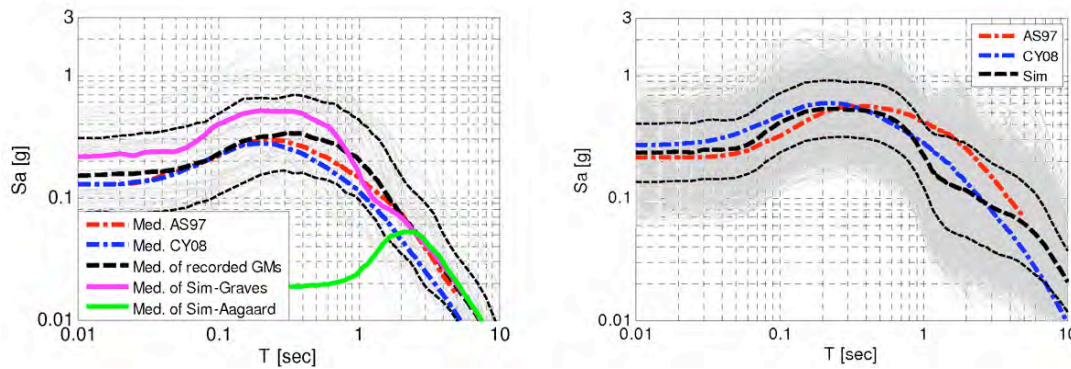


Figure 50. Left panel shows geometric mean response spectra of 83 recorded motions (gray lines) from 1989 Loma Prieta earthquake along with their geometric mean (thick dash-dash line) and \pm one sigma (thin dash-dash lines) compared with the geometric mean of the predicted spectra from both the GMPEs and the simulations. Right panel compares simulated and GMPE predictions for 1906 earthquake scenario.

Figure 50 compares 5% damped elastic response spectra from the earthquake simulations with that predicted from the GMPEs of Abrahamson and Silva [1997] and Chiou and Youngs [2008]. The left panel is for the 1989 Loma Prieta earthquake, which also includes the median of the actual observations, and the right panel is for the 1906 scenario. For the Loma Prieta earthquake, the

simulation predicts higher motions on average for periods less than about 1 sec. Between 1 and 2 seconds the simulated motions under-predict the median observations, and then above 2 sec the simulations are at the same level as the median observations. For 1906, the simulation and GMPE predictions are quite similar except for the dip in the simulations seen between periods of 1 and 4 seconds. As discussed in the next section, recent refinements to the simulation methodology have been focused on correcting the deficiencies illustrated by these comparisons. These include the implementation of a more accurate non-linear site response model, and the use of a sharper slip rate function, both of which significantly improve the fit to the Loma Prieta observations (Figure 52).

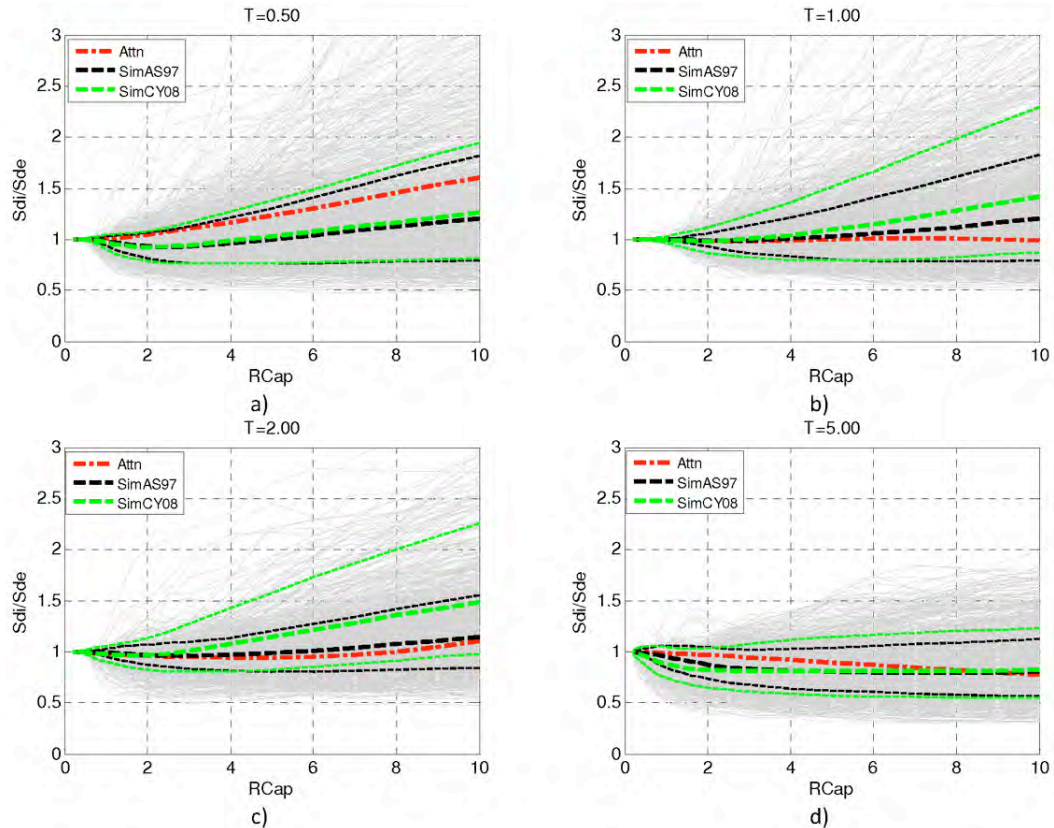


Figure 51. Comparison of inelastic displacement ratio for multiple periods between simulated records for the 1906 earthquake scenario and those predicted by the GMPE of Tothong and Cornell [2006].

Figure 51 compares the inelastic response for the 1906 simulation. The results are displayed as the ratio of inelastic to elastic spectral displacement plotted as a function of the expected level of nonlinearity (RCap). At longer periods, the simulation is consistent with the empirical prediction from Tothong and Cornell [2006]; however, at shorter periods the simulations show lower inelastic response ratios than the empirical model. Interestingly, Baker [2007] used a similar procedure to analyze simulations for a Mw 7.15 Puente Hills scenario generated using the same methodology employed for the 1906 simulation and also found good agreement at the longer periods. However, at shorter periods Baker [2007] found that the simulations predicted higher inelastic response ratios than the empirical model. This apparent discrepancy can be explained by examining the scenario

specific rupture characteristics employed in each simulation. The Puente Hills scenario analyzed by Baker [2007] was a high dynamic stress drop event that produced quite strong short period motions [Graves and Somerville, 2006], and consequently generated large inelastic response ratios at the shorter periods. On the other hand, the 1906 scenario is modeled as a low dynamic stress drop event (due to the presence of surface rupture), which consequently produces relatively weak short period motions and lower inelastic response ratios.

The results from this study highlight the benefits of utilizing statistical analyses to validate and guide the improvement of the simulation methodologies. In addition, they also illustrate the need to consider potential biases introduced by event- and/or scenario specific characteristics included in the simulations.

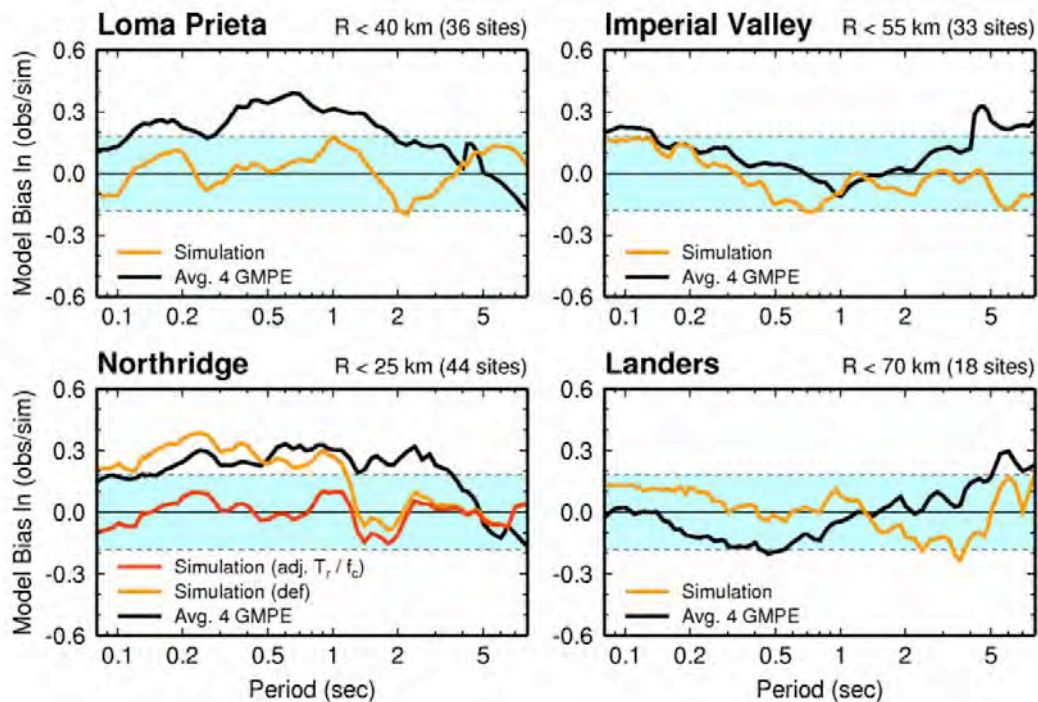


Figure 52. Mean model bias of average horizontal component spectral acceleration for simulations of four large California earthquakes. Blue shading indicates +/-20% variance. The black lines are predictions from empirical ground motion attenuation models.

Broadband Simulations. (Graves and Pitarka). Current work on this project is aimed at refinements to the hybrid broadband ground motion simulation methodology of Graves and Pitarka [2004], which combines a deterministic approach at low frequencies ($f < 1$ Hz) with a semi-stochastic approach at high frequencies ($f > 1$ Hz). The high frequency approach assumes a random phase omega-squared radiation spectrum and generic ray-path Green's functions. The low frequency motions are computed using a 3D viscoelastic finite difference algorithm. Fault rupture is represented kinematically and incorporates spatial heterogeneity in slip, rupture speed and rise time.

Recent source characterization improvements are guided by rupture model inversions and dynamic rupture simulations. The prescribed slip distribution is constrained to follow an inverse wavenumber-squared falloff and the average rupture speed is set at 80% of the local shear wave

velocity, which is then adjusted based on the slip distribution such that the rupture propagates faster in regions of high slip, and slower in regions of low slip. The slip rate function is a Kostrov-like pulse having a rise time proportional to the square root of slip, with the average rise time across the entire fault constrained empirically. Recent observations from large earthquakes show that surface rupturing events generate relatively weak high frequency ground motions compared to buried ruptures. Dynamically, this behavior can be reproduced by including a zone of velocity strengthening in the upper few km of the rupture. Kinematically, this leads to a reduction of rupture propagation speed and a lengthening of the rise time, which we model by applying a 70% reduction of the rupture speed and increasing the rise time by a factor of 2 in a zone extending from the surface to a depth of 5 km.

Another refinement is the use of near surface response factors developed from equivalent linear response analysis. These factors are based on V_{s30} as implemented in the empirical model of Campbell and Bozorgnia [2008]. First, ground motions are simulated for a reference site condition, which is typically set at $V_{s30} = 865$ m/s for the high frequency portion of the simulation. Next, using the peak ground acceleration (PGAR) measured from the reference waveform, the reference V_{s30} (VREF) and the site V_{s30} (VSITE), a frequency dependent amplification spectrum is constructed. This amplification spectrum is then applied to the Fourier amplitude spectrum of the simulated waveform. Inverse transformation back to the time domain yields the site-specific broadband waveform. Non-linear effects are incorporated through the use of PGAR, which adjusts the level of amplification depending on the strength of the reference motions. For large PGAR, the amplification functions can be less than one, particularly at high frequencies. Although the factors are strictly defined for response spectra, the application in the Fourier domain appears to be justified since the functions vary slowly with frequency. The use of V_{s30} is attractive because this parameter is readily available and the amplification functions are easy to compute and apply to large-scale simulations.

The fidelity of the simulation technique is demonstrated in Figure 51, which compares the spectral acceleration goodness-of-fit against the strong motion recordings from the Imperial Valley, Loma Prieta, Landers, and Northridge earthquakes.

b. Dynamic Rupture Effects on High Frequency Ground Motions

Rough Faults. (Dunham and Rice). This work utilizes numerical simulations to explore how ruptures propagate along rough faults [Belanger and Dunham, 2008]. Measurements indicate that natural fault surfaces are rough at all scales; more specifically, deviations from planarity are evident at all wavelengths with an amplitude-to-wavelength ratio that is scale independent (i.e., fault surfaces are self-similar fractals). Part of the effort over the past year has been devoted to development of a numerical method that offers more flexibility in terms of incorporating other bulk rheologies (including plasticity) and geometrical complexity of faults. This has led to the development of a block-structured finite difference code that is capable of handling curved boundaries/faults. Irregular geometries in the physical domain are mapped onto a rectangular computational domain via a coordinate transformation; the governing equations are solved in the computational domain. For these simulations, band-limited self-similar fault profiles are generated with the maximum roughness wavelength corresponding to the fault length and the minimum taken to be about ~ 10 times larger than the grid spacing to ensure proper numerical resolution of all modeled roughness wavelengths. The top panels of Figure 53 shows an example of a synthetically generated fault surface as well as the location of a station where synthetic seismograms are computed; rupture is nucleated in the center of the domain.

One important result shown by the simulations is that increasing the fault roughness, while keeping all other parameters (initial stresses, friction law parameters, etc.) fixed, ultimately inhibits rupture propagation by creating extremely large stress perturbations. These stress perturbations are, for sufficiently short roughness wavelengths, capable of completely relieving normal stress over small portions of the fault, at least when assuming linear elastic material response as was done in these simulations.

In addition to influencing rupture propagation, roughness alters the characteristics of radiated ground motion. This is most easily illustrated for faults with a single Fourier mode of roughness at a given wavelength (bottom panels of Figure 53). One might speculate that faults with a single Fourier mode of roughness will only excite waves at a single frequency; these would appear as a single peak in ground motion spectra. However, this is not the case. Instead, the frequency of waves also depends upon the speed of the rupture relative to the station. That is, the excited waves exhibit a Doppler shift; if the rupture is receding from the station, then the frequency decreases as a function of time, as illustrated in Figure 53. Hence, there is no single, distinct peak in the Fourier spectrum.

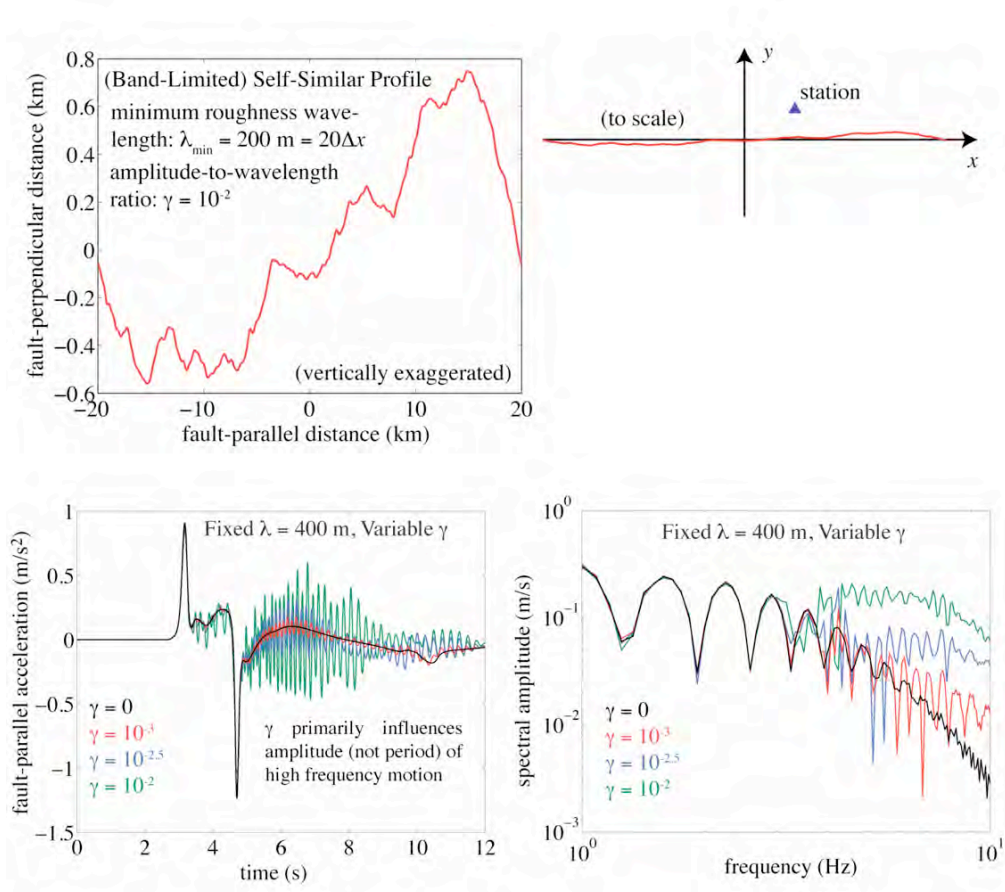


Figure 53. Top panels show non-planar fault model used to explore influence of fault roughness on rupture propagation and production of high frequency ground motion. Bottom panels show Ground acceleration and its Fourier transform for ruptures on sinusoidal faults having various levels of roughness for a given wavelength. Note how the period of the high frequency oscillations in the seismograms increases with time. This is the Doppler shift caused by the rupture propagating away from the station.

Heterogeneous Initial Stress. (Ampuero, Ruiz, and Mai). The main goal of this project is to design efficient procedures to generate realistic initial stress conditions for dynamic earthquake source simulations tailored to ground motion prediction. The scope of the work this year was to formulate a stress generation procedure based on additive residual stresses from background Gutenberg-Richter seismicity, and explore its properties through extensive 2D simulations. Of particular interest was to examine the ability of the model to radiate high frequencies with ω^{-2} spectral decay throughout the whole rupture surface. This is a major improvement with respect to usual dynamic models in which high frequencies come mainly from stopping phases at arbitrarily abrupt rupture ends.

In crack models, the two major mechanisms to produce rupture speed jumps and strong high-frequency radiation are abrupt heterogeneities of fracture energy and inverse square root concentrations of initial stress. The latter, which is the focus of the current study, arises naturally at the edge of previous ruptures. In this study, it is assumed that the heterogeneous fault stress emerges from the background seismicity. A large number of such initial stress distributions are generated by stochastically varying the locations of the hypocenters in the background seismicity. These initial stresses are then taken as initial conditions for 2D rupture simulations on a planar fault governed by slip-weakening friction. The problem is solved numerically with a spectral boundary integral equation method. Finally, the statistical properties of the resulting ruptures are examined, in particular macroscopic source properties such as the far-field radiation spectra derived from the seismic potency rate functions.

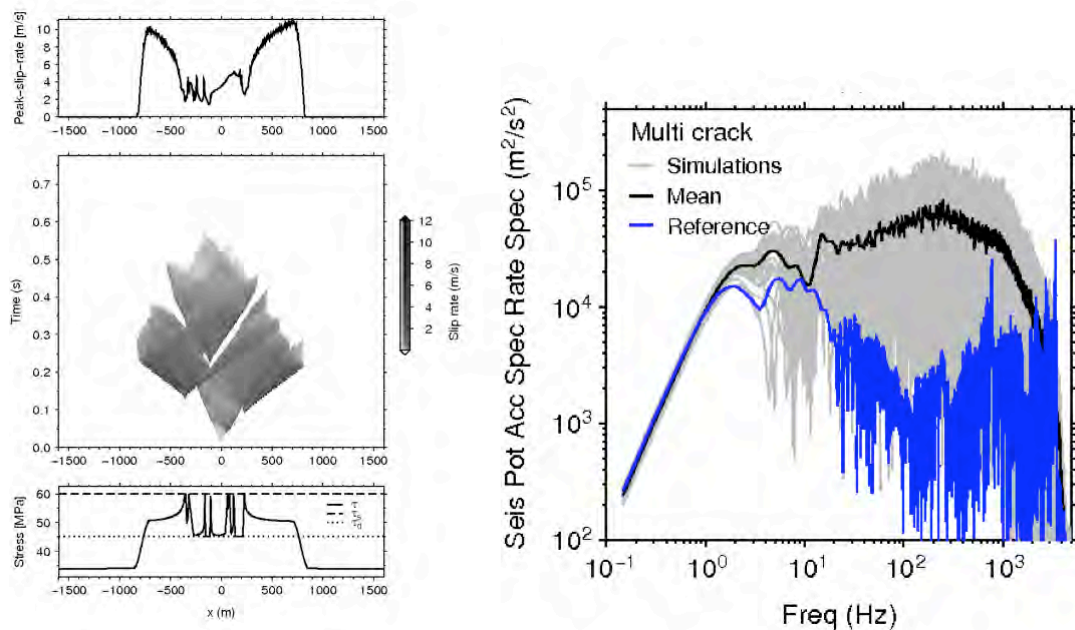


Figure 54. Example of 2D dynamic rupture under heterogeneous initial stress containing a multiple initial cracks (left panels). Each panel on the left shows the assumed initial stress (bottom), the resulting space-time distribution of slip rate (middle) and the spatial distribution of peak slip rate (top). Right panel shows spectra of far-field acceleration derived from the seismic potency rate of 30 simulations with the multi-crack model. The reference model (blue) has uniform initial stress.

This process involves the fitting of a basic spectral model to estimate seismic potency, corner frequency and high-frequency spectral fall-off exponent. Three models are considered: (1) a reference model with very smooth initial stresses, (2) a single-crack model with only one pair of initial stress concentrations from a single previous rupture and (3) a multi-crack model. The single-crack and multi-crack models generate spectra with the usual ω^{-2} high-frequency decay (Figure 54). In contrast, the reference model is deprived of high frequencies, its spectrum falls off as ω^{-3} . The multi-crack model is richer in high frequencies than the single-crack model, it generates higher corner frequencies for the same event magnitude (Figure 54). The enhanced high-frequency content is generated by the multiple strong phases present all along the rupture.

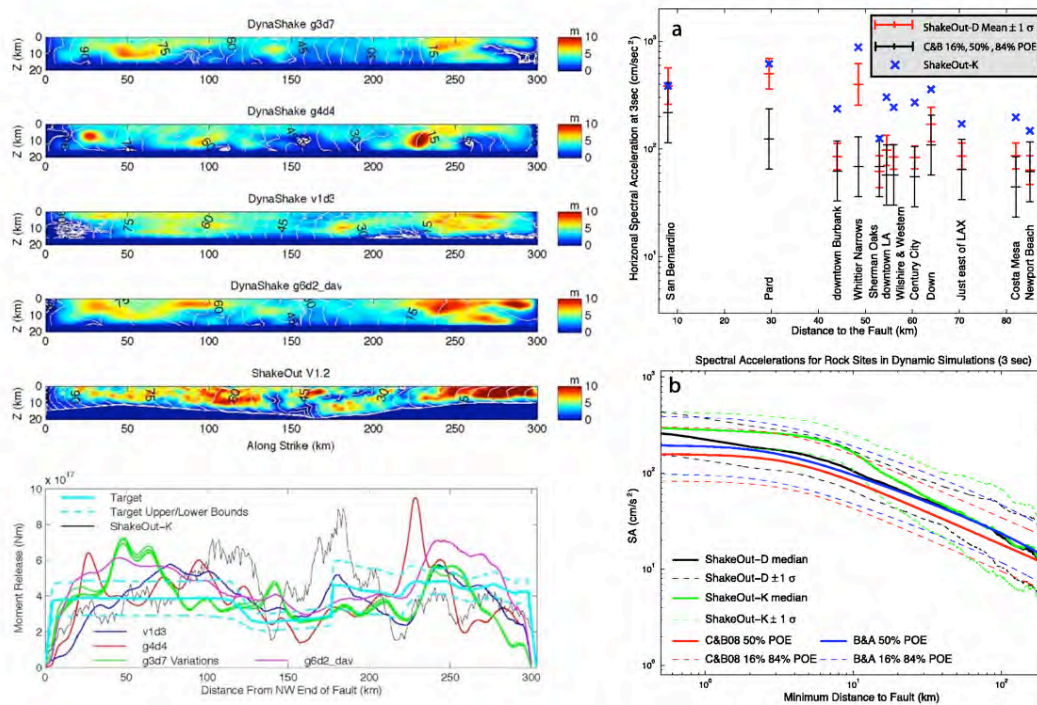


Figure 55. Left panels show slip distributions for 4 of the 7 ShakeOut-D sources and ShakeOut-K. The white contours and contour labels depict the rupture times. The bottom left panel shows distributions of depth-integrated moment density along the fault. Right panels show comparison between 3s-SA at rock sites (top) for 12 selected sites and (bottom) for the mean of ShakeOut-D, for ShakeOut-K, and for CB08 and BA08.

c. Large Scale Ground Motion Simulations

Spontaneous ShakeOut Rupture. (Olsen, Day, Dalguer, Mayhew, Cui, Cruz-Atienza, Roten, Maechling, Jordan, Okaya, and Chourasia). This collaborative effort simulated ground motion in southern California from an ensemble of 7 spontaneous rupture models of large (Mw7.8) northwest-propagating earthquakes on the southern San Andreas fault (ShakeOut-D). Each ShakeOut-D dynamic source was modeled via a slip-matching technique constraining the initial (shear and normal) stress conditions. This technique allowed us to iteratively perform kinematic and dynamic simulations to find initial distributions that approximately conform to the kinematic ShakeOut static slip distribution. The distributions of depth-integrated moment density (left panels

of Figure 55) all reproduce the ShakeOut scenario relatively well. Nonetheless, as Figure 55 illustrates, 4 of the 7 dynamic rupture models vary greatly in their fault-plane spatial-temporal distributions of final slip and rupture time, even though averages are nearly identical. The remaining 3 ShakeOut-D sources are variants of the rupture model 'g3d7', with initial stress conditions that yield similar slip (but somewhat different slip-rate distributions).

The right panels of Figure 55 compare 3s-SA values for the mean of the ShakeOut-D ensemble with those of our ShakeOut-K simulation, at all rock sites within 200 km of the fault rupture. The rock-site distance dependences of ShakeOut-K and ShakeOut-D are very different. While the medians agree well for distances less than about 1 km and larger than about 30 km from the fault, the ShakeOut-K medians are up to 60% larger than those from ShakeOut-D between 1 km and 30 km from the fault. The larger values for ShakeOut-K in this range must reflect characteristics of the ShakeOut-K source model that differ systematically from the ShakeOut-D ensemble. A possible source of this difference would be the presence of strong rupture-induced directivity in ShakeOut-K, which has rupture velocities that are often near or above the Rayleigh velocity. In contrast, rupture-front coherence, and therefore directivity effects, are likely to be substantially reduced by the complex dynamic ruptures that emerge in the ShakeOut-D simulations. Moreover, the ShakeOut-D sources satisfy local energy conservation, which puts constraints on possible rupture velocities, for example, the preclusion of rupture velocities between the Rayleigh and S velocities. ShakeOut-K, being kinematically prescribed, need not obey these energy constraints.

Graves et al. [2008] demonstrate that predicted ground motions in Los Angeles are significantly reduced if one introduces relatively moderate reductions in the average rupture speed of the ShakeOut-K scenario. It is possible that this sensitivity reflects, in part, the presence in ShakeOut-K of segments rupturing at velocities between the local Rayleigh and S-wave velocities, i.e., the range that is energetically precluded. Dynamically simulated sources will naturally avoid the energetically-precluded regime.

Kinematic ShakeOut Comparison. (Bielak, Graves, Olsen, Taborda, Ramirez-Guzman, Day, Ely, Roten, Jordan, Maechling, Urbanic, Cui, and Juve). This project involves a verification of three simulations of the ShakeOut scenario, an Mw 7.8 earthquake on a portion of the San Andreas fault in southern California, conducted by three different groups at the Southern California Earthquake Center using the SCEC Community Velocity Model for this region. Two of these sets were obtained using the finite difference method, and the third, the finite element method. Qualitative and quantitative comparisons were performed. The results are in good agreement with each other: only small differences occur both in amplitude and phase between the various synthetics at ten observation points located near and away from the fault, as far as Santa Barbara. Using the goodness-of-fit criteria proposed by Anderson [2004], all the comparisons scored above 8, with most above 9.2. This score would be regarded as excellent if the measurements were between recorded and synthetic seismograms. Results are also very good for comparisons based on the misfit criteria of Kristekova et al. [2006]. Results from these two criteria can be used for calibrating the two methods for comparing seismograms. In those cases in which noticeable discrepancies occurred between the seismograms generated by the three groups, we found that they are the product of intrinsic differences between the numerical methods used and their implementation. In particular, we found that the major source of discrepancy lies in the difference between mesh and grid representations of the same material model. These differences notwithstanding, the three schemes are consistent, reliable, and sufficiently accurate and robust for use in future large-scale simulations.

Figure 56 shows snapshots at different times of the magnitude of the horizontal velocity at the free surface, calculated as the square root of the sum of squares of the two horizontal components, for

the three groups. Although smaller and larger values are present in the results, the color limits in the figure were set to 0.05 and 2.0 m/s for visual convenience. Other than the differences derived from URS/USC using a smaller domain, all triplets are in good agreement with each other at all times. Discrepancies are practically unnoticeable unless one zooms in and examines the triplets carefully. Those small differences are more visible in wave fronts with amplitudes close to the lower limit of the color scale. See, for example, the back front moving along to the right side of the fault by 60 and 90 s, the frontal wave at 120 s, or the remaining trapped waves in San Fernando Valley by 150 s. Still, these differences are insignificant. One can confidently say that, judging by this comparison, the results of the three sets are, from a regional perspective, equivalent.

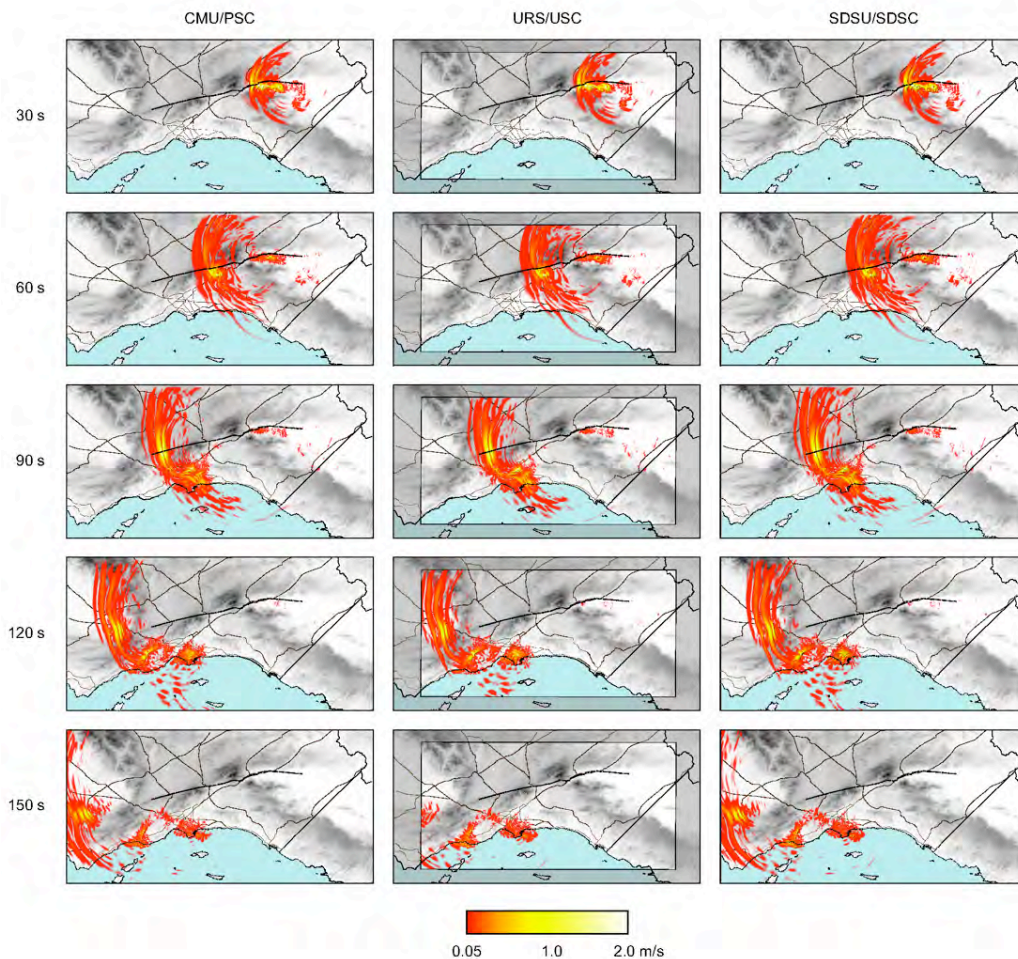


Figure 56. Snapshots of surface horizontal magnitude velocity for the three simulation sets at different times. Left to right shows Carnegie-Mellon group’s simulation running at the Pittsburgh Supercomputing Center, URS group’s simulation running at USC, and San Diego State’s group running at San Diego Supercomputing Center.

d. References

- Baker, J.W., Validation of Ground Motion Simulations for Engineering Applications. Annual report, 2007 Project #07069, 2007.
- Ma, S., G.A. Prieto, and G. C. Beroza, Testing Community Velocity Models for Southern California Using the Ambient Seismic Field, *Bull. Seismol. Soc. Am.*, **98**, 2694-2714, DOI: 10.1785/0120080947, 2008.
- Olsen, K. B., S.M. Day, L.A. Dalguer, J. Mayhew, Y. Cui, J. Zhu, V.M. Cruz-Atienza, D. Roten, P. Maechling, T.H. Jordan, D. Okaya & A. Chourasia, ShakeOut-D: Ground motion estimates using an ensemble of large earthquakes on the southern San Andreas fault with spontaneous rupture propagation, *Geophys. Res. Lett.*, **36**, L04303, doi:10.1029/2008GL036832, 2009.
- Prieto, G. A., and G. C. Beroza, Earthquake Ground Motion Prediction Using the Ambient Seismic Field, *Geophys. Res. Lett.*, **35**, L14304, doi:10.1029/2008GL034428, 2008.
- Purvanche, M.D., A. Anooshehpour, and J.N. Brune, Freestanding Block Overturning Fragilities: Numerical Simulation and Experimental Validation, *Earthquake Engineering and Structural Dynamics* **37**, 791-808, 2008.
- Rood, D.H., J.N. Brune, K. Kendrick, M.D. Purvanche, A. Anooshehpour, L. Grant-Ludwig, and G. Balco, How do we Date a PBR?: Testing Geomorphic Models using Surface Exposure Dating and Numerical Methods. Proceedings 2008 SCEC Meeting, Palm Springs, Ca., Sept. 6-11, 2008.

7. Seismic Hazard and Risk Analysis

The purpose of the Seismic Hazard and Risk Focus Group is to apply SCEC knowledge to the development of information and techniques for quantifying earthquake hazard and risk. Projects in this focus group can have relationships with most of the other focus groups. The strongest linkages are with the Ground Motion Prediction Focus Group, as well as to SCEC special projects such as the Extreme Ground Motion Project, and to PEER special projects such as the Tall Buildings Initiative. Projects that involve interactions between SCEC scientists and members of the community involved in earthquake engineering research and practice are especially encouraged in SHRA. The following three SCEC reports summarize some of the activities in SHRA during 2008-09. A very large number and variety of SCEC projects relate in some way to the goals of SHRA. This report briefly reviews a selection of projects that span this wide range of topics.

a. The Earthquake Source

Seismic Energy, Stress Drop, and the Limits of Strong Ground Motion. (Beroza). A long-standing discrepancy exists in studies of the radiated seismic energy. Some studies find that the scaled energy - the ratio between seismic energy and seismic moment - varies systematically with earthquake size, while others find that it does not. The scaling of seismic energy is an important issue for both the physics of earthquake faulting and for strong ground motion prediction. For earthquake physics, a break in scaling might be diagnostic of a characteristic length scale in the faulting process. For strong ground motion prediction, if large earthquakes radiate seismic energy more efficiently than do small earthquakes, then they have the potential to generate more intense strong ground motion. It is this latter issue that is important for the extreme ground motion project.

This study used an empirical Green's function (eGf) method on the seismic coda in order to investigate possible scaling of the radiated seismic energy with earthquake size. Path effects in the spectra of earthquakes were corrected using a stack of closely located, small earthquakes as an eGf. This approach was applied to four earthquake sequences in western North America that span a magnitude range from Mw 3.0 – Mw 7.1. The estimates of scaled energy are consistent with independent measurements, where available. No dependence in individual seismic energy

estimates on source-station distance was found, which validates the eGf approximation. Energy estimates for the larger events compare with those made independently. A constant scaled energy of 2.4×10^{-5} provides a reasonable fit to all the data, with no systematic variation of the scaled energy with seismic moment required (Figure 57).

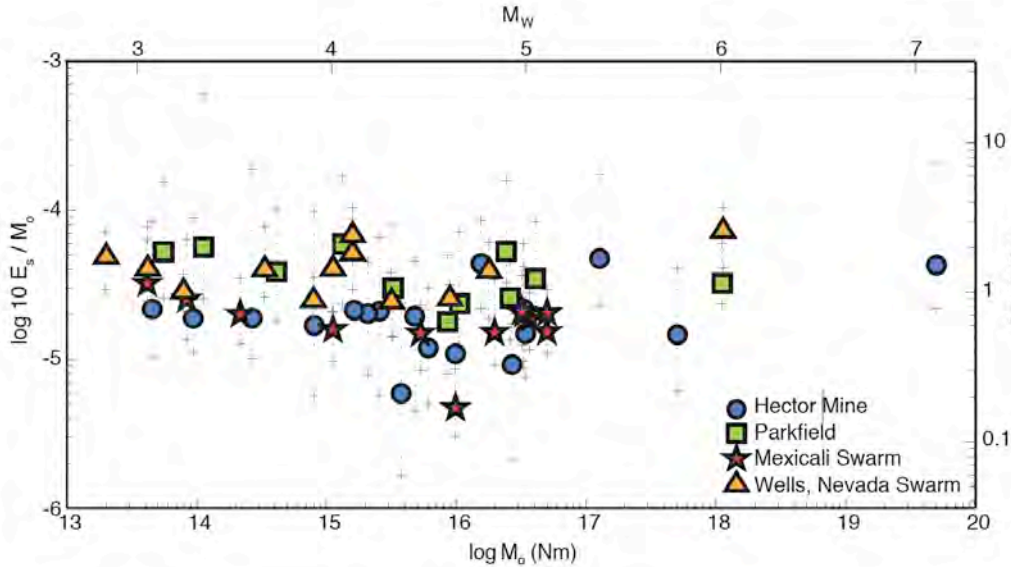


Figure 57. Scaled energy for four earthquake data sets. Large symbols show mean value of scaled energy for each location and event. Grey error bars show 5% and 95% intervals on the interstation scatter. Estimates from this study fall within the range of previous results.

Constant Stress Drop from Small to Great Earthquakes in Magnitude-Area Scaling. (B. Shaw).

Earthquakes span a tremendous range of scales, more than 5 orders of magnitude in length. This study addressed the question whether earthquakes are fundamentally the same across this huge range of scales, or whether great earthquakes are different from small ones. All of the leading magnitude-area scaling relations used in the most recent US national seismic hazard maps assume a breakdown of the scaling seen in small earthquakes, with stress drops increasing for the largest earthquakes. This poses a challenge for earthquake physics and for seismic hazard estimation: what is different in the physics of great earthquakes, and how can we extrapolate from the much more numerous moderate and destructive large earthquakes to the rare and devastating great earthquakes if the physics differs? The study showed that the simplest hypothesis, that earthquake stress drops are constant from the smallest to the largest events, when combined with a more thorough treatment of the geometrical effects of the finite seismogenic layer depth, gives a magnitude area scaling which matches the data very well, and better than the currently used scaling laws which have non-constant stress drop scaling (Figure 58).

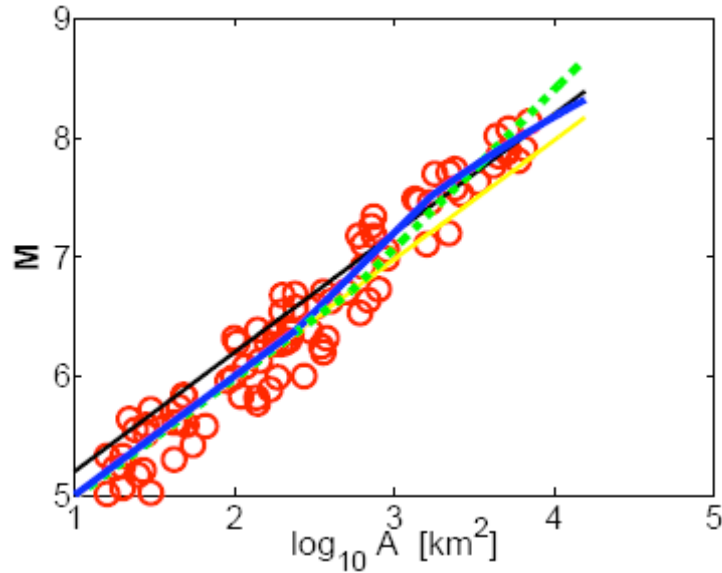


Figure 58. Magnitude area relations for large strike-slip events. Red dots denote magnitude and area of events from [Hanks and Bakun, 2008] database. Solid yellow line is linear [Wells and Coppersmith, 1994] magnitude-area relation, solid black line is linear Ellsworth-B [WGCEP, 2003] magnitude-area relation. Dashed green line is [Hanks and Bakun, 2002] bilinear relation. Blue line is our new proposed scaling relation. Note excellent agreement of solid blue line with data across the whole range of magnitudes. From [Shaw, 2009]

b. Earthquake Ground Motion

The highlights of the 2008-09 research into ground motions are described in the Ground Motion Prediction Report. Important topics at the interface between strong motion seismology and earthquake include the study by Tothong et al. on validation of synthetic ground motions via spectral response quantities, described in that report, and the study on nonlinear response described below.

Nonlinear Site Response Uncertainty in “Rupture-to-Rafters” Broadband Ground Motion Simulations. (*Assimaki*). To quantify the conditions under which nonlinear effects significantly affect the ground surface response, two indexes were developed to describe the near surface soil stratification and the characteristics of input seismic motion at each site during each scenario. Note that the site conditions describe which layers are susceptible to nonlinear effects, while the amplitude and frequency content of input motion identify whether the seismic waves will “see” the soft layers and whether they “carry” sufficient energy at the corresponding frequencies to impose large strains in the soft layers. More specifically, the intensity of incident seismic motion was described by the level of PGA (Peak Ground Acceleration) on rock outcrop (i.e. on ground surface for BS boundary soil conditions), and the frequency content of ground motion was characterized relative to the amplification potential (or transfer function) of the soil profile by means of the so-frequency index which is defined as the normalized cross correlation between the linear elastic transfer function of the profile and the Fourier amplitude of the input seismic motion (Figure 59).

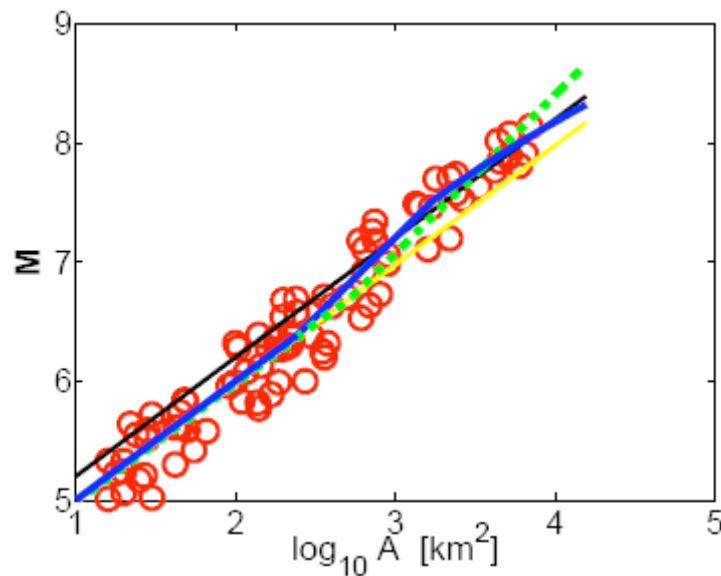


Figure 59. Contour maps of the prediction error (ERR) as a function of the peak ground acceleration (PGARO) on rock-outcrop and frequency index (IF) for selected sites.

c. Modeling of Earthquake Occurrence

ALLCAL – An Earthquake Simulator for All of California. (S. Ward). This physics-based earthquake simulator produces spontaneous, dynamic rupture on geographically correct and complex system of interacting faults. ALLCAL computations now involve a truly 3-dimensional fault system including thrust faults and variable slip down dip. Fault geometry, fault rake, fault slip rate, fault strength and a two parameter velocity weakening friction law are all that ALLCAL requires to generate spontaneous dynamic rupture catalogs that include all fault stress interactions. Fault geometry, rake and slip rate are considered to be data, so fault strength and the two frictional parameters are the only adjustable quantities in the simulator.

The primary product of earthquake simulators is a long series of earthquakes that act as surrogates for real, but time limited catalogs. ALLCAL simulations provide all details of every rupture. For example, earthquake scaling laws, M_{\max} and b-value that are input into most earthquake hazard estimates are outputs of the simulator. Agreements between observed and synthetic scaling relations such as Area versus Moment, give evidence that ALLCAL results are meaningful. The earthquake potential for California derived from the earthquake simulator is shown in Figure 60.

The model is tuned with real earthquake data. Largely, the tuning is accomplished by comparing computed earthquake recurrence intervals versus magnitude to observed intervals. Paleoseismic data constrain earthquake simulators in two ways: 1) through input of measured slip rates, and 2) by comparison of computed recurrence interval and slip per event with field measurements provided through projects like SoSAFE. While fault slip rate is a direct constraint, slip per event and recurrence interval are applied indirectly. In the simulator, these observables spring from the fundamental physics of the system through fault slip rate, fault strength and friction law parameters. Like slip rate, fault strength is thought to be preserved through many earthquake cycles. Strong fault segments tend to have larger slip per event earthquakes with longer recurrence intervals, but the correlation is imperfect because of the non-linear nature of the system and the

complex memories of all preceding earthquakes. For these reasons, iterative segment strength adjustments are made to the model to match reasonably well paleoseismic recurrence data.

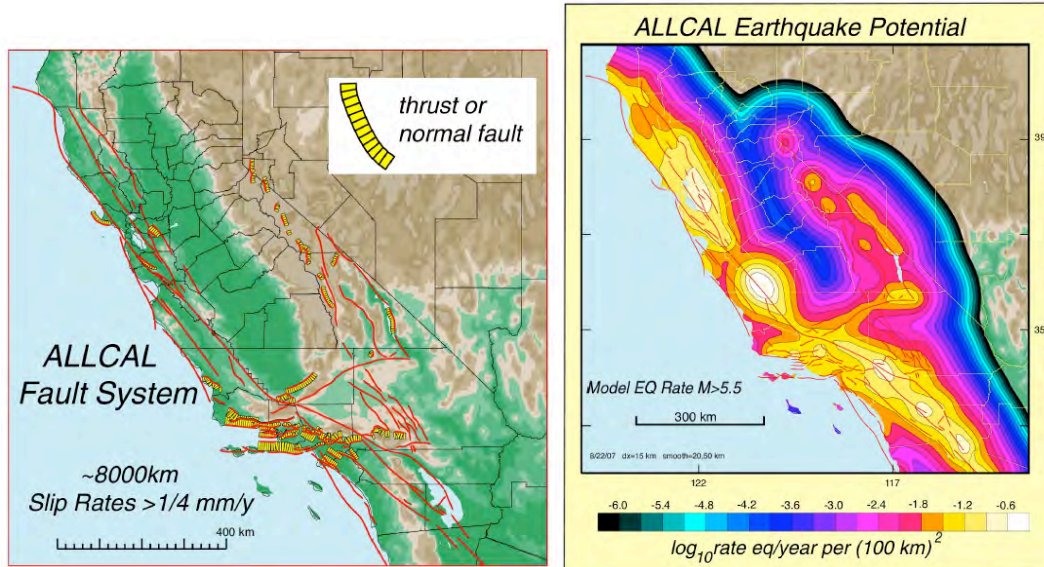


Figure 60. Earthquake potential (right) derived directly from the ALLCAL earthquake simulator (left). In the simulator, earthquakes occur only on the specified faults. Earthquake hazard and potential have been windowed off fault. Instead, geodetic information is used to fill in off fault hazard.

Modeling Seismic Moment Rate in San Andreas Fault – Great Basin System: Combination of Seismological and Geodetic Approaches. (Zaliapin, Anderson, Kreemer, Pancha). It has been shown that the geodetic and seismological estimations of moment release may differ significantly on a regional level: the ratio between the observed and geodetically predicted moment releases varies from 0.1 to 100. Such discrepancies can be explained by the heavy-tailed distribution of seismic moment [Zaliapin et al., 2005a,b; 2006; 2007].

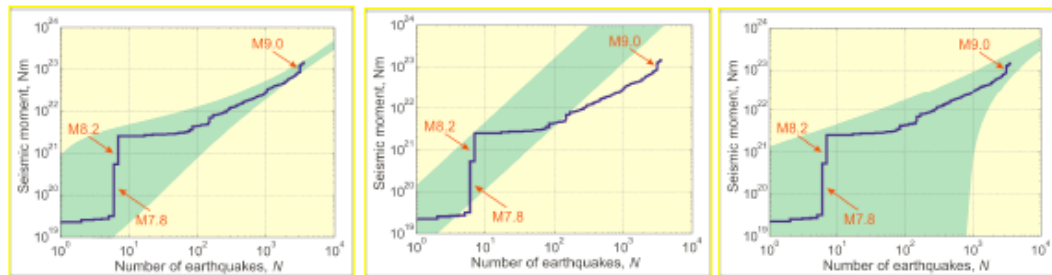


Figure 61. Alternative models for seismic moment release: tapered Pareto model (left panel), pure Pareto model (center panel), and the classical Normal model (right panel).

The practical necessity of the tapered Pareto distribution is illustrated in Figure 61, which compares the long-term moment distribution predictions based on Normal, Pure Pareto, and tapered Pareto distributions and the observed world-wide seismic moment release during 1976-2008 according to the NEIC catalog. The tapered Pareto model (left panel) correctly accounts for short-term and long-term moment release. The pure Pareto model (center panel) overestimates the long-term release, and the classical Normal model (right panel) underestimates the short-term release. The validity of a moment release model is based on the seismic coupling ratio that is defined as the ratio between the observed and predicted moments. Under this study's approach, the predicted moment is the geodetic long-term moment release according to our strain model. The currently accepted probabilistic approximation to the long-term release is given by the expected moment according to the tapered Pareto distribution. It has been shown by the PIs during previous SCEC projects that the approximation is very close for large regions and long time-intervals. This year investigation has shown though that this approximation overestimates the moment release in small regions, which is illustrated on the left side of Figure 61.

The currently accepted model for moment release gives wrong estimations within small regions. Each point in the figure corresponds to an observed regional seismic coupling; shades depict the model predictions. To account for this discrepancy, the investigators suggest a modified model that takes into account the fact that the observed number N of earthquakes in a region is also random and obeys a heavy-tailed discrete distribution. The distribution of N is chosen based on the observed seismicity within the SAF-GB region. The results of this modified model are illustrated on the right side of Figure 62.

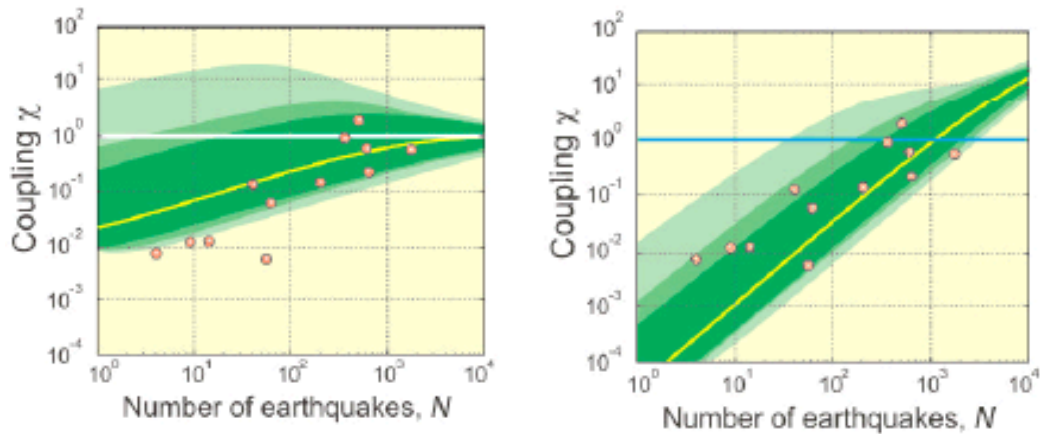


Figure 62. Distribution of seismic coupling ratio, defined as the ratio between the observed and predicted moments, for tapered Pareto distribution (left) and modified tapered Pareto distribution (right).

d. Building Response and Loss Estimation

Response of Steel Buildings to the Ground Motions of the ShakeOut Scenario. (Krishnan, Muto, Graves). The scenario earthquake, chosen based on a wide variety of observations and constraints, was a magnitude 7.8 earthquake on the San Andreas fault with rupture initiating at Bombay Beach and propagating northwest through the San Geronio Pass a distance of roughly

304 km, terminating at Lake Hughes near Palmdale, sections of the San Andreas fault that last broke in 1680, 1812, and 1857. Through community participation in two Southern San Andreas Fault Evaluation (SoSAFE) workshops organized by the Southern California Earthquake Center (SCEC), a source model specific to the southern San Andreas fault was constructed with constraints from geologic, geodetic, paleoseismic, and seismological observations.

Using this source model, Rob Graves simulated 3-component seismic waveforms on a uniform grid covering southern California (Graves et al. 2008). Peak velocities of the synthetic ground motion were in the range of 0-100 cm/s in the San Fernando Valley, and 60-180 cm/s in the Los Angeles basin (Figure 63). Corresponding peak displacement ranges were 0-100 cm and 50-150 cm. For the shakeout drill, USGS commissioned the investigators to provide a realistic picture of the impact of such an earthquake on the tall steel buildings in southern California. They selected 784 sites across southern California to place 3-D computer models of three steel moment frame buildings in the 20-story class (an existing building designed according to the 1982 UBC, the same building redesigned using the 1997 UBC, and a hypothetical L-shaped building also designed according to the 1997 UBC, and analyzed these models subject to the simulated 3-component ground motion, orienting them in two different directions, considering perfect and imperfect realizations of beam-to-column connection behavior.

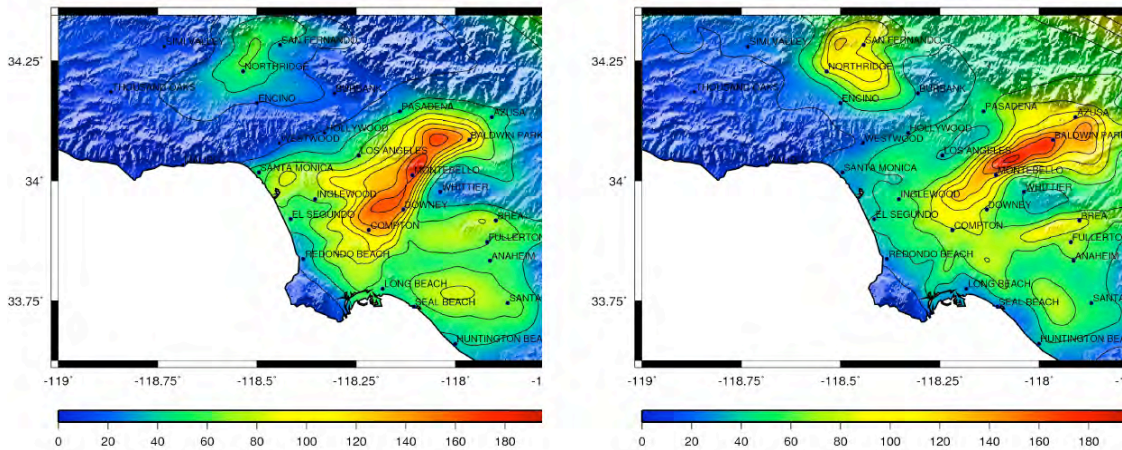


Figure 63. San Andreas fault shakeout scenario earthquake simulation: Peak ground motion under a S-to-N rupture (east and north components of velocity in cm/s.)

Figure 64 shows a map of average peak interstory drift ratios for the 12 structural models considered in this study (3 buildings x 2 orientations x 2 connection susceptibility assumptions). Structural models hypothetically located at 784 analysis sites spread across the Los Angeles basin were analyzed. The results indicated that 7% of these could be immediately occupied after the earthquake (IO, blue zone); 34% would have damage requiring building closure, but no loss of life (LS, green zone); 35.8% would have serious damage resulting in loss of life, but collapse would be prevented (CP, yellow zone); 10.5% would have to be red-tagged and may be on the verge of collapse (RT, red zone); and 12.7% would have collapsed (CO, pink zone).

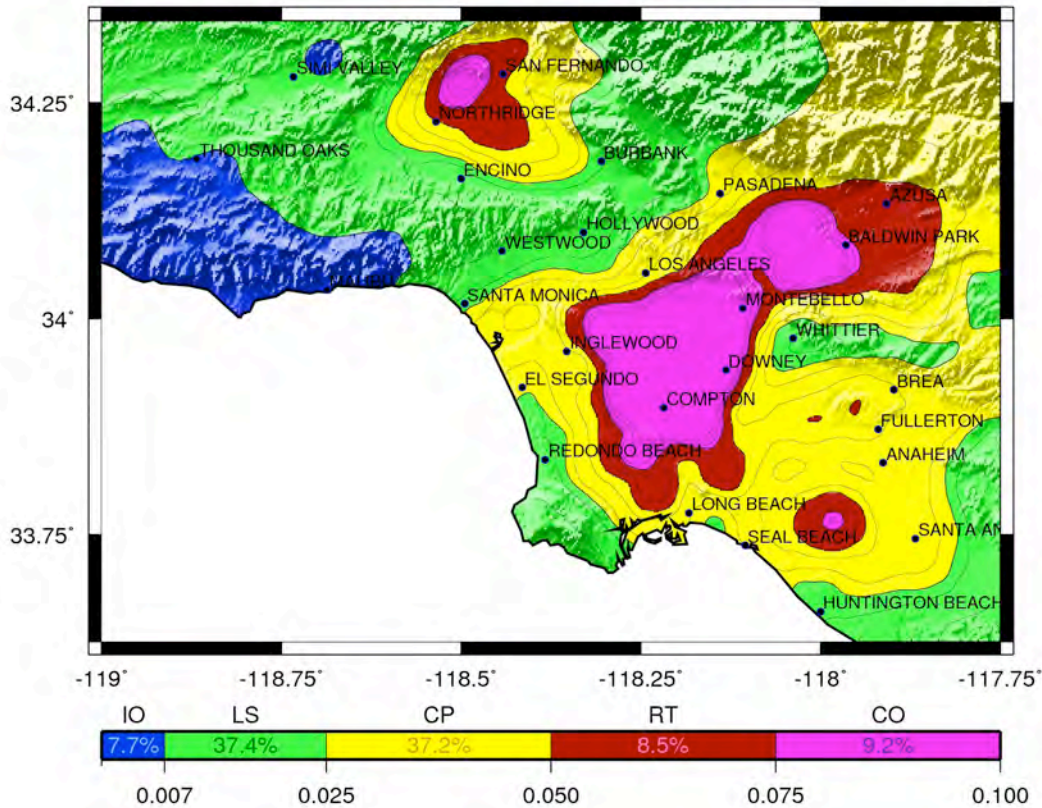


Figure 64. Distribution of peak interstory drift ratios, demarked into building damage states.

Implementation of HAZUS® to Evaluate Societal Impacts Associated with the Uniform California Earthquake Rupture Forecast (UCERF) Model & the Next Generation of Attenuation (NGA) Relationships. (Seligson). The objectives of the reframed study were two-fold; to re-visit HAZUS® loss estimates for a Puente Hills scenario earthquake (studied extensively under SCEC funding in 2004-2005) relative to 1) recently developed physics-based ground motions developed by Rob Graves, and 2) recent enhancements made to HAZUS® inventory data for southern California for the “ShakeOut” earthquake scenario.

Figure 65 provides a comparison of HAZUS® total direct economic losses estimated for the various M7.15 Puente Hills scenario ground motions (for the area within the Graves’ study limits), using the enhanced “ShakeOut” inventory data. Within HAZUS®, total direct economic loss includes building and content losses, as well as inventory loss and income losses (which includes relocation costs, income losses, wage losses and rental income losses). For the physics-based ground motions, losses are largest for V2 and V5, the scenarios with the shortest rise time (V2) and the largest rupture velocity (V5). The only attenuation-based ground motions producing losses on the same order of magnitude as the largest physics-based ground motions are BJJ 1997; the NGA ground motions produce losses approximately half as large as the largest physics-based ground motions.

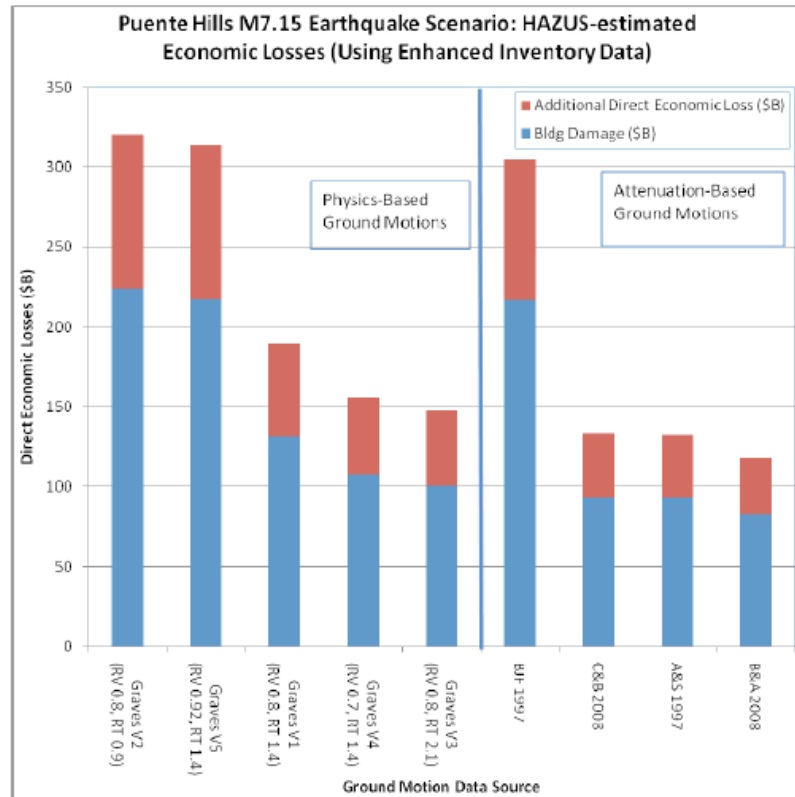


Figure 65. Comparison of Total HAZUS®-estimated Direct Economic Losses (within the Graves’ grid limits) for the M7.15 Puente Hills Scenario Earthquake for various Sources of Input Ground Motion Data

e. References

Hanks, T. C. and W. H. Bakun, M-logA Observations for Recent Large Earthquakes, *Bull. Seismol. Soc. Am.*, 98, 490-494; DOI: 10.1785/0120070174, 2008.

Wells, D. L., and Coppersmith, K. J., New empirical relationships among magnitude, rupture length, rupture width, rupture area, and surface displacement, *Bull. Seismol. Soc. Am.*, 84, , p. 974-1002, 1994.

Zaliapin, I.V., Kagan, Y.Y., and Schoenberg, F.P., Approximating the distribution of Pareto sums, *Pure Appl. Geophys.*, 162, 1187-1268, 2005a.

Zaliapin, I.V., Kagan, Y.Y., and Schoenberg, F.P., Evaluating the rate of seismic moment release: A curse of heavy tails. Abstract of the Annual 2005 SCEC meeting, Palm Springs, September 11-14, 2005b.

Zaliapin, I.V., Kumar, S., Kagan, Y.Y., and Schoenberg, F.P., Statistical Modeling of Seismic Moment Release and Moment Deficiency. Southern California Earthquake Center (SCEC) 2006 Annual Meeting, September 10-13, Palm Springs, California, 2006.

Zaliapin, I.V., Kumar, S., Kagan, Y.Y., and Schoenberg, F.P., Statistical Modeling of Seismic Moment Release in San Andreas Fault System. Southern California Earthquake Center (SCEC) 2007 Annual Meeting, September 9-12, Palm Springs, California, 2007.

C. Special Projects

In addition to the disciplinary groups, and cross-cutting focus groups, SCEC has undertaken a number of special projects, which are focused on problems with well-defined short-term research objectives, but are nevertheless consistent with SCEC goals. These include the *Southern San Andreas Fault Evaluation (SoSAFE)*, the *Collaboratory for the study of Earthquake Predictability (CSEP)*, the *Working Group on California Earthquake Probabilities (WGCEP)*, the *Extreme Ground Motion Project (ExGM)*, and the *Community Modeling Environment (CME)*.

1. Southern San Andreas Fault Evaluation

The Southern San Andreas Fault Evaluation (SoSAFE) Project is in its third year of work towards better defining the past 2000 years of earthquake occurrence, as well as slip rates along this hazardous and intensively scrutinized fault system. The information obtained is enhancing our ability to forecast the occurrence of future destructive earthquakes along the fault system and to better predict aspects of fault system behavior. Work conducted by SoSAFE researchers is being funded by the USGS Multi-Hazards Demonstration Project (MHDP) through SCEC. SoSAFE paleoseismologists are now making systematic use of the NSF-funded B4 Project LiDAR data set along the entire southern San Andreas and San Jacinto, throughout the B4 coverage area. The SoSAFE Project furthermore links with NSF's GeoEarthScope and its funding of geochronological support, using radiocarbon and other new dating facilities and methods. GeoEarthScope has recently also acquired LiDAR along many other major faults, hence SoSAFE work with B4 data has proven to be pioneering integrative science within the SCEC framework.

On January 8-9, 2007 for the sesquicentennial commemoration of the great 1857 Fort Tejon earthquake on the southern San Andreas fault, the Southern California Earthquake Center (SCEC) held a SoSAFE science workshop. Four SoSAFE workshops have been held so far - one at each SCEC Annual Meetings; 2006, 2007, and 2008; the latest one was held jointly with Fault Systems in early 2008.

The next SoSAFE workshop will be held at the SCEC Annual Meeting in 2009. Discussion at the upcoming SoSAFE workshop in Sept. 2009 will consider the future direction of this special project in this context, as did the Sept. 2008 workshop. The leadership transition from Ken Hudnut, who led SoSAFE from its inception in Sept. 2006 through March 2009, to Co-Leaders Tom Rockwell and Kate Scharer, has begun and the new Co-Leaders will lead the upcoming workshop.

Coordinated studies employ novel dating methods and emphasize cross-validation of methods and field sampling techniques to gain a better understanding of actual uncertainties in geologically estimated slip rates over time spans of up to several tens of thousands of years. For example, studies on the San Andreas and San Jacinto faults have used cosmogenic and U-series dating, as well as soils analysis.

Another SoSAFE highlight is the exciting result from Zielke and Arrowsmith [2008] that numerous, subtle 5m offsets are present along the Carrizo Plain section of the San Andreas fault (Figure 65). These offsets are about half the ~10 m slip attributed to the 1857 Fort Tejon earthquake by Sieh [1978]. This new result agrees well with new paleoseismic recurrence from the Bidart fan paleoseismic site [Akciz et al., 2009]. The net impact of these findings is that great earthquakes on the southern San Andreas fault are about twice as frequent as previously thought (Figure 66). Slip-rate studies within the Big Bend and south have focused on longer time-scales that integrate earthquake behavior. One of these sites, near Palmdale, promises to resolve a long-standing debate on the rate of slip (25 vs. 35 mm/yr) of the San Andreas through the Transverse Ranges [Sgriaccia and Weldon, research in progress].

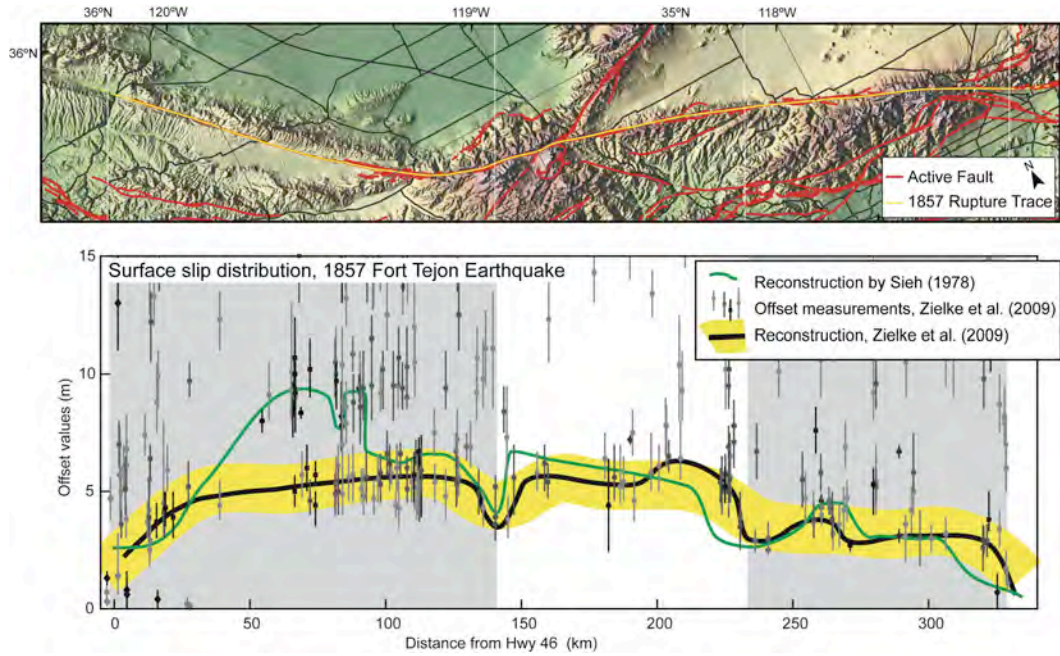


Figure 66. Results from Akciz et al. showing 1857 fault rupture yellow (upper panel). Lower panel shows previous slip reconstruction in Green [Sieh, 1978] and revised reconstruction in black [Zielke, Arrowsmith, Grant-Ludwig, and Akciz] of slip in the 1857 Fort Tejon earthquake.

(Grant & Sieh, 1994)		(Akciz et al., in review)		Average time interval is 137±44 years
3 trenches		Same 3 trenches		
14 C-14 analyses		28 new C-14 analyses		
Events	Dates	Events	Dates	
A	1857	A	1857	
B	1405-1510	B	1640-1857	
C	1277-1510	C	1545-1630	
D	1277-1510	D	1370-1425	
E	1218-1276	E	1285-1340	
F	after 200 BC	F	after 200 BC	
G	after 200 BC	G	after 200 BC	

Figure 67. Old vs. new San Andreas Fault earthquakes and dates based on paleoseismological work at the Bidart fan. The revised record indicates more frequent earthquakes and is corroborated by geomorphic analysis of offset features.

In the San Andreas case, a group worked to re-examine the age of an offset alluvial fan at Biskra Palms Oasis that had been previously dated by similar cosmogenic methods. At this location, the geodetic slip rate is nearly twice as high as geologic; both rates are reasonably well constrained. This site therefore provides a testing ground for studying the uncertainties in all methods used, and in addressing possible slip rate variation through time. At Biskra Palms, two papers have reached the point of completion and will be published together soon in GSA Bulletin. – notably, both papers are first-authored by graduate students, Whitney Behr at USC and Kate Fletcher at U. C. Berkeley. In the slip rate studies on the San Jacinto, special emphasis is being given to the question of whether slip rates vary through time.

Work at the Frazier Mountain site has been another major highlight of SoSAFE-funded research. SoSAFE has funded a series of other trenching studies at sites along the San Andreas and San Jacinto faults during the past two years and more in the present third year. In addition to workshops, numerous field site visits and field trips to foster collegial discussion at sites of active trenching and studies of offset channels have been conducted through SoSAFE as well. Part of the emphasis of the early 2008 workshop was on the in-field scientific review process, as well. Through these interactions, the paleoseismic community within SCEC has been able to reach consensus on a number of high priorities for future research. The highest priority identified at the first SoSAFE workshop, of obtaining more and better data in the northern Big Bend, has already been addressed well by the progress at Frazier Mountain.

In its first year, the SoSAFE group contributed heavily to definition of the ShakeOut earthquake scenario source description. Along with the more recent work highlighted here, these early successes of SoSAFE have been followed by much work that is still in progress.

We note that many other projects were also funded by the SCEC regular core funds, and also that many studies being conducted as part of the larger SoSAFE effort are also funded by the NSF and USGS NEHRP external program. SoSAFE workshops typically present research results from broad studies that are being conducted with support from these other sources as well as from the USGS MHDP special project funds.

Special project funding has been provided by USGS MHDP for the originally agreed-upon 3 years, and it should be expected to taper down after the end of the third year of funding. The USGS MHDP is necessarily moving on to emphasize other priorities, and the FY10 budget allocation for MHDP was not increased. Contingent on the amount of support the SoSAFE investigators are able to match against the USGS MHDP funds, the ramp-down rate may vary; that is, continued or increased matching would be taken as a healthy indication, and would encourage USGS to maintain ongoing support rather than ramp it down sooner.

2. Collaboratory for the Study of Earthquake Predictability

The special project Collaboratory for the Study of Earthquake Predictability (CSEP) is developing a global program of research on earthquake predictability through prospective, comparative testing of scientific prediction hypotheses in a variety of tectonic environments. CSEP is an open, international partnership, and our purpose is to encourage participation by scientists and research groups from other countries who are interested in the scientific study of predictability. To understand earthquake predictability, scientists must be able to conduct prediction experiments under rigorous, controlled conditions and evaluate them using accepted criteria specified in

advance. Retrospective prediction experiments, in which hypotheses are tested against data already available, have their place in calibrating prediction algorithms, but only true (prospective) prediction experiments are really adequate for testing predictability hypotheses.

The CSEP core group at USC developed during the year 2007 the first two released versions of the CSEP Testing Center Software. At the beginning of 2008, the testing center (Schorlemmer & Gerstenberger, 2007) at USC was hosting several experiments for the testing area of California: First, CSEP inherited a variety of forecasts created for the RELM (Field et al., 2007) experiment (5-year forecasts). Second, two 1-day forecast models were installed in the testing center, ETAS and STEP. Third, for intermediate-term forecast testing, CSEP started a new 3-month model class and seven forecast models were installed in the testing center. CSEP was able to complete the initial phase of the collaborative development in 2007 with an operational testing center and different experiments underway.

In 2008-09, CSEP kept the pace and expanded into all directions. New testing regions were established (Western Pacific, Japan, and a global testing program). New testing procedures were introduced and the testing center software was optimized for processing speed and memory usage. Several meetings were held at USC and INGV, Rome, and a collaboration between SCEC and the Earthquake Research Institute (ERI) of the University of Tokyo was established for erecting a testing center at ERI.

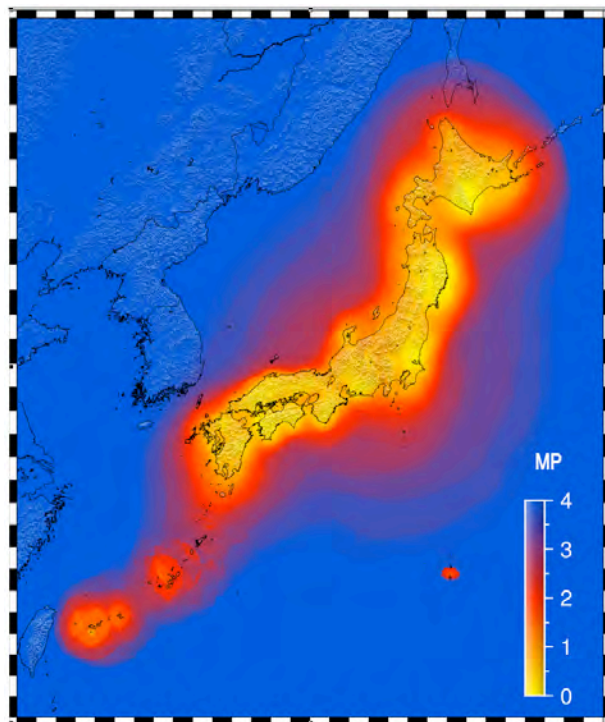


Figure 68. Probability-based magnitude of completeness of the JMA network on 1 April 2008.

a. Collaboration Between SCEC and ERI

D. Schorlemmer was invited as research fellow to spend the summer at ERI. During this visit, he conducted a full characterization of the network recording completeness of the network of the Japan Meteorological Agency (JMA), employing the PMC method (Schorlemmer & Woessner,

2008). The results of this study were used to define the Japanese testing region. Although the results confirmed that the JMA network is a high-quality network with a completeness magnitudes spatially below (Figure 68), the CSEP group in Japan (N. Hirata, K. Nanjo, H. Tsuruoka) decided to first mimic the experiments from California and to use the same magnitude ranges for forecasting and testing. Analogous to the procedure in Italy and California, the testing region was defined to capture not only Japan but also a region of approx. 100 km around it to allow testing of hazard-relevant forecasts.

ERI established an agreement with JMA for the use of the JMA catalog data for the forecast experiments in CSEP. This agreement also includes that CSEP researchers can freely use the JMA data for model development. ERI also invited software engineer F. Euchner from the European CSEP team at ETH to help installing the CSEP testing center software. The installation was finished during the visit of both CSEP members and the system went operational as a prototype on 1 September 2008, the Japanese Earthquake Preparedness Day, with three 1-year models: A “Relative Intensity” (RI) model provided by K. Nanjo, “TripleS” by J. Zechar, and “JALM” by D. Schorlemmer. All three models are essentially smoothed seismicity models, except for JALM, which additionally uses spatially varying b-values for forecast generation. Because the latency of the JMA catalog is up to 6 months before the final publication of earthquake locations, the CSEP group decided to first run a retrospective experiment to test the functionality of the Japanese testing center.

b. Other Testing Regions

Besides the new Japanese testing region, CSEP established two new testing regions for which experiments are hosted at the testing center at USC: The Western Pacific region and global testing (see Figure 69).

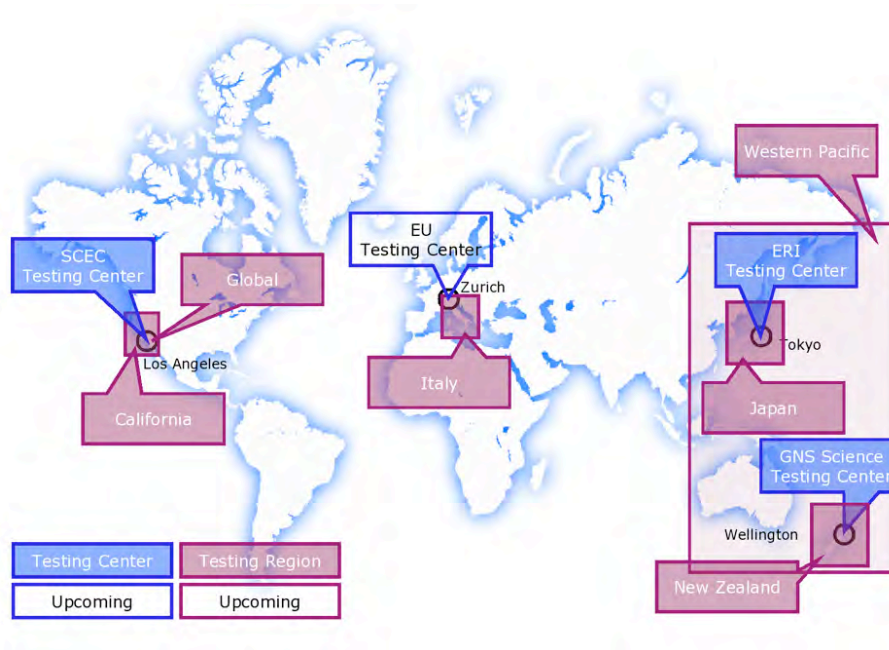


Figure 53. Distribution of CSEP testing regions and testing centers at the end of 2008.

Because Y. Kagan and D. Jackson were performing earthquake forecasting and testing in the Western Pacific region, CSEP decided to include this experiment in the testing center to ensure long-term processing of this ongoing experiment and to open this experiment to other researchers with competing models. Furthermore, this testing region can be considered a blueprint for global testing as it already covers 55% of global seismicity and only a global catalog can be used for the experiment. In addition to the models by Y. Kagan and D. Jackson, W. Marzocchi and A. Lombardi installed their Double-Branching Model, and J. Zechar provided the TripleS model. For historical reasons the Western Pacific region is divided into a northern and a southern part; CSEP decided to not change the original setup.

After successful implementation of the Western Pacific region, CSEP implemented a prototype global testing region. A consensus between modelers was reached to start global testing with a low-resolution but regular grid. Several other possibilities were discussed during the Global Testing Meeting, from high-resolution grids to a grid with varying resolution to allow for detailed forecasts in high-seismicity areas but to not force modelers to provide high-resolution forecasts in areas of sparse seismicity. Two models were submitted: TripleS and Double-Branching.

To prepare the future extension of the global program to high-resolution testing, a 0.1x0.1 degree grid was proposed but is still debated. The primary goal of such a regular high-resolution grid is to match with local testing regions such that each global model can be automatically used as a regional model. For this purpose, all local testing regions were designed to exactly match with this proposed global grid. The California, Italy, and Japan grid were originally defined in a way that they match, but the New Zealand testing was shifted by 0.5 degrees in latitude and longitude. Because only preliminary testing was underway in New Zealand, no experiment had to be stopped or canceled.

c. Developments in Italy

The Italian CSEP group organized a meeting on 27 October 2008 to solicit model submissions for the upcoming experiments and to reach a consensus of the rules for each of the proposed experiments. Because the RELM experiment received a high attention due to the large variety of submitted forecasts, the CSEP group decided to repeat such an experiment in Italy. For the RELM forecasts, researchers were able to use input data for their forecasts that are currently not provided by CSEP for models running in the testing center. This allows for the large variety of forecasts because geodetic and geologic data were also used. Furthermore, providing only a forecast (as numbers) is easier for modelers than to install codes in the testing center. Two experiments will be conducted, one for 5-year forecasts and the second one for 10-year forecasts. A deadline for model submission was set to July 2009 and testing is projected to start in August 2009. Besides the experiment for RELM-type forecasts, the European testing center will open for model installation. Defined experiments encompass 1-day, 3-month, and 1-year tests.

d. New Testing Procedures

In early 2008, the CSEP development team improved the testing codes implemented in the CSEP testing center software distribution for speed and memory usage. This, and the previous improvement accomplished in 2007, helped to reduce the computer time for performing all tests and to allow for easier recomputations.

On the scientific side, alarm-based testing was introduced using different testing procedures: Molchan Test (Molchan, 1990, 1991), ROC Diagram (Mason, 2003), and the Area Skill Score (Zechar & Jordan, 2008, 2009). Alarm-based testing was introduced to the testing regions of California, Western Pacific, and the global program. The new tests were formulated in a way such that they

are also used for evaluating the rate-forecasting models (Schorlemmer et al., 2007); this provides further evaluations of the models and will help better understand the performances of the various models.

e. Software Development

The software development is the main focus of the current CSEP development as a functioning infrastructure is the base line for any CSEP related operation. The software development team decided to release new testing center software versions in a 3-month cycle. One month before the release, no new features will be added to the system and the particular system will be tested and checked for roughly one month. Only after successfully passing the acceptance tests for the software system, the new codes will be released.

A large portion of the time of the CSEP main developer M. Liukis was needed to support modelers installing their earthquake forecast codes in the system and to adapt the system capabilities to support the models such that they can be seamlessly integrated.

In parallel to the development of the operational system, J. Yu worked on the result viewing component of the CSEP website to improve the user experience for this website.

f. Results

In mid-2008, the first half of the RELM experiment was accomplished (2.5 years of the 5-year experiment). The CSEP group decided to prepare an intermediate report to inform the modelers and the wider scientific community about the results and the experiment. This report was presented at many meetings and was also submitted to the special volume of Pure and Appl. Geophys. about the Evison symposium held in early 2008 in Wellington, New Zealand, and covering many aspects of statistical seismology (Schorlemmer et al., in print).

In February 2008, a swarm of several M5+ earthquakes hit the Baja California area. Fortunately for CSEP, this swarm was in the southern part of the California testing region and offered a great opportunity to evaluate the two 1-day models for California. The surprising result was that, although the STEP model was more strongly focusing the projected aftershock area, the ETAS model clearly showed better performance. This is because the STEP model's forecasts were off by some tens of kilometers to the east (see Figure 3). Discussion with the author M. Gerstenberger revealed that most likely a software bug caused the model to shift the forecast in the grid. As a consequence, M. Gerstenberger is working on a new version of the model for later submission. This result was also reported to the USGS that currently uses the STEP model for their "tomorrow's earthquake forecast" webpage.

g. Outreach and Communication

CSEP held three meetings during the year 2008: A testing meeting to discuss ongoing testing procedure developments and to agree on future tests to be implemented; a global testing meeting to prepare a global testing program; and a meeting in Rome to prepare testing in Europe, to solicit models, and to find a consensus in the testing rules for Europe.

Besides these meetings, CSEP was present at all major conferences and hosted several scientific sessions at these meetings. In 2008, CSEP sessions were held at the Evison symposium in Wellington, New Zealand and at the SSA annual meeting in Santa Fe, USA. Results of CSEP testing were presented at all of these meetings and a report about the first half of the RELM experiment was compiled.

h. References

- Field, E. H., Overview of the Working Group for the Development of Regional Earthquake Likelihood Models (RELM), *Seismol. Res. Lett.* **78**, 7–16, 2007.
- Mason, I. B., Binary events, in Forecast Verification, 37–76, eds. Jolliffe, I.T. & Stephenson, D.B., Wiley, Hoboken, 2003.
- Molchan, G. M., Strategies in strong earthquake prediction, *Phys. Earth Planet. Inter.*, **61**, 84–98, 1990
- Molchan G. M., Structure of optimal strategies in earthquake prediction, *Tectonophysics*, **193**, 267–276, 1991.
- Schorlemmer, D., & M. Gerstenberger, RELM Testing Center, *Seismol. Res. Lett.*, **78**, 30–36, 2007.
- Schorlemmer, D., M. Gerstenberger, S. Wiemer, D. Jackson, & D. Rhoades, Earthquake Likelihood Model Testing, *Seismol. Res. Lett.*, **78**, 17–29, 2007.
- Schorlemmer, D., & J. Woessner, Probability of Detecting an Earthquake, *Bull. Seismol. Soc. Am.*, **98**, 2103–2117, 2008.
- Schorlemmer, D., J. Zechar, M. Werner, E. Field, D. Jackson, T. Jordan, & the RELM Working Group (in print), First Results of the Regional Earthquake Likelihood Models Experiment, *Pure and Appl. Geophys.*, 2009.
- Zechar, J. D., and T. H. Jordan, Testing alarm-based earthquake predictions, *Geophys. J. Int.*, **172**, 715–724, doi 10.1111/j.1365-246x.2007.03676.x, 2008.
- Zechar, J. D., and T. H. Jordan, The area skill score statistic for evaluating earthquake predictability experiments, *Pure Appl. Geophys.*, 2009 (in press).

3. Extreme Ground Motion

Extreme ground motions are the very large amplitudes of earthquake ground motions that can arise at very low probabilities of exceedance, as was the case for the 1998 PSHA for Yucca Mountain. The Extreme Ground Motion (ExGM) project, is a three-year study, sponsored by the Department of Energy, that investigates the credibility of such ground motions through studies of physical limits to earthquake ground motions, unexceeded ground motions, and frequency of occurrence of very large ground motions or of earthquake source parameters (such as stress drop and faulting displacement) that cause them. A particular interest to ExGM, which applies more generally to the Fault and Rupture Mechanics, Ground Motion Prediction, and Seismic Hazard and Risk Analysis focus groups, is why crustal earthquake stress drops are so sensibly constant and so much less than the frictional strength of rocks at mid-crustal depths. The main SCEC disciplinary and focus groups that work on this project are Geology – especially fault zone geology; Faulting and Mechanics of Earthquakes, Ground-Motion Prediction, and Seismic Hazard and Risk Analysis. Elements of this project are discussed above within these focus group reports.

a. 3D Rupture Dynamics Code Validation Workshop

Numerical simulations of earthquake rupture are used by SCEC researchers for a variety of purposes – from ground motion prediction, such as in the Extreme Ground Motion and PetaSHA DynaShake projects, to the basic goal of a better understanding of earthquake source physics. In either case, it is critical for the simulations to be numerically accurate and reproducible. For some types of geophysics and seismology problems, tests of numerical accuracy are simple, since the codes can be compared with analytical solutions. For dynamic earthquake rupture simulations however, there are no analytical solutions, and code testing must be performed by other means, such as with a code comparison exercise.

Within SCEC, rupture dynamics modelers who consider the physics of earthquakes will continue to use a range of computational methods to simulate earthquake behavior. No single numerical method has been shown to be superior for all problems. Therefore a number of numerical codes are

being used, each with its own advantages. These include finite-difference, finite-element, spectral element, and boundary integral techniques. Whereas some of the methods are extremely accurate and computationally efficient at certain types of problems, for example investigating a range of earthquake friction mechanisms, others are better at simulating realistic fault geometry or the propagation of waves through the heterogeneous crust.

The November 17, 2008 3D Rupture Dynamic Code Workshop was led by Ruth Harris included approximately 34 participants, and was funded by the Extreme Ground Motion Project due to the need to have verified codes for simulations of dynamic rupture and ground motions at Yucca Mountain. The workshop was described in detail in the FARM focus group session, but here we note that inclusion of tests on a dipping normal fault was important for the Extreme Ground Motion project. Also relevant was the decision to work towards benchmark simulations that included the effects of realistic off-fault yielding as part of the rupture process.

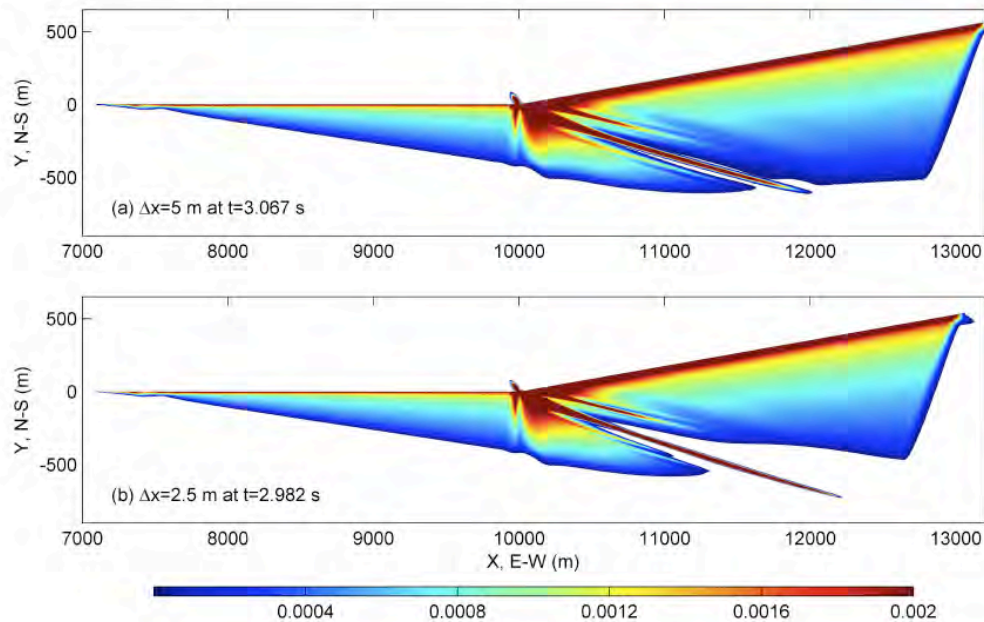


Figure 70. Distribution of off-fault plastic strain magnitude due to rupture on a fault with a kink (at $x = 10$ km, $y = 0$ km). Plastic strain localizes into bands and lobes near the kink, and the solution of the localization is apparently convergent when the element size is reduced. (From Duan and Day [2008]).

b. Non-Planar Faulting and Off-Fault Damage

Dynamic rupture modeling usually assumes planar faulting, but this clearly violates observations of faulting in the Earth. Non-planar faulting is interesting to the extreme ground motion because it may lead to strong high-frequency radiation in earthquakes. Another aspect of real faults that is increasingly being incorporated into models of dynamic rupture is the effect of off-fault yielding on earthquake rupture. This will have a strong effect on high frequency radiation as well, so the two issues are intertwined.

Duan and Day [2008] completed a study of elasto-plastic dynamics of non-planar faults. They examined inelastic strain near a fault kink and how it affects both rupture dynamics and seismic radiation from the kink. They found extensive inelastic deformation near a restraining bend,

particularly on the side of the fault associated with rupture-front extensional strains (Figure 70). The extensive inelastic deformation reduced high-frequency radiation from the kink and the reduction is significant above several Hz. They also found that plastic strain sometimes localizes spontaneously during rupture along a planar fault; however, the details of the shear banding change with element size, indicating the challenge of numerically simulating inelastic off-fault deformation. They continue their work on this problem, and are including pore pressure effects, with an eye towards the specifics of the Solitario Canyon fault. They anticipate that off-fault yielding, and its effect on rupture, will help place upper bounds on ground motion.

Duan also worked on the challenging problem of modeling kinked faults, with both a material contrast and off-fault yielding. Previously, he had found that bi-material ruptures lead to asymmetric damage [Duan, 2008]. In this study he found that releasing bends suppress the bi-material effect, whereas restraining bends reinforce it.

Dmowska, Templeton, and Rice studied dynamic rupture with fault branching in a configuration of specific interest for the Solitario Canyon Fault. They also initiated more general studies on rupture through (or arrest at) complex fault junctions that involve branches and damaged fault bordering zones. The studies allowing for Mohr-Coulomb type elastic-plastic response in the simplified Drucker-Prager formulation. Their results on the effect of off-fault yielding, and fault branching, on ground motion for this specific configuration are shown in Figure 28.

Goldsby and Tullis continued their work to understand fault weakening mechanisms including: flash heating, silica gel lubrication, and thermal pressurization that may be operative at high slip speeds. All of these could have profound implications for the magnitude of stress-drop, and thus for the intensity of strong ground motion. This information is important for resolving questions concerning stress levels in the crust. If coseismic friction is low, and the magnitudes of dynamic stress drops are constrained to modest values by seismic data, then the tectonic stress acting on faults must also be modest. We may have a strong crust that is nevertheless able to deform by faulting under modest tectonic stresses if the strength is overcome at earthquake nucleation sites by local stress concentrations and at other places along the fault by dynamic stress concentrations at the rupture front. Thus, understanding high-speed friction is important not only for predicting strong ground motion, but also for answering major scientific questions receiving considerable attention and funding, e.g. the strength of the San Andreas fault and the stress-heat flow paradox.

c. Precariously Balanced Rocks

Where they are available, precariously balanced rocks (PBRs) have the potential to provide unique constraints on long-term levels of strong ground motion. So they are of particular interest to the Extreme Ground Motion project. A key issue in using PBRs for this purpose, is in determining how long they have been precarious. For that reason, a key concern of PBR research in 2008-09 was age dating.

Grant Ludwig and her collaborators [Grant Ludwig et al., 2007; Rood et al., 2007; Scholm et al., 2008] focused on constraining the age and exhumation or “renewal” rates of PBRs. They identified PBRs with good potential for dating at sites that are important for ground motion validation (Figure 71). In 2007 and 2008, they collected samples from 9 rocks at 6 sites for ^{10}Be analysis, and obtained preliminary exposure ages of four PBRs near the southern San Andreas. In early 2009, they collected additional samples to refine model dependent (Figure 72) exposure ages of rocks at these sites, and to investigate activity of the Cleghorn fault at the critical Grass Valley site in order to interpret results relative to ground motions from San Andreas and/or San Jacinto earthquakes.



Figure 71. Rocks sampled at Lovejoy Buttes, Pacifico, Grass Valley and Beaumont South for 2007-2008 pilot study (Rood et al., 2008).

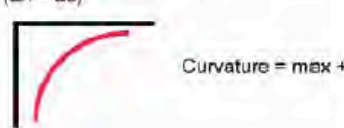


Scenario	E_A (m/Myr)	E_B (m/Myr)	T_{EXP} (yr)
1 FAST EXHUMATION ($E_A > E_B$) 	2000	32	22000
2 EQUAL EXHUMATION RATES ($E_A = E_B$) 	50	50	31000
3 SLOW EXHUMATION ($E_A < E_B$) 	15	500	46000

Figure 72. (left). Model ^{10}Be profiles for different exposure scenarios, erosion rates, and exposure times. In profiles (red), x-axes are ^{10}Be concentration (N) and y-axes are depth/height (Z). Note curvature and magnitude of erosion rate differences that can be used to test geomorphic models and refine exposure times.

2009 will mark the 3rd year of the 3-year Extreme Ground Motion project. A final report summarizing the results of the project is planned to be submitted to SCEC for review by December, 2009.

d. References

- Duan, B. Asymmetric off-fault damage generated by bilateral ruptures along a bimaterial interface, *Geophys. Res. Lett.*, 35, L14306, doi:10.1029/2008GL034797, 2008.
- Duan, B., and S. M. Day, Inelastic strain distribution and seismic radiation from rupture of a fault kink, *J. Geophys. Res.*, 113, B12311, doi:10.1029/2008JB005847, 2008.
- Grant Ludwig, L., K. Kendrick, L. Perg, J.N. Brune, M.D. Purvance, A. Anooshehpour, S. Akciz, and D. Weiser (2007). Preliminary Sample Collection and Methodology for Constraining Age of Precariously Balanced Rocks (PBR), Proceedings 2007 SCEC Conference, Palm Springs, Ca, Sept. 9-12.
- Rood, D., Brune, J., Kendrick, K., Purvance, M., Anooshehpour, R., Grant Ludwig, L. and Balco, G. (2008). "How do we date a PBR?: Testing geomorphic models using surface exposure dating and numerical methods", presentation at the Southern California Earthquake Center 2008 Annual Meeting Extreme Ground Motion Workshop, Sept. 7, 2008.
- Schlom, T. M., Grant Ludwig, L. B., Kendrick, K. J., Brune, J. N., Purvance, M. D., Rood, D. H. and Anooshehpour, R. (2008). An initial study of precariously-balanced rocks at the Grass Valley site, and their relevance to Quaternary faults in an near the San Bernardino Mountains, CA, Southern California Earthquake Center 2008 Annual Meeting, Proceedings and Abstracts, v. XVIII, p. 103.

4. Community Modeling Environment

The Southern California Earthquake Center (SCEC) Community Modeling Environment (SCEC/CME) collaboration is an inter-disciplinary research group that includes geoscientists and computer scientists from University of Southern California, San Diego State University, University of Wyoming, Stanford University, San Diego Supercomputer Center (SDSC), the University of California at San Diego, Carnegie Mellon University (CMU), Pittsburgh Supercomputer Center (PSC), and USC Information Sciences Institute (USC/ISI). The CME collaboration develops computational models of earthquake processes and uses high performance computing (HPC) systems to run these predictive numerical models and produce physics-based seismic hazard estimates for California.

Many SCEC researchers use numerical modeling in their work. However, complex system science calculations such as seismic hazard analysis calculations for California require expertise in several geoscientific specialties as well as several computer science specialties. The CME collaboration enables SCEC to conduct computational research at scales and complexity levels that exceed what individual researchers or small research groups can typically accomplish.

Several recent scientific advisory and workshop reports including Living on the Active Earth (National Research Council – 2003) and Long Range Science Planning for Seismology (NSF – 2009) have discussed how numerical modeling techniques can be used to improve current seismic hazard analysis estimates. In order perform large-scale seismic hazard calculations, geoscientific expertise from SCEC collaborate with computer scientists that specialize in high performance scientific computing. The CME has produced a series of significant scientific results since its inception in 2001. In this SCEC/CME Project report for 2009, we present an overview of CME research activities and summarize some of the research results obtained by the group this year.

a. CME Science and Computational Goals

The scientific goals of the CME Project have been defined to support the scientific goals of the core SCEC program. Many of the SCEC 3 science objectives require the use of computer modeling and the CME is developing the scientific computing systems needed for SCEC reach those objectives. At the start of the CME program, SCEC researchers defined four SCEC Computational Pathways for seismic hazard analysis (Figure 73). These Pathways represent increasingly complex and

computational expensive ways to calculate ground motion predictions. The CME scientific software and computer system developments are designed to help SCEC researchers perform one or more of the SCEC Seismic Hazard Computational Pathway calculations.

The SCEC Computational Pathways calculations produce predictive seismological parameters with broad impact. These predictive seismic hazard parameters include scenario ground motion maps (used in emergency management exercises), scenario broadband seismograms (used in seismic engineering of tall buildings), and probabilistic seismic hazard curves (used in insurance loss estimations). Groups such as emergency management organizations, building engineers, and insurance organizations will benefit if SCEC science can improve these predictive data products. By integrating new SCEC science results into highly-scalable computational models and running seismic hazard calculations on national supercomputer facilities, the CME simulation results help the SCEC science program have an immediate societal impact.

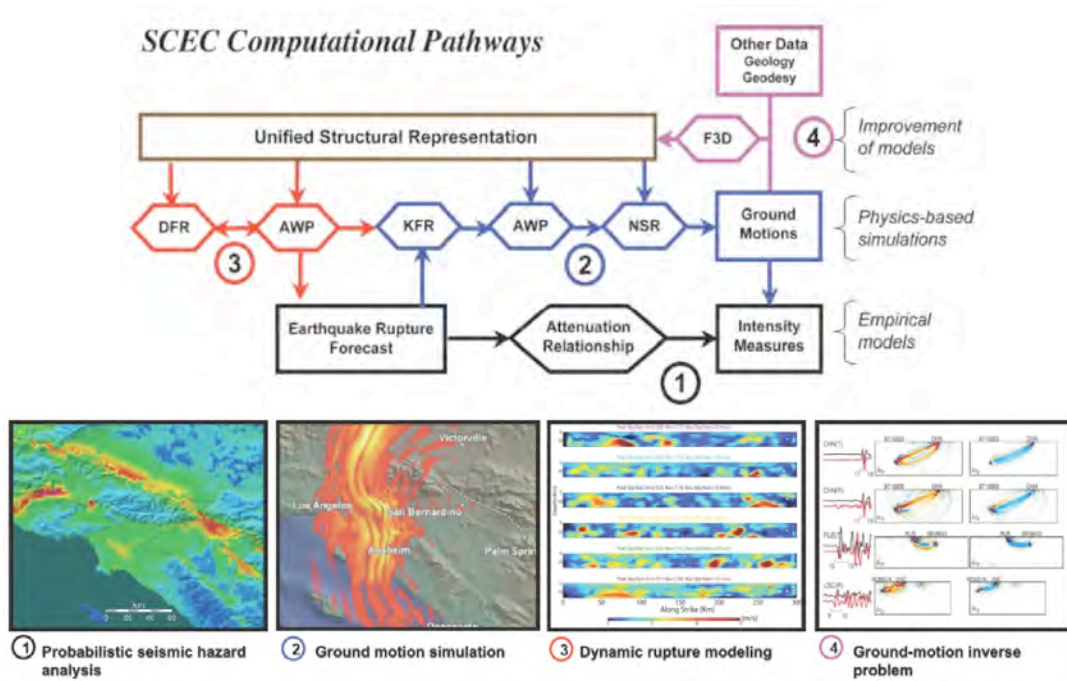


Figure 73. A wiring diagram for the SCEC computational pathways in seismic hazard analysis (upper diagram) and large-scale calculations (lower panels). The computational modules with three-letter abbreviations are described in Box 1. (1) High-resolution seismic hazard map for the Los Angeles region using the UCERF2 model. (2) Simulation of a M 7.8 earthquake on the southern San Andreas Fault for the 2008 ShakeOut exercise. (3) Dynamic rupture models for a M 7.8 earthquake on the southern San Andreas Fault used in the ShakeOut-D simulations. (4) Frechet kernels used in full 3D waveform tomography to improve seismic velocity models in Southern California.

The CME collaboration has identified four specific computational improvements that are needed to advance the SCEC science program towards its goal of improving ground motion predictions. The following four scientific and computational goals identify specific computational improvements that the CME is pursuing in order to improve the accuracy of ground motion predictions for California.

Goal 1: Improve the resolution of dynamic rupture simulations by an order of magnitude to investigate realistic friction laws, near-fault stress states, and off-fault plasticity.

Goal 2: Investigate the upper frequency limit of deterministic ground-motion prediction by simulating strong motions up to 3 Hz using realistic 3D structural models for Southern California.

Goal 3: Validate and improve the Southern California structural models using full 3D waveform tomography.

Goal 4: Transform probabilistic seismic hazard analysis (PSHA) by using wave propagation modeling rather than empirical attenuation relationships in PSHA calculations.

These goals provide the CME with specific scientific and computational improvements that are needed to improve seismic hazard numerical modeling efforts. In particular, these goals address the seismic hazard issues of broad impact including development of accurate source descriptions, verification and validation of 3D structural models, and the integration of state-of-the-art numerical modeling techniques into standard PSHA calculations.

b. CME Simulation Planning and Results

As SCEC researcher develops new insights into earthquake processes and improves earth structural models, these scientific improvements are integrated into computational models and used for large-scale seismic hazard simulations. The CME collaboration together with researchers from SCEC and other research organizations has performed a series of significant simulation results over the last several years.

The planning and performance of large scale simulations go through a similar process. First, CME geoscientists identify an important scientific issue relating to our understanding of seismic hazards in California that can be investigated through numerical modeling. Then, in situations where the computational requirements exceed the capabilities of our numerical modeling tools, CME researchers extending and improving current CME computational capabilities. Once all the seismological and high performance software is integrated to work together we consider it a computational platform. Then the computational platform must be re-verified and re-validated which is typically done by using the system to run reference problems with known good solutions. Once the platform is confirmed ready for use, the large scale simulations are run. Planning, development, testing, and running of a CME simulation often takes 6 months of consistent team work. Once the simulation is completed, researchers require additional time to analyze and publish the results. It is common for three or four such large simulations to be underway in the CME collaboration at any one time.

When the SCEC simulation goals exceed the capabilities of our current numerical modeling tools, we work with CME computer scientists to develop the required computational capabilities. The CME computer scientists have greatly improved the scalability of SCEC wave propagation codes. SCEC is now qualified to run on the world's largest supercomputers. The CME computer scientists have automated our distributed computing using scientific workflows that enable us to perform probabilistic seismic hazard calculations requiring 100M+ jobs and 100M+ files. By repeating the project phases including; a) definition of new scientific questions, b) HPC cyberinfrastructure development, and then c) integration of new scientific computational capabilities into a practical PSHA framework, the CME project produces important new results and establish the numerical

c. CME Communication, Education, and Outreach

The SCEC CEO Program helps the CME collaboration communicate SCEC and CME research results. CME collaborators participate in SCEC intern programs including UseIT and ACCESS. The 2009 UseIT program recently concluded another successful summer in the IT lab at SCEC (Figure 74).

ACCESS-G students working with CME are conducting projects on (a) Vector and tensor Visualization (McQuinn, Minster, Chourasia – UCSD/SDSC), (b) Building Response Animation (Fu, Krishnan - USC/Caltech), and (c) Data Management and Data Access Tools for SCEC simulation archives (Pechprasarn, Maechling – USC/USC) (Figure 75).

The CME helps to provide SCEC researchers with access to HPC systems. SCEC numerical modeling researchers can make use of the CME computer allocation on the USC High Performance Computing and Communication (HPCC) system. When the CME simulations need more computer power than available at USC, we move simulations to NSF TeraGrid facilities onto system that exceed 60K cores. Beginning in January 2009, the CME was awarded computer time and has begun to run simulations on a Department of Energy (DOE) Leadership class computer called Intrepid at Argonne National Laboratory’s (ANL) which exceeds 130K cores. The CME’s computational results and accomplishments have raised SCEC’s profile in the national and international high performance computing community. SCEC’s computational science program now approaches the scale of other large-scale HPC scientific users including high energy physics, chemistry, and atmospheric science.



Figure 74. The SCEC Undergraduate Studies in Earthquake Information Technology (UseIT) attracts students from around the country to study earthquake system science. Over 140 students have successfully complete their SCEC internship in the last 6 years of the program. The twenty three on the left are participating in the 2009 summer UseIT program are supervised by the PI and SCEC Educational specialist (Robert de Groot, PhD). The interactive 3D visual earth environment software developed by the group under the name SCEC Virtual Display of Objects (SCEC-VDO) has been used frequently to display earthquake information for the public media. The SCEC-VDO development has also been used in a USC multi-media literacy program conducted by the USC college of Letters, Arts, and Sciences in collaboration with the USC School of Cinematic Arts.

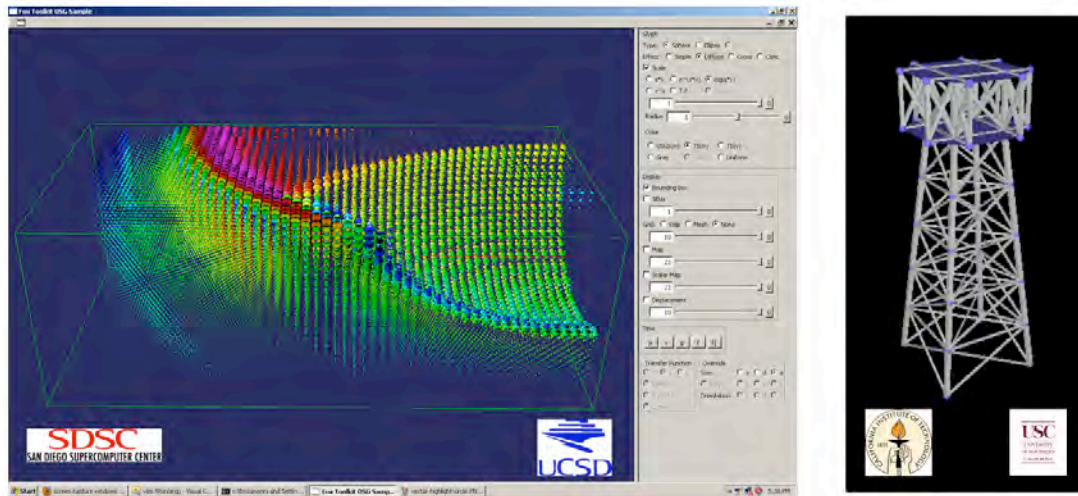


Figure 75. SCEC Access-G CME related projects include (left) development of new techniques for visualizing volumetric data from wave propagation simulations. Images shows acceleration vectors in a volume rendering of acceleration vectors during a SORD simulation (McQuinn, Minster, Chourasia - UCSD/SDSC) and (right) an animation frame from a 3D rendering of a Caltech Virtual Shaker structural response simulation (Fu, Krishnan - USC/Caltech).

CME project members regularly present SCEC research at computer science and HPC conferences such as Supercomputing and TeraGrid. This year, multiple articles about CME research were written and presented on NSF TeraGrid web sites including Texas Advanced Computer Center (TACC) and National Institute for Computational Sciences (NICS) at Oak Ridge National Laboratory. These articles about SCEC research were picked up and used by public science outlets including Live Science and US News and World Report. CME simulations are featured in a number of widely used scenario earthquake animations. CME ShakeOut simulation images were used in USGS literature and on public television. SCEC Intern animations from SCEC-VDO are distributed by new agencies from the news agency web sites. Visualizations of CME simulations produced by Amit Chourasia and others at San Diego Supercomputer Center (SDSC) continue to with awards for scientific visualizations including recent awards from DOE Scientific Discovery through Advanced Computing (SciDAC) in 2009 and ACM SIGGRAPH 2009.

SCEC, as a system science organization with broad research goals, has a wide variety of computational science research needs. SCEC's computer science capabilities, including the CME, rates with the best in any geophysical research group in the world. In particular, SCEC has developed one of the most scalable wave propagation codes (AWP-Olsen) and one of the largest and most complex scientific workflow systems (CyberShake1.0) in existence. Also, the CME work on full 3D Tomography has identified SCEC as one of the most data intensive computational groups in any NSF research domains. As the CME research program improves SCEC's scientific computing capabilities it helps to establish a leadership role for SCEC in national scientific computing.

d. SCEC Projects Organization

SCEC/CME activities were initiated in 2001 under a five-year NSF Information Technology Research (ITR) award. Through the CME ITR Project, SCEC was able to establish collaborative research activities with computer scientists and through these geoscience/computer science collaborations the scale and capabilities of the SCEC computational science program greatly increased. Since the NSF ITR program ended in 2006, CME activities have been supported through NSF OCI and EAR awards under Project names including PetaSHA-1, PetaSHA-2, PetaShake-1, and PetaShake-2. Detailed information about each of the awards is posted on the CME project web site (<http://www.scec.org/cme>).

Current funding for the CME is approximately 1.6M/year under two different NSF awards. These awards are (1) Petascale Cyberfacility for Physics-Based Seismic Hazard Analysis (PetaSHA-2) (EAR – 074493 – May 1, 2008 to April 30, 2010), and (2) Outward on the Spiral: Petascale Inference in Earthquake System Science (SCEC PetaShake Project) (OCI-0905019 - August 1, 2009 to July 31, 2011). The CME collaboration awards augments core SCEC research funds and provide a way for SCEC to rapidly migrate new research results into useful seismic hazard products.

CME Project funds are allocated to ten different research groups each of which has budget under the CME NSF awards. Some of the CME funded groups are led by computer scientists. The CME's collaborative work with computer scientists has been of great benefit to the SCEC computational modeling work. CME computer science groups have contributed great improvements in the scalability, automation, data management, and reliability of many SCEC simulations. We also believe there is wide recognition within NSF, and other scientific organizations, in the value of interdisciplinary collaborations between domain scientists and computer scientists. The CME collaboration provides an outstanding example of how such interdisciplinary groups can collaborate to good effect.

CME Projects are conducted under the scientific leadership of Principal Investigator (PI), Thomas H. Jordan. Day-to-day CME project operations are managed by Philip Maechling, SCEC IT Architect. The CME holds annual All-Hand Meetings (separate from the annual SCEC meeting) and collaborative CME project goals are coordinated by the CME senior scientists. CME Project coordination teleconference calls are held on a regular basis and CME Project results are posted on the CME web site and are presented as abstracts, posters, and talks at conferences including the SCEC annual meeting.

e. Anticipated Growth in Computational Science

Both the NSF and DOE are building very large-scale HPC systems, which will become available for open-science research within the next two years. The NSF is building a sustained Petaflops system that they call a Track 1 computer (Blue Waters at NCSA). DOE is deploying what they call Leadership Class Petascale computers for open-science research including Intrepid at Argonne National Lab and Jaguar at Oak Ridge National Lab. As these HPC systems become available, the sponsoring organizations will be very interested in using them to perform important scientific research. SCEC, as a large, deep, inter-disciplinary research consortium is one of the few groups capable of performing computational science at petascale. And current CME HPC capabilities have positioned SCEC as one of the few groups qualified to run on these largest systems.

Because this new class of supercomputers is about to become available, the time may be right to for SCEC to identify one or more seismological computational "Grand Challenges" and collaborate with geoscientific groups and HPC system operators to attempt some highly challenging, computationally intensive, and transformative research. If the SCEC science planning committee

identified a computational challenge that is currently well outside the scale of any computer or research group, it might be possible to collaborate with the NSF and DOE to obtain the computer time needed attempt the computational challenge. As an example, SCEC researchers might decide what is needed to advance national seismological research is a full 3D velocity model from 0 to 100 km for all of North America using full 3D tomography. As another example of a “grand challenge” problem, SCEC researchers might decide there is great scientific value in a physics-based PSHA map for all of North America at 1 Hz. These calculations are currently well out of range of any group or any available NSF or DOE supercomputers. However, these calculations may not be out of range for long. Within 5 years, calculations at these scales may be possible if a consistent focused effort were made to achieve them.

The CME collaboration currently contains an exceptional group of HPC experts, and it is highly likely that these HPC experts would enthusiastically approach a large scale computational challenge if the anticipated scientific result has broad significance.

f. CME Research Using SCEC Computational Platforms

The science goal of the SCEC/CME collaboration is to transform seismic hazard analysis (SHA) into a physics-based science through high-performance computing (HPC). The CME is working to develop computational programs and techniques needed by SCEC to produce this transformation. SCEC’s experience performing numerical modeling research has taught us that, in nearly all cases, several different codes must be run in order to produce a significant computational research result.

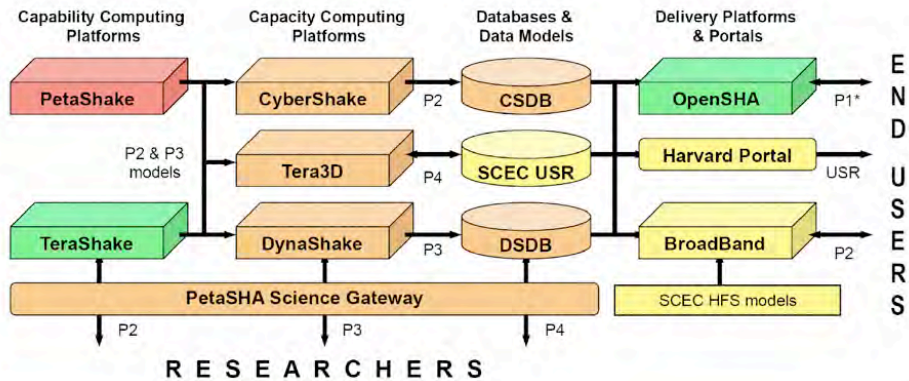


Figure 76. Computational platforms of the PetaSHA cyberfacility. Terashake and OpenSHA were developed under ITR funding (green). Cybershake and Dynashake and their databases, CSDB and DSDB, as well as the full-3D inversion platform, Tera3D (orange) are being developed under NSF/EAR funding. Petashake is a new petascale capability computing platform supported by NSF/OCI funding (red box). Other components supported by the SCEC base grants are shown in yellow. P1* and P2-P4 are the computational pathways diagramed in figure 1 and described in Box 1. The P2 and P3 models developed on PetaShake will be migrated to the capacity-computing platforms for full-scale production of seismic hazard maps. Researchers access codes and results from the PetaSHA science gateway, and users will access validated models and data products through the three delivery platforms: OpenSHA, Broadband, and the Harvard USR portal.

The CME uses high performance software and supercomputers that we call *computational platforms* to perform SCEC’s computationally intensive seismic hazard research. We define a computational platform as a vertically integrated collection of hardware, software, observational data, structural models, and people that can perform a useful research calculation. A SCEC computational platform

assembles and integrates all the software, hardware, middleware, input parameters, and structural models needed to perform a useful research calculation and it also includes all the observational data needed to verify and validate the functioning of the platform. A computational platform may require a large collection of software programs and these programs are carefully configured to work together.

The CME currently uses six computational platforms (Figure 76). Each platform performs a specific type of seismic hazard research calculation. The research capabilities of the computational platforms include: (1) Dynamic Rupture simulations (DynaShake Platform), (2) Earthquake Wave Propagation Simulations (TeraShake Platform), (3) Calculate high frequency synthetic seismograms (Broadband Platform), (4) Velocity Model Validation and Optimization (Full 3D Tomography (F3DT Platform)), (5) Traditional probabilistic seismic hazard analysis (OpenSHA Platform), and (6) Physics-based PSHA using full 3D wave propagation (CyberShake Platform). Other computational platforms including highly scalable and capable wave propagation codes (PetaShake Platform) and data management tools (PetaSHA Science Gateway) are in development.

The CME collaboration seeks to perform very large-scale simulations that exceed the capabilities of our current computational platforms. To accomplish these research goals, we work to improve and optimize the computational platforms until they are capable of performing the desired research calculations. As we scale-up the CME computational platforms, our goal is to make effective use of NSF petascale computing for SCEC research when such computing resources become available. An NSF Track 1 computer system (Blue Waters – NCSA) capable of sustained Petaflops/s performance is expected to go online in 2011. Properly used, petascale computing will help study geosystems and other complex natural phenomena in more detail, at higher resolution, using more realistic physics, for larger geographical regions.

g. CME Scientific Research Results

CME project activities are science driven with CME research focused on science issues relating to seismic hazard analysis. CME research remains coordinated with SCEC science objectives because scientific needs precede CME software or system development. Given specific science goals, the CME evaluates its current software and computer tools to determine if it can perform the necessary computation. If the simulation exceeds the capabilities of our current platforms, we work on improving the scalability of the necessary platform until it is capable of running the needed simulation. We iterate between scientific software development, cyberinfrastructure development, and application of our Platforms to run milestone simulations. By combining software development, system improvements, and milestone research runs, the CME improves the capabilities of our computational platforms and produces significant research results.

Dynamic Rupture Research. The DynaShake Platform is designed to run large-scale (>300km rupture length) dynamic rupture simulations. The DynaShake Platform development is currently led by Steve Day and his team at SDSU. The DynaShake platform serves two important purposes in CME research. First, it is used to investigate the physics of fault ruptures. This is done by developing numerical models of rupture processes including friction laws on fault surfaces during an earthquake rupture. Second, DynaShake dynamic rupture simulations are also used to produce kinematic source descriptions by capturing rupture parameters produced by the dynamic simulation.

The DynaShake platform is used to investigate high-frequency seismic energy generation. The challenge is that the relevant phenomena (e.g., frictional breakdown, shear heating, effective normal-stress fluctuations, material damage, etc.) controlling ruptures are strongly interacting and span many orders of magnitude in spatial scale, requiring high-resolution simulations that couple

disparate physical processes (e.g., elastodynamics, thermal weakening, pore-fluid transport, heat conduction). In dynamic rupture simulations, friction coefficient at sliding velocities above roughly 0.1 m/s are likely to be sharply weakened by flash heating of asperities. Compounding the computational challenge, natural faults are not planar, but instead have roughness that can be approximated by power laws with ratio of amplitude to wavelength typically in the range of roughly 0.01 – 0.001, potentially leading to large, multiscale fluctuations in normal stress. The capacity to perform 3D rupture simulations that couple these processes while capturing outer/inner spatial-scale ratios of 104 – 105 will enable significant advances in our fundamental understanding of high-frequency seismic wave excitation. The DynaShake software can simulate flash heating in a fully regularized form by embedding it in a rate- and state-dependent friction formulation using a well-verified and efficient numerical method. In this model, dynamic weakening will occur if the effective normal stress is reduced by shear heating of pore fluids the effect being controlled by the balance between pore pressurization by shear heating and depressurization by fault-normal Darcy flow. This effect can be included in simulations by coupling frictional dissipation with fault-normal heat conduction and pore-fluid diffusion models.

DynaShake-based dynamic rupture sources were used in both the TeraShake-2 research study (Olsen et al – 2007) and ShakeOut-D (Olsen et al – 2009). In 2007, the DynaShake development group developed a technique for constraining dynamic rupture simulations so that the final slip exhibited by the simulation matched slip (for example, surface or depth-averaged) proscribed by the modelers. Then, these DynaShake produced source descriptions were used in the ShakeOut-D study. The CME dynamic rupture research is also involved with the rupture research ongoing within SCEC. The DynaShake developers participated in the SCEC Dynamic Rupture Verification Exercise.

An important aspect of the CME dynamic rupture research is the development of pseudo-dynamic rupture generators. Due to the complexity and large computational requirements of dynamic rupture simulations, kinematic rupture descriptions will continue to be used in seismic hazard research for several years to come. Pseudo-dynamic rupture generators that produce kinematic rupture descriptions with parameters consistent with dynamic rupture simulations are being developed in order to integrate advances in our understanding of dynamic ruptures into seismic hazard calculations. Both the Broadband and the CyberShake Platforms use rupture generators to produce source descriptions. Improvements in rupture parameterization produced by the DynaShake Platform will provide guidance for constructing appropriate pseudo-dynamic source models for high-frequency ground motion simulations and will be quickly migrated to other computational platforms. CME DynaShake research and other rupture modeling researchers including Beroza (Stanford), Archuleta (UCSB), and Graves (URS) are developing pseudo-dynamic rupture generators designed to produce kinematic rupture descriptions that are consistent with results from large-scale dynamic rupture models.

The DynaShake platform can simulation large magnitude (M8.0+), long rupture surface (>300km), long duration (> 60seconds) dynamic ruptures needed for simulations of regional scale earthquakes and worst-case Southern California earthquakes. The most scalable dynamic rupture modeling software in the DynaShake platform is a finite difference dynamic rupture code (Day et al) that uses a regular grid. To model many earthquakes in Southern California, the dynamic rupture simulations must work properly for complex faults such as multi-segment dipping faults. A number of dynamic rupture codes that support complex fault geometries are under evaluation for this purpose including SORD (Ely - USC) and DR-FE (Ma - SDSU). The SORD code was developed to handle the sort of complex fault geometry noted above, while retaining very good computational scalability and sufficient flexibility to accommodate the appropriate rupture physics. The DR-FE code can simulation ruptures on complex fault geometries and it can also

model wave propagation in models that contain other geometrical complexities including topography.

High Frequency Wave Propagation Simulations. The CME Collaboration has developed the TeraShake Computational Platforms in order to run deterministic wave propagation simulations on regional scales at frequencies above 1Hz. Civil and building engineers, important users of CME seismic hazard modeling results want synthetic seismograms containing higher frequencies (up to 10Hz) for use in seismic hazard analysis ground motion studies.

The CME Collaboration has developed the TeraShake Computational Platforms in order to run deterministic wave propagation simulations on regional scales at frequencies above 1Hz. Civil and building engineers, important users of CME seismic hazard modeling results want synthetic seismograms containing higher frequencies (up to 10Hz) for use in seismic hazard analysis ground motion studies.

In 2007 and 2008, three CME research groups (Graves, Olsen, and Bielak) ran wave propagation simulations at 1Hz for the ShakeOut scenario M7.8 event in a large southern California region. In 2009, CME researchers once again double the frequency at which wave propagation simulations are performed. The 2009 TeraShake Platform development focused on running 2.0Hz simulations of historical earthquakes (e.g. Chino Hills). The 2.0Hz synthetic waveforms produced by these simulations have been compared against observed seismograms for this event in order to validate the simulation.

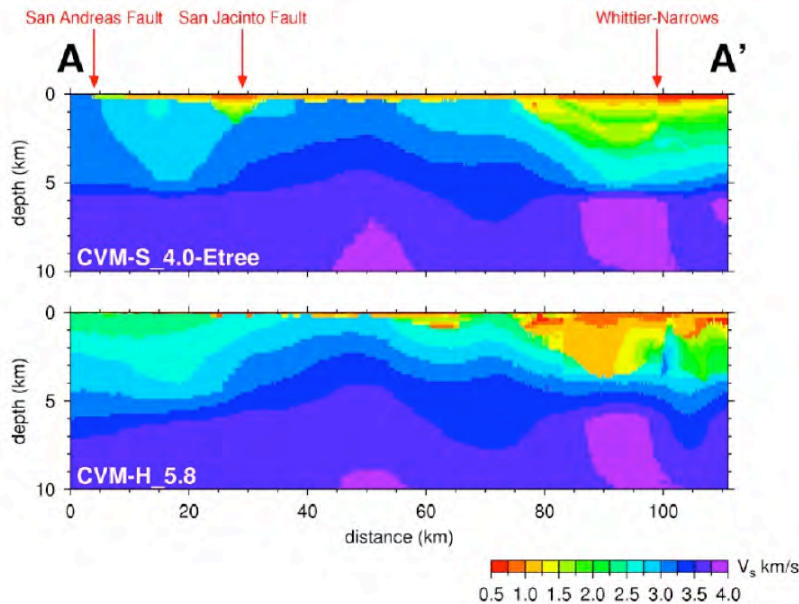


Figure 77. Comparable V_s profiles across the Los Angeles Basin are shown with CVM4.0 (top) and CVM-H (bottom). The differences between the CVM 4.0 and CVM-H velocity models contribute to uncertainties in high frequency simulations. The CME collaboration is working with both velocity models in order to determine which produces best match to observation or if a new combined or merged model will be required for 2.0 Hz and higher frequency deterministic wave propagation simulations for Southern California.

When simulation results match observational results, it indicates that each aspect of the simulation including the simulation software, the source description used, and the velocity model are valid for the region and frequencies involved. When earthquake wave propagation simulation results do not

match observational results, differences are usually attributed to one or two inputs, either (1) the velocity model (e.g. CVM4.0), or (2) the source description. In order to identify the most accurate simulation configuration, we must analyze the sensitivity of our Southern California simulation results to the different 3D velocity models, which are available for this region including both the CVM4.0 and CVM-H. A comparison between the CVM4.0 and CVM-H 5.7 for a profile across the Los Angeles Basin indicating significant differences between the models that will affect ground motion simulations is shown in Figure 76.

In 2009, the CME has begun to integrate the SCEC CVM-H (v5.7 and later) into our numerical modeling work. The CME is running simulations using alternative velocity models and comparing the differences between simulation results. During this evaluation process, we identified the need for a numerical measurement that indicates how well seismograms match. Several characteristics of seismograms may be significant in a comparison including time of phase arrivals, amplitude and duration of motions, and frequency content. To improve the process of comparing seismograms, we have developed a Goodness of Fit (GOF) (Mayhew, Olsen – SDSU) algorithm that compares each of these aspects of two seismograms and produces a single numerical value on a 0-100 scale (a perfect match produces a 100 results) that is intended to represent how well the two seismograms fit. We are using this Goodness of fit measure to analyze the differences in simulation results between the CVM4.0 and CVM-H. Goodness of Fit results that compare observational data for the Chino Hills M5.4 earthquake to 2Hz simulation results are shown in Figure 78.

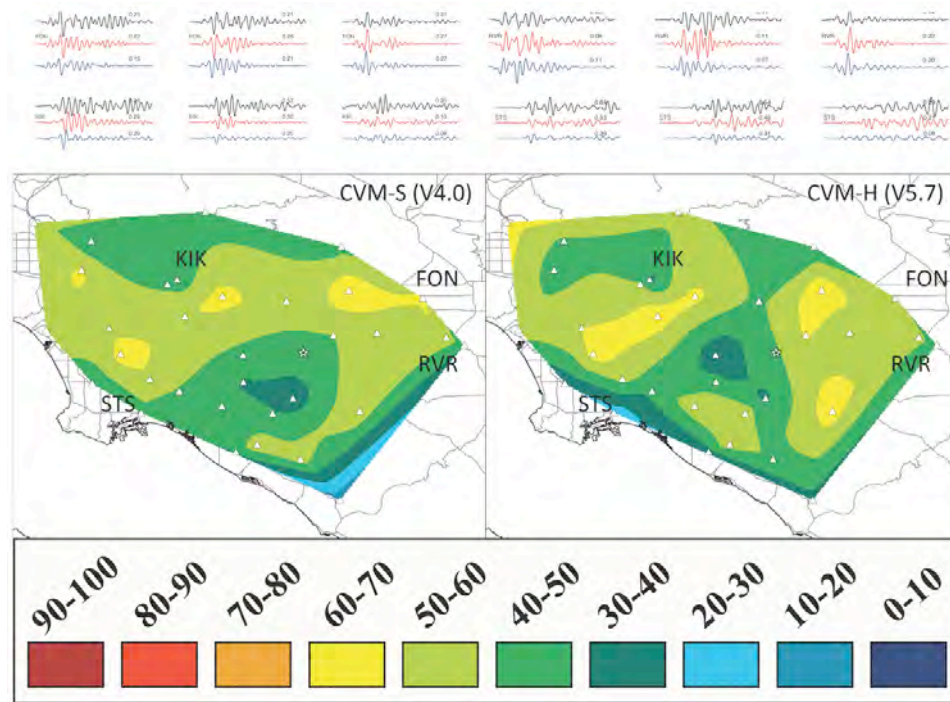


Figure 78. Validating regional scale wave propagation simulation results against observed data may require thousands of comparisons between observed and simulated data. The CME has developed an initial implementation of a Goodness of Fit (GOF) measurement system and is applying these new tools to help evaluate the 2Hz Chino Hills simulations. In this GOF scale, 100 is a perfect fit. The maps (left) show how GOF values vary geographically for AWP-Olsen, Chino Hill M5.4 event, and two different SCEC Community Velocity Models, CVM4.0 (left) and CVM-H 5.7 (right).

In HPC terminology, the largest and most parallel simulations are called *capability* simulations. In order to obtain computational time on the world's largest supercomputers, scientific groups must demonstrate their capability codes produce useful science results and make efficient use of the supercomputers. Under our current OCI PetaShake-2 award, the CME is working to improve the performance of our dynamic rupture and wave propagation codes so that we are ready to use the upcoming NSF Track 1 petascale computer (Blue Waters NCSA) when it becomes available in 2011.

The CME's most scalable code, the AWP-Olsen-Day-Cui software, is capable of scientific runs at using all available cores on the system at the same time on the nation's largest supercomputers including both NSF Track 2 machines (TACC Ranger - 50K cores) and NICS Kraken - 63K cores) as well as DOE's leadership class computer (ANL Intrepid - 130K cores). The CME capability computing developments have been led by Yifeng Cui (SDSC) who has improved the parallel performance SCEC software until it scales efficiently on more than 130,000 cores. The SCEC wave propagation software is in a small and select category of supercomputer applications that have been shown to produce well-verified scientific results at this scale. Scalability plots for three of the SCEC Computation codes (AWP-Olsen, Hercules, and SORD) are shown in Figure 79.

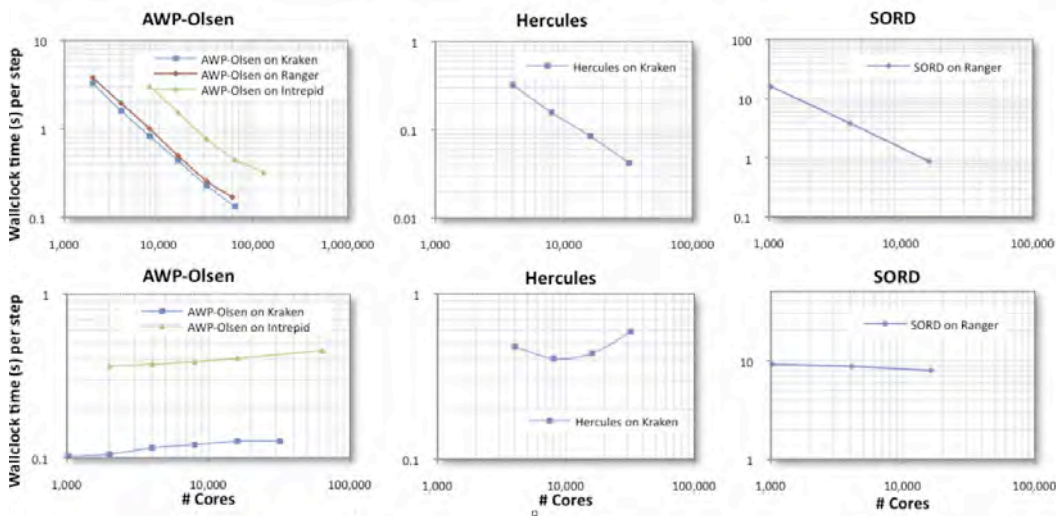


Figure 79. Plots show strong scaling (top) and weak scaling (bottom) for out two optimized codes AWP-Olsen (left) and Hercules (center). Yifeng Cui and his team at SDSC has optimized the AWP-Olsen software and it now shows excellent scaling up to 130k cores on DOE leadership class system Intrepid. Hercules shows excellent scaling up to 32k cores on NSF Track 2 system Kraken. We have begun optimization of SORD code (right) to support dynamic rupture and wave propagation simulations with more complex structural geometries including dipping faults and topography.

NSF's HPC organization, the TeraGrid, has supported our development of the TeraShake Platform and its highly scalable software. Over the last four years, each time a new NSF supercomputer became available, the NSF TeraGrid Advanced Support for TeraGrid Applications (ASTA) program collaborated with the CME by providing highly specialized HPC technical support to ensure our software ran efficiently on the new HPC system.

The NSF HPC community defined performance goals for hardware and software a few years ago as it embarked on the current NSF HPC development program. Science users together with NSF decided that the NSF HPC should enable scientific numerical modeling research at sustained Petaflops performance. Scientific applications groups such as SCEC expect to continue to improve

our software until it is capable of sustained Petaflops performance. The CME has made outstanding progress in its code development. Current maximum sustained code performance for our CME software is approximately 50 TFlops indicating that we must improve the performance of our CME software by a factor of 20 to achieve this national scientific and HPC performance goal.

Full 3D Tomography (F3DT) Platform. The CME Full 3D Tomography (F3DT) Platform is a platform for executing Pathway 4 (inverse) calculations. The F3DT platform provides the means for updating the CVMs using seismic observations—an important validation step for predictive ground motion simulations.

In F3DT, the starting velocity model as well as the model perturbation is 3D and the sensitivity (Fréchet) kernels are computed using numerical simulations that incorporate the full physics of 3D wave propagation. F3DT can account for the nonlinearity of structural inverse problem through iteration. SCEC researchers have been developing F3DT algorithms that fall into two classes: the adjoint wavefield (AW) formulation, and the scattering integral (SI) formulation. The two are closely related, but their relative efficiency depends on the problem geometry, particularly on the ratio of sources to receivers. The SI method, which computes Fréchet kernels for individual measurements by convolving source wavefields with RGTs, is computationally more efficient than the AW method in regional waveform tomography using large sets of natural sources, although it requires more storage.

A CME group led by Po Chen (University of Wyoming) and Thomas Jordan (USC) have successfully applied a scattering-integral (SI) formulation of F3DT to improve CVM3.0 in the Los Angeles region (Figure 80). They have inverted time- and frequency-localized measurements of waveform differences to obtain a revised 3D model that provides substantially better fit to the observed waveform data than the 3D starting model. In 2009, Po applied this technique to an inversion CVM4.0 for a 300km x 600km region of Southern California. In this work, performed largely on the DOE Incite computer Intrepid, he produced both a catalog of refined focal mechanisms and a perturbation model for CVM4.0 at 5 seconds period.

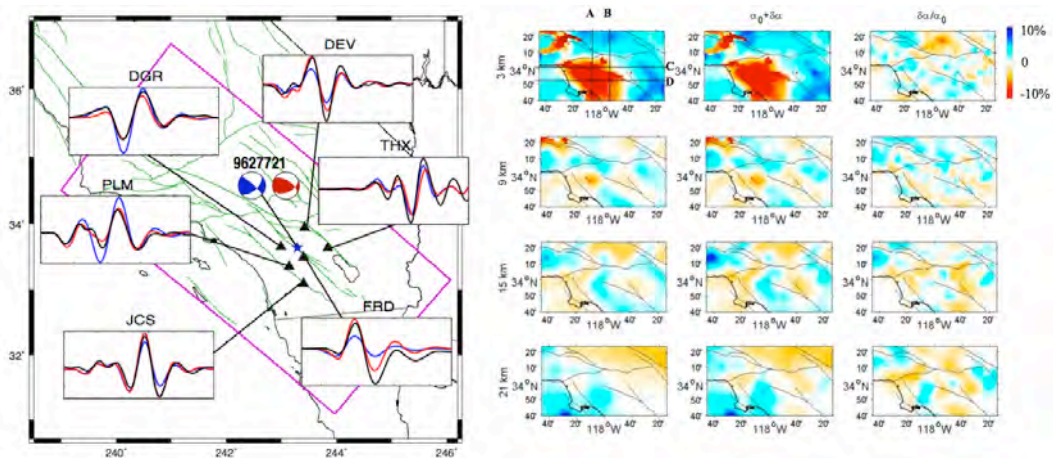


Figure 80. Full 3D Tomography (F3DT) Platform is used to validate and improve the 3D velocity models for California. The F3DT Platform can produce improved focal mechanisms (left) and improved 3D velocity models (right) by comparing simulation results to data. (Po Chen, U. of Wyoming)

Other geoscience groups including SCEC members are also developing 3D inversion techniques including both the SI and the AW methods. Carl Tape (Harvard) and Jeroen Tromp (Princeton) are using the AW method to improve an earlier version of CVM-H. Greg Beroza (Stanford) and others are developing techniques that use ambient noise recorded at seismic stations to calculate kernels that can be used to improve velocity models at low frequencies.

F3DT inversions together with new seismic observations (including new earthquakes and new recording stations) can be used to improve velocity models. So, in the future, it is likely that ground motion modeling groups will base their seismic hazard calculations on the best available version of the SCEC CVM. This introduces the challenges of creating, maintaining, and using a time dependent community velocity model. The CME is working to support such a system in a number of ways. First, we have developed software tools capable of creating very large (>1B mesh points) velocity meshes from any of the current SCEC velocity models. Next, we are developing techniques to integrate inversion results into a velocity model and deliver the updated models for use in ground motion simulations. The CME is also working to define a “standard” inversion problem for California by defining an initial starting model, the region and maximum frequency, and validation criteria. The intent is for different groups to perform comparable inversion and then to compare the inversion results to determine whether the methods converge. In the long term, it should be possible to automate the inversion process, using the most efficient inversion technique available, and to repeat the inversion and deliver an updated and improved CVM whenever new observations are available.

OpenSHA Platform. OpenSHA is a Probabilistic Seismic Hazard Analysis (PSHA) computational platform. The CME developed the OpenSHA Platform in collaboration with USGS under the leadership of Ned Field (USGS). The OpenSHA Platform implements traditional PSHA calculations which use two critical inputs; (1) an Earthquake Rupture Forecast (ERF), and (2) a Ground Motion Prediction Equation (GMPE), typically an attenuation relationship. An ERF provides a list of possible future earthquakes, their magnitudes, and a probability that the earthquake will occur in a given time span (e.g. within 1 year). OpenSHA is object-oriented and it implements both (1) specific seismic hazard models such as earthquake rupture forecasts, and (2) specific seismic hazard algorithms such as attenuation relationships. Users can combine alternative models and algorithms to produce PSHA hazard curves and PSHA hazard maps for California.

OpenSHA is highly integrative platform because it relies on valid implementations of many modeling components include fault models, velocity models, rupture models, and ground motion prediction equations. In order to produce valid PSHA hazard curves maps, all of these seismic hazard modeling elements must work correctly. Despite this complexity, PSHA seismic hazard predictions are highly significant because they represent a critical interface between seismology and engineering. In the foreseeable future, it is likely that SCEC will continue to communicate our understanding of seismic hazards using PSHA techniques. As SCEC improves its understanding of earthquake processes, these scientific advances are used to improve PSHA results.

In 2007, a new Unified California Earthquake Rupture Forecast (UCERF2) was released by USGS. OpenSHA was used to define the reference implementation of this ERF and it also includes implementations of several recent (2008) attenuation relationships. OpenSHA was used by SCEC and the USGS in the development of UCERF2. Software implementations of the proposed forecast models were developed within OpenSHA (Figure 81). The OpenSHA software enabled UCERF2 scientists to easily test the prototype Earthquake Rupture Forecast models with established PSHA codes. OpenSHA proved a significant value during the development of UCERF2 and it will likely be used again during UCERF3 development.

The OpenSHA development group is developing new capabilities so OpenSHA can support global seismic hazard calculations for use on the Global Earthquake Modeling (GEM) project. GEM is an international collaboration working to produce a seismic hazard and loss calculations on a global scale. OpenSHA’s object-oriented design, and its ability to perform very large-scale PSHA calculations using distributed computing, makes it an excellent basis for the large-scale PSHA calculations needed by GEM.

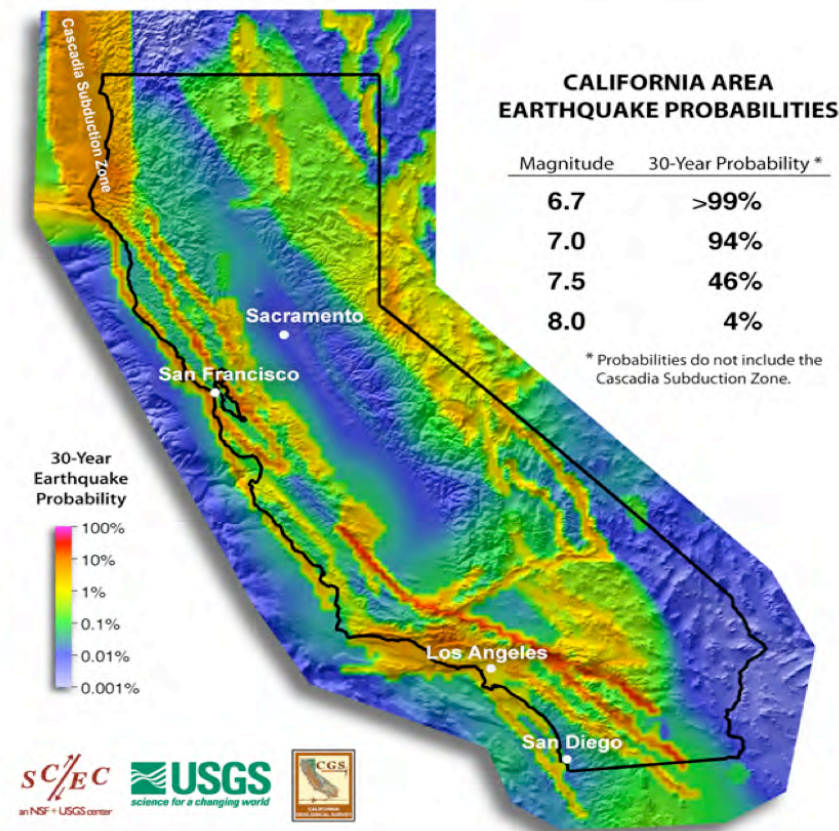


Figure 81. The colors on this California map represent the UCERF2 probabilities of having a nearby earthquake rupture (within 3 or 4 miles) of magnitude 6.7 or larger in the next 30 years. As shown in the table, the chance of having such an event somewhere in California exceeds 99%. The 30-year probability of an even more powerful quake of magnitude 7.5 or larger is about 46%. The CME OpenSHA computational platform was used in the development of the UCERF2 model with funding support from the California Earthquake Authority (an insurance consortium). The OpenSHA platform demonstrates the value of integrating geological and structure models with computational capabilities. New computational models can be added to the platform and immediately used in PSHA calculations with other existing PSHA components.

Physics-Based PSHA Curves Using UCERF2.0. Traditional PSHA calculations calculate ground motions at a site for a particular earthquake by using an attenuation relationship as a ground motion prediction equation (GMPE). This approach is computationally efficient but produces only an approximation of ground motions at the sites under study and these standard GMPE calculations do not produce seismograms so certain information about the ground motions is not

available. PSHA researchers on the CME have implemented the CyberShake Platform in order to replace existing GMPE in standard PSHA calculations with 3D wave propagation modeling. Integrating 3D waveform modeling into standard PSHA calculations is an interesting scientific challenge as well as a very large computational challenge. The CyberShake PSHA technique promises to deliver new insights about how rupture directivity and sedimentary basin effects can modify hazard curves. CyberShake is the capacity-computing platform for executing and managing the large number of Pathway 2 simulations needed to construct physics-based PSHA maps.

A CME team led by R. Graves (URS) and Scott Callaghan (USC) developed the CyberShake Platform over the last few years. The current CyberShake implementation samples ~13,000 distinct sources in the UCERF2.0 ERF for Southern California. For each large ($M > 6.5$) source, the hypocenter, rupture rise-time and velocity distributions, and final slip distribution are varied according to a pseudo-dynamic model, producing a total catalog of more than 400,000 ruptures for each site. To make the calculations feasible, the Graves AWP codes has been modified and optimized to calculate “receiver Green tensors” (RGTs). Using seismic reciprocity, we can now efficiently post-process the RGTs to synthesize a site’s ground motions for the full suite of rupture variations and, from this database, compute hazard curves for spectral accelerations below 0.5 Hz.

In previous years, the CME developed the basic CyberShake computational approach and calculated a number of PSHA hazard curves in order to validate our methodology. In 2009, based on satisfactory verification and validation results for a small number of trial CyberShake hazard curves, we scaled our CyberShake calculations up to produce a physics-based PSHA hazard map for part of Southern California. Using TeraGrid computer resources at TACC, we used the CyberShake computational platform to calculate physics-based (3D waveform modeling based) probabilistic seismic hazard curves. When then combined these hazard curves into the first ever physics-based PSHA map for Southern California as shown in Figure 82.

This CyberShake1.0 PSHA hazard map required an enormous calculation involving both parallel earthquake wave propagation codes and serial post-processing codes. The CME was able to perform this calculation by using a workflow system based on NSF-funded tools including Pegasus-WMS, Condor DAGManager, and Globus. The CyberShake1.0 Map calculation required more than 60 days of processing on one of the NSF’s largest supercomputers and used more than 6 million CPU hours to complete.

This CyberShake 1.0 map represents the initial implementation of an important new technique for improving PSHA hazard curves. The official USGS PSHA hazard curves impact billions of dollars of construction each year. Improvements in PSHA hazard curves can have a very broad societal impact. Until now, physics-based PSHA calculations have been beyond the computational capabilities of SCEC and other seismic hazard research groups. The CME work has shown this type of calculation is possible. Now, we anticipate that SCEC researchers will help to evaluate the results and to determine whether the level of improvement produced by CyberShake justifies the computational effort needed by new PSHA technique.

CyberShake’s PSHA calculations integrate elements from most of the other CME ground motion modeling simulations. As the other CME computational platforms such as the DynaShake Platform, the TeraShake Platform, and the F3DT Platform produce improved ground motion modeling results, these improvements will be integrated into the CyberShake Platform so that CyberShake physics-based PSHA calculations continue to improve in accuracy and/or efficiency of calculation.

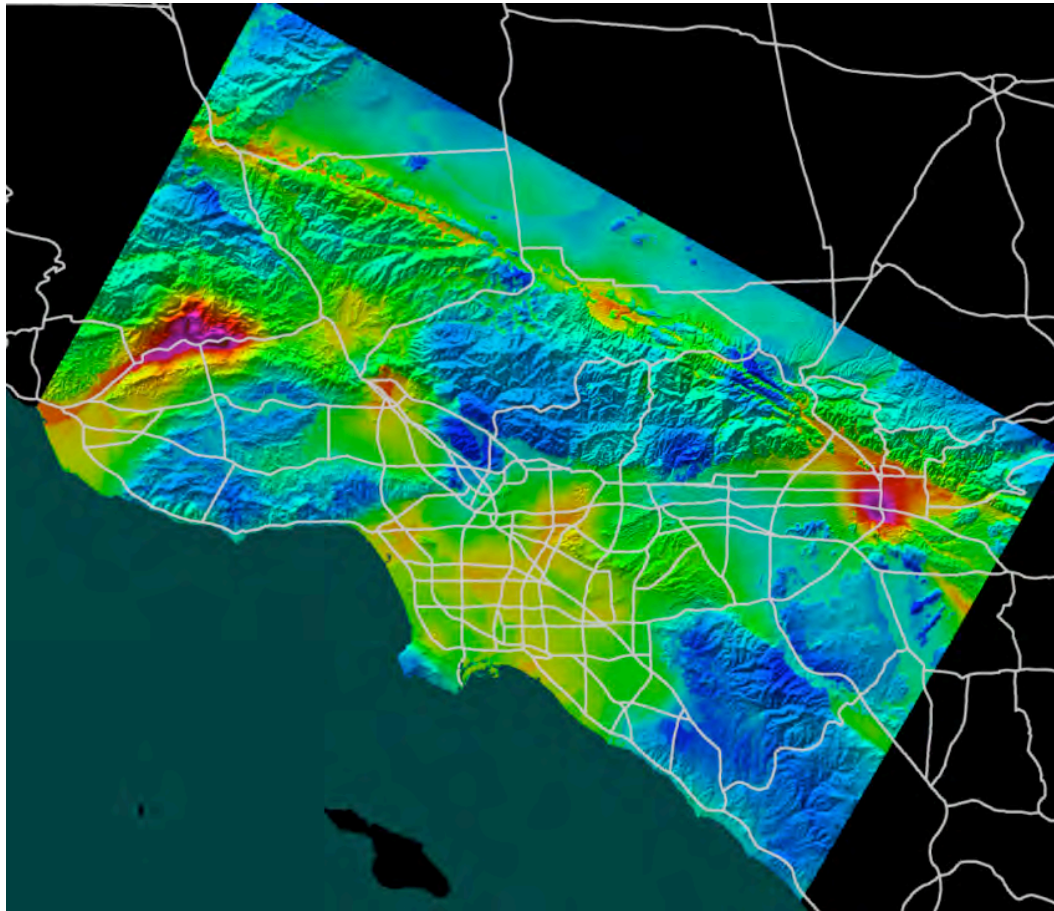


Figure 82. More than 220 CyberShake v1.0 physics-based PSHA hazard curves are assimilated into a background UCERF2 (2008) and NGA-based (2008) PSHA map (left) Peak SA3.0 (0.1 blue to 1.2 indigo) at 2% in 50 years tends to raise hazard estimates in the Los Angeles and Ventura Basins and reduce hazard estimates for mountainous regions in southern California. The CyberShake capacity computational platform calculated this map over approximately 50 days of production runs on NSF Track 2 Ranger system. Scientific workflow technologies, including Globus, Condor, and Pegasus were used to submit, run, and monitor more than 100M tasks and 100M files during the calculation. The CME workflow system was able to use an average of 4000 cores at all times on TACC Ranger for 50 days in order to complete this calculation. This capacity run represents a transformative use of NSF HPC facilities by NSF/EAR research groups. The technologies developed by the CME collaboration run at this scale include general purpose geoinformatics and cyberinfrastructure tools valuable to both solid earth researchers as well as other domains including atmosphere, high energy physics, and medical research.

The CyberShake1.0 map calculation was possible only because of the advanced IT capabilities of the CME. Several computational trends for the CME indicating significant improvements during the last few years (Figure 83). These plots show that the CME has produced steady improvements in the scientific tools, the speed of processing, and the cyberinfrastructure used in the CyberShake Platform. The CyberShake1.0 calculations show how the CME applies HPC tools and techniques to PSHA enabling SCEC to produce improved seismic hazard information for southern California.

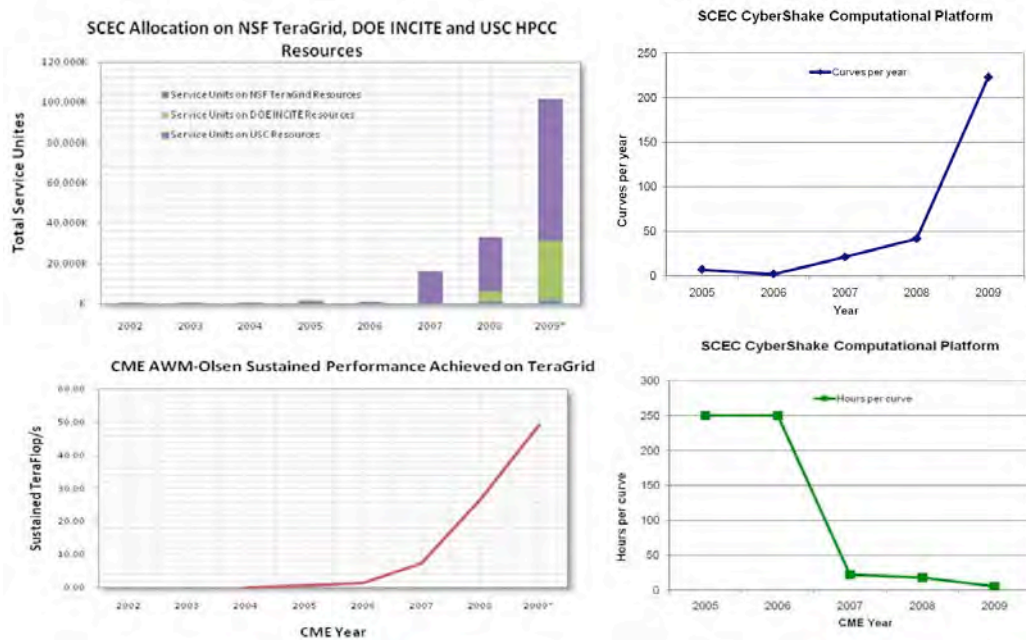


Figure 83. CME supercomputer allocations (top left) now include resources from NSF TeraGrid, USC HPCC, and DOE INCITE program. Peak performance of our capability code AWP-Olsen (bottom left) has risen as performance improvements and larger HPC system have become available. The number of physics-based PSHA hazard curves calculated with the CyberShake platform has risen by two orders of magnitude (top right), and the time required to calculate a hazard curve (bottom right) has fallen by two orders of magnitude.

h. Upcoming CME Research

The SCEC system science approach continues to integrate better physics into seismic hazard calculations and the CME continues to improve the efficiency of SCEC calculations on open-science high performance computers. The overall goal of improving seismic hazard calculations remains constant but the CME improvements change year by year. This upcoming year, the CME will run several large-scale scenario earthquake simulations for southern California that we call the Big Ten (Figure 84).

The Big Ten is a collection of large magnitude (>M7.5), high probability ruptures defined in UCERF2. All Big Ten events represent significant seismic hazards for Southern California. The Big Ten event set has been carefully selected to confront seismologists and numerical modelers with a wide variety of scientific and computational challenges. Issue the modeling groups must address include modeling of high frequency sources and wave propagation, use of multiple velocity models, simulation regions so large that earth curvature must be considered, modeling of topography, important of low minimum S wave velocities in velocity models, dipping faults, fault to fault stress transfer, and long rupture surface, long duration, M8.0+ events. The Big Ten simulations will involve all of the SCEC computational platforms. The Big Ten simulations are representative of earthquake simulations used in seismic hazard calculations and this CME research will help SCEC determine how to get valid scientific results from large seismic hazard calculations.

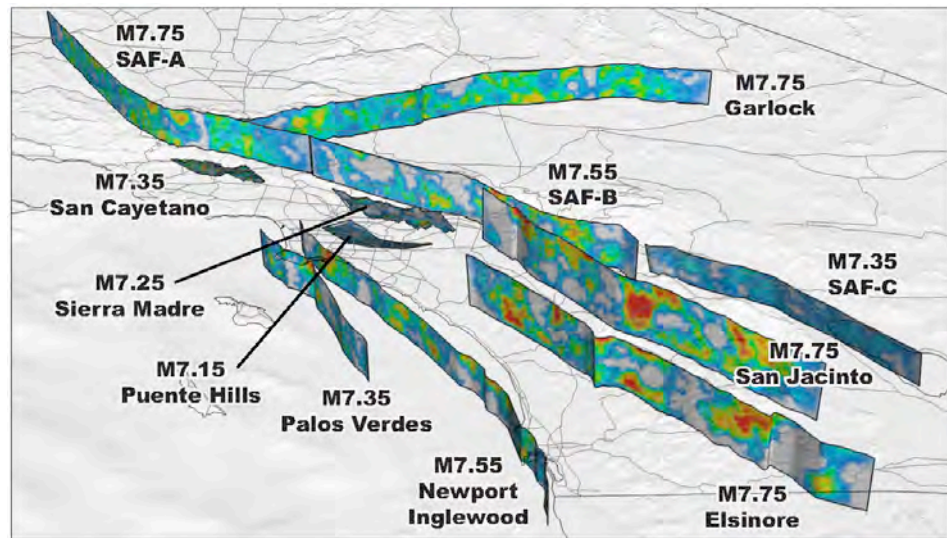


Figure 84. The Big Ten events are a collection of large magnitude, high probability ruptures defined in UCERF2.0. The CME will integrate new capabilities into our computational platforms including simulation of dynamic ruptures on dipping faults and higher frequency (>2Hz) wave propagation simulations. Once our computational platforms run at the required scale with the required capabilities, we will simulate the Big Ten events and analyze the impact of these scenario on seismic hazards in Southern California (Image: Ely, Jordan - USC).

i. References

- Bielak, J., Graves, R., Olsen, K., Taborda, R., Ramirez-Guzman, L., Day, S., Ely, G., Roten, D., Jordan, T., Maechling, P., Urbanic, J., Cui, Y. and Juve, G.: The ShakeOut Earthquake Scenario: Verification of Three Simulation Sets, submitted to Geophysical Journal International, March, 2009.
- Callaghan, S., P. Maechling, E. Deelman, K. Vahi, G. Mehta, G. Juve, K. Milner, R. Graves, E. Field, D. Okaya, D. Gunter, K. Beattie, and T. Jordan, 'Reducing Time-to-Solution Using Distributed High-Throughput Mega-Workflows -- Experiences from SCEC CyberShake', Fourth IEEE International Conference on eScience, IEEE, Indianapolis, IN, 2008.
- Cui, Y., Chourasia, A., Moore, R., Olsen, K., Maechling, P., Jordan, T., The TeraShake Computational Platform, Advances in Geocomputing, Lecture Notes in Earth Sciences 119, DOI 10.1007/978-3-540-85879-9_7, pp229-278, editor H. Xing, Springer-Verlag Berlin Heidelberg, 2009.
- Dalguer, L. A., H. Miyake, S. M. Day, and K. Irikura, Calibrated surface and buried dynamic rupture models constrained with statistical observations of past earthquakes, *Bull. Seism. Soc. Am*, Vol. 98, doi: 10.1785/0120070134, pp. 1147-1161, 2008.
- Day, S. M., R. W. Graves, J. Bielak, D. Dreger, S. Larsen, K. B. Olsen, A. Pitarka, and L. Ramirez-Guzman (2008). *Model for basin effects on long-period response spectra in southern California*, Earthquake Spectra (in press).
- Doser, D.I., K.B. Olsen, F.F. Pollitz, R.S. Stein, and S. Toda, The 1911 M~6.6 Calaveras earthquake: Source parameters and the role of static, viscoelastic and dynamic Coulomb stress changes imparted by the 1906 San Francisco earthquake, *Bull. Seis. Soc. Am.* 99, 1746-1759, 2009.
- Duan, B., and S.M. Day, *Inelastic strain distribution and seismic radiation from rupture of a fault kink* J. Geophys. Res., in review.

Report | SCEC Research Accomplishments

- Ely, G., S.M. Day, and J-B. Minster *Dynamic rupture models for the southern San Andreas fault*, Bull. Seism. Soc. Am., in review, 2008.
- Ely, G. P., S. M. Day, and J. B. Minster, *A support-operator method for viscoelastic wave modeling in 3D heterogeneous media*, Geophys. J. Int. , 172, doi: 10.1111/j.1365-246X.2007.03633.x, 331-344, 2008.
- Graves, R. W., The seismic response of the San Bernardino Basin region during the 2001 Big Bear Lake earthquake, *Bull. Seismol. Soc. Am.*, **98**, 241– 252, doi:10.1785/0120070013, 2008.
- Graves, R.W., B. Aagaard, K. Hudnut, L. Star, J. Stewart & T. H. Jordan, Broadband simulations for Mw 7.8 southern San Andreas earthquakes: Ground motion sensitivity to rupture speed, *Geophys. Res. Lett.*, submitted, Sept. 2008.
- Graves, R., S. Callaghan, E. Deelman, E. Field, N. Gupta, T. H. Jordan, G. Juve, C. Kesselman, P. Maechling, G. Mehta, D. Meyers, D. Okaya and K. Vahi, Physics Based Probabilistic Seismic Hazard Calculations for Southern California, 14th World Conference on Earthquake Engineering, October, 2008, Beijing China
- Ma, S., G.A. Prieto, and G. C. Beroza, Testing Community Velocity Models for Southern California Using the Ambient Seismic Field, *Bull. Seismol. Soc. Am.*, **98**, 2694-2714, DOI: 10.1785/0120080947, 2008
- Maechling, P., E. Deelman, Y. Cui, Implementing Software Acceptance Tests as Scientific Workflows, Proceedings of the IEEE International Parallel & Distributed Processing Symposium 2009, Las Vegas Nevada, July, 2009 (in press), 2009.
- Olsen, K. B., Dalguer, L., Day, S., Cui, Y., Zhu, J., Cruz, V.M., Roten, D., Mayhew, J., Maechling, P., Jordan, T., Chourasia, A. and Okaya, D. ShakeOut-D: Ground Motion Estimates Using an Ensemble of Large Earthquakes on the Southern San Andreas Fault With Spontaneous Rupture Propagation, *Geophysical Research Letters*, doi:10.1029/2008GL036832, in press, 2009.
- Olsen, K.B., W.J. Stephenson, and Andreas Geisselmeyer, *3D Crustal Structure and Long-period Ground Motions From a M9.0 Megathrust Earthquake in the Pacific Northwest Region*, Jour. Seismol. DOI 10.1007/s10950-007-9082-y, 2008.
- Olsen, K.B. and J.N. Brune, *Constraints from precariously balanced rocks on preferred rupture directions for large earthquakes on the southern San Andreas Fault*, Jour. Seismol. DOI 10.1007/s10950-007-9078-7, 2008.
- Prieto, G.A. & G. C. Beroza, Earthquake ground motion prediction using the ambient seismic field, *Geophys. Res. Lett.* **35**, L14304, doi:10.1029/2008GL034428, 2008.
- Star, L.M., J. P. Stewart, R. W. Graves & K. W. Hudnut, Validation against NGA empirical model of simulated motions for M7.8 rupture of San Andreas Fault, Proceedings of the 14th World Conference on Earthquake Engineering , Beijing, China, Paper No. 02-0070, 2008.
- Stewart, J.P., L. M. Star & R. W. Graves, Validation against NGA empirical model of simulated motions for M7.15 rupture of Puente Hills fault, preprint, 2008.

Draft 2010 Science Plan

SCEC Planning Committee

September 2009 Meeting

I. Introduction

On February 1, 2002, the Southern California Earthquake Center (SCEC) changed from an entity within the NSF/STC program to a freestanding center, funded by NSF/EAR and the U.S. Geological Survey. SCEC2 was funded for a five-year period, February 2002 to January 2007. SCEC was renewed for the period February 2007 through January 2012, referred to now as SCEC3. This document solicits proposals from individuals and groups to participate in the second year of the SCEC3 research program.

II. Guidelines for Proposal Submission

Due Date. Friday, November 6, 2009, 5:00 pm PST. Late proposals will not be accepted. Note the different deadline for submitting annual progress reports below.

Delivery Instructions. Proposals must be submitted as PDF documents via the SCEC Proposal web site at <http://www.scec.org/proposals>. Submission procedures, including requirements for how to name your PDF files, will be found at this web site.

Formatting Instructions.

- **Cover Page.** The cover page should be headed with the words "2010 SCEC Proposal" and include the project title, Principal Investigator(s), institutional affiliation, amount of request, and proposal categories (from types listed in Section IV). List in order of priority three science objectives (Section VII) that your proposal addresses, for example A3, A5 and A11. Indicate if the proposal should also be identified with one or more of the SCEC special projects (see Section VIII). Collaborative proposals involving multiple investigators and/or institutions should list all Principal Investigators. Proposals do not need to be formally signed by institutional representatives, and should be for one year, with a start date of February 1, 2010.
- **Technical Description.** Describe in up to five pages (including figures) the technical details of the project and how it relates to the short-term objectives outlined in the SCEC Science Objectives (Section VII). References are not included in the five-page limit.
- **Budget Page.** Budgets and budget explanations should be constructed using NSF categories. Under guidelines of the SCEC Cooperative Agreements and A-21 regulations, secretarial support and office supplies are not allowable as direct expenses.
- **Current Support.** Statements of current support, following NSF guidelines, should be included for each Principal Investigator.
- **2009 Annual Report.** Scientists funded by SCEC in 2009 must submit a report of their progress by 5 pm February 28, 2010. 2010 proposals approved by the PC will not be funded until all progress reports are submitted. Reports should be up to five pages of text and figures. Reports should include bibliographic references to any SCEC publication during the past year (including papers submitted and in review), including their SCEC contribution number. Publications are assigned numbers when they are submitted to the SCEC publication database at <http://www.scec.org/signin>.

Draft 2010 Science Plan

- **Labeling the Submitted PDF Proposal.** PI's must follow the proposal naming convention. Investigators must label their proposals with their last name followed by 2010, e.g., Archuleta2010.pdf. If there is more than one proposal, then the file would be labeled as: Archuleta2010_1.pdf (for the 1st proposal) and Archuleta2010_2.pdf (for the 2nd proposal).

Principal Investigator Responsibilities. PI's are expected to interact with other SCEC scientists on a regular basis (e.g., by attending workshops and working group meetings), and contribute data, analysis results, and/or models to the appropriate SCEC data center (e.g., Southern California Earthquake Data Center—SCEC), database, or community model (e.g., Community Velocity Model—CVM). Publications resulting entirely or partially from SCEC funding must include a publication number available at <http://www.scec.org/signin>. By submitting a proposal, investigators are agreeing to these conditions.

Eligibility. Proposals can be submitted by eligible Principal Investigators from:

- U.S. Academic institutions
- U.S. Private corporations
- International Institutions (funding will mainly be for travel)

Collaboration. Collaborative proposals with investigators from the USGS are encouraged. USGS employees should submit their requests for support through USGS channels. Collaborative proposals involving multiple investigators and/or institutions are strongly encouraged; these can be submitted with the same text, but with different institutional budgets if more than one institution is involved.

Budget Guidance. Typical SCEC grants funded under this Science Plan in the past have fallen in the range of \$10,000 to \$35,000. This is not intended to limit SCEC to a fixed award amount, nor to a specified number of awards, rather it is intended to calibrate expectations for proposals written by first-time SCEC investigators.

Award Procedures. All awards will be funded by subcontract from the University of Southern California. The Southern California Earthquake Center is funded by the National Science Foundation and the U.S. Geological Survey.

III. SCEC Organization

A. **Mission and Science Goal.** SCEC is an interdisciplinary, regionally focused organization with a mission to:

- Gather data on earthquakes in Southern California and elsewhere
- Integrate information into a comprehensive, physics-based understanding of earthquake phenomena
- Communicate understanding to the world at large as useful knowledge for reducing earthquake risk

SCEC's primary science goal is to develop a comprehensive, physics-based understanding of earthquake phenomena in Southern California through integrative, multidisciplinary studies of plate-boundary tectonics, active fault systems, fault-zone processes, dynamics of fault ruptures, ground motions, and seismic hazard analysis. The long-term science goals are summarized in Appendix A.

B. **Disciplinary Activities.** The Center sustains disciplinary science through standing committees in seismology, geodesy, and geology. These committees will be responsible for planning and coordinating disciplinary activities relevant to the SCEC science plan, and they will make recommendations to the SCEC Planning Committee regarding

support of disciplinary research and infrastructure. High-priority disciplinary activities are summarized in Section VII.A.

- C. **Interdisciplinary Focus Areas.** Interdisciplinary research is organized within five science focus areas: 1) Unified Structural Representation (URS), 2) Fault and Rupture Mechanics (FARM), 3) Crustal Deformation Modeling (CDM), 4) Lithospheric Architecture and Dynamics (LAD), 5) Earthquake Forecasting and Predictability (EFP), 6) Ground Motion Prediction (GMP) and 7) Seismic Hazard and Risk Analysis (SHRA). High-priority activities are listed for each of these interdisciplinary focus areas in Section VII.B.
- D. **Special Projects.** SCEC supports eleven special projects that will advance designated research frontiers. Several of these initiatives encourage further development of an advanced IT infrastructure for system-level earthquake science in Southern California. High-priority initiatives are listed and described in Section VIII.
- E. **Communication, Education, and Outreach.** SCEC maintains a strong Communication, Education, and Outreach (CEO) program with four principal goals: 1) coordinate productive interactions among SCEC scientists, and with partners in science, engineering, risk management, government, business, and education; 2) increase earthquake knowledge and science literacy at all educational levels; 3) improve earthquake hazard and risk assessments; and 4) promote earthquake preparedness, mitigation, and planning for response and recovery. Opportunities for participating in the CEO program are described in Section IX. Current activities are described online at <http://www.scec.org/ceo>.

IV. Proposal Categories

- A. **Data Gathering and Products.** SCEC coordinates an interdisciplinary and multi-institutional study of earthquakes in Southern California, which requires data and derived products pertinent to the region. Proposals in this category should address the collection, archiving and distribution of data, including the production of SCEC community models that are on-line, maintained, and documented resources for making data and data products available to the scientific community.
- B. **Integration and Theory.** SCEC supports and coordinates interpretive and theoretical investigations on earthquake problems related to the Center's mission. Proposals in this category should be for the integration of data or data products from Category A, or for general or theoretical studies. Proposals in Categories A and B should address one or more of the goals in Section VII, and may include a brief description (<200 words) as to how the proposed research and/or its results might be used in a special initiative (see Section VIII) or in an educational or outreach mode (see Section IX).
- C. **Workshops.** SCEC participants who wish to host a workshop between February 2009 and February 2010 should submit a proposal for the workshop in response to this RFP. This includes workshops that might be organized around the SCEC annual meeting in September. Workshops in the following topics are particularly relevant:
 - Organizing collaborative research efforts for the five-year SCEC program (2007-2012). In particular, interactive workshops that engage more than one focus and/or disciplinary group are strongly encouraged.
 - Engaging earthquake engineers and other partner and user groups in SCEC-sponsored research.

Draft 2010 Science Plan

- Participating in national initiatives such as EarthScope, the Advanced National Seismic System (ANSS), and the George E. Brown, Jr. Network for Earthquake Engineering Simulation (NEES).
- D. **Communication, Education, and Outreach.** SCEC has developed a long-range CEO plan and opportunities for participation are listed in Section IX. Investigators who are interested in participating in this program should contact Mark Benthien (213-740-0323; benthien@usc.edu) before submitting a proposal.
- E. **SCEC/SURE Intern Project.** If your proposal includes undergraduate funding, please note this on the cover page. Each year SCEC coordinates the SCEC Summer Undergraduate Research Experience (SCEC/SURE) program to support one-on-one student research with a SCEC scientist. See <http://www.scec.org/internships> for more information. SCEC will be recruiting mentors in November, 2008, and will request descriptions of potential projects via email. In December, these descriptions will be published on the SCEC Internship web page to allow applicants to identify their preferred projects.

Mentors will be required to provide at least \$2500 of the \$5000 intern stipend, and SCEC will pay the balance. Mentor contributions can come from any source, including SCEC-funded research projects. Therefore, interested SCEC scientists are encouraged to include at least \$2500 for an undergraduate intern in their 2009 SCEC proposals, and then respond to the recruitment emails.

Questions about the SCEC/SURE Intern Project should be referred to Robert de Groot, degroot@usc.edu.

- F. **SCEC Annual Meeting participation.** Investigators who wish to only request funding to cover travel to the annual meeting can participate in a streamlined review process with an abbreviated proposal. Investigators who are already funded to study projects that would be of interest to the SCEC community, and investigators new to SCEC who would benefit from exposure to the annual meeting in order to fine-tune future proposals are encouraged to apply.

V. Evaluation Process and Criteria

- A. Proposals should be responsive to the RFP. A primary consideration in evaluating proposals will be how directly the proposal addresses the main objectives of SCEC. Important criteria include (not necessarily in order of priority):
- Scientific merit of the proposed research
 - Competence and performance of the investigators, especially in regard to past SCEC-sponsored research
 - Priority of the proposed project for short-term SCEC objectives as stated in the RFP
 - Promise of the proposed project for contributing to long-term SCEC goals as reflected in the SCEC science plan (see Appendix).
 - Commitment of the P.I. and institution to the SCEC mission
 - Value of the proposed research relative to its cost
 - Ability to leverage the cost of the proposed research through other funding sources
 - Involvement of students and junior investigators
 - Involvement of women and underrepresented groups

- Innovative or "risky" ideas that have a reasonable chance of leading to new insights or advances in earthquake physics and/or seismic hazard analysis.
- B. Proposals may be strengthened by describing:
- Collaboration
 - Within a disciplinary or focus group
 - Between disciplinary and/or focus groups
 - In modeling and/or data gathering activities
 - With engineers, government agencies, and others. (See Section IX)
 - Leveraging additional resources
 - From other agencies
 - From your institution
 - By expanding collaborations
 - Development and delivery of products
 - Community research tools, models, and databases
 - Collaborative research reports
 - Papers in research journals
 - End-user tools and products
 - Workshop proceedings and CDs
 - Fact sheets, maps, posters, public awareness brochures, etc.
 - Educational curricula, resources, tools, etc.
 - Educational opportunities
 - Graduate student research assistantships
 - Undergraduate summer and year-round internships (funded by the project)
 - K-12 educator and student activities
 - o Presentations to schools near research locations
 - o Participation in data collection
- C. All research proposals will be evaluated by the appropriate disciplinary committees and focus groups, the Science Planning Committee, and the Center Director. CEO proposals will be evaluated by the CEO Planning Committee and the Center Director.
- D. The Science Planning Committee is chaired by the Deputy Director and comprises the chairs of the disciplinary committees, focus groups, and special projects. It is responsible for recommending a balanced science budget to the Center Director.
- E. The CEO Planning Committee is chaired by the Associate Director for CEO and comprises experts involved in SCEC and USGS implementation, education, and outreach. It is responsible for recommending a balanced CEO budget to the Center Director.
- F. Recommendations of the planning committees will be combined into an annual spending plan and forwarded to the SCEC Board of Directors for approval.
- G. Final selection of research projects will be made by the Center Director, in consultation with the Board of Directors.
- H. The review process should be completed and applicants notified by the end of February, 2010.

VI. Coordination of Research Between SCEC and USGS-EHRP

- A. Earthquake research in Southern California is supported both by SCEC and by the USGS Earthquake Hazards Reduction Program (EHRP). EHRP's mission is to provide the scientific information and knowledge necessary to reduce deaths, injuries, and economic losses from earthquakes. Products of this program include timely notifications of

Draft 2010 Science Plan

- earthquake locations, size, and potential damage, regional and national assessments of earthquakes hazards, and increased understanding of the cause of earthquakes and their effects. EHRP funds research via its External Research Program, as well as work by USGS staff in its Pasadena, Menlo Park, and Golden offices. The EHRP also supports SCEC directly with \$1.1M per year.
- B. SCEC and EHRP coordinate research activities through formal means, including USGS membership on the SCEC Board of Directors and a Joint Planning Committee, and through a variety of less formal means. Interested researchers are invited to contact Dr. Ken Hudnut, EHRP coordinator for Southern California, or other SCEC and EHRP staff to discuss opportunities for coordinated research.
 - C. The USGS EHRP supports a competitive, peer-reviewed, external program of research grants that enlists the talents and expertise of the academic community, State and local governments, and the private sector. The investigations and activities supported through the external program are coordinated with and complement the internal USGS program efforts. This program is divided into six geographical/topical 'regions', including one specifically aimed at Southern California earthquake research and others aimed at earthquake physics and effects and at probabilistic seismic hazard assessment (PSHA). The Program invites proposals that assist in achieving EHRP goals.
 - D. The EHRP web page, <http://earthquake.usgs.gov/research/external/>, describes program priorities, projects currently funded, results from past work, and instructions for submitting proposals. The EHRP external funding cycle is several months offset from SCEC's, with the RFP due out in February and proposals due in May. Interested PI's are encouraged to contact the USGS regional or topical coordinators for Southern California, Earthquake Physics and Effects, and/or National (PSHA) research, as listed under the "Contact Us" tab.
 - E. USGS internal earthquake research is summarized by topic at <http://earthquake.usgs.gov/research/topics.php>

VII. SCEC3 Science Priority Objectives

The research objectives outlined below are priorities for SCEC3. They carry the expectation of substantial and measurable success during the coming year. In this context, success includes progress in building or maintaining a sustained effort to reach a long-term goal. How proposed projects address these priorities will be a major consideration in proposal evaluation, and they will set the programmatic milestones for the Center's internal assessments. In addition to the priorities outlined below, the Center will also entertain innovative and/or "risky" ideas that may lead to new insights or major advancements in earthquake physics and/or seismic hazard analysis.

There are four major research areas with the headings A, B, C and D with subheadings given by numbers. The front page of the proposal should specifically identify subheadings that will be addressed by the proposed research.

- A. Develop an extended earthquake rupture forecast to drive physics-based SHA
 - A1. Define slip rates and earthquake history of southern San Andreas fault system for the last 2000 years
 - A2. Investigate implications of geodetic/geologic rate discrepancies
 - A3. Develop a system-level deformation and stress-evolution model

- A4. Statistical analysis and mapping of seismicity and source parameters with an emphasis on their relation to known faults
- A5. Develop a geodetic network processing system that will detect anomalous strain transients
- A6. Test scientific prediction hypotheses against reference models to understand the physical basis of earthquake predictability
- A7. Determine the origin, evolution and implications of on- and off-fault damage
- A8. Test hypotheses for dynamic fault weakening
- A9. Assess predictability of rupture extent and direction on major faults
- A10. Develop statistical descriptions of heterogeneities (e.g., in stress, strain, geometry and material properties) in fault zones, and understand their origin and implications for seismic hazard by observing and modeling single earthquake ruptures and multiple earthquake cycles.
- A11. Constrain absolute stress and understand the nature of interaction between the faulted upper crust, the ductile crust and mantle, and how geologic history helps to resolve the current physical properties of the system.
- B. Predict broadband ground motions for a comprehensive set of large scenario earthquakes
 - B1. Develop kinematic rupture representations consistent with observations and realistic dynamic rupture models of earthquakes.
 - B2. Investigate bounds on the upper limit of ground motion
 - B3. Develop high-frequency simulation methods and investigate the upper frequency limit of deterministic ground motion predictions
 - B4. Validate earthquake simulations and verify simulation methodologies
 - B5. Improve our understanding of nonlinear effects and develop methodologies to include these effects in broadband ground motion simulations.
 - B6. Collaborate with earthquake engineers to develop rupture-to-rafters simulation capability for physics-based risk analysis
- C. Improve and develop community products (data or descriptions) that can be used in system-level models for the forecasting of seismic hazard. Proposals for such activities should show how they would significantly contribute to one or more of the numbered goals in A or B.
- D. Prepare post-earthquake response strategies

Some of the most important earthquake data are gathered during and immediately after a major earthquake. Exposures of fault rupture are erased quickly by human activity, aftershocks decay rapidly within days and weeks, and post-seismic slip decays exponentially. SCEC solicits proposals for a workshop to plan post-earthquake science response. The goals of the workshop would be to: 1) develop a post-earthquake science plan that would be a living document such as a wiki; 2) identify permanent SCEC and other science facilities that are needed to ensure success of the science plan; 3) identify other resources available in the community and innovative ways of using technology for

Draft 2010 Science Plan

coordination and rapid data processing that will allow for rapid determination of source parameters, maps, and other characteristics of the source and ground motion patterns.; 4) develop plans for use of simulations in post-earthquake response for evaluation of short-term earthquake behavior and seismic hazards; and 5) develop mechanisms for regular updates of the SCEC post-earthquake response plan.

VII-A. Disciplinary Activities

The Center will sustain disciplinary science through standing committees in seismology, geodesy, and geology. These committees will be responsible for planning and coordinating disciplinary activities relevant to the SCEC science plan, and they will make recommendations to the SCEC Planning Committee regarding the support of disciplinary infrastructure. High-priority disciplinary objectives include the following tasks:

1. Seismology

- A. **Objectives.** The objectives of the Seismology group are to gather data on the range of seismic phenomena observed in southern California and to integrate these data into physics-based models of fault slip. Of particular interest are proposals that foster innovations in network deployments, data collection, real-time research tools, and data processing. Proposals that provide community products that support one or more of the numbered goals in A, B, C or D or those that include collaboration with network operators in Southern California are especially encouraged.

Proposers should consider the SCEC resources available including the Southern California Earthquake Data Center (SCEDC) that provides extensive data on Southern California earthquakes as well as crustal and fault structure, the network of SCEC funded borehole instruments that record high quality reference ground motions, and the pool of portable instruments that is operated in support of targeted deployments or aftershock response.

- B. **Research Strategies.** Examples of research strategies that support the objectives above include:
- Enhancement and continued operation of the SCEDC and other existing SCEC facilities particularly the near-real-time availability of earthquake data from SCEDC and automated access.
 - Real-time processing of network data such as improving the estimation of source parameters in relation to known and unknown faults (A3, A4, A10), especially evaluation of the short term evolution of earthquake sequences and real-time stress perturbations on nearby major fault segments (D).
 - Enhance or add new capabilities to existing earthquake early warning (EEW) systems or provide new EEW algorithms. Develop real-time finite source models constrained by incoming seismic and GPS data to estimate evolution of the slip function and potentially damaging ground shaking (D).
 - Advance innovative and practical strategies for densification of seismic instrumentation, including borehole instrumentation, in Southern California and develop innovative algorithms to utilize data from these networks. Develop metadata, archival and distribution models for these semi-mobile networks.
 - Develop innovative new methods to search for unusual signals using combined seismic, GPS, and borehole strainmeter data (A5, A6); collaborations with EarthScope or other network operators are encouraged.
 - Investigate near-fault crustal properties, evaluate fault structural complexity, and develop constraints on crustal structure and state of stress, and (A7, A10, C).
 - Collaborations, for instance with the ANSS and NEES projects, that would augment existing and planned network stations with downhole and surface

instrumentation to assess site response, nonlinear effects, and the ground coupling of built structures (B4, B6).

- Preliminary design and data collection to seed future passive and active experiments such as dense array measurements of basin structure and large earthquake properties, OBS deployments, and deep basement borehole studies.

C. **Priorities for Seismology in 2010:**

- Earthquake early warning research. In the next few years, earthquake early warning (EEW) systems will be installed in California. The seismology group seeks proposals that will provide new algorithms, enhance or add new capabilities to existing EEW algorithms. The development of Bayesian probabilities that would take advantage of the extensive knowledge developed by SCEC about fault structures and spatial and temporal seismicity patterns are needed to make EEW algorithms more robust. Similarly, high-sample rate GPS 1 second solutions are being made available real-time for EEW development. Using these new data to develop new EEW algorithms for finite sources is a new area of research for SCEC scientists. For instance, we seek proposals that will provide algorithms for real-time finite source models constrained by incoming real-time seismic and GPS data to predict spatial and temporal development of the slip function, as well as the resulting potentially damaging ground shaking.
- Low-cost dense sensor networks. Several low cost seismic sensors networks are being developed in California. We seek proposal that would address development of seismological algorithms to utilize data from these networks in an innovative way. We also seek proposals that would develop metadata and archiving models for these new semi-mobile networks, as well as archive and serve these data to the SCEC user community.
- Near Real-time earthquake sequence source processes. Two recent earthquake sequences (in Italy and near Bombay Beach in the Salton Sea area of southern California) highlight the need for rapid evaluation of earthquake probabilities and to identify the onset of a significant events within evolving earthquake sequences. We seek proposals that would address the earthquake statistics aspects of earthquake sequences, and quantifying source processes that may have value for predicting short term evolution of earthquake sequences. In addition, small sequences may perturb the state of stress on nearby major fault segments. We seek proposals that would provide quantitative evaluation of such processes, and possibly provide near real-time estimates of changes in earthquake probabilities for these major fault segments.

2. Tectonic Geodesy

- A. **Objectives.** The broad objective of SCEC's Tectonic Geodesy disciplinary activities is to foster the availability of the variety of geodetic data collected in Southern California and the innovative and integrated use of these observations, in conjunction with other relevant data (e.g., seismic or geologic information), to address the spectrum of deformation processes affecting this region. Topics of interest include, but are not limited to, rapid earthquake response, transient deformation, anthropogenic or nontectonic effects, and the quantification and interpretation of strain accumulation and release, with one goal being the increased use of insights from geodesy in seismic hazard assessment. Proposed work may overlap with one or more focus areas, such as Crustal Deformation Modeling (CDM).
- B. **Research Strategies.** The following are research strategies aimed at meeting the broad objective:
- Develop reliable means for detecting, assessing, and interpreting transient deformation signals and for using this information in monitoring and response activities. (A5).

Draft 2010 Science Plan

- Develop detection algorithms. Work that extends the demonstrated capability of such algorithms to real data, that utilizes other data types in addition to or instead of GPS, or that explores means for incorporating such algorithms into monitoring systems is encouraged, as is participation in the ongoing Transient Detection Blind Test Exercise.
- Generate sets of real or synthetic GPS or other types of data for the Transient Detection Blind Test Exercise.
- Investigate processes underlying detected signals and/or their seismic hazard implications.
- Extend methods for estimating crustal motion and refine such estimates for southern California (A1, A2, A3, B1, C, D). In all cases, work should include assessment of the sources of uncertainty in the analysis and quantification of uncertainties in results (especially those relating to model uncertainty). Proposals for the development of new data products or collection of new data must explicitly motivate the need for such efforts and state how the resulting data or products will be used. Data collected with SCEC funding must be made publically-available in an online archive within two years of its collection, although PIs may choose to share data on a case-by-case basis earlier than the two-year deadline.
 - Collaborate on the generation and maintenance of an up-to-date consensus velocity field for southern California.
 - Improve vertical velocity estimates, for example by refining or extending data processing and analysis strategies or approaches for the combined use of multiple data types.
 - Identify possible trade-offs in regional slip rate models, conduct quantitative comparison of such models, and/or develop new models.
 - Develop methods for combining data types (e.g., GPS, InSAR, strainmeter, and/or other data) that have differing spatial and temporal apertures, sampling frequencies, and sensitivities, and assess the utility of such combinations for interpreting tectonic or nontectonic signals.
 - Develop tools for using high-rate and real-time GPS positions and demonstrate application of these data to address topics such as rapid earthquake response, postseismic analysis, or the combined use of GPS and seismic data.

3. Earthquake Geology

- A. **Objectives.** The Earthquake Geology group promotes studies of the geologic record of the Southern California natural laboratory that advance SCEC science. Geologic observations can provide important contributions to nearly all SCEC objectives in seismic hazard analysis (A1-A3, A6-A11) and ground motion prediction (B2-B5). Studies are encouraged to test outcomes of earthquake simulations and crustal deformation modeling. Earthquake Geology also fosters data-gathering activities that will contribute demonstrably significant geologic information to (C) community data sets such as the Unified Structural Representation. The primary focus of the Earthquake Geology is on the Late Quaternary record of faulting and ground motion in southern California. Collaborative proposals that cut across disciplinary boundaries are especially competitive.
- B. **Research Strategies.** Examples of research strategies that support the objectives above include:
 - Paleoseismic documentation of earthquake ages and displacements, including a coordinated effort to develop slip rates and earthquake history of southern San Andreas fault system (A1).
 - Evaluating the potential for 'wall-to-wall' rupture or a brief cluster of major earthquakes on the San Andreas fault system (A1, A9).
 - Investigating the likelihood of multi-segment and multi-fault ruptures on major southern California faults (A1, A9).

- Testing models for geologic signatures of preferred rupture direction (A9).
 - Development of slip rate and slip-per-event data sets, taking advantage of newly collected GeoEarthScope LiDAR data, and with a particular emphasis on documenting patterns of seismic strain release in time and space (A1-A3, A5, A6, A9).
 - Development of methods to evaluate multi-site paleoseismic data sets and standardize error analysis (A1, A9).
 - Characterization of fault-zone geology, material properties, and their relationship to earthquake rupture processes, including studies that relate earthquake clustering to fault loading in the lower crust (A7, A8, A10).
 - Quantitative analysis of the role of distributed deformation in accommodating block motions, dissipating elastic strain, and modifying rheology (A2, A3, A7, A10, A11).
 - Development of constraints on the magnitude and recurrence of strong ground motions from precarious rocks and slip-per-event data (B2-B5).
- C. **Geochronology Infrastructure.** The shared geochronology infrastructure supports C-14, optically stimulated luminescence (OSL), and cosmogenic dating for SCEC-sponsored research. The purpose of shared geochronology infrastructure is to allow flexibility in the number and type of dates applied to each SCEC-funded project as investigations proceed. Investigators requesting geochronology support must estimate the number and type of dates needed in their proposal. For C-14 specify if sample preparation will take place at a location other than the designated laboratory. For cosmogenic dating, investigators are required to arrange for sample preparation. These costs must be included in the proposal budget unless preparation has been pre-arranged with one of the laboratories listed. Investigators are strongly encouraged to contact the investigators at the collaborating laboratories prior to proposal submission. Currently, SCEC geochronology has established relationships with the following laboratories:
- C-14: University of California at Irvine (John Southon, jsouthon@uci.edu) and Lawrence Livermore National Laboratory (Tom Guilderson, tguilderson@llnl.gov).
 - OSL: University of Cincinnati (Lewis Owen, lewis.owen@uc.edu) and Utah State University (Tammy Rittenour, tammy.rittenour@usu.edu)
 - Cosmogenic: Lawrence Livermore National Laboratory (Tom Guilderson, tguilderson@llnl.gov).

Investigators at collaborating laboratories are requested to submit a proposal that states the cost per sample analysis and estimates of the minimum and maximum numbers of analyses feasible for the upcoming year. These investigators are also strongly encouraged to request for funds to support travel to the SCEC annual meeting. New proposals from laboratories not listed above will be considered, though preference will be given to strengthening existing collaborations.

Investigators may alternatively request support for geochronology outside of the infrastructure proposal for methods not listed here or if justified on a cost-basis. These outside requests must be included in the individual proposal budget. Please direct questions regarding geochronology infrastructure to the Earthquake Geology group leader, Mike Oskin (meoskin@ucdavis.edu).

VII-B. Interdisciplinary Focus Areas

Interdisciplinary research will be organized into seven science focus areas: 1) Unified Structural Representation (USR), 2) Fault and Rupture Mechanics (FARM), 3) Crustal Deformation Modeling (CDM), 4) Lithospheric Architecture and Dynamics (LAD), 5) Earthquake Forecasting and Predictability (EFP), 6) Ground Motion Prediction (GMP) and 7) Seismic Hazard and Risk Analysis

Draft 2010 Science Plan

(SHRA). High-priority objectives are listed below for each of the seven interdisciplinary focus areas. Collaboration within and across focus areas is strongly encouraged.

1. Unified Structural Representation (USR)

The Structural Representation group develops unified, three-dimensional representations of active faults and earth structure (velocity, density, etc.) for use in fault-system analysis, ground motion prediction, and hazard assessment. This year's efforts will focus on making improvements to existing community models (CVM-H, CFM) that will facilitate their uses in SCEC science, education, and post-earthquake response planning.

- A. **Community Velocity Model (CVM).** Improve the current SCEC CVM-H model, with emphasis on more accurate representations of V_p , V_s , density structure, and basin shapes, and derive models for attenuation. Generate improved mantle V_p and V_s models, as well as more accurate descriptions of near-surface property structure that can be incorporated into a revised geotechnical layer. Evaluate the existing models with data (e.g., waveforms, gravity) to distinguish alternative representations and quantify model uncertainties. Establish an evaluation procedure and benchmarks for testing how future improvements in the models impact ground motion studies. Special emphasis will be placed on developing and implementing 3D waveform tomographic methods for evaluating and improving the CVM-H.
- B. **Community Fault Model (CFM).** Improve and evaluate the CFM, placing emphasis on defining the geometry of major faults that are incompletely, or inaccurately, represented in the current model. Evaluate the CFM with data (e.g., seismicity, seismic reflection profiles, geodetic displacement fields) to distinguish alternative fault models. Integrate northern and Southern California models into a statewide fault framework, and update the CFM-R (rectilinear fault model) to reflect improvements in the CFM.
- C. **Unified Structural Representation (USR).** Develop better IT mechanisms for delivering the USR, particularly the CVM parameters and information about the model's structural components, to the user community for use in generating and/or parameterizing computational grids and meshes. An example of such IT mechanism is a web-based system that allows plot and download of profiles and cross sections of the CVMs and related data (i.e., V_s30) at desired locations. Generate maps of geologic surfaces compatible with the CFM that may serve as strain markers in crustal deformation modeling and/or property boundaries in future iterations of the USR.

2. Fault and Rupture Mechanics (FARM)

The primary mission of the Fault and Rupture Mechanics focus group in SCEC3 is to develop physics-based models of the nucleation, propagation, and arrest of dynamic earthquake rupture. We specifically solicit proposals that address this mission through field, laboratory, and modeling efforts directed at characterizing and understanding the influence of material properties, geometric irregularities, and heterogeneities in stress and strain over multiple length and time scales (A7-A10, B1, B4), and that will contribute to our understanding of earthquakes in the Southern California fault system.

We invite proposals to:

- A. Investigate the relative importance of different dynamic weakening and fault healing mechanisms, and the slip and time scales over which these mechanisms operate (A7-A10).

- B. Determine the properties of fault cores and damage zones and characterize their variability with depth and along strike to constrain theoretical and laboratory studies, including width and particle composition of actively shearing zones, signatures of temperature variations, extent, origin and significance of on- and off-fault damage, healing, and poromechanical behavior (A7-A11).
- C. Determine the relative contribution of on- and off-fault damage to the total earthquake energy budget, and the absolute levels of local and average stress (A7-A11).
- D. Develop realistic descriptions of heterogeneity in fault geometry, properties, stresses, and strains, and tractable ways to incorporate heterogeneity in numerical models of single dynamic rupture events and multiple earthquake cycles (A10-11, B1, B4).
- E. Understand the significance of fault zone characteristics and processes on fault dynamics and formulate constitutive laws for use in dynamic rupture models (A7-11, B1, B4).
- F. Assess the predictability of rupture direction and directivity of seismic radiation by collecting and analyzing field and laboratory data, and conducting theoretical investigations to understand implications for strong ground motion (A7-A10, B1).
- G. Evaluate the relative importance of fault structure, material properties, interseismic healing, and prior seismic and aseismic slip to earthquake dynamics, in particular, to rupture initiation, propagation, and arrest, and the resulting ground motions (A7-A10, B1).
- H. Characterize earthquake rupture, fault loading, degree of localization, and constitutive behavior at the base of and below the seismogenic zone. Understand implications of slow events and non-volcanic tremors for constitutive properties of faults and overall seismic behavior. Use these data to evaluate seismic moment-rupture area relationships (A3, A11).

3. Crustal Deformation Modeling (CDM)

We seek proposals aimed at resolving the kinematics and dynamics of southern California faults over time scales ranging from hours to thousands of years. Our long-term goal is to contribute to the SCEC objective of developing a physics-based probabilistic seismic hazard analysis for southern California by developing and applying system-wide deformation models of processes at time-scales of the earthquake cycle. Our immediate goals include assessing the level of detail necessary in deformation models to achieve the broader SCEC objectives. Collaborations with geologists and researchers in other SCEC groups are strongly encouraged.

System-Wide Deformation Models:

- A. Develop kinematic models of interseismic deformation or the earthquake cycle to estimate slip rates on primary southern CA faults, fault geometries at depth, and spatial distribution slip or moment deficits on faults. Compare with or refine SCEC CFM and assess discrepancies of the kinematic models with geodetic, geologic, and seismic data (A1, A3).
- B. Develop a system-wide model of southern California faults, incorporating the SCEC CFM, properties derived from the SCEC CVM, and realistic inferred rheologies, to model interseismic deformation, including transfer of stress across the fault system (A3).
- C. Develop simpler models to compare with the system-wide deformation model above for benchmarking purposes and to assess the degree of detail needed to adequately represent interseismic deformation and stress transfer. Various modeling approaches are requested

Draft 2010 Science Plan

and might include boundary element methods, 2D simplifications, and analytical or semi-analytical methodology (A10, A3).

- D. Assess whether stress transfer implicitly assumed in earthquake simulator models is similar to stress transfer estimated from either category of deformation model mentioned above (A11).

More Focused Deformation Models:

- A. Determine the extent to which rheological heterogeneity (including damage) influences deformation and stress transfer at various spatial and temporal scales. What level of detail will be required for the system-wide model (A7, A10, A11, A3)?
- B. Evaluate spin-up effects for viscoelastic models and methods to accelerate this process. How much does deep viscoelastic relaxation influence interseismic deformation and stress transfer? Can it be neglected or “worked around” in a southern-California-wide stress transfer model (A11, A3)?
- C. Evaluate whether nonlinear rheologies be represented with heterogeneous distributions of linearly viscoelastic material (A11, A3).
- D. Investigate causes of discrepancies between geologic and geodetic slip rate estimates (A2).
- E. Investigate possible causes and effects of transient slip and earthquake clustering (A1, A11).

4. Lithospheric Architecture and Dynamics (LAD)

The lithospheric architecture and dynamics group (LAD) seeks proposals that will contribute to our understanding of the structure, geologic provenance and physical state of the major southern California lithospheric units, and how these relate to absolute stress in the crust and the evolution of the lithospheric system (A3, A11).

The principal objective of this group is to understand the physics of the southern California system, the boundary conditions and internal physical properties. Special attention is given to constraining the average absolute stress on southern California faults. Our general approach is to use 3D geodynamic models to relate the various forces loading the lithosphere to observable fields such as geodetic and geologic strain, seismic anisotropy and gravity. Of particular importance are: how flow in the sub-seismogenic zone and the asthenosphere accommodates plate motion, constraints on density structure and rheology of the southern California lithosphere, and how the system loads faults.

Physics models will be developed that use the paleo-history of the 3D geology to infer how present physical conditions were created, such as depths of Moho, the seismogenic layer, base of the lithosphere, topography and basin depths, rock type, temperature, water content, rheology and how these relate to mantle flow, velocity, anisotropy and density.

The LAD work will interface with the geology group to better understand crustal structure and North America mantle lithosphere. Of particular interest are the distribution of the underplated schist and the fate of Farallon microplate fragments and their relation to inferred mantle drips. We will interact with FARM to obtain constraints on rheology and stress (absolute and dynamic), with the USR and seismology groups on 3D structure, and CDM on current stress and strain rates.

In this context, proposals are sought that contribute to our understanding of geologic inheritance and its relation to the three-dimensional structure and physical properties of the crust and lithosphere. Proposals should indicate how the work relates to stress evolution (A2, A3, A11) as

well as the current geological structure (C). A primary goal is to generate systems-level models that describe southern California dynamics against which hypotheses can be tested regarding the earthquake mechanism, fault friction, seismic efficiency, the heat flow paradox and the expected evolution of stress and strain transients (A5).

The LAD group will be involved in the USGS-NSF Margins/Earthscope Salton Trough Seismic Project and will interface to the southern California offshore seismic (OBS) experiment, and will consider proposals that piggyback these experiments and integrate the results into LAD goals.

5. Earthquake Forecasting and Predictability (EFP)

In general we seek proposals that will increase our understanding of how earthquakes might be forecast and whether or not earthquakes are predictable (A6). Proposals of any type that can assist in this goal will be considered. We are especially interested in proposals that will utilize the Collaboratory for the Study of Earthquake Predictability (CSEP). In order to increase the number of earthquakes in the data sets, and so decrease the time required to learn about predictability, proposals are welcome that deal with global data sets and/or include international collaborations.

For research strategies that plan to utilize CSEP, see the description of CSEP under Special Projects to learn of its capabilities. Successful investigators proposing to utilize CSEP would be funded via core SCEC funds to adapt their prediction methodologies to the CSEP framework, to transfer codes to the externally accessible CSEP computers, and to be sure they function there as intended (A6). Subsequently, the codes would be moved to the identical externally inaccessible CSEP computers by CSEP staff who will conduct tests against a variety of data as outlined in the CSEP description. In general, methodologies will be considered successful only if they do better than null hypotheses that include both time-independent and time-dependent probabilities. Proposals aimed toward developing useful measurement/testing methodology that could be incorporated in the CSEP evaluations are welcomed, including those that address how to deal with observational errors in data sets.

Proposals are also welcome that assist in attaining the goals of these two Special Projects: WGCEP (the Working Group on California Earthquake Probabilities) and SoSAFE (the Southern San Andreas Evaluation), especially if the proposals focus on understanding some physical basis for connections between earthquakes. Proposals to utilize and/or evaluate the significance of earthquake simulator results are encouraged. Investigation of what is an appropriate magnitude-area relationship, including the maximum depth of slip during large earthquakes, is encouraged. Studies of how to properly characterize the relationship between earthquake frequency and magnitude for use in testing prediction algorithms are also encouraged.

Proposals that can lead to understanding whether or not there exists a physical basis for earthquake predictability (A6) are welcome, even if they are not aimed toward, or are not ready for, tests in CSEP, or are not aimed toward assisting WGCEP or SoSAFE. For example, proposals could include ones that connect to objectives A1, A2, A3, A5, A9, A10 and A11, as well as ones focused on understanding patterns of seismicity in time and space, as long as they are aimed toward understanding the physical basis of some aspect of extended earthquake predictability (A6). Development of methods for testing prediction algorithms that are not yet in use by CSEP is encouraged.

Proposals for workshops are welcome. Specific workshops of interest include one on earthquake simulators and one on setting standards that could be used by CSEP for testing and evaluation, data, and products.

6. Ground Motion Prediction (GMP)

The primary goal of the Ground Motion Prediction focus group is to develop and implement physics-based simulation methodologies that can predict earthquake strong motion waveforms over the frequency range 0-10 Hz. Source characterization plays a vital role in ground motion prediction. At frequencies less than 1 Hz, the methodologies should deterministically predict the amplitude, phase and waveform of earthquake ground motions using fully three-dimensional representations of the ground structure, as well as dynamic or dynamically-compatible kinematic representations of fault rupture. At higher frequencies (1-10 Hz), the methodologies should predict the main character of the amplitude, phase and waveform of the motions using a combination of deterministic and stochastic representations of fault rupture and wave propagation.

Research topics within the Ground Motion Prediction program include:

- A. Developing and/or refining physics-based simulation methodologies, with particular emphasis on high frequency (1-10 Hz) approaches (B3)
- B. Incorporation of non-linear models of soil response (B2, B4, B5);
- C. Development of more realistic implementations of dynamic or kinematic representations of fault rupture. In collaboration with FARM, this research could also include the examination of current source-inversion strategies and development of robust methods that allow imaging of kinematic and/or dynamic rupture parameters reliably and stably, along with a rigorous uncertainty assessment. (B1, B2).
- D. Verification (comparison against theoretical predictions) and validation (comparison against observations) of the simulation methodologies with the objective of being to develop robust and transparent simulation capabilities that incorporate consistent and accurate representations of the earthquake source and three-dimensional velocity structure (B4, C).

It is expected that the products of the Ground Motion Prediction group will have direct application to seismic hazard analysis, both in terms of characterizing expected ground motion levels in future earthquakes, and in terms of directly interfacing with earthquake engineers in the analysis of built structures (B6). Activities within the Ground Motion Prediction group will be closely tied to several special projects, with particular emphasis on addressing ground motion issues related to seismic hazard and risk. These special projects include the Extreme Ground Motion Project and the Tall Buildings Initiative (see SHRA below).

7. Seismic Hazard and Risk Analysis (SHRA)

The purpose of the SHRA Focus Group is to apply SCEC knowledge to the development of information and techniques for quantifying earthquake hazard and risk, and in the process to provide feedback on SCEC research. Projects in this focus group will in some cases be linked to the Ground Motion Prediction Focus Group, to SCEC special projects such as the Extreme Ground Motion Project, and to Pacific Earthquake Engineering Research Center (PEER) special projects such as the Tall Buildings Initiative (TBI) and Reference Buildings and Bridges Project. Projects that involve interactions between SCEC scientists and members of the community involved in earthquake engineering research and practice are especially encouraged. Examples of work relevant to the SHRA Focus Group follow.

Improved Hazard Representation

- A. Develop improved hazard models that consider simulation-based earthquake source and wave propagation effects that are not already well-reflected in observed data. These could

include improved methods for incorporating rupture directivity effects, basin effects, and site effects in the USGS ground motion maps, for example. The improved models should be incorporated into OpenSHA.

- B. Use broadband strong motion simulations, possibly in conjunction with recorded ground motions, to develop ground motion prediction models (or attenuation relations). Broadband simulation methods must be verified (by comparison with simple test case results) and validated (against recorded strong ground motions) before use in model development. The verification, validation, and application of simulation methods must be done on the SCEC Broadband Simulation Platform. Such developments will contribute to the future NGA-H Project.
- C. Develop ground motion parameters (or intensity measures), whether scalars or vectors, that enhance the prediction of structural response and risk.
- D. Investigate bounds on the variability of ground motions for a given earthquake scenario.

Ground Motion Time History Simulation

- A. Develop acceptance criteria for simulated ground motion time histories to be used in structural response analyses for building code applications or risk analysis.
- B. Assess the advantages and disadvantages of using simulated time histories in place of recorded time histories as they relate to the selection, scaling and/or modification of ground motions for building code applications or risk analysis.
- C. Develop and validate modules for the broadband simulation of ground motion time histories close to large earthquakes, and for earthquakes in the central and eastern United States, for incorporation in the Broadband Platform.

Collaboration in Building Response Analysis

- A. Tall Buildings. Enhance the reliability of simulations of long period ground motions in the Los Angeles region using refinements in source characterization and seismic velocity models, and evaluate the impacts of these ground motions on tall buildings. Such projects could potentially build on work done in the TBI Project.
- B. End-to-End Simulation. Interactively identify the sensitivity of building response to ground motion parameters and structural parameters through end-to-end simulation. Buildings of particular interest include non-ductile concrete frame buildings.
- C. Reference Buildings and Bridges. Participate with PEER investigators in the analysis of reference buildings and bridges using simulated broadband ground motion time histories. The ground motions of large, rare earthquakes, which are poorly represented in the NGA strong motion database, are of special interest. Coordination with PEER can be done through Yousef Bozorgnia, yousef@berkeley.edu.
- D. Earthquake Scenarios. Perform detailed assessments of the results of scenarios such as the ShakeOut exercise, and the scenarios for which ground motions were generated for the Tall Buildings Initiative (including events on the Puente Hills, Southern San Andreas, Northern San Andreas and Hayward faults) as they relate to the relationship between ground motion characteristics and building response and damage.

Ground Deformation

Draft 2010 Science Plan

- A. Investigate the relationship between input ground motion characteristics and local soil nonlinear response, liquefaction, lateral spreading, local soil failure, and landslides.

Risk Analysis

- A. Develop improved site/facility-specific and portfolio/regional risk analysis (or loss estimation) techniques and tools, and incorporate them into the OpenRisk software.
- B. Use risk analysis software to identify earthquake source and ground motion characteristics that control damage estimates.

Other Topics

Proposals for other innovative projects that would further implement SCEC information and techniques in seismic hazard and risk analysis, and ultimately loss mitigation, are encouraged.

VIII. Special Projects and Initiatives

The following are SCEC special projects with which proposals in above categories can be identified.

1. Southern San Andreas Fault Evaluation (SoSAFE)

The SCEC Southern San Andreas Fault Evaluation (SoSAFE) Project will continue to increase our knowledge of slip rates, paleo-event chronology, and slip distributions of past earthquakes, for the past two thousand years on the southern San Andreas fault system. From Parkfield to Bombay Beach, and including the San Jacinto fault, the objective is to obtain new data to clarify and refine relative hazard assessments for each potential source of a future 'Big One.' Most work to be funded is expected to involve paleoseismic and geological fault slip rate studies.

Past SoSAFE workshops have led to a focused research plan, and further discussion at the SoSAFE workshop prior to the 2009 SCEC Annual Meeting will allow for refinement of group objectives for the fourth year. Research by single or multi-investigator teams will be supported to rapidly advance SCEC research towards meeting priority scientific objectives related to the mission of the SoSAFE special project. Research will address significant portions of the fault system, and all investigators will agree to collaboratively review one another's progress. We welcome requests for infrastructure resources, for example geochronology support. That is, an investigator may ask for dating support (e.g., to date 12 radiocarbon samples). Requests for dating shall be coordinated with Earthquake Geology and a portion of SoSAFE funds will be contributed towards joint support for dating.

We also welcome proposals that investigate methodologies for using paleoseismic and geologic data to develop rupture histories. For example, ongoing interaction between SoSAFE and the scenario rupture modeling activities of SCEC will continue beyond the ShakeOut, as we continue to develop constraints such as dating or slip data that can be used to eliminate the scenario of a "wall-to-wall" rupture (from Parkfield to Bombay Beach). SoSAFE will also work to constrain scenario models by providing the best possible measurements of actual slip distributions from past earthquakes on these same fault segments as input, thereby enabling a more realistic level of scenario modeling. Use of novel methods for estimating slip rates from geodetic data would also potentially be supported within the upcoming year. Slip rate studies will continue to be encouraged, and for these it is understood that support may be awarded to study offset features that may be older than 2000 yrs., perhaps as old as 60,000 yrs. in some cases. It is expected that much support will go towards improved dating (e.g., radiocarbon and OSL) of earthquakes within

the past 2000 yrs., so that event correlations and coefficient of variation in recurrence intervals may be further refined.

SoSAFE objectives also foster common longer-term research interests and engage in facilitating future collaborations in the broader context of a decade-long series of interdisciplinary, integrated and complementary studies on the southern San Andreas fault system.

The fourth year of SoSAFE may again be funded at \$240K by USGS, depending on 1) the report on progress in the first three years, 2) effective leveraging of USGS funds with funds from other sources, 3) level of available funding from USGS for the year, and 4) competing demands for the USGS Multi-Hazards Demonstration Project funding.

2. Working Group on California Earthquake Probabilities (WGCEP)

Following the 2008 release of the Uniform California Earthquake Rupture Forecast version 2 (UCERF2), the WGCEP is now working on adding some major enhancements in a forthcoming UCERF3. Our primary goals are to relax segmentation, add multi-fault ruptures, and include spatial-temporal clustering (earthquake triggering). As the latter will require robust interoperability with real-time seismicity information, UCERF3 will bring us into the realm of operational earthquake forecasting. This model is being developed jointly by SCEC, the USGS, and CGS, with tight coordinated with the USGS National Seismic Hazard Mapping Program. The following are examples of SCEC activities that could make direct contributions to WGCEP goals:

- A. Reevaluate fault models in terms of the overall inventory, and specify more precisely fault endpoints in relationship to neighboring faults (important for multi-fault rupture possibilities)
- B. Reevaluate fault slip rates, especially using more sophisticated modeling approaches (e.g., that include GPS data, generate kinematically consistent results, and perhaps provide off-fault deformation rates as well).
- C. Help determine the average along-strike slip distribution of large earthquakes, especially where multiple faults are involved (e.g., is there reduced slip at fault connections?)
- D. Help determine the average down-dip slip distribution of large earthquakes (the ultimate source of existing discrepancies in magnitude-area relationships).
- E. Contribute to the compilation and interpretation of mean recurrence-interval constraints from paleoseismic data.
- F. Develop earthquake rate models that relax segmentation and include multi-fault ruptures.
- G. Develop ways to constrain the spatial distribution of maximum magnitude for background seismicity (for earthquakes occurring off of the explicitly modeled faults).
- H. Answer the question of whether every small volume of space exhibits a Gutenberg Richter distribution of nucleations?
- I. Develop methods for quantifying elastic-rebound based probabilities in un-segmented fault models.
- J. Help quantify the amount of slip in the previous event (including variations along strike) on any major faults in California.
- K. Develop models for fault-to-fault rupture probabilities, especially give uncertainties in fault endpoints.

Draft 2010 Science Plan

- L. Determine the proper explanation for the apparent post-1906 seismicity-rate reduction (which appears to be a statewide phenomenon)?
- M. Develop applicable methods for adding spatial and temporal clustering to the model.
- N. Develop easily computable hazard or loss metrics that can be used to evaluate and perhaps trim logic-tree branch weights.
- O. Develop techniques for down-sampling event sets to enable more efficient hazard and loss calculations.

Further suggestions and details can be found at <http://www.WGCEP.org>, or by speaking with the project leader (Ned Field: field@usgs.gov; (626) 644-6435).

3. Next Generation Attenuation Project, Hybrid Phase (NGA-H)

The NGA-H Project is currently on hold, but it is hoped that it will go forward at some point in the future in conjunction with PEER. It will involve the use of broadband strong motion simulation to generate ground motion time histories for use, in conjunction with recorded ground motions, in the development of ground motion attenuation relations for hard rock that are based on improved sampling of magnitude and distance, especially large magnitudes and close distances, and improved understanding of the relationship between earthquake source and strong ground motion characteristics. Broadband simulation methods are verified (by comparison of simple test case results with other methods) and validated (against recorded strong ground motions) before being used to generate broadband ground motions for use in model development. These simulation activities for verification, validation, and application are done on the SCEC Broadband Simulation Platform. The main SCEC focus groups that are related to this project are Ground Motion Prediction and Seismic Hazard and Risk Analysis.

4. End-to-End Simulation

The purpose of this project is to foster interaction between earthquake scientists and earthquake engineers through the collaborative modeling of the whole process involved in earthquake fault rupture, seismic wave propagation, site response, soil-structure interaction, and building response. Recent sponsors of this project have been NSF (tall buildings) and CEA (woodframe buildings), and new sponsors are being sought. The main SCEC discipline and focus groups working on this project are Geology, especially fault models; Unified Structural Representation; Faulting and the Mechanics of Earthquakes; Ground Motion Prediction; Seismic Hazard and Risk Analysis; and PetaSHA – Terashake and Cybershake.

5. Collaboratory for the Study of Earthquake Predictability (CSEP)

CSEP is developing a virtual, distributed laboratory—a collaboratory—that supports a wide range of scientific prediction experiments in multiple regional or global natural laboratories. This earthquake system science approach seeks to provide answers to the questions: (1) How should scientific prediction experiments be conducted and evaluated? and (2) What is the intrinsic predictability of the earthquake rupture process? Contributions may include:

- A. Establishing rigorous procedures in controlled environments (testing centers) for registering prediction procedures, which include the delivery and maintenance of versioned, documented code for making and evaluating predictions including intercomparisons to evaluate prediction skills;
- B. Constructing community-endorsed standards for testing and evaluating probability-based and alarm-based predictions;

- C. Developing hardware facilities and software support to allow individual researchers and groups to participate in prediction experiments;
- D. Providing prediction experiments with access to data sets and monitoring products, authorized by the agencies that produce them, for use in calibrating and testing algorithms;
- E. Intensifying the collaboration between the US and Japan through international projects, and initiating joint efforts with China;
- F. Developing experiments to test basic physical principles of earthquake generation (e.g., models for estimating the largest possible earthquake on a given fault are important to earthquake scenarios like ShakeOut and to earthquake hazard models. We seek proposals to develop quantitative tests of such models); and
- G. Conducting workshops to facilitate international collaborations.

A major focus of CSEP is to develop international collaborations between the regional testing centers and to accommodate a wide-ranging set of prediction experiments involving geographically distributed fault systems in different tectonic environments.

6. National Partnerships through EarthScope

The NSF Earthscope project provides unique opportunities to learn about the structure and dynamics of North America. SCEC encourages proposals to the NSF Earthscope program that will address the goals of the SCEC Science Plan.

7. Extreme Ground Motion Project (ExGM)

Extreme ground motions are the very large amplitudes of earthquake ground motions that can arise at very low probabilities of exceedance, as was the case for the 1998 PSHA for Yucca Mountain when extended to 10^{-8} /yr. This project investigates the credibility of such ground motions through studies of physical limits to earthquake ground motions, unexceeded ground motions, and frequency of occurrence of very large ground motions or of earthquake source parameters (such as stress drop and faulting displacement) that cause them. Of particular interest to ExGM (and more generally to ground-motion prediction and SHRA) is why crustal earthquake stress drops are so independent of earthquake size (amidst considerable scatter) and so much less than the frictional strength of rocks at mid-crustal depths.

Since the summer of 2005, the DOE-funded Extreme Ground Motion (ExGM) program has supported research at SCEC, both institutionally and individually. ExGM funding has been dramatically cut in the current year, and prospects for the future are uncertain. Available funds will be directed to ground-motion simulations in accord with the original ExGM prospectus and schedule. While the status of ExGM as a separately funded, Special Project is thus uncertain, the research imperatives of ExGM remain significant to several of the SCEC focus and disciplinary groups, including, Geology – especially fault zone geology; Faulting and Mechanics of Earthquakes, Ground-Motion Prediction, and Seismic Hazard and Risk Analysis. This project is also discussed above within SHRA.

8. Petascale Cyberfacility for Physics-Based Seismic Hazard Analysis (PetaSHA)

SCEC's special project titled "A Petascale Cyberfacility for Physics-based Seismic Hazard Analysis" (PetaSHA) aims to develop and apply physics-based predictive models to improve the practice of seismic hazard analysis. This project will utilize numerical modeling techniques and high

Draft 2010 Science Plan

performance computing to implement a computation-based approach to SHA. Three scientific initiative areas have been identified for this project to help to guide the scientific research. The PetaSHA initiative areas are: (1) development of techniques to support higher frequencies waveform simulations including deterministic and stochastic approaches; (2) development of dynamic rupture simulations that include additional complexity including nonplanar faults, a variety of friction-based behaviors, and higher inner /outer scale ratios (e.g. (fault plane mesh dimension) / (simulation volume dimension)); and (3) physics-based probabilistic seismic hazard analysis including probabilistic seismic hazard curves using 3D waveform modeling. All of these modeling efforts must be accompanied by verification and validation efforts. Development of new techniques that support the verification and validation of SCEC PetaSHA modeling efforts are encouraged.

The SCEC PetaSHA modeling efforts address several of the SCEC3 objectives. Development of new verification and validation techniques (B4) are common to each of the PetaSHA initiative areas. Research activities related to the improved understanding and modeling of rupture complexity (A8, B1) support the PetaSHA initiatives. In addition, research into the upper frequency bounds on deterministic ground motion predictions (B2, B3) are SCEC3 science objectives that are important work areas in the PetaSHA Project.

9. Advancement of Cyberinfrastructure Careers through Earthquake System Science (ACCESS)

Project goal. Provide students with research experiences in earthquake system science to advance their careers and creative participation in cyberinfrastructure (CI) development.

Three programmatic elements:

- A. ACCESS-U: One-term undergraduate internships to support CI-related senior thesis research in the SCEC Collaboratory
- B. ACCESS-G: One-year graduate internships to support CI-related master thesis research in the SCEC Collaboratory
- C. ACCESS Forum: a new CEO working group to promote CI careers in earthquake system science

IX. SCEC Communication, Education, and Outreach

SCEC maintains a Communication, Education, and Outreach (CEO) program with four long-term goals:

- Coordinate productive interactions among a diverse community of SCEC scientists and with partners in science, engineering, risk management, government, business, and education.
- Increase earthquake knowledge and science literacy at all educational levels, including students and the general public.
- Improve earthquake hazard and risk assessments
- Promote earthquake preparedness, mitigation, and planning for response and recovery.

Short-term objectives are outlined below. These objectives present opportunities for members of the SCEC community to become involved in CEO activities, which are for the most part coordinated by CEO staff. As project support is very limited, budgets for proposed projects should be on the order of \$2,000 to \$5,000. Hence proposals that include additional sources of support (cost-sharing, funding from other organizations, etc.) are highly recommended. Smaller activities

can be supported directly from the CEO budget and do NOT need a full proposal. Those interested in submitting a CEO proposal should first contact Mark Benthien, associate SCEC director for CEO, at 213-740-0323 or benthien@usc.edu. There may be other sources of funding that can be identified together.

CEO Focus Area Objectives

1. SCEC Community Development and Resources (activities and resources for SCEC scientists and students)
 - SC1 Increase diversity of SCEC leadership, scientists, and students
 - SC2 Facilitate communication within the SCEC Community
 - SC3 Increase utilization of products from individual research projects
2. Education (programs and resources for students, educators, and learners of all ages)
 - E1 Develop innovative earth-science education resources
 - E2 Interest, involve and retain students in earthquake science
 - E3 Offer effective professional development for K-12 educators
3. Public Outreach (activities and products for media reporters and writers, civic groups and the general public)
 - P1 Provide useful general earthquake information
 - P2 Develop information for the Spanish-speaking community
 - P3 Facilitate effective media relations
 - P4 Promote SCEC activities
4. Knowledge transfer (activities to engage other scientists and engineers, practicing engineers and geotechnical professionals, risk managers, government officials, utilities, and other users of technical information.)
 - I1 Communicate SCEC results to the broader scientific community
 - I2 Develop useful products and activities for practicing professionals
 - I3 Support improved hazard and risk assessment by local government and industry
 - I4 Promote effective mitigation techniques and seismic policies

Appendix: SCEC3 Long-Term Research Goals

This section outlines the SCEC science priorities for the five-year period from February 1, 2007, to January 31, 2012. Additional material on the science and management plans for the Center can be found in the SCEC proposal to the NSF and USGS (<http://www.scec.org/aboutscec/documents/>).

Basic Research Problems

SCEC is, first and foremost, a basic research center. We therefore articulate our work plan in terms of four basic science problems: (1) earthquake source physics, (2) fault system dynamics, (3) earthquake forecasting and predictability, and (4) ground motion prediction. These topics organize the most pressing issues of basic research and, taken together, provide an effective structure for

Draft 2010 Science Plan

stating the SCEC3 goals and objectives. In each area, we outline the problem, the principle five-year goal, and some specific objectives. We then assess the research activities and the new capabilities needed to attain our objectives.

1. Earthquake Source Physics

Problem Statement. Earthquakes obey the laws of physics, but we don't yet know how. In particular, we understand only poorly the highly nonlinear physics of earthquake nucleation, propagation, and arrest, because we lack knowledge about how energy and matter interact in the extreme conditions of fault failure. A complete description would require the evolution of stress, displacement, and material properties throughout the failure process across all relevant scales, from microns and milliseconds to hundreds of kilometers and many years. A more focused aspect of this problem is the physical basis for connecting the behavior of large ruptures at spatial resolutions of hundreds of meters and fracture energies of megajoules per square meter with laboratory observations of friction at centimeter scales and fracture energies of kilo-joules per square meter. Two further aspects are the problem of stress heterogeneity—the factors that create and maintain it over many earthquake cycles—and the related problem of defining the concept of strength in the context of stress and rheological heterogeneity.

Goal and Objectives. The goal for SCEC3 will be to discover the physics of fault failure and dynamic rupture that will improve predictions of strong ground motions and the understanding of earthquake predictability. This goal is directly aligned with our mission to develop physics-based seismic hazard analysis. Specific objectives include:

- A. Conduct laboratory experiments on frictional resistance relevant to high-speed coseismic slip on geometrically complex faults, including the effects of fluids and changes in normal stress, and incorporate the data into theoretical formulations of fault-zone rheology.
- B. Develop a full 3D model of fault-zone structure that includes the depth dependence of shear localization and damage zones, hydrologic and poroelastic properties, and the geometric complexities at fault branches, step-overs, and other along-strike and down-dip variations.
- C. Combine the laboratory, field-based, and theoretical results into effective friction laws for the numerical simulation of earthquake rupture, test them against seismological data, and extend the simulation methods to include fault complexities such as bends, step-overs, fault branches, and small-scale roughness.
- D. Develop statistical descriptions of stress and strength that account for slip heterogeneity during rupture, and investigate dynamic models that can maintain heterogeneity throughout many earthquake cycles.

2. Fault System Dynamics

Problem Statement. In principle, the Southern California fault system can be modeled as a dynamic system with a state vector S and an evolution law $dS/dt = F(S)$. The state vector represents the stress, displacement, and rheology/property fields of the seismogenic layer as well as its boundary conditions. Its evolution equation describes the forward problem of fault dynamics. Many of the most difficult (and interesting) research issues concern two inference or inverse problems: (1) model building—from our knowledge of fault physics, what are the best representations of S and F ?—and (2) data assimilation—how are the parameters of these representations constrained by the data D on the system's present state S_0 as well as its history?

The SCEC approach is not to proceed by trying to write down general forms of S and its rate-of-change F . Rather, we use judicious approximations to separate the system evolution into a series of numerical simulations representing the interseismic, preseismic, coseismic, and postseismic behaviors. In particular, the natural time-scale separation between inertial and non-inertial dynamics usually allows us to decouple the long-term evolution of the state vector from its short-term, coseismic behavior. Therefore, in describing many interseismic and postseismic processes, we can treat the fault system quasi-statically, with discontinuous jumps in S at the times of earthquakes. On the other hand, the dynamics of earthquake rupture is clearly important to the basic physics of fault system evolution. In the modeling of stress heterogeneity, for example, the coupling of inertial and non-inertial dynamics must be addressed by integrating across this scale gap.

Goal and Objectives. The principal SCEC3 goal for fault system dynamics is to develop representations of the postseismic and interseismic evolution of stress, strain, and rheology that can predict fault system behaviors within the Southern California Natural Laboratory. The SCEC3 objectives are sixfold:

- A. Use the community modeling tools and components developed in SCEC2 to build a 3D dynamic model that is faithful to the existing data on the Southern California fault system, and test the model by collecting new data and by predicting its future behavior.
- B. Develop and apply models of coseismic fault slip and seismicity in fault systems to simulate the evolution of stress, deformation, fault slip, and earthquake interactions in Southern California.
- C. Gather and synthesize geologic data on the temporal and spatial character and evolution of the Southern California fault system in terms of both seismogenic fault structure and behavior at geologic time scales.
- D. Constrain the evolving architecture of the seismogenic zone and its boundary conditions by understanding the architecture and dynamics of the lithosphere involved in the plateboundary deformation.
- E. Broaden the understanding of fault systems in general by comparing SCEC results with integrative studies of other fault systems around the world.
- F. Apply the fault system models to the problems of earthquake forecasting and predictability.

3. Earthquake Forecasting and Predictability

Problem Statement. The problems considered by SCEC3 in this important area of research will primarily concern the physical basis for earthquake predictability. Forecasting earthquakes in the long term at low probability rates and densities—the most difficult scientific problem in seismic hazard analysis—is closely related to the more controversial problem of high-likelihood predictions on short (hours to weeks) and intermediate (months to years) time scales. Both require a probabilistic characterization in terms of space, time, and magnitude; both depend on the state of the fault system (conditional on its history) at the time of the forecast/prediction; and, to put them on a proper science footing, both need to be based in earthquake physics.

Goal and Objectives. The SCEC3 goal is to improve earthquake forecasts by understanding the physical basis for earthquake predictability. Specific objectives are to:

Draft 2010 Science Plan

- A. Conduct paleoseismic research on the southern San Andreas and other major faults with emphasis on reconstructing the slip distributions of prehistoric earthquakes, and explore the implications of these data for behavior of the earthquake cycle and time-dependent earthquake forecasting.
- B. Investigate stress-mediated fault interactions and earthquake triggering and incorporate the findings into time-dependent forecasts for Southern California.
- C. Establish a controlled environment for the rigorous registration and evaluation of earthquake predictability experiments that includes intercomparisons to evaluate prediction skill.
- D. Conduct prediction experiments to gain a physical understanding of earthquake predictability on time scales relevant to seismic hazards.

4. Ground Motion Prediction

Problem Statement. Given the gross parameters of an earthquake source, such as its magnitude, location, mechanism, rupture direction, and finite extent along a fault, we seek to predict the ground motions at all regional sites and for all frequencies of interest. The use of 3D velocity models in low-frequency (< 0.5 Hz) ground motion prediction was pioneered in SCEC1 (§II.A), and this type of simulation, based on direct numerical solution of the wave equation, has been taken to new levels in SCEC2 (§II.B.6). The unsolved basic research problems fall into four classes: (a) the ground motion inverse problem at frequencies up to 1 Hz; (b) the stochastic extension of ground motion simulation to high frequencies (1-10 Hz); (c) simulation of ground motions using realistic sources; and (d) nonlinear wave effects, including nonlinear site response. In addition, there remain scientific and computational challenges in the practical prediction of ground motions near the source and within complex structures such as sedimentary basins, as well as in the characterization of the prediction uncertainties.

Goal and Objectives. The principal SCEC3 goal is to predict the ground motions using realistic earthquake simulations at frequencies up to 10 Hz for all sites in Southern California. The SCEC3 objectives are:

- A. Combine high-frequency stochastic methods and low-frequency deterministic methods with realistic rupture models to attain a broadband (0-10 Hz) simulation capability, and verify this capability by testing it against ground motions recorded at a variety of sites for a variety of earthquake types.
- B. Use observed ground motions to enhance the Unified Structural Representation (USR) by refining its 3D wavespeed structure and the parameters that account for the attenuation and scattering of broadband seismic energy.
- C. Apply the ground-motion simulations to improve SHA attenuation models, to create realistic scenarios for potentially damaging earthquakes in Southern California, and to explain the geologic indicators of maximum shaking intensity and orientation.
- A. Investigate the geotechnical aspects of how built structures respond to strong ground motions, including nonlinear coupling effects, and achieve an end-to-end simulation capability for seismic risk analysis.

SCEC Annual Meeting Abstracts

Plenary Presentations

Horizon Ballroom, Hilton Palm Springs Resort

MONDAY, SEPTEMBER 14, 2009 – 11:00

DECIPHERING TECTONIC TREMOR BENEATH THE SAN ANDREAS FAULT NEAR PARKFIELD: REPEATING EVENTS, MIGRATION, AND POSSIBLE DEEP SLIP PRECEDING THE 2004 M 6.0 EARTHQUAKE

Shelly DR (Berkeley)

The San Andreas Fault (SAF) is one of the most extensively studied faults in the world, yet its physical character and deformation mode beneath the relatively shallow earthquake-generating portion remain largely unconstrained. Tectonic “non-volcanic” tremor can provide new insight into the deep processes that drive the SAF near Parkfield. Here, I examine continuous seismic data from mid-2001 through 2008, identifying tremor and decomposing the signal into different families of activity based on the shape and timing of the waveforms at multiple stations. This approach allows differentiation between families of activity on nearby patches of the deep fault and begins to unveil rich and complex patterns of tremor occurrence not previously observed in this area. I find that tremor is located at ~25 km depth, near the Moho in this area. Tremor sources are long-lived, with no discernable evolution in waveform shape of individual families over the 7+ year study period. Activity in some families occurs semi-regularly, with recurrence times as short as two days. Tremor exhibits nearly constant migration, with the most extensive episodes propagating more than 20 km along fault strike at rates of 15-80 km/hr. This suggests that the San Andreas Fault remains a localized through-going structure at least to the base of the crust in this area. Of particular interest are newly resolved changes in tremor behavior related to the 2004 M 6.0 Parkfield earthquake. While there is no obvious short-term precursor, I find unidirectional tremor migration accompanied by elevated tremor rates in the 3 months prior to the earthquake, which suggests accelerated creep on the fault ~16 km beneath the eventual earthquake hypocenter [Shelly, 2009, GRL in press]. After the earthquake, tremor rates increased and recurrence times decreased in many areas, but these changes were not uniform within the tremor zone. The systematic recurrence of tremor shown here suggests great potential to monitor detailed time-varying deformation on this portion of the deep SAF.

MONDAY, SEPTEMBER 4, 2009 – 16:00

BRIDGING THE GAP BETWEEN SEISMOLOGY AND ENGINEERING: AVENUES FOR COLLABORATIVE RESEARCH

Goulet C (URS)

Research and practice in seismic hazard and risk analyses would benefit from increased interaction between engineers and scientists. Although collaboration has become more frequent in recent years, there are still many gaps to fill at the interface. As with any type of collaboration, communication is a controlling factor in the success or failure of the joint venture. Efficient communication requires the use of a common language, but even more importantly, it requires a genuine desire to understand the goals and perspectives of each party. The different languages used by both communities is often at the source of a disconnect, but scientists and engineers also tend to have different overall objectives. Scientists are after a better understanding of the world

while engineers are after a designed product, which often requires the use of simplifying models and assumptions. Because of these intrinsic differences in language and perspective, technology transfer at the interface is not always achieved. Through effective collaboration, there are benefits to be gained for all. Engineers will benefit from a better understanding of the science of earthquakes, which can be transferred directly into their designs. Scientists will improve the impact of their findings into the built world and through a better understanding of engineering applications and needs, develop new research ideas. In this presentation, I illustrate some of the practical challenges we face with regard to collaboration and how we can overcome them. I will then present a few specific problems which will help both groups understand gains to be realized from collaborative efforts.

TUESDAY, SEPTEMBER 15, 2009 – 08:00

FAULT LUBRICATION DURING EARTHQUAKES

Di Toro G (INGV), Han R (Korea), Hirose T (Kyoto), De Paola N (Durham), Nielsen S (Johnson & Nielsen), Mizoguchi K (NIED), Ferri F, Cocco M, and Shimamoto T (Hiroshima)

The determination of rock friction at seismic slip rates (about 1 m/s) is of paramount importance in earthquake mechanics, as fault friction controls the stress drop, the mechanical work and the frictional heat adsorbed during slip. Given the lack of determination through seismological methods, elucidating constraints arise from experimental studies. Here we show that a review of a large set of published and unpublished experiments (~300) performed in rotary shear apparatuses at slip rates of 0.1 – 2.6 m/s indicates a significant decrease in friction (up to one order of magnitude) for cohesive (silicate-, quartz- and carbonate-built) and non-cohesive (clay-rich, anhydrite, gypsum and dolomite gouges) rocks typical of crustal seismogenic sources. The temperature rise in the slipping zone triggers thermally activated physico-chemical processes (production of nanopowders, decarbonation and dehydration reactions, flash heating, melt lubrication, etc.) responsible for fault lubrication. The comparison between (1) experimental and natural fault products and (2) mechanical work measures resulting from these laboratory experiments and seismological estimates allows the extrapolation of experimental data to conditions typical of earthquake nucleation depths (7-15 km). Dynamic fault weakening inferred by these experiments implies large coseismic dynamic stress drops (> 70 MPa), irrespective of the fault rock composition and of the specific weakening mechanism involved.

TUESDAY, SEPTEMBER 15, 2009 – 10:30

MAGNITUDE-FREQUENCY STATISTICS ON A SINGLE FAULT: DOES GUTENBERG-RICHTER SCALING APPLY?

Page MT (Caltech), Felzer KR (USGS), Weldon RJ (Oregon), Biasi GP (UNR), Alderson D (Naval Postgraduate School), Doyle J (Caltech), and Field EH (USGS)

The characteristic earthquake hypothesis posits that large earthquakes on major faults occur at a higher rate than a Gutenberg-Richter (G-R) extrapolation from small events would predict (Wesnousky and Scholz, 1983; Schwartz and Coppersmith, 1984). The primary evidence for such a scaling break is an apparent mismatch between instrumental and paleoseismic earthquake rates in several major fault zones. This mismatch, however, can also be explained as a rate change rather than a deviation from G-R statistics. We show that the largest instrumental events in the major fault zones of Southern California are consistent with G-R scaling. For the Southern San Andreas fault in particular, the instrumental and historic catalogs are internally G-R, as is, most importantly, a catalog for the Southern San Andreas fault formed by linking paleoseismic event evidence. Characteristic events are not needed to explain these observations; in fact, the available catalogs leave few gaps in the magnitude distribution where possible characteristic events could reside. A related idea that often follows from the characteristic earthquake hypothesis is that regional G-R

scaling is the result of “characteristic” contributions from individual faults that have a power-law distribution of fault lengths (see e.g., Wesnousky, 1999). However, this idea is inconsistent with the observation that earthquake size in Southern California does not correlate with hypocenter distance from the major mapped faults. Surprisingly, fault demarcations that are clear in the geology and in the seismicity rate are not apparent in the magnitude distribution itself. Lastly, we present an entropic explanation for G-R size scaling on a single fault. While there are many possible sets of earthquakes that can satisfy a given slip rate on a fault, a strong degeneracy of solutions that have G-R scaling makes other size distributions improbable. This entropic push combined with the paleoseismic and instrumental evidence provides compelling evidence that earthquakes on individual faults follow the Gutenberg-Richter relationship.

TUESDAY, SEPTEMBER 15, 2009 – 15:30

SEISMIC TOMOGRAPHY AND IMAGING OF THE SOUTHERN CALIFORNIA CRUST

Tape C, Liu Q, Maggi A, and Tromp J

The ability to accurately simulate seismic waves from strong ($M_w > 7$) earthquakes depends on the qualities of the earthquake rupture model, the three-dimensional (3D) structural model, and the numerical method for seismic wave simulations. Using seismograms from moderate ($M_w < 5$) earthquakes, we iteratively improve a 3D structural model of the southern California crust. The initial 3D model, CVM-H, is provided by the Southern California Earthquake Center. The dataset comprises three-component seismic waveforms (i.e., both body and surface waves), filtered over the period range 2-30 s, from 143 local earthquakes recorded by 203 stations. Time windows for measurements are automatically selected by the FLEXWIN algorithm. The misfit function in the tomographic inversion is based upon frequency-dependent multitaper traveltimes differences. The gradient of the misfit function for each earthquake is computed using an adjoint method. The inversion included 16 iterations, which required 6800 wavefield simulations and a total of 0.8 million CPU hours. Our new crustal model, m16, is described in terms of independent shear (V_s) and bulk-sound (V_b) wavespeed models. It reveals strong heterogeneity, including local changes of +/- 30% with respect to the initial 3D model. The model reveals several features that relate to geologic observations, such as sedimentary basins, exhumed batholiths, and contrasting lithologies across faults. The quality of the new model is validated by the waveform misfit reduction of full-length seismograms from 91 earthquakes that were not used in the tomographic inversion. The new model provides more accurate synthetic seismograms that will benefit assessments of seismic hazard. Its synthetics match observed waveforms that have reflected from complicated interfaces. We will use such waveforms to image prominent interfaces in the southern California crust. "Adjoint tomography" is a powerful tool for improving 3D structural models that can be independently assessed or constrained with additional geological, geophysical, and seismic observations.

WEDNESDAY, SEPTEMBER 16, 2009 – 08:00

LONG- AND SHORT-TERM OPERATIONAL EARTHQUAKE FORECASTING IN ITALY: THE CASE OF THE APRIL 6, 2009, L'AQUILA EARTHQUAKE

Marzocchi W (INGV), and Lombardi AM (INGV)

The recent large earthquake that devastated the city of L'Aquila (located in the Abruzzo region, with a population of about 73,000) gave us a unique opportunity to check our operational long- and short-term earthquake forecasting capability. Here, we describe this experience discussing in detail three issues. First, we analyze the performances of the available long- and short-term forecasting models in a real prospective experiment. Specifically, we compare the long-term forecasts of different time-dependent and time-independent models (the new official hazard map included) that were proposed in the last few years for that region. For the short-term, immediately

following the April 6 event, we began producing daily earthquake forecasts for the region, and we provided these forecasts to Civil Protection - the agency responsible for managing the emergency. The forecasts are based on a stochastic ETES (Epidemic-Type Earthquake Sequence) model that combines the Gutenberg-Richter distribution of earthquake magnitudes and power-law decay in space and time of triggered earthquakes. After one month we compare the forecasts and the real observations in order to evaluate our operational ability to track the evolution of an earthquake sequence in real-time. Second, we discuss the practical problems - and solution adopted - encountered in providing short-term forecasts, mostly due to the limitations of the real-time seismic catalog. Third, we discuss how these probabilistic estimations have been practically used to manage the crisis. In particular, this experience demonstrates an urgent need for a connection between probabilistic forecasts and decision-making in order to establish - before crises - quantitative and transparent protocols for decision support.

Group 1. Poster Abstracts

Plaza Ballroom, Hilton Palm Springs Resort

Communication, Education, and Outreach (CEO)

1-001

NEW PRODUCTS AND PROGRAMS FROM SCEC'S COMMUNICATION, EDUCATION, AND OUTREACH (CEO) PROGRAM *Dansby B (USC), Gotuaco C (SCEC), Yamashita W (USC), Coss Y Leon D (New Mexico Tech), de Groot RM (SCEC / USC), and Hwang G (USC)*

In order to promote improved earthquake awareness and preparedness the SCEC CEO program and the Earthquake Country Alliance (ECA) are in the process of creating three new standards-based educational resources. The "Take on the Quake" program aims to educate several target audiences about earthquake science and preparedness through interactive activities and experiences. The "Take on the Quake" program is ideal for use in many learning environments and contexts such as museums, scouting, and in parks. The program facilitator has a choice to present "Take on the Quake" as a 20-minute overview (Express), a one-hour workshop (Explore), or as a half-day program (Experience). The "Take on the Quake" program can be used any time of the year. The "ShakeOut Curriculum" is designed for use classroom settings during the weeks leading up to, and immediately following the ShakeOut drill. This program takes consideration the time and logistical constraints in school environments. Activities for the "ShakeOut Curriculum" are designed to be flexible and are not sequence-bound. Educators can select the activities they want to use in any order and the lesson length can be easily modified. The maximum time required for any one lesson is thirty minutes. "Take on the Quake" and the "ShakeOut Curriculum" are aligned with the ECA mission by fostering a culture of earthquake and tsunami readiness in California. The materials for these programs will be available on the ECA website. The Plate Tectonics Learning Kit is an expansion and reimagining of an activity created by Professor Larry Braile at Purdue University. At the core of the kit is the USGS Dynamic Planet Poster that is cut into pieces and used as a "puzzle" activity. While extremely effective as a learning tool educators have often commented on the difficulty of knowing where to make the cuts on the map to create the puzzle. SCEC CEO team members have created a simplified version of the map with the map on one side and the cut

lines for the plates and the plate names on the back. This innovation allows the facilitator to use the activity out of the box. The full Plate Tectonics Learning Kit contains the poster and an array of learning tools that provide a cross-curricular learning experience. Additionally, several of the puzzle pieces are easily misplaced and SCEC has responded to this problem by providing templates for the most easily misplaced plates (e.g. Juan de Fuca) without having to purchase a new map.

1-002

USEIT MEDIA GROUP *Howard DM (Wilberforce)*

The Undergraduate Studies in Earthquake Information Technology (USEIT) is an internship program that works out of the Southern California Earthquake Center (SCEC) located at the University of Southern California (USC). USEIT for the past seven years has brought together a diverse group of interns majoring in all areas to collaborate on one big aspect surrounding the summer called The Grand Challenge. For summer 2009, the grand challenge focused on the delivery aspect of SCEC-VDO and its functionalities, as well as developing a viable portal to view such processes and information, and to create an innovative movie as visual data for scientists and the general public of California. This movie would be comprised as visual metadata to show how interns work around the clock to bring forth a feasible, interactive program and website to be used by both science professionals and the general population.

1-003

USEIT DRUPAL WEBSITE DEVELOPMENT *Montes de Oca JS (USC), Rodriguez V (LMU), and Fei Y (ELAC)*

The Undergraduate Studies in Earthquake Information Technology (USEIT) program unites undergraduates to participate in a leading-edge internship that enables them to work in teams to tackle a scientific “Grand Challenge.” The 2009 “Grand Challenge” appointed the task of delivering SCEC-VDO visualizations via a content management system. The Website Development Group utilized an open source content management system called Drupal to create a website that delivers USEIT created content over the internet.

In order to accomplish the difficult task of building a user-friendly website, the team underwent a process of learning unfamiliar computer languages to manipulate Drupal’s already robust set of features.

The goal was to make SCEC-VDO products more accessible to a broader audience. The website’s main feature is the ability to stream visualizations online. The team also revolutionized the way metadata for visualizations is managed and displayed. After refining the metadata rubric, it became more precise and organized. Also, the website provides USEIT interns a portal for team members and directors to interact and enhances the ability to document the internship.

Ultimately, the website will serve as a window into the work of the USEIT internship program. This easily navigated website connects the interns to the public.

1-004

SCEC-VDO DEVELOPMENT *Armstrong JS (ASU), Boyd EE (UT Austin), Brown JF (USC), Patino AJ (USC), and Welch KB (Univ. of Cincinnati)*

The Southern California Earthquake Center's Virtual Display of Objects (SCEC-VDO) is an object-oriented, open-source, internet-enabled software package showing interactive 3D displays of diverse data. Developed by SCEC Undergraduate Studies in Earthquake Information Technology (UseIT) interns in 2002, SCEC-VDO continues to be improved each summer. It is currently being used by a growing number of SCEC scientists and in a multi-media curriculum at USC.

The Software development team of UseIT focused on the implementation of new tools into SCEC-VDO to create visualizations that will be targeted to a general audience in accordance with the Great California ShakeOut. One feature created was the Shake Map representation on the 2D surface of the earth, allowing users to see shake maps of earthquakes within the 3D world. To show population density in relation to fault systems and earthquakes a feature was created using Census Tract data. To give the public a point contact for their region, the Earthquake Country Alliance Regional Areas feature was added. A new 3D slip rate model feature was created to display fault ruptures underneath the earth's surface. The Cascadia Subduction zone was modeled in 3D to show the threat it poses to residents in the northwest United States.

1-005

INTERACTIVE DISPLAYS OF COMPLEX GEOLOGIC DATA ON A WEBSITE *Berti RW (USC)*

The SCEC-VDO software has become large and complicated. Because of this users must take time to learn about its available features and specific abilities. During the summer, the focus of my research was the display of interactive 3D scenes on a website. These scenes are derived directly from the SCEC-VDO software, and allow users of the web display to interact with complex data sets in an intuitive manner. The process to produce these displays is simple. A user familiar with the SCEC-VDO software can produce a meaningful display and export it as a binary file. This file is then uploaded to the server. The end user downloads this file through a Java applet, displays its contents on the web page, and is allowed full interactivity. This makes the production of scenes in SCEC-VDO accessible by end users without the process that is downloading and installing the software.

1-006

2009 SCEC-VDO PRODUCTION TEAM PROJECT *Barba M (UC Berkeley), Garcia S (USGS), Kim C (PCC), Lopez HK (PCC), Oliver BK (Cal Poly Pomona), Quiroz R (ELAC), and Zhang Z (PCC)*

The Grand Challenge of the 2009 Undergraduate Studies in Earthquake Information Technology (USEIT) Program is to deliver Southern California Earthquake Center - Virtual Display of Objects (SCEC-VDO) images and animations of faults and earthquake sequences to SCEC, the Earthquake Country Alliance, and other virtual organizations via a content management system that captures the metadata and guides the user. For the production team, the primary focus was on the development and delivery of useable visualizations using SCEC-VDO as well as the creation of metadata associated with the visualizations. The production team was also tasked with helping to improve SCEC-VDO by identifying limitations and bugs within the software. During the research into the individual alliances, within the Earthquake Country Alliance (ECA), the production team encountered several challenges. These challenges included the need for relocated earthquake catalogs, a visualization of the Cascadia Subduction Zone, a rubric for creating consistent SCEC-

VDOs, a uniform format for gathering and submitting metadata, and several limitations within the software. One of the challenges was met by researching and locating better datasets. Once the datasets were obtained, the production team converted them into formats that were compatible with SCEC-VDO or they were sent to the development team for implementation into SCEC-VDO. The result was a new relocated earthquake catalog and a visualization of the Cascadia Subduction Zone. A rubric and metadata sheet was also created for current and future SCEC USEIT interns with the goal of creating both professional and consistently accurate movies. After overcoming these challenges, the production team was able to produce professional movies. Two movies were created for SCEC scientists, four movies for the alliances, and three movies for other virtual organizations.

1-007

BOMBAY BEACH EARTHQUAKE SWARM SEQUENCES *Oliver BK (Cal Poly Pomona), and Barba M (UC Berkeley)*

The Bombay Beach earthquake swarms of 2001 and 2009 concern seismologists because of their potential to initiate the Great Southern California Shakeout Scenario, a magnitude 7.8 earthquake along the southernmost San Andreas Fault. Using the Southern California Earthquake Center's Virtual Display of Objects (SCEC-VDO) software, a visualization was created to help identify other possible swarms and to better understand the swarms' behavior. Relocated earthquake catalogs for Southern California were obtained from Dr. Peter Shearer, Dr. Egill Hauksson, and Guoqing Lin. The relocated catalogs were then plotted in graphs displaying magnitude versus time and number of earthquakes versus time to identify potential swarms in the Bombay Beach region. The identified potential swarms were displayed in SCEC-VDO in sequence to define their behavior through time. Earthquake swarms in April and June 1984, November 2001, and March 2009 were identified and animated in a visualization created to demonstrate the swarm's behavior. The SCEC-VDO visualization is a resource for seismologists in its ability to aid in explaining the possible trigger of the Great Southern California Shakeout Scenario.

1-008

PREPARING FOR POST-EARTHQUAKE RESPONSE: A TOOL TO FACILITATE INFORMATION SHARING AND COORDINATION *Chen S (Caltech), Huynh TT (SCEC), Marquis JE (SCEC), Yu E (Caltech), and Yu J (USC)*

The Southern California Earthquake Center (SCEC) has launched a website to facilitate earthquake response coordination between SCEC institutions and its agency partners. The website enables users to create, edit, review, search, and archive various kinds of information relating to significant earthquake activity. It is designed to be a virtual meeting place for SCEC scientists to gather and share information and coordinate activities in a post-earthquake environment. It can be used as a living document for the SCEC response coordination plan. The website is hosted at the University of Southern California, with backup mirror sites residing at two other facilities: the Southern California Earthquake Data Center (SCEDC) at Caltech and Stanford University.

During the Great Southern California ShakeOut Exercise, SCEC scientists, agency liaisons, and other members of the SCEC community first used the SCEC Earthquake Response website to (a) post information, (b) discuss unfolding events, and (c) coordinate response activities and deployment of institutional resources in response to the virtual M7.8 that struck southern California on November 13, 2008. Information about other significant earthquake activity in southern California has been discussed since, including the Bombay Beach swarm in March 2009 and the Newport-Inglewood events of May 2009. A failover exercise to test the resiliency of the

SCEC Earthquake Response site is planned for the 2009 ShakeOut in October. The website continues to be developed, and further feedback is welcome: <http://response.scec.org>

1-009

THE HALL OF GEOLOGICAL WONDERS AND THE QUAKE CATCHER NETWORK – EARTHQUAKE SCIENCE EDUCATION IN A MUSEUM SETTING THROUGH THE USE OF REAL TIME DATA COLLECTION INTERACTIVES *Springer KB (San Bernardino County Museum), Cochran ES (UCLA), Sagebiel JC (San Bernardino County Museum), Scott E (San Bernardino County Museum), Lawrence JF (Stanford), and de Groot RM (SCEC / USC)*

The San Bernardino County Museum in Redlands, California, the largest museum in inland California, is designing and installing exhibits in our new 12,000 square foot three-story expansion, the Hall of Geological Wonders. We devote significant space in the new Hall to explaining the evolution of southern California's landscape. Visitors will learn about the geologic forces at work beneath their feet – forces that explain the shape of the Earth, its landforms and its sometimes violent nature. The evolution of plate tectonics theory will be placed in the context of scientific discovery via the scientific method. The San Andreas Fault will be interpreted in a manner no other museum ever has attempted. The Hall is designed so that visitors will observe the San Andreas Fault zone from our "Earth's Cylinder" – below ground in a re-created excavation of the fault, and above ground in a viewing tower. The viewing tower then segues to an immersive exhibit where the visitors will feel a simulated earthquake in a recreated mountain cabin in our "San Andreas Fault Earthquake Experience".

As the southern California nexus of the EPIcenter (Education and Public Information Centers) concept in free-choice learning environments, the Museum is partnering with the Southern California Earthquake Center's Communication, Education and Outreach program and the Quake-Catcher Network (QCN) to provide a unique educational experience. The QCN uses sensors and interactive displays to allow visitors to see visualizations of the shaking they are experiencing in real time. The Hall will integrate these technologies, encouraging visitors to become a part of the scientific process through interactives such as "Did You Feel It?" and the QCN, thereby duplicating a real-time earthquake experience in a museum exhibit setting. In addition, visitors can observe how the QCN is being used throughout Southern California to increase the number of seismograms of moderate to large earthquakes to aid in the study of earthquake rupture and wave propagation, as well as being encouraged to participate in this "citizen science" endeavor. The goal of the collaboration is to improve knowledge outcomes, encourage community participation in science data collection, and promote earthquake preparedness.

LOBBY

POINT-BASED VISUALIZATION AND ANALYSIS OF LIDAR DATA *Kreylos O (UC Davis), Bawden GW (USGS), Bowles CJ (UC Davis), Cowgill ES (UC Davis), Elliott AJ (UC Davis), Gold RD, Hamann B, Kellogg LH (UC Davis), and Oskin ME (UC Davis)*

The recent proliferation of high-resolution and large-extent topography data, gathered by terrestrial LiDAR scanning or airborne laser swath mapping (e.g. "B4" and GeoEarthscope), has created a need for visualization and analysis software going beyond the capabilities of existing tools. LiDAR scans pose significant analysis challenges due to their size (tens to hundreds of gigabytes) and their unstructured, point-based nature. Data size means that existing tools can typically only handle small subsets of an entire data set at a time, and LiDAR data's point-based nature means that the first step in most processing pipelines is to resample the data onto a regular grid, thereby losing salient information, such as the presence of vegetation or engineered

structures. Gridding also implies that a LiDAR data set's varying resolution -- especially in the case of terrestrial LiDAR -- must be resampled to a uniform resolution, thereby downsampling data in high-resolution areas and filling in areas of low resolution or holes. Finally, terrestrial LiDAR data can scan true 3D features such as overhangs, which cannot be represented in a 2D grid of elevation values.

We present LiDAR Viewer, a custom visualization application addressing both major challenges. LiDAR Viewer works directly on "raw" LiDAR point clouds, while still providing the visualization methods typically seen in other tools, such as interactive navigation and real-time hill shading from arbitrary light directions. At the same time, LiDAR Viewer provides out-of-core, multiresolution, view-dependent visualization, which means it can visualize entire LiDAR scans covering hundreds of square kilometers at sub-meter resolution interactively, even on mid-range or low-end computers. Besides visualizing point clouds, LiDAR Viewer enables simple interactive analysis methods, such as accurately selecting and exporting point subsets, and fitting simple geometric primitives to selected point subsets. Additionally, the LiDAR Viewer package contains a batch processing framework, which enables users to quantitatively analyze the data. Users can develop their own analysis algorithms in the Python programming language, and then apply them to LiDAR data sets while exploiting LiDAR viewer's optimized data storage and access methods.

LiDAR Viewer is one member of a suite of related applications for geoscience visualization. We will also present an interactive fault editor and an analysis program for volumetric 3D data.

Community Modeling Environment (CME)

1-010

A HYBRID MPI/OPENMP IMPLEMENTATION OF AN EXPLICIT FINITE ELEMENT DYNAMIC CODE - EQDYNA *Duan B (Texas A&M), Wu X (Texas A&M), and Taylor VE (Texas A&M)*

Finite element method (FEM) can deal with complexity in both fault geometry and material property and is thus capable of simulating dynamic rupture along nonplanar fault systems and wave propagation in complex geological structure. EQdyna is an explicit finite element code, which has been verified in the SCEC/USGS dynamic earthquake rupture code verification exercise. To apply this code to regional-scale simulations (such as in Southern California) of rupture and wave propagations for strong ground motion prediction, we parallelize the code so that it can run on modern high performance computing systems. The current trend in high performance computing systems has been shifting towards cluster systems with multicores. These systems provide a natural programming paradigm for hybrid MPI/OpenMP applications. We develop an element-based partitioning scheme for parallelizing EQdyna. We explore how efficiently to use hybrid MPI/OpenMP to achieve multiple levels of parallelism of the code, and to reduce the communication overhead of MPI within a multicore node, by taking advantage of the shared address space and on-chip high inter-core bandwidth and low inter-core latency. We have verified our implementation on two dynamic rupture models. One is the SCEC/USGS code verification benchmark problem TPV11. The other is a dynamic source model of the 2008 Wenchuan earthquake. We have conducted performance analysis on Pangu, a SUN server with 8 cores on one node, and Hydra, an IBM POWER5+ cluster with 40 p5-575 nodes and 16 cores on each node. Our experimental results show that the hybrid MPI/OpenMP implementation of EQdyna obtains accurate simulation results and has good scalability on multicore systems. We will test the scalability of the parallelized EQdyna on larger scale multicore supercomputers, such as BlueGene/P at Argonne National laboratory. This parallelized version of EQdyna has application potential in next generations of the SCEC strong ground motion prediction to more accurately capture complex fault geometry and velocity structure in dynamic rupture and wave propagation models of Southern California.

1-011

GATHERING CRITICAL DATA TOWARD THE WESTERN BASIN AND RANGE CVM *Louie JN (UNR), Tibuleac I, Cashman P, Trexler J, Stephenson WJ (USGS), Odum J (USGS), Pullammanappallil SK (Optim), Pancha A (UNR), and Magistrale M (SDSU)*

In January 2008, a Western Great Basin Community Velocity Model (WGBCVM) Working Group was formed at a workshop sponsored by the USGS-NEHRP National Intermountain West Program with the goal of creating a CVM for calculating earthquake ground motions in the Reno/Tahoe and Las Vegas metropolitan areas. The WGBCVM group developed a list of priorities; the primary priority has been funded, that a WGBCVM be assembled on a similar basis as the SCEC and Wasatch Front CVMs. Building this initial WGBCVM with new data from Reno is a crucial step toward development of an urban hazard map for the city, and will contribute directly toward reducing earthquake losses in this region.

The University of Nevada, Reno (UNR) and Optim Seismic Data Solutions will measure shear-velocity profiles at twelve previously unmeasured ANSS stations in the Reno, Carson City, Carson Valley, and Tahoe areas. At some of the sites, long refraction microtremor arrays will be deployed to determine shear velocity to 300-m depths. We will merge these results with prior

results into a Reno metro area geotechnical model, for delivery to the team assembling the WGBCVM.

During June 2009 we collected 12 km of seismic reflection profiles in the Reno-area basin. The data were collected in collaboration with the nees@UTexas project, who provided the “Thumper” mini vibe, with a 141-kg reaction mass. Property owners, local businesses and the cities of Reno and Sparks allowed us to complete one profile through downtown Reno east to Rock Blvd. along the Truckee River. A second W-E profile along Manzanita Ln., 4.5 km south of the River, crosses numerous mapped faults including the Virginia Lake fault. In field stacked sections, internal basin stratigraphy is clearly visible as well as a reflection from the base of the sediments across both profiles at 0.2-1.0 km depth. The Truckee River profile suggests several faults from diffractions and reveals moderate east-dipping stratigraphic deformation, while the Manzanita profile bears sidewall reflections from a potentially significant, vertically dipping fault zone. We will further process and interpret the seismic sections in light of local structural and stratigraphic knowledge, gravity interpretations, and borehole analyses to extrapolate a 3-d basin model from the 2-d seismic sections and deliver these results to the team assembling the WGBCVM. CVM assembly activities may be taken up by UNR next year.

1-012

CHINO HILLS --- A HIGHLY COMPUTATIONALLY EFFICIENT 2 HZ VALIDATION EXERCISE *Taborda R (Carnegie Mellon), Karaoglu H (CMU), Bielak J (CMU), Urbanic J (PSC), Lopez J (Carnegie Mellon), and Ramirez-Guzman L (CMU)*

The 2008 Chino Hills earthquake was the largest earthquake in the Los Angeles metropolitan region since the 1994 Northridge earthquake. With a magnitude M_w 5.4, the July 29, 2008 Chino Hills earthquake was recorded by most networks in the area. Its occurrence constitutes an excellent opportunity to study the response of the greater Los Angeles basin and to test the most common assumptions for crustal structure and material properties under ideal conditions of anelastic modeling due to a kinematic point source excitation. We present here a preliminary validation study for a set of simulations of the Chino Hills earthquake using Hercules—the parallel octree-based finite element simulator developed by the Quake Group at Carnegie Mellon University. In the past, we have reported on the simulation capabilities of Hercules for more complex—yet hypothetical—earthquake scenarios such as TeraShake and ShakeOut. For the latter, we have also conducted a comprehensive verification of results in collaboration with other SCEC simulation groups, using different methodologies. With this new simulation we attempt to come full circle in the verification and validation paradigm as understood by the modeling and simulation community. The results presented here correspond to a set of four different simulations, the most challenging one with a maximum frequency of 2 Hz and a minimum shear wave velocity of 200 m/s. These particular values of these two critical parameters help us explore the influence of higher frequencies and lower velocity profiles on ground motion. The extension to these parameters is becoming possible in our simulations thanks to the latest computational improvements we are implementing into Hercules. While our focus is on the physical interpretation of the results of our simulations and their comparison with observations, we also report on the computing resources employed. Our preliminary results suggest that extending the maximum frequency beyond the de facto assumed barrier of 1 Hz for deterministic simulations is an effort worth pursuing.

1-013

SCEC PETASHA-2 AND PETASHAKE-2 PROJECTS: LARGE-SCALE NUMERICAL MODELING IN SUPPORT OF SCEC EARTHQUAKE SYSTEM SCIENCE *Maechling PJ (SCEC / USC), Jordan TH (USC), Beroza GC (Stanford), Bielak J (CMU), Chen P (LDEO), Cui Y (SDSC), Day S, Deelman E, Graves R, Minster JB, Olsen KB, and the CME Collaboration*

The SCEC Community Modeling Environment (CME) collaboration performs basic scientific research using high performance computing with the goal of developing a predictive understanding of earthquake processes and seismic hazards in California. CME research areas including dynamic rupture modeling, wave propagation modeling, probabilistic seismic hazard analysis, and full 3D tomography.

CME research activities are currently funded through two NSF awards, the NSF-EAR PetaSHA-2 project, and the NSF-OCI PetaShake-2 projects. PetaSHA-2 focuses on integrating SCEC's basic seismic hazard research into computational models. PetaShake-2 focuses on increasing the scale and resolution of SCEC computational codes to use petascale supercomputers when available for open-science research in 2011. Seismic hazard calculations of ground motions including large-scale rupture simulations, broadband seismograms from scenario earthquakes, scenario ShakeMaps, and probabilistic seismic hazard analysis (PSHA) hazard curves represent critical seismological data products. These types of science-based ground motion estimates represent important interfaces between seismologists and broader groups including emergency management, building engineers, and governmental planning organizations. The PetaSHA-2 and PetaShake-2 projects science plans use a science-based framework, called the SCEC computational pathways, to guide the scientific techniques which we use to improve ground motion calculations. As we implement SCEC computational pathways as numerical models, we improve the accuracy and resolution of ground motion simulations. The core SCEC research program continues to produce important new seismic hazard research that can be used to improve numerical models including improvements in structural models for Southern California, improved understanding of the physics of ruptures, and improved understanding of long term fault behaviors. In this poster, we describe how the CME numerical modeling program can provide a migration path for basic SCEC research as this research is integrated and incorporated into widely used seismic hazard data products with broad impact. More information about the SCEC/CME research is available at www.scec.org/cme.

1-014

COMMUNICATION OPTIMIZATIONS OF SCEC PETASHAKE APPLICATION *Lee K (Jet Propulsion Laboratory), Cui Y (SDSC), Maechling PJ (SCEC / USC), Olsen KB (SDSU), and Jordan TH (USC)*

The Southern California Earthquake Center AWP-Olsen code has been considered to be one of the most extensive earthquake applications in supercomputing community. The code is highly scalable up to 128k cores and portable across wide variety of platforms. However, as the problem size grows, more processors are required to effectively parallelize workloads. The scalability of the code is highly limited by the communication overhead in the NUMA-based systems such as TACC Ranger and NICS Kraken which exhibit highly unbalanced memory access latency based on the location of the processors. The asynchronous communication model effectively removes interdependence between nodes which does not show any temporal dependence. Consequently, the efficiency of utilizing system communication bandwidth is significantly improved by efficiently parallelizing all the communication paths between cores. Furthermore, this optimized code performed large scale scientific earthquake simulation and reduced the total simulation time to 1/3 of the time of the synchronous code.

1-015

CALCULATING CYBERSHAKE MAP 1.0 *Callaghan S (USC), Maechling PJ (SCEC / USC), Deelman E (ISI), Small P (SCEC), Vahi K (USC / ISI), Mehta G (ISI), Juve G (USC), Milner K (USC), Graves R (URS), Field E (USGS), Okaya D (USC), Gunter D, Beattie K, Brooks C, and Jordan TH (USC)*

Current Probabilistic Seismic Hazard Analysis (PSHA) calculations produce predictive seismic hazard curves using an earthquake rupture forecast (ERF) and a ground motion prediction equation (GMPE) that defines how ground motions decay with distance from an earthquake. Traditionally, GMPEs are empirically-based attenuation models. However, these GMPEs have important limitations. The observational data used to develop the attenuation relationships do not cover the full range of possible earthquake magnitudes. These GMPEs predict only peak ground motions, and do not produce ground motion time series. Phenomena such as rupture directivity and basin effects may not be well captured with these GMPEs.

SCEC researchers on the CyberShake project are implementing physics-based PSHA calculations by using full 3D waveform modeling as the GMPE. CyberShake performs PSHA hazard curve calculations for various sites in Southern California, using the UCERF 2.0 ERF. For each rupture, we capture rupture variability by varying the hypocenter, slip distribution, and rise times to produce about 410,000 different events per site of interest. The goal of CyberShake is to calculate more accurate hazard curves using high performance computing tec

1-016

COULOMB STATIC STRESS INTERACTIONS BETWEEN M>7 EARTHQUAKES AND MAJOR FAULTS IN SOUTHERN CALIFORNIA *Rollins JC (USC), Ely GP (USC), and Jordan TH (USC)*

Using the SCEC CyberShake project's variable-slip models for eleven hypothetical M>7 southern California earthquakes, we calculate the Coulomb stress changes that each earthquake imparts to major local faults. Strong stress interactions are found between the San Andreas and subparallel right-lateral faults, the northward-dipping thrust faults under the Los Angeles basin, and the left-lateral Garlock Fault. M>7 earthquakes rupturing sections of the southern San Andreas fault decrease Coulomb stress on the San Jacinto and Elsinore faults and impart localized Coulomb stress increases and decreases to the Garlock, San Cayetano, Puente Hills and Sierra Madre faults. M>7 earthquakes rupturing the San Jacinto, Elsinore, Newport-Inglewood and Palos Verdes faults decrease Coulomb stress on parallel right-lateral faults. A M=7.35 earthquake on the San Cayetano fault decreases stress on the Garlock fault and imparts stress increases and decreases to nearby sections of the San Andreas. A M=7.15 earthquake on the Puente Hills fault increases stress on the San Andreas and San Jacinto faults, decreases stress on the Sierra Madre fault and imparts localized stress increases and decreases to the Newport-Inglewood and Palos Verdes faults. A M=7.25 shock on the Sierra Madre fault increases stress on the San Andreas and decreases stress on the Puente Hills fault. These are the most robust findings derived from calculations using a single variable-slip model for each of the eleven earthquakes. We plan to use several models for each earthquake in order to assess the effect that variations in the distribution of slip have on the magnitudes of these stress interactions.

1-017

MONITORING LARGE DISTRIBUTED HIGH PERFORMANCE COMPUTING (HPC) SIMULATIONS ON THE SCEC CYBERSHAKE PROJECT *Small P (SCEC), Callaghan S (USC), Milner KR (SCEC), Maechling PJ (SCEC / USC), and Yu J (USC)*

On the CyberShake Project, SCEC researchers run a particular type of serial, seismological calculation repeatedly with different input data sets in order to calculate Probabilistic Seismic Hazard Analysis (PSHA) hazard curves using full 3D waveform modeling. SCEC runs these scientific calculations on thousands of processing nodes at a time using grid-based workflow technologies including Globus, Condor DAGManager, and Pegasus-WMS. The SCEC calculations have increased to include hundreds of thousands, and now hundreds of millions, of calculations. It has become difficult to track the execution progress of these complex distributed scientific workflows as they run on SCEC, USC High Performance Computing and Communications (HPCC), and Texas Advanced Computing Center (TACC) computer resources.

In support of this year's CyberShake 1 Map calculation, the CyberShake group developed an extensive workflow monitoring framework called the CyberShake Run Manager to quickly assess the progress of dozens of high core-count workflows running across many different computational resources. The Run Manager also provided users with an automatically updated view of new simulation results as they were completed to help with error checking and initial evaluation of results.

A CyberShake simulation is primarily comprised of two Pegasus workflows, the first for Strain Green Tensor generation and the second for spectral peak amplitude computation, with follow-on computation to generate the hazard curve plots and overall scatter maps. The Run Manager tracks a CyberShake simulation end-to-end, from the moment the initial SGT Pegasus DAX is created to the final verification of hazard curve charts. Workflow statistics are updated in real-time on a SCEC website so that developers may view current operational status. Once peak amplitudes and hazard curves are generated for a site, these are immediately viewable on the website.

In our poster, we provide additional details about the design and implementation of the Run Manager and we describe which aspects of the Run Manager proved the most valuable during this year's sixty day long CyberShake Map calculation.

1-018

IMPROVING PERSISTENT STORAGE OF SCEC SIMULATION RESULTS *Pechprasarn T (USC), Maechling PJ (SCEC / USC), Small P (SCEC), Callaghan S (USC), Milner KR (SCEC), and Jordan TH (USC)*

The SCEC Community Modeling Environment computational science research group has run several important simulations over the last few years. SCEC researchers need to save important simulation results so that these results are available, intact, and accessible to researchers. In this poster, we describe our work on the SCEC Data Management System (SDMS). Our SDMS development has two primary goals: (1) Help SCEC researchers save important simulation results into persistent storage, and (2) Help SCEC researchers discover and access existing SCEC simulation results.

To support the first goal, the SDMS provides software tools which researchers can use to request creation of a simulation "archive." An archive should be a simulation result, or other digital data. When the user declares a SCEC archive, the SDMS tools create an inventory of directories and files that are included in the archive and the SDMS codes apply integrity checks on the files in the

archive. The archive is assigned a persistent identifier, and an entry is made into a centralized SCEC Simulation Archive Database. Once a simulation archive has been created, the SDMS is defined to help to manage that archive. For example, copies of a simulation archive can be created and distributed to any available storage. The SDMS integrity checks help to confirm that a simulation archive copy is intact and can be safely used even after years of storage.

To support the second goal, the SDMS provides an online catalog that summarizes the available SCEC simulation archives and it provides tools to help users request some, or all, of the different archives.

To guide our technical development of the SDMS, we have used the CyberShake 1 Map simulation results as a working example. We are developing an inventory of the files and directories in this simulation result and we are establishing an initial SDMS Simulation Archive catalog accessible through the SCEC web site. We have developed SDMS tools that help user access data in the CyberShake 1 Map simulation result including hazard curve sites, peak ground motions for a site, source and rupture lists, and seismograms and slip-time histories that produced specific peak amplitudes. Once we can show that the SDMS provides tools to help SCEC manage the persistent storage of the CyberShake 1 Map results, we will apply this system to support storage of other important SCEC simulation results including the ones listed above.

1-019

AUTOMATIC END-TO-END WORKFLOW TO SUPPORT SCEC CAPABILITY SIMULATIONS ON TERAGRID *Zhou J (SDSC), Cui Y (SDSC), and Lee K (SDSC)*

We present an automatic end-to-end workflow approach for the Southern California Earthquake Center (SCEC) capability simulations on Teragrid, where large-scale earthquake data processing and transfer, scientific simulation, visualization and outputs archival can be processed automatically and robustly incorporating resources available on Teragrid. SCEC PetaSHA capability simulations are growing in size exponentially each year, automatic processing becomes necessary. This workflow is a combined process in a configurable and structured set of steps to support dynamic rupture and wave propagation simulations using AWP-Olsen-Day code. First the workflow transfers earthquake datasets between different machines on Teragrid on demand and validates transferred data in parallel, then executes the AWP-Olsen simulation code and keeps tracking of the simulation results, finally it generates derived products such as seismograms based on simulation outputs and backups simulation dataset into tape archive. Automatic notification is then sent to users on status of the progress. One challenge and primary goal of the workflow is to ensure the correctness of input and output data and detect errors occurred during the process and recover automatically. We will describe software tools employed in the workflow, component parts of the workflow such as Globus and high performance GridFTP and how the workflow meets the computational requirements. We also discuss factors that might affect the workflow efficiency and our approaches to optimize the overall performance. The workflow presented is highly configurable, reliable and easy to utilize. Experiment results will be demonstrated and further optimization functions of the workflow will be discussed.

1-020

GENERATING 3D ANIMATIONS OF GROUND MOTIONS AND STRUCTURAL RESPONSE *Fu J (USC), Krishnan S (Caltech), Maechling PJ (SCEC / USC), Chourasia A (SDSC), and Jordan TH (USC)*

Earthquake animations are widely used to help people analyze and understand the impact of historical and scenario earthquakes. In the recently concluded ShakeOut exercise, ground-shaking

animations were used effectively to communicate the nature of seismic hazard to all stakeholders including the general public. The Caltech ShakeMovie (<http://shakemovie.caltech.edu>) site automatically creates movies of long-period seismic waves radiating from the source of each local event in southern California and propagating into the Los Angeles basin. While these animations are useful in gauging the extent of ground-shaking, the burden of envisioning the earthquake effects is put upon the viewing audience, thus severely limiting their impact. To overcome this, the Southern California Earthquake Center has undertaken an interdisciplinary effort to integrate the visualization of earthquakes and its effects on the built environment.

We start by developing a workflow which includes both ground motions and structural response to the ground motions. Using the Caltech VirtualShaker (<https://virtualshaker.caltech.edu>) we calculate the response of various structures to specific earthquake ground motion waveforms. The VirtualShaker is an e-analysis facility containing a collection of structural models. To compute the response of a given model to a particular event, we upload the 3-component recorded or synthetic seismograms to the VirtualShaker, select the structural model of interest, and through the web-interface issue a command for VirtualShaker to perform the corresponding response-history analysis. Using the deformed configuration of the structural model at each instant of time returned by VirtualShaker, we create a synthesized animation of the ground shaking and the structure responding. To demonstrate the value of such an integrated visualization, we have developed a “virtual” building collection that we call a Digital City block. Our Digital City block contains a set of eight different buildings. We have developed an initial animation that shows the response of the Digital City block, hypothetically located in Thousand Oaks, during a southern San Andreas fault rupture. By relocating the block to various sites in southern California and repeating this exercise, one can visualize the impact of a major earthquake on the entire Los Angeles metropolitan region. This standardized workflow can be easily duplicated in other parts of the world.

1-021

THE BIG TEN EARTHQUAKE SCENARIOS FOR SOUTHERN CALIFORNIA *Ely GP (USC), Jordan TH (USC), Maechling PJ (SCEC / USC), Olsen KB (SDSU), Day SM (SDSU), Minster JB (UCSD), Graves R (URS), Bielak J (Carnegie Mellon), Taborda R (Carnegie Mellon), Beroza G (Stanford), Ma S (Stanford), Cui Y (SDSC), Urbanic J (PSC), and Callaghan S (USC)*

The Big Ten project is generating a hierarchy of simulations for ten of the most probable large ($M > 7$) ruptures in Southern California, with the objective of understanding how source directivity, rupture complexity, and basin effects control ground motions. The ruptures and moment-magnitudes are selected from events with relatively high probability rates in the UCERF2 model. Feedback on and refinement of the selected event set from the SCEC community is encouraged. The event set is being used to coordinate multiple types of large-scale simulations (requiring high performance computing), as well as multiple groups of researchers around a common set of earthquake scenarios. The geoscience goals of the Big Ten project are to: (1) Understand the roles of source directivity, rupture complexity, and basin effects on ground motions, and evaluate how these factors control the CyberShake hazard curves; (2) Improve PetaSHA simulation capabilities by incorporating new codes that can model geologic complexities including topography, geologic discontinuities, and source complexities such as irregular, dipping, and offset faults; (3) Use dynamic rupture simulations to investigate the effects of realistic friction laws, geologic heterogeneities, and near-fault stress states on seismic radiation and thereby improve pseudo-dynamic rupture models of hazardous earthquakes; and (4) Use realistic earthquake simulations to evaluate static and dynamic stress transfer and assess their effects on strain accumulation,

rupture nucleation, and stress release. Examples of some preliminary Big Ten simulations will be displayed.

1-022

PARALLEL IO OPTIMIZATIONS FOR SCEC SHAKEOUT-D SIMULATIONS *Lee K (Jet Propulsion Laboratory), Cui Y (SDSC), Kaiser TH (SDSC), Maechling PJ (SCEC / USC), Olsen KB (SDSU), and Jordan TH (USC)*

The Southern California Earthquake Center (SCEC) AWP-Olsen code has been considered to be one of the most extensive earthquake applications in supercomputing community. Currently, the code has been used to run large-scale earthquake simulations, for example, the SCEC ShakeOut-D wave propagation simulations using 14.4 billion mesh points with 100-m spacing on a regular grid for southern California region, and benchmarked 50-m resolution simulations with challenging 115.2 billion mesh points. Consequently, along with the computational challenges in these scales, IO emerges the most critical component to make the code highly scalable. A new MPIIO scheme in preserving high IO performance and incorporating data redistribution enhances the IO performance by providing contiguous data with optimal size, and effectively redistributing sub-data through highly efficient asynchronous point-to-point communication with minimal travel time. This scheme has been used for SCEC large-scale data-intensive seismic simulations, with reduced IO initialization time to 1/7 for SCEC ShakeOut-D run.

1-023

SINGLE CPU OPTIMIZATIONS OF SCEC AWP-OLSEN APPLICATION *Nguyen HT (UCSD), Cui Y (SDSC), Olsen KB (SDSU), and Lee K (SDSC)*

Reducing application time-to-solution has been one of the grand challenges for scientific computing, especially at large-scale. This also applies to simulating earthquake using the Southern California Earthquake Center (SCEC) AWP-Olsen code. The SCEC 100-m resolution ShakeOut-D wave propagation simulations, conducted on Kraken at NICS using 64k cores with 14.4 billion mesh points for southern California region, consume hundreds of thousands of allocation hours per simulation. There has been an urgent need of reducing time spent on each individual processor since saving 1% execution time on each processor can save thousands of allocation hours per simulation. This work introduces single CPU optimization as a very effective solution.

Single CPU Optimization is a process of modifying a code focusing on selected portion where most of computation is executed to make it work more efficiently. Profiling tools such as CrayPat on NICS Kraken machine indicates that the “hot spots” of the AWP-Olsen are six subroutines which account for about 45% of the execution time. On the first attempt, some expensive formulas are rewritten to use inexpensive operators. Further analysis suggests the optimal strategy of storing frequently used parameter arrays can greatly reduce the cost of computation. In addition, for some critical loop structures, look-up table and loop-unrolling technique is utilized to trade memory usage for lower cache-miss, and to increase cache reusability. The improvements from these changes have been significant with a speed-up of more than 30% in computational time with latest SCEC capability simulations.

1-024

TERA3D: A COMPUTATIONAL PLATFORM FOR TERA-SCALE FULL-3D WAVEFORM TOMOGRAPHY (F3DT) IN SOUTHERN CALIFORNIA *Lee E (Wyoming), Chen P (LDEO), Jordan TH (USC), and Maechling PJ (SCEC / USC)*

We are automating our full-3D waveform tomography (F3DT) based on the scattering-integral (SI) method and applying the automated algorithm to iteratively improve the 3D SCEC Community Velocity Model Version 4.0 (CVM4) in Southern California. In F3DT, the starting model as well as the derived model perturbation is 3D in space and the sensitivity kernels are calculated using the full physics of 3D wave propagation. The SI implementation of F3DT is based on explicitly constructing and storing the sensitivity kernels for individual misfit measurements. Compared with other F3DT implementations, the primary advantages of the SI method are its high computational efficiency and the ease to incorporate 3D Earth structural models into very rapid seismic source parameter inversions. So far, over 3,500 phase delay measurements are used to invert for 3D velocity perturbations to the 3D reference model, SCEC CVM4 using the Tera3D platform. After the first iteration, the updated model, CVM4SI1, reduced the variance of the phase delay measurements by about 29% and the synthetics generated by the updated model generally provide better fit to the observed waveforms. In this poster we will report our recent progresses on automating the complete F3DT workflow, the updated velocity model, CVM4SI1, and waveform improvements produced by the updated model.

1-025

SORD AS A COMPUTATIONAL PLATFORM FOR EARTHQUAKE SIMULATION, SOURCE IMAGING, AND FULL 3D TOMOGRAPHY Wang

F (VPAC), Ely GP (USC), and Jordan TH (USC)

Earthquake simulations in 3D structures are currently being used for forward prediction of ground motions, imaging of sources, and structure refinement (full 3D tomography). The computational platform for such simulations requires the accurate location of sources and receivers within the computational grid; the flexibility to represent geological complexities, such as topography, non-planar faults, and other distorted surfaces; and the facility to calculate Fréchet kernels for source and structural perturbations. We are adapting the Support Operator Rupture Dynamics (SORD) code for these purposes. SORD is an efficient numerical code developed by Ely, Day, and Minster (2008), which employs a structured but distortable mesh that can handle non-planar surfaces, such as topography. We represent point sources of arbitrary location as mesh-distributed sources of finite duration that match the travel-time and amplitude centroids of radiated waves; similarly, we represent receivers as centroid-preserving summations on a distributed mesh. We compute synthetic seismograms for a 3D spherical model of Southern California that includes topography and compare the travel-times and amplitudes with those computed for 3D Cartesian-mesh models, such as the “squashed topography” approximation in common use; we show the differences can be significant in tomographic inversions. We also use SORD to calculate Fréchet kernels, and demonstrate how these kernels can be used to understand wave propagation complexities, such as basin excitations.

1-026

VISUALIZATION OF VECTOR FIELDS OF SEISMIC DATA McQuinn E (UCSD), Chourasia A (SDSC), Minster JB (UCSD), and Schulze JP (Calit2)

Earthquake simulations produce vast amounts of surface and volumetric temporal data. We have implemented methods to visualize scalar and vector data that allows comprehension of the large amount of information. We leverage advances in graphics processors to draw oriented and textured geometry interactively.

We have developed four glyphs to depict the underlying vector data: spheres, ellipsoids, lines, and voxels. The glyphs can be switched interactively and offer multiple visual representations where each glyph enhances different underlying property. Additionally, we have developed

highlighting mechanisms to enhance comprehension of direction of vector data. For instance, a sphere would ordinarily not provide directional cues but with our method of highlight the sphere can indicate the direction. We have also developed interactively tunable methods to resolve occlusion of volumetric data. We present multimodal visual representations that provide an array of interactive and flexible visualization techniques to the scientists for scientific investigation through visualization.

The visualization tool can be run on a laptop, desktop or virtual reality (VR) environment. We are leveraging one such state-of-the-art system called “StarCAVE”. The StarCAVE surrounds the user with seamless, immersive and stereoscopic virtual environment. This VR environment provides the capability to view the volumetric data from inside the volume in an immersive manner, which is similar to witnessing the earthquake event from inside earth from any vantage point.

Project URL: <http://visservices.sdsc.edu/projects/scec/vectorviz>

Ground Motion Prediction (GMP) Seismic Hazard and Risk Analysis (SHRA)

1-027

LONG PERIOD STRONG GROUND MOTION MODELING USING THE AMBIENT SEISMIC FIELD *Denolle M (Stanford), Prieto GA (Stanford), Lawrence JF (Stanford), and Beroza GC (Stanford)*

Modeling wave propagation through the complex geology of the Earth's crust is one of the foremost challenges to a physics-based approach to seismic hazard analysis, largely because we lack the complete and accurate description of elastic and anelastic structure needed to ensure accurate ground motion simulations. We use information derived from the ambient seismic field to improve the prospects for these simulations in several ways. First, we have test the technique against several earthquakes for which there are nearby broadband instruments: the M 4.1 earthquake occurring on 10/2/2008 near Seven Oaks Dam and the M 5.0 earthquakes on 12/6/2008 near Hector Mine. Despite the difference in depth (surface vs. buried source) and mechanism (point force vs. double-couple) the ambient-noise results and the earthquake records show very similar amplitude variations and duration for the 4-10 s period band we have focused on. The strongly directional nature of ambient field excitation (from the Pacific) complicates its application. We have developed a higher order correlation approach (correlation of correlations) that helps overcome the problem of directional excitation while preserving amplitude information. A second component of our research is to recover three-dimensional anelastic structure. Towards this end we interpret coherency measurements from all station pairs to estimate spatially variable anelastic structure. Finally, we note that ambient-field measurements can be used both for direct ground motion predictions, and to constrain crustal structure, for targets of particular interest, such as long period ground motions in the Los Angeles Basin resulting from a great earthquake on the southern San Andreas Fault.

1-028

SYSTEMATIC ANALYSIS OF TEMPORAL CHANGES IN SITE RESPONSE ASSOCIATED WITH STRONG GROUND MOTION IN JAPAN *Wu C (Georgia Tech), Peng Z (Georgia Tech), and Asimaki D (Georgia Tech)*

We analyze temporal changes in site response associated with the strong ground motion of the Mw6.6 2004 Mid-Niigata earthquake sequence in Japan. The seismic data is recorded at a site with accelerometers at the surface and the 100-m-deep borehole. We compute the empirical surface-to-borehole spectral ratios and use them to track temporal changes in the top 100 m of the crust. We observe that the peak spectral ratio decreases by 40-60% and the peak frequency drops by 30-70% immediately after large earthquakes. The coseismic changes are followed by apparent recoveries with the time scale ranging from several tens to more than one hundred of seconds. The coseismic peak frequency drop, peak spectral ratio drop, and the postseismic recovery time roughly scale with the input ground motions when the peak ground velocity is larger than ~5 cm/s (or the peak ground acceleration is larger than ~100 gal). Our results suggest that at a given site the input ground motion plays an important role in controlling both the coseismic change and postseismic recovery in site response.

1-029

"SITE EFFECTS" IN NONLINEAR STRUCTURAL PERFORMANCE PREDICTIONS *Asimaki D (Georgia Tech), and Li W (Georgia Tech)*

The computationally efficient and credible evaluation of site response has been debated in the recent years both in the engineering and seismological communities. In turn, the selection of site response prediction methodology is critical for the estimation of structural performance in the occurrence of an earthquake. We here investigate the uncertainty introduced in nonlinear structural analyses by the site response modeling variability. For the latter, we consider elastic, equivalent linear and nonlinear site response simulations. We quantify the ground response variability by means of the COV of site amplification, defined as the ratio of the predicted PGA and SA to the corresponding ground motion intensity measures on rock-outcrop. Next, we subject a series of bilinear and multilinear SDOF oscillators to the ground motions computed using the alternative site response methodologies, and evaluate the variability introduced in structural response predictions. Results show high bias and uncertainty of the inelastic structural displacement ratio for periods near the fundamental period of the site. Furthermore, the amount of bias and period range where uncertainty manifests is shown to be a function of the soil stiffness. Empirical correlations between Vs30 and the variability introduced in structural analyses as a result of the site response model selection are presented in the end of our work.

1-030

REPORT ON GEOTECHNICAL SITE CHARACTERIZATIONS IN CALIFORNIA: IN-SITU VS30 MEASUREMENTS AND PROXY-BASED VS30 MODELS *Khan M (USGS), Yong A (USGS), and Schwarz S (USGS)*

Many predictive models have been developed to characterize geotechnical site conditions that use the average shear wave velocity in the upper 30 m (Vs30) as a proxy for site amplification. Several recent models use geology (Wills et al., 2000; Wills and Clahan, 2006; BSSA), topographic-slope (Wald and Allen, 2007; BSSA), and terrain-type (Yong et al., 2009; SRL) to develop site characterization maps. A common method to evaluate the accuracy of these models is to compare the predicted values to in-situ measurements. In 2007, a site characterization table (<http://sitechar.gps.caltech.edu/table2.php>) containing 782 seismographic station sites with predicted Vs30 values (Wills and others) was made openly available for California □ included were 69 Vs30 measurements at southern California station sites. Recently, an additional 854 measurements was added to this table through the PEER-NGA database. The availability of these 923 actual measurements provides an opportunity to better evaluate the reliability of each prediction model. As a first cut, for each model we assess the coefficient of determination (R2) to investigate if the proportion of variance explained by the linear fits in each regression is an appropriate measure of each relationship. By regressing the 923 observations on both models by Wills et al. (2000) and Wills and Clahan (2006), we find the R2 values to be around 0.5, which is down from 0.6 when 69 observations were used in a previous study (Yong et al., 2008; SCEC). Applying the same analytic technique to the topographic-slope and

1-031

SPATIAL ANALYSIS OF SHEAR-VELOCITY MEASUREMENTS IN SOUTHERN CALIFORNIA FOR PREDICTION UNCERTAINTIES *Thompson M (UNR), Louie JN (UNR), Dhar M (UNR), Pancha A (UNR), Pullammanappallil SK (Optim), and Yong A (USGS)*

In the western U.S., the average shear-wave velocity in the upper 30 m (Vs30) is currently the most popular predictor of ground motions in probabilistic models that estimate earthquake hazards. Because the coverage of Vs30 measurements in southern California is sparse, researchers have proposed various methods to predict Vs30 where there are few direct measurements. We apply the kriging method to 391 direct Vs30 measurements made by UNR and Optim, and from the NGA database to produce several first-order Vs30-estimate maps that address spatial variance and likelihood models of potentially hazardous soil classes. We divide the 391 measurements into

"soil", "basin", or "rock" categories based on the site class map assembled by Wills et al. (2000; BSSA). Statistical analysis of the data shows that the direct measurements closely fit a log-normal type of distribution. The first-order Vs30 predictions look sensible, match much of the geology, and thus, these results can be used as preliminary hazard maps. These maps created from the log-transformed Vs30 data show NEHRP site class E sites likely in certain parts of the Los Angeles Basin, and in the Imperial Valley. As expected, NEHRP site class D sites are very likely in these and many additional areas. In the Los Angeles basin portions of the SCEC CVM v4 (Magistrale et al., 2000; BSSA), the square root of the spatial variance or standard deviation reaches 0.3 natural log units for predicted values. In areas that have fewer direct measurements, the standard deviation exceeds 0.38 natural log units for the predictions. The spatial variance is less for the "soil" and "basin" subsets when compared to the "rock" subset or the complete data set; this is because the kriged spatial variance does not appear to reflect the variance of the direct measurements. The analysis clearly indicates that there is a need for many more measurements at "rock" sites. This need is exemplified in areas between San Clemente and San Diego, CA, where only one direct Vs30 measurement west of the Elsinore fault zone currently exists in these data sets. It is also clear that additional direct and denser measurements will decrease the spatial variance and standard deviation that should be associated with predictive models, and make probabilistic models more realistic.

1-032

THE EFFECT OF FAULT STEPOVERS ON GROUND MOTION *Lozos JC (UCR), Oglesby DD (UCR), and Brune JN (UNR)*

We investigate the effect of fault stepovers on ground motion. We use the 3D finite element method (Whirley and Engelmann, 1993; Oglesby, 1999) to model the dynamics of two parallel strike-slip faults with an unlinked stepover of variable width and an overlap of 5 km between the ends of the two segments. The overall length of the fault system, encompassing both segments, is 60 km. We modeled this system as both an extensional and a compressional stepover. We also compared these models to the ground motion from a planar fault of the length of a single segment (30 km) and one the length of the entire system (60 km). We found that, overall, the presence of a stepover along the fault trace reduces the maximum ground motion when compared to the long planar fault. In addition, the compressional stepover exhibited a higher maximum ground motion than the extensional stepover. In both cases, the stepover (overlapping) region itself had significantly lower ground motion than along the sections of fault that did not overlap. Also in both cases, the ground motion distribution after the rupture jumped to the second segment was highly asymmetrical, with lower motions between the fault segments, but the distribution became more symmetrical again as rupture progressed down the second segment. The overall distribution of ground motion was slightly more asymmetrical in the compressional stepover. The results may have implications for ground motion prediction in future earthquakes on geometrically complex faults.

1-033

A NEW KINEMATIC RUPTURE MODEL GENERATOR INCORPORATING SPATIAL INTERDEPENDENCY OF EARTHQUAKE SOURCE PARAMETERS *Schmedes J (UCSB), Archuleta RJ (UCSB), and Lavallee D (UCSB)*

Based on the results obtained by analyzing a large number of dynamic strike slip rupture models (Schmedes et al., 2009, subm. to JGR) we construct a kinematic rupture model generator that incorporates the key characteristics extracted from the dynamic rupture models. The source parameters that are used to construct the slip rate function at each sub-fault are final slip, rise time, local rupture velocity, and the peak time, which is a measure of the impulsive part of the slip

rate function. A four-dimensional correlation matrix is used to describe the spatial interdependency between the four source parameters that are modeled as correlated random fields. Each parameter has a different marginal distribution obtained from the analysis of the dynamic models. The marginal distributions are allowed to change as a function of the propagation distance, for example the rupture velocity increases as the rupture propagates along the fault. The autocorrelation of each parameter is modeled to have a power spectrum that follows a power-law, i.e. the source parameters are self-similar. The value of the power spectral decay for the different source parameters are based on the results obtained from the dynamic rupture models. Finally, the values of rise time and peak time are adjusted such that the moment rate function fits a Brune spectrum for a specified corner frequency. We validate the rupture model generator using observed strong motion near field recording for the 1994 Northridge earthquake and the 1989 Loma Prieta earthquake. The synthetic broadband seismograms are computed using the method of Liu et al. (2006, BSSA).

1-034

THE SCEC/USGS RUPTURE DYNAMICS CODE COMPARISON EXERCISE *Harris RA (USGS), Barall M (Invisible Software, Inc.), Archuleta RJ (UCSB), Andrews DJ (USGS), Dunham EM (Harvard), Aagaard B (USGS), Ampuero J, Atienza V, Dalguer L, Day S, Duan B, Ely G, Kaneko Y, Kase Y, Lapusta N, Ma S, Noda H, Oglesby D, Olsen K, Pitarka A, Song S, and Templeton-Barrett E*

Computer simulations of earthquake source rupture physics started three decades ago, with a few researchers developing and using their own methods to solve problems of mostly theoretical interest. In contrast, in current times numerous spontaneous rupture computer codes are being developed and used by researchers around the world, and the results are starting to be used in earthquake hazard assessment, for both seismological and engineering applications. Since most of the problems simulated using these numerical approaches have no analytic solutions, it is essential to compare, verify, and validate the various versions of this research tool. To this end, a collaborative project of the Southern California Earthquake Center, that has also received some funding from the DOE Extreme Ground Motion project, has been underway. We started with the basic problem of earthquake nucleation and spontaneous rupture propagation on a vertical strike-slip fault in a homogeneous material and subsequently moved on to problems with slightly more heterogeneous stresses and with differing material properties on opposite sides of the fault. Last fall we simulated 1) the case of rupture on a dipping fault, which is relevant to Yucca Mountain fault-rupture scenarios, and 2) the case of rate-weakening friction, rather than the slip-weakening friction used in most of our previous exercises. Our upcoming exercises are 1) rupture on a dipping fault with plastic-yielding and slip-weakening friction, and 2) rate-state friction or thermal pressurization on a vertical strike-slip fault. We have a website that enables easy comparisons of the results, and also supplies information about the benchmarks and codes. Our overall objective is a complete understanding of the simulation methods and their ability to faithfully implement our assumptions about earthquake rupture physics and calculate the resulting ground motion.

1-035

BROADBAND GROUND MOTIONS COMBINING LOW-FREQUENCY DETERMINISTIC SIMULATIONS AND HIGH-FREQUENCY SCATTEROGRAMS: VALIDATION AGAINST THE 1994 NORTHRIDGE EARTHQUAKE *Imperator W, Olsen KB (SDSU), and Mai PM (ETH)*

Mai and Olsen (2009) proposed a method to generate synthetic broadband ground motions by combining low-frequency (LF, $< \sim 1$ -2Hz) deterministic simulations and high-frequency (HF, $> \sim 1$ -

2Hz) point scatterograms from the theory by Zeng et al. (1991) and Zeng (1993). The method combines the LFs and HFs at a selected merging frequency minimizing the error in both amplitude and phase between the deterministic and stochastic time series (Mai and Beroza, 2003). Mena et al. (2009) extended this method to distribute the moment of the event to that of a finite-fault, and included a dynamically-consistent source-time function. Using this updated BB code, Mena et al. obtained an unbiased comparison to peak ground motions and spectral accelerations from NGA relations for the TeraShake simulations of large earthquakes on the southern San Andreas fault (Olsen et al., 2006, 2008) at precariously-balanced rock locations.

Here, we validate the most recent version of our BB method against strong-motion data from the 1994 Northridge earthquake. Validations are carried out using both strong-motion data (to isolate the accuracy of the HFs) and 3D finite-difference simulations (source model by Hartzell et al., 1996) as LFs. The goodness-of-fit between BB synthetics and data is estimated using the method by Mayhew and Olsen (2009), as well as by the bias (response spectral residuals). We estimate the site-specific kappa values that generate the optimal spectral fit between BB synthetics and data. The resulting distribution of kappa (average value of about 0.028 at 133 strong motion sites) show little or no correlation to V_s , or to the distance from the event. This distribution of kappa values is then used to compute a preferred set of BB synthetics for the Northridge earthquake. We find the best overall fit to data for the BBs generated using LFs up to 2Hz, as f_{max} (the frequency beyond which the spectral velocity decay follows $1/f$) at many stations is higher than 1 Hz. Our BB method is validated by a very good fit between observed and synthetic HFs for 2-10Hz using the observed data as LFs. Using simulated LFs we also obtain generally favorable fit between observed and synthetic BB peak ground accelerations, peak ground velocities, and spectral accelerations. However, our BB synthetics tend to slightly underpredict the strong-motion amplitudes between 2 and 10 Hz, primarily due to lack of complexity in our LF source model between 1 and 2 Hz.

1-036

GOODNESS-OF-FIT CRITERIA FOR BROADBAND SYNTHETIC SEISMOGRAMS, WITH APPLICATION TO THE 2008 MW5.4 CHINO HILLS, CA, EARTHQUAKE
Mayhew JE (SDSU), and Olsen KB (SDSU)

We present a goodness-of-fit measure (GOF_MO) for broadband ground motion time histories. As is the case with the goodness-of-fit measure proposed by Anderson (2004), our method includes a set of user-weighted metrics such as peak ground motions, response spectrum, the Fourier spectrum, cross correlation, and energy release measures. The scale for the goodness-of-fit ranges from near 0 to 100 (perfect fit). We apply the method to synthetic seismograms for the 2008 Mw5.4 Chino Hills, CA, earthquake, simulated in two different velocity models: CVM-4 and CVM-H. The two CVMs generate similar (and generally high) long-period ($< \sim 1$ Hz) levels of goodness-of-fit for this event. However, at selected sites, one of the two CVMs tends to generate a slightly better fit to data than the other, and thus providing guidance for improvement in accuracy of the velocity structure. Of particular importance, relatively good fits obtained in the Chino basin provide some observational support for the strong wave-guide effects from this area obtained for scenarios of northwestward-propagating ruptures on the southern San Andreas fault (TeraShake, ShakeOut). Other areas, such as part of Orange and Riverside counties and western Mojave Desert locations produce less favorable GOF values and suggest that improvement of the crustal structure is needed here.

The long-period synthetics for Chino Hills were combined with high-frequency scattering functions to generate broadband (BB) synthetics (0-10Hz) using the method by Mai and Olsen

(2009). At shorter periods, the goodness-of-fits fall above our general acceptance level (as well as that proposed by Anderson, 2004) at about 2/3 of the selected sites for the event. In addition to the metrics used for the long-period synthetics, we computed the goodness-of-fit for the Chino Hills event including an additional metric with specific interest for structural engineers, the ratios of inelastic/elastic displacements (IE ratios). We find a good fit between IE ratios for synthetics and data at long periods, which degrades at shorter periods, in agreement with Baker and Jayaram, 2008. It is possible that the use of site-specific parameters (kappa, scattering coefficient) may improve the fit for the shorter periods of the synthetics. Our results suggest that broadband synthetic seismograms for small earthquakes can be generated in relatively close agreement with data for the greater Los Angeles area, with some room for improvement.

1-037

THE SOUTHERN CALIFORNIA ARCHIVE OF PRECARIOUSLY BALANCED ROCKS: POTENTIAL FOR CONSTRAINING EARTHQUAKE RECURRENCE AND GROUND MOTION ATTENUATION *Brune JN (UNR), Anooshehpour A (UNR), Purvance MD (UNR), Brune RS (UNR), and Brune RJ*

Reconnaissance surveys over the past 15 years in arid regions of Southern California have located over a thousand precariously or semi-precariouly balanced rocks useful for constraining both components of earthquake hazard: earthquake recurrence models and ground motion attenuation models.

We have tested approximately 20 boulders in Southern California with experiments and numerical simulations in order to improve the observations of precariously balanced rocks as a quantitative tool for assessing seismic hazards. The cosmogenic and rock varnish surface age dates invariably proved to be older than 10,500 years. In this poster we discuss only the general distribution and fragility of the precarious rocks (based on photographic observation) to estimate the future value of the archive for constraining earthquake hazard. We present a rough estimate of how many of the documented rocks will eventually be consistent with the 2008 USGS-CGS seismic hazard maps for 10%, 2%, and 1% in 50 year probabilities. Essentially all rock sites are approximately consistent with the 10% map and inconsistent with the 1% map. Results for 2% in 50 year maps are shown in table 1.

TABLE 1

SP=Semi-precariouly, P=Precariouly, C=consistent at 2%, I=Inconsistent at 2%.

Aliso Canyon	SP	I
Anza	SP	I
Beaumont South	SP	I >10%g
Benton Rd	SP	I
Black Mtn Rd	SP	I
Comanche Pt road	SP	I
Cottonwood Oasis	SP	C
Culp Valley	SP	I >10g
Gibraltar	SP	I
Gopher gulch	SP	C
Granite Pass	P	C
Grass Valley /MarieLouise	SP	I >10%g
Indian flats Campground	SP	C

Poster Abstracts | Group 1 – GMP, SHRA

Jacumba	SP	I	
Jarupa	SP	C	
Joshua Tree	SP	C	
Juniper flats road	SP	I >10%g	
Lake Mathews Drive	SP	I	
Lake Perris North	SP	I >10%g	
Lovejoy Buttes	SP	I	
Mill Creek	SP	I	
Mirage West	SP	C	
Mockingbird/Cajalco	SP	I	
Moreno	SP	I >10%g	
Perris	SP	I	
Pinyon Crest	SP	I >10%g	
Pioneertown	P	I >10%g	
Santa Ynez Mtns	SP	I >10%g	
Silverwood Lake	SP	I >10%g	
UCR	SP	I	
White Wolf Fault	SP	I	
Yucca Valley	P	I	>10%g

We point out particular areas which are most likely to be of most importance to future seismic hazard maps. Important questions which the rocks have the potential answering include: Are some of the faults in UCERF2 less active than assumed?; What level of background seismicity should be assumed?; Which attenuation curves are more appropriate?; Is there a preferred rupture direction for large earthquakes?; Is the ergodic assumption appropriate?

1-038

FIELD-TEST OF PRECARIOUSLY BALANCED ROCKS NEAR YUCCA VALLEY CALIFORNIA: SEISMIC HAZARD RAMIFICATIONS *Anooshehpour A (UNR), Brune JN (UNR), and Purvance MD (UNR)*

The 2008 hazard maps for the Yucca Valley region indicate a very high hazard yet we find a number of precariously balanced rocks there, indicating there has been no strong shaking for the last few thousand years. The 2008 hazard estimate for this area is influenced by proximity to the San Andreas Fault (SAF), the Eastern California Shear Zone (ECSZ site of the 1992 Mw=7.3 Landers earthquake) the Pinto Mountain Fault (PMF), the Burnt Mountain Fault (BMF) the Eureka Peak Fault (EPF, site of the 1992 Mw=6.1 Joshua Tree Earthquake) and the Morongo Valley Fault (MVF) all of which converge in the area. To improve on the constraint on ground motion for this interesting and complex area we have tested the fragility of 6 precariously balanced rocks (PBR) just a few kilometers NW of the town of Yucca Valley. These field tests consisted of taking photographs of the rocks for accurate determination of their shapes using photogrammetry and quasi-static tilt-testing of a subgroup of them to determine accurate restoring force versus tilt curves. This information is important for accurate PBR fragility determination. Preliminary estimates of the quasi-static toppling accelerations for four of these rocks suggest that they could topple with ground accelerations less than 0.35 g inconsistent with the 2008 hazard maps. Therefore we discuss several possibilities for this discrepancy: (1) such complex areas typically do not produce very strong ground motions because large ruptures do not get organized; (2) the PMF and perhaps other faults in the area are less active than assumed in the hazard map. (The PMF slip rate is given a very large uncertainty); (3) since the PMF is not offset by the ECSZ there may be a detachment slab under the area which isolates the surface faults from the regional shear

(Doug Morton, personal communication), (4) the SAF does not form an organized rupture through San Geronio Pass; (5) there is a strong Vs30 PGA or PGV site effect.

1-039

PROPOSED GUIDELINES FOR THE SCIENTIFIC STUDY AND PRESERVATION OF PRECARIOUS ROCKS *Anderson JG (UNR), Brune JN (UNR), Anooshehpour A (UNR), and Purvance MD (UNR)*

Precarious rocks are irreplaceable. They are geological structures that are fragile enough that they could be destroyed by earthquakes. They have been formed over thousands of years by gradual geological processes. The observation that they are still standing provides irreplaceable information on past earthquakes that have occurred over their lifespan.

Precarious rocks should be seen as a finite and non-renewable resource. They are by definition fragile and vulnerable to destruction. Appropriate protection and management is therefore essential. In particular care must be taken to ensure that precarious rocks are not needlessly or thoughtlessly destroyed. With that purpose, we propose guidelines for their scientific study and preservation.

Because the precarious rocks are an irreplaceable resource scientists who engage in their study both corporately and individually have a responsibility to help conserve the resources to use them economically in their work, to conduct their studies in such a way that reliable information may be acquired, and to disseminate the results of their studies. Our proposed guidelines recognize the importance of scientific integrity in studying the rocks, steps for conserving the resource principles for field studies and the importance of promptly communicating the results.

A key element of our suggestions for conserving the resource, and the one that is the most controversial is nondisclosure of the rock locations except in selected cases. While some balanced rocks are well known features of the landscape the primary protection for most of them is their lack of visibility. For the obscure ones, resources are not available to protect them or even to post adequate signs with the intent of educating those who encounter the feature of their scientific value. A non-disclosure guideline would obviously require a two-tier system in which precise coordinates are available to scientists who need the information for their research but the community would agree that it is irresponsible to publish locations with a precision that makes for easy discovery.

1-040

GRAIZER-KALKAN GROUND MOTION PREDICTION MODEL BASED ON USGS GLOBAL ATLAS DATABASE *Kalkan E (USGS), Graizer V (USNRC), and Lin K (USGS)*

An alternative approach to ground motion prediction modeling based on representation of attenuation function as a combination of filters was introduced by Graizer & Kalkan (2007). In this model, each filter is a module calibrated separately to represent a certain physical phenomenon on seismic radiation (e.g., magnitude scaling site-correction basin effect, directivity Moho reflection etc.). This modular approach allows to isolate the influence of each phenomenon on prediction of ground motion intensity thus provides an enhanced robustness and stability to ground motion prediction equation (GMPE). In this paper, our GMPE and its modules are tested on USGS – Global Atlas database which has about 14,000 data points from 244 worldwide shallow crustal events including the 2008 M7.9 Wenchuan (China) and 2009 M6.3 L'Aquila earthquakes (Italy). Comparison of actual data with predictions demonstrates a very good match up to about 100 km for a range of magnitudes (M4.2 - 7.9). In order to achieve a better fit at far distances (>100 km)

where generally a fast attenuation is observed two coefficients in our original GMPE are modified and a new module is implemented. The resultant GMPE is tested to be used reliably for ground motion predictions from shallow crustal tectonic regions.

1-041

CALCULATING THE SOURCE SENSITIVITY OF BASIN GUIDED WAVES BY TIME-REVERSED SIMULATIONS *Day SM (SDSU), Roten D (SDSU), and Olsen KB (SDSU)*

Simulations of earthquake rupture on the southern San Andreas fault (SAF) reveal large amplifications associated with channeling of seismic energy along contiguous sedimentary basins. The Shakeout simulations, for example have shown that Love wave-like energy with a predominant period around 4 seconds is channeled southwestwardly from the San Gabriel basin (SGB) into the Los Angeles basin (LAB). While these channeling effects are repeatedly observed from different SAF simulations, the actual amount of amplification is sensitive to details of the source, such as slip distribution and direction and velocity of the rupture.

Day et al. (2008) proposed a numerical method that evaluates the sensitivity of a given wavefield pattern to perturbations of the source kinematics. Their method is based on isolating the wavefield feature of interest and calculating its pullback onto the source by means of a single time-reversed (i.e. adjoint) simulation. This allows calculation of the feature excitation resulting from any source perturbation without actually running a forward simulation. By applying this method to the SGB/LAB channeled waves Day et al. (2008) showed that the excitation of the waveguide is highly sensitive to slip on the ~100km long central SAF segment (Bombay Beach to Indio) but relatively insensitive to rupture on the northern and southern SAF segments. They successfully verified these findings through direct (forward-time) simulations.

Here we present additional results obtained from applying this approach to the SGB/LAB and Ventura basin waveguides. We analyze the sensitivity of the SGB/LAB waveguide to perturbations in the rupture velocity and rupture direction. Compared to the southeast-northwest rupture direction, the sensitivity analysis shows that excitation of surface waves in SGB/LAB are about a factor of 10 smaller for rupture from northwest to southeast, which confirms results obtained from the Terashake simulations. We find that the highest basin excitation occurs for rupture from southeast to northwest with super-shear rupture velocities between 3750 and 4000 m/s in the central SAF segment. Rupture speeds between the Rayleigh and S-wave velocities, i.e. the range that is energetically precluded, generate a basin excitation nearly as high as super-shear speeds. This result emphasizes the need for constraining kinematic source parameterizations from spontaneous rupture models, which naturally avoids the energetically-precluded regime.

1-042

GROUND MOTION HAZARD FROM SUPERSHEAR RUPTURE *Andrews DJ (USGS)*

An idealized rupture, propagating smoothly near a terminal rupture velocity, radiates energy that is focused into a beam. For rupture velocity less than the S-wave speed, radiated energy is concentrated in a beam of intense fault-normal velocity near the projection of the rupture trace. Although confined to a narrow range of azimuths, this beam diverges and attenuates. For rupture velocity greater than the S-wave speed, radiated energy is concentrated in Mach waves forming a pair of beams propagating obliquely away from the fault. These beams do not attenuate until diffraction becomes effective at large distance. Events with supershear and sub-Rayleigh rupture velocity are compared in 2D plane-strain calculations with equal stress drop, fracture energy, and rupture length; only static friction is changed to determine the rupture velocity. Peak velocity in the sub-Rayleigh case near the termination of rupture is larger than peak velocity in the Mach

wave in the supershear case. The occurrence of supershear rupture propagation reduces the most intense peak ground velocity near the fault, but it increases peak velocity within a beam at greater distances.

1-043

MINIMUM SURFACE EXPOSURE AGES OF MOJAVE PRECARIOUSLY BALANCED ROCKS *Purvance MD (UNR), Brune JN (UNR), and Anooshehpour A (UNR)*

Precariously balanced rocks (PBRs) are relic geomorphic features which have survived the actual ensembles of ground motions at their sites during their residence times. Thus PBRs can be utilized to constrain the levels of unexceeded ground motion amplitudes while they have persisted in their fragile states. Efforts to constrain the ground motions required to overturn PBRs have resulted in quantitative nonexceedence constraints which have been validated via shake table experiments. In order to fully utilize PBRs to constrain seismic hazard estimates, though, one must also estimate the PBR residence times. This work documents recent efforts to constrain the ages of granitic PBRs near the Mojave section of the San Andreas Fault via the varnish microlamination (VML) method. The VML method exploits the strong correlation between climatic variations and the deposition of surface varnish layering to estimate the minimum rock surface exposure ages. The resulting surface exposure estimates are true minimum exposure estimates due to the possibility that surface weathering has destroyed previous varnish. VML samples have been collected on numerous granite rock surfaces at sites within ~ 15-30 km of the Mojave section of the San Andreas Fault. Sample locations range from PBR pedestals to adjacent rock surfaces below nearby PBR bases to the lowest rock exposures in the local vicinities of PBRs. The VML analyses strongly indicate that the Mojave PBRs have survived without overturning for greater than ~ 14,000 years. These VML results demonstrate that the Mojave PBRs represent important data tools useful to constrain seismic hazard estimates. These data will be utilized to compare these PBR constraints with the 2009 USGS National Seismic Hazard Maps.

1-044

THE ECHO CLIFFS PRECARIOUSLY BALANCED ROCK; DISCOVERY AND DESCRIPTION BY TERRESTRIAL LASER SCANNING *Hudnut KW (USGS), Amidon W (Caltech), Bawden GW (USGS), Brune JN (UNR), Bond S, Graves RW (URS), Haddad D (ASU), Limaye A, Lynch DK (Caltech), Phillips D (UNAVCO), Pounders E (USGS), Rood D (LLNL), and Weiser D (UCLA)*

We investigate a previously undocumented Precariously Balanced Rock (PBR) located above Echo Cliffs in the western Santa Monica Mountains, using Terrestrial Laser Scanning (TLS). We present the initial merged and aligned point cloud of TLS data (over 42 million points) and selected photos to document the Echo Cliffs PBR site. We also present our initial interpretations of the site, of its geomorphic development, and its possible significance for seismic hazards in the Los Angeles region.

The rock lies above the ramp in the fault propagation fold structure that has been interpreted by Davis and Namson as an active structure that may pose a major seismic hazard to the Los Angeles area. The Echo Cliffs PBR stands at just over 14 meters in height, so assuming it acts as an inverse pendulum, it has a 3 to 4 second period of oscillation (the period is square root of height). This period corresponds to the oscillatory period of a 30 to 40 story building. The rock withstood ground motions during the 1994 Northridge earthquake that we estimate to have been 0.2 g (PGA) and 12 cm/sec (PGV) at this site. We also show our modeled ground motions from scenario earthquakes at this site, such as the Puente Hills Thrust and ShakeOut models. It is

expected that the Echo Cliffs PBR may provide important constraints on such scenario ground motions and may also help improve such simulations in the future.

We believe that this is the first application of TLS methods on PBR's, and we find that the high resolution and spot density provided by TLS allows us to characterize the detailed shape of the PBR itself, as well as key details of the interface between the rock and pedestal at the centimeter level. In addition, the cliff band near the PBR and the geomorphic context of the surrounding hill slope area was also scanned at a coarser resolution, providing data that help to understand the processes by which the PBR formed.

An advantage of TLS is that it provides an image of the outline of the rock-pedestal contact surface and adjacent non-contacting surfaces. This and other details provided by TLS are expected to enhance the accuracy with which simulations of rocking motions with respect to the pedestal may be computed, and hence refine toppling ground motion criteria. The TLS also helps with quantifying shielding of cosmogenic nuclides, and will therefore enhance the accuracy of surface exposure age dating that we are applying to the rock and pedestal here.

1-045

CHARACTERIZING THE GEOMORPHIC SITUATION OF PRECARIOUSLY BALANCED ROCKS IN SEMI-ARID TO ARID LANDSCAPES OF LOW-SEISMICITY REGIONS *Haddad DE (ASU), and Arrowsmith JR (ASU)*

Granitic precariously balanced rocks (PBRs) are a subset of spheroidally weathered boulders formed in upland drainage basins and pediments of the Southwest. They are used as negative indicators of earthquake-generated extreme ground motions to evaluate seismic hazard analyses for Southern California and Nevada. Current understanding of PBR formation and preservation is derived from a two-stage conceptual model that involves (1) corestone production by subsurface chemical weathering of bedrock along joint surfaces, followed by (2) corestone exhumation and placement in precarious positions. The primary factors that control PBR formation are joint density, spacing, and geometry. However, the geomorphic agents that exhume, and subsequently produce, PBRs are insufficiently understood. For example, what geomorphic processes control the spatial distribution of PBRs in a landscape, and where do these processes dominate? Are PBRs located on steep or gentle hillslopes? Are they located near drainages or hillslope crests?

We propose a process-based conceptual model for PBR production and preservation that quantitatively describes the geomorphic agents acting in the PBR life cycle. Subsurface corestone production from bedrock during wetter climatic conditions was facilitated by high soil production rates, resulting in soil-mantled and transport-limited hillslopes. The transition to arid climatic conditions introduced short-lived, high-intensity precipitation events that were conducive to corestone exhumation and PBR production. Precarious rock development is therefore a result of the coupling of subsurface corestone formation, soil production, and downslope transport of hillslope materials.

Our latest efforts utilize the innovative combination of terrestrial and airborne light detection and ranging (LiDAR) technology to acquire research-grade digital topographic data for a precarious rock zone. These data permit submeter-scale morphometric computations of local slope and relief. Because the fundamental mechanistic hillslope transport laws are controlled by local hillslope gradient and contributing area, the locations of PBRs in a landscape have important controls on their exhumation rates and histories. Therefore, characterizing the geomorphic situation of PBRs is critical to guiding interpretations of PBR surface exposure ages that are used to formulate

statistical simulations of earthquake-generated extreme ground motions for seismic hazard analyses.

1-046

HOW DO WE DATE A PBR? : A ROBUST METHOD USING BE-10 SURFACE EXPOSURE DATING WITH NUMERICAL MODELS *Rood DH (LLNL), Balco GA (LLNL), Purvance MD (UNR), Anooshehpour A (UNR), Brune JN (UNR), Grant Ludwig LB (UCI), and Kendrick K (USGS)*

Be-10 geochronology of precariously balanced rocks (PBRs) is a powerful tool for constraining unexceeded ground motions, but surface exposure dating of PBRs can only be successful if the geomorphic history of the rock is known. In order to reduce uncertainty in interpreted ages, we must develop a more accurate geomorphic model for PBR formation processes. Our approach is to (1) collect profile samples of the PBRs and pedestals at various heights above the ground surface and (2) sample saprolite and stream sediment to constrain surface denudation rates. We measured Be-10 concentrations in 30 samples from 8 PBRs along a 150-km transect near the San Andreas, San Jacinto, and Elsinore faults in southern California. In all cases, pedestal samples yield lower Be-10 concentrations than their associated PBR, and nuclide concentrations show an exponential increase with increasing height above the ground surface. This observed pattern among rock and pedestal Be-10 concentrations indicates that the exhumation history must be carefully considered. We use a forward model and compare our Be-10 data to predicted profiles for a range of surface denudation rates and exposure times. The total Be-10 concentration is the sum of nuclides produced before (i.e. subsurface) and after exhumation, with different ratios of pre- and post-exhumation erosion rates yielding different nuclide concentrations as a function of depth.

Using simplified shielding corrections and assuming rapid exhumation, our model predicts surface exposure ages for 4 PBRs that range from 23-16 ka, consistent with minimum exposure ages from varnish microlamination dating results. However, because the cosmic ray flux is only partly attenuated by the rock, to accurately interpret PBR profiles requires that the model include a shielding correction that accounts for the shape of the PBR. Three-dimensional models for PBRs were constructed using photogrammetric and ground-based LiDAR data. Using a model with the more realistic shielding correction, one PBR in the San Bernardino Mountains gives best-fit parameters that indicate that the entire rock and pedestal was exhumed rapidly at 27 +/- 2 ka. Furthermore, saprolite and stream sediment samples associated with this PBR indicate surface denudation rates of 0.1 mm/yr following rapid exhumation. To refine our exposure ages, ongoing work will apply our model to additional PBRs and constrain PBR rock erosion rates using in-situ C-14.

1-047

ASSESSING FEMA HAZUS-MH MR3: CONSTRAINING SEISMIC HAZARD ESTIMATES FOR RIVERSIDE COUNTY USING PRECARIOUSLY BALANCED ROCKS *Neighbors CJ (UCR), and Cochran ES (UCLA)*

We will assess and validate ground motion, earthquake hazard, and potential loss estimates employed in FEMA (Federal Emergency Management Agency) HAZUS-MH MR3 (Hazards United States - Multi-Hazards Maintenance Release 3) by testing precariously balanced rocks (PBRs) and by examining seismic amplification. The study region will be the University of California, Riverside (UCR) campus, which provides an excellent natural laboratory to assess HAZUS-MH expected ground motions due to its proximity to several major active faults and precariously balanced rocks located adjacent to a shallow sedimentary basin. For UCR campus,

two faults pose significant hazard: the San Andreas fault and the San Jacinto fault; both faults are right-lateral, strike slip with slip rates of 25 mm/yr and 12 mm/yr, respectively.

Precariously balanced rocks help to constrain maximum ground shaking in a region over the time period that the rocks have been exposed. For each PBR a toppling velocity will be determined by calculating toppling accelerations based on the rock's center of mass and pedestal configuration and by field testing some PBRs. Digital photogrammetry performed on one PBR provides a preliminary estimate of a calculated toppling accelerations of 7.7 m s^{-2} . Cosmogenic radionuclide dating will be used to constrain a specific age of the rock's surface exposure, or the length of time the rock has been precarious.

To constrain local amplification and subsurface structure, we will deploy temporary seismometers and refraction microtremor (ReMi) instruments. Seismic data will be used to compare ground motions from regional earthquakes and will aid in the investigation of coherence of ground motions both at small scales on hard rock sites (<1 km) and across medium scale distances (<5 km) of varying foundations (hard rock and thin sediment layer). ReMi arrays will allow us to determine the 3-D subsurface structure. We will compare the subsurface structure with local site effects to determine if a simple relationship exists between them.

To assess the FEMA HAZUS-MH MR3 Earthquake Model, we plan to run various earthquake scenarios for UCR campus. Peak ground accelerations (PGA) calculated from HAZUS-MH empirical attenuation relationships will be compared to PGA needed to topple PBRs. With constraints on maximum ground shaking determined from PBRs and local path and site effects, we will evaluate the existing HAZUS-MH MR3 Earthquake Model.

1-048

CAN PRECARIOUSLY BALANCED ROCKS (PBRs) PROVIDE IMPORTANT CONSTRAINTS ON FAULT RUPTURE HAZARD FOR UNIFORM CALIFORNIA EARTHQUAKE RUPTURE FORECAST 3 (UCERF3)? *Grant Ludwig LB (UCI), Kendrick KJ (USGS), Brune JN (UNR), Anooshehpour A (UNR), Purvance MD (UNR), Rood DH (LLNL), and Schlom T (CSU Fullerton)*

Hazard maps are developed from two basic components: fault rupture probability and ground motion attenuation. Precariously balance rocks (PBRs) constrain ground motions and thereby provide implicit constraints on rupture probability of nearby faults. In specific cases where PBRs are located close to an active fault, the precarious age of the rock constrains the time since the last significant ground motion generated by that fault, and by extension, provides constraint on Holocene slip rate. In our recent work we found that the pre-Holocene age of a PBR in the western San Bernardino Mountains <1 km from the Cleghorn fault is inconsistent with the 3 ± 2 mm/yr slip rate used in the 2008 National Seismic Hazard Maps (NSHMs) and UCERF2. Rood et al. (companion abstract) report a preliminary exhumation age of approximately 27 ± 2 ka, implying that the rock has not experienced strong ground motions during the Holocene. Similarly along the western Pinto Mountain fault near Yucca Valley, Anooshehpour et al (companion abstract) report 6 PBRs located ~ 1 km from the mapped t

1-049

THE ALPINE FAULT: CONSTRAINTS ON THE UPPER LIMITS ON NEAR-FAULT EARTHQUAKE MOTIONS FROM FRAGILE GRANITIC LANDFORMS *Stirling MW (IGNS New Zealand), Langridge RM (USGS), and Massey C (IGNS New Zealand)*

We have recently commenced a study of fragile bedrock landforms to constrain the upper-bounds of near-field earthquake motions from great Alpine Fault earthquakes. There is a paucity of instrumental strong motion data close to major earthquake epicentres and ruptures, and a relatively few well-instrumented events dominate the worldwide strong motion datasets (e.g. Chi-Chi, Taiwan). There are currently no strong motion records for near-field Alpine Fault earthquake motions, and our application of standard methods of probabilistic seismic hazard assessment (PSHA) predict increasingly stronger motions as a function of return period close to the fault (peak ground accelerations of c. 0.9g, 1.4g and 1.6g at the 475 year, 2500 year and 5000 year return periods, respectively). There is currently no procedure for verifying whether these hazard estimates are realistic for the Alpine Fault, a mature plate boundary fault with nearly 500 km of accumulated offset.

Our approach to constraining the upper-bounds of Alpine Fault ground motions is to use natural bedrock landform features as low resolution seismoscopes that have “recorded” past Alpine Fault events. Specifically, we seek to quantify the age and fragility of certain fragile landforms to establish the likely ground motions required to initiate their failure. The methodology of using fragile landforms in this manner was originally developed in the USA, and has also been applied to New Zealand in EQC/SCEC co-funded work. The co-funded studies of precariously-balanced rocks (PBRs) at a near-fault site in central Otago established the PBRs to be of Holocene age (i.e. considerably younger than PBRs in arid USA environments), too young to be useful for testing ground motions at active faults with recurrence intervals of greater than 10kyrs. PBRs and fragile bedrock landforms will instead be useful near faults with short recurrence intervals such as the Alpine Fault (3 to 5 ground-rupturing earthquakes in the last 1000 years).

The Hohonu Range has been chosen for this study based on proximity to the well-studied central section of the Alpine Fault (5 to 10km distance), and the presence of fragile granitic outcrops (with no associated scree deposits) and precariously perched boulders on summit ridges and cirque headwalls. Weathering features on the granite surfaces appear old enough for the outcrops and boulders to have survived repeated nearby Alpine Fault earthquakes.

1-050

COMMUNITY-OUTREACH EFFORTS IN DATA COLLECTION AND ANALYSIS FOR THE 2008 MOGUL EARTHQUAKE SEQUENCE *Kell-Hills AM (UNR), Dhar MS (UNR), Thompson M (UNR), Louie JN (UNR), and Smith KD (UNR)*

Beginning February 28, 2008 the residents of west Reno and Sparks, Nevada experienced continuous earthquakes ranging in magnitude from M1.0 to M5.0, centered in the west Reno neighborhoods of Mogul and Somerset. The occurrence of these earthquakes within residential areas stimulated the attention of the public and the media, providing an opportunity for the Nevada Seismological Laboratory (NSL) to involve the public in earthquake research. The NSL invited the public to host single-channel USArray Flexible Array RefTek RT-125A (Texan) recorders in their homes during May and June of 2008. Reno and Sparks residents volunteered to attend training sessions on installing and hosting recorders at their private residence, filling the many gaps in NSL’s permanent and RAMP station arrays. The volume of public interest allowed a density of seismograph coverage unprecedented in U.S. aftershock response, with 106 deployed locations. Evaluation of recorded seismograms for a M3.1 event display atypical responses for

areas of bedrock and basin fill in that bedrock seismograms in the north of Reno displayed higher than expected amplitudes and long durations, and that some regions of basin fill showed lower than expected amplitudes. Comparing these seismograms allows us to better interpret basin depths and bedrock locations for the Reno basin and allows us to develop a model for local earthquake hazard. Analyses of the recorded data include time delay calculations and straight-ray tomography. A back-projection of pick delays indicate positive delays north of Reno, atypical of bedrock settings. Curve fitting on a time vs. distance plot on the M3.1 event calculated a hypocentral depth greater than the depth derived from NSL's permanent stations, motivating a study relocating the event depths. These results are presented in this meeting in a poster titled "Station Delays and Their Variance in the Reno-Area Basin from a Dense Deployment During the 2008 West Reno Earthquake Swarm."

1-051

THE CALTECH VIRTUAL SHAKER ([HTTPS://VIRTUALSHAKER.CALTECH.EDU](https://virtualshaker.caltech.edu))
Krishnan S (Caltech)

The Caltech Virtual Shaker (<http://virtualshaker.caltech.edu>) is an online science gateway to facilitate the sharing and exchange of structural models and ground motion waveforms between various research groups, and the transfer of simulation technology to various stake-holders. The unique feature of this interface is the facility to remotely analyze structural models on a high-performance computing cluster (HPCC) at Caltech, dedicated to earthquake engineering simulations. It consists of the following modules:

Ground motion database: Simulated ground motion waveforms from various scenarios and recorded waveforms from recent earthquakes are archived in this database and available for remote analysis of structural models through the E-Analysis facility.

Structural model database: One of the difficulties facing the structural engineering research community is the lack of detailed design information on existing building models. This database collates and archives models of existing buildings as well as newly designed buildings accessible to the entire community to conduct structural engineering studies. Models of buildings that are submitted for remote analysis through the E-analysis facility are automatically added to the database and are publicly available for researchers to access.

E-analysis facility: This module facilitates the remote analysis of structural models on the dedicated high-performance computing cluster for earthquake engineering simulations at Caltech. Registered users are able to submit structural models for analysis under earthquake ground motion submitted by them or taken from the ground motion database. Upon completion, an email is sent to the user with information on how to download the results. The results can be interpreted through a comprehensive User Guide also available online.

The SCEC Community can make use of this facility in the following ways:

1. Contribute ground motion waveforms (recorded or simulated) for others to use.
2. Contribute structural models for others to use.
3. Analyze any of the structural models in the database under any waveform from the ground motion database to get a feel for the response of structures under various kinds of earthquake motions.

4. Visualize the structural response through animations (coming soon).

NO USE FEE, NO SOFTWARE OR HARDWARE REQUIRED. SIMPLY REGISTER AND START SHAKING.

1-052

HAZUS LOSS ESTIMATION FOR CALIFORNIA SCENARIO EARTHQUAKES *Chen R (CGS), Branum D (CGS), and Wills CJ (CGS)*

Comprehensive estimate of the scale and extent of damage, social disruption, and economic losses due to potential earthquakes is useful information in preparing emergency response plans and developing earthquake hazard mitigation strategies. Using HAZUS, loss estimation software developed by the Federal Emergency Management Agency, we estimated economic losses, social impact, and structural damage for over fifty scenario earthquakes developed by the United States Geological Survey (USGS) (referred to as USGS scenarios). These scenarios were developed using ground motion prediction equations from Boore et al. 1997 and Joyner and Boore 1988 and source parameters of the 2002 probabilistic seismic hazard assessments for California. Significant research developments have occurred in the past few years in both ground motion prediction and rupture source characterization. To estimate the effects of these latest developments on HAZUS loss estimates, we developed and analyzed ten scenarios based on source parameters and probability results of the Uniform California Earthquake Rupture Forecast Version 2 (UCERF 2) and three Next Generation Attenuation (NGA) models (referred to as UCERF 2-based scenarios). Estimated losses for USGS scenarios and UCERF 2-based scenarios are summarized and compared. Comparison is also made with a 2005 study by California Geological Survey (CGS) using an earlier version of HAZUS.

The predicted three most damaging USGS scenario earthquakes in Northern California involve co-seismic rupture of different combinations of at least three Northern San Andreas Fault segments, resulting in an estimated economic loss ranging from nearly \$70 billion to over \$80 billion. In southern California, the most damaging scenario is the M7.1 earthquake on the Puente Hills fault with total predicted economic loss reaching \$83 billion. Comparison of estimated building-related losses for the USGS scenarios from the current study with those from the CGS 2005 study does not show a consistent trend. Instead, the difference varies significantly with geographical locations. There are, however, significant and consistent differences in the estimated building related losses for the UCERF 2-based scenarios compared to the USGS scenarios. In general, the estimated building-related loss for a UCERF 2-based scenario is 30 to 60 percent lower than that for the comparable USGS scenario. This difference is mainly due to the use of NGA models in the UCERF 2-based scenarios.

1-053

SEISMIC PERFORMANCE OF REINFORCED CONCRETE FRAME BUILDINGS IN SOUTHERN CALIFORNIA IN THE MAGNITUDE 7.8 SHAKEOUT SCENARIO EARTHQUAKE *Lynch KP, Rowe K, and Liel AB (Colorado)*

This study assesses the seismic performance of reinforced concrete (RC) frame buildings in Southern California due to a magnitude 7.8 earthquake on the southern San Andreas Fault, with the goal of predicting the impact of this scenario event on RC frame structures built in the Los Angeles region over the past 40 years. The investigation is based on RC office buildings typical of those found in California, including both older non-ductile RC frame buildings (constructed pre-1970) and modern code-conforming special moment frame structures.

We utilize broadband ground motion simulations at more than 700 evenly-spaced sites in Southern California, developed by researchers at SCEC (Graves et al. 2008), to predict damage and collapse risk in a set of typical RC frame structures. Seismic response parameters (e.g. interstory drifts, peak floor accelerations, etc.) are predicted from nonlinear dynamic analysis of simulation models of each building at each site. Each building is modeled in OpenSees, with material and geometric properties capable of capturing possible strength and stiffness deterioration as the structure becomes damaged and potentially collapses under large ground motions.

The final study will include 20 modern and older RC frame buildings, varying in height from 1 to 20 stories, and including both space and perimeter frame systems. At this time, preliminary results of the analysis of 4- and 8-story RC frame buildings will be presented to illustrate the distribution of damage over the study region and differences in damage and collapse risk between older (pre-1970) and modern, seismically-designed RC frame buildings. These results illustrate damage and casualties in the scenario earthquake, which can be used to identify types of buildings and sub-regions that may be particularly vulnerable in future earthquakes in Los Angeles. The study also demonstrates how ground motion time history simulations can be used in rupture-to-rafters simulation to assess seismic risk in a particular region.

1-054

MODELING ELASTIC AND INELASTIC, CRITICAL- AND POST-BUCKLING BEHAVIOR OF BRACING MEMBERS - A PREREQUISITE FOR THE STUDY OF TALL BRACED FRAME BUILDINGS *Krishnan S (Caltech)*

Analyzing tall steel braced frame buildings with thousands of degrees of freedom in three dimensions subject to strong earthquake ground motion requires an efficient brace element that can capture the overall features of its elastic and inelastic response under axial cyclic loading without unduly heavy discretization. A modified elastofiber (MEF) element has been developed to efficiently model the elastic and post-critical buckling of braces and buckling-sensitive slender columns in such structures. The MEF element consists of three fiber segments, two at the member ends and one at mid-span, with two elastic segments sandwiched in between. The segments are demarcated by two exterior nodes and four interior nodes. The fiber segments are divided into 20 fibers in the cross-section that run the length of the segment. The fibers exhibit nonlinear axial stress-strain behavior akin to that observed in a standard tension test in the laboratory, with a linear elastic portion, a yield plateau, and a strain hardening portion consisting of a segment of an ellipse. The elastic buckling of a member is tracked by updating both exterior and interior nodal coordinates at each iteration of a time step, and checking force equilibrium in the updated configuration. Inelastic post-buckling response is captured by fiber yielding in the nonlinear segments. A user-defined probability distribution for the fracture strain of a fiber in a nonlinear segment enables the modeling of premature fracture, observed routinely in cyclic tests of braces. Handling geometric and material nonlinearity in such a manner allows the accurate simulation of member-end yielding, mid-span elastic buckling and inelastic post-buckling behavior, with fracture or rupture of fibers leading to complete severing of the brace. The element is integrated into the nonlinear analysis framework for the 3-D analysis of steel buildings, FRAME3D. A series of simple example problems with analytical solutions, in conjunction with data from a variety of cyclic load tests, is used to calibrate and validate the element. A FRAME3D model of a full-scale 6-story braced frame structure that was pseudodynamically tested by the Building Research Institute of Japan subjected to the 1978 Miyagi-Ken-Okai earthquake record, is analyzed and shown to closely mimic the experimentally observed behavior.

1-055

ON THE MECHANISM OF COLLAPSE OF TALL STEEL MOMENT FRAME BUILDINGS *Krishnan S (Caltech), and Muto M (Caltech)*

How would tall steel moment frame buildings collapse under seismic loading? Steel moment frame exhibit shear beam type behavior. It is well known that when a two-sided pulse travels through a uniform shear beam, strain doubling occurs due to constructive interference of the reverse phase of the incident wave with the forward phase that is reflected off the free end. Such strain doubling can lead to damage localization. Moment frame buildings differ from uniform shear beams in two important ways- first, the buildings are not uniform, there is typically stiffness gradation and mass variation over the height of the structure; second, gravity is not present in the shear beam wave propagation problem, whereas, it plays a dominant role in the response of moment frame buildings. Not only do building columns carry axial loads, but gravity also causes second-order overturning moments associated with the self-weight of the structure acting through its deformed configuration under lateral loading, the so-called P-Delta effect. As a consequence, damage localization in moment frame buildings can result in the formation of a slider-block collapse mechanism, consisting of column yielding at floors corresponding to the top and bottom of the slider-block, with significant yielding of the beams or columns or panel zones at each joint in each of the intermediate floors. We demonstrate that such a compliant slider block, driven by P-Delta effects from the over-burden dead weight of the floors above the slider-block, is the fundamental mode of collapse of tall steel moment frame buildings. Through parametric studies of 3-D finite element models of tall (approximately twenty story) steel moment-frame buildings subjected to idealized pulses, we show that for moderate loading (motions that are not strong enough to cause structural collapse), the region of dominant damage is controlled by the period of the input ground motion relative to the fundamental period of the structures, with behavior that is very similar to that of an idealized shear beam. However, the response to "collapsogenic" input motions, i.e., motions with larger amplitudes or long-duration pulse-train loading, shows a "convergence" of the region of dominant damage. This implies that there is a special preferred mechanism of collapse for a given building regardless of the frequency-duration characteristics of the incident ground motion. This preferred collapse mechanism happens to be a function of the structural system alone and can be predicted using its basic properties. Analyses performed using recorded near-source ground motion waveforms from recent events, as well as simulated motions from a larger (magnitude 7.9) far-source event support this idea of a preferred collapse mechanism.

1-056

GEOLOGIC STUDIES AND SEISMIC SOURCE MODEL FOR A PROPOSED NEW OCEAN OUTFALL, SAN PEDRO SHELF, CALIFORNIA *Hogan PJ (Fugro West, Inc.), Varnell SL (Fugro West, Inc.), Smith PM (Fugro West, Inc.), and McNeilan TW (Fugro West)*

The Sanitation Districts of Los Angeles County (Districts) are evaluating the feasibility of a new tunnel and ocean outfall for its Joint Outfall System. Fugro performed offshore geotechnical and seismic survey campaigns for the project between 2004 and 2008. Based on these new data, we describe structural and stratigraphic conditions on the Palos Verdes (PV) and San Pedro (SP) Shelves and adjacent slopes.

The offshore stratigraphy consists of a sequence of Cenozoic marine strata overlying Mesozoic basement rocks consisting of Catalina Schist. Soil and rock units present beneath portions of the shelf and slope in the survey area include: 1) Catalina Schist, 2) Monterey Formation, 3) Malaga Mudstone, 4) Fernando Formation, 5) Late Pleistocene sediments, and 6) Holocene sediments. Miocene basaltic intrusions are found within the lower Monterey Formation.

The PV Anticlinorium (PVA) dominates the structure of the Project Area. The PVA extends onshore and offshore for approximately 30 miles, from Santa Monica Bay to SP Bay, and is associated with a broad zone of uplift adjacent to the Palos Verdes Fault Zone (PVFZ). The PVFZ is an inverted Miocene normal fault that has been reactivated as a transpressional structure in the Plio-Pleistocene (Brankman and Shaw, 2009). We interpret the PVA as a broad hanging-wall anticline above the southwest-dipping PVFZ. Our current seismic source model, including segmentation of the PVFZ is presented.

Shorter faults, such as the Cabrillo fault and other faults on the continental shelf and slope to the southwest of the Project Area are considered secondary structures related to the PVFZ, PVA, and a deep basal decollement underlying the southern LA Basin and SP Shelf. The Cabrillo fault and numerous other short faults may have formed as bending moment faults as a consequence of folding during uplift of the PVA concurrently with shortening across the LA Basin.

Potentially active and inactive southwest-dipping reverse faults are present beneath the SP Slope, creating a stable buttress against slope failures. This appears to have resulted in relatively stable bedding conditions on the outer SP Shelf and Slope. Potential fault rupture and seismicity present geohazard challenges to the project. Geohazards will be mitigated through appropriate engineering design of the facilities.

1-057

EARTHQUAKE EARLY WARNING USING TOTAL DISPLACEMENT WAVEFORMS FROM REAL-TIME GPS NETWORKS *Crowell BW (UCSD), Bock Y (UCSD), and Squibb MB (UCSB)*

We have created the framework for an earthquake early warning (EEW) system based upon the use of high-rate (1-Hz) measurements from dense regional GPS networks such as Japan's GEONET and the California Real Time Network (CRTN) run by the Scripps Orbit and Permanent Array Center (SOPAC). This system utilizes the method of precise instantaneous GPS positioning [Bock et al., 2000] and the resulting total (dynamic and static) displacement waveforms to compute a strain rate Delaunay triangulation throughout the entire network of stations and searches for anomalous strain activity. Email alerts are sent to key personnel during when strain exceeds a prespecified threshold. Once high strain is obtained, earthquake source modeling begins. A real-time network adjustment is performed to reference the entire network to the station farthest away from seismic activity to ensure a stable reference station. Earthquake hypocenter is determined through a grid search algorithm with aims to minimize the L1 and L2 norms of travel time difference and total travel time, respectively, once 4 stations have encountered total peak ground displacement (PGD) greater than 0.1 meters. Scaling laws are then used to determine the moment magnitude and a full coseismic inversion is performed after the event to assist first responders. Integration of geodetic and seismic warning systems can currently be accomplished with existing infrastructure through the use of a multi-rate Kalman filter as evidenced from outdoor shake table results.

1-058

RECENT DEVELOPMENTS IN CISN EARTHQUAKE EARLY WARNING TESTING FOR CALIFORNIA *Boese M (Caltech), Hauksson E (Caltech), Solanki K (Caltech), Heaton TH (Caltech), and EEW group C*

Over the past three years the California Integrated Seismic Network (CISN) has been testing the real-time performance of three algorithms for earthquake early warnings (EEW) in California. The algorithms have successfully detected many earthquakes and in some cases predicted the peak

ground shaking a few seconds before it was felt. We are now beginning to build a prototype alert system that will provide warnings to a small group of test users. We will present basic ideas of this system.

In addition, we show the real-time performance of the single-sensor based τ -Pd on-site warning algorithm in California during the past three years. The algorithm has detected ~140 local earthquakes in California and Mexico Baja with moment magnitudes of $3.5 \leq M_w \leq 5.4$. Combined with newly derived station corrections the algorithm rapidly determines moment magnitudes M_w and Modified Mercalli Intensities with uncertainties of $\sigma=0.5$ and $\sigma=0.7$ units, respectively. In the past reporting delays ranged from 9 sec to 16 sec, but were recently reduced to 4 sec to 11 sec, including 3 sec waveform data required by the current algorithm.

Particularly in regions with sparse instrumentation, the τ -Pd algorithm usually provides faster information than the regional warning approaches. However, the algorithm has (1) a higher probability of false triggers, and (2) there is a significant amount of scattering in the $\log_{10}(\tau)$ - M_w relation. The main causes for false triggers are temporally increased levels of noise, e.g. caused by construction, malfunctioning stations, or mass-recentering. We have developed several tools, such as (1) a two-station approach for trigger confirmation, (2) a Black List to deactivate noisy channels manually, (3) a real-time notification system to halt data flow temporally from sensors to the EEW algorithm during mass-recentering.

Recently, we discovered systematic trends in the spatial distribution of the τ residuals in California: e.g. the magnitude of earthquakes in the Imperial Valley or LA Basin usually were overestimated by up to 1.5 units, whereas magnitudes of earthquakes in the Big Bend of the San Andreas Fault were similarly underestimated. A likely explanation is the existence of spatial differences in the seismic stress drops as reported previously. Based on a new tool to replay the records of past earthquakes from SCEDC/NCEDC as simulated real-time data streams, we are currently working on a detailed analysis of these uncertainties.

1-059

DEVELOPING PERFORMANCE MEASURES FOR THE CISN EARTHQUAKE EARLY WARNING (EEW) TESTING CENTER (CTC) *Maechling PJ (SCEC / USC), Jordan TH (USC), Liukis M (SCEC), and Callaghan S (USC)*

Researchers with the California Integrated Seismic Network (CISN) recently began a three year USGS funded effort to integrate Earthquake Early Warning (EEW) processing into the CISN real-time earthquake monitoring system. SCEC is collaborating with CISN and USGS on this project by developing tools and techniques needed to perform independent evaluation of EEW system performance.

Independent, and collaborative, testing of scientific forecasts can help to accelerate broader acceptance of such forecasts. As one example, the Collaboratory for the Study of Earthquake Predictability (CSEP) implements independent, and collaborative, testing of short-term earthquake forecasts. The CISN EEW Testing Center (CTC) will implement independent, and collaborative, testing and evaluation of CISN EEW forecasts and CISN EEW system performance.

An important benefit of independent forecast testing as implemented by the CTC is to reduce controversy around stated forecast results. Retrospective testing, that is forecasting a past event from historical data, is commonly used during forecast development. However, the broader scientific community may not accept retrospective forecast results due to the possibility that the

Poster Abstracts | Group 1 – GMP, SHRA

forecasts were biased because the actual values were known when the forecast was made. The CTC's use of prospective testing for CISON EEW forecasts builds confidence in the CTC EEW performance results.

The CTC will be designed to assess both the seismological accuracy and the system performance of CISON EEW. CISON EEW algorithms can forecast seismological information such as final magnitude and peak ground motions for an event and the CTC will compare the accuracy of these forecasts against the final observational results for the event. The CTC will also evaluate the CISON EEW system performance and reliability by collecting and summarizing speed of performance, false alarm rate, and missed event rate during CISON EEW system operations. Performance measurements recorded by the current CISON EEW testing system will be used to describe the performance metrics that will be gathered by the CTC during upcoming CISON EEW developments.

Earthquake Forecasting and Predictability (EFP)

1-060

THE GLOBAL EARTHQUAKE MODEL: PHASE I *Monelli D (ETH Zurich), Wiemer S (ETH), Pagani M, Crowley H, Giardini D (Institute of Geophysics), and Team G*

The Global Earthquake Model (GEM, www.globalquakemodel.org) is a public-private partnership initiated by the OECD to build an independent standard for modeling, monitoring, and communicating earthquake risk worldwide. GEM will provide authoritative, open information about seismic risk and decision tools to support mitigating actions. GEM will raise risk awareness and help post-disaster economic development, with the ultimate goal of reducing the toll of future earthquakes. One of GEM's central initiatives is to develop software and online tools as required to achieve its overall goals. As the first step in the development of GEM, a team of scientists is building a prototype for GEM software and models, with the working name of "GEM1." The GEM1 effort is carried out by five core institutions: ETHZ, EUCENTRE, GFZ, NORSAR and the USGS in Golden. In addition, GEM1 will be issuing a number of subcontracts to data and software providers. More information on GEM1 can be found on the GEM1 wiki (<http://gemwiki.ethz.ch/wiki>). In this presentation we will highlight the current status and future plans for GEM1.

1-061

LESSONS FROM CSEP APPLIED TOWARDS A GLOBAL EARTHQUAKE MODEL *Holliday JR (UCD), and Rundle JB (UCD)*

Repeating the CSEP calculations and performing additional tests, we analyzed the forecasts submitted to the RELM experiment to determine which assumptions could best forecast locations of actual, future seismicity. In this poster we itemize our findings and discuss a path forward for creating a global earthquake forecast.

1-062

CSEP-EU: THE EUROPEAN NODE OF THE COLLABORATORY FOR THE STUDY OF EARTHQUAKE PREDICTABILITY *Euchner F (ETH Zurich), Marzocchi W (INGV), Schorlemmer D (USC), Liukis M (SCEC), Yu J (USC), Christophersen A, Werner M (ETH Zurich), Zechar J (Columbia), Wiemer S (ETH Zurich), Woessner J (Caltech), Maechling P (USC), and Jordan TH (USC)*

The objective of the Collaboratory for the Study of Earthquake Predictability (CSEP, www.cseptesting.org) is to provide a controlled environment in which earthquake forecasting experiments can be conducted. CSEP established rigorous procedures for registering and evaluating experiments, as well as community standards for comparative testing of predictions. Forecasting experiments are run on a well-defined computing infrastructure (testing center), based on the computer codes that are the central component of CSEP.

We report on the implementation of a testing center at ETH Zurich/Switzerland, which will host forecasting experiments for testing regions in Europe. The first region that has been implemented is Italy, since it is one of the most seismically active regions in Europe and is well instrumented by the network of the Istituto Nazionale di Geofisica e Vulcanologia (INGV) to ensure high data quality. For that region, eighteen long-term forecast models have been submitted. Forecasts start on 1 August 2009 and cover 5-year and 10-year periods, respectively. Furthermore, three models providing three-month forecasts and five models providing daily forecasts have been submitted. Model evaluations are based on the official Seismic Bulletin published by INGV. As a requirement, the computer codes of the three-month and one-day models have been installed in

the testing center. They are periodically invoked in order to update the forecasts without manual interaction. The testing center provides full reproducibility of the experiments, because forecast creation and evaluation can be rerun automatically at any later time. Thus, not only prospective, but also retrospective testing can be performed in the testing center.

1-063

RETROSPECTIVE TESTING OF THE LONG-TERM EARTHQUAKE FORECASTS SUBMITTED TO THE ITALIAN CSEP PREDICTABILITY EXPERIMENT *Werner MJ (UCLA), Zechar JD (Columbia), Marzocchi W (INGV), and Wiemer S (ETH)*

The international Collaboratory for the Study of Earthquake Predictability (CSEP, www.cseptesting.org) recently initiated a new prospective earthquake forecasting experiment in Italy. Eighteen different earthquake forecasts were submitted by a variety of researchers to the CSEP-EU Testing Center at ETH Zurich. As a sanity check of the submitted forecasts and to ensure that forecasts were correctly registered by the testing center, we performed a simple analysis and a retrospective test of the forecasts on past seismicity in the testing region. As a result of this feedback, 6 forecasts were modified before the final deadline for submission. Prospective testing of the five-year and ten-year forecasts started on 1 August 2009. Here, we present the results from retrospective tests of the 18 final long-term forecasts on the Italian CSI and the CPTI earthquake catalogs. We use the evaluation method proposed by the Working Group on Regional Earthquake Likelihood Models (RELM), as well as modified and improved versions thereof, and alarm-based tests. We discuss the fluctuations in the models' performances with varying target periods and catalogs. Retrospective tests allow us to gain an understanding of the models and their differences, of the performance metrics and their shortcomings, of the potential observations, and of the robustness of potential outcomes of the prospective experiment.

1-064

RETROSPECTIVE TESTING IN THE NEW ZEALAND EARTHQUAKE FORECAST TESTING CENTER *Gerstenberger MC (GNS Science), and Rhoades DA (GNS Science)*

We have retrospectively tested thirteen earthquake forecast models within the New Zealand Earthquake Forecast Testing Centre (NZTC). Separating the models into four model classes (one-day, three-month, six-month, and five-year) we have evaluated the performance of the models using three likelihood-based tests from CSEP. In the L-Test and the R-Test the forecasts are evaluated using 0.1 degree cells and all classes are tested against observed data of magnitudes 5.0 to 9.0 except the one-day class which includes magnitudes as small as 4.0.

The tests of the one-day models were hampered by an error in the CSEP testing procedure that was discovered during the testing, and the results were inconclusive. In this class the we tested STEP (Gerstenberger, et al, 2005), ETAS (Rhoades, et al, 2008), Abundance (Christophersen, 2005) and a New STEP model (Christophersen and Gerstenberger, in prep). Five models, EEPAS-0F, EEPAS-0R, EEPAS-1F, EEPAS-1R and PPE (Rhoades and Evison, 2004) were tested in the three-month category using data from 1996 to 2007, and all but EEPAS-1R were shown to be consistent with the data. In a relative comparison test of the five models, the EEPAS-0F model was shown to provide a statistically significant improvement over the other four models. Only one model, M8 (Harte, et al, 2007) was tested in the six-month category and it was shown to be inconsistent with the earthquake data between 1996 to 2007. The five-year models were tested using observed earthquake data from 1984 to 2009 and all three models, a uniform Poisson model, a smoothed seismicity model (Rhoades and Evison, 2004), and the National Seismic Hazard Model (Stirling, et al, 2002), were shown to be consistent with the data. In a comparison test the smoothed seismicity model was able to significantly reject the other two models.

Additionally we report the results of the development of two alternative testing routines for the NZTC. First, we have developed alternatives to the L and N-Tests in CSEP that remove unnecessary calculations and speed up the computational time significantly. Secondly we have developed a protocol for testing long-term forecasts (100 years or more) based on historical Modified Mercalli Intensity information and recorded ground-shaking amplitude data.

1-065

TOWARD CONSTRUCTING EARTHQUAKE FORECAST SYSTEMS FOR JAPAN
Nanjo KZ (Tokyo), Tsuruoka H (Tokyo), Hirata N (Tokyo), Schorlemmer D (USC), and Euchner F (ETH Zurich)

Past Japanese research projects aiming at the realization of scientific earthquake prediction have focused on better understanding of the mechanism of earthquake occurrence and the development of forecast simulation technologies based on physical modeling of earthquakes. One part of the newly-introduced main activities under the current Japanese "Observation and Research Program for Prediction of Earthquakes and Volcanic Eruptions (2009-2013)" is to construct forecast systems of earthquake occurrence for Japan. This activity aims to quantitatively forecast time, place, and magnitude of future earthquakes in and around Japan. Our approach is based on the following three steps: (1) developing the Testing Center, a framework that quantifies the performance of registered earthquake forecast methods; (2) conducting comparative testing experiments within this framework to determine the registered forecast model's accuracy; and (3) aiming at the creation and buildup of sophisticated forecast models, based on results obtained from multiple experiments. To smoothly start this new research program, the Earthquake Research Institute (ERI) joined the global "Collaboratory for the Study of Earthquake Predictability" (CSEP). ERI implemented the Japanese Testing Center and started on 1 September 2008 a prototype experiment for evaluating a set of three one-year forecast models. We will formally start conducting the comparative forecast research in 1 November 2009. Here, we first present our recent progress which consists of two elements: quality characterization of the earthquake catalog data from the Japan Meteorological Agency (JMA) and first results of the prototype experiment. We next present the "rules of the game" of the forthcoming experiments to invite earthquake forecast models. Our testing experiment is becoming a good baseline for model development in order to move toward constructing earthquake forecast systems for Japan.

1-066

THE SCEC COLLABORATORY FOR THE STUDY OF EARTHQUAKE PREDICTABILITY (CSEP) TESTING CENTER
Liukis M (SCEC), Schorlemmer D (USC), Yu J (USC), Maechling PJ (SCEC / USC), Zechar JD (Columbia), Jordan TH (USC), Euchner F (ETH Zurich), and the CSEP Working Group

SCEC began development of the Collaboratory for the Study of Earthquake Predictability (CSEP) in January of 2006 with funding provided by the W. M. Keck Foundation. Since that time, a large group of scientists and software engineers have translated the scientific and computational concepts of CSEP into several operational testing centers. The initial implementation of the W. M. Keck Foundation Testing Center at SCEC for the California natural laboratory became operational on September 1, 2007 and has since been further improved, optimized, and extended over the past two years. The design and implementation of the SCEC Testing Center have been guided by four design goals that were originally identified as objectives for the RELM testing center which are: (1) Controlled Environment, (2) Transparency, (3) Comparability, and (4) Reproducibility. By meeting these goals, the CSEP Testing Center can provide clear descriptions of how all registered earthquake forecasts are produced and how each of the forecasts are evaluated. As of September 2009, there are four testing centers established around the globe. The SCEC Testing Center hosts

alarm-based and rate-based forecasts models for California, Western Pacific and global testing regions. The forecasts under evaluation are mostly seismicity-based forecasts models. We describe how the currently operational CSEP Testing Center at SCEC has been constructed to meet the design goals; we also present new capabilities and development of the Testing Center, and we share our experiences operating the center since its inception.

1-067

RESULTS FROM EARTHQUAKE FORECAST TESTING IN THE COLLABORATORY FOR THE STUDY OF EARTHQUAKE PREDICTABILITY *Schorlemmer D (USC), Zechar JD (Columbia), Gerstenberger MC (GNS Science), Hirata N (Tokyo), Jordan TH (USC), and the CSEP Working Group*

The Collaboratory for the Study of Earthquake Predictability (CSEP) aims to improve our understanding about the physics and predictability of earthquakes through rigorous and prospective testing of earthquake forecast models. The system-science character of earthquake prediction research demands an open and collaborative structure for experimentation in a variety of fault systems and tectonic regions. Several CSEP Testing Centers are being developed to provide adequate infrastructure for predictability research. The first began operations at the Southern California Earthquake Center on 1 September 2007, and we are currently running prospective, automated evaluations of more than 40 models for California, the western Pacific region, and globally. During the last year, CSEP Testing Centers in New Zealand and Japan started operations and participation in CSEP, complemented this year by a center in Europe. In this presentation, we provide an overview of the testing metrics employed and share and discuss initial results from all testing regions.

1-068

QUAKEML: A COMMUNITY-CREATED SEISMOLOGICAL DATA EXCHANGE STANDARD *Euchner F (ETH Zurich), Schorlemmer D (USC), Kästli P (ETH Zürich), and Working Group Q*

QuakeML is an XML-based exchange format for seismological data. Version 1.1 has been released as a Proposed Recommendation in 2008. An updated version 1.2 is under revision by the Working Group and is available as a release candidate. The current release is based on contributions from a global community which have been collected in a public Request for Comments process. Contributions have been made from ETH, GFZ, USC, SCEC, USGS, IRIS DMC, EMSC, ORFEUS, GNS, ZAMG, BRGM, Nanometrics, and ISTI. The current release of QuakeML covers a basic description of seismic events including picks, arrivals, amplitudes, magnitudes, origins, focal mechanisms, and moment tensors. Future QuakeML development will include an extension for macroseismic information. Furthermore, development on seismic inventory information, resource identifiers, and resource metadata is under way. QuakePy is a Python-based seismicity analysis toolkit which is based on the QuakeML data model. It is used in the Collaboratory for the Study of Earthquake Predictability (CSEP) testing center software developed by SCEC. QuakeML finds acceptance as a distribution format for earthquake catalog data at an increasing number of institutions around the globe. At SCEC, efforts to establish an earthquake catalog web service providing QuakeML are under way. Prototype web services are available from GNS Science, New Zealand, and the European-Mediterranean Seismological Centre (EMSC).

Online resources: <http://www.quakeml.org>, <http://www.quakepy.org>.

1-069

PRELIMINARY RESULTS FROM THE FIRST 3.5 YEARS OF THE REGIONAL EARTHQUAKE LIKELIHOOD MODELS EXPERIMENT *Zechar JD (Columbia), Schorlemmer D (USC), Werner MJ (UCLA), and Jordan TH (USC)*

One of the primary objectives of the Regional Earthquake Likelihood Models (RELM) working group was to formalize earthquake occurrence hypotheses in the form of prospective earthquake rate forecasts in California. RELM scientists developed more than a dozen 5-year forecasts; they also outlined a performance evaluation method and provided a conceptual description of a Testing Center in which to perform predictability experiments. Subsequently, researchers working within the Collaboratory for the Study of Earthquake Predictability (CSEP) have begun implementing Testing Centers in different locations worldwide, and the RELM predictability experiment—a truly prospective earthquake prediction effort—is underway within the U.S. branch of CSEP. The experiment, designed to compare time-invariant 5-year earthquake rate forecasts, is now approximately seventy percent complete. Here, we present the forecasts under evaluation and the preliminary results of this unique experiment. We discuss the sample of observed target earthquakes in the context of historical seismicity within the testing region, highlight potential pitfalls of the current tests, and present plans for future revisions to experiments such as this one.

1-070

LIKELIHOOD-BASED TESTS FOR EVALUATING SPACE-RATE-MAGNITUDE EARTHQUAKE FORECASTS *Zechar JD (Columbia), Gerstenberger MC (GNS Science), and Rhoades DA (GNS Science)*

The five-year experiment of the Regional Earthquake Likelihood Models (RELM) working group was designed to compare several forecasts of earthquake rates in latitude-longitude-magnitude bins in and around California. This forecast format is being used as a blueprint for many other earthquake predictability experiments around the world, and therefore it is important to consider how to evaluate the performance of such forecasts. Currently, two tests are used to measure the likelihood of the observed distribution of target earthquakes given each forecast; one test compares the binned space-rate-magnitude observation and forecast, and the other compares only the rate forecast and the number of observed target earthquakes. In this paper, we point out a subtle flaw in the current test of the rate forecast, and we propose new tests that isolate the spatial and magnitude components of a space-rate-magnitude forecast. As an illustration, we consider the target earthquake distribution observed during the first half of the ongoing RELM experiment. We find that a space-rate-magnitude forecast may appear to be consistent with the distribution of target earthquakes despite the spatial forecast being inconsistent with the spatial distribution of target earthquakes, and we argue that these new tests should be used to provide increased detail in earthquake forecast evaluation.

1-071

A SUITE OF REFERENCE MODELS FOR THE EVALUATION OF EARTHQUAKE FORECASTS *Goebel T (USC), Schorlemmer D (USC), Becker TW (USC), Gerstenberger MC (GNS Science), and Zechar JD (Columbia)*

Results from the collaborative efforts of both the Regional Earthquake Likelihood Model (RELM) group and the Collaboratory for the Study of Earthquake Predictability (CSEP) have made the difficult task of validating earthquake forecasting models less intimidating.

Available now is a streamlined, community-accepted and relatively user-friendly computational environment that allows efficient testing of multiple forecasting models; this structure paves the

way for testing of basic hypotheses that have, in the past, been advanced in the earthquake hazard and forecasting community.

We are developing a suite of models starting at a basic, fundamental level with subsequently adding more complexity. We are starting with simple smoothed seismicity models with varying smoothing kernels, e. g., 5-50 km Gaussian or inverse-biquadratic.

The next steps include the testing of declustering algorithms for particular catalogs, uniform and spatial varying b-values and adaptive smoothing kernels. Each step is documented and optimized in regard of its forecast potential of historic events. These models will serve as possible null hypotheses in the CSEP Testing Center software. They will be fully implemented in the CSEP software distribution and development will be done with the target of testing the models in the CSEP global testing center; however development will proceed with the intent of potentially testing the models at the various CSEP regional testing centers such as California, New Zealand, Europe, and Japan.

1-072

TESTING EARTHQUAKE FORECASTS USING RELIABILITY DIAGRAMS *Holliday JR (UCD), Gaggioli WJ (UC Davis), and Knox LE (UC Davis)*

Empirically-derived earthquake forecasting methods are difficult to test. There are many different types of forecasts, and each type requires its own methods of testing and verification. Similarly, for a given forecast there are many different types of tests which can be performed, and the forecast may perform differently on different tests. Care must be taken to choose an appropriate test and to interpret the results correctly. In this poster we introduce reliability diagrams, a standard forecast evaluation tool, as a useful tool for earthquake forecast testing. As a case study, we present results from our extensive efforts to test a modified version of the Holliday et al. (2006) temporal earthquake forecasting method.

1-073

A LONG-TERM FORECAST OF SHALLOW SEISMICITY BASED ON THE GLOBAL STRAIN RATE MAP *Bird P (UCLA), Kreemer C (UNR), and Holt WE (SUNY-Stony Brook)*

The Global Strain Rate Map (GSRM) of Kreemer et al. (2003) was project II-8 of the International Lithosphere Program; it describes the spatial variations of horizontal strain rate tensor components, rotation rates, and velocities for the whole Earth. The model consists of 25 rigid spherical plates and ~25,000 0.6 x 0.5-degree deformable grid areas within the diffuse plate boundary zones.

We convert GSRM to a forecast of long-term shallow seismicity by applying the hypotheses and equations of Bird and Liu (2007), known as the Seismic Hazard Inferred From Tectonics (SHIFT) hypotheses: (1) The long-term seismic moment rate of any tectonic fault, or any large volume of permanently-deforming lithosphere, is approximately that computed using the coupled seismogenic thickness of the most comparable type of plate boundary; and (2) The long-term rate of earthquakes generated along any tectonic fault, or within any large volume of permanently-deforming lithosphere, is approximately that computed from its moment rate by using the frequency/magnitude distribution of the most comparable type of plate boundary.

We faced 4 difficulties: First, the GSRM strain-rates are largely elastic and thus have smoother map patterns than long-term permanent strain-rates. However, on the scale of global maps and forecasts this is relatively insignificant. Second, GSRM treats plate interiors as rigid. Our solution

is to forecast a uniform low seismicity rate in all plate interiors, based on their collective frequency/magnitude distribution. Third, the basic SHIFT hypotheses do not specify how to decide which is the “most comparable type of plate boundary” at each grid point. We use the global map of deformation regimes by Kreemer et al. (2002), and in some cases also use the tectonic style of the local strain-rate tensor. Finally, we found that our uncorrected forecast was underpredicting global shallow seismicity (by a factor of 2) and that this was primarily due to underpredictions of subduction seismicity (by a factor >3). We identified three sources of underprediction in subduction zones; compounding these corrections requires scaling-up the forecast seismicities of all subduction zones by about a factor of 3. We also apply smaller empirical correction factors to each of the other three deformation regimes. This yields an adjusted forecast that is reasonably consistent with the map-pattern and frequency/magnitude graph of the 32-year-old Global Centroid Moment Tensor catalog.

1-074

SYNTHETIC SEISMICITY AND THE PRECURSORY SCALE INCREASE PHENOMENON *Rhoades DA (GNS Science), Robinson R (IGNS), and Gerstenberger MC (GNS Science)*

The Every Earthquake a Precursor According to Scale (EEPAS) model has performed well as a long-range forecasting model for the larger earthquakes in a number of real seismicity catalogues. It is based on the precursory scale increase phenomenon and associated predictive scaling relations, the detailed physical basis of which is not well understood. Synthetic earthquake catalogues generated from stress interactions on a fault network have been analysed using the EEPAS model, to better understand the physical process responsible for the precursory scale increase phenomenon. In a generic fault network with a small number of parallel faults, the performance of the EEPAS model is poor. But in a more elaborate network involving major faults at a variety of orientations and a large number of small randomly oriented faults, the performance of the EEPAS model is similar to that in real catalogues, such as that of California, albeit with some differences in the scaling parameters for precursor time and area. The richness and variety of fault orientations therefore appear to be responsible for conformity to the EEPAS model. Tracking the stress evolution on individual cells in the synthetic seismicity model gives insights into the origin of the precursory scale increase phenomenon.

1-075

ASSESSING PREMONITORY POWER OF VARIATIONS IN THE EARTHQUAKE MAGNITUDE DISTRIBUTION *Olsen S (UNR), and Zaliapin I (UNR)*

The premonitory changes of the magnitude distribution have been described in many observational and synthetic seismic studies; moreover, a similar phenomenon has been observed in the systems of statistical physics and in fracturing of steel samples. However, the intrinsic data quality problems in statistical analysis of seismic data have so far prevented this phenomenon from being rigorously confirmed and employed for earthquake forecasting. We propose to overcome the existing difficulties in testing the premonitory changes in the magnitude distribution by (i) Developing a robust Bayesian filtering scheme for estimating the relevant magnitude distribution parameters, (ii) Considering several alternative parameterizations of a potential premonitory phenomenon, and (iii) Developing novel spatio-temporal statistical methods for assessing the power of premonitory signals. Here we show the first results using the seismicity of California.

Seismology

1-076

CORRELATIONS BETWEEN SEISMIC CLUSTERING AND PROPERTIES OF THE CRUST *Zaliapin I (UNR), and Ben-Zion Y (USC)*

We attempt to establish correlations between spatio-temporal patterns of seismicity and geophysical properties of the crust. In particular, we examine the relations between properties of foreshock-mainshock-aftershock sequences and heat flow data, and the relations between asymmetric dynamic triggering pattern along faults and velocity structure images. We use the regional southern CA catalog of Lin et al. (2007) and the catalogs of Power and Jordan (2009) for various specific fault-zones in CA. The analyses are based on the earthquake clustering technique of Zaliapin et al. (2008) that employs the Baiesi-Paczuski distance between earthquakes and allows one to distinguish between the clustered (foreshocks-aftershock) and homogeneous (mainshocks) parts of an earthquake catalog. The initial results indicate the presence of asymmetric triggering in early-time aftershocks along the creeping section of the San Andreas fault, as well as spatial correlations between aftershock productivity and heat flow. Updated results will be presented in the meeting.

1-077

PROBABILISTIC SEISMIC NETWORK COMPLETENESS STUDIES AROUND THE WORLD *Schorlemmer D (USC)*

An important characteristic of any seismic network is its detection completeness, which should be considered a function of space and time. Many researchers rely on robust estimates of detection completeness, especially when investigating statistical parameters of earthquake occurrence.

We present the Probability-based Magnitude of Completeness (PMC) method for computing the spatial variation and temporal evolution of detection capability of seismic networks based on empirical data only: phase data, station information, and the network specific attenuation relation.

We present studies of regional networks from California, Switzerland, Italy, Japan, and compare the result with estimated completeness levels of other methods. We report on the time evolution of monitoring completeness in these regions and show the depth dependence of detection probabilities. Scenario computations show the impact of different possible network failures and offer estimates of possible network optimization strategies. All presented results are published on the CompletenessWeb (www.completenessweb.org) from which the user can download completeness data from all investigated regions, software codes for reproducing the results, and publication-ready and customizable figures.

1-078

EARTHQUAKE SIZE DISTRIBUTION: POWER-LAW WITH EXPONENT $\beta = 1/2$ *Kagan YY (UCLA)*

We propose that the widely observed and universal Gutenberg-Richter relation is a mathematical consequence of the critical branching nature of earthquake process in a brittle fracture environment. These arguments, though preliminary, are confirmed by recent investigations of the seismic moment distribution in global earthquake catalogs and by the results on the distribution in crystals of dislocation avalanche sizes. We consider possible systematic and random errors in determining earthquake size, especially its seismic moment. These effects increase the estimate of the parameter β of the power-law distribution of earthquake sizes. In particular we find that the decrease in relative moment uncertainties with earthquake size causes inflation in the β -

value by about 1-3%. Moreover, earthquake clustering greatly influences the beta-parameter. If clusters (aftershock sequences) are taken as the entity to be studied, then the exponent value for their size distribution would decrease by 5-10%. The complexity of any earthquake source also inflates the estimated beta-value by at least 3-7%. Taking all these effects into account, we propose that the recently obtained beta-value of 0.63 could be reduced to about 0.52-0.56: near the universal constant value (1/2) predicted by theoretical arguments. We also consider possible consequences of the universal beta-value and its relevance for theoretical and practical understanding of earthquake occurrence in various tectonic and Earth structure environments. Using comparative crystal deformation results may help us understand the generation of seismic tremors and slow earthquakes.

1-079

QUANTIFICATION OF THE LOSS IN DETECTION CAPABILITIES AT THE FRINGES OF SEISMIC NETWORKS *Lewis MA (USC), Schorlemmer D (USC), and Euchner F (ETH Zurich)*

We calculate detection probabilities for any given magnitude and completeness magnitudes for selected probability levels for the Southern California Seismic Network (SCSN) between 1967 and 2008 using the Probability-based Magnitude of Completeness (PMC) method. We then separate the network into selected regions to test the impact on the completeness, particularly near the boundary of the regions, that occurs from calculating the completeness magnitude from a subset of stations. This is to simulate the loss effects on event detection and completeness magnitudes of having two adjoining networks. Many areas of research rely on correct estimates of detection completeness, particularly those involving statistical parameters of earthquake occurrence.

We divide the SCSN in half and treating each subset the same as the whole, calculating which events would have been detected based on 4 stations needing to be triggered. Detection probabilities are calculated using the events and stations in each of the subsets of the SCSN. Near the boundary between the two regions, the completeness magnitude is reduced. However the distance probability plots for each station are different in the entire data set compared to the subsets. In the subsets of the data the distance from a station to which events are detected with a low probability level (0.1) is further for lower magnitude events (3 and below) and shorter for higher magnitude events. At a higher probability (0.9) of detecting events the changes are on average smaller with a slight increase in the distance to which magnitude 4-5 events are detected. This could be an effect of removing smaller events not detected at some stations in the subsets thus increasing the detection probability while the latter may be a result of making the area covered by the stations smaller thus reducing the distance out to which large events are detected.

1-080

THE EFFECT OF EARTHQUAKE STATISTICS OF CENSORED TIME, SPACE AND MAGNITUDE *Wang Q (CSB), and Jackson DD (UCLA)*

The Epidemic-type Aftershock Sequence (ETAS) model is widely used in seismic studies. The observations used for estimating the ETAS parameters will always be limited in space, time, and magnitude, yet unobserved earthquakes affect the probabilities of events in the observable region. Simulations based on the ETAS model are used in this study to explore how significantly the effect caused by censoring of time, space and magnitude in earthquake statistics. Log-likelihood values of the ETAS model contributed by each pair of earthquakes are studied. The effect of the censoring window will affect the pair statistics to which the ETAS model will be fit, so the effects of this window must be incorporated in parameter estimation. A larger time, space and

magnitude window could be helpful to get better estimates of the parameters in the ETAS model. The size of the larger window is discussed in this study.

1-081

BAYESIAN EARTHQUAKE SOURCE MODELING *Minson SE (Caltech), Simons M (Caltech), Beck JL (Caltech), Owen SE (USC / JPL), and Genrich JF (UCSD)*

Traditional optimization techniques are designed to produce a single model which fits data well under a very specific set of conditions, e.g., the classic least-squares solution with Gaussian noise on the data and Gaussian expectations on parameter values. However, most geophysical problems are under-determined and their solutions are not well characterized by a single model. Instead, the ensemble of all possible models, or all acceptable models, expressed as a Bayesian a posteriori probability density function (PDF), can be sampled using numerical methods. The entire ensemble can then be analyzed to determine which model features are well characterized. Since only the forward model is evaluated during the Bayesian sampling process, these techniques can solve nonlinear problems as efficiently as they can solve linear problems. This approach has the advantage that all a priori information about the geophysical process being modeled can be used to inform the a posteriori PDF. However, the usefulness of Bayesian techniques is limited by the "curse of dimensionality", and are only computationally tractable in low-dimensional spaces, i.e., they are only usable for problems with a small number of unknown parameters. The tempered Markov chain Monte Carlo (tempered MCMC or TMCMC) method uses principles derived from genetic algorithms, the Metropolis algorithm for MCMC simulation, and simulated annealing to increase the efficiency of sampling in higher dimensions. The TMCMC algorithm has previously been successfully applied to sample solution spaces of as many as 30 parameters, which is currently a large number of parameters to be sampled using Bayesian techniques but is still far smaller than the number of free parameters in a finite-fault kinematic earthquake source inversion. Here, we present new computational techniques for Bayesian sampling in high-dimensional spaces. We have modified the TMCMC method both by parallelizing the algorithm and increasing its efficiency in high-dimensional spaces. These improvements allow us to efficiently sample parameters spaces with many hundreds of dimensions, sufficient to generate kinematic earthquake source models. We present performance tests of our new technique using synthetic data and apply our new methodology to the 2007 Tocopilla, Chile earthquake.

1-082

WHAT DO WE LEARN FROM THE EXERCISE OF THE SOURCE INVERSION VALIDATION BLIND TEST I? *Shao G (UCSB), Ji C (UCSB), and Lavallee D (UCSB)*

We participated in the Blind Test I exercise of the Source Inversion Validation project (<http://www.seismo.ethz.ch/staff/martin/BlindTest.html>), in which researchers are asked to invert the rupture process of a pseudo source using noise-free synthetic seismic waveforms at an ideally distributed near-fault strong motion network. Previously, nine groups had participated in this exercise, but "4 out of 9 inversion results are, statistically speaking, not better than a random model with somehow correlated slip!" (Mai et al., 2007). Since the earth structure and fault plane geometry were given in the test, the discrepancies between the inverted models and the target may reflect the errors in source representations or the intrinsic non-uniqueness of the finite fault inverse methods. Here we attempt to verify this counterintuitive result, investigate the causes, and explore the potential ways to improve the inversion.

We have used as many as 41 crustal layers to precisely approximate the given continuous velocity model in calculating reflectivity synthetics (<2 Hz). . The slip pattern of our preliminary inversion

result looks similar to the target, but its slip and total seismic moment are roughly a factor of two larger. The later analysis reveals that the amplitudes of waveform data posted online are twice of what they should be, likely caused by a mistake in applying the target model. Furthermore, the velocity data had been contaminated by constant offsets, which have been corrected as well in our computation. Our forward calculations, based on the target model, are matching the corrected synthetic data with a 99.91% average variance reduction. We divide the fault plane into 1 km by 1 km subfaults. We invert the slip and the shape of the asymmetric cosine slip rate function simultaneously (Ji et al., 2003) by matching the broadband velocity waveforms (<2 Hz) at all 33 stations. Our inversion results indicate: 1) the target model could be well retrieved by matching the broadband seismic data 2) By just matching the bandpass filtered strong motion waveforms from 0.1 Hz to 1 Hz, as typically applied in the previous studies, however, cannot guarantee that the inverted model closely reproduce the target model. 3) The fault-plane spatial resolution and ground-motion temporal resolution are correlated. Using a larger subfault reduces not only the spatial resolution but also the reliability of the high frequency temporal variation.

1-083

ON THE QUANTIFICATION OF ROBUSTNESS WHEN COMPARING KINEMATIC INVERSION MODELS: NEW TOOLS FOR THE SOURCE INVERSION VALIDATION PROJECT *Lavallee D (UCSB), Shao G (UCSB), and Ji C (UCSB)*

With the goals of improving the reliability and consistency of source parameter computations, a group of researchers created the Source Inversion Validation (SIV) project. Recently a blind test exercise was held where researchers were invited to compute a slip model from ground motions generated from a synthetic model. Statistical tools are thus needed for the inter-comparison of the computed slip models as well as for the comparison of the computed slip models to the original synthetic model. In this presentation, we adapted tools used in signal processing to capture and quantify the quality of the fit when comparing different slip spatial distributions.

The tools are the 2D spatial cross spectrum and the 2D coherence function (a generalization of the coherence function used in signal processing). The two methods are complementary in their scopes and thus needed to best quantify and understand the "difference" (or misfits) between two slip models. The cross spectrum provides information that is "global" that is, across the range of wavenumbers- as it compares and weights the relative contribution of two slip models at different wavenumbers (or wavelengths or scale lengths). On the other hand, the 2D coherence function is designed to estimate the linear dependence between the two models. The linear dependence is estimated at every wavenumber. It thus provides information that is "local in nature" that is specific to a given wavelength- when compared to the 2D spatial cross spectrum. When applied to two slip models, the 2D coherence function allows one to measure the degree of linearity between two slips models at different wavelengths. To take into account that the quality of the match between two slip models may depend on the areas considered, the 2D spatial cross spectrum and the 2D coherence function are computed over a moving window. We compute the 2D spatial cross spectrum and the 2D coherence function for different pairs of slip models taken from a bank of slip models computed by Shao et al. 2009 (see abstract in this volume). We also compute the 2D spatial cross spectrum and the 2D coherence function for slip models selected from the same bank and the original slip model used in the blind test exercise discussed above. We interpret and discuss the consequences of the estimated spatial cross spectrum and of the 2D coherence in assessing the quality of fitness between different slip models.

1-084

FINITE FAULT STUDIES OF INTERMEDIATE EARTHQUAKES IN SOUTHERN CALIFORNIA *Ji C (UCSB), and Shao G (UCSB)*

We have developed a quick finite fault inversion system to study the rupture process of intermediate earthquakes using the body waves recorded by local strong motion stations. Here we present the results of three recent earthquakes, 2008 Mw 5.4 Chino Hill earthquake and its largest aftershock, 2009 Mw 4.7 Ingerwood earthquake. The inferred static and dynamic stress drops will be addressed.

1-085

ESTIMATION OF EARTHQUAKE SPECTRUM CORNER FREQUENCY USING A NEW 'SQUARE-DECONVOLUTION' TECHNIQUE *Hillers G (UCSB), and Prieto GA (Stanford)*

The analysis of earthquake source spectra permits estimates of fundamental physical source properties. To obtain the true source spectrum, influences of path and receiver have to be removed from the recorded signal. This is typically done by spectral deconvolution for one large event, where the signal is deconvolved with the signal of a small nearby earthquake. Alternatively, when analyzing events over a range of sizes, the raw spectra are stacked as a function of size, and the smallest bin is used as an average EGF for the entire earthquake population. Once the true source spectrum is obtained, the source parameters have to be determined by fitting the measurement to a spectral source model. This requires the fitting to an at least three-parameter model including relative seismic moment, corner frequency (f_c), and the high frequency fall-off rate. We introduce a new technique by which we can determine the spectral corner frequency of an event of size M_c (e.g., M_2)---or a stack of collocated events with size similar to M_c ---without the need of a fitting procedure. It requires, however, recordings of events that ruptured the same fault---or stacks thereof---with smaller and larger magnitudes, M_- and M_+ , respectively. The magnitude difference $\Delta M = |M_c - M_{\pm}|$ (e.g., $\Delta M=0.5$) is ideally symmetric, but we can evaluate the degree of over- or under estimation in the asymmetric case. We show that the minimum of our analysis function, $\Lambda(f)$, coincides with the corner frequency of the M_c event. The method is independent of fitting the source spectra to a spectral model; the only implicit assumption is the self-similarity of ruptures for the range M_- to M_+ . To demonstrate the capability of our method, we verify the theoretical analysis by analyzing data from locally confined earthquake clusters in Southern California, recorded at 200 Hz sampling borehole stations. The values for f_c that are determined by a single borehole sensor are verified using a number of collocated surface broadband stations, that sample at 100 Hz. This clearly demonstrates the utility of our approach, since we can robustly identify f_c of $M_c=2$ events in the 35 Hz range using data up to only 40 Hz, which would be difficult to obtain by robustly fitting the entire spectrum including the high frequency fall-off rate above 35 Hz. Analyzing spectra of a $M_c=4$ cluster recorded at a 200 Hz station, the analysis function suggests the identification of two corner frequencies at 25 and 45 Hz.

1-086

SCALED SEISMIC ENERGY IN JAPAN AND THE US BY EMPIRICAL GREEN'S FUNCTION ANALYSIS *Baltay AS (Stanford), Prieto GA (Stanford), Ide S (Stanford), and Beroza GC (Stanford)*

We estimate seismic energy and apparent stress to explore the relationship between radiated seismic energy and moment. Some studies indicate that scaled seismic energy, or apparent stress, increases with increasing moment, while others indicate it is constant across many orders of magnitude. The relatively sparse strong motion data set seems to support self-similarity, leading

us to reexamine results that find strong scaling of apparent stress. Our empirical Green's function method uses time-averaged coda spectra, to exploit the stability and averaging effects of the seismic coda. In each region, we choose events that are nearly co-located so that the path term to any station is constant. Small events are used as empirical Green's functions to correct for propagation effects. Results from the western US and Mexico do not show strong evidence for systematic scaling of radiated seismic energy with moment. Recent results from the Kamaishi sequence of repeating events in Honshu, Japan, have a higher apparent stress than the earthquakes in the western United States, and the 2008 Mw 4.7 event has an apparent stress of about 10 MPa. These results agree with other analysis of the same region. Overall, our results support earthquake self-similarity, and are consistent with studies of radiated energy determined from other methods.

1-087

TOWARDS UNDERSTANDING THE ORIGIN OF CODA FROM LOCAL EARTHQUAKES AND EXPLOSIONS *Dominguez Ramirez LA (UCLA), and Davis PM (UCLA)*

We examine waveforms from both local events and explosion in Southern California. The objective of this work is to understand the mechanisms that determine S wave coda and consequently a reliable method to obtain estimates of the trade offs between intrinsic and scattering Q as well as geometric spreading. Our initial hypothesis considers that scattering effects concentrate in the uppermost crust where the impedance contrasts are greatest. Since earthquakes occur at depths >3km but explosions are restricted to a maximum of a few hundreds of meters below the surface, a longer coda is expected for explosions than for earthquakes, because the waves reverberate in two surface scattering layers, one at the source and one at the receiver. We compare coda decay in seismic records from quarry blasts and nearby earthquakes for eight mines along Southern California from 1981 through 2005. In addition, we compute the spectral ratio for SAFOD borehole station and a surface Central California station to examine vertical variation of the Q. In this preliminary work, we attempt to establish the possible relationships to give insight into the factors that generate coda of earthquakes and explosions. To analyze differences, we select seismic stations in a radio of 40 km from the mines and fit the coda decay to our initial model, $\log_{10} y = (mc+a) - q\log_{10}(t - tp)$ where y is the amplitude of the record; mc is the magnitude of the event; and q accounts for geometric spreading and a0 account for site effects parameters that are adjusted at each station. Furthermore, we examine the spectral ratio as a function of depth to detect changes due to the changes in heterogeneities. These preliminary results will be used as a base for comparing models of coda decay.

1-088

A NEW INTERPRETATION ON THE SCATTERING ORIGIN OF SEISMIC CODA *Zeng Y (USGS), and Jing Y*

The study of seismic scattering has been an effective tool to investigate the inhomogeneity of the earth. By assuming the earth as a random scattering medium, Aki (1969), Aki and Chouet (1975), and Sato (1977) have studied the seismic coda waves as single backscattered waves. Since then it is generally believed that seismic coda waves are formed by backscattered waves. In this paper, we will show that the seismic coda waves are not from backscattered waves, instead they are from energy that leak out from the forward scattered waves. First we developed a numerical technique to simulate non-isotropic scattering waves based on the 3-D non-isotropic scattering theory proposed by Sato (1995). This is obtained by improving the numerical instability problem of the hyper-geometrical function computation in the solutions of the non-isotropic scattering equations. By applying the simulation to the 2008 Wells earthquakes, Nevada, we find that the traditional

backscattering theory does not explain the observations. A forward non-isotropic scattering model provides the best fit to the observed high frequency direct and coda wave energy envelopes. The results also successfully explain the broadening effect that is commonly observed in the high frequency direct wave trains. We have evaluated the contribution of single and multiple scattering in early seismic coda and find that the single non-isotropic scattering provides an excellent fit to the observations for stations within 100 km of the source. For source-station distances larger than 100 km, multiple scattering becomes very important.

1-089

SYSTEMATIC ESTIMATION OF CORNER FREQUENCY RATIOS OF P AND S WAVES GENERATED BY AFTERSHOCKS AROUND THE KARADERE-DÜZCE BRANCH OF THE NORTH ANATOLIAN FAULT *Yang W (USC), Ben-Zion Y (USC), and Peng Z (Georgia Tech)*

We propose a method to systematically estimate the corner frequency ratios of P and S waves, and apply the method to obtain corner frequency ratios generated by ~9000 aftershocks of the 1999 İzmit and Düzce earthquakes recorded at 10 seismic stations along the Karadere-Düzce branch of the North Anatolian Fault. The analysis is associated with separation of source, travel-time and station spectra terms and stacking results at several stages to enhance the signal-to-noise ratio. We analyze source spectra of P waves selected from a 1.28-second window around the P arrival, and examine results associated with S wave signals selected using the following 5 choices: (A) A single 1.28-second time window for S wave. (B) A single 10-second time window for S wave. (C1-C3) Stacked S wave spectra in N (N = 15) 1.28 second consecutive S wave windows, where the spectral amplitudes are stacked according to travel-time normalization (C1), amplitude normalization (C2), and without any normalization (C3). The corner frequency ratios and relative strain-drops are obtained by fitting iteratively the separated P and S source spectra of 201 nearest neighboring events in different amplitude bins to the ω^{-2} source spectral model. The mode values of the obtained P/S corner frequency ratios are 1.52, 1.57, 1.89, 1.47 and 1.56 for each of the five schemes, respectively. The obtained mode values for \log_{10} relative strain-drops for all schemes are -4.35. This corresponds to a stress drop of 1.34 MPa assuming a nominal rigidity of 30 GPa. Schemes A and B have larger fitting errors compared with scheme C1-C3. Scheme C1 over-estimates the corner frequency ratio compared with the other four schemes, and the obtained corner frequency ratios given by scheme C3 are less concentrated compared with the other schemes. The variations of the P/S corner frequency ratios obtained for different groups of events may be related to changes in average azimuths between the event locations and stations, variable focal mechanisms spatial changes of fault heterogeneities, and rupture directivity effects. Updated results will be presented in the meeting.

1-090

COMPARING 3D HETEROGENEOUS STRESS/RATE-STATE FRICTION MODELS OF AFTERSHOCK SEQUENCES WITH LANDERS *Smith DE (UCR), and Dieterich JH (UCR)*

We have implemented simulations of seismicity that integrate 3D spatially heterogeneous stress on geometrically complex faults with rate-state seismicity equations to simulate different parts of the seismic cycle, especially aftershock sequences. The model generates both temporal and spatial characteristic of real aftershocks, including scattered aftershocks in traditional Coulomb “stress shadow” zones, and it produces a focal mechanism orientation for each simulated event. Significantly, rotations of failure orientations in the aftershocks sequences are biased by the stress perturbation of the mainshock – this bias can lead to under-estimates of crustal stress based on stress rotations. We have begun modeling of specific seismic events and their associated

aftershock sequences, such as Landers earthquakes. In this modeling, we also incorporate effects of off-fault stress relaxation. Some key observables we are investigating include: 1) the percentage of events in Coulomb stress increase vs. decrease area, 2) stress heterogeneity based on seismicity statistics, 3) seismic moment partitioning between off-fault seismicity vs. on-fault moment, and 4) spatial and temporal rotation of focal mechanisms. Comparisons of observed and simulated focal mechanism data will be used to evaluate biasing effects in the focal mechanism rotations, which will permit estimates of average crustal stress with an associated uncertainty.

1-091

REMOTELY TRIGGERED SEISMICITY IN CONTINENTAL CHINA BY THE 2008 MW7.9 WENCHUAN EARTHQUAKE *Jiang T (Georgia Tech), Peng Z (Georgia Tech), Wang W (City of Pasadena), and Chen Q (State Seismological Bureau)*

We perform a systematic search of remotely triggered seismicity in Continental China following the 2008 Mw7.9 Wenchuan earthquake. We visually identify earthquakes as impulsive seismic energies with clear P and S arrivals on 5 Hz high-pass-filtered three-component velocity seismograms 1 hour before and after the Wenchuan earthquake. Out of the 280 stations in the updated Chinese digital Seismic Network (CSN), 17 stations show statistically significant seismicity increase with β -statistic values larger than 2 following the Wenchuan earthquake. These include 12 stations in North China block, which is seismically active and is in the rupture propagation direction of the Wenchuan earthquake, 3 stations along the coastal lines in the relatively stable South China block, 1 station near the Haiyuan fault zone in northwest China and 1 station near the Longgang volcanoes in northeast China. The tectonic environments near the sites with clear triggered activity range from transpressional to tranextensional, and most of the regions are not associated with active geothermal or volcanic activities, indicating that dynamic triggering is ubiquitous and could occur in a wide range of tectonic environments. In some cases, the onset of the triggered activity coincides with the first few cycles of the Love waves, while in other cases, there is no correlations between the triggered activity and surface waves. The dynamic stresses estimated from the peak ground velocities at stations showing triggered activity range from 0.01 to 0.09 MPa. Our observations suggest that dynamic triggering in intraplate regions tends to occur near active faults that have ruptured in historic times, and in the rupture propagation directions of the mainshock. However, it is worth noting that many sites that satisfy the criteria are not triggered, suggesting that these conditions would help, but are not sufficient enough to guarantee remote triggering in intraplate regions.

1-092

SYSTEMATIC SEARCH OF REMOTELY TRIGGERED EARTHQUAKES AND NON-VOLCANIC TREMOR ALONG THE HIMALAYA/SOUTHERN TIBET AND NORTHERN CALIFORNIA *Ojha L (Arizona), and Peng Z (Georgia Tech)*

Non-volcanic tremor is a seismic signal observed away from volcanoes, and is characterized with long durations and no clear body wave arrivals. Recent studies have found that non-volcanic tremor can be triggered instantaneously during the surface waves of large teleseismic events along the circum-Pacific subduction zones, California, and Taiwan. However, it is still not clear whether triggered tremor could occur at other tectonic environments, and what are the necessary conditions for tremor to occur. Here we conduct a systematic search for triggered tremor around the Himalayan region for 30 teleseismic events since 2002, based on the continuous seismic data recorded by the temporary PASSCAL project HiCLIMB. We find many local earthquakes in southern Tibet triggered by the 2004 Mw9.2 Sumatra and 2005 Mw8.7 Nias earthquakes. However, we did not identify any triggered tremor along the Himalayan Fold-Thrust Belt in Nepal. This is mainly due to a lack of available seismic recordings in Nepal that are generated by

large-size events. We also perform a similar search for additional triggered tremor in Northern California, focusing on the Central Calaveras fault, where triggered tremor has been identified previously. Out of the 29 teleseismic events with $M \geq 7.5$ since 2000, our visual inspection shows that only the 2002 Denali Fault earthquake have triggered clear tremor in the central Calaveras fault. These observations are similar with a companion study (Fabian and Peng, 2009), where only the Denali Fault earthquake have triggered clear tremor in three regions in Southern California. In comparison, many large teleseismic events have triggered tremor in Japan, Cascadia, central California and Taiwan. Possible reasons for a lack of widespread triggering in these regions include: elevated background noises for surface stations that may hide weak triggered tremor signals, different ambient tremor rate, or different tremor triggering threshold in different regions. Updated results will be presented at the meeting.

1-093

STUDY OF TRIGGERED TREMOR CHARACTERISTICS AND TRIGGERING THRESHOLD IN ANZA REGION, SOUTHERN CALIFORNIA *Wang T (UCR), and Cochran ES (UCLA)*

Non-volcanic tremor have been widely observed at subduction zones (e.g. SE Japan, Nankai and Cascadia) and, more recently, along strike-slip faults in California (e.g. central to southern San Andreas and San Jacinto fault). In southern California, both ambient tremor and tremor triggered by distant large earthquakes have been observed close to well-developed faults. Tremor triggered by passing teleseismic waves suggests that tremor can be triggered by low stress changes.

We examine data of the Anza seismic network to determine the characteristics of tremor along crustal faults. The data we examine are continuous broadband waveforms from the Southern California Seismic Network (SCSN), along with the borehole station data around Anza, from 2002 to 2007. The borehole seismometers provide high signal-to-noise data that is an important dataset to assist in tremor detection and analysis. Before utilizing the borehole data for tremor detection, we had to determine the orientation of the horizontal components. Using 25 regional earthquakes in 2007, we found the best-fit P-onset polarization azimuths.

To systematically search and document tremor locations, we implemented an automatic detection program. In this preliminary work, we found two episodes of triggered tremor observed by most of the stations near Anza. The most obvious triggered tremor episode occurs during passage of surface waves from the Denali earthquake (M_w 7.9), 2002, out of 41 potential triggering wave passages ($M_w > 7.0$) examined. Overall, tremor found in southern California is less periodic and more impulsive compared to subduction zone tremor. We plan to survey tremor triggered by teleseismic events to determine the stress change on the fault needed to trigger tremor. If tremor is triggered at a critical stress level we can better understand the underlying physical processes driving tremor. The particular section of San Jacinto fault where we detect tremor is described as Anza seismic gap due to an absence of large ($M > 6$) earthquakes since 1790. If tremor is constrained to the Anza Gap section, this might imply unusual frictional properties that favors tremor generation and perhaps precludes larger earthquakes.

1-094

SYSTEMATIC SEARCH FOR TRIGGERED NON-VOLCANIC TREMOR IN SOUTHERN CALIFORNIA *Fabian AR (South Carolina), and Peng Z (Georgia Tech)*

We perform a systematic search of triggered non-volcanic tremor in Southern California. Our study area includes the San Jacinto Fault near Hemet and the Simi Valley, where tremor triggered by the 2002 Denali Fault earthquake has been reported previously, and the San Gabriel

Mountains. We examined 36 teleseismic earthquakes with $M_w \geq 7.5$, and 44 regional earthquakes with $M_w \geq 5.0$ since 2001 that were recorded by the Southern California Seismic Network (SCSN) broadband and short period seismometers. So far we have only been able to definitely identify tremor associated with the 2002 $M_w 7.9$ Denali Fault earthquake, which is seen in all three regions. This includes the San Gabriel Mountains, where either ambient or triggered tremor has not been observed before. The tremor observed near Hemet appears to be initiated by Love waves and becomes more intensified during the large amplitude Rayleigh waves. The tremor triggered in the other two regions is rather weak, and hence such a pattern is not clear. Our results suggest a lack of wide spread triggering of tremor in Southern California. This is consistent with a similar study in Northern California (Ojha and Peng, 2009), indicating that either weak triggered tremor is hidden behind elevated background noises recorded by surface stations, or the ambient tremor rate and the tremor triggering threshold is low in these regions. Our results could be used to further constrain the necessary conditions to generate tremor in a strike-slip environment, and improve our understanding of the fundamental processes in deep fault zones.

1-095

TRIGGERED TREMOR ON THE SAN JACINTO FAULT FROM THE 3 AUGUST 2009 MW 6.9 GULF OF CALIFORNIA EARTHQUAKE *Brown JR (Stanford), Shelly DR (Berkeley), Aguiar AC (Stanford), and Beroza GC (Stanford)*

Recent studies show that non-volcanic tremor can be triggered by the passing of surface waves of large earthquakes at great distances. In this study we examine the excitation of non-volcanic tremor in southern California following the August 3, 2009 $M_w 6.9$ Gulf of California earthquake. Similar to non-volcanic tremor activity in multiple subduction zones (e.g. SW Japan, Cascadia, Costa Rica), the triggered tremor in southern California appears to consist of a series of low-frequency earthquakes (LFEs). The LFEs are detected using a running autocorrelation approach successfully employed to study subduction zone tremor. Once identified, we cross-correlate the events and use the differential times as data for hypoDD in order to locate their source. Our preliminary locations reveal LFE activity between 15 and 20 km depth in vicinity of the San Jacinto fault west of the Salton Sea. The concentration of events in this depth range may illuminate the transition zone between stable and unstable sliding on the San Jacinto fault. The template events of LFEs within triggered tremor can be used to search continuous data for LFEs/ambient tremor.

1-096

EFFECTS OF DYNAMIC TRIGGERING ON PATTERNS OF SEISMICITY IN VIRTUAL CALIFORNIA EARTHQUAKE SIMULATION *Yikilmaz MB (UCD), Turcotte DL (UCD), Yakovlev G (UCD), Rundle JB (UCD), and Kellogg LH (UCD)*

In order to better understand the behavior of seismicity simulations, we have carried systematic studies of relatively simple fault models using the Virtual California earthquake simulation. Here we consider a straight strike-slip fault with a length of 480 km and a depth of 12 km, meshed in 1×1 km elements. Our first study is of a uniform fault with a mean recurrence interval of 200 years. An important parameter in the simulation is the dynamic triggering factor F which can be described as the fractional decrease in failure stress due to the high stress at the tip of the propagating rupture. With $F = 1$, no reduction in stress occurs and a near Gutenberg-Richter (GR) distribution of earthquakes in the range $M = 5.4$ to 8.1 is obtained. As F is decreased characteristic earthquakes in the range $M = 7.8$ to 8.1 become dominate but with a GR background of smaller events. We have also carried out simulations where the recurrence interval varied linearly from 200 at one end of the fault to 1000 years at the other. Interesting pattern of seismicity is obtained.

1-097

NON-VOLCANIC TREMOR NEAR THE CALAVERAS FAULT TRIGGERED BY MW~8 TELESEISMS *Aguiar AC (Stanford), Brown JR (Stanford), and Beroza GC (Stanford)*

Deep, non-volcanic tremor has been shown to accompany large, slow slip events on subduction zones, such as Cascadia and SW Japan. It has also been found to be triggered by the passing of surface waves from distant large earthquakes. Triggered tremor has been identified in several areas of California, including an area centered on the Calaveras fault. In subduction zones, studies have shown that tremor is a superposition of many small low frequency earthquakes (LFEs). Ongoing, non-triggered tremor near Cholame has also been shown to be comprised of LFEs. Due to the strong similarities between triggered and spontaneous tremor, we hypothesize that triggered tremor is also a superposition of LFEs. We test this idea using data from the Calaveras Fault because it is very well instrumented and has significant micro-earthquake activity. We have analyzed data from ~25 stations around the Calaveras fault for the time periods of four different $M_w \geq 8$ earthquakes. So far, these data show tremor triggered by the 2001 Peru ($M_w=8.4$), 2002 Denali ($M_w=7.9$), 2004 Sumatra ($M_w=9.1$) and 2007 Kuriles ($M_w=8.1$) earthquakes. We use a match filter method that correlates the waveforms of each station with itself across the networks of stations; we have found more than a dozen signals that repeat during a period of 500 s for each earthquake. This strongly suggests that triggered tremor is comprised of many low frequency earthquakes. We also find that potential LFEs triggered by different earthquakes correlate with each other, indicating that the source location of triggered tremor is persistent between triggering events. Identifying LFEs within triggered tremor should allow us to develop greatly improved locations, which in turn should greatly increase our understanding of this phenomenon.

1-098

DEPTH EXTENT OF DAMAGE ZONES AROUND THE CENTRAL CALAVERAS FAULT FROM WAVEFORM ANALYSIS OF REPEATING EARTHQUAKES *Zhao P (Georgia Tech), and Peng Z (Georgia Tech)*

We systematically investigate spatial variations of temporal changes and depth extent of damage zones along the Calaveras fault that ruptured during the 1984 Morgan Hill earthquake by the waveform analysis of 333 sets of repeating earthquakes. We use a sliding window waveform cross-correlation technique to measure travel time changes in waveforms generated by each repeating cluster. We find clear travel time delays in the S- and early S-coda waves for events immediately after the Morgan Hill mainshock. The amplitudes of the time delays decrease logarithmically with time since the mainshock, indicating a time-dependent recovery (healing) process following the abrupt co-seismic temporal changes. The largest temporal changes are observed at station CCO that is the closest to the rupture zone of the Morgan Hill mainshock. The time delays at this station are larger for clusters in the top 6 km, and decrease systematically at larger depth. In comparison, the time delays observed at other 5 stations are much smaller, and do not show clear relationship with hypocentral depth. We suggest that the temporal changes at these 5 stations mostly occur in the top few hundred meters of the near-surface layers, while the temporal changes at station CCO is likely associated with the damage zone around the Calaveras fault that is well developed in the top few kms of the upper crust. Our results are consistent with the inference of a widespread damage and nonlinearity in the near-surface layers associated with strong ground motions of nearby large earthquakes, and localized damages and flower-type structures around active faults based on previous studies of fault zone structures and recent 3D numerical simulations.

1-099

AUTOMATICALLY DEFINED CATALOGS AND IMPROVED MOMENT ESTIMATES REVEAL THAT REPEATING EARTHQUAKES ARE SOMETIMES TIME- AND SLIP-PREDICTABLE *Rubinstein JL (Washington), and Ellsworth WL (USGS)*

Using continuous waveforms, we have implemented a cross-correlation-based method to automatically identify repeating earthquakes near Parkfield, CA. Starting with template waveforms from sequences defined from a relocated earthquake catalog, we are able to construct a catalog of individual repeating events (and their near neighbors) by waveform correlation and careful relocation. This method is highly robust: it reproduces catalog results where available. Additionally, this method does not rely on the preexistence of earthquake catalogs nor is it susceptible to errors in initial locations.

We then analyze the repeating events with a new, SVD-based technique for determining relative earthquake size. We find that errors in catalog magnitudes may exceed ± 0.3 magnitude units, or approximately a factor of 2 in moment. The results of our method have uncertainty of 11% in moment or equivalently 0.03 magnitude units.

Using these newly defined repeating earthquake sequences and a precise measurement of their moments, we revisit simple models of earthquake recurrence: the time-predictable and slip-predictable models. Previous studies of earthquake recurrence of larger events show that these models do not perform well, but with precise magnitude estimates and locations we show that both of these models work well for many repeating earthquakes. Other sequences do not appear to be time- or slip-predictable at all.

Additionally, we study the evolution of slip behavior following the Parkfield earthquake. Parts of the fault see a rapid increase in slip rate and no change in fault strength as evidenced by reduced recurrence intervals and stable magnitudes following the Parkfield mainshock. Other parts of the fault appear to have been weakened by the mainshock; in these locations we identify repeating events where both moment and recurrence times of repeating earthquakes were reduced following the Parkfield mainshock.

1-100

TRIGGERING EFFECT OF 2004 M6 PARKFIELD EVENT ON EARTHQUAKE CYCLE OF SMALL REPEATING EVENTS *Chen KH (Berkeley), Bürgmann R (Berkeley), and Nadeau RM (Berkeley)*

Stress fluctuations caused by nearby events may influence the timing of earthquakes and complicate earthquake recurrence. After the 29 September 2004, M 6.0 Parkfield, California earthquake, a large number of postseismic repeats of small earthquakes are observed. We analyze a subset of 25 M -0.4 ~ 1.7 repeating earthquake sequences (RES) from 1987-2008 at Parkfield to examine the variation of recurrence properties in space and time. The response of the repeating events to the occurrence of large earthquakes provides the clearest documentation of the interaction process. Accelerations of repeating sequences are associated with the 2004 Parkfield earthquake, which reflect accelerated aseismic afterslip surrounding the rupture. The clear acceleration in earthquake recurrences only appears at depths of < 7 km, whereas the selected RES from below 7 km do not reveal a clear dependence of recurrence interval on elapsed time since the mainshock. The healing rates measured by seismic moment versus recurrence interval scaling relation also reveal a likely depth-dependent trend. The temporal variation in recurrence of repeating sequences is found to be correlated with each other when the RES are close enough in space. Spatially clustered repeating sequences show evidence of strong interaction in time,

reflected in temporally clustered event recurrences and similar recurrence history. The temporal correspondence appears to be a function of separation distance from nearby repeaters, where the dependence is evident for the repeaters with similar magnitude.

1-101

SEARCHING FOR EVIDENCE OF A PREFERRED RUPTURE DIRECTION IN SMALL EARTHQUAKES AT PARKFIELD *Kane DL (SIO / UCSD), Shearer PM (UCSD), Allmann BP (UCSD), and Vernon FL (UCSD)*

Theoretical modeling of strike-slip ruptures along a bimaterial interface suggests that the interface will have a preferred rupture direction and will produce asymmetric ground motion (Shi and Ben-Zion, 2006). This could have widespread implications for earthquake source physics and for hazard analysis on mature faults because larger ground motions would be expected in the direction of rupture propagation. Studies have shown that many large global earthquakes exhibit unilateral rupture, but a consistently preferred rupture direction along faults has not been observed. Some researchers have argued that the bimaterial interface model does not apply to natural faults, noting that the rupture of the M 6 2004 Parkfield earthquake propagated in the opposite direction from previous M 6 earthquakes along that section of the San Andreas Fault (Harris and Day, 2005).

We analyze earthquake spectra from the Parkfield area to look for evidence of consistent rupture directivity along the San Andreas Fault. We separate the earthquakes into spatially defined clusters and quantify the differences in high-frequency energy among earthquakes recorded at each station. Propagation path effects are minimized in this analysis because we compare earthquakes located within a small volume and recorded by the same stations. By considering a number of potential end-member models, we seek to determine if a preferred rupture direction is present among small earthquakes at Parkfield.

1-102

MIGRATION OF THE PARKFIELD EARLY AFTERSHOCK SEQUENCE *Peng Z (Georgia Tech), and Zhao P (Georgia Tech)*

A large shallow earthquake is immediately followed by numerous aftershocks with a significant portion missing in existing earthquake catalogs, mainly due to masking of the mainshock coda and overlapping arrivals. Recovering these missing early aftershocks is important for understanding the physical mechanisms of earthquake triggering, and tracking post-seismic deformation around the mainshock rupture zone. Here we use waveforms of relocated events along the Parkfield section of the San Andreas Fault (SAF) as templates, and scan through continuous waveforms for 3 days around the 2004 Mw6.0 Parkfield earthquake to detect missing aftershocks. We identify 11 times more aftershocks than reported in the standard Northern California Seismic Network (NCSN) catalog. The newly detected aftershocks show clear migration in both along-strike and down-dip directions with logarithmic time since the mainshock, consistent with the numerical simulations on expansions of aftershocks caused by propagating afterslip. The cumulative number of early aftershocks increases linearly with postseismic deformation in the first 2 days, suggesting that early aftershocks could be driven by significant afterslip along the SAF induced by the Parkfield mainshock.

1-103

MICROSEISMICITY AND PETROLOGY OF THE SALTON BUTTES REGION, CA *Simila G (CSUN), Vazquez J, and McStroul G*

We will be participating in the January 2010 Salton Trough Seismic Project, funded by NSF (Margins/Earthscope) and the USGS. In the Salton Trough, however, the 20-22 km thick crust is composed entirely of new material added by magmatism from below and Colorado River sedimentation from above. The adopted model of magmatic addition to the crust is from A. Schmitt and J. Vazquez (2006), where mafic magma reaches neutral buoyancy in the lower to middle crust. Rhyolite lavas and xenoliths from the Salton Sea geothermal field (Southern California) provide insights into crustal compositions and processes during continental rupture and incipient formation of oceanic crust. Salton Buttes rhyolite lavas contain xenoliths that include granophyres, fine-grained altered rhyolites ("felsite"), and amphibole-bearing basalts. Zircon is present in lavas and xenoliths, surprisingly even in the basaltic xenoliths, where it occurs in plagioclase-rich regions interpreted as pockets of crystallized partial melt. Zircons in the xenoliths are exclusively Late Pleistocene-Holocene in age and lack evidence for inheritance. This is evidence for deep-reaching hydrothermal circulation and indicates rhyolite genesis by episodic remelting of altered basalts instead of fractional crystallization of unaltered basaltic magma.

For the Salton Trough project, we are analyzing the microseismicity from the SCSN database of the region around the Salton Buttes, five rhyolite domes, at the southern end of the Salton Sea and near the Brawley seismic zone. In fall 2009, we will install five digital seismographs to supplement the existing network for a more detailed study related to subsurface structures. Then in January 2010, we will participate in the main north-south seismic reflection/refraction line. In addition, samples of the rhyolite have been collected with Jorge Vazquez and students for petrologic and P wave velocity analyses.

1-104

ANALYSIS OF THE MICROSEISMICITY (1996-2007) OF THE SANTA MONICA MOUNTAINS AND ASSOCIATED MALIBU COAST, SANTA MONICA-DUME, AND SANTA MONICA BAY FAULTS *Green J (Antelope Valley Press), Simila G (CSUN), and Sorlien CC (UCSB)*

The Santa Monica Mountains, in the western Transverse Ranges, are separated from Los Angeles and offshore Santa Monica sedimentary basins by the E-W, now predominantly left-lateral Raymond-Hollywood-Santa Monica-Dume fault system. The western ~80 km-long stretch of this fault system has been investigated by Sorlien et al (2006) using seismic reflection and earthquake data. Previous investigators proposed thrust slip on a low-angle blind fault beneath the Santa Monica-Dume fault to account for the Santa Monica anticlinorium. The onshore Malibu Coast fault (MCF) and the onshore Santa Monica fault are probably oblique left-reverse faults. The Malibu Coast fault shows evidence of reverse-oblique slip with a left-lateral strike-slip component along north-dipping strands ranging from 30-70 degrees. The convergence rate across the MCF is estimated to be about 18 mm/yr, and the slip rate is estimated to be between 0.04 to 1.5 mm/yr. Convergence is evident in focal mechanisms showing mostly reverse faulting. Though Holocene surface displacements have been officially recognized across only two strands of the MCF zone to date, the MCF is still considered active and capable of producing a magnitude 6.5 to 7.0 earthquake. The microseismicity (1996-2007; M=1-3, 307 events) for the region has been relocated using HYPOINVERSE 2000 and the SCEC/LARSEII crustal velocity structure. The results show seismicity (map view and cross-sections) associated with the Malibu Coast, Santa Monica-Dume, and Santa Monica Bay faults, as well as scattered events in the eastern region of the Santa Monica Mountains. The focal mechanisms show primarily reverse and some left-lateral slip faulting.

1-105

PRELIMINARY CATALOG OF FOCAL MECHANISMS (1981 TO 2009) FOR SOUTHERN CALIFORNIA: SEISMOTECTONIC AND EARTHQUAKE PHYSICS IMPLICATIONS *Hauksson E (Caltech), Yang W (USC), Shearer PM (UCSD), and Hardebeck JL (USGS)*

We analyze first motion data for ~480,000 earthquakes recorded by the Caltech/USGS Southern California Seismic Network (SCSN) from 1981 to present. We apply the HASH method of Hardebeck and Shearer (2002) to determine two catalogs of first motion mechanisms. First, we apply the same data-quality constraints used in the J. Hardebeck 1983-2004 catalog, and determine an expanded catalog (1981-2009) of ~37,000 well-resolved focal mechanisms. Second, we relax most constraints and determine a bulk catalog of ~137,000 first motion mechanisms. We compare and analyze these two catalogs.

Both catalogs show very similar temporal behavior from 1981 to 2009. Time series of the rake and dip show minimal variations with time, with a consistent average dip of 70 degrees. The rake shows a similar constant temporal average of ± 180 degrees, with only minor fluctuations suggesting the presence of a small extensional stress component. However, during the 1994 Northridge sequence the overall stress field appears to be slightly more compressional. Similarly, the three measures of quality, average number of first motions per event, the station distribution ratio, and the average plane errors only exhibit minor fluctuations with time. Thus neither the occurrence of major events such as the 1992 Mw7.3 Landers earthquake nor changes in the configuration of the seismic network seem to have affected the average properties of the focal mechanisms or their quality.

Strike-slip faulting occurs across southern California as demonstrated in both catalogs. Strike-slip with some normal faulting occurs along the San Jacinto fault, in the Mojave Desert, and in the southern Sierras. In contrast, the western Transverse Ranges, including the Los Angeles basin, are characterized by a mixture of strike-slip and thrust-faulting earthquakes. Plots of the rake versus dip values show three distributions corresponding to right-lateral strike-slip, normal faulting, and dip-slip faulting. These distributions are overlapping and indicate a continuous merging of one style of faulting to the next. Similarly, the rake values versus the dip directions show the same three distributions with strike-slip faulting being most prominent. We also compare the style of faulting with the distribution of stress drops. In the near future, we plan to improve these catalogs by adding P/S amplitude ratios as additional constraints.

1-106

PRODUCTS AND SERVICES AVAILABLE FROM THE SOUTHERN CALIFORNIA EARTHQUAKE DATA CENTER (SCEDC) AND THE SOUTHERN CALIFORNIA SEISMIC NETWORK (SCSN) *Yu E (Caltech), Chen S (SUNY Buffalo), Chowdhury F (Caltech), Bhaskaran A (Caltech), Hutton K (Caltech), Given D (USGS), Hauksson E (Caltech), and Clayton R (Caltech)*

Currently the SCEDC archives continuous and triggered data from nearly 3000 data channels from 375 SCSN recorded stations. The SCSN and SCEDC process and archive an average of 12,000 earthquakes each year. The SCEDC provides public access to these earthquake parametric and waveform data through its website www.data.scec.org and through client applications such as STP and DHI. This poster will describe the most significant developments at the SCEDC in the past year.

New data products:

- The SCEDC is planning to distribute synthetic waveform data from the 2008 ShakeOut scenario (Jones et al., USGS Open File Rep., 2008-1150) and (Graves et al. 2008; Geophys. Res. Lett.) This is a M 7.8 earthquake on the southern San Andreas fault. Users will be able to download 40 sps velocity waveforms in SAC format from the SCEDC website. The SCEDC also plans to distribute synthetic GPS data (Crowell et al., 2009; Seismo. Res. Letters) for this scenario as well.
- The SCEDC has added a new web page to show the latest tomographic model of Southern California. This model is based on Tape et al., 2009 Science.

New data services:

- The SCEDC plans to export earthquake parametric data in QuakeML format. This is an xml format that has been adopted by the ANSS. This data will also be available as a web service.
- The SCEDC plans to export data in StationXML format. This is an xml format created by the SCEDC to fully describe station metadata. This data will also be available as a web service.
- The stp 1.6 client can now access both the SCEDC and the NCEDC waveform archives.

In progress – SCEDC to distribute 1 sps GPS data in miniSEED format:

- As part of a NASA/ AIST project in collaboration with JPL and SIO, the SCEDC will receive real time 1 sps streams of GPS displacement solutions from the California Real Time Network (<http://sopac.ucsd.edu/projects/realtime>; Genrich and Bock, 2006, J. Geophys. Res.). These channels will be archived at the SCEDC as miniSEED waveforms, which then can be distributed to the user community via applications such as STP.

1-107

THE QUAKE-CATCHER NETWORK: SENSOR DISTRIBUTION AND TESTING
Cochran ES (UCLA), Lawrence JF (Stanford), and Christensen C (Kleinfelder, Inc)

The goal of the Quake-Catcher Network (QCN) is to dramatically increase the number of sensors by exploiting recent advances in sensing technologies and cyberinfrastructure. Triaxial Micro-Electro-Mechanical Systems (MEMS) sensors are very low cost (\$50-\$100), interface to any desktop computer via USB cable, and provide high-quality acceleration data. Distributed computing provides a mechanism to expand seismology with minimal infrastructure costs, while promoting community participation in science. The increased seismic observations will yield unprecedented resolution of rupture mechanics, leading to increased understanding of how earthquakes evolve from initiation to termination. These same observations will provide new images of the subsurface, which will improve earthquake hazard scenarios by predicting shaking outcomes from a dynamic rupture through the earth.

Preliminary shake table tests comparing the response of two MEMS sensors with the Kinematics EpiSensor show the MEMS accelerometers can record high-fidelity seismic data and provide linear phase and amplitude response over a wide frequency range. QCN began distributing external MEMS sensors to K-12 schools and the general public in January 2009 and quickly distributed more than 200 sensors. We recently started outreach program to K-12 schools to provide hands-on activities, sensors and software with the goal of improving student

understanding of seismology. Additionally, we are working to provide displays to public centers, such as museums and libraries, to improve community understanding of seismic hazard and earthquakes. QCN has the potential to produce wide-reaching outcomes for: earthquake physics research, distributed sensor networks, improved seismic safety, and increased public knowledge of earthquakes.

1-108

A WEB-BASED BOREHOLE DATA DISSEMINATION PORTAL *Steidl JH (UCSB), Ratzesberger L, Seale S, Civilini F, and Vaughan N*

Data from instrumented boreholes in southern California are producing very interesting observations from a large data set that includes 100's of earthquake observations each month. While the majority of these are very small events, they provide the control data that represents the linear behavior of the site. The largest motions recorded to date, $\sim 10\%g$, are only just getting to the regime where nonlinear effects become important. In order to make these data more accessible to the seismology and earthquake engineering research community, software development of a web-based data dissemination portal has taken place under the George E. Brown Jr., Network for Earthquake Engineering (NEES) program. This development includes processing and analysis tools, and web-based data dissemination available through the NEES@UCSB website [<http://nees.ucsb.edu>]. Of interest to the research community are the tools developed to provide search and download capabilities for access to data recorded through the various borehole-monitoring programs at UC Santa Barbara, including the SCEC borehole program. Researcher interested in obtaining data recorded at the various field sites can use the map-based event search tool to select a particular station and instrument, and show the records available at the site. These records can then be downloaded in a number of common formats, including MSeED, SAC, and an ASCII text-based real-time data viewer (RDV) format. The last format allows the data to be viewed in the NEES developed RDV tool, a platform independent JAVA program that can display both real-time streaming data, or playback data that has been downloaded through the web-based event search tool.

1-109

CALIFORNIA FAULT ZONE ORPHAN BOREHOLE DATABASE *Avila JA (UCSC), and Brodsky EE (UCSC)*

California is tectonically active and has many abandoned boreholes across the state. With information on these boreholes provided by the Division of Oil, Gas, and Geothermal Resources (DOGGR), we have been able to create several interactive maps on Google Earth for a public website and database accessible at: <http://www.pmc.ucsc.edu/~rapid/>. These maps locate abandoned and adoptable wells near active quaternary fault traces and are linked to relevant subsurface information. The links on the website include complete histories, logs, lithologies, stratigraphic columns, and casing information (when available). Earthquake scientists may utilize these wells for monitoring subsurface changes prior, during, and after an earthquake in California. The boreholes could be used for the measurements of several subsurface observables, including: repeat temperature logs, stress measurements, geophysical logging, repeat active-source seismic experiments, sampling of mud/ gas/ fluids, long-term monitoring of temperature and pore fluid pressure, passive seismicity, etc. The "Adopt a Well Program" with DOGGR allows the orphaned well to be tested for 90 days without liability then purchased upon approval. With the science of seismology expanding its limits, these boreholes offer the depth necessary to have accurate subsurface data in order to make informed implications about what occurs deep beneath the surface.

1-110

3D GEOLOGICAL MODEL OF THE CRUSTAL STRUCTURE IN THE SOUTHEAST CARIBBEAN *Whitesides AS (USC), and Miller MS (USC)*

From the NSF funded BOLIVAR (Broadband Onshore-offshore Lithosphere Investigation of Venezuela and the Antilles arc Region) project from 2003-2005 in the southeast Caribbean, onshore-offshore seismic multi-channel (MSC) reflection data was collected as part of a multi-disciplinary investigation to examine how island arcs, marginal basins, and oceanic plateaus become accreted to continents. Through the use of Dynamic Graphics software EarthVision, the seismic data profiles that were collected were to be imported, compiled, and viewed in a three-dimensional environment. From the interpreted data profiles, the stratigraphic architecture and faults throughout the region were to be connected to help form a subsurface map and interpretation. Due to technical problems and limitations in the current version of EarthVision, a subsurface map for the seismic profiles from the BOLIVAR project was not fully completed, but initial modeling results will provide a framework for further development of the 3D mapping project. Initial results include a 3D model of topography and bathymetry of the southeast Caribbean as well as the interpreted Moho discontinuity. In the future, it is planned to either import the 2D seismic profiles in an alternative format or drape images of the reflection profiles into the model. The best alternative to using image files would be to build a 3D reference grid in which the 2D seismic profiles are imbedded and then import these grids into EarthVision for 3D interpretation.

Earthquake Geology Southern San Andreas Fault Evaluation (SoSAFE)

1-121

INTERNATIONAL COLLABORATION IMAGES THE NORTH ANATOLIAN FAULT SYSTEM IN MARMARA SEA, TURKEY: SUBSIDED LOWSTAND DELTAS, ONLAPPING BASIN FILL, THRUST-FOLD TRANSVERSE RIDGES, TRANSTENSION, AND DISTRIBUTED ACTIVE FAULTING *TAMAM Scientific Party**

We collected high-resolution multichannel seismic reflection (MCS) data to image the North Anatolian Fault (NAF) and basin sediments in the Marmara Sea. The North strand of the NAF, passing closest to Istanbul, is considered to carry most of the current and late Holocene plate motion, based on GPS data, historic seismicity and onshore trenching. Three >1200 m-deep bathymetric basins and the 800 m-deep Kumburgaz basin are arrayed along the northern NAF. Our results may support long-standing yet still controversial suggestions that the NW-SE releasing segment of the northern NAF is non-vertical with a normal component of slip, and that this ongoing process is responsible for the basin. However, additional advanced data processing (migration) is planned to better image the fault geometry. Extension or transtension, however, are by no means universal within Marmara Sea. We image transverse (NE-SW) ridges between the basins to be thrust-related anticlines. We also imaged large-scale deep-seated landslide complexes on the basin flanks that are important contributors to basin fill.

Our chirp data image several strands of the southern fault system, 50 km south of the northern NAF, to offset strata above the Last Glacial Maximum unconformity. A WNW-striking segment of the intervening Imrali fault system is associated with normal-separation, 300 m-high sea floor scarps, and numerous young secondary faults in its hanging-wall. There, stacked low-stand shelf edge deltas, whose tops were formed near sea level or lake level, are now >400 deep. Sea level and climate cycles control delivery of sediment to the deep basins, resulting in a repeating pattern of onlapping fill on the progressively-tilting basin flanks. We will attempt to relate the onlapping fill events to the succession of low-stand deltas by tracing horizons via regional strike profiles.

MCS profiles with simple migrations indicate that the E-W segment of the NAF through Kumburgaz basin adjacent to western Istanbul is associated with shortening structures. The deep part of a N-dipping transpressional fault there would be closer to western Istanbul than would a south-dipping transtensional NAF.

*Selin D. Akhun, A. Evren Buyukasik, Melis Cevatoglu, Günay Çifçi, Süleyman Coskun, Emin Demirbag, John Diebold, Derman Dondurur, Savas Gurcay, Caner Imren, H. Mert Kucuk, Hülya Kurt, Pinar G. Özer, Emre Perinçek, Leonardo Seeber, Donna Shillington, Christopher C. Sorlien, Michael Steckler, and Duygu Timur

1-122

SOUTHERN CALIFORNIA MODELING OF GEODYNAMICS IN 3D (SMOG3D): TOWARD QUANTIFYING THE STATE OF TECTONIC STRESS IN THE SOUTHERN CALIFORNIA CRUST *Fay NP, Becker TW, and Humphreys ED*

We present results from numerical modeling of three-dimensional geodynamics of the southern California lithosphere. Our primary objective is to quantify how faults are loaded and, more generally, the state of stress in the southern California crust. We evaluate how buoyancy and rheology control this stress state, and aim to better understand the relationships to active deformation and earthquakes, horizontal coupling between tectonic plates, and the vertical

coupling between the lithosphere and upper mantle. We use a 3D finite element approach incorporating visco-elastic-plastic rheology to model the viscous and frictional behavior of the crust and mantle lithosphere. Density heterogeneities within the crust and upper mantle (surface topography, Moho topography, and mantle seismic/density anomalies) produce a state of deviatoric horizontal tension in the Transverse Ranges with principal stresses of ~5-20 MPa. These stresses must be balanced by compression caused by crustal block motions related to plate interaction. We also present results of modeling the southern California lithosphere under shear (representing relative Pacific Plate motion) with embedded faults of the San Andreas system. We find that if all the faults of the San Andreas system are of similar long-term shear strength, deviatoric tension is produced in the central and eastern Transverse Ranges. Models with the San Andreas weaker than other major faults (e.g., 10 MPa San Andreas, 30 MPa San Jacinto, depth-averaged shear strength) produce compression in the Transverse Ranges suggesting the San Andreas may be weaker than other faults in the system. Further work will include incorporating lateral variations in lithospheric viscosity and self-consistent determination of the effects of buoyancy variations on lithospheric viscous flow.

1-123

THE MECHANICS OF CONTINENTAL TRANSFORMS: IMPLICATIONS FOR THE TECTONICS OF CALIFORNIA *Platt JP, Becker TW, and Kaus BJ*

Displacement on intracontinental transforms is commonly distributed over a zone several hundred km wide, and may incorporate large regions of transtensional and transpressional strain, but no consensus exists on what controls the distribution and style of this deformation. We model the transform boundary as a weak shear zone of finite length that exerts shear stress on the deformable continental lithosphere on either side. Strain rate decreases away from the shear zone on a scale related to its length. Force balance in this system requires gradients in shear-strain rate normal to the shear zone to be balanced by gradients in stretching rates parallel to the zone. The shear-zone parallel gradients create zones of lithospheric thickening and thinning distributed anti-symmetrically about the shear zone. Simple analytical estimates, two-dimensional (2D) spectral models, and 2D/3D numerical models give consistent indications of the spatial scales and magnitudes of the zones of uplift and subsidence. Using reasonable parameter values, the models yield geologically relevant rates. Strain-rate components inferred from the GPS-determined 2-D velocity field, and analysis of seismicity using Kostrov's method, taken together with the geological data on the distribution of active faults, uplift, and subsidence, suggest that the distribution and rates of active deformation in California are consistent with our predictions. This validates the assumptions of the continuum approach, and provides a tool for predicting and explaining the tectonics of California and of other intracontinental transform systems.

1-124

EFFECTS OF LATERAL VISCOSITY VARIATIONS ON THE DYNAMICS OF

WESTERN NORTH AMERICA *Ghosh A, Becker TW, and Humphreys ED*

We investigate the effects of lateral viscosity variations (LVVs) and long-range force transmission on the dynamics of the deforming North American lithosphere, with focus on the western region close to the plate boundary. We address the question how the basal shear tractions as generated by mantle convection affect the stress field in North America on top of the inherited gravitational potential energy variations. Our goal is to find a model that self-consistently explains both kinematic surface constraints and internal deformation indicators. For the latter, our efforts are partially motivated by the finding of Humphreys & Coblenz (2007) that an inversion for plate

forcing requires cratonic drag and mantle tractions, but at a reduced amplitude from the predictions of an earlier model without LVV by Becker & O'Connell (2001). Traction amplitude variations can be induced by LVVs, and a major source of such variations underneath North America is the presence of old continental lithosphere with underlying cratonic keels. Those keels are inferred to be high viscosity and reach deep into the mantle, up to a depth of ~300 km. The presence of the thick high viscosity keel, along with weak plate boundaries, likely creates large LVVs, which will potentially have long-range effects on the deformation of the North American plate. We quantify these effects by computing the basal tractions globally using a high resolution finite element mantle convection code, CitcomS, that can take into account several orders of lateral viscosity variations. The flow in the model is driven by density anomalies, as imaged by seismic tomography. Since the relative viscosities of the stiff keel and the weak plate boundaries are poorly constrained, a number of models with varying viscosities are tested. The stress fields associated with these predicted tractions are then compared with stress observations such as the World Stress Map and strain-rates from the Global Strain Rate Map. The ultimate goal is to construct a global, spherical geodynamic model that is adapted to the North American plate. This background model can provide information on how long-distance forcing affects regional tectonics, such as in southern California. This will in turn provide a deeper understanding of how faults in this region are loaded and how strain is localized on the plate boundary.

1-125

CONSTRAINING THE EVOLVING ARCHITECTURE OF THE PLATE BOUNDARY ZONE THROUGH 3D SEISMIC VELOCITY AND ANISOTROPY MAPPING *Kosarian M, Davis PM, Clayton RW, and Tanimoto T*

The two main data sources for seismic anisotropy in Southern California, SKS splitting data and surface wave data, show inconsistent patterns. The primary goal of this project is to understand the source of this discrepancy and to obtain a seismic structure that satisfies both sets of data. The key must be in the depth variations in anisotropy, as the two types of data have different depth sensitivities. We formulated a scheme to invert surface waves and obtained S-wave velocity anisotropy maps. We present results of crust and mantle anisotropy derived from measurements of core-refracted phases (SKS and SKKS) recorded at stations in Southern California. We calculated splitting parameters using a single layer anisotropy model. We have made new shear wave splitting measurements for 126 seismic stations with best data (50 earthquakes out of 190 earthquakes) for the period of 1990-2008. On average, fast directions are east-west with about 1 second delay. For the surface wave anisotropy model we computed predicted SKS splitting times from the mantle-lithosphere. We find that predicted splitting times are much less than SKS splitting times. The surface wave fast axes directions are also different in that our results are mostly parallel to the relative plate motion direction. Larger variations closer to the major faults also seem to be a new observation. Anisotropic structure derived from surface waves clearly cannot explain SKS splitting data. We suggest that the SKS waves are sensitive to the deeper parts of the upper mantle.

1-126

ANELASTIC EARTH STRUCTURE FROM THE AMBIENT SEISMIC FIELD *Prieto GA, Beroza GC, and Lawrence JF*

Cross correlation of the ambient seismic field is now routinely used to measure seismic wave travel times; however, relatively little attention has been paid to other information that could be extracted from these signals. In this paper we demonstrate the relationship between the spatial coherency of the ambient field and the elastodynamic Green's function in both time and frequency domains. Through measurement of the frequency domain coherency as a function of distance, we sequentially recover phase velocities and attenuation coefficients. From these measurements we

generate 1D shear wave velocity and attenuation models for southern California. The ambient field measurements of attenuation and the exceptional path coverage that results from the many inter-station measurements, allow us to extend Q estimates to higher frequencies than has previously been possible using earthquake data. Measurements from paths that cross major sedimentary basins show both slower wave speeds and lower quality factors than other paths, as expected. Our results indicate that there is a wealth of information available in the spatial coherency of the ambient seismic field.

1-128

UPPER MANTLE P VELOCITY STRUCTURE BENEATH SOUTHERN CALIFORNIA FROM TELESEISMIC TOMOGRAPHY USING LOCAL AND REGIONAL ARRAYS

Schmandt B, and Humphreys ED

Strong seismic heterogeneity in the upper mantle beneath Southern California has been revealed by several tomographic studies. Previous models require complex seismic structure on a variety of length-scales, and include high amplitude velocity anomalies at depths ranging from near Moho to greater than 200 km. Resolution of such structures is limited by the depth distribution of crossing rays, and modeling of finite frequency and ray bending effects on travel times. We use broadband data from USArray, permanent regional networks, and temporary deployments spanning 1997 through 2008 to create a new model of upper mantle P velocity. Our tomographic imaging method uses ray-theoretical travel time sensitivity kernels, and we are currently working on iterative 3-D ray tracing to mitigate ray bending effects. In the future we plan to model S velocity and incorporate new 3-D crustal velocity models in our analysis.

1-129

BASAL CRUSTAL ANISOTROPY BENEATH THE SAN GABRIEL MOUNTAINS AND ADJACENT INNER BORDERLAND: A FOSSIL REGIONAL DETACHMENT? *Zandt G,*

Porter RC, and Ozacar AA

Receiver functions calculated for long-operating seismic stations in southern California located in the San Gabriel Mountains (MWC, CHF) and adjacent Inner Borderland (RPV) exhibit converted phases from the mid- to lower-crust and Moho with large variations in amplitude and polarity reversals on both the radial and transverse components. These data characteristics are similar to those observed at station PKD located in the Salinian terrane near Parkfield, central California. The large amplitudes and small move-out of the phases, and the broad similarity of data patterns on widely separated stations support an origin primarily from a sub-horizontal layer of hexagonal anisotropy with a dipping symmetry axis, rather than planar dipping interfaces. However, in some cases, localized dip or offsets on the interfaces may contribute to complexity in the data (Yan and Clayton, 2007).

Neighborhood algorithm searches for depth and dip of interfaces, and trend and plunge of anisotropy symmetry axis have been completed for station PKD and are in progress for the other stations. At PKD, the best fitting models require a 6-km-thick, high V_p/V_s layer at the base of the crust with slow axis hexagonal anisotropy $> 15\%$ and a slow axis orientation consistent with ENE dipping (~ 35 degree) rock fabric. A very similar anisotropy model is recovered from the preliminary MWC data inversion and is anticipated for the other stations with similar data characteristics.

The orientation of the anisotropy is consistent with a fossilized fabric created from top-to-the-west sense of shear that existed along the length of coastal California during past subduction. Under MWC the top of the anisotropic layer is at ~ 20 km, the approximate depth of the San Gabriel Bright

Spot (SGBS) observed in LARSE I reflection data ~20 km to the east, and modeled by a 500-m-thick, low-velocity layer. Ryberg and Fuis (1998) interpreted it as a possible “master” decollement for active thrust faults in the area. A possible explanation for this apparent age contradiction is that the SGBS is a young feature that was localized at the top of an older and thicker regional detachment layer.

1-130

MARINE SEISMIC STUDY OF THE PACIFIC-NORTH AMERICAN PLATE BOUNDARY *Kohler MD, and Weeraratne D*

To study the Pacific-North America plate boundary in southern California, a diffuse, transpressional, 500+ km wide interplate zone of deformation, we present plans to deploy 24 ocean bottom seismometers (OBS) in a passive seismic experiment offshore. This experiment will complement the simultaneous recording of excellent land based instruments provided by arrays such as the California Integrated Seismic Network (CISN) and the recent occupation of USArray and improve our understanding of the physical properties and deformation style of the Pacific plate contributing to plate boundary dynamics. The marine seismic experiment, to be deployed in July 2010 for a 12 month period, will extend westward across the borderlands, cover the Arguello and Patton microplates, and include relatively undisturbed ~9 My Pacific seafloor at its western most extent. Data and results from this work will be integrated with crustal and lithospheric studies in the SCEC program to improve our understanding of the plate boundary considering both North American and Pacific plate dynamics and deformation. Three-dimensional variations in upper mantle seismic velocity, seismic anisotropy, and improved local earthquake location by surface wave, body wave, and shear wave splitting analysis will be used to identify variations in lithospheric plate thickness, faulting, plate fracture, rotational dynamics, and mantle flow patterns at mantle depths for comparison with surface observables and styles of deformation on the North American crust and lithosphere. Seismic anisotropy will also be utilized to differentiate between recent models for asthenospheric flow in western north America. Extended seismic coverage by OBS's offshore is also expected to produce a more accurate offshore hypocenter catalog that can be used to identify spatial relationships between background seismic activity with mapped offshore faults.

1-131

MODELING SOUTHERN CALIFORNIA CRUSTAL ANISOTROPY USING TELESEISMIC RECEIVER FUNCTIONS *Culp DB, Sheehan AF, Schulte-Pelkum V, and Shearer PM*

The detection and modeling of seismic anisotropy is a powerful tool for mapping 3-dimensional crustal fabrics in a variety of tectonic settings. Crustal deformation can lead to fabric development in the middle and deep crust, which may result to zones of seismic anisotropy, detectable by a variety of methods. Recent improvements in teleseismic converted wave (receiver function) techniques can be used to provide insight into kilometer-scale crustal structures under Southern California. While there have been numerous studies of receiver functions in Southern California in the past, few have emphasized features in the midcrust or anisotropic signatures from the converted waves. The current research builds upon our previous work with crustal anisotropy and converted waves in the Himalaya and New Zealand, with new applications to the broadband seismic stations of the Southern California Seismic Network. Focusing on the highest quality long-term stations in the greater Los Angeles area, which are most likely to have a good distribution of teleseismic events with backazimuth, we have begun to model crustal features, including depth to Moho, midcrustal arrivals, and possible anisotropic structures. Anisotropic features can be modeled using the observed backazimuthal variations in the radial and transverse receiver

functions. Strong patterns with back-azimuth have been recognized at a number of stations, which we will model in terms of underlying structure. Our ultimate plan is to trace the structures modeled at the long-term seismic stations to those from dense shorter-term deployments in order to create a map of midcrustal interfaces beneath the Los Angeles region. These analyses will help determine the extent that detachment surfaces found in 1D reflection/refraction profiles in the Los Angeles region continue laterally, and will provide information complementary to ongoing seismicity, structure, and deformation modeling studies of the region.

1-132

SUBSURFACE STRUCTURE BENEATH SAN FERNANDO VALLEY, SOUTHERN CALIFORNIA, BASED ON SEISMIC, POTENTIAL-FIELD, AND WELL DATA

Langenheim VE, Okaya DA, Wright TL, Fuis GS, Thygesen K, and Yeats RS

We provide new perspectives on the subsurface geology of San Fernando Valley, home of two of the most recent damaging earthquakes in southern California, from analysis of multichannel seismic profiles acquired by the petroleum industry, interpretation of potential-field data, and the LARSE (Los Angeles Regional Seismic Experiment) II deep-crustal profiles. The combined geological and geophysical datasets permit a new 3-D analysis of this basin, with structure contour maps of various Quaternary to Miocene horizons providing insight into the bounding structures of this valley.

Seismic reflection data are primarily located in the north central and southwestern parts of the valley and provide depths to four Quaternary to Miocene horizons, showing in greater detail the Northridge Hills anticline and the Mission Hills syncline as well as additional smaller folds throughout the valley. These data also reveal a down-to-the-north fault beneath the Northridge Hills thrust fault that corresponds to thinning of the Neogene section and narrowing of the Northridge Hills anticline and a north-dipping unconformity at the base of the Plio-Pleistocene Saugus Formation. Beneath the base of the late Miocene Modelo formation are largely non-reflective rocks of the Topanga and older formations. Crystalline basement is only imaged on one profile in the SE part of the valley, revealing a down-to-the-north fault that does not offset the top of the Modelo. Gravity data show that this fault strikes NW and bounds a concealed basement high, which influenced the Miocene Tarzana fan. LARSE refraction data image basement.

Gravity and seismic-refraction data indicate that the basin underlying San Fernando Valley is asymmetric, with the north part of the basin reaching depths of 5-8 km. LARSE II data show that the basin fill in the north part of the valley has higher velocity than that south of the Mission Hills fault. Magnetic data suggest a major boundary at or near the Verdugo fault, the SE margin of the basin, and show a change in the dip sense of the fault along strike. The western margin of the basin as defined by gravity data is linear and strikes about N45E. The NE-trending gravity gradient follows part of the 1971 San Fernando aftershock distribution called the Chatsworth trend and the aftershocks of the 1994 Northridge earthquake. These data may suggest that the 1971 San Fernando and 1994 Northridge earthquakes may have reactivated portions of Miocene normal faults.

1-133

NON-VERTICAL DIPS OF THE SOUTHERN SAN ANDREAS FAULT AND THEIR RELATIONSHIPS TO MANTLE VELOCITIES, CRUSTAL TECTONICS, AND EARTHQUAKE HAZARD *Scheirer D, Fuis GS, Langenheim VE, and Kohler MD*

The San Andreas Fault (SAF) in southern California is in most places non-vertical, based on seismic-imaging, potential-field, earthquake-aftershock, and selected microseismicity studies of the crust. The dip of the SAF changes from SW (55-75 degrees) near the Big Bend to NE (10-70 degrees)

southeastward of the eastern San Gabriel Mountains, forming a crude propeller shape. The uncertainty of most of the dip observations is about 5-10 degrees. To examine the geometry of the fault surface, we have developed a three-dimensional model of a dipping SAF, extending from Parkfield in central California to the SAF's southern termination at the Salton Sea. Knowledge about the dip of the SAF is important for estimating shaking potential of scenario major earthquakes and for calculating geodetic deformation.

In sections across the SAF, P-wave tomographic images of the mantle beneath southern California (Kohler et al., 2003) suggests that the plate boundary extends into the mantle and is continuous with the SAF in the crust. The dip of the plate boundary appears to steepen in the mantle. Seismicity sections across the locked part of the SAF, from Indio towards the northwest, reveal different seismicity regimes on either side of our model SAF surface, but do not reveal the fault itself. These differences include changes in the maximum depth of the seismogenic zone and in the abundance of seismicity over the past ~20 years. The different seismicity regimes may reflect changes in physical properties and/or stress state of the crust on either side of the SAF at seismogenic depths. Mantle velocities southwest of this projected plate boundary, within the Pacific Plate, are relatively high and constitute the well documented upper-mantle high-velocity body of the Transverse Ranges. This relationship is similar, in some ways, to that between the Alpine fault of New Zealand and its underlying mantle, and suggests that in both California and New Zealand, Pacific lithospheric mantle is downwelling along the plate boundary (Fuis et al., 2007).

1-134

GEOLOGY AND TECTONICS OF THE CHOCOLATE MOUNTAINS *Powell RE, and Fleck RJ*

The Chocolate Mountains (CM), situated along the NE margin of the southern Salton Trough, lie NE of the post-5-Ma San Andreas (SA) fault and SW of the southeastward projection of the early and middle Miocene Clemens Well (CW)-Fenner-San Francisquito-SA strand of the SA system. The CM are the western part of a highly extended terrain in SE CA and SW AZ that evolved during the late Oligocene-middle Miocene and is bounded to the NE by the CW-SA fault.

The principal structural feature in the CM is a complexly faulted, NW-trending array of en echelon antiforms that runs the length of the range and continues into AZ. Orocochia Schist in the core of the antiforms is structurally overlain by Proterozoic rocks (augen/pelitic/layered gneiss; anorthosite-syenite) and Mz mylonite, orthogneiss, and plutonic rocks (TR Mt Lowe, J mafic and intermediate rocks) at the ductile CM thrust.

All these units are intruded by a late Oligocene composite batholith comprising plutons of gabbrodiorite, granodiorite, and granite. Dacitic to rhyolitic hypabyssal, volcanic, and pyroclastic rocks cap the batholith, and are coeval with it. Younger Miocene volcanic rocks also are present.

Structure in the CM manifests late Oligocene-middle Miocene extensional tectonism that culminated in exhumation of Orocochia Schist by tectonic denudation. Tectonism was accompanied by sedimentation and by magma-generation forming the batholith and its volcanic cap. Brittle extensional faulting has largely reactivated and cut out the ductile CM thrust and has created a stack of fault plates in the basement rocks above the thrust and in a superjacent steeply west-tilted section of syntectonic Oligocene-Miocene redbeds, megabreccia, and volcanic and volcanoclastic rocks. Along the NE flank of the CM, the extensional fault stack was dropped to the NE along a normal fault representing final phase of extension.

Field relations and dating the widespread Cz igneous rocks allows us to bracket intervals of extensional deformation between the late Oligocene and middle Miocene. In the context of an ongoing or intermittent extensional regime between about 28 and 13 Ma, our ^{40}Ar - ^{39}Ar dates and many published K-Ar dates indicate intervals of extensional faulting ca 28-24 Ma, 24 to 20 Ma, and 19 to 13 Ma. The latter interval is coeval with displacement on the CW-SA strand of the early SA system, suggesting that diminishing strike-slip displacement on that fault is accommodated southeastward on CM normal faults.

1-135

DOES THE WEST SALTON DETACHMENT EXTEND THROUGH SAN GORGONIO PASS, SOUTHERN CALIFORNIA? *Matti JC, and Langenheim VE*

We use geologic and geophysical data to speculate on continuation of the West Salton Detachment (WSD)—a key element of the early San Andreas Fault system—northwestward beyond its last known occurrence along the east side of the Santa Rosa Mts. We propose that the WSD originally extended from the NW head of Coachella Valley west into San Gorgonio Pass (SGP), where the detachment probably forms the base of the late Cenozoic marine and terrestrial sedimentary sequence south of the Banning strand of the San Gabriel Fault. The WSD probably continues west beyond SGP, with extensional translation decreasing until the detachment intersects the Banning Fault near Calimesa. There, we propose that the WSD bounds a subsurface sedimentary package north of the San Timoteo badlands and south of the Banning Fault that a gravity low suggests is 2 km thick, and that purportedly contains marine sediment penetrated in boreholes. When ~44 km of right-slip is restored on the Banning Fault (Matti and Morton, 1993), the gravity low restores opposite a similar low in the northwestern Coachella Valley. The juxtaposed gravity lows thus mark a late Cenozoic depocenter that formed at the northwestern head of the nascent Salton Trough during evolution of the San Gabriel and San Andreas Faults (10 Ma to 1.2 Ma).

This reconstruction has several implications: (1) the WSD was active while the late Cenozoic sedimentary sequence in SGP accumulated in its hangingwall at 7 Ma (marine Imperial Fm) and probably as early as 8-9 Ma (Hathaway Fm); (2) At that time the San Jacinto Mts (SJM) began to rise in the WSD footwall, shedding sediment and landslide breccia into the SGP basin. Simultaneously, Transverse Ranges sources shed sediment southwest, south, and southeast into the SGP basin and the adjoining San Timoteo basin; (3) Prior to disruption by right-slip on the Banning Fault, the WSD probably extended around the NW head of the nascent Salton Trough, where the detachment would have separated crystalline rock of SGP from hangingwall deposits of the Salton Trough (Coachella Fanglomerate, Imperial and Painted Hill fms). The enigmatic Whitewater Fault in the SE San Bernardino Mts may be the WSD. (4) Because extensional translation on the WSD diminished westward through SGP, it is doubtful that >3 km of topographic relief on the WSD footwall in the SJM resulted only from footwall uplift during the period 8-9 Ma to 1.2 Ma. Quaternary uplift must account for an unknown component of this relief.

1-136

CONTROLLED-SOURCE SEISMIC IMAGING OF RIFT PROCESSES AND EARTHQUAKE HAZARDS IN THE SALTON TROUGH *Hole JA, Stock JM, and Fuis GS*

The NSF MARGINS program, the NSF EarthScope program, and the U.S. Geological Survey have funded a large seismic refraction and reflection survey of the Salton Trough in southern California and northern Mexico, including the Coachella, Imperial, and Mexicali Valleys. The goals of the project include both rifting processes at the northern end of the Gulf of California extensional province and earthquake hazards at the southern end of the San Andreas fault system. In the central Salton Trough, the 20-22 km thick rifted crust is apparently composed entirely of new crust

Poster Abstracts | Group 1 – Geology, SoSAFE

added by magmatism from below and sedimentation from above. The seismic survey will image the effects of rapid sedimentation upon extension and magmatism during continental rifting. The vertical and lateral partitioning of strain will be investigated in this oblique rift. The southernmost San Andreas Fault is considered at high risk of producing a large damaging earthquake, yet structure of the fault and adjacent basins are not currently well constrained. The seismic survey will image the structure of the San Andreas and Imperial Faults, structure of sedimentary basins in the Salton Trough, and three-dimensional seismic velocity of the crust and uppermost mantle. Fieldwork is tentatively scheduled for January 2010. The purpose of this poster and a workshop to be held immediately after the 2008 SCEC meeting is to communicate plans for the seismic project and encourage synergy with piggyback and complementary studies.

Group 2. Poster Abstracts

Plaza Ballroom, Hilton Palm Springs Resort

Unified Structural Representation (USR)

2-019

MOMENT TENSOR INVERSIONS FOR ADJOINT TOMOGRAPHY OF SOUTHERN CALIFORNIA *Liu Q (Caltech), Tape CH (Caltech), Maggi A (EOST), and Tromp J (Princeton)*

We compute source mechanisms and depths for earthquakes used in adjoint tomography studies of the southern California crust (Tape et al., 2009), including 143 crustal earthquakes used in the tomographic inversions as well as 91 earthquakes that are used in the subsequent validation of the tomographic model. Our source inversions use Green's functions computed based on the latest 3D adjoint tomographic model and require 7-9 spectral-element simulations per earthquake (Liu et al., 2004). We fit synthetic and observed waveforms filtered between 2 and 30 seconds to achieve optimal source mechanisms. These 3D moment-tensor inversions are incorporated within the tomographic inversion, and they also provide a robust catalog of source mechanisms. These source mechanisms in most cases are similar to those inverted by other methods (e.g., "cut-and-paste" method), but in some cases show significant differences that can be validated using 3D forward simulations. We plan to routinely invert for southern California earthquakes with $M_w \geq 3.5$ using the latest tomographic model.

2-020

SEISMIC TOMOGRAPHY OF THE SOUTHERN CALIFORNIA CRUST BASED ON SPECTRAL-ELEMENT AND ADJOINT METHODS *Tape CH (Caltech), Liu Q (Caltech), Maggi A (EOST), and Tromp J (Princeton)*

We iteratively improve a three-dimensional tomographic model of the southern California crust using numerical simulations of seismic wave propagation based upon a spectral-element method (SEM) in combination with an adjoint method. In Tape et al. (2009) we presented the tomographic technique and a succinct analysis of misfit and resolution. Here we present a detailed misfit analysis that considers three different measures of misfit: a simple waveform difference and frequency-dependent traveltime and amplitude differences. We illustrate several key aspects of the tomographic technique using selected seismograms. For example, some seismic waveforms that are not present in our initial-model synthetics are revealed using the final-model synthetics. Our simulations produce seismic waveforms due to strong 3D heterogeneity, such as basin resonance and laterally reflected surface waves. Earthquakes occurring in the upper 8 km of the crust excite numerous sedimentary basins and provide the most challenging tests for wavefield simulations. Future efforts will incorporate lateral and vertical interfaces, 3D-varying anisotropy, and a more detailed attenuation model.

2-021

CVM-H 6.0: INVERSION INTEGRATION, THE SAN JOAQUIN VALLEY AND OTHER ADVANCES IN THE COMMUNITY VELOCITY MODEL *Plesch A (Harvard), Tape CH (Caltech), Shaw JH (Harvard), and of the USR working group m*

We present a new version of the Community Velocity Model CVM-H (CVM-H 6.0). Responding to community feedback, we implemented a number of incremental improvements to the velocity

Poster Abstracts | Group 2 – USR

model and to its delivery format. In addition, there are two fundamental improvements to the model. First, the background model incorporates the results of Tape et al. (2009) ("model m16"), who used an adjoint-based iterative tomographic inversion. Second, we include a velocity description for the San Joaquin sedimentary basin. These major changes are delivered in alternative velocity models.

Based on feedback by users at the 2008 meeting and over the course of the year, a number of improvements were made. We adjusted the V_s background model in the crust in such a way that the V_p/V_s ratio is geophysically sensible everywhere in the model including interpolated transition zones. We also adjusted the density scaling relationship from one based on well log calibration in the L.A. basin to the widely used Nafe-Drake curve which delivers reasonable densities over a wider range of velocities including the middle and lower crust. We assessed the difference between our own calibration and the Nafe-Drake curve at sedimentary velocities (< 3 km/s) and found that it is too small to warrant a composite description. The background model was further improved by removing an artificial discontinuity at the boundary between the tomographic model and the mantle model at 30 km depth. The models transition now more smoothly. Finally, the GTL in the Salton Trough was improved by removing velocity inversions which had been introduced by sampling the SCEC CVM 4.0. On the delivery side, we adjusted the query and delivery code to provide higher precision in its coordinate handling and output so that input coordinates can be precisely repeated.

The CVM-H has long been used to forward model waveforms using various techniques such as the spectral-element method (SEM). One of the stated objectives of developing a data-driven velocity model is to integrate the results of such modeling back into the CVM-H. Here, we provide an alternative model (CVM-H 6.0b) which feeds back model m16 into the background model, which is used outside and below the sedimentary basin in CVM-H. The integration of m16 included representing the Moho discontinuity as a variable depth interface in the model. For this purpose we compiled a surface based on several published data sets (e.g., Yan and Clayton, 2007) and an overall understanding of how the Moho tapers from continental to oceanic crust. Above the Moho surface, model m16 was used to populate the model whereas below the Moho T. Tanimoto's mantle model continued to be used. Finally, the replacement of the background model required a reparametrization of the GTL in the basement areas.

The second major improvement in CVM-H is the representation of the San Joaquin Valley, a sedimentary basin, in the model. The San Joaquin Valley is one of the defining tectonic units of southern and central California, houses population and economic centers, and has experienced significant historical earthquakes. Our representation consists of a basement surface as a main velocity interface, a well-log and stacking velocity based basin velocity model, and a tomographic background model. We defined the basement surface using ca. 540 wells which record the position of the top of the basement, as well as dozens of published maps and cross sections from local studies. The velocity model in the basin was constructed by kriging of sonic logs from ca. 250 wells and of stacking velocities along ca. 1200 line kilometers of reflection seismic. Below the basement interface the background velocity field is provided by model m16 where available or a 1-d velocity model. The resulting velocity model for the San Joaquin Valley was combined with CVM-H 6.0b and is available as CVM-H 6.0c.

2-022

CENTRAL UNITED STATES VELOCITY MODEL VERSION 1: DESCRIPTION AND VALIDATION *Ramirez-Guzman L (CMU), Williams R (Univ. of Tennessee), Boyd OS (USGS), and Hartzell S (USGS)*

We describe and test via numerical simulations a velocity model of the Central United States (CUSVM Version 1). Our model covers an area of 650,000 km² and includes parts of Arkansas, Mississippi, Alabama, Illinois, Missouri, Kentucky and Tennessee. The model represents the compilation of research carried out for decades consisting of seismic refraction and reflection lines, geophysical logs, and inversions of the regional seismic properties. The CUSVM has a higher resolution description around Memphis and St. Louis, two of the largest urban areas in the Central United States. The density, p- and s-wave velocities are synthesized in a stand-alone spatial data base that can be queried to generate the required input for numerical simulations. We calibrate the CUSVM using three earthquakes located N, SW and SE of the zone encompassed by the model to sample different paths of propagation. The selected stations in the comparisons reflect different geological site conditions and cover distances ranging from 50 to 450 km away from the epicenters. The results indicate that both within and outside the Mississippi embayment, the CUSVM satisfactorily reproduces: a) the body wave arrival times and b) the observed regional variations in ground motion amplitude and duration in the frequency range 0-0.75Hz.

2-023

A 3-D SEQUENCE-BASED STRUCTURAL MODEL FOR THE QUATERNARY LOS ANGELES BASIN, CALIFORNIA *Ponti DJ (USGS), and Ehman KD*

A 3-D sequence-based structural/stratigraphic model for the Los Angeles Basin is being developed by the USGS for use in earthquake hazards and ground water resources research. The model builds upon the Quaternary sequence-stratigraphic framework developed in Long Beach (Ponti and others, 2007) and incorporates the entire LA County portion of the basin, much of Santa Monica and San Pedro bays, and a small portion of northwestern Orange County from La Habra southwest to Sunset Beach.

The model comprises 8 Quaternary and 3 late-Pliocene units. All but two of the units are unconformity-bound stratigraphic sequences that can be correlated throughout the basin and consist primarily of sea-level high-stand tract deposits. The other two units occur in the central basin only and are identified based on their distinctive hydrologic properties. Structural control for the model is obtained from oil-industry seismic-reflection data (central LA basin), high-resolution marine seismic-reflection data (San Pedro Bay) and more than 680 water and oil well electric logs. Age control and relevant stratigraphic information are derived from core samples obtained from several dozen water wells and geotechnical borings throughout the basin, although the cored holes are concentrated in the Long Beach and north-central LA basin areas.

The Quaternary section reaches a maximum thickness of more than 1280 m in the Lynwood area east of the Newport-Inglewood (N-I) fault zone. In the west basin, the Quaternary section reaches its greatest thickness (>410 m) in San Pedro Bay just east of the Palos Verdes fault. Of the inter-basin structures that impact the Quaternary section, the Compton-Alamitos fault (Wright, 1991) is the most prominent. Discreet faulting of mid-late Pleistocene deposits and structural relief of up to 300 m is suggested by the seismic data and by anomalous water levels near Los Alamitos. West of the N-I fault, two W-NW-trending inter-basin faults offset mid-late Pleistocene sediments and may serve to consume slip from the N-I. The M4.7 Hawthorne earthquake of May 18, 2009 was located near the northernmost of these structures and has a fault-plane solution consistent with the geometry and kinematics of this fault as evidenced in the geology.

Development of the model is ongoing. Next steps are incorporation/reconciliation of the SCEC CFM and the addition of lithologic facies as a preface to a revised geologically-based shear-wave model for the upper 400 m of the LA basin.

2-024

MERGENCE OF THE PALOS VERDES, SAN PEDRO BASIN, AND SAN DIEGO TROUGH FAULT ZONES: A 220+ KM-LONG FAULT SYSTEM *Alward WS (Missouri), Sorlien CC (UCSB), Bauer RL (Missouri), and Campbell BA (Missouri)*

The Palos Verdes fault (PVF) extends from Santa Monica Bay southward to Lasuen Knoll, cutting onshore from Redondo Beach to Long Beach. It has previously been shown to be a right-lateral fault with over 3 mm/yr of Holocene slip and over 5 km of post-Miocene right slip near and offshore of Long Beach (McNeilan et al., 1996 JGR; Brankman & Shaw, 2009 BSSA). Previous workers also have interpreted the southern extension of the PVF zone to terminate south-southeast of Lasuen Knoll, with a total fault length of approximately 100 km. Employing high resolution USGS and petroleum industry seismic reflection data, we have evaluated the southern PVF and both the San Pedro Basin and San Diego Trough faults. The focus of the study has been in the offshore region extending from Newport Beach to San Diego. Top Repetto (~2.5 Ma), Top Delmontian (~4.5 Ma), and Top Lower Pico (~1.8 Ma) stratigraphic horizons were correlated and digitally represented to help constrain timing and kinematics.

We have interpreted a revised southern continuation for the PVF. Instead of terminating just south of Lasuen Knoll, it bends and continues due south to merge with the NNW-striking San Diego Trough fault. This newly mapped releasing segment is associated with up to a 3 km-wide zone of normal-separation faults, especially near the northern bend. Additionally, the San Pedro Basin fault merges with the San Diego Trough fault and PVF near the northern end of San Diego Trough. This zone of mergence is in agreement with the linkage of San Pedro Basin and San Diego Trough faults mapped by Conrad and others (2008, AGU Fall Meeting). Our digital horizon maps do not reveal transverse folds or extension that could absorb several km of post-Miocene right slip near the previously proposed southern termination of the PVF. No significant through-going faults are imaged that could carry such slip southeastward. A trend of anticlines and discontinuous shallow faults connects the Lausen segment of the PVF southeastwards to the Coronado Bank fault zone. Because the strand that connects to the San Diego Trough fault is more through-going, we hypothesize that the majority of PVF displacement is carried by this releasing segment. Multibeam bathymetry images scarps along the San Diego Trough fault into Mexican waters. The PVF -San Diego Trough fault is thus a 220 km minimum length system.

2-025

QUATERNARY DEFORMATION RELATED TO 3D GEOMETRY OF THE CARLSBAD FAULT, OFFSHORE SAN CLEMENTE TO SAN DIEGO *Campbell BA (Missouri), Sorlien CC (UCSB), Cormier M (Missouri), and Alward WS (Missouri)*

This study examines the Quaternary deformation between the Newport-Inglewood fault and the basin southwest of the Carlsbad fault, offshore San Clemente to San Diego. Industry and high-resolution USGS seismic reflection surveys were used, complemented by a 100m bathymetric grid. The ~1.8 Ma Top Lower Pico of Wright (1991) was correlated through the dataset. It is an unconformity which truncates minor extensional faults throughout the basin. An ~2.5 Ma unconformity was also correlated through the area.

Interpretation reveals NW-striking faults, including the Carlsbad fault which outcrops intermittently along the base of the slope and the Newport-Inglewood fault along the Continental

Shelf. The interpreted 55 km-long segment of the Carlsbad fault displays a moderate dip to the northeast. This fold-fault trend continues an additional 20 km to offshore Newport Beach. Quaternary horizons exhibit a varying degree of reverse separation across this segment, though underlying Miocene horizons display normal separation. Preliminary interpretation of thickness variations between the ~1.8 Ma and ~2.5 Ma horizons suggests that transpressional folding initiated ~end Pliocene in the hanging-wall of the Carlsbad fault, synchronous with transtension in the footwall basin. At the southeast terminus of this segment, the fault bends 70 degree, stepping right by 17 km, and merges with the Coronado Bank Miocene detachment fault. Parts of this Carlsbad-Coronado Bank fault system coincide with the Oceanside thrust and Carlsbad thrust of Rivero et al. (2000). Near the 70 degree bend, Quaternary separation shifts abruptly from reverse to normal, and faults within the stepover have consistent normal separation in Quaternary strata.

In addition to the major right-stepover, more subtle bends characterize the NNW-striking segment. Overall, the deformation along the fault is typical of a moderately dipping right lateral fault, showing reverse structural relief in the left-stepping bends and reacting more sedately near right-stepping bends. The right-lateral Newport-Inglewood fault is located in the hanging-wall of the Carlsbad fault. Evidence for at least a component of right-lateral slip on the Carlsbad fault implies incomplete partitioning of right-lateral motion. Trigonometric analysis will quantify the finite Quaternary displacement along the Carlsbad fault and test whether it is a right-lateral fault or a right-reverse oblique-slip fault.

2-026

TRANSPRESSION ALONG STRIKE-SLIP RESTRAINING SEGMENTS VS. REGIONAL THRUSTING IN THE INNER CALIFORNIA CONTINENTAL BORDERLAND *Sorlien CC (UCSB), Campbell BA (Missouri), Alward WS (Missouri), Seeber L (LDEO), Legg MR (Legg Geophysical), and Cormier M (Missouri)*

Quaternary contractional anticlines and anticlinoria are present in and around Los Angeles basin and throughout the California Continental Borderland. There is wide agreement that the Puente Hills are folding above an active deeply-rooted blind thrust fault. In contrast, there is disagreement on the extent and cause of the Palos Verdes anticlinorium. It has been described as several anticlines, with Palos Verdes Hills associated with a non-vertical restraining segment in the right-lateral Palos Verdes fault, or as a single anticlinorium folding above a SW-directed thrust wedge. We interpret it as a single anticlinorium formed both by the Palos Verdes Fault restraining segment and a regional thrust fault rooted beneath Los Angeles. The belt of contractional folding steps left and continues along the continental shelf and slope to Oceanside.

We interpreted multiple dense grids of industry and high resolution USGS seismic reflection data together with a 100 m bathymetric grid. Digital ~1.8 Ma, ~2.5 Ma, and ~4.5 Ma horizons were created over a large part of the Inner Borderland. We also interpreted most of the significant offshore Quaternary faults between Long Beach and San Diego west to Catalina Island and San Diego Trough.

Many of the seafloor knolls are associated with local restraining segments in the linked right-lateral San Pedro Basin, Palos Verdes, and San Diego trough faults (Alward et al., this meeting). We have investigated the SCEC Community Fault Model Oceanside thrust and found it to coincide with parts of the Carlsbad fault and the Coronado Bank detachment (Campbell et al., this meeting). The Oceanside thrust cuts north between these 2 faults, where it is generally normal-separation, has little effect on the ~2.5 Ma horizon above its shallow tip, and a regional anticline expected due to deeper blind thrust slip beneath the Gulf of Santa Catalina is lacking. Adjoining faults with north

strikes are right-lateral. Significant Plio-Quaternary folding is only present where the Oceanside thrust bends to merge with the Carlsbad fault. Quaternary slip on the moderately NE-dipping Carlsbad fault is oblique-right reverse between Oceanside and San Clemente. It flattens between San Clemente and Newport Beach, with steeply progressively tilted Pliocene and Quaternary strata above it. This suggests that SW-verging thrust slip contributes to uplifting the continental shelf above the subsiding basin, as well as to uplift of the San Joaquin Hills.

2-027

REVISED 3D FAULT MODELS FOR CFM ALONG THE SOUTHERN SAN ANDREAS AND ELSINORE-EARTHQUAKE VALLEY FAULT SYSTEMS *Nicholson C (UCSB), Hauksson E (Caltech), Plesch A (Harvard), and Shearer PM (UCSD)*

Hypocenter and focal mechanism nodal plane alignments are used to identify the geometry and sense of slip of active fault segments at depth. At issue is whether these more complex models defined by the microearthquakes are necessarily representative of the primary, through-going slip surface, or whether these structures illuminated by seismicity only represent adjacent secondary faults. This issue is particularly important along the San Andreas fault (SAF), where various sections are largely aseismic and where various fault models -- both simple and complex -- have been proposed. In the northern Coachella Valley, however, seismicity indicates that the Garnet Hill and Banning fault strands are most likely sub-parallel (with dips of $\sim 70^\circ$ NE) to depths of 8–10 km, where they intersect and possibly merge with a stack of low-angle thrust faults. Gravity and water well data confirm that these faults are sub-parallel and near vertical in the upper 2–3 km, suggesting that these faults tend to decrease dip with depth. The active Mission Creek fault (MCF) appears to increase dip along strike SE from $\sim 60^\circ$ NE to $\sim 80^\circ$ NE in the Indio Hills. Gravity and velocity modeling also suggest that the Mission Creek fault is moderately NE-dipping, although this modeled velocity/density contrast likely reflects an older ancestral(?) basin-bounding MCF, which tends to act as the lower bound to adjacent seismicity located farther east. SE to North Shore and at Bombay Beach, a few events do locate directly beneath the SAF surface trace, suggesting that a vertical SAF is permissible here. Through the Mecca Hills, seismicity east of the surface trace is clearly related to adjacent secondary faults. Although clusters of hypocenters and nodal planes near North Shore and Salt Creek project to the SAF surface trace with dips $\sim 65^\circ$ NE, these events also appear to be more closely related to slip on intervening secondary fault splays, and not necessarily to slip on the SAF itself. Along the Elsinore-Earthquake Valley fault system, hypocenter and nodal plane alignments exhibit a similar pattern of active multiple fault strands that are often sub-parallel throughout the seismogenic zone, and that change dip and dip direction along strike and with depth. As a result, we have developed alternative 3D fault models for these various active fault segments, and have relaxed the assumption that strike-slip faults are necessarily vertical, or exhibit constant dip and dip direction either along strike or down dip.

2-028

CALIBRATION SHOTS RECORDED FOR THE SALTON SEISMIC IMAGING PROJECT, SALTON TROUGH, CALIFORNIA *Murphy JM (USGS), Rymer MJ (USGS), Fuis GS (USGS), Stock JM (Caltech), Goldman MR (USGS), Sickler RR (USGS), Miller SA, Criley CJ, Ricketts J, and Hole JA (Virginia Tech)*

The Salton Seismic Imaging Project (SSIP) is a collaborative venture between the U.S. Geological Survey, Caltech, and Virginia Tech, to acquire seismic reflection/wide angle refraction data, and currently is scheduled for data acquisition in 2010. The purpose of the project is to get a detailed subsurface 3-D image of the structure of the Salton Trough (including both the Coachella and Imperial Valleys) that can be used for earthquake hazards analysis, geothermal studies, and studies of the transition from ocean-ocean to continent-continent plate-boundary.

In June 2009, a series of calibration shots were detonated in the southern Imperial Valley with specific goals in mind. First, these shots were used to measure peak particle velocity and acceleration at various distances from the shots. Second, the shots were used to calibrate the propagation of energy through sediments of the Imperial Valley. Third, the shots were used to test the effects of seismic energy on buried clay drainage pipes, which are abundant throughout the irrigated parts of the Salton Trough. Fourth, we tested the ODEX drilling technique, which we had not used in past projects. Information obtained from the calibration shots will be used for final planning of the main project.

The shots were located in a unused field adjacent to Hwy 7, about 6 km north of the U.S. /Mexican border (about 18 km southeast of El Centro). Three closely spaced shot points (16 meters apart) were aligned N-S and drilled to 21-m, 23.5-m, and 27-m depth. The holes were filled with 23-kg, 68-kg, and 123-kg of ammonium-nitrate explosive, respectively. Four instruments types were used to record the seismic energy – six RefTek RT130 6-channel recorders, seven RefTek RT130 3-channel recorders, 35 Texans, and a 60-channel 40-Hz cabled array.

Irrigation districts in both the Coachella Valley and Imperial Valley use clay drainage pipes buried beneath fields to remove irrigation water and prevent ponding. To determine the effect of seismic energy on the drain pipes, we exposed sections of pipe several meters long with a backhoe at distances of 7-15 meters from the shot holes, and, after each shot, visually inspected the pipes. Our shots produced no pipe damage.

2-029

CONSTRAINING SEDIMENTARY BASIN-BASEMENT INTERFACE WITH CONVERTED BODY WAVES: A CASE STUDY AT CHINO *Ni S (UNR), Luo Y (Caltech), Zeng X (University of Science and Technology of China), and Graves RW (URS)*

Deterministic ground motion simulation in southern California has been quite successful for frequencies below 0.5HZ, and pushing to higher frequency (1Hz or higher) requires better understanding of short scale crust structure. In particular, the velocity structure of sedimentary basins, the velocity contrast across them, and the geometry of the basin-basement interface have a controlling influence on the ground motions. Situated in the Chino basin and just north of the Chino fault, the CHN station recorded high quality three-component waveforms from the 2008 Chino Hills earthquake aftershocks, with typical predominant frequency of 2Hz and above. Most of the records show clear P and S waves, yet between the P and S arrivals we also observe signals almost as strong as the P waves but weaker than S waves. The horizontal signals appear on both radial and tangential components, suggesting an origin due to non 1D structure. With a dozen events from the 2008 Chino Hills as an “event array”, we are able to demonstrate that these signals are converted waves when P and S waves cross the bottom of the Chino basin. The signals on the vertical components are Sp waves (converted to P waves when S crosses the interface), arriving before the S wave, and the signals on the horizontal components are Ps waves, which lag the P wave with almost the same time interval as the interval between Sp and S. The Ps on the tangential component can be explained by a dipping interface. The strong amplitudes of these converted waves indicate a strong velocity contrast across the interface. Finite difference calculations with the SCEC CVM do not adequately match the timing interval between Ps and P (or Sp and S) or the amplitude ratio of Ps/P (or Sp/S). We also attempt to model these converted waves with 3D ray-based synthetic seismograms for a few forward models. Models of the dipping interface with appropriate velocity contrast will be presented. Our modeling suggests that deterministic waveform at high frequency (>1HZ) is possible for close-in records where waves are converted only once or twice, when the basin structure is well understood. Conversely, those close-in records

are valuable for constraining the geometry of and velocity contrast across basins, thus contributing to more accurate ground motion simulation.

2-030

S-WAVE VELOCITY STRUCTURE WITHIN THE LA BASIN USING AMBIENT NOISE
Yano TE (UCSB), and Tanimoto T (UCSB)

The shallow S-wave velocity structure, in particular within the LA basin, will provide improvement of community velocity models (CVM-H 5.2) used for strong ground-motion prediction for future earthquake scenarios in southern California. We are attempting to establish such shallow structure using phase velocity and particle motion data of Rayleigh waves.

For phase velocity measurement, first we correlate the vertical component of ambient seismic noise data to determine station-to-station Green's functions. These Green's functions let us measure a phase velocity of each path between stations. We used records on 82 broadband stations for at most 4 years, with dense coverage in the greater Los Angeles area. In addition to phase velocity, we also measured ZH ratio of 158 broadband stations within 0.13 Hz and 0.37 Hz for at most 2 years. ZH ratio provides an ellipticity of Rayleigh wave particle motion which relates to its local structure. We investigate shallow S-wave velocity structures and basin determined by using these two independent methods.

Phase velocities for dominant Rayleigh waves between 0.13 Hz and 0.2 Hz were measured by an ambient-noise Green's function for more than 1000 paths. Ray paths are approximated by straight lines. Phase velocities we measured on path through the basin are usually slower, suggesting a strong path dependency. However, this dependency becomes weaker as higher the frequency. We will also investigate the lower frequency around 0.06 Hz where another dominant Rayleigh waves exist in southern California.

We obtained ZH ratio measurements by the ratio between vertical and horizontal eigenfunctions of Rayleigh waves. In southern California, stable ZH ratio can be obtained between 0.13 Hz and 0.37 Hz although sharp dominant Rayleigh waves exist at 0.15 Hz. These measurements show systematically different pattern depending on the local structure, basin or non-basin region.

Comparing the velocity pattern of CVM-H 5.2 to phase velocity and ZH ratio pattern, slower region should be larger towards east and west than CVM-H 5.2. We take advantage of the fact that ZH ratio has upper 5km sharp sensitivity and phase velocity has sensitivity down to at least 20km, we will perform the joint-inversion using phase velocity and ZH ratio measurement and investigate the difference between CVM-H 5.2 and our result. Getting a clear image of the basin will provide important information for improving future community velocity models.

2-031

IMPLICATIONS OF THE DIFFERENCE IN LOCATIONS BETWEEN QUATERNARY AND GEOPHYSICALLY-MAPPED FAULTS IN THE EASTERN TRANSVERSE RANGES, SOUTHERN CALIFORNIA
Langenheim VE (USGS), Powell RE (USGS), Menges CM (USGS), and Matti JC (USGS)

Comparing locations of faults mapped in Quaternary deposits with those mapped by potential-field techniques offers insight into the evolution of left-oblique transtensional basins that formed along the east-trending fault zones in the Eastern Transverse Ranges. These fault zones occupy a sinistral domain immediately east of the dextral San Andreas transform boundary. A previous study using primarily gravity data defined left-stepping strands of the main through-going

sinistral faults that traverse the Eastern Transverse Ranges north of the Orocopia Mountains. The left steps produce strike-slip basins along the Pinto Mountain, Blue Cut, and Chiriaco faults, with 16-20 km, 5-10 km, and 8-11 km of left slip, respectively. Interpretation of the geophysical data (1) show that the strike-slip basins are significantly narrower than the alluviated valleys along the fault zones and (2) more clearly define the position of these basins by delineating the bounding faults where surficial deposits largely or completely cover the evidence for the surface traces.

New detailed gravity data across the Smoke Tree Wash fault zone, a subsidiary sinistral fault with 1-1.5 km of offset, suggest a small basin that is bounded on the north by the southern strand of the fault zone mapped in surficial deposits. This is consistent with the previous study in that not all the basin boundaries defined by gravity and aeromagnetic data correspond in location with faults mapped in Quaternary deposits. The lack of correspondence could reflect the abandonment of left steps in favor of straighter fault traces, the clockwise rotation of these fault sets into a different stress regime, uplift along the San Andreas fault at the western end of the sinistral domain, or partitioning of slip in space and time. On the northern boundary of the sinistral domain, a location mismatch exists between basins and mapped surface faults along the Pinto Mountain fault zone. Gravity data indicate that a narrow elongate subsurface basin lies south of the transpressive surface faults. The center and southern edge of the buried basin lack surface structural, topographic or depositional expression. These features suggest a shift from transtension to transpression along the fault related to internal fault reorganization, boundary effects of fault-block rotations to the south, and (or) transverse contraction related to intersection with the Mojave domain of NW-trending dextral faults to the north.

Lithospheric Architecture and Dynamics (LAD) Crustal Deformation Modeling (CDM)

2-032

TECTONICS OF THE WESTERN UNITED STATES ILLUMINATED BY SEISMIC SURFACE-WAVE IMAGING *Pollitz FF (USGS), and Snoke JA (VPI & SU)*

We utilize two-and-three-quarter years of vertical-component recordings made by the Transportable Array component of Earthscope in order to constrain three-dimensional (3D) seismic shear-wave velocity structure in the upper 200 km of the western US. Single-taper spectral estimation is used to compile measurements of complex spectral amplitudes from 44,317 seismograms generated by 123 teleseismic events. To determine Rayleigh-wave phase velocity structure in a first step, we implement a new imaging method, which is simpler and more robust than scattering-based methods (e.g. multi-plane surface-wave tomography). The Transportable Array is effectively implemented as a large number of local arrays by defining a horizontal Gaussian smoothing distance that weights observations near a given target point. The complex spectral amplitude measurements are interpreted with the spherical Helmholtz equation using local observations about a succession of target points, resulting in Rayleigh wave phase velocity maps at periods 18 to 125 sec. The derived maps depend on the form of local fits to the Helmholtz equation, which generally involve the non-plane-wave solutions of Friederich et al. (1994). In a second step, the phase velocity maps are used to derive 3D shear-velocity structure. The 3D velocity images confirm details witnessed in prior body wave and surface wave studies and reveal new structures, including a deep (>~ 100 km deep) high-velocity lineament, of width ~200 km, stretching from the southern Great Valley to northern Utah that may be a relic of plate subduction or, alternatively, a remnant of the Mojave Precambrian Province or a mantle downwelling. Mantle seismic velocity is highly correlated with heat flow, Miocene-Present volcanism, elastic plate thickness, and seismicity, suggesting that shallow mantle structure provides the heat source for associated magmatism as well as thinning of the thermal lithosphere, leading to relatively high stress concentration. Our images also confirm the presence of high-velocity mantle at >~100 km depth beneath areas of suspected mantle delamination (southern Sierra Nevada; Grande Ronde uplift), low velocity mantle underlying active rift zones, and high velocity mantle associated with the subducting Juan de Fuca plate. Structure established during the Proterozoic appears to exert a lasting influence on subsequent volcanism and tectonism up to the Present.

2-033

MAPPING OF GEOLOGY AND GEOPHYSICAL DATA OFFSHORE SOUTHERN CALIFORNIA *Shintaku N (CSUN), Weeraratne DS (CSUN), and Kohler MD (UCLA)*

We present preliminary maps of seafloor bathymetry, gravity, and magnetics for the Continental Borderlands and older seafloor west of the southern California coastline. Seafloor geophysical data is compiled from current data sets stored at the NGDC (National Geophysical Data Center). We seek to develop high resolution maps to study surface geomorphology, seismicity, fault structure, crustal, and lithospheric data of the western side of the wide, diffuse, transpressional Pacific-North America plate boundary. The shear complexity of this diffuse plate boundary motivates the need for analysis of offshore geology and geophysics. The complex fault dynamics of the non-uniform San Andreas Fault and multitude of juxtaposed fault systems extend over a 400 km wide region on land. This crustal structure and fault system is at the core of SCEC research for the Community Fault Model, studies of interactive rupture dynamics, and hazard analysis for southern California. These fault models dominantly stop at the coastline, however, although physical stresses across the plate boundary do not. We are interested in collaborating with SCEC community models and other agencies who may have offshore data which may contribute to this offshore mapping project.

Ultimately we also seek to improve the locations of offshore earthquakes, seafloor fault structures, and seismic imaging of crustal-lithospheric dynamics using geophysical data from previous and future data sets for improved understanding of the Pacific side of the southern California plate boundary.

2-034

SEISMIC CONSTRAINTS ON SMALL-SCALE CONVECTION IN THE SOUTHERN CALIFORNIA UPPER MANTLE *Schmandt BM (Oregon), and Humphreys ED (Oregon)*

New P- and S-wave upper mantle tomography images provide strong constraints on the form and magnitude of small-scale convection active beneath southern California. We invert travel-time residuals from the EarthScope Transportable Array, SCSN broadband and short-period arrays, and previous temporary networks for three-dimensional (3-D) velocity structure. Our tomographic inversion method uses approximate finite-frequency sensitivity kernels to interpret travel-time residuals in multiple frequency bands and 3-D crust thickness and velocity models to better isolate the mantle component of travel-time residuals. Use of all available data, a wider aperture array, and P- and S-wave data results in improved lateral, depth, and magnitude resolution, and provides a new level of constraint on the physical state of the southern California upper mantle. The new images more clearly define the extent and density structure of the Transverse Ranges (TR) and southern Great Valley (sGV) high-velocity anomalies, allowing better estimates of the negative buoyancy and thus the load applied to the base of the southern California lithosphere by convective downwelling. The magnitude and prevalence of low-velocity structures surrounding the TR and sGV anomalies suggests infilling asthenosphere that is partially melting as it rises. Coupling V_p and V_s structure also allows improved estimates of the buoyancy/vertical load provided by upwelling asthenosphere. Disparity in magnitude between V_p and V_{sh} ($dV_{sh} \gg dV_p$) in the low-velocity upper mantle beneath the Salton Trough suggests partially molten asthenosphere, but comparison with previous Rayleigh-wave tomography suggests that radial anisotropy may locally complicate the relationship between V_p , V_{sh} , and V_{sv} . Currently, we are working toward a joint inversion of body- and surface-waves to better distinguish lithospheric and asthenospheric structure and better constrain the effects of anisotropy.

2-035

PERVASIVE LOWER CRUSTAL SEISMIC ANISOTROPY IN SOUTHERN CALIFORNIA: A FOSSIL RECORD OF PRE-TRANSFORM SUBDUCTION *Porter RC (Arizona), and Zandt G (Arizona)*

Understanding lower crustal deformational processes and the related features that can be imaged by seismic waves is an important goal in active tectonics. We demonstrate that teleseismic receiver functions calculated for broadband seismic stations in southern California reveal a signature of pervasive seismic anisotropy in the lower crust. The large amplitudes and small move-out of the diagnostic converted phases, and the broad similarity of data patterns on widely separated stations support an origin primarily from a basal crustal layer of hexagonal anisotropy with a dipping symmetry axis. Neighborhood algorithm searches for depth and thickness of the anisotropic layer, and the trend and plunge of the anisotropy symmetry (slow) axis have been completed for 41 stations. The search identified a wide range of results but a dominant SW-NE trend of the symmetry axis emerged, consistent with shearing at the base of the crust oriented in that direction. When the results are divided into crustal blocks and restored to their pre-36 Ma locations using the tectonic reconstructions of McQuarrie and Wernicke (2005), including the $>100^\circ$ rotation of the western Transverse Ranges, the regional scale SW-NE trend becomes even more consistent. We interpret this dominant trend as a fossilized fabric created from top-to-the-southwest sense of shear that existed along the length of coastal California.

2-036

NEOGENE BASIN AND TERRANE BOUNDARY DEVELOPMENT IN THE OUTER CALIFORNIA CONTINENTAL BORDERLAND *De Hoogh GL (CSULB), Nicholson C (UCSB), Sorlien CC (UCSB), and Francis RD (CSU Long Beach)*

Extensive grids of recently released industry multichannel seismic reflection data, together with bathymetry and well data, are used to map stratigraphic reference horizons and 3D fault surfaces in the central Outer Continental Borderland offshore of southern California. Post-subduction transtension associated with the initiation and development of the Pacific-North American plate boundary resulted in large-scale oblique crustal rifting and translation of this area away from the Peninsular Ranges located to the east.

The Nicolas terrane is the inner of two tectonostratigraphic regions that compose the Outer Borderland and represents the forearc basin of the former subduction margin. Our mapping of the Nicolas terrane extends from San Nicolas Island south to the offshore US-Mexico border, and includes San Nicolas, East and West Cortes, and Velero basins, the intervening highs, and parts of Cortes and Tanner Banks.

This mapping shows that the eastern boundary of the Nicolas terrane is marked by an unconformity that apparently formed shortly after the widespread deposition of a volcanic sequence of early Miocene age, and that cuts down through the pre-Miocene forearc basin strata to acoustic basement. This suggests the boundary is related more to crustal uplift associated with continental rifting and lower crustal exhumation than to large-scale oblique translation of the Borderland characterized by a major strike-slip or normal fault, as previously hypothesized. Mapping also reveals a pattern of significant post-early Miocene basin subsidence (as much as 3-4 km), as well as later basin inversion and the creation of major fold structures with anticlines as wide as 50 km and up to 200 km along trend. A ~3.8 Ma horizon dates the onset of this extensive folding, as well as reverse-fault reactivation, showing that the current basin and ridge topography of the Borderland is relatively young, and not related to earlier tectonic events such as Miocene rifting or ridge subduction. Later tilted horizons and offset bathymetry suggest that this subsequent folding and faulting has continued through the Quaternary.

2-037

MODELING OF MULTIPLE EARTHQUAKE CYCLES IN SOUTHERN CALIFORNIA USING THE CFM AND CVM-H *Williams CA (RPI), Gable CW (LANL), Hager BH (MIT), and Meade BJ (Harvard)*

To understand the complicated fault interactions in southern California, one useful approach is to create simulations that examine a long history of interseismic and coseismic slip on a large number of faults. Each of these faults will have different slip rates and average earthquake recurrence times, providing different time-varying contributions to the predicted surface deformation field as well as the overall stress field. When viscoelastic behavior is considered, it is necessary to 'spin up' such models so that near steady-state behavior is achieved. As a first step in providing such simulations we have computed several simulations using a subset of the faults in the Community Fault Model (CFM).

We use the analytical block model of Meade and Hager (JGR, 2005) to compute a consistent set of block rotation poles for a subset of the blocks defined in their model. Although these rotation poles were computed using a simplified rectangular fault geometry, our finite element simulations use the full geometry defined by the CFM. Our present model consists of 11 blocks, which are bounded by 55 of the faults from the CFM. The model is purely kinematic, and is driven by a combination of

co-seismic slip above the 15 km locking depth and velocity boundary conditions consistent with the computed rotation poles applied along the lateral boundaries of the mesh.

We examine five different rheological models: homogeneous elastic, heterogeneous elastic using the Community Velocity Model (CVM-H), Maxwell viscoelastic, generalized Maxwell viscoelastic (two Maxwell models in parallel), and power-law viscoelastic. We also explore the effects of including topography in our models. We use published recurrence times for the main faults, and use a simple empirical rule to assign recurrence times for the additional faults. The simulations are run for a sufficient period of time to allow each fault to experience several coseismic events. Since the faults of the CFM do not form closed blocks, we also examine the effects of allowing stress and strain dissipation using viscoelastic behavior in the upper crust.

2-038

INTERPRETATION OF ANISOTROPIC STRUCTURES BENEATH CALIFORNIA DERIVED FROM SKS-SKKS SPLITTING AND SURFACE WAVES *Kosarian M (UCLA), Davis PM (UCLA), Tanimoto T (UCSB), Clayton RW (Caltech), and Prindle K (UCSB)*

The objective is to use measurements of seismic anisotropy to infer flow in the mantle, and how such flow relates to loading of faults. We calculated SKS splitting parameters for all available data at all broadband stations in California. In southern California, where the density of stations is greatest, we calculated azimuthal anisotropy in the upper 150 km using surface waves. The results show that splitting in the mantle lithosphere is small (about 0.2 sec) compared with SKS splitting (about 1.5 sec) and obtains a maximum value (0.4 sec) in the transpressive region of the Big Bend, south of, and aligned with, the San Andreas Fault. This suggests that most of the SKS splitting is generated in the asthenosphere. SKS splitting shows a remarkable parallelism with absolute plate motion in northern and central California and east-southern California, but in west-southern California there is a notable discrepancy. We interpret the parallelism as indicating the SKS anisotropy is caused by drag of the asthenosphere imposed by the overlying plates. The discrepancy in west-southern California is interpreted as due to the transition to a wide plate margin and asthenospheric flow westward around the drip-structure associated with the Big Bend. The results are consistent with a passive upper mantle responding to the motions of the overlying plates.

2-039

MODELING SEISMIC MOMENT RELEASE: TOWARD RESOLVING THE SEISMIC MOMENT DEFICIT PARADOX *Zaliapin I (UNR), Kreemer C (UNR), Anderson JG (UNR), and Pancha A (UNR)*

An important part of physics-based Seismic Hazard Assessments (SHA) is the estimation of regional earthquake occurrence rate and seismic moment release rate. The ultimate goal is to connect the moment release from the observed seismicity to its long-term predictions based on geodetic and geological information. During the previous SCEC projects we have demonstrated that (i) the reported discrepancies between the observed moment release and its geodetic/geological predictions (including the seismic moment deficit) at large spatial scales are a consequence of a power-law moment distribution and may not imply an increased risk of a large earthquake, and (ii) it is necessary to explicitly account for seismic clustering for explaining the moment release within small regions and at short time intervals. Here we incorporate the seismic cluster properties into the existing seismic moment modeling framework to consistently describe the moment release in the SAF-GB system on spatial scales down to tens of kilometers and temporal scales down to years.

2-040

THE INFLUENCE OF SPATIAL VARIATIONS IN FAULT FRICTION ON EARTHQUAKE RUPTURES AND INTERSEISMIC COUPLING Kaneko Y (*Caltech*), Avouac J (*Caltech*), and Lapusta N (*Caltech*)

Patterns of earthquakes and interseismic fault deformation provide ample observational evidence for spatial variations in fault friction. The pattern of interseismic coupling (ISC) is generally found to be heterogeneous and, to some degree, coincides with the pattern of large earthquakes. For example, the distribution of seismic asperities in the Kurile-Japan trench seems to be relatively stationary and lie within a zone with high ISC (Ito et al., 2000). Similarly, large earthquakes offshore of Sumatra appear to have ruptured areas that had remained locked during the interseismic period (Chlieh et al., 2008; Konca et al., 2008). These observations can be interpreted as evidence for heterogeneous fault friction properties. However, how spatial variation of friction properties translates into the pattern of ISC and complexity of earthquake ruptures is still poorly understood.

Here we quantify the effect of variations in fault friction on rupture patterns and interseismic coupling (ISC) using numerical simulations. We consider 2D and 3D fault models that contain both seismogenic velocity-weakening (VW) and rupture-impeding velocity-strengthening (VS) areas. We find that ISC and the probability that an earthquake breaks through a VS patch are correlated and that they both depend on a nondimensional parameter that incorporates properties of VS and VW segments. Our results further suggest that a patch with relatively high values of ISC ($ISC > 0.6$) can systematically arrest coseismic ruptures. This has important implications for seismic hazard, since areas of low ISC can be found from geodetic or remote-sensing measurements. The presented work provides physical insights into how spatial heterogeneities in fault friction properties observed through seismic, postseismic, and interseismic slip can influence future earthquakes.

2-041

SEMI-ANALYTIC MODELS OF POSTSEISMIC DEFORMATION DUE TO FAULT AFTERSLIP AND NONLINEAR VISCOELASTIC FLOW Barbot SD (*UCSD*), and Fialko Y (*UCSD*)

We present a unified representation of two important mechanisms that are thought to participate in postseismic relaxation. The model employs a generalized viscoelastic rheology that includes a power-law flow in the ductile substrate and fault creep. The unified representation allows one to model each mechanism individually as well as in combination. We use a Fourier-domain semi-analytic Green's function for an elastic half space in the presence of gravity. Our treatment of the restoring buoyant tractions at the surface of the halfspace is an approximation to the full effect of gravity (in particular, it neglects the perturbation of the gravitational potential). We present benchmarks of static deformation due to fault slip and magmatic intrusions. We also show examples of time-dependent deformation, including linear and power-law viscoelastic flow below the brittle-ductile transition for strike-slip and dip-slip faults. We illustrate the effect of gravity on surface deformation due to viscoelastic response to rupture on a dip-slip fault. We also present example simulations of afterslip governed by a generalized rate-and-state friction law. Our benchmarks reveal a good agreement with other analytic, as well as fully numerical (e.g., finite-element) solutions. The proposed semianalytic approach is fast and readily parallelized to deal with large computational domains. It can be used in forward and inverse models of postseismic deformation involving geometrically complex earthquake ruptures, and laboratory-derived constitutive laws for fault friction and bulk ductile deformation.

2-042

HYDRAULIC DIFFUSIVITY AROUND THE KAMIOKA MINE ESTIMATED FROM BAROMETRIC RESPONSE OF PORE PRESSURE *Kano Y (Kyoto), and Yanagidani T (Kyoto)*

The frequency response of monitoring of pore pressure inside rock mass is significantly improved by closing the well. Pore pressure of the rock mass is successfully measured at higher frequencies (0.1 Hz ~ 2 Hz) using closed borehole well in contrast to using open wells that may have a high-cut response by wellbore storage effect. We closed the wellhead of the four artesian borehole wells that was drilled at the Kamioka mine, central Japan, and carried out the pressure measurement. We obtained that the pore pressure response both to barometric pressure change and to earth tides, which is in agreement with theoretical model derived from the linear poroelasticity. The amplitude of tidal response of the wells is consistent with those of response to seismic waves. We determined local shear modulus and loading efficiency, which correlates to the Skempton coefficient, from the observed data. The result suggested that the local shear modulus corresponding to borehole well tapped near fault zone is smaller than that corresponding to borehole well tapped into host rock that is away from the Mozumi-Sukenobu fault. We also estimated hydraulic diffusivity from the low-cut frequency of the barometric response of pore pressure. For the wells drilled near the Mozumi-Sukenobu fault, the in situ value of hydraulic diffusivity is 0.1 m²/s, which is consistent with that determined by core measurement. At the site near the Atotsugawa fault, hydraulic diffusivity is estimated to be 0.1 m²/s in one well. Pore pressure in the other well responds to barometric pressure in period range above 1 day, which implies that the aquifer is unconfined.

2-043

SECULAR STRESS ACCUMULATION ON LOS ANGELES REGIONAL FAULTS: PRELIMINARY RESULTS AND IMPLICATIONS *Marshall ST (Appalachian State), and Cooke ML (UMass)*

Earthquakes occur when accumulated stress is rapidly released in the form of radiated energy and slip on a discrete surface. Yet despite this, very little is known about the rates of stress accumulation on active faults. Stress triggering models have been used to determine locations of increased stress and thus areas likely to produce aftershocks, but how these stress changes affect the timing of large events on nearby active faults is enigmatic. To better understand the rates of secular tectonic stress accumulation along faults in the Los Angeles region, we use an established CFM-based three-dimensional Boundary Element Method deformation model of the Los Angeles region to calculate stress accumulation along Los Angeles regional faults. Rock properties in the model are derived from the SCEC CVM, which indicates a relatively uniform rheology at seismogenic depths (~15-18km). To calculate secular stressing rates, we apply a regional geodetic strain rate determined from corrected GPS velocities to a model with all fault elements locked. We then calculate the area-weighted average annual shear stress accumulation on each fault surface. Because stress drops are relatively invariant for a large range of earthquake magnitudes, these secular stressing rates could be useful for estimating recurrence rates and maximum potential earthquake magnitudes. Furthermore, if secular tectonic stressing rates are known, stress changes after coseismic events can be directly converted into clock advances and clock delays for future events on nearby faults.

2-044

PYLITH: A FINITE-ELEMENT CODE FOR MODELING QUASI-STATIC AND DYNAMIC CRUSTAL DEFORMATION *Aagaard B (USGS), Williams CA (RPI), and Knepley MG (Argonne)*

We have developed open-source finite-element software for 2-D and 3-D dynamic and quasi-static modeling of crustal deformation. This software, PyLith (current release is version 1.4), combines the quasi-static viscoelastic modeling functionality of PyLith 0.8 and its predecessors (LithoMop and Tecton) and the wave propagation modeling functionality of EqSim. The target applications contain spatial scales ranging from tens of meters to hundreds of kilometers with temporal scales for dynamic modeling ranging from milliseconds to minutes and temporal scales for quasi-static modeling ranging from minutes to thousands of years. PyLith development is part of the NSF funded Computational Infrastructure for Geodynamics (CIG) and the software runs on a wide variety of platforms (laptops, workstations, and Beowulf clusters). Binaries and source code are available from geodynamics.org. It uses a suite of general, parallel, graph data structures called Sieve for storing and manipulating finite-element meshes. This permits use of a variety of 2-D and 3-D cell types including triangles, quadrilaterals, hexahedra, and tetrahedra.

Current features include kinematic fault ruptures with multiple sequential earthquakes and aseismic creep, time-dependent Dirichlet and Neumann boundary conditions, absorbing boundary conditions, time-dependent point forces, linear elastic rheologies, generalized Maxwell and Maxwell linear viscoelastic rheologies, power-law rheologies, and gravitational body forces. Current development focuses on implementing dynamic fault interface conditions (employing fault constitutive models) and additional viscoelastic and viscoplastic materials. Future development plans include support for large deformation and automated calculation of suites of Green's functions. We also plan to extend PyLith to allow coupling multiple simultaneous simulations. For example, this could include (1) coupling an interseismic deformation simulation to a spontaneous earthquake rupture simulation (each using subsets of the software), (2) coupling a spontaneous earthquake rupture simulation to a global wave propagation simulation, or (3) coupling a short-term crustal deformation simulation to a mantle convection simulation and an orogenesis and basin formation simulation.

2-045

MODELING EARTHQUAKE-INDUCED CRUSTAL DEFORMATION WITH MESHFREE FINITE ELEMENT TECHNIQUE *Tsukanov I (FIU), and Wdowinski S (Miami)*

Meshfree (or meshless) Finite Element (FE) may sound as an oxymoron, but it is an emerging modeling technique with many advantages. The method still uses elements, just as the standard (meshed) techniques. However, the elements are set by a grid that does not necessarily conform to the geometry of the modeled object. In the contrast to standard FEMs, in our meshfree method the object's geometry is represented by the distances to the boundaries. Distance to the boundary is an intrinsic property of any geometric object, and it provides a natural way to represent the geometric information and satisfy boundary conditions exactly. Because meshfree methods do not require spatial meshing that conforms to the geometric model, they provide the needed geometrical flexibility lacking in standard FE methods. However, the treatment of boundary conditions becomes more challenging. The meshfree FE technique is used in variety of engineering applications, such as heat transfer, structural analysis, shape-material optimization and stress analysis of acquired models. So far, this very promising technique had a very minor impact in geoscience research. Only three geoscience papers used the meshfree technique in their research.

We have started utilizing this flexible numerical modeling tool to study earthquake-induced crustal deformation. So far, we used 3-D elastic models to simulate interseismic deformation due to a buried dislocation. Our preliminary results show an excellent fit with analytical dislocation models. We plan to continue developing the application of the meshfree technique to crustal deformation studies, in order to generate a modeling tool that can easily incorporate complicated geometries

(faults, topography, and crustal units), geometrical changes over time, complicated rheologies, and heterogeneous crustal properties.

2-046

GEOFEST QUASI-STATIC SIMULATIONS FOR CALIFORNIA - AND CERES *Parker JW (JPL), Lyzenga GA (Harvey Mudd), Norton CD (JPL), and Raymond CA (Jet Propulsion Laboratory)*

The simulation software GeoFEST (Geophysical Finite Element Simulation Tool) has been released for widespread free source download in a substantial upgrade for reliability and important features (v4.8). GeoFEST now uses Pyramid library features to automatically perform parallel mesh refinement, using strain energy from a scratch solution on the initial coarse mesh to drive the refinement by subdivision of those regions of the mesh most in need of increased accuracy. This allows problems with at least 120,000,000 finite elements, sufficient for modeling a tectonic region such as southern California, including dozens of faults and material layers. Setup for large problems has been simplified. Refinement is based on initial elastic strain energy, and the user may set a threshold percentage of elements for refinement. The matrix solution convergence has been greatly improved for reliable, accurate solutions. Fault slip may be specified as separate slip schedules for individual strands, and specified slip variation along the length of each fault. Buoyancy restoration forces are now included. The result is that GeoFEST is now effective and convenient for performing regional simulations of earthquake stress transfer, deformation, and strain from immediate earthquake response, post-event relaxation and fault afterslip, and multiple-earthquake cycles. Such simulations are useful in developing and assessing seismic hazard and for enhancing scientific understanding of earthquakes and interactions of systems of earthquake faults, in conjunction with deformation data collection efforts. GeoFEST simulated deformation data compares directly with regional GPS network data and with differential InSAR observations; we show tests of Mojave post-earthquake transients that verify essential correctness of the viscoelastic algorithm.

New work is implementing support for temperature diffusion and temperature-dependent viscosity, spherical shell geometry (including radial gravity), and improved nonlinear viscosity evolution, in preparation for supporting observations from the DAWN mission encounter with Ceres in 2015.

2-047

MIXED LINEAR-NONLINEAR FAULT SLIP INVERSION: BAYESIAN INFERENCE OF MODEL, WEIGHTING, AND SMOOTHING PARAMETERS *Fukuda J (Indiana), and Johnson KM (Indiana)*

Studies utilizing inversions of geodetic data for the spatial distribution of coseismic slip on faults typically present the result as a single fault plane and slip distribution. Commonly the geometry of the fault plane is assumed to be known a priori and the data are inverted for slip. However, sometimes there is not strong a priori information on the geometry of the fault that produced the earthquake and the data is not always strong enough to completely resolve the fault geometry. We develop a method to solve for the full posterior probability distribution of fault slip and fault geometry parameters in a Bayesian framework and Monte Carlo methods. The slip inversion problem is particularly challenging because it often involves multiple data sets with unknown relative weights (e.g. InSAR, GPS), model parameters that are related linearly (slip) and nonlinearly (fault geometry) through the theoretical model to surface observations, prior information on model parameters, and a regularization prior to stabilize the inversion. We present the theoretical framework and solution method for a probabilistic inversion that can handle all of these aspects of

the problem. The method handles the mixed linear/nonlinear nature of the problem through combination of both analytical least-squares solutions and Monte Carlo methods. We first illustrate and validate the inversion scheme using synthetic data sets. We then apply the method to inversion of geodetic data from the 2003 M6.6 San Simeon, California earthquake. We show that the uncertainty in strike and dip of the fault plane is over 20 degrees. We characterize the uncertainty in the slip estimate with a volume around the mean fault solution in which the slip most likely occurred. Slip likely occurred somewhere in a volume that extends 5-10 km in either direction normal to the fault plane. We implement slip inversions with both traditional, kinematic smoothing constraints on slip and a simple physical condition of uniform stress drop.

2-048

LIMITATIONS OF STRAIN ESTIMATION TECHNIQUES FROM SPARSELY SAMPLED GEODETIC OBSERVATIONS *Baxter SC (JPL), Parker JW (JPL), Kedar S (JPL), Webb FH (JPL), Owen SE (USC / JPL), Dong D (JPL), and Sibthorpe A (JPL)*

Using an interactive Strain Analysis Tool we have conducted an analysis of two classes of strain estimation techniques from geodetic measurements: (1) Least squares estimation of regional strain directly from the deformation measurements, as has been traditionally done with geodetic data, and (2) Calculation of the strain using an interpolated velocity field.

Our analysis shows that both techniques are limited by the sampling of the field, and by the orientation of the geodetic network relative to the tectonic deformation field that it samples. We demonstrate that without a-priori knowledge of the deformation field, artifacts emerge that are dominated by the spatial scale of the sampling, and which are impossible to distinguish from real features in the strain field. This is due to the sensitivity of the deformation field derivatives (from which the strain is constructed) to the assumptions that are made in their estimation. In either case, implicit assumptions about the linearity or smoothness of the derivatives are made, that inevitably misrepresent the real-world case, which is typically highly non-linear particularly near faults. Without a-priori knowledge of that non-linear behavior our analysis is limited to visualizing only large scale features of the strain field. The current GPS networks, although providing unprecedented coverage of tectonic deformation, are still too sparse to reliably depict small-scale strain behavior within or near fault zones.

This will be demonstrated using an ideal situation in which a simple tectonic deformation field is sampled by a dense and regular grid of stations. The Strain Analysis Tool, which will be on display, will be interactively used to demonstrate the dependence of artifacts in the strain field on grid sampling and network orientation, and to provide explanation for these artifacts. We conclude by exploring these same effects in a more realistic tectonic setting and GPS station distribution.

2-049

INTERSEISMIC FAULT LOCKING DEPTH ESTIMATES FOR SOUTHERN CALIFORNIA *Chuang YR (Indiana), and Johnson KM (Indiana)*

The parameters of active faults in southern California such as fault slip rates and interseismic fault locking depths are important for seismic hazard assessments. However, estimates of fault slip rates and locking depths using geodetic data are model dependent. Previous fault slip rate estimates using GPS data for southern California are derived from elastic block models. These models assume that tectonic blocks bounded by faults move as undeformed bodies over the long-term. During the interseismic period, elastic strain accumulation due to locking of faults is modeled as a perturbation to this long-term block motion and steady fault slip with back-slip on locked portions of faults using dislocations in an elastic half-space.

In order to better estimate the distribution of locking depths, we designed two classes of lithosphere block models to examine the effect of model assumptions on slip rate and locking depth estimates. Our models can solve for the distribution of interseismic fault locking depths and fault slip rates in the inversion. In the “steady” model, faults are either creeping or locked during the interseismic period and creep occurs at constant resistive shear stress. This model assumes deformation is steady over time. In inversions with this model, we solve for the distribution of locked and creeping patches on faults. In the “earthquake cycle” class of lithosphere block models, we impose periodic earthquakes and consider time-variable viscous flow of the asthenosphere. In this model we assume that faults are locked above some depth during the interseismic period and creep below this depth at the long-term fault slip rate. Preliminary results show that the steady model favors deep locking depths for the San Andreas fault, and the earthquake cycle model prefers moderate locking depths for the San Andreas fault system.

2-050

INTERSEISMIC DEFORMATION OF THE DEATH VALLEY FAULT ZONE *Del Pardo C (UTEP), Smith-Konter BR (UTEP), and Serpa LF (UTEP)*

The Death Valley Fault Zone (DVFZ), located in southeastern California, is an active fault system with an evolved pull-apart basin that has been deforming over the last 15 million years. The main processes in the evolution of the structures of the DVFZ are poorly understood and may not be well connected to faulting. Our objectives are to study the interseismic motion of DVFZ in order to better understand the nature of present-day loading conditions of the fault zone. Using a 3-D semi-analytic viscoelastic deformation model, constrained by geodetic velocities, we aim to establish best-fitting model parameters for interseismic slip rate, apparent locking depth, elastic plate thickness and mantle viscosity. We divide the DVFZ into three primary sections for this study, the Southern Death Valley Fault Zone, the pull-apart basin in Central Death Valley, and the Northern Death Valley Fault Zone and simulate interseismic motion on vertical interacting fault segments with 1 km spacing. We allow the model to accommodate variable locking depths (5-12 km) and slip rates (2-5 mm/yr) and tune the model to fit a set of local continuous and campaign geodetic velocities, including data from the SCEC3 Crustal Motion Map. Our best fitting preliminary model, consisting of 200 fault elements, provides an excellent fit to the data (0.64 mm/yr fault-perpendicular RMS misfit, 1.03 mm/yr fault-parallel RMS misfit, 1.26 mm/yr vertical RMS misfit) and reveals an appropriate sensitivity to fault geometry. The model predicts 0.6 mm/yr of subsidence and 1.5 mm/yr of extension in the Death Valley pull-apart basin, corresponding to the extensional component of the fault system as it bends eastward. The fundamental model parameters obtained by this study will ultimately be applied to a 3-D finite difference model we are constructing using FLAC3D, in which we plan to further investigate the formation and evolution of the pull-apart basin in the DVFZ.

2-051

Sandwell DT (UCSD), Becker TW (USC), Bird P (UCLA), Fialko Y (UCSD), Freed A (Purdue), Holt WE (SUNY-Stony Brook), Kreemer C (UNR), Loveless J (Harvard), Meade B (Harvard), McCaffrey R (RPI), Pollitz F (USGS), Smith-Konter B (UTEP), and Zeng Y (USGS)

GPS measurements across the North American - Pacific Plate boundary are providing decade and longer time series at 2 to 3 millimeter-level precision from which surface velocity estimates are derived. Several geodetic research groups have used these point velocity measurements to construct large-scale maps of crustal strain rate. Since the typical spacing of GPS stations is 10 km or greater, an interpolation method or physical model must be used to compute a continuous vector velocity model that can be differentiated to construct a strain-rate map. Four approaches are used to develop strain maps: isotropic interpolation, interpolation guided by known faults,

interpolation of a rheologically-layered lithosphere, and analytically determined strain rates derived from a geodetically constrained block model in an elastic half space. This poster compares the strain-rate maps of several groups using these different methods to define common features as well as differences among the maps. The differences reveal the spatial resolution limitations of GPS arrays, as well as assumed fault locations and the effects of differing assumptions about crustal rheology. Moreover the comparisons promote collaboration among the various groups to develop the best possible strain-rate map. Our first analysis only compares the magnitude of the strain rate given by the following formula $\sqrt{\epsilon_{xx}^2 + \epsilon_{yy}^2 + 2\epsilon_{xy}^2}$.

2-052

FAULT INTERACTION AND STRESSING RATES IN SOUTHERN CALIFORNIA

Loveless JP (Harvard), and Meade BJ (Harvard)

Relative motion between the Pacific and North American plates is accommodated in southern California through slip partitioning across a ~200 km wide fault system. We simultaneously estimate microplate rotations, fault slip rates, elastic strain accumulation rates, and spatially variable coupling on fault surfaces using a block model, based on the Community Fault Model Rectilinear geometry and GPS data combined from six networks. We use the catalog of derived fault slip rates to analytically calculate stressing rates on the San Andreas fault (SAF) from Parkfield to south of the Salton Sea, resolving the shear stress rate on the SAF by rotating the full 3D stress tensor calculated at each segment centroid. We compare shear stress rates resulting from slip on all fault segments in the block model (“total stress”) to those due to slip on only SAF segments (“self stress”). Differences between total and self stress rates of up to 200% are most evident at intersections between the SAF and the White Wolf, Garlock, North Frontal, Eureka Peak, San Jacinto, and Elsinore faults; these differences are expected given abrupt along strike changes in SAF slip rate that occur at fault junctions. However, differences of up to 30% exist between these intersections along the Mojave and San Bernadino segments of the SAF, indicating that interaction amongst all faults in the network plays a substantial role in dictating stress accumulation. We compare stressing rates to on-fault seismicity and find that seismicity rates correlate best with the stress rate difference, suggesting that fault system interaction also influences patterns of earthquake rupture. These results have direct application to evaluation of seismic hazard, calculation of earthquake recurrence intervals on the SAF, and segmentation patterns along the SAF and other seismogenic faults.

2-053

MAPPING SLOW SLIP EVENTS AND ASPERITIES IN JAPAN *Kawasaki I (Kyoto)*

During the past decade, we have observed many types of slow slip events in seismo-geodetic band from tens of seconds to years in Japan: afterslips (Kawasaki et al., 1995; Miura et al., 1995; Heki et al., 1995; Yagi et al., 2001; Miyazaki et al., 2004), silent slow slip events (Hirose et al., 1999; Ozawa et al., 2003) and very low frequency earthquakes (Ito and Obara, 2006) in the so-called seismogenic zone and their borders on the subduction interfaces of the Pacific plate along the Japan trench in the northeastern Japan and the Philippine sea plate along the Nankai trough in the southwest Japan.

Following numerical simulation by Yoshida and Kato (2003) based on Dieterich and Ruina law, we can categorize the seismogenic zone into four subzones of (K1) to (K4) characterized by friction properties, $a-b$, stiffness K and critical stiffness K_c as

(K1) $a-b < 0$ and $K < K_c$: seismic asperity where dynamic ruptures occur,

(K2) $a-b < 0$ and $K \sim K_c$: stability transition subzone where episodic slow slip events occur

(K3) $a-b < 0$ and $K > K_c$: substable sliding subzone where is locked in the interseismic period, stable slip before dynamic rupture and afterslip immediately after dynamic rupture occur,

(K4) $a-b > 0$; stable sliding subzone where stable slip in the interseismic period is dominant and afterslip immediately after earthquake may occur.

We plot the source areas of slow slip events and seismic asperities in association with (K1) to (K4). We recognize

(1) major element is afterslip zone (K4) along the Japan trench in the so-called seismogenic zone at depths from 20 km to 35 km along the Nankai trough. It is seismic asperity (K1) along the Nankai trough.

(2) many and little slow slip events occur along the Japan and Nankai trenches, implying the narrow stability transition zone (K2) along Japan trench and the broad (K2) along Nankai trough.

(3) there is a gap between (K1) and (K2) subzones along the Nankai trough. This may suggest that the zone of non-volcanic tremors at depths from 30 km to 35 km discovered by Obara (2002?) is a part of broader stability transition subzone (K2). The 1944 Tonankai (Mw8.3) and the 1946 Nankai (Mw8.3) earthquakes broke the corresponding asperities plotted but the slip of the super giant Hiei Tokai earthquake (Mw8.6?) in 1707 might break the asperities of the Tonankai and Nankai earthquakes and the stability transition zone (K2) along the Nankai trough.

One of notable events was the afterslip that started immediately after the Tokachi earthquake (Sept. 25, 2003, Mw8.3), south-off Hokkaido, and propagated eastward by about 200 km to trigger the Nemuro-oki earthquake (Nov. 28, 2004, Mw7.0). The other was a succession of silent slow slip events which started in the beginning of Jan., 2006, in the middle of the Kii-peninsula in the Kinki district, to propagate northeastward by about 200 km and stopped within the month in the Tokai district, close to the supposed rupture area of the Tokai earthquake but did not trigger the Tokai earthquake. We know little about interaction between the episodic slow slips and M8 class giant earthquakes who are neighbors on the subduction interface.

2-054

PRESENT-DAY CRUSTAL DEFORMATION OF TAIWAN *Ching K, Rau RJ (National Cheng-Kung University, Taiwan), Hu J (National Taiwan University), Lee J, and Johnson KM (Indiana)*

Taiwan, seated at the junction of the Manila and the Ryukyu subduction systems, is a classical case of the ongoing arc-continent collision due to convergence between the Eurasian and the Philippine Sea plates. We analyzed 601 GPS observations in Taiwan to understand the kinematics of present-day crustal deformation of the Taiwan mountain belt. Horizontal GPS velocities, relative to the Chinese continental margin station, S01R, represent a fan-shaped pattern and gradually decrease northwestward from ~82 mm/yr in SE Taiwan to nearly no deformation in NW coastal area. Directions of the horizontal velocities are dominantly toward NW in central Taiwan and the clockwise rotation and counterclockwise rotation are occurring in northern and southern Taiwan, respectively. For stations between the Chishan fault and the western flank of the southern Central Range in southern Taiwan, most station velocities are consistent (51.9 ± 6.6 mm/yr) and, from east to west, the azimuths change gradually from 277° to 247° . In northern Taiwan, magnitudes of

northwestward velocities are 0.3-7.8 mm/yr in NW part of this area and vectors of 9.3-41.2 mm/yr from 53° to 146° occur in the Ilan area. Three significant features are characterized based on the analyses of velocities and 3-D block modeling results. First, tectonic block rotations are mostly concentrated on the northern Taiwan, which correspond to the transition from the Ryukyu subduction to the Taiwan collision zone. The roll-back of Ryukyu trench and the opening of Okinawa trough are probably superposed on the arc-continent collision-induced rotation in northern Taiwan mountain belt. Second, block translations are mainly occurred in southern Taiwan. The interaction between the Peikang basement high and the westward propagation of the accretionary wedge results in the material across southern Taiwan to move toward WSW, sub-parallel to the southern edge of the continental margin, via the strain partitioning along several major structures. Third, high slip rate deficits are mainly derived along the active faults in the Ilan area and along the northern Longitudinal Valley fault, which may correspond to the areas with high earthquake potential.

2-055

AFTERSHOCK DISTRIBUTION AS A CONSTRAINT FOR THE 2004 PARKFIELD EARTHQUAKE COSEISMIC SLIP MODEL *Bennington N (Wisconsin), Thurber CH (Wisconsin), Feigl K (Wisconsin), and Murray-Moraleda J (USGS)*

Several studies of the 2004 Parkfield earthquake have linked the spatial distribution of the event's aftershocks to the mainshock slip and/or stress drop distribution on the fault. We present a coseismic slip model for the 2004 Parkfield earthquake with the constraint that the edges of coseismic slip patches align with aftershocks. Two strategies for applying the constraint were compared, cross-gradient and anti-parallel gradient. The cross-gradient constraint failed to align coseismic slip patches with aftershock clusters, but the anti-parallel constraint led to slip patches whose edges coincided with areas of high aftershock density. The latter also improved fit of the geodetic data compared to the unconstrained case. The large patch of peak slip about 15 km northwest of the 2004 hypocenter observed in the anti-parallel constrained model is in good agreement in location and amplitude with previous geodetic studies and the majority of strong motion studies. The anti-parallel constrained solution shows the continuation of moderate levels of slip to the southeast, in agreement with strong motion studies but inconsistent with the majority of published geodetic slip models. Southeast of the 2004 hypocenter, a patch of peak slip observed in strong motion studies is absent from our anti-parallel constrained model, but the available GPS data do not resolve slip in this region.

Tectonic Geodesy

2-056

USE OF INTERSEISMIC GPS VELOCITY FIELD IN SOUTHERN CALIFORNIA FOR THE DETERMINATION OF PLATE RIGIDITY VARIATION *Joulain C, Chéry J (Université Montpellier 2), Mohammadi B, and Peyret M*

Interseismic velocity field provided by geodetic methods in tectonically active areas is often interpreted using the concept of thick elastic blocks cut by slipping faults at depth. This approach is purely kinematical and the best adjustment between observed and modeled velocity fields is obtained by searching the fault slip rate distribution along the block boundaries below the seismogenic depth. We assume here that interseismic strain occurs in response to remote forces or velocities imposed by the plates. In this case, lithosphere and faults rheology control interseismic strain rate. If faults are fully locked within the seismogenic zone, strain rate variations must occur in response to lateral variations in the elastic rigidity of the lithosphere. In line with this view, low rigidity zones should lead to high interseismic strain while high rigidity areas remain weakly deformed.

We present here a mathematical method to approximate the observed GPS velocity field by a mechanical model displaying a horizontally variable plate rigidity. We adopt an optimisation scheme that aims to minimize a cost function representing the offset between a forward elastic model and the GPS data (interseismic velocity field). The plate rigidity is described by a small number of parameters defined on control points. This way, it is tractable to compute the cost function gradient in the parameter space. An optimization algorithm allows to minimize the cost function. We first apply this method to search the rigidity distribution in the case of a well-posed problem for which 1) the rigidity map is a priori known 2) the data velocity field is the FEM solution of the direct problem. This approach allows us to define a suitable parametrization in which the parameter space can be progressively enriched during the optimization process.

We then use the southern California zone in the vicinity of the San Andreas fault to test the ability of the method to solve the rigidity distribution over an intraplate region. This zone is of a special interest because it includes different tectonical areas such as the border of the Pacific plate, the San Andreas fault zone and the Mojave region. Therefore, one can expect that the analysis of the continuous GPS velocity field (CMM3) should lead to contrasted rigidities across the studied domain. We discuss the rigidity distribution obtained by our method in the light of heat flow, seismology and tectonic knowledge of southern California.

2-057

REAL TIME DATA FROM SOUTHWEST REGION OF PLATE BOUNDARY OBSERVATORY GPS NETWORK *Walls C (UNAVCO), Lawrence S (Parsons Infrastruc. & Tech Group Inc.), Basset A (UNAVCO), Borsa A (UCSD), Feaux K (UNAVCO), and Jackson ME (UNAVCO)*

Plate Boundary Observatory (PBO) is the geodetic component of EarthScope. PBO maintains a network of 1,100 continuously operating GPS stations in the western US and Alaska, consisting of 891 PBO GPS stations constructed from 2003 to 2008 and 209 pre-existing GPS stations from preceding geodetic networks. Most stations feature drill-braced GPS monuments designed by the Southern California Geodetic Network (SCIGN). All stations have been built or upgraded with Trimble NetRS receivers and IP based communications. Fifteen second data for each station is archived daily and available through the EarthScope Data Portal. In addition 1 and 5 sample per second data is buffered for download in case of an earthquake.

The Southwest Region of PBO is a new management area consisting of 453 GPS stations formerly included in parts of the Northern and Southern California Regions of PBO. The Southwest Region extends from San Diego to Sonoma County in the west and includes the Eastern California Shear Zone south of Long Valley in the east. Three engineers maintain stations in the Southwest Region with a Regional Office in the Los Angeles area. The Southwest Region includes 319 PBO GPS stations, 123 stations acquired from SCIGN, and 10 stations from the BARD network.

PBO has the potential to provide real-time GPS data for the science and survey communities. PBO is supporting the USGS in the development of earthquake early warning (EEW) networks based on real-time GPS data streams. In addition PBO is a potential data provider for California based real-time GPS networks used by surveyors. PBO currently runs a pilot program which streams 1 sample per second data from 60+ stations in the Southwest Region. Data is provided in BINEX and RTCM formats via the NTRIP protocol. Data streams are currently freely available to the public. Requests for access to data can be made at <http://pboweb.unavco>.

2-058

REAL-TIME HIGH-RATE GPS AT USGS PASADENA *King NE (USGS), Langbein J (USGS), Lisowski M (USGS), Hudnut KW (USGS), Stark KF (SCIGN), and Aspiotes AG (USGS)*

Recent advances in hardware, telemetry, and processing software make real-time geodetic monitoring possible. These developments allow monitoring of fault-crossing lifelines, further the integration of geodetic and seismic networks, and improve geodetic response to large earthquakes. USGS Pasadena operates 97 permanent continuously-operating GPS stations in southern California. To further the earthquake-response mission of USGS, these stations are in the heavily-populated urban area and along the southern San Andreas fault. With support from city and county land surveyors, USGS Pasadena has been upgrading its stations to real-time (1 second sampling interval), and broadcasting RTCM streams, for several years. With recent funding from the USGS MultiHazards Demonstration Project, USGS Pasadena recently co-located GPS at four new or upgraded seismic stations along the southern San Andreas fault. Partnerships to implement real-time monitoring at locations where lifelines cross the fault are being explored; one such partnership is underway. USGS Pasadena currently operates 30 stations in real time, and anticipates upgrading many more in the next year or two. Testing of real-time processing (both point positioning and real-time-kinematic), technical development, and research (precision, outlier detection, and signal discrimination) indicate that high-rate and real-time GPS results will significantly improve our capacity to monitor fault slip and respond to southern California earthquakes.

2-059

WHERE IS THE TRUE TRANSFORM BOUNDARY IN CALIFORNIA? *Platt JP (USC), and Becker TW (USC)*

An intriguing aspect of the geodetically defined velocity field in California is that the zone of highest strain-rate does not everywhere coincide with the surface trace of the San Andreas fault (SAF). In southern California it is centered between the SAF and the San Jacinto Faults, and north of the San Francisco Bay area it lies up to 40 km E of the SAF. This effect could be (i) a transient aspect of interseismic strain accumulation, (ii) an intermediate-term effect of the interaction of the visco-elastic response of numerous faults throughout the western US, or (iii) a reflection of the long-term distribution of strain-rate within the transform zone. To distinguish among these possibilities we have analyzed the velocity field on swaths across the transform system, avoiding intersections among the major fault strands, so as to minimize transform-parallel variations in slip-rate within each swath. This allows us to define the velocity profile within each swath with a high

degree of precision. Slip rates and flexural parameters for each fault were determined by finding the best fit to the velocity profile of a simple arctan function for the velocity distribution. Our estimated slip rates are then compared with current geologic estimates. Fit is generally good, although our estimates are significantly lower than geologic estimates for some sections of the SAF, and the cumulative slip rate across the Mojave Desert is about twice current geologic estimates. We suggest that the present-day velocity field is reasonably representative of the long-term field, and that it provides an image of the long-term response of the continental lithosphere to relative plate motion. This leads to the following conclusions.

1. The lithospheric transform is a zone of high strain-rate up to 80 km wide that is not everywhere centred on the surface trace of the San Andreas Fault. It is straighter than the SAF, and has an overall trend closer to the plate motion vector than the SAF.
2. Most sections of the SAF take up less than 50% of the total slip rate, and slip is transferred from one part of the system to another in a way that suggests the SAF should not be considered as a unique locator of the plate boundary.
3. 35-50% of the total plate boundary displacement takes place outside the high strain-rate zone, and is distributed over a region several hundred km on either side, including the Eastern California Shear Zone.

2-060

CONTEMPORARY BLOCK TECTONICS AND KINEMATICS OF SOUTHERN CALIFORNIA DERIVED FROM GPS-DATA *Gaydalenok O (Moscow State), and Simonov D (Moscow State)*

Southern California attracts great interest from scientists all over the world due to its complicated tectonics. Because it has one of the best GPS networks it allowed us to apply our original methods for the analysis of the velocity data. We classified GPS-vectors according to the similarity of their Euler poles, and calculated the relative motions of the resulting clusters. Thus we obtained statistical clusters (Model of GPS-derived Clusters) that could be interpreted as belonging to different rigid blocks where confirmed with geologic data. We matched our Model of Clusters with Quaternary faults and found that not all boundaries coincide with faults. For this reason we mapped lineaments using Shuttle Radar Topography Mission data. Thus we made a general Block Tectonic Model that shows (a) boundaries based on Quaternary faults, (b) boundaries based on lineaments, and (c) inferred boundaries without topographic expression. We suggest that some boundaries do not express in topography because the displacements are so recent and topography has not developed yet, or it they may be caused by creep or by localized stress accumulation.

The main conclusions from our Block Tectonic Model are as follows:

1. The model suggest that there is the kinematically stable zone along the San Andreas fault between its interaction with the Garlock and San Jacinto faults. The fault is locked and a strong earthquake can be expected in this area, but the model shows that stress on this segment is significantly decreased due to nearby block interactions, where reverse motions are expressed widely.
2. Block boundaries which display transpressional kinematics mostly coincide with Quaternary faults (Santa Susana reverse fault), while boundaries with strike-slip character do not coincide with faults (Elsinore, San Gabriel faults).

3. Block kinematics suggested by the model correlate well with seismicity, which that could provide a test of the validity of our Model and our methods.

Additionally, we compared our Block Tectonic Model with previous block models. The main difference between the models is in approaches. Other authors first derive the block boundaries based on previously identified faults, and then they calculate GPS velocities of the blocks. We do the opposite – first we divide the area into blocks using statistical methods and then we try to confirm the resulting block boundaries geologically.

2-061

DECORRELATION OF ALOS AND ERS INTERFEROMETRY OVER VEGETATED AREAS IN CALIFORNIA *Wei M (SIO / IGPP), and Sandwell DT (UCSD)*

Temporal decorrelation over vegetated areas is the main limitation for recovering interseismic deformation along the San Andreas Fault system. To assess the improved correlation properties of L-band with respect to C-band, we analyzed ALOS PALSAR interferograms over three vegetated areas in California and compared them with corresponding C-band interferograms from Remote Sensing Satellite (ERS) of European Space Agency. Both ALOS and ERS interferograms have various temporal baselines with a maximum of two-year and various spatial baselines. (1) In the highly vegetated Northern California forests in the Coast Range area, ALOS remained remarkably well correlated over a two-year winter-to-winter interferogram (~0.27), while an ERS interferogram with a similar temporal and spatial baseline lost coherence (<0.13). (2) In central California near Parkfield, we found similar pattern. Four ALOS interferograms with a two-year temporal baseline all had adequate correlation (0.16-0.25) over vegetated mountain areas, while the ERS interferogram had much lower inadequate correlation (0.13-0.16). This improvement in correlation at L-band revealed creep along the San Andreas Fault that was not apparent at C-band. (3) In the Imperial Valley of Southern California, ALOS had higher correlation in the urban area (0.4 versus 0.3) and lightly irrigated area (0.18 versus 0.16). However, it had lower correlation over some sandy surfaces (0.2 versus 0.4). Interferograms with similar season acquisitions has higher correlation compared to that with dissimilar season even the time interval of the similar season is much longer. For both ALOS and ERS have lower correlation over vegetated areas and the correlation decreases with time when the time interval is less than 1 year on all types of areas. After that, the correlation stays the same level or even higher. In the vegetated areas, ALOS has higher correlation while they both decorrelated on farmlands in the Imperial Valley. We also found in some cases that the correlation of FBS-FBS interferograms was slightly better than that of mix-mode interferograms, i.e. FBD-FBS. These results suggested that ALOS remains correlated much longer than ERS in vegetated areas in California. New L-band observation including ALOS and future US mission DESDynl will be especially valuable for study the long-term slow motion, such as interseismic slip and fault creep, over vegetated areas in California.

2-062

TESTING DEM-BASED ATMOSPHERIC CORRECTIONS TO SAR INTERFEROGRAMS OVER THE LOS ANGELES BASIN *Jin L (UCR), and Funning GJ (UCR)*

Atmospheric water vapor delay is the major source of noise in SAR interferograms. Without the atmospheric delay being corrected, it is hard to see any slow surface movements of the ground; and it is impossible to validate PS-InSAR method either. If the water vapor delay is quantified, not only can we solve the previous two problems, but also reduce the errors in geodetic measurements, and improve the accuracy in generating Digital Elevation Models (DEMs).

In order to reduce water vapor delay, there are some possible solutions. This project is a method based on DEMs. It intends to find the relationship between topography and water vapor delay in interferograms so the water vapor signals can be reduced. It is assumed that the water vapor delay is linearly related to the topography over a certain distance. For example, the low phase delay appears over the places where the elevation is high; or low elevation leads to high phase delay.

We tested 17 interferograms over the LA basin--5 from the ERS-1/2 tandem mission between 1995 and 1996; 12 from EnviSAT between 2005 and 2007 with the time spans from 35 to 245 days. The basic idea was to divide each interferogram and DEM into a series of small windows. Then the coefficients of the relationship between the phase and the elevation in each same window were found. After interpolating these coefficients across the interferogram area, we obtained the water vapor corrections. In this project, we tested three interpolation methods--linear, spline, and cubic, but we found that there was little difference among them. To test the result, we calculated the root mean square phase of the data before and after correcting, and assessed the similarity of the correction between neighboring windows (i.e. the 'coherence'). We varied the size of windows to find the one which was most effective in removing signals. However, the result was that: the smaller the window sizes the more signals it removed. Furthermore, when we conducted the same procedures using 10 other DEMs (i.e. DEMs of other places), we found the wrong DEMs also removed signals at a similar level of success to the correct one. In only 3 cases could we separate the correct DEM from the wrong ones. Another thing worth mentioning is the method also removed the real deformation signals. In conclusion then, the DEM-based corrections alone are not sufficient to correct for water vapor delay. The incorporation of GPS data into these models would be necessary.

2-063

OPTIMAL DESIGN OF GEODETIC NETWORKS: A NEW MEASURE OF PERFORMANCE, WITH APPLICATION TO THE SOUTHERN CALIFORNIA FAULT SYSTEM *Lipovsky BP (UCR), and Funning GJ (UCR)*

There are over 10,000 geodetic monuments listed in the UNAVCO repository as of August 2009. Given this ubiquity, the optimal design of these networks is paramount. Where geodetic observations should be made is a question of general interest in geodesy, and is relevant to geophysical geodesy for crustal deformation in particular. We build on prior work in this field (e.g., Blewitt, 2000; Segall and Schmidt, 2003; Gerasimenko et. al., 2000) in two regards: we devise a method to account for stochastic variability in observations, and we consider fault zones of realistic geometry.

We use a new statistical measure to evaluate the quality of a geodetic network with respect to geophysical model parameters. This new measure, Weighted D-Optimality, accounts for stochastic variability in deformation data through a method similar to Principal Component Analysis.

We also consider optimal network configuration with respect to models of elastic deformation on single finite (map view) faults and in fault systems. We find that ideal detection of fault length occurs at the fault's endpoints, and that observation of fault locking depth is optimized at perpendicular distance D (depth of locking) from the fault trace endpoints.

We produce a map of choice locations for detection of fault parameters in the southern California fault system. We use a synthetic deformation record created by the physics-based Earthquake simulator RSQSim (Dieterich and Richards-Dinger, manuscript submitted). Our model geometry is

derived from the Community Fault Model (Plesch et al., 2007). Both stochastic variability and complex optimization geometry are fully utilized in the creation of this map.

2-064

AIRBORNE AND TERRESTRIAL LASER SCANNING ACTIVITIES AT UNAVCO: PROJECT HIGHLIGHTS AND NEW SUPPORT RESOURCES *Phillips DA (UNAVCO), Jackson ME (UNAVCO), and Meertens CM (UNAVCO)*

UNAVCO leads and supports airborne and terrestrial laser scanning (ALS and TLS, also referred to as airborne and ground-based LiDAR) activities in support of a wide range of Earth science applications. UNAVCO acquired nearly 6,000 km² of high resolution ALS data as part of the EarthScope Facility construction project funded by the National Science Foundation. ALS data from southern and eastern California include 0.5 meter DEM's covering the Elsinore, Garlock, Calico, Lenwood, Blackwater, Helendale, Panamint Valley, Ash Hill, Owens Valley and San Andreas faults. EarthScope ALS data products are freely available from the Open Topography portal (<http://opentopography.org>). UNAVCO is also significantly expanding support resources for TLS, including the procurement of five new TLS instruments that will be available to researchers as part of the UNAVCO Facility pool. UNAVCO currently coordinates and conducts TLS activities through Polar Services support and through INTERFACE (INTERdisciplinary alliance for digital Field data ACquisition and Exploration), a collaborative project funded by NSF that includes specialized TLS data processing and visualization software tools developed specifically for geoscience applications, as well as community outreach and training. We will present an overview of ALS and TLS project highlights and available resources.

2-065

SOLID EARTH SCIENCE DATA SYSTEM FOR EXPLORATION OF LITHOSPHERIC DEFORMATION IN THE WESTERN US *Webb FH (JPL), Bock Y (UCSD), Kedar S (JPL), Owen SE (USC / JPL), Dong D (JPL), Jameson P, Fang P (UCSD), Squibb M (SDSC), and Crowell B (UCSD)*

The primary objective of this project is to generate long-term consistent surface deformation Earth Science Data Records (ESDRs) by infusing science product generation, visualization, and manipulation tools and information technology, prototyped in the past 5 years under a variety of NASA Earth Science programs, into an end-to-end operational Science Data System. The products include geodetic daily position time series, crustal motion velocities, and strain and strain rate maps. High-rate (1 Hz and higher) position time series and tropospheric calibration products for remotely sensed deformation from InSAR will be added through a sister NASA project that began in May 2009. By the end of the project these products will provide nearly two decades of consistent and calibrated GPS deformation products. These data products will be at the level just below interpretation and will make scientific discoveries from PBO and other networks more accessible to the broad community of geophysics researchers and students by generating high level deformation products from the raw geodetic data and providing the through a science data portal with integrated product exploration and modeling tools.

Data products and web-based modeling tool are made accessible through a portal called GPS

Explorer (<http://geoapp03.ucsd.edu/gridsphere/gridsphere>, see below) that allows scientific users to explore and manipulate these products and data sets in a workbench-like environment. The tools allow users to explore geophysical parameters in response to earthquakes and volcanic events within the PBO and greater western North America region.

The project brings prototype IT infrastructure and product generation tools to a mature, flexible and expandable science data system providing high-level (Level-1C to Level-3) data products to the scientific community of geophysicists studying earthquake processes, crustal evolution, and magmatic systems in Western North America.

The project is funded through NASA's Making Earth System data records for Use in Research

Environments (MEaSURES) program.

2-066

A PRELIMINARY WESTERN US CRUSTAL MOTION MAP *Shen Z (UCLA), and Zeng Y (USGS)*

We have collected from numerous data archive centers all the available GPS data (both campaign mode and continuous) observed in the western US from October 1999 to present, and processed them in a homogeneous way. We have used the same software (GAMIT/GLOBK for daily GPS data processing and QOCA for final combination), employed the same processing strategy and parameterization, and estimated station secular velocities and coseismic and postseismic displacements due to large earthquakes simultaneously. A preliminary version of Crustal Motion Map for the western continental US has been produced, which includes secular velocities of 1689 stations, coseismic displacements at 93 sites caused by 3 earthquakes that occurred during this time period, and postseismic displacements of 313 sites whose positions were affected by postseismic deformation from 4 earthquakes.

2-067

AUTOMATED FAULT RESAMPLING FOR COSEISMIC SLIP INVERSIONS USING THE MODEL RESOLUTION MATRIX *Barnhart WD (Cornell), and Lohman RB (Cornell)*

We present an automated method of quadtree fault resampling for use in coseismic slip inversions from InSAR and GPS data sets. Our method allows for optimization of fault patch size given a particular data distribution with minimal user interaction. This method relies on the model resolution matrix to iteratively reduce fault patch size in well-resolved regions by calculating the spatial scale of smoothing between the centers of adjacent patches. Patches with scale lengths smaller than their current size are subdivided into four equal size patches while patches that are smoothed over a distance approximately equal to their size are retained. The method is done recursively until all scale lengths are consistent with the model resolution. This method differs from manual fault discretization algorithms in that it considers the entire model resolution matrix, not just the diagonal; thus, it more completely samples error and noise which play into the data's ability to resolve slip on a given patch. We apply this method to a variety of synthetic data tests as well as InSAR data for the 1995 Mw 8.1 Antofagasta subduction zone event. Our coseismic slip inversions agree well with published slip inversions that used variable fault discretization done arduously by hand, demonstrating the usefulness of our automated algorithm.

2-068

INTERCOMPARISON OF PBO BOREHOLE-STRAINMETERS AND -SEISMOMETERS IN ANZA, CALIFORNIA WITH NEARBY SURFICIAL BROADBAND SEISMOMETERS *Barbour AJ (PFO/IGPP at SIO), and Agnew DC (UCSD)*

Many of the PBO installations of borehole strainmeters and seismometers in the Anza region were made at sites of the Anza Seismic Network, which is instrumented with broadband seismometers in surface vaults. We compare the noise levels of these sensors from 10⁻³ to 10 Hz. The borehole strainmeters are 4-component Gladwin Tensor Strainmeters which should measure the horizontal

strain tensor; the borehole-seismometers are three orthogonal GS-1 2 Hz seismometers; and the surface instruments are Streckeisen STS-2's, with one STS-1 (located at the Pinon Flat Observatory). To evaluate relative sensitivities of these instruments, we examine relative noise levels, and use these to form a plot of phase velocity as a function of frequency. Such a plot allows us to identify which instrument has the best signal-to-noise ratio for a signal with given frequency and phase velocity. Generally speaking, the borehole strainmeter is preferable to the seismometers only for extremely low phase velocities: less than 100 m/s across the entire band, and less than 1 km/s at periods between 0.3 to 10 seconds.

2-069

ARE THERE GEOLOGIC/GEODETTIC FAULT SLIP RATE DISCREPANCIES IN SOUTHERN CALIFORNIA? *Johnson KM (Indiana), and Chuang YR (Indiana)*

The short answer to the title question is 'no'. We show that a viscoelastic earthquake cycle model constrained by GPS data predicts slip rates that are entirely consistent with geologic slip rate estimates on all major faults in southern California. However, the more nuanced answer to the title question is 'it depends on the model used to fit GPS data'. Previous inversions of GPS data in southern California illustrate not only discrepancies between geodetic and geologic estimates of fault slip rates, but also discrepancies between different models. Inversions using elastic half-space block models by Becker et al. [2004] and Meade and Hager [2005] result in fault slip rates that are a factor of two or more lower than geologic estimates on the Garlock Fault and the Mojave and San Bernardino (San Geronimo knot) segments of the San Andreas Fault. These models also predict a composite slip rate across faults in the southern Mojave section of the Eastern California Shear Zone that is 2-3 times faster than geologic estimates. In contrast, a joint inversion of GPS, geologic, and focal mechanism data by McCaffrey [2005] using an elastic block model with additional inelastic uniform block strain produces slip rate estimates that are mostly consistent with the geologic estimates.

Our viscoelastic earthquake cycle model consists of fault-bounded blocks in an elastic crust overlying a viscoelastic lower crust and uppermost mantle. It is a kinematic model in which long-term motions of fault-bounded blocks is imposed. Interseismic locking of faults and associated deformation is modeled with steady back-slip on faults and imposed periodic earthquakes.

Based on comparisons of an elastic block model and our viscoelastic cycle model, we conclude that elastic block models tend to underpredict slip rates on the Mojave and Carrizo segments of the San Andreas Fault and the Garlock Fault because these faults are mid to late in the earthquake cycle and current strain rates across these faults are lower than average due to viscous relaxation of the lower crust. We conclude that elastic block models overpredict the composite slip rate across the southern Mojave ECSZ because these faults are in the early phase of the composite earthquake cycle and current deformation rates across this region are higher than average because of accelerated viscous flow in the lower crust.

2-070

NEW GPS FAULT SLIP RATES FOR IMPROVED EARTHQUAKE HAZARD ASSESSMENT IN SOUTHERN CALIFORNIA *Thatcher W (USGS), and Murray-Moraleda J (USGS)*

Modeling GPS velocity fields in seismically active regions worldwide indicates deformation can be efficiently and usefully described as relative motions among elastic, fault-bounded crustal blocks. However, subjective choices of block geometry are unavoidable and introduce significant uncertainties in model formulation and in the resultant GPS fault slip rate estimates.

To facilitate comparison between GPS and geologic results in southern California we use the SCEC Community Fault Model (CFM) and geologic slip rates tabulated in the 2008 Uniform California Earthquake Rupture Forecast (UCERF2) report as starting points for identifying the most important faults and specifying the block geometry. We then apply this geometry in an inversion of the SCEC Crustal Motion Model (CMM4) GPS velocity field to estimate block motions and intra-block fault slip rates and compare our results with previous work.

In many parts of southern California—for example, north of the San Andreas Big Bend and SE of Los Angeles—our block geometry closely resembles that assumed in previous studies (McCaffrey 2005 JGR; Meade & Hager 2005 JGR; Becker et al. 2005 GJI). In these regions GPS slip rates on individual faults generally agree from one study to another and are also consistent with geologic slip rate estimates. However, there is no consensus on block geometry in the Transverse Ranges, Los Angeles Basin and Central Mojave Desert, where CFM faults are densely distributed, UCERF2 slip rates on several faults are comparable, and a simple block description may not be useful. It is notable that a number of documented disagreements between GPS and geologic slip rates occur on faults in these complex deforming zones (e.g. central Garlock fault, Eastern California Shear Zone, Big Bend San Andreas), in part reflecting the substantial epistemic uncertainty in GPS rate estimates for these faults.

Application of GPS data to hazard assessment in regions of densely distributed faulting may best be accomplished by alternative approaches such as estimating cumulative slip rates across several faults or simply using the average geodetic strain rate within each complex deforming zone. Elsewhere in southern California, slip rates may be used directly in hazard calculations once GPS rates are agreed to among geodesists and are judiciously incorporated with geological estimates to obtain consensus rates.

2-071

TRANSIENT DETECTION WORKSHOP RESULTS: PHASE II *Lohman RB (Cornell), Murray-Moraleda J (USGS), and Agnew DC (UCSD)*

The Transient Detection Test Exercise is a project in support of one of SCEC III's main science objectives, to "develop a geodetic network processing system that will detect anomalous strain transients." Fulfilling this objective is a high priority for SCEC and will fill a major need of the geodetic community. A means for systematically searching geodetic data for transient signals has obvious applications for network operations, hazard monitoring, and event response, and may lead to identification of events that would otherwise go (or have gone) unnoticed.

As part of the test exercise test datasets are distributed to participants who then apply their detection methodology and report back on any transient signals they find in the test data. Phase I of the exercise ran from January 15 to March 15, 2009; the test data and results are posted at <http://groups.google.com/group/SCECtransient>. Phase II of the test exercise has begun with the distribution of test data and results due on August 24, 2009. Both Phase I and II have used synthetic GPS datasets, but we plan to expand this to include real data and other data types in future phases. Here we show the results of the blind test exercise for both of the first two phases, including details of the synthetic examples that we drew from.

2-072

PCA-BASED TRANSIENT DETECTION: APPLICATION TO SCEC PHASE II DATA *Ji KH (MIT), and Herring TA (MIT)*

The detection algorithm in the analysis is based on the sequential application of state estimation smoother and principal component analysis (PCA). The state parameters are an initial offset, velocity, annual and semi-annual sinusoids, and the first-order Gauss-Markov (FOGM) process. The FOGM process accounts for not only time-correlated noise but also transient signals, however, the FOGM (random) process may not fully account for a (systematic) transient signal. If such signal is detected, we re-estimate the FOGM states by increasing process noise within signal time interval. PCA uses only FOGM estimates. Principal components (PCs) from time-correlated noise show sinusoidal temporal patterns similar to Fourier series expansion, which can make a transient signal unclear. Furthermore, large temporal variation not coherent in space possibly appears in first a few PCs, which may also hide a transient signal. We increase the signal-to-noise ratio by focusing a target signal in both space and time. We use spatial distribution of PCs for space focusing and a stack of the FOGM estimates for time focusing. The algorithm detected transient signals in cases 003923 (2003.4 ~ 2004.6) and 010157 (2001.6 ~ 2002.6 and 2003.0 ~ 2003.2) in Group A and cases 010056 (2002.13 ~ 2002.18) and 010731 (2004.0 ~ 2004.7) in Group B. All signals detected originate in the Los Angeles area. The signal in case 003923 propagates in both space and time, which is described by first two PCs. There are two events with time interval of 0.4 year in case 010157. The cases in Group B are more subtle. In case 010056, large fast slip is detected but missing at some sites. The signal in case 010731 is noisy in space but we believe this signal to be a transient because it is localized.

2-073

INSTANTANEOUS DEFORMATION FROM GPS: RESULTS FOR THE SCEC TRANSIENT DETECTION EXERCISE *Holland AA (Arizona)*

We applied a technique to model instantaneous velocities from GPS position time-series to the SCEC transient detection exercise. The SCEC transient detection exercise provides a unique opportunity to benchmark and evaluate different techniques designed to examine time-dependent deformation processes against a set of synthetic coordinate time-series from continuous GPS (CGPS). The dataset is carefully constructed to mimic Southern California CGPS distribution and operating times. Unknown noise sources were inserted into the data, and deformation transients were also inserted into some of the simulated time-series. Our technique models the best fitting smooth spline and the secular velocity to the coordinate time-series. This smooth spline provides a continuous representation of the instantaneous velocity. This velocity function integrates to zero over the duration of the observation period. We must select a proper amount of smoothing to constrain our model to a single solution from the infinite set of possible solutions. We do this by simply examining the averaging kernel width associated with our basis functions and possible choices of damping values. This allows us to select an averaging kernel width, which is appropriate for the potential transients. This time-dependent velocity field can then be used to provide time dependent strain rate by determining the spatial gradient of the velocity field. We present our results from the SCEC transient detection exercise using our smoothing spline determination for instantaneous velocity.

2-074

DETECTING STRAIN TRANSIENTS IN THE SALTON TROUGH *McGuire JJ (WHOI), Segall P (Stanford), and Herring TA (MIT)*

The Salton Trough region routinely experiences fault creep transients with time-scales of days to weeks, and previous studies have documented a temporal relationship between these aseismic transients and earthquake swarms. The Plate Boundary Observatory has greatly increased the density of continuous geodetic data available in the Salton Trough, and we are analyzing this dataset to detect time periods when aseismic transients occurred in the Salton Trough.

We are searching the daily GPS solutions for the time period from 2005-2009 for transients using Kalman Filter based detection algorithm called the Network Strain Filter [Ohtani, McGuire, and Segall, 2009]. The NSF solves for estimates of the secular velocity field and a time-vary transient displacement field that are expanded in basis functions. We utilize two dimensional wavelets as the basis functions. Spatial smoothing of the transient and secular velocity field are achieved by weighting the prior covariance matrix elements based on the scale of the individual wavelet basis. Site specific colored noise (seasonal terms, etc) is estimated as an random walk for each component.

The vast majority of the Salton Trough GPS records are well explained by a combination of secular velocity and seasonal terms. However, we do find two spatially coherent transient episodes visible at multiple stations in the GPS data. The largest occurs near the southern extension of the Superstition Hills fault (Weinert Fault) during the second half of 2007. About 1 cm of extra motion to the northwest is observed at station P494, P496, and P497. The time scale of this transient is a few months. A second, smaller more abrupt transient is observed at stations P500 and P744 at the time of the February 2008 earthquake swarm at Cerro Prieto. We are investigating whether these two transients can be explained by slip on the Superstition Hills and Imperial faults respectively.

2-075

SEISMICITY-BASED TRANSIENT DETECTION IN THE SALTON TROUGH *Llenos AL (MIT/WHOI), and McGuire JJ (WHOI)*

Aseismic processes such as fluid flow, magma migration, and slow slip can trigger changes in seismicity rate. To detect these processes in space and time, we have developed a method that can map these seismicity rate variations to the stressing rate changes due to these processes. Because aftershocks often obscure changes in the background seismicity caused by these processes, we combine two models commonly used to estimate the time dependence of underlying driving mechanisms, the stochastic Epidemic Type Aftershock Sequence model (Ogata, 1988; Ogata, 1998) and the physically based rate- and state-dependent friction model (Dieterich, 1994), into a single seismicity rate model that can explain both aftershock activity as well as changes in background seismicity rate. We then implement this model into a data assimilation algorithm that inverts seismicity catalogs for stressing rate variations, resulting in space-time estimates of the state variables in our model (background stressing rate, aseismic stressing rate, and rate-state variable γ) as well as maximum likelihood estimates of the ETAS and rate-state parameters.

We apply our method to a catalog of $M > 1.8$ events occurring in the Salton Trough from 1982-2009. A number of geodetic studies have detected several transient stressing events in this region, including for example afterslip following the 1987 Superstition Hills earthquake (e.g., Williams and Magistrale, 1989), dynamic triggering following the 1992 Landers and 1999 Hector Mine earthquakes (Gomberg et al., 2001), and shallow aseismic creep on the Obsidian Buttes fault (Lohman and McGuire, 2007). The seismicity rate anomalies detected by our algorithm can in many cases be linked to geodetically-observed stressing rate transients. We calibrate our stressing rate

estimates by calculating the Coulomb stress change due to a shallow aseismic slip event on the Obsidian Buttes fault (Lohman and McGuire, 2007). The results suggest that our method can be a useful tool to detect and map transient deformation strictly from seismicity catalogs.

2-076

TRANSIENT DETECTION IN GEODETIC DATA: A COMPARISON OF MODAL DECOMPOSITION METHODS *Lipovsky BP (UCR), Floyd MA (UCR), and Funning GJ (UCR)*

Motivated by the SCEC transient detection exercise, we have explored several general methods for the analysis of geodetic time series. Our research goal is to define algorithms which will eventually lead to the automation of transient motion detection in much the same way that seismic data is currently automatically aggregated and analyzed in near real time. All of our methods intend to isolate signals which may be any combination of low amplitude (near noise level), temporally transient, unaccompanied by seismic emissions, and heretofore unnoticed.

All of the modal decomposition methods discussed represent geodetic data as linear combinations of temporal and spatial information (modes). We use the technique of mode rotation to find physically meaningful combinations of modes. We also compare several methods of handling missing data within the framework of PCA.

Strictly speaking, PCA is not defined on datasets with missing values. We use a Maximization-Expectation (ME) implementation of probabilistic PCA (pPCA) to estimate the equivalent to principal components for the missing data case. For methods of handling missing data which do not result in a true covariance matrix, we evaluate the method of Higham to find the "nearest" covariance matrix. Several heuristic solutions to the missing data problem are also evaluated.

We show the geophysical relevance of these techniques by comparing the results of each method. Results are compared by inverting modes of deformation to estimate temporally varying fault slip.

2-077

MODEL-BASED GEODETIC TRANSIENT DETECTION *Ohlendorf SJ (Berkeley), Feigl KL (Wisconsin), and Thurber CH (Wisconsin)*

We describe the initial evaluation of a model-based approach to the detection of geodetic transients. The basic strategy is to use the triangular element geodetic inversion code of Murray and Langbein (2006) and an a priori fault geometry model to develop a "reference" fault slip model using GPS data from a selected "quiet" time interval. For a subsequent time period, which we call the "evaluation" interval, we solve for a new slip model and evaluate the fit of the original "reference" model to the data from the "evaluation" interval. This approach provides two measures for detecting possible transients: changes in the slip model and changes in the data misfit. It allows the use of statistical tests to evaluate the significance of the results. Our approach is being applied to the Parkfield area, where seismic and aseismic events are well characterized and can be used to test the sensitivity of our approach.

2-078

ANOMALY DETECTION IN PROBLEMATIC GPS TIME SERIES DATA AND MODELING *Avraham DR (UCLA), and Bock Y (UCSD)*

Detecting anomalies in Global Positioning System (GPS) time series is a matter of considerable importance and concern in geodetic research. The Scripps Orbit and Permanent Array Center (SOPAC) generates continuous and daily time series in three-dimensions for over 1400 global GPS stations, focusing on Southern California and Western North America. The time series are automatically analyzed using a computerized modeling program, which is limited to fitting slopes (velocities), offsets, periodic (annual and semiannual terms), and (exponential) postseismic decays, for entire time series, but anomalous events are not adequately recognized or considered. Therefore, we have developed anomaly detection algorithms specifically for GPS time series that are capable of detecting signals, outliers, and trends in the data, as well as modeling problems. The algorithms are inspired by time series analysis techniques and anomaly detection methods from various other fields, including statistics, econometrics, and mathematical sciences, and therefore contain modified versions of noise analysis, correlation statistics, and threshold utility. The algorithms run on the complete set of global GPS time series, successfully uncovering a majority of the previously undetected anomalies. Furthermore, we spatially cluster the types of anomalies in order to gain insight into the geophysical factors that contribute to the occurrence of such incongruities.

We are developing a new interactive environment that will allow users to analyze on-the-fly temporal and spatial subsets of GPS time series in various ways, and to detect anomalous events using the methods described above. This is being incorporated into the GPS Explorer data portal (<http://geoapp.ucsd.edu>), a joint project of SOPAC and JPL to provide user-friendly GPS data products and on-line modeling applications.

2-079

ESTIMATING TIME-DEPENDENT VELOCITY GRADIENT TENSOR FIELDS AS A METHOD FOR RECOGNIZING STRAIN RATE TRANSIENTS *Holt WE (SUNY-Stony Brook), and Hernandez D (City of San Fernando)*

We are continuing work on developing and refining a tool for recognizing strain rate transients as well as for quantifying the magnitude and style of their temporal and spatial variations. We determined time-averaged velocity values in 0.05 year epochs using time-varying velocity estimates for continuous GPS station data from the Southern California Integrated GPS Network (SCIGN) for the time period between October 1999 and February 2004. A self-consistent model velocity gradient tensor field solution is determined for each epoch through bi-cubic Bessel interpolation to the GPS velocity vectors whereby we determine model dilatation strain rates, shear strain rates, and the rotation rates. Departures of the time dependent model strain rate and velocity fields from a master solution, obtained from a time-averaged solution for the period 1999-2004, with constraints provided by imposed plate motion and Quaternary fault data, are evaluated in order to best characterize the time dependent strain rate field. A particular problem in determining the transient strain rate fields is the level of smoothing or damping that is applied. Our current approach is to choose a damping that both maximizes the departure of the transient strain rate field from the long-term master solution and achieves a reduced chi-squared value between model and observed GPS velocities of around 1.0 for all time epochs. We present results from the SCIGN data, which are dominated by the Hector Mine earthquake, as well as results obtained to date on the SCEC transient II detection exercise.

2-080

ABNORMAL STRAIN CHANGES REVEALED FROM NATIONAL GPS NETWORK IN JAPAN *Ohya F (Kyoto)*

The dense national GPS network, GEONET, has been operated in Japan since middle of the nineteen-nineties. At the Kinki district in southwest Japan, the seismicity in the highland area in the northern part of this district decreased slightly but clearly and suddenly at the beginning of 2003. I will present the anomalous strain rate change in GEONET data related to this quiescence in the seismic activity.

Strain rate is evaluated from the distance changes between two stations. The pairs of stations are configured with not only the locally nearest two stations but also the longer distanced pairs over the neighbor station, and the length of baselines is limited about 40km. The time series data are smoothed by extracting the median values in the moving time windows, what we call running median data series. This procedure makes the data series linear with few noisy deflections. The processed data of all pairs in the Kinki district, over 550 pairs, are tested whether the folding point are exist or not on their line graph by the successive linear regression approximation in each part of the graph divided by the moving point. If the line is folded exactly at a point, two regression lines on each segment intersect closely near the dividing point. However in most cases two regression coefficients do not differ from each other significantly, it is the case of no folding point. This procedure will be expanded to the case of three line segments with two folding points, and so on.

In the time-space distribution of the baselines with folded line graph, they concentrated in the northern part of this district and to the latter half of 2002 in time, which preceded the seismic quiescence. The amounts of strain rate changes at the folding point depend on the direction of the lines. At the baseline in ESE-WNW direction, the strain rate decreased in the maximum value. At the lines perpendicular to the former direction, the strain rate decreased in the minimum value. The direction of the maximum strain rate decrease is consistent to the direction of P-axis of the focal mechanism in this area. This fact reveal that the stress change which forced strain rate decrease in this area caused the following quiescence in the seismic activity, and the time delay of the beginning of decreasing in the seismic activity from that of the surface crustal strain change suggest the effect of the viscosity or fluid at the seismogenic depth.

Fault Rupture and Mechanics (FARM)

2-001

RECORD BREAKING EARTHQUAKE INTERVALS IN GLOBAL CATALOGS AND AFTERSHOCK SEQUENCES *Yoder MR (UCD), Turcotte DL (UCD), and Rundle JB (UCD)*

Inter-occurrence times are the time intervals between successive earthquakes with magnitudes greater than a specified value in a specified region. A record-breaking inter-occurrence time interval is defined to be larger (or smaller) than all previous intervals; a starting date must be specified. In this paper, we show that the succession of record-breaking intervals for random background seismicity is very different from the succession for aftershocks. Specifically, we consider the number of record breaking interval times as a function of the number of events that have occurred. We first consider earthquakes on a world-wide basis with moment magnitudes greater than 5.5 for the years 1977 to 2006. We determine the number of record breaking earthquakes, n_{rb} , during 10,592 successive periods of 1024 events and average the results for sub-intervals. For a random (iid) process, the prediction is $n_{rb} \sim \ln(n)$ where n is the number of events. Our results are in excellent agreement with this prediction.

We next consider the sequence of record breaking time intervals in the aftershock sequences following the Parkfield earthquake. As the aftershock sequence decays in time, it is expected that there will be a strong increase in record-breaking intervals. For the example considered, we find that $n_{rb} \sim n$ is a good approximation. Thus, there is a strong statistical difference between the behavior of aftershock and background random seismicity.

2-002

SEISMIC RADIATION FROM REGIONS SUSTAINING MATERIAL DAMAGE *Ben-Zion Y (USC), and Ampuero J (Caltech)*

We discuss analytical results for seismic radiation during rapid episodes of inelastic brittle deformation that include, in addition to the standard moment term, a damage-related term stemming from changes of elastic moduli in the source region. The radiation from the damage-related term is associated with products of the changes of elastic moduli and the total elastic strain components in the source region. Order of magnitude estimates suggest that the damage-related contribution to the motion in the surrounding elastic solid, which is neglected in standard calculations, can have appreciable amplitude that may in some cases be comparable to or larger than the moment contribution. A decomposition analysis shows that the damage-related source term has an isotropic component that can be larger than its DC component.

2-003

STUDY OF FRICTIONAL PROPERTIES OF GRANITE OVER A TEMPERATURE RANGE OF 15 – 500 °C *Mitchell EK (UCSD), Brown KM (UCSD), and Fialko Y (UCSD)*

We investigate frictional properties of K-feldspar granite using a heated direct shear apparatus. We study the effects of temperature, applied forcing velocity and normal stress on the evolution of friction. In particular, we measure peak friction coefficient, velocity, amplitude and duration of individual slip events. We perform two types of tests in this study: hold tests and high sample rate tests. In a hold test the rock sample is allowed to remain in quasi-stationary contact under a constant normal load for a given time. The sample is then rapidly loaded at a constant forcing velocity until it slips. We measure peak friction coefficient as a function of hold time at 15, 300 and 500 °C. Static coefficient of friction increases as a logarithm of hold time with a pre-multiplying coefficient, in rough agreement with results of Dieterich (1972). The effect of increasing temperature is to increase the value and rate of change of the static friction coefficient as a function

of hold time. This suggests that post slip fault strengthening is enhanced at higher temperatures. Our observations indicate that the thermally-activated flattening of the asperities and concomitant increases in the actual contact area dominate over decreases in the shear strength of the asperities to produce a noticeable strengthening effect. We also performed a series of high sample rate (10,000 Hz) tests to study the effects of varying normal stress, forcing velocity, and temperature on the velocity, amplitude and duration of individual slip events. Increasing temperature increases slip distance and decreases slip duration so that slip rate increases. We observe a dramatic jump in slip characteristics as temperatures rise from 300 °C to 400 °C: both slip time reduces and slip rate increases by two orders of magnitude. With increasing normal stress or decreasing forcing velocity we measure an increase in slip duration and amplitude, but the rate of amplitude increase is higher still so that slip velocity increases. We speculate that the jump in slip velocities of individual slip events as background temperature changes from 300 to 400 °C is related to the weakening of the quartz mineral phase. Also, we surprisingly observe stick-slip behavior at temperatures as high as 500 °C. This may highlight the importance of water in the stick-slip/creep transition at the bottom of the seismogenic zone since all of our tests were conducted at dry conditions.

2-004

PARTICLE SIZE DISTRIBUTIONS, MICROSTRUCTURES AND CHEMISTRY OF FAULT ROCKS IN A SHALLOW BOREHOLE ADJACENT TO THE SAN ANDREAS FAULT NEAR LITTLE ROCK, CA *Wechsler N (USC), Chester JS (Texas A&M), Rockwell TK (SDSU), and Ben-Zion Y (USC)*

In mapping the distribution of fractured crystalline rocks along the Mojave section of the San Andreas Fault (SAF), Dor et al. (2006) found that almost all of these rocks within 50 to 300 m from the fault are pulverized to some degree. In an effort to characterize the role of surface weathering, and quantify the mesoscale and microscale deformation of these rocks as a function of depth in the shallow subsurface environment, we have collected a nearly continuous, 42 meter-deep core from pulverized rocks adjacent to the main strand of the SAF near Little Rock, California. The Little Rock site is characterized by extensive outcrops of granitic rock displaying varying degrees of damage up to a few hundreds of meters from the fault's primary active strand. The cored section is composed primarily of pulverized granites and granodiorites, and is cut by numerous mesoscopic secondary shears. Medium to coarse silt- and fine sand-size particles dominate throughout the cored section; very few micron-scale particles are observed and only minor amounts of clay weathering products are present. Mapping on optical and SEM images of core samples at various depths and magnifications defines the distribution of two main fault rock types, pulverized zones displaying primarily opening-mode fractures, and cataclastic fault zones. The pulverized regions display large host-rock crystals that are fractured to produce angular particles often ranging from 10-100 microns in diameter. The fractured parts display optical continuity and a high density of fluid inclusion trails suggesting episodes of fracture healing. The cataclastic zones are characterized by smaller (0.5-10 microns) and more rounded grains, a greater clay content, and sometimes show repeated stages of calcite cementation and shear. The distribution of pulverized particles and cataclastic zones indicate multiple fracture-healing cycles to produce an outcrop that reduces to powder when dug out with a hammer. Most samples analyzed to date suggest that cataclastic grain size reduction and shear at the microscale are significant processes in the formation of this pulverized zone. Currently, we are quantifying the particle size distribution and aerial extent of representative cataclastic zones in this region.

2-005

VOLUMETRIC EXPANSION AND THE ORIGIN OF POTASSIUM FELDSPAR MEGACRYSTS IN THE DAMAGE ZONE OF THE SAN ANDREAS FAULT NEAR LITTLE ROCK, CALIFORNIA *Anderson KM (SDSU), Rockwell TK (SDSU), Girty GH (SDSU), and Wechsler N (USC)*

In order to determine the origin of pink potassium feldspar megacrysts in a tabular zone of biotite granodiorite within the damage zone and fault core of the San Andreas fault, an ~400 m transect normal to the trace of the fault near Little Rock, California was sampled and studied. Bulk and grain densities of samples were determined using the modified wax-clod method and a helium pycnometer respectively. Porosity was then determined by the relationship $1 - (\rho_{bl}/\rho_g)$ where ρ_{bl} is the bulk density and ρ_g is the grain density. Within the transect, the porosity of the parent rock varies from 0 to ~1.5%. In contrast, measured porosity within the damage zone reaches ~17%, but then falls to ~9% within the fault core. Volumetric strain, bulk mass change, and elemental mass change were all calculated using Al₂O₃ as the immobile element. Results indicate positive volume strain throughout the damage zone and fault core with a volumetric expansion of ~42% within the damage zone and ~10% within the fault core. Rocks of the damage zone display a bulk mass gain of up to ~17% while rocks of the fault core lost ~2% of their bulk mass. Changes in elemental mass are believed to be due to the alteration of minerals by fluid migration through the damage zone as indicated by petrologic data observed in thin section and mass balance relationships. For example, the elemental mass of SiO₂ increases within the damage zone to values as high as ~28%, but then decreases in the fault trench to values as low as ~6%. This relationship may suggest that fluids leached silica from the fault core and then transferred it to the damage zone. In addition, the most dramatic increase in elemental mass is displayed by K₂O. Throughout the damage zone and fault core K₂O mass is increased by ~78%. This dramatic increase appears to correlate to an increase in pink potassium feldspar within the damage zone. The above results support numerical models which suggest volumetric expansion within fault damage zones around the principal slip surface creating a "flower-like" structure composed of minimal damage around the fault at depth which then fails by dilation at the earth's surface. A second transect was completed near Lake Hughes, California and data derived from this phase of our study will be presented at the meeting.

2-006

CHAOS AND LOCALIZATION IN DIETERICH-RUINA FRICTION *Erickson BA (UCSB), Birnir B (UCSB), and Lavallee D (UCSB)*

We consider two models derived from a 1-D Burridge-Knopoff chain of spring connected blocks subject to the nonlinear Dieterich-Ruina (D-R) friction law. We analyze both the discrete ordinary differential equations, as well as the continuum model. Preliminary investigation into the ODEs shows evidence of the Dieterich-Ruina law exhibiting chaos, dependent on the size of the system. Periodic behavior occurs when considering chains of 3 or 5 blocks, while a chain of 10 blocks with the same parameter values results in chaotic motion. The continuum model (PDE) undergoes a transition to chaos when a specific parameter is increased and the chaotic regime is reached for smaller critical values than in the case of a single block (see Erickson et. al. 2008). This parameter, epsilon is the ratio of the stress parameters (B-A) and A in the D-R friction law. The parameter A is a measure of the direct velocity dependence (sometimes called the "direct effect") while (A-B) is a measure of the steady-state velocity dependence. When compared to the slip weakening friction law, the parameter (B-A) plays a role of a stress drop while A corresponds to the strength excess. In the case of a single block, transitions to chaos occur when epsilon = 11, a value too high for applications in seismology. For the continuum model however, the chaotic regime is reached for epsilon = 1. That the transition to chaos ensues for smaller parameter values than in the case of a single block may also be an indication that a careful rescaling of the friction law is necessary,

similar to the conclusions made by Schmittbuhl et. al. (1996) who studied a "hierarchical array of blocks" and found that velocity weakening friction was scale dependent. We also observe solutions to both the discrete and the continuous model where the slip remains localized in space, suggesting the presence of solitonic behavior. Initial data in the form of a gaussian pulse tends to remain localized under certain parameter values and we explore the space of values for which this occurs. These solitonic or localized solutions can be understood as proxy for the propagation of the rupture across the fault during an earthquake. Under the Dieterich-Ruina law we may have discovered only a small subset of solutions to both the discrete and the continuous model, but there is no question that even in one spatial dimension, a rich phenomenology of dynamics exists.

2-007

RHEOLOGY AT THE BASE OF THE SEISMOGENIC ZONE *Hirth G (Brown), Behn M (WHOI), and McGuire JJ (WHOI)*

While debate continues on the stress state on seismogenic faults, a combination of experimental and geological and geophysical observations show good agreement between the rheology of rocks predicted by extrapolation of lab data and that inferred based on microstructural observations of natural mylonitic rocks. These types of studies indicate stresses on order of 100 MPa are common near the base of the seismogenic zone in several lithologies and tectonic environments. Some of the best constraints on rheology at these conditions come from mantle rocks. Geophysical observations indicate that

seismicity in the oceanic lithosphere is generally limited to depths above the 600C isotherm. This relationship is in good agreement with extrapolation of experimental data on the frictional behavior of olivine (Boettcher et al., 2007). Under laboratory conditions, a transition from unstable to stable frictional sliding is observed at a temperature of approximately 1000C. By accounting for the rate-dependence of crystal plasticity at asperities, the same transition is predicted to occur at a temperature of ~600C in the Earth. A unique aspect of many oceanic earthquakes is that they likely occur in what was previously undamaged rock. Owing to upwelling and corner flow, the mantle rocks cool below the 600C isotherm prior to any brittle deformation. Thus, rocks in the source regions for these earthquakes are likely intact at relatively high pressure with no pore fluids present. In other words, almost all the mechanisms hypothesized to produce weakening along faults in continental settings are unlikely to be active prior to an earthquake in the oceanic lithosphere. These rocks could thus be capable of supporting differential stresses in the range of 500 MPa at depths of 20 to 30 km. Microstructural observations of mylonitic peridotites from the oceanic lithosphere, interpreted to reflect deformation at the base of the seismogenic zone, are consistent with stresses of this magnitude (Warren and Hirth, 2006). Similarly, the "apparent stress" estimated for some earthquakes from oceanic lithosphere can be quite high, and based on scaling arguments, are also consistent with these estimates of differential stress (Choy and McGarr, 1999). We will review these rheological constraints, and outline the evidence (or lack thereof) for high stresses based on earthquake seismology.

2-008

MICROMECHANICAL DAMAGE MECHANICS OF WESTERLY GRANITE *Sammis CG (USC), Bhat HS (Harvard), and Rosakis AJ (Caltech)*

We have derived an energy function for the micromechanical damage mechanics formulated by Ashby and Sammis (PAGEOPH, 1990) and used it to calculate the stress-strain curves for Westerly granite. The strain due to crack growth in this model is an order of magnitude smaller than the non-linear strain measured by Lockner (JGR, 1998) – even after we extended the Ashby-Sammis model to include the observed distribution of initial flaw sizes and orientations. These extensions

also failed to produce the observed curvature in the failure envelope. We were, however, able to reproduce the experimental curvature by considering a two-mineral model for granite in which a stronger mineral obeys damage mechanics at all stresses up to failure while a weaker mineral deforms by a low-temperature obstacle-controlled flow law at lower stresses. Flow of the weaker mineral concentrates stress on the stronger one such that the apparent failure stress is an average of the failure stress of the strong mineral and the flow stress of the weaker one. This apparent failure stress has the experimentally observed curvature. At very high confining stress, the stronger mineral also flows, as originally proposed by Ashby and Sammis. The non-linear flow of the weaker mineral produces the extra strain necessary to match the data. In fact the functional form of obstacle-controlled flow predicts the observed logarithmic relation between shear stress and non-linear strain using physically reasonable parameters in the flow law. Such stress transfer from weak to strong minerals may explain the commonly observed preferential shattering of quartz grains in pulverized rock adjacent to major faults.

2-009

LABORATORY INVESTIGATIONS OF MICROCRACKING AND FRAGMENTATION IN WESTERLY GRANITE *Yuan F (CWRU), and Prakash V (CWRU)*

Zones of pulverized rock have been observed in surface outcrops adjacent to the fault cores of the San Andreas and other major faults in Southern California. The origin of these pulverized rocks is not clear, but their structural context indicates that they are clearly associated with faulting. In the present study, a series of laboratory experiments are conducted on Westerly granite rock samples to investigate the critical conditions for initiation of microcracking and subsequent fragmentation under stress-wave loading conditions. In the first series of experiments a Split Hopkinson pressure bar (SHPB) is utilized to subject cylindrical rock specimens to well defined uniaxial compressive stress-wave loading. In these experiments the amplitude as well as the duration of the compressive loading pulse is systematically varied to study the initiation and progression of fragmentation in both confined and unconfined granite samples. Well-characterized lateral confinement can be generated in the cylindrical specimens during SHPB testing by utilizing metal sleeves/jackets around the specimens during the dynamic loading process. In the second series of experiments, plate-impact experiments are conducted to obtain the stress threshold for inelasticity in Westerly granite by estimating its Hugoniot Elastic Limit (HEL) under shock-induced compression. These experiments are designed to also provide spall (tensile) strength following shock-induced compression in the granite samples. In addition, soft recovery plate-impact experiments have been conducted to better understand the threshold for initiation of microcracking in the granite. The results of the SHPB experiments indicate that the peak stress for Westerly granite under uniaxial compression is ~ 210 MPa (with a strain to failure of about 0.7%) in the unconfined state; the peak stress increases to 1 GPa with a confinement pressure of 60 MPa. The HEL for the granite is estimated to be between 4.2 to 5.0 GPa. The spall strength following the shock-compression is measured to be small (~ 50 MPa), and nearly independent of the applied compression level in the range 1.2 to 5.0 GPa. The post-impact samples show a well-defined spall plane with no apparent fragmentation at a shock compression level of 1.2 GPa. At higher impact velocities, fragmentation is observed up to 1.8 GPa, and the rock samples are reduced to a powder at impact stress levels of above 2.6 GPa.

2-081

SYSTEMATIC SEARCH FOR SPONTANEOUS NON-VOLCANIC TREMOR NEAR HEMET AND SIMI VALLEY, SOUTHERN CALIFORNIA *Hillers G (UCSB), and Ampuero J (Caltech)*

Since its discovery in Japan, non-volcanic tremor (NVT) signals have been detected in virtually all circum-Pacific subduction zones where sufficient instrumentation exists. Furthermore, tremor bursts have been identified beneath the central section of the SAF over a time span of several years. Tremor swarms were also detected in southern California at different locations, triggered by the passage of surface waves from the 2002 Denali earthquake. These observations warrant a systematic search for tremor signals in southern California using continuous recordings by the available dense seismic network.

Focusing on six-hour night time data segments from selected station subsets of the Southern California Seismic Network (SCSN), we implemented a transient detection algorithm based on similarity across station clusters of seismogram envelopes in the 2 to 8 Hz frequency band.

The detection efficiency depends on parameters that determine the temporal scale of transients and the exclusion of earthquake signals. To achieve a relatively large ratio of positive to false detections, we experiment with a range of minimum-transient durations and max-to-mean amplitude ratios per correlation window.

Processing data from the HRSN borehole stations that include tremor signals originating on the SAF in the Cholame region, we tune the algorithm by comparing results to higher resolution tremor detections by D. Shelly.

We find that our method reliably detects tremor signals that last longer than one minute; allowing shorter durations leads to increased indications of earthquake waveforms. Analyzing the same data set using a few nearby surface broadband stations with significantly larger inter station distances, strong, long duration tremor signals are also detected with a high success rate.

This benchmarking warrants detections of similar signals at other places in southern California.

We apply our strategy to clusters of stations distributed around the reported triggered tremor sources in the Simi Valley and around Hemet, analyzing data from 2000 to 2008. Signals that match the automated tremor characteristics are individually inspected and selected for further analysis. We present statistics of the temporal distribution of selected signals. We apply a 3D grid search technique to locate the origin of the tremor signals by minimizing the errors in the inter station differences of peak-envelope arrival times. Preliminary results of these efforts will be reported.

2-082

OVERESTIMATIONS OF THE WIDTH OF LOW-VELOCITY FAULT ZONES IN INSAR ANALYSES BY STATIC STRESS CHANGES *Duan B (Texas A&M), and Kang J (Texas A&M)*

Low-velocity fault zones (LVFZs) have been detected along active faults by seismic investigations (trapped waves and travel time analysis) and InSAR observations. However, the width of LVFZs estimated from these two types of data is significantly different: seismic investigations generally give a value of several hundred meters, while InSAR analyses obtain a value of 1.5~3 km. Although a recent study on the Calico fault (Cochran et al., 2009) attempts to reconcile this discrepancy, the 1.5-km-wide fault zone along the fault appears to be dominantly determined by the InSAR data

analysis. In this study, we use numerical models to show that the width of LVFZs obtained by previous InSAR analyses may be significantly overestimated. We construct 2D plane-strain models of a strike-slip fault with three LVFZs. One LVFZ (II) surrounds the fault, and the other two (I and III) are 10 km away from the fault. Each of the LVFZs is 200 wide with a reduction in shear wave velocity of 40% relative to wall rock. We use an explicit finite element dynamic code EQdyna to simulate rupture propagation on the fault and wave propagation in the inhomogeneous medium. We find strain localizations around the LVFZs I and III in the final displacement field. We measure these residual displacements caused by the LVFZs in our models. Predictions of residual displacements by the static stress change hypothesis proposed in previous InSAR analyses (e.g., Fialko et al., 2002; Cochran et al., 2009) are only a small fraction (25% or less) of those observed in our models. To fit observed residual displacements by the hypothesis, one would need much wider LVFZs (4 times or wider). This suggests that the width of LVFZs may be overestimated by a factor of 4 or larger in previous InSAR analyses. Dynamic waves appear to play a much more important role in strain localizations around LVFZs induced by nearby ruptures than static stress changes.

2-083

CONSTRAINING THE FRICTIONAL BEHAVIOR OF THE SOUTHERN SECTION OF THE HAYWARD FAULT *Kanu CO (Indiana), and Johnson KM (Indiana)*

Since at least the 1920's, sections of the Hayward fault (HF) have exhibited nearly steady surface creep of 5-10mm/yr. However, theodolite surveys of monuments spanning ~100m across the fault show changes in creep rates on the HF following the 1989 Loma Prieta (LP) earthquake on the San Andreas Fault. These changes have been explained as a response to change in the stress state of the fault as a result of 1989 LP earthquake. The theodolite data show that the southern portion of the HF essentially stopped creeping or even reversed sense of creep for about 6 yrs immediately after the 1989 earthquake. Following this period of near-quiescence, a rapid transient creep event was observed in this section of the fault accumulating an average of 20-25mm of slip. This creep response to a sudden shear stress reduction is consistent with predictions from spring-slider (SS) models with slip governed by rate-state (RS) friction. To study this transient behavior and infer friction parameters on the fault, we model the data with a triple SS model coupled with the rate- and state-dependent friction laws. This model is supported by various studies which have successfully linked the connection between slip behaviors to their governing frictional properties. The normal stress change along the fault surface resulting from the 1989 earthquake is also incorporated into the model as an instantaneous change immediately after the earthquake. We inverted the data using a Monte Carlo Metropolis algorithm to obtain the posterior probability distributions for RS friction parameters. We find that the model provides an acceptable fit to the creep evolution within 1989-2007. We find a critical slip distance, d_c , of order $10^{-4.3}$ to $10^{-3.5}$ which is 2-3 orders of magnitude larger than typical lab values from small rock samples. The incorporation of the instantaneous change in effective normal stress allowed for an independent estimation of effective normal stress which is within the range of 5-85MPa. The range of values we found for a , $a-b$, L (patch radius) and V (long-term slip rate) are 0.0025 to 0.035, 10^{-6} to 10^{-4} , 3.5-8.5km, and 4-7.5mm/yr respectively. Estimates of a and $a-b$ fall within the range of values inferred from lab experiments. The inferred patch radius implies surface creep on the southernmost HF extends to a depth of ~10km with a low effective normal stress. These friction parameter estimates are similar to estimates from the creeping section of Parkfield California.

2-084

CHARACTERIZING MICRO-SCALE FAULT ROUGHNESS USING LIDAR AND INTERFEROMETRY *Muirhead AC (UCSC), Brodsky EE (UCSC), and Savage HM (Penn State)*

Faults are often considered planar, but numerous field and seismologic studies show that faults can be highly irregular, with bumps, striations, and larger-scale bends. Stress concentrates at surface asperities so that fault roughness undoubtedly plays a role in the initiation and/or arrest of earthquakes. Studies have shown that roughness of a fault at the centimeter to meter scale is directly related to total displacement along the fault, with faults surfaces generally becoming smoother with increasing displacement. Here we measure fault roughness with centimeter to 200 micron wavelengths to determine if smoothing processes continue down to the grain scale. A white-light interferometer was used to measure the topography of hand samples by emitting a broadband light source along the sample and mapping the constructive and destructive interference of the return signal to the topography. In this study, the roughness is quantified by calculating the power spectral density (PSD) along transects of the surface roughness. We measure surface roughness on several faults, as well as a surface of the solid extrusion from the 2004-2007 Mt. St. Helen's eruption which is hypothesized to have sustained stick-slip and stably sliding frictional motion for approximately 1 km of displacement. Previous studies of larger-scale fault roughness have shown that while fault roughness decreases with displacement in the slip-parallel direction, roughness in the slip-perpendicular direction is similar on most faults (Sagy et al. 2007). Preliminary data of small-scale roughness show that roughness in the perpendicular direction is similar across some faults. These preliminary results suggest that processes controlling surface roughness at the centimeter to meter scale may differ from those at the centimeter to micron scale.

2-085

THERMAL PRESSURIZATION EXPLAINS ENHANCED LONG-PERIOD MOTION IN THE CHI-CHI EARTHQUAKE *Andrews DJ (USGS)*

Ground motion recorded in the 1999 M 7.6 Chi-chi, Taiwan, earthquake provides evidence on the process of thermal pressurization. Spectral response velocity near the southern portion of the rupture was roughly flat at periods from 1 s to 10 s, while spectral velocity near the northern portion was about the same at 1 s, but increased with period to be several times larger than the southern response value at 10 s. The fault is in different lithologic units in the north and south, being within low-permeability shale in the north. This spatial correlation strongly suggests that properties of the shale determined the enhanced long-period motion. Shale is both less permeable and less subject to dilatant damage than other rocks.

Thermal pressurization of pore fluid due to frictional heating during fault slip reduces effective pressure and so reduces shear stress resisting slip. For given heat input, fluid pressure rise is inversely proportional to the thickness of the pressurized zone. Pressurized thickness will be larger than the slip zone thickness, due both to fluid diffusion and to dilatant damage produced by the stress wave at the rupture front. Shear stress will decay by $1/e$ at a critical slip value (D_c) about 4 times the pressurized thickness. Slip zone thickness observed in core samples is 1-2 cm. Laboratory measurements of permeability in the Chinshui shale imply that fluid pressure will diffuse only 2.5 cm in 10 s. Therefore, critical slip displacement is expected to be roughly $D_c = 0.1$ m, if there is no dilatant damage.

Dynamic simulations of the Chi-chi earthquake have been performed. Average initial stress is constrained by the geometry of the accretionary prism. Self-similar spatial fluctuations in initial stress over the entire fault produce ground motions that match the southern spectra. Thermal

pressurization at shallow depths in the north produces complete stress drop there and matches long period amplitudes. In order not to amplify short-period amplitudes, it must be assumed that the pressurized fluid is promptly spread through a damage zone 1.25 m thick, so that $D_c = 5$ m, a large fraction of the final slip.

Thermal pressurization is a mechanism to increase the magnitude of an event without increasing short-period motion.

2-086

EARTHQUAKE SOURCE CHARACTERIZATION BY THE ISOCHRONE BACK PROJECTION METHOD USING NEAR-SOURCE GROUND MOTIONS *Jakka RS (UCR), Cochran ES (UCLA), and Lawrence JF (Stanford)*

Rapid and accurate assessment of source (rupture) characteristics of a moderate to large earthquake is of great value for rapid hazard assessment and guidance of emergency services. With the recently developed Back Projection Method (BPM) [e.g. Ishii et al., 2005; Festa and Zollo, 2006; Allmann and Shearer, 2007; Pulido et al., 2008], it is possible to obtain the image of the source rupture very rapidly, within minutes after the initiation of rupture. Here, we suggest some modifications to the formulation of earlier BPM to improve its computational efficiency. We determine both slip amplitudes and slip distribution of the source rupture. We explored the utility and limitations of the BPM using a series of synthetic examples. Further, to test the its applicability to real events, we apply the method to the 2004 Mw 6.0 Parkfield earthquake using available near source seismic data. The method, using either P-wave or S-wave displacement records, identifies slip distributions comparable with slip maps from previous studies. For reliable results, a large number of stations with good azimuthal distribution around the source are needed. Due to the simplicity and computational efficiency of the method, we plan to develop the algorithms for a quasi-real time system, that work with QCN network to provide rapid source characterization. The QCN, with the potential for thousands to hundreds of thousands of sensors, can provide the ample number of seismograms that are required for the successful application of the BPM method.

2-087

EFFECTIVE EARTHQUAKE SOURCE CHARACTERIZATION AND MODELING WITH GEOSTATISTICS FOR STRONG MOTION SIMULATION *Song S (URS), and Somerville P (URS)*

Physics-based ground motion simulation requires the development of physically self-consistent source modeling tools to emulate the essential physics of earthquake rupture. We apply 2D spatial data analysis tools, commonly used in Geostatistics, to characterizing earthquake rupture process and developing an effective source modeling tool for strong motion simulation. The earthquake source process is described by key kinematic source parameters, such as static slip, rupture velocity, and slip duration. The heterogeneity of each source parameter is characterized with auto-coherence while the linear dependency (coupling) between parameters is characterized with cross-coherence. Both zero and non-zero offset spatial coherence can be considered in the form of cross-coherence. We analyzed several kinematic and dynamic rupture models (e.g., synthetic asperity rupture models, both kinematic and dynamic rupture models for the 1992 Landers event, and several Mw 7.8 rupture models generated by the SCEC Dynashake project) to demonstrate the efficiency of these new techniques and found that many interesting features of earthquake rupture can be captured in this way, which may be difficult to analyze, or even detect by zero offset coherence only. For instance, the correlation maximum between slip and rupture velocity can be shifted from the zero offset, i.e., large slip may generate faster rupture velocity ahead of the current rupture front, which may be important for rupture directivity. We demonstrate that we can

generate a number of realizations of earthquake source models to reproduce the target coherence using stochastic modeling techniques (e.g., sequential Gaussian simulation) once coherence structures in earthquake rupture are well understood. This type of coherence analysis may provide the potential for improved understanding of earthquake source characteristics, and how they control the characteristics of near-fault strong ground motions.

2-088

QUANTIFICATION OF VELOCITY REDUCTION IN FAULT ZONES BY DAMAGE RHEOLOGY *Zhong J (Texas A&M), and Duan B (Texas A&M)*

Low-velocity fault zones, in which seismic velocities are reduced significantly relative to surrounding wall rocks, are widely observed around active faults. The presence of such a zone will affect rupture propagation, near-field ground motion, and off-fault damage in subsequent earthquakes. In this study, we attempt to quantify the reduction of seismic velocities caused by the dynamic rupture on a 2D planar fault surrounded by a low-velocity fault zone. First, we implement the damage rheology (Lyakhovsky et al. 1997) in EQdyna (Duan and Oglesby 2006), an explicit finite element code used in the dynamic code verification in SCEC. Then, we quantify off-fault continuum damage based on a quantitative measure in damage rheology. In particular, damage is investigated in terms of velocity reduction in the low-velocity fault zone and the surrounding rocks. Slip velocity, slip, and near-field ground motions computed from damage rheology are also compared with those from off-fault elastic or elastoplastic responses. Effects of low-velocity fault zones on the tempo-spatial distributions of continuum damages are also investigated.

CONTACTS

Jinquan Zhong: Postdoctoral Research Associate, Department of Geology and Geophysics, Texas A&M University, College Station, TX, E-mail: zhong@geo.tamu.edu

Benchun Duan: Assistant Professor, Department of Geology and Geophysics, Texas A&M University, College Station, TX, E-mail: duan@geo.tamu.edu

2-089

SUDDEN AND GRADUAL COMPACTION OF SHALLOW BRITTLE POROUS ROCKS *Sleep NH (Stanford)*

Porous brittle rocks fail in shear and compaction. Rate and state friction describes such failure on a planar surface while end-cape failure describes the failure of a continuum. Both formalisms include Coulomb failure in shear at low normal tractions. Rate and state friction includes slow compaction of gouge by normal traction when shearing is not occurring. It also represents slow compaction of porous sandstone. End-cap failure includes both grain crushing and shear. Micromechanically, all these mechanisms involve exponential creep at stresses of a few GPa. Rate and state friction is modeled by tabular real contacts where shear and extrusion occur. The observed compaction rate depends on the normal traction to a modest power ~ 27 for gouge and ~ 10 for sandstone. End-cap failure involves grain cracking in the neighborhood of the grain-grain contact. Its rate should depend on the normal traction raised to a power of ~ 100 . This strong rate dependence is not measurable in practice as a failure cascade commences once some grains crack. Materials with pointy contacts including unwelded tuff and "regolith" in the uppermost 10s of meters that has repeatedly been damaged by strong seismic waves compact in this manner at dynamic stresses modestly above their ambient lithostatic stress. This produces significant nonlinear attenuation of compressional P-waves with sustained dynamic accelerations that are a modest fraction of the ambient acceleration of gravity.

2-090

RUPTURE DYNAMICS ON NONPLANAR FAULTS WITH STRONGLY RATE-WEAKENING FRICTION AND OFF-FAULT PLASTICITY *Dunham EM (Harvard)*

Natural fault surfaces are nonplanar at all scales. Slip on such faults induces local stress perturbations that lead to irregular rupture propagation and potentially activate off-fault inelastic deformation. Using 2D plane-strain finite difference simulations, we study rupture phenomenology on nonplanar faults in elastic-plastic (Drucker-Prager) media. Motivated by high-velocity friction experiments, we use a strongly rate-weakening friction law formulated in a rate-and-state framework. Studies of ruptures on planar faults in elastic media show how strongly rate-weakening friction laws can lead to rupture propagation in the form of slip pulses, provided that the background stress level on the fault is below a critical value. At higher stress levels, ruptures generally take the form of cracks, which can produce several times more slip than slip pulses, even though the differences in dynamic stress drop are minor. This phenomenology holds also for ruptures in elastic-plastic media, though the minimum background stress required for slip pulses to be self-sustaining is increased relative to that in an elastic medium. Plastic deformation generally occurs in the extensional quadrants unless the maximum principal compressive stress is oriented at a low angle to the fault. This is consistent with Templeton and Rice's (JGR, 2008) results with slip-weakening friction laws (which produce crack-like ruptures). However, the extent of plastic deformation (and amount of slip) is reduced when rupture occurs in the slip-pulse instead of crack-like mode. The addition of fault roughness, having amplitude-to-wavelength ratios of 10^{-3} to 10^{-2} , does not greatly change the overall distribution or extent of plastic deformation, but instead modulates its amplitude. This spatial variability of plastic deformation enhances the irregularity of rupture propagation due to fault roughness.

2-091

SLIP MODES AND PARTITIONING OF ENERGY DURING DYNAMIC FRICTIONAL SLIDING BETWEEN IDENTICAL ELASTIC-VISCOPLASTIC SOLIDS *Shi Z (USC), Needleman A (Brown), and Ben-Zion Y (USC)*

The effect of plasticity on properties of dynamic frictional sliding along an interface between two identical elastic-viscoplastic solids is analyzed. Two solids are held together by a compressive stress and one is subject to shear loading imposed by edge impact near the interface. Plane strain analyses are carried out for this configuration and bulk material plasticity is accounted for. The material on each side of the interface is modeled as an isotropically hardening elastic-viscoplastic solid. The interface is characterized as having an elastic response together with a rate- and state-dependent frictional law for its inelastic response. Depending on bulk material properties, interface properties and loading conditions, frictional slip along the interface can propagate in a crack-like mode, a pulse-like mode or a train-of-pulses mode. Results are presented for the effect of material plasticity on the mode and speed of frictional slip propagation as well as for the partitioning of energy between stored elastic energy, kinetic energy, plastic dissipation in the bulk and frictional dissipation in the interface. Some parameter studies are carried out to explore the effects of varying the interface elastic stiffness and the impact velocity.

2-092

TO BRANCH OR NOT TO BRANCH: NUMERICAL MODELING OF DYNAMICALLY BRANCHING FAULTS *DeDontney N (Harvard), Templeton-Barrett EL (Harvard), Dmowska R (Harvard), and Rice JR (Harvard)*

Branched fault geometries occur in strike-slip as well as dip-slip settings [Poliakov et al., 2002; Kame et al., 2003]. The Wenchuan earthquake illustrates such branched geometry [Hubbard and Shaw, 2009] in a fold and thrust belt, and a branched structure, the Central Basin Decollement

[Shaw & Suppe, 1996], underlies the Los Angeles Basin. By simulating dynamic rupture path selection at branch junctions with explicit finite element (FE) methods here, we are able to estimate which faults should be activated.

Factors that influence coseismic branch activation have been extensively studied [Poliakov et al.; Kame et al.; Oglesby et al., 2003, 2004; Bhat et al., 2004, 2007]. The results show that the rupture velocity, pre-stress orientation and fault geometry influence rupture path selection. We show further that the ratio of σ_1/σ_3 (equivalently, the seismic S ratio) and the relative frictional fault strength also play a significant role in determining which faults are activated.

Our methodology has recently included the use of a regularized friction routine [Ranjith & Rice, 2001; Cochard & Rice, 2000] which reduces the growth of numerical noise throughout the simulations. A difficulty arises in the treatment of surface interactions at the branch junction. When local opening does not occur there, slip on the branch fault must vanish at the junction, a constraint that we impose on the FE model. However, the FE contact routine used demands that slip always be constrained to zero on one or the other fault at such a junction, which is problematic when opening occurs. There is then no fundamental basis for constraining slip at the junction to zero on either fault, and the choice made affects the slip distributions and rupture path selection.

Material contrasts across a fault are common, so we consider the effect of a bimaterial interface. Also inelastic off-fault deformation may be extensive in the area of the fault junction, and therefore important in determining fault activation. By incorporating plasticity in the modeling, we are able to determine its effect on the branching behavior. Templeton et al. [subm. 2009] examine the role of plasticity in the context of normal faults at Yucca Mtn. and focus on branches on the extensional side of the main fault. They found that inclusion of plasticity affected strong ground motion but not branch activation in that particular case. We investigate a broader range of parameters and fault geometries.

2-093

HIGH-ORDER TREATMENT OF FAULT BOUNDARY CONDITIONS USING SUMMATION-BY-PARTS FINITE DIFFERENCE METHODS *Kozdon JE (Stanford), Dunham EM (Harvard), and Nordström J (Uppsala)*

High-order numerical methods are ideally suited for earthquake problems, which are primarily limited by available memory rather than CPU time, since they require fewer grid points to achieve the same solution accuracy as low-order methods. Though it is relatively straightforward to apply high-order methods in the interior of the domain, it can be challenging to maintain stability and accuracy near boundaries (e.g., the free surface) and internal interfaces (e.g., faults and layer interfaces). This is particularly problematic for earthquake models since numerical errors near faults degrade the global accuracy of the solution, including ground motion predictions. Despite several efforts to develop high-order fault boundary conditions, no codes have demonstrated greater than second-order accuracy for dynamic rupture problems, even on rate-and-state friction problems with smooth solutions.

In this work we use summation-by-parts (SBP) finite difference methods along with a simultaneous approximation term (SAT) to achieve a truly high-order method for dynamic ruptures on faults with rate-and-state friction laws [Carpenter et al., JCP 1999; Nordström & Gustafsson JSC 2003; Nordström SISC 2007]. SBP methods use centered spatial differences in the interior and one-sided differences near the boundary. The transition to one-sided differences is done in a particular manner that permits one to provably maintain stability as well as high-order accuracy. In many

methods the boundary conditions are strongly enforced by modifying the difference operator at the boundary so that the solution there exactly satisfies the boundary condition. This approach often results in instability when combined with high-order difference schemes. In contrast, the SAT method enforces the boundary conditions in a weak manner by adding a penalty term to the spatially discretized governing equations.

Additional complications arise with rate-and-state friction laws, and several finite difference implementations [Bizzarri et al., GJI, 2001; Rojas et al., GJI, 2009] suffer from extreme stiffness that requires the use of implicit time integration schemes for fields on the fault. This is also the case for the SAT method unless the boundary condition is formulated in terms of characteristic variables (i.e., the combination of stresses and velocities associated with waves entering and exiting the fault). With this formulation, the solution can be advanced using fully explicit time-stepping methods.

2-094

ALLCAL EARTHQUAKE SIMULATOR - RECENT PROGRESS *Ward SN (UCSC)*

In the past year ALLCAL, the earthquake simulator for all of California, has undergone some improvements:

(1) The geometry of the fault elements has evolved from "picket fence" type (short dimension along strike and full dimension down dip, roughly 4 km x 12 km) to a more square type (roughly 4 km x 3 km). This offers a better representation of smaller quakes (~M5.5) and allows ruptures with variable slip down dip, but it increases the computational effort by about a factor of four. The current simulator uses 8000 fault elements arranged in such a manner as to avoid most large tears and overlaps with depth on contorted faults.

(2) The component fault system has been vetted to a degree to more closely conform to the faults used in the UCERF program. Several questionable faults have been removed and several others, mostly in northern California, have been added. With ALLCAL faults now virtually the same as the UCERF faults, the integration of simulator results to UCERF products should be achievable.

(3) A new method to drive the system has been devised such that stresses and displacements, both on and off the faults, can be tracked. This involves finding a continuous interseismic velocity / stress field for Western North America that: (1) gives no shear stress on the free surface, (2) satisfies the static equations of force balance, (3) reasonably reproduces interseismic surface velocities at all geodetic sites and (4) stresses the faults such that they slip at rates close to those estimated geologically. The goal here is to employ both geological and geodetic data to constrain ALLCAL and to progress toward a self-consistent system level model for stress accumulation by tectonic deformation and subsequent release by slip on faults.

2-095

EARTHQUAKE RECURRENCE IN SIMULATED FAULT SYSTEMS *Dieterich JH (UCR), and Richards-Dinger KB (UCR)*

We employ a computationally efficient fault system earthquake simulator, RSQSim, to explore effects of earthquake nucleation and fault system geometry on earthquake occurrence. The simulations incorporate rate- and state-dependent friction, high-resolution representations of fault systems, and quasi-dynamic rupture propagation. Faults are represented as continuous planar surfaces, surfaces with a random fractal roughness, and discontinuous fractally segmented faults. Simulated earthquake catalogs have up to 10^6 earthquakes that span a magnitude range from

$\sim M4.5$ to $M8$. The seismicity has strong temporal and spatial clustering in the form of foreshocks and aftershocks and occasional large-earthquake pairs. Fault system geometry plays the primary role in establishing the characteristics of stress evolution that control earthquake recurrence statistics. Empirical density distributions of earthquake recurrence times at a specific point on a fault depend strongly on magnitude and take a variety of complex forms that change with position within the fault system. Because fault system geometry is an observable that has a great impact on recurrence statistics, we propose using fault system earthquake simulators to define the empirical probability density distributions for use in regional assessments of earthquake probabilities.

2-096

COMPARISON OF EARTHQUAKE SIMULATORS EMPLOYING RATE AND STATE FRICTION *Tullis TE (Brown), Noda H (Caltech), Richards-Dinger KB (UCR), Lapusta N (Caltech), Dieterich JH (UCR), Kaneko Y (Caltech), and Beeler NM (USGS)*

This is a progress report on comparing and validating earthquake simulators, i.e. computer models in which a series of earthquakes spontaneously occur. This particular study is a joint effort to compare the behavior of three independently devised earthquake simulators that employ rate and state friction. The three simulators are 1) one from Caltech that uses the boundary element method and can use either the fully elastodynamic equations or a quasidynamic approximation (radiation damping) and an FFT approach to reduce computation time; the fully elastodynamic implementation of this simulator neither makes compromises in the equations of motion nor in the friction equations and thus can be considered the 'correct' numerical solution for a whole space, 2) one from Brown (PARK) that uses the boundary element method, radiation damping, and a fast multipole approach to reduce computation time, and 3) one from UCR (RSQSim) that uses quasidynamics and a simplified three-condition representation of rate and state friction to reduce computation time. Here we study one simple problem, termed Problem 2b. Previously we studied a similar problem in less detail in a comparison with 6 other earthquake simulators that represent friction in a simpler way. During that comparison the problem was not adequately specified for rate and state friction. The problem involves a strike slip fault, with a bi-linear asymmetrically peaked initial stress distribution, and a constant loading rate. The original problem, termed Problem 2, was defined with fault constitutive properties having a fixed failure stress, higher than the peak in the initial stress, and a fixed dynamic sliding stress. Our simulations utilizing rate and state friction approximated this description, but the initial state was not specified; Caltech, Brown, and UCR used different values.

One problem in making an exact comparison is that fully dynamic Green's functions do not exist for a half space. Thus in this study we compare not only three independently calculated solutions using rate and state friction, we also compare the behavior of half and full space solutions by all three groups, compare quasi-dynamic solutions by all three groups, and compare the full elastodynamic and quasidynamic solutions by the Caltech group. We also investigate the role of the size and shape of the elements.

2-097

OBSERVED SCALING REPRODUCED IN A MODEL OF SMALL REPEATING EARTHQUAKES WITH THE SLIP FORM OF RATE AND STATE FRICTION LAWS *Chen T (Caltech), and Lapusta N (Caltech)*

Small repeating earthquakes have short recurrence times and known locations, and hence they present an excellent target for observations and studies of earthquake physics. We have previously shown that a model based on the aging form of rate and state friction laws reproduces the observed

scaling of the repeat time and seismic moment of small repeating earthquakes. This is noteworthy since the observed scaling is different from the one in a simple conceptual model that treats repeating earthquakes as circular ruptures with only seismic slip and stress drop independent of the seismic moment. In our model, a small circular patch with rate-weakening friction is surrounded by a much larger region with rate-strengthening friction. For a range of realistic parameters, we have shown that the observed scaling can be reproduced by varying the size of the rate-weakening patch. The difference between our model and the simple conceptual model is in the occurrence of aseismic slip at the location of repeating earthquakes.

In this study, we investigate the behavior of the model with the slip form of the rate and state friction laws, since recent experimental results have favored the slip form over the aging form and theoretical studies have shown that the two forms result in significant differences for earthquake nucleation. We find that the scaling of the repeat time with seismic moment in the model with the slip law also matches the observed scaling, for the values of the velocity-weakening parameter ($b - a$) of 0.008 or larger. Values of $(b - a)$ of 0.004 or smaller result in a different scaling. Since the value of 0.008 is about twice larger than typically inferred from slow-velocity friction experiments, this finding motivates consideration of a more realistic friction law, with additional weakening at seismic slip rates. For both types of friction laws, the source spectra of our simulated events resemble that of a Brune-type source. The observed scaling is also reproduced (i) in a model with a rectangular instead of circular velocity-weakening patch, and (ii) in 2D fault models with an adjusted moment computation that reinterprets slip in terms of a 3D model. We will report on our current efforts to construct a theoretical explanation of the scaling produced by our model.

2-098

3D EARTHQUAKE SEQUENCE SIMULATIONS THAT ACCOUNT FOR THERMAL PRESSURIZATION OF PORE FLUIDS: EFFECTS OF HETEROGENEOUS FRICTIONAL AND POROELASTIC PROPERTIES Noda H (Caltech), and Lapusta N (Caltech)

We have developed a three-dimensional methodology for simulating earthquake sequences that accounts for evolution of temperature and pore pressure due to frictional heating and their diffusion normal to the fault, with the potential thermal pressurization (TP) of pore fluids during seismic events. Diffusion equations are integrated with a spectral method using a Fourier basis. This method is unconditionally stable, accurate with affordable computational resources, and highly suitable to earthquake sequence calculations in which timesteps vary. The methodology incorporates full wave effects during seismic slip [Lapusta et al., 2000; Lapusta and Liu, 2009]

We use the methodology to investigate the effect of heterogeneous frictional and hydraulic fault properties. For a single velocity-weakening region of homogeneous properties, the model produces earthquake cycles with one model-spanning event. Introduction of two regions of different properties makes the earthquake cycle more complex. A region of lower permeability and hence more efficient TP produces larger displacements during model-spanning events, and thus does not rupture in several subsequent events, creating multiple events of different sizes. The location of the maximum temperature rise in our simulations is not associated with the location of maximum slip, as the location of maximum slip experiences significant dynamic weakening and hence slips under low levels of stress. The region of more efficient TP has lower interseismic shear stress which discourages earthquake nucleation, even though the theoretical estimate of the nucleation size is smaller there [Segall and Rice, 2006]. Our models indicate that hypocenters of large events do not correlate with a region of large slip or large stress drop. When the region of more efficient TP is assigned rate-strengthening friction properties, as motivated by lab measurements on borehole

samples from the Chelungpu fault, Taiwan [Tanikawa and Shimamoto, 2009], the two fault regions generate motions with different high-frequency content. In model-spanning events, the rate-strengthening region of more efficient TP has larger slip but lower high-frequency content, as observed in 1999 Chi-Chi, Taiwan, earthquake [e.g., Dalguer et al., 2001; Huang et al., 2001; Ma et al., 2003]. Our simulations show that differences in hydraulic and friction properties of the two parts of the fault may explain such observations.

2-099

DILATANT STABILIZATION VS THERMAL PRESSURIZATION: CONTROL ON SLOW VS FAST FAULT SLIP? *Segall P (Stanford), and Bradley AM*

We explore the hypothesis that at low effective normal stress dilatancy stabilizes velocity weakening faults against dynamic slip, whereas at higher effective stress thermal pressurization overwhelms dilatancy leading to dynamic ruptures. Our two-dimensional quasi-dynamic simulations include rate-state friction, a dilatancy law linked to state evolution, and heat and pore-fluid flow normal to the fault. The fault is loaded by down-dip slip at an imposed rate, and effectively locked up-dip.

The numerical scheme solves: ODE's in slip and state on the fault; the algebraic stress balance on the fault with the radiation damping approximation; and PDE's in pressure and temperature normal to the fault for both zero- and finite-width shear zones. The spatially discretized system of equations is a semiexplicit index-1 differential-algebraic equation (DAE). To increase speed and accuracy, we discretize the fault normal direction using logarithmic spacing; use explicit-implicit integration in time; and minimize the number of LU factorizations of the Jacobians of the nonlinear systems solved at each ODE stage by using fast factorization updates.

For a preferred set of parameters, spatially uniform frictional and transport properties, the zero-width shear zone limit, and an effective stress of 1 MPa, the model exhibits a series of propagating slow slip events. These events are stabilized by pore-pressure drops at the rupture tips. For faults long compared to the drained critical nucleation length we observe slow-slip events driven both by imposed down-dip sliding that occur without stress drop, as well as faster (but quasi-static) events that relax the accumulated stress.

At 10 MPa effective stress, the models exhibit slow-slip and dynamic ruptures. Following large stress drops associated with dynamic events, a sequence of slow slip events is driven from the down-dip end of the fault. Temperature changes on the fault are < 0.1 degrees C, and the behavior mimics isothermal calculations. With time the slow slip events propagate further into the low stress zone left by the dynamic rupture. During this slow-slip phase, the maximum slip-speeds and moment rates increase. Ultimately, slip-speeds reach sufficiently high rates ($\sim 10^{-4}$ m/s) to allow thermal pressurization to dramatically weaken the fault, leading to dynamic rupture. Further work will be required to determine whether this behavior could lead to observable changes prior to dynamic ruptures.

2-100

THERMAL PRESSURIZATION DURING "SLIP LAW" FRICTIONAL EARTHQUAKE NUCLEATION *Schmitt SV (Stanford), and Segall P (Stanford)*

Recent work has suggested that shear heating-induced thermal pressurization may become the dominant fault weakening mechanism during the quasi-static nucleation phase of an earthquake, well before the onset of seismic radiation. In the last two years, we have performed numerical simulations of rate- and state-dependent frictional nucleation with the aging form of the state

evolution law, coupled with shear heating and heat/fluid transport with diffusivities inferred from laboratory observations of fault zone materials. For hydraulic diffusivities ranging from 10^{-8} to 10^{-4} m^2/s , we have shown that thermal pressurization dominates frictional weakening when slip attains speeds greater than 0.02 to 2 mm/s [Schmitt & others, SCEC, 2008].

Nucleation with the aging law form of rate-state friction is "cracklike," in that the interior of the nucleation zone continues slipping at nearly the maximum slip speed, with the greatest cumulative slip located at its center. Thermal pressurization is effectively a slip weakening mechanism that feeds back into itself, and therefore rapidly dominates in the center of an aging law nucleation zone. This effect leads to dramatic along-strike localization of the nucleation zone at its midpoint.

With the slip (logarithmic) friction evolution law, however, nucleation is "quasi-pulselike," in that the fastest-slipping portion of the nucleation propagates unidirectionally, with velocity decaying behind [for example, Ampuero & Rubin, JGR, 2008]. Under this regime, the relative importance of thermal pressurization is diminished since most of the frictional weakening occurs in locations with limited amounts of slip. Despite the hindered effect of thermal pressurization, numerical simulations indicate that it dominates frictional weakening at slip speeds in the range of 1-300 mm/s. These speeds range from well below to just above the initiation of seismic radiation, well before an earthquake becomes large.

We also observe changes to the behavior of the nucleation pulses with the added effect thermal pressurization. Pulse width decreases with increasing slip speed, unlike the self-similar growth under slip law friction alone. The propagation of the pulse front slows, and the pulse front may even halt at some time after thermal pressurization has become the dominant weakening mechanism. In that case, the nucleation zone becomes a narrow, stationary instability that accelerates toward seismic radiation.

2-101

SEMI-EMPIRICAL CONSTITUTIVE RELATIONS FROM HIGH SPEED FRICTION EXPERIMENTS *Beeler NM (USGS)*

To date laboratory-observed dynamic weakening mechanisms can be classified into three types, flash weakening (e.g., flash melting, Tullis and Goldsby, 2003), shear-induced weakening (e.g., gel weakening, Goldsby and Tullis, 2000) and thermal weakening from bulk phase changes (e.g., melting, Tsutsumi and Shimamoto, 1997). Using dimensional analysis from rudimentary theory and direct observations from the lab tests, the different classes can be distinguished on the basis of mechanical data. In this study I illustrate the differences, focusing particularly on the dependence of shear resistance on slip velocity, post-weakening strength recovery, and the dependencies of the slip weakening distance on slip velocity and normal stress. In addition to cataloging the differences between mechanism types, semi-empirical constitutive relations for thermal-weakening are developed.

References

Goldsby, D., and T. E. Tullis (2002), Low frictional strength of quartz rocks at subseismic slip rates, *Geophys. Res. Lett.*, 29(17), 1844, doi:1810.1029/2002GL015240.

Tsutsumi, A., and T. Shimamoto, (1997) High-velocity frictional properties of gabbro, *Geophys. Res. Lett.*, 24, 699-702.

Tullis, T. E., and D. L. Goldsby (2003), Flash melting of crustal rocks at almost seismic slip rates, *Eos. Trans. Am. Geophys. Union, Fall Meeting Suppl.*, 84(46), Abstract S51B-05.

2-102

DIVERSITY OF FAULT ZONE DAMAGE AND TRAPPING STRUCTURES IN THE PARKFIELD SECTION OF THE SAN ANDREAS FAULT FROM COMPREHENSIVE ANALYSIS OF NEAR FAULT SEISMOGRAMS *Lewis MA (USC), and Ben-Zion Y (USC)*

We perform comprehensive analyses of trapped waves and time delays of body waves for the Parkfield section of the San Andreas Fault. Waveforms generated by thousands of earthquakes and recorded by near fault stations in several deployments are examined, with attention to the possible influence of a lithology contrast across the fault on signals of the low velocity damage zone. Clear candidate trapped waves are identified at only 3 stations, MM and 2 of the other near fault stations (FLIP and PIES) further to the NW. Clear candidate trapped waves are not seen at any of the near fault stations SE of MM. The locations of events generating good candidate trapped waves are not evenly distributed in space, but clustered in limited locations. Moreover, events that generate clear candidates for trapped waves at one station do not typically generate trapped waves at the other 2 stations. The observations imply that the damage zone is highly variable along strike and that a connected wave guide does not exist for distances along strike larger than at most 3-5 km. Synthetic waveform fits to trapped waves at stations MM and FLIP indicate that the most likely parameters of the trapping structures at these locations are widths of 100-200 m, velocity reductions of 40-50%, Q values of 20-40, and depths of about 3 km. Synthetic calculations of trapped waves demonstrate that a contrast of seismic velocity across the fault produces a delay between the trapped and regular S waves. Trapped waves at MM, and to a lesser extent at FLIP and PIES, show this characteristic. This suggests a lithology contrast in the top few km at these locations, in agreement with results from tomography and studies of head waves in the Parkfield area. At fault zone station NE1C in the SE section, where trapped waves are not observed, the low velocity damage zone layer is detected from the delay in the arrival time of body wave phases relative to a nearby off-fault station. The observed delay of the S wave is greater than the P wave delay, consistent with the existence of a damage zone with Poisson ratio of about 0.33. The observation of a time delay without the generation of trapped waves indicates that parts of the damage zone are insufficiently coherent to generate trapped waves. The results highlight the diversity of damage structures along the ~40 km of the SAF examined in this study, and imply that fault imaging based on data at single sites does not necessarily apply to a larger section.

2-103

DYNAMIC RUPTURE ON A FRICTIONAL INTERFACE WITH OFF-FAULT DAMAGE *Xu S (USC), Ampuero J (Caltech), Ben-Zion Y (USC), and Lyakhovskiy V (Geological Survey of Israel)*

The high stress concentration in the front of dynamic rupture is expected to produce rock damage (reduction of elastic moduli) in the material surrounding the main fault plane. The off-fault yielding of materials and energy absorption in the damage process may reduce the amplitude of near-fault ground motion. However, the local low-velocity zone produced by damage can amplify the motion locally and create a waveguide which will allow the motion to propagate with little geometric attenuation. In addition, the asymmetrical distribution of damage across the fault may produce localized bimaterial interface that could reduce frictional dissipation and increase radiation efficiency.

Previous studies incorporated plastic yielding in simulations of dynamic rupture while keeping the elastic moduli unchanged (Andrews, 1975, 2005; Ben-Zion and Shi, 2005; Templeton et al., 2008). In

our model, dynamic ruptures are simulated on a frictional fault surrounded by media with elastic moduli that can evolve spontaneously during off-fault inelastic deformation. The partitioning of elastic strain energy during rupture propagation among frictional heat, plastic yielding, rock damage (evolution of elastic moduli), and seismic radiation is examined quantitatively to clarify how damage generation under different conditions influence the maximum ground motion. We also attempt to clarify the conditions where spontaneous generation of asymmetric damage and the resulting bimaterial interface lead to generation of wrinkle-like rupture pulses. Updated results will be presented in the meeting.

2-104

HOW QUICKLY DOES THE SUBSURFACE DAMAGE INDUCED BY THE 1999 CHI-CHI EARTHQUAKE HEAL? *Chen KH (Berkeley), and Rau RJ (National Cheng-Kung University, Taiwan)*

Observation of six M 4.6 repeating earthquakes from 1991 to 2007 reveals a unique temporal and spatial variation in seismic wave character associated with the 1999 Mw 7.6 Chi-Chi earthquakes that occurred ~90 km away. Post-Chi-Chi events have reduced waveform similarity, suggesting a sudden change of seismic wave propagation properties after the Chi-Chi event. The changes in seismic character are widely distributed over Taiwan and remain significant in 5 years after Chi-Chi. Since 2004, the waveform similarity gradually recovered to the pre-Chi-Chi level. The most recent repeating event occurred on 15 November 2007 reveals only a subtle variation in seismic character compared to the pre-Chi-Chi event, indicating that the damaged rock has been regaining the strength with time. The healing of subsurface damage zone, however, is not fully complete even 8 yr after the Chi-Chi earthquake. Using waveform cross correlation, we also identify a ~1 sec delay in S-wave arrival for the 2001 repeating event. The large delay at S-wave arrival is found to be localized at stations south of the mainshock rupture (the Chiayi area) and offshore Penghu island (>100 km travel distance) This suggests that the scatterer is not located in the immediate vicinity of mainshock rupture, besides, the post-seismic change in crustal property is likely to occur in the lower crust. The significant delay in S-wave arrival time may imply the presence of widely distributed fluid-filled fractures underneath the Chiayi area.

2-105

LABORATORY EXPERIMENTS TO UNDERSTAND DYNAMIC SLIP WEAKENING IN ROCKS AND ANALOG MATERIALS AT CO-SEISMIC SLIP RATES *Yuan F (CWRU), and Prakash V (CWRU)*

In the present study plate-impact pressure-shear friction and the modified torsional Kolsky bar friction experiments are employed to investigate the frictional slip resistance in fine-grained Arkansas Novaculite rock, quartz and soda lime glass, at relevant normal stresses and co-seismic slip rates. The motivation of these experimental studies is to gain a better understanding of dynamic fault weakening due to flash heating of asperity contacts, so as to further delineate the conditions for which this mechanism is expected to control fault strength. The results of the plate impact experiments on soda-lime glass indicate that a wide range of frictional slip conditions exist at the frictional interface. These range from initially no-slip, followed by slip-weakening, slip-strengthening, and eventually seizure, all during a single slip event. The initial slip-weakening is most likely due to thermally-induced flash-heating and incipient melting at asperity junctions, and requires only a fraction of a mm of slip to be effective; the slip strengthening is understood to be aided by the coalescence and solidification of local softened/melt patches, which leads to continuous healing and eventual seizure of the slip interface. The maximum bulk temperature rise

is attained at the frictional interface, and occurs during the slip strengthening phase (prior to the seizure of the interface). It is to be noted that during the slip-weakening phase, even though the bulk temperature rise is small, the flash temperatures at the asperity contacts are expected to approach near-melt temperatures of soda-lime glass. As slip precedes these soft near-melt asperity junctions continuously increase in size by local plastic flow leading to an increase in effective area of contact, leading to healing and eventual seizure of the slip interface. Seizure of the interface is also aided by the increase in shear-strength of the flattened asperity junctions as they are rapidly quenched by the surrounding lower temperature material. Re-initiation of slip occurs with the drop in normal st

2-106

SUPERSHEAR NUCLEATION OF THE 2009 MW 6.3 L'AQUILA, ITALY EARTHQUAKE *Ellsworth WL (USGS), and Chiaraluze L (INGV)*

The L'Aquila region of central Italy was devastated when a Mw 6.3 normal faulting earthquake ruptured directly beneath the city on April 6, 2009. More than 300 people perished in the earthquake, and both culturally significant and modern buildings suffered substantial damage. Nearfield recordings of the earthquake the Italian National Strong Motion Network and MedNet station AQU show that the earthquake began with a weak nucleation phase followed 0.6 s later by a strong breakaway phase of the type documented by Ellsworth and Beroza (*Science*, 1995; *Tectonophysics*, 1996).

To study the nature of the nucleation and breakaway we image the rupture process using both displacement and velocity seismograms from the nearfield accelerometers. The overall rupture is well-imaged by the network, and the final offsets and seismic moment agree well with results obtained from InSAR interferograms (Atzori et al., GRL in press). Focusing on the nucleation process, we model the first 4 s of rupture using just 4 s of seismogram sampled at 0.1 s. The initial 0.5 s of the nucleation process cannot be resolved with confidence at present, but appears to involve primarily down-dip rupture. The breakaway phase initiates at the base of the ruptured fault surface and propagates up-dip through the just-ruptured fault surface at a supershear velocity (4.1 – 4.3 km/s). Slip concentrates in the narrow rupture front and little, if any slip follows in its wake.

Previously, the breakaway phase was proposed to represent either 1) the growth of the rupture beyond the boundaries of an initial rupture in which aseismic preslip had lowered the stress, or 2) a statistical manifestation of a cascading rupture growing in an irregular manner. The L'Aquila nucleation process suggests a third possibility, that the breakaway represents initiation of a supershear slip pulse that forms through re-rupture of the initial slip area. As pointed out to us by Eric Dunham, the conditions for formation of a supershear rupture that also propagates as a slip pulse are restrictive. Transition to supershear by itself requires the initial stress to be relatively closer to the failure stress than to the residual stress (Dunham, *JGR*, 2007), while the conditions favoring development of a slip pulse generally require a low stress (Zheng and Rice, *BSSA*, 1998). Evolution of the peak strength to a lower value within the area of the initial rupture would satisfy both conditions in immediate re-rupture.

2-107

EXPERIMENTAL INVESTIGATION OF RADIATED GROUND MOTION DUE TO SUPERSHEAR EARTHQUAKE RUPTURES *Mello M (Caltech), Bhat HS (Harvard), and Rosakis AJ (Caltech)*

Recent theoretical and numerical investigation of supershear ruptures in 2D (Dunham and Archuleta, 2004 and Bhat et al., 2007) and in 3D (Dunham and Bhat, 2008) have shown that ground motion due to the passage of the Mach front is virtually unattenuated at large distances from the fault. In the 2D steady-state supershear rupture model, the Mach front carries the ground motion unattenuated to infinity. Bhat et al., 2007 estimate that the actual distance should be of the order of the depth of the seismogenic zone. This has been partly observed by Bouchon and Karabulut, 2008 who showed that the aftershocks cluster in a region away from the fault at distances comparable to the depth of the seismogenic zone after a supershear rupture. Numerical simulations of supershear earthquake ruptures by Aagaard and Heaton, 2004 also show that in the supershear regime the fault parallel component of particle velocity dominates over the fault normal one whereas in the sub-Rayleigh regime the opposite is true. These two results combined could be seen as distinguishing signatures of a supershear earthquake rupture. We characterize these two effects experimentally using laser interferometry to measure fault particle velocity and high speed imaging of Photo elastic fringes to characterize super shear rupture in a laboratory earthquake setup (Xia et al., 2004, 2005). We observe that ground motion is less attenuated due to supershear rupture compared to its sub-Rayleigh analogue. We also verify, experimentally, some of the key signatures of supershear rupture related ground motion that has been previously identified by analytical and numerical models.

2-108

STRAIN LOCALIZATION IN A MODEL OF COSEISMIC SLIP BELOW THE SEISMOGENIC ZONE *Daub EG (UCSB), and Carlson JM (UCSB)*

We study the impact of strain localization on dynamic rupture propagation below the seismogenic zone. Field studies show that rocks that were deformed below seismogenic depths exhibit both broad and localized shear. We model the deformation of the fault materials using STZ Theory, a physics-based constitutive law that resolves the spontaneous localization of strain in sheared amorphous solids. STZ Theory incorporates the physics of localization through the dynamic evolution of an effective disorder temperature. For rate strengthening parameters, which are appropriate for fault zones below the seismogenic zone, steady sliding with a spatially uniform effective temperature is linearly stable. This indicates that long-term strain during the interseismic period is accommodated in a broad manner. Shear bands can form in rate strengthening materials due to transient effects, and thus coseismic slip that drives the material away from steady sliding causes localization of strain in the STZ model. We test the fault scale consequences of localization by studying a 2D depth-dependent dynamic rupture model. We compare a model where coseismic deformation below the seismogenic zone is uniform across the width of the fault zone to a model where coseismic strain dynamically localizes. We find that when strain can dynamically localize, coseismic deformation occurs in a narrow shear band that persists for the duration of coseismic slip. This shows that our model is able to capture the localization observed in deformed rocks. Localization does not lead to a significant difference in the fault scale propagation of rupture when compared to deformation that is uniform across the width of the fault gouge, as the localization effects increase the negative stress drop that occurs when faults slip below the seismogenic zone.

2-109

FINITE DIFFERENCE MODELING OF RUPTURE PROPAGATION WITH STRONG VELOCITY-WEAKENING FRICTION *Rojas OJ (SDSU), Dunham EM (Harvard), and Day SM (SDSU)*

We incorporate rate- and state-dependent (RS) friction in finite difference simulations of mode II ruptures in elastic media, using the Mimetic Operators Split-Node (MOSN) method, with consistent fourth-order spatial accuracy in the whole domain. At fault points, the RS equations

combined with the spatially discretized momentum conservation equations form a coupled system of ODE for slip velocity and state variable, which exhibits numerical stiffness that is inversely proportional to velocity squared. Approximate solutions to this velocity-state system are achieved by two different implicit schemes: (i) a multistep Rosenbrock integration of the full system, and (ii) one-step integrations (backward Euler and trapezoidal) of the velocity equation, time-staggered with analytic integration of the state equation under the approximation of constant slip velocity over the time step. In assessing the numerical schemes, we use reference solutions from a spectral boundary integral equation method (BIEM) to a test problem with state evolution given by a slip law with strong velocity-weakening behavior at high slip rates, representing flash heating (FH) of microscopic asperity contacts. Both MOSN methods, Rosenbrock and trapezoidal, show the same convergence rates as BIEM: second-order convergence for fault-slip and state-variable misfits, with slower (at least linear) convergence for slip-rate and shear-traction errors. The Euler MOSN method yields lower fault-slip and state-variable convergence rates relative to alternative MOSN schemes. We next use MOSN schemes to study supershear ruptures on RS-FH faults. The propagation speed and rupture mode (crack .vs. slip pulse) are determined by two parameters: the initial background stress T_0 , and a generalization of Andrew's (1976, 1985) seismic S ratio between strength excess and dynamic stress drop to RS laws. To construct the S ratio, the strength excess is estimated as the strength change resulting from an increase in slip velocity, in the absence of state evolution, from T_0 to one consistent with coseismic sliding. The dynamic stress drop is taken to be the difference between T_0 and the residual fault strength under fully weakened conditions. Rupture modes evolve from cracks to pulses via reduction of background stress, as predicted by the understressing theory of Zheng and Rice (1998). We also report on how the supershear transition distance depends on S and T_0 .

2-110

ENERGETICS OF STRAIN LOCALIZATION IN A MODEL OF SEISMIC SLIP
Hermundstad AM (UCSB), Daub EG (UCSB), and Carlson JM (UCSB)

We quantify the energy dissipated to heat and to local disorder in a sheared layer of granular fault gouge. Local disorder is modeled using Shear Transformation Zone (STZ) Theory, a continuum model of non-affine deformation in amorphous solids that resolves spontaneous localization of strain. Strain localization decreases the total energy dissipated during slip. A fraction of this energy is dissipated to increasing local disorder as the material is sheared, thereby decreasing the amount of energy dissipated as thermal heat. We quantify the heat dissipated per unit area as a function of total slip in the presence and absence of strain localization and test the dependence of these calculations on poorly constrained parameters. We find that less heat is dissipated per unit area when compared to results obtained using a traditional heuristic energy partition.

2-111

ACOUSTIC EMISSIONS DURING FRACTURE AND SLIDING OF ROCK SURFACES – PRELIMINARY RESULTS
Goebel T (USC), Stanchits SA (GFZ), Becker TW (USC), Dresen G (GeoForschungsZentrum Potsdam), and Schorlemmer D (USC)

Frictional properties of rock surfaces have a large influence on their behavior under variable differential and confining stress regimes. To understand seismicity patterns and rupture initiation in upper crustal regimes, we deploy sets of experiments with different rock types.

We investigate fracture and sliding on fault surfaces in Aue Granite under 20 and 75 confining pressure. The experiments were performed with a 4600 kN loading frame that enables hydrostatic and axial loading. We start by creating an initial fault in originally intact rock samples without recognizable cracks under low confining pressure (20 MPa). To control the rupture nucleation

process, we use an acoustic emission feedback system. After fracturing, the confining pressure is increased to 75 and 150 MPa, respectively, in the attempt to lock the fault. During all experiments, stress, strain, and bulk velocities are continuously monitored. To characterize the fault propagation and the development of surface sliding, acoustic emissions (AE) are recorded with high sensitivity, piezoceramic sensors and digitized by a state of the art data acquisition system which enables us to analyze complete waveforms during the entire experiment.

We compare acoustic emission rates with stress levels and select events that are connected to accelerated stress decrease. Location of AE event clusters are possibly connected to local asperities. b-value maps and regional acoustic emission rates are analyzed before and after the initiation of accelerated stress release. Frequency-magnitude distributions of larger events show Gutenberg-Richter scaling with b-values larger than unity. Regions of high seismic activity could be linked to asperity grinding which takes place in a steady (approximately continuous sliding) or an accelerated displacement mode. Both modes, and transitions between them, have been observed on the same fault plane. The overall shear strength of rough faults is highly dependent on properties of larger asperities.

Preliminary experiments show a good correlation between fault smoothness and the acoustic emission activity during stick-slip events.

2-112

ON STEADY SELF-HEALING RUPTURE MODES IN CONTINUUM FAULT MODELS

Elbanna AE (Caltech), Lapusta N (Caltech), and Heaton TH (Caltech)

Seismic inversions indicate that earthquake ruptures may propagate in a self-healing pulse-like mode. Prior numerical simulations of dynamic rupture on rate and state interfaces with velocity-weakening friction and uniform prestress found either growing or decaying pulse-like ruptures. Such simulations employed an overstressed region, usually of uniform prestress, to nucleate dynamic ruptures.

Here we show that steady pulse-like ruptures can be produced by a nucleation procedure that involves a more complex stress distribution in the nucleation region. This allows us to study properties of steady pulses and their response to changes in prestress. In particular, we find that such solutions lose their steadiness once they enter areas of different constant prestress. Our simulations are done in a 2D antiplane fault model with constant normal stress and rate and state friction that involves enhanced weakening at seismic slip velocities motivated by flash heating. We find that, for given friction properties, steady pulses can propagate for a range of shear prestress levels, with different prestress levels corresponding to different shapes and overall slip of the resulting steady pulse-like ruptures. We also show that the generated steady pulses are stable to short-wavelength perturbations of small amplitude and unstable otherwise, where the wavelength is compared with the pulse width and the amplitude is compared with the steady-state pre-stress level, which is in turn comparable to dynamic stress variations. If the prestress ahead of the steady pulse is abruptly changed to a different constant level that also supports steady pulses, the slip pulse does not change to a different steady shape; instead, the pulse either grows or dies, depending on whether the new prestress level is higher or lower.

Our future goals include determining whether a given prestress can correspond to multiple steady pulse solutions that depend on the nucleation procedure, studying properties of slip pulses nucleated as a result of a slow quasi-static process, and investigating pulse propagation with more complex prestress distributions. Ultimately, we would like to understand whether it is possible to

formulate a simplified approach, based on energy-related or other considerations, which would allow us to predict the distribution of slip accumulated for a given prestress distribution without conducting a full elastodynamic simulation.

2-113

FORMATION OF PULSE-LIKE RUPTURES ON VELOCITY-WEAKENING INTERFACES AND ITS RELATION TO STABILITY PROPERTIES OF STEADY-STATE SLIDING *Elbanna AE (Caltech), Lapusta N (Caltech), and Heaton TH (Caltech)*

Prior studies have shown that velocity-weakening interfaces can produce both crack-like ruptures, for higher prestress levels, and pulse-like ruptures, for lower prestress levels and sufficient amounts of weakening. More complex rupture patterns, such as multiple pulses of slip, may result for intermediate levels of prestress. Such multiple pulses occur due to destabilization of steady sliding behind the front of the crack-like rupture that forms after the nucleation stage. The spacing of the multiple pulses can be predicted from linearized stability analysis of the steady sliding; it corresponds to the wavelength of the perturbation with the maximum growth rate. Whether the transition from the crack-like rupture to multiple pulses occurs within the rupture duration depends on the growth rates, which are higher for more pronounced velocity weakening.

Here we explore the possibility that transition from the initial crack-like rupture to a self-healing pulse can also be understood based on such stability analysis. We conduct simulations of dynamic ruptures in a 2D antiplane fault model with rate and state friction that involves enhanced weakening at seismic slip velocities motivated by flash heating. The fault has uniform prestress, except in a small overstressed region with Gaussian prestress distribution used for rupture nucleation. For a range of model parameters that favors slip pulses, we find that the decrease of sliding velocity behind the front of the initial crack causes significant increase in the maximum growth rate of unstable modes and increase in their phase velocities. The combination of these effects, we hypothesize, leads to the local arrest of rupture and formation of slip pulses. Phase velocities of the growing wavelengths also influence the speed of the healing front of the resulting slip pulses and hence influence how the width of the pulse changes with its propagation. We will report on our current efforts to turn these observations into a predictive theory of rupture mode selection on uniformly pre-stressed velocity-weakening interfaces. The effect of the nucleation procedure, which is clearly present in the formation of self-healing pulses (please see a companion abstract on steady pulse-like ruptures), may be possible to incorporate through the different characteristics of the initial crack-like rupture.

2-114

DYNAMIC WEAKENING DURING EARTHQUAKES BY SOLID LUBRICATION *Reches Z (Oklahoma), and Lockner DA (USGS)*

We present new experimental results of fault friction in a slip velocity range of 0.001-1.0 m/s, and normal stress up to 7.0 MPa performed with a rotary shear apparatus. The experiments with dry, solid, granite samples show intensive wear of the sliding surfaces to form fine-grain gouge powder even under modest stresses and displacements. The experiments reveal systematic trends of rate-dependent weakening and strength-recovery in the studied velocity range. The observed rate- and slip- dependent trend of weakening and strengthening, and the observation of the gouge formed during the experiments, suggest that the experimental faults are lubricated and dynamically weakened by the fine-grain gouge. Gouge lubrication is expected to be a common, efficient mechanism for earthquake instability as gouge forms along all brittle faults in the earth crust.

Numerous mechanisms have been proposed for dynamic weakening of faults when shearing occurs in a particulate gouge layer. For example, flash melting at grain contacts, or bulk melting due to frictional heating of the melt zone. Other proposed mechanisms are related to heating of trapped fluids (thermal pressurization) or formation of gel. In our experiments, heating to approximately 140°C eliminates the fault weakening and suggests a weakening mechanism related to adsorbed water on ultrafine gouge particles.

2-115

EARTHQUAKE-LIKE SLIP EVENTS ON AN ANALOG LABORATORY FAULT *Reches Z (Oklahoma), Lockner DA (USGS), Chang J (Oklahoma), and Totten MW (Oklahoma)*

We generated dynamic slip events with prescribed total energy on an experimental fault. Sliding occurred between granite rings, in a rotary shear apparatus driven by a 100 hp motor and a massive flywheel (225 kg) at normal stress up to 7 MPa. In the experiments, the motor first brought the flywheel to a pre-selected angular velocity. Then, the motor was disengaged and the flywheel was connected to one granite block through a fast-acting clutch, initiating slip between the rotating and stationary blocks. The rate- and slip- dependent friction of the simulated fault surface controlled the slip velocity and slip distance until the kinetic energy of the flywheel was consumed.

The flywheel kinetic energy density (per unit area of the sliding surfaces) ranges from 75 J/m², which is insufficient to initiate slip, to 3.6×10^6 J/m², which generates slip events with duration of ~2 s, maximum slip velocity 0.6-0.7 m/s, and slip distance 0.6-0.9 m. The main observations are: (1) Rise-time < 0.1s for all events; (2) Fault locked until the shear stress reaches yield stress (sliding friction of 0.65-0.8); (3) Significant weakening at slip velocity greater than 0.4 m/s leading to chattering slip (=high-frequency stick-slip events); (4) power law relations between total sliding distance and flywheel energy.

2-116

A MICROMECHANICAL MODEL FOR DEFORMATION IN SOLIDS WITH UNIVERSAL PREDICTIONS FOR STRESS-STRAIN CURVES AND SLIP AVALANCHES *Dahmen KA (Illinois), Ben-Zion Y (USC), and Uhl JT*

A basic micromechanical model for deformation of solids with only one tuning parameter (weakening ϵ) is introduced. The model can reproduce observed stress-strain curves, acoustic emissions and related power spectra, event statistics, and geometrical properties of slip, with a continuous phase transition from brittle to ductile behavior. Exact universal predictions are extracted using mean field theory and renormalization group tools. The results agree with recent experimental observations and simulations of related models for dislocation dynamics, material damage, and earthquake statistics.

2-117

ON THE ENERGY BUDGET AND CONFIGURATIONAL FORCE ASSOCIATED WITH A PROPAGATING SELF-HEALING PULSE IN DISCRETE AND CONTINUUM FAULT MODELS *Elbanna AE (Caltech), and Heaton TH (Caltech)*

We study the energy budget and construct an equation of motion for a self-healing pulse propagating on a frictional interface in a 1D spring block slider model. The energy of the pulse is defined as the sum of the kinetic energy of the masses contained in that pulse at a given time plus the change in potential energy in the springs within the pulse region at that instant. The pulse motion is driven by the difference between the change in the potential energy of the springs that have been displaced by the passage of the slip pulse and the frictional work that have been dissipated throughout the propagation of this pulse. We derive a differential equation that can

track this transport of energy by the slip pulse as it propagates on the fault and augment it with two constitutive equations describing empirically the dependence of the pulse energy and the frictional work on the slip left behind the pulse. The result is a highly nonlinear ODE whose solution can approximate the final slip distribution in large and moderate sized events if the pre-stress distribution that existed before that event is given.

We extend our study to a 2D anti-plane continuum fault model with a rate and state friction law and strong velocity weakening at seismic slip rates. For low pre-stress values, we observe slip pulses. We calculate the seismic efficiency for some of these pulse like ruptures and report values greater than 0.7. We find the seismic efficiency to increase with increasing the rate of velocity weakening as well as the value of the confining normal stress. We also derive an expression for the configurational force associated with the pulse and show that its evolution as the pulse propagates is strongly correlated with the final slip distribution of the event.

Finally we hypothesize a definition for the pulse energy in a continuum setting based on the kinetic energy of the waves set up by the propagating pulse. We study the spatial variation of the kinetic energy density as the pulse width changes, using simple kinematic models, and conclude that for a given slip the narrower the pulse the higher the kinetic energy associated with it and the smaller the region in which this energy is concentrated in. We also examine the relation between the pulse energy defined this way and the seismic radiated energy and propose an energy balance equation, analogous to the one derived for the spring block model, with the pulse energy as one of its components. Our future plans include investigating how to approximate the various terms in this equation and examining the properties of its different solutions and its implications for dynamic rupture.

2-118

STATISTICS OF A DYNAMICAL SYSTEM FAILING AT MULTIPLE LENGTH SCALES AND ITS IMPLICATIONS ON MODELS FOR MATERIAL STRENGTH

Elbanna AE (Caltech), and Heaton TH (Caltech)

Systems failing at multiple length scales are abundant in nature from dislocations to earthquakes. We here present a parametric study for a 1D spring block slider model as an idealization of such systems. Due to its discreteness and lacking of long range interaction, the spring block slider model can not represent accurately the dynamics of a single rupture in a continuum. Nonetheless, the spring block slider can capture reasonably well the long time statistics of complex systems with multiple repeated ruptures since the collective behavior of those systems is independent of the physics of individual event (as long as ergodicity holds at least in an approximate sense).

Our parametric study includes the investigation of the influence of changing of the following parameters on patterns of ruptures obtained: 1)The loading speed of the driving plate 2)The ratio of the coil spring to the leaf spring stiffnesses, and 3) The amount of frictional weakening. In an earthquake setting those parameters will correspond to the rate of tectonic loading, the ratio of the length to the depth of the seismogenic region and the amount of steady state velocity weakening relative to the radiation damping, respectively. We find that smaller driving speeds, higher ratios of leaf spring to coil spring stiffness and smaller frictional weakening favor the generation of smaller ruptures and vice-versa. By tuning the different parameters we can find a region in the parameter space where events of all sizes are produced with statistics similar to Gutenberg-Richter scaling law with a b-value of 1. We show that for this range of parameters we obtain a number of scaling laws similar to what is observed in real life such as potency-length scaling, constant average stress drop scaling and Poisson statistics for stress increments between successive events. We also

show that there is no correlation between the stress increment and the size of the next event, the thing which complicates models for earthquake prediction, and that in general the duration of the earthquake is proportional to its size reflecting a nearly constant rupture velocity independent of the event size.

We study the long time properties of the prestress due to the accumulation of repeated ruptures of different sizes. We conclude that the prestress evolved into a heterogeneous distribution with a power law Fourier spectrum and non-Gaussian statistics. By defining the material strength as the change in potential energy during an event per unit slip per unit rupture length we find the strength to be dependent on the size of rupture with smaller ruptures showing higher values of strength. We show that the size dependence of strength has a power law character with the power law exponent dependent on the b-value in the Gutenberg-Richter scaling. In the plastic limit where most of the energy is dissipated in a large number of small events, $b \gg 1$, the strength is nearly independent of the rupture size. Whereas in the brittle limit where most ruptures are catastrophic events spanning the whole system length, $b \sim 0$, the strength is inversely proportional to the rupture length. For intermediate values of "b" the strength scaling exponent varies between 0 and -1.

2-119

ELEVATED HIGH-FREQUENCY SIGNALS DURING THE LARGE-AMPLITUDE SURFACE WAVES IN SOUTHERN CALIFORNIA: WIDESPREAD TRIGGERING, INSTRUMENTAL CAUSE, OR FILTERING EFFECT? *Peng Z (Georgia Tech), Long L, Fabian AR (South Carolina), and Ohja L*

Recently studies have shown that non-volcanic tremor can be triggered instantaneously during the surface waves of large teleseismic events in Japan, Cascadia, California, and Taiwan. The triggered tremor is characterized by the elevated high-frequency signals during large-amplitude surface waves, which are coherent among different stations and show moveout with increasing distances. Here we compute the spectrograms from the seismic recordings in southern California generated by the 2002 Mw7.8 Denali Fault earthquake. We find elevated high-frequency signals from the spectrograms during large-amplitude surface waves for most stations that are equipped with broadband seismometer/digitizer systems. In comparison, such signals are absent in the co-located short-period instruments. Sometimes bursts of high-frequency signals can be identified from the 2-16 Hz band-pass-filtered seismograms, which correspond to the triggered tremor reported previously. Because such elevated high-frequency signals shown in the spectrograms only correspond to the broadband but not the short-period recordings, we can rule out the possibility that they are caused by widespread triggering of deep tremor or near-surface events. Potential sources of such signals include high-frequency noise within the broadband seismometer/digitizer system, or the short-duration time window used in the generating the spectrograms.

2-120

EARTHQUAKE NUCLEATION ON TWO PARALLEL FAULTS *Fang Z (UCR), Dieterich JH (UCR), and Xu G (UCR)*

Previous nucleation studies employ highly idealized models of single planar fault surfaces. However, natural faults show non-planar features and segmentation at all scales. Slip of non-planar faults results in complex stress interactions that may significantly alter nucleation processes. We employ rate- and state-dependent friction to model nucleation on an idealized fault model consisting two parallel planar faults with step-over features. The geometry of the step-over is described by overlap length d and offset h . In this study, we focus on investigating how nucleation is affected by d and h . For simulations with homogeneous initial conditions both d and h are found to strongly affect the nucleation location. For a specific d , when h is small, earthquakes tend to

nucleate near the end of the overlapping zone for both compressive and extensional stopovers. As h gets larger, earthquakes generally nucleate further away from the overlapping ends for compressive stop-overs. However, for extensional stop-overs, nucleation always occurs in the vicinity of overlapping ends for all offsets studied. Both compressive and extensional step-overs have the same shear stress change profiles but reversed normal stress change profiles for the same geometric configuration, leading to different modified Coulomb stress change profiles. Nucleation locations are found to coincide with the peaks of modified Coulomb stress changes, which explains why nucleation locations migrates in different ways with d and h for compressive and extensional step-overs. However, when heterogeneous initial conditions are applied, the effect of the step-over is significantly diminished. Instead, earthquakes tend to nucleate at the location that has the largest initial friction except when the offset h is extremely small.

2-121

SHEAR-RATE DEPENDENT COMPACTIVITY IN GRANULAR MEDIA *van der Elst NJ (UCSC)*

Granular media exhibit different behaviors depending on the rate of deformation. In particular, the compactivity (the inverse of compaction) of certain media has been observed to depend on shear rate. At low shear rates, the media deforms with constant compactivity over many orders of magnitude in shear rate. At high velocities, where inertial collisions begin to dominate, compactivity increases as the square of shear rate. Between these regimes, there is an unexpected transitional regime, where compactivity decreases over several orders of magnitude in shear rate before increasing into the inertial regime.

The transitional regime is here investigated using a torsional rheometer and angular, polydisperse beach sand with grain sizes between 250-500 microns. Shear rate steps demonstrate that: 1) shear-induced compactivity changes are reversible and reproducible, and 2) the characteristic lengthscale for the evolution of compactivity is much larger than the particle size or the thickness of the localized boundary shear zone. The long displacement lengthscale for the evolution of compactivity is hence inferred to be associated with the slowly deforming bulk. We speculate that the transitional decrease in compactivity reflects a transition in the fabric of the media as force chains lose stability in the presence of inertial collisions.

2-122

SOURCE MECHANISMS AND RUPTURE PROPERTIES OF THE 05/17/2009 INGLEWOOD EARTHQUAKE SEQUENCE *Luo Y (Caltech), Tan Y (Caltech), Zhan Z (Caltech), Ni S (UNR), Hauksson E (Caltech), and Helmberger DV (Caltech)*

On May 18, 2009, an Mw 4.7 event occurred in the LA basin, followed by an aftershock sequence. Waveform inversions using the Cut-And-Paste(CAP) technique with various combinations of data sets yield self consistent results. The results indicate the centroid depth of the main shock is around 8km, with a fault plane of 246/50/17 (strike/dip/rake). The focal mechanism is consistent with slip on the Newport-Inglewood fault. The centroid depth is much shallower than catalog depth from travel times (12.6km), and deeper than SCEC centroid depth from moment tensor inversion (5km).

For the smaller aftershocks, we use the newly developed CAP+ method, where magnitude ~ 4 events with well-known mechanisms are used to calibrate paths for the first few seconds of P-waves in the 0.5 to 2Hz range. These corrections, Amplitude Amplification Factors (AAFs), can then be used to model the smaller events. In this case, we used the events 10410337 (Mw 4.7), 10411545 (Mw 4.0) and 9716853 (Mw 3.8) as references to derive the AAFs and obtained the solutions for 13 smaller events. These events have similar mechanisms to the main event. Then we

used the small aftershocks to study rupture properties of the larger aftershocks (Tan and Helmberger, 2009). The preliminary results indicate that the main event ruptures to the northwest.

2-123

RAPID CENTROID MOMENT TENSOR (CMT) INVERSION IN 3D EARTH STRUCTURE MODEL FOR EARTHQUAKES IN SOUTHERN CALIFORNIA *Lee E (Wyoming), Chen P (LDEO), Jordan TH (USC), and Maechling PJ (SCEC / USC)*

Accurate and rapid CMT inversion is important for seismic hazard analysis. We have developed an algorithm for very rapid CMT inversions in a 3D Earth structure model and applied it on small to medium-sized earthquakes recorded by the Southern California Seismic Network (SCSN). Our CMT inversion algorithm is an integral component of the scattering-integral (SI) method for full-3D waveform tomography (F3DT). In the SI method for F3DT, the sensitivity (Fréchet) kernels are constructed through the temporal convolution between the earthquake wavefield (EWF) and the receiver Green tensor (RGT), which is the wavefield generated by 3 orthogonal unit impulsive body forces acting at the receiver location. The RGTs are also the partial derivatives of the waveform with respect to the moment tensors. In this study, our RGTs are computed in a 3D seismic structure model for Southern California (CVM4SI1) using the finite-difference method, which allows us to account for 3D path effects in our source inversion. We used three component broadband waveforms below 0.2 Hz. An automated waveform-picking algorithm based on continuous wavelet transform is applied on observed waveforms to pick P, S and surface waves. A multi-scale grid-searching algorithm is then applied on the picked waveforms to find the optimal strike, dip and rake values that minimize the amplitude misfit and maximize the correlation coefficient. In general, our CMT solutions agree with solutions inverted using other methods and provide better fit to the observed waveforms.

2-124

EXPERIMENTAL INVESTIGATION OF FLASH WEAKENING IN LIMESTONES *Tisato N, Di Toro G (INGV), De Rossi N, and Quaresimin M (Padova)*

Flash heating and weakening is one of the possible weakening mechanisms operating during earthquake nucleation and propagation. In particular, frictional properties of limestone and dolostone are of interest to earthquake mechanics where seismic ruptures nucleate and propagate in carbonate-bearing rocks (e.g., Mw 6.3 L'Aquila 2009 earthquake).

We performed 27 rock friction experiments in a compression-torsion apparatus on ring-shaped (50/60 and 70/80 mm in diameter) limestone samples (100% CaCO₃) at sub-seismic to seismic slip rates (0.05 to 350 mm/s), small displacements (30-40 mm) and under normal stresses (3-8 MPa). The experiments involved an initial 'loading' followed by a low-speed slip to verify the low-speed friction behaviour and a 'high-speed' step to determine the velocity dependence. The friction coefficient gradually increased from 0 to 0.7-0.8, a typical value for friction in limestone, during the low-speed step (0.05 mm/s and at least 7 mm displacement). In the high-speed step, slip rate was abruptly increased to 250 mm/s for 30 mm displacement (samples 50/60 mm in diameter) and to 350 mm/s for 40 mm displacement (samples 70/80 mm in diameter). All experiments show a dramatic decrease, up to 60%, in friction for slip rates > 100 mm/s.

A possible weakening mechanism is flash heating-induced thermal decomposition of calcite (CaCO₃ → CaO + CO₂) at asperity contacts. In the experiments, weakening was contemporaneous with a peripheral temperature increase of 60-170°C measured with an infrared camera. This temperature range yields a lower limit to the temperature achieved in the slipping zone and at the asperity contacts. Energy Dispersive Spectroscopy equipped with Field Emission Scanning Electron

Microscope (FE-SEM), X-Ray powder diffraction and Raman Spectroscopy analyses rule out the presence of decarbonation products (CaO, Ca(OH)₂) in the slipping zone. Instead, FE-SEM observation reveals the presence of CaCO₃ nano-particles (< 40 nm in size) decorating the slipping zone after the experiments. We conclude that flash heating and, more reasonably, nano-powder lubrication may operate together to decrease fault dynamic friction in limestone rocks in experiments and likely in nature.

2-125

SURFACE SLIP ROUGHNESS OF LARGE EARTHQUAKES *Shaw BE (LDEO)*

For earthquakes which are large enough to break the Earth's surface, slip can be measured directly, providing model-independent information of spatially varying behavior in earthquakes. Here, we develop and apply new scale-free spatial techniques to extract robust measures of surface slip. In particular, we examine how differences in slip scale with differences in separation. Examining slip distributions of 7 large earthquakes in a digital database we find collapse of the curves onto a common behavior showing increasing strain (slip/separation) at decreasing separations, over kilometer lengthscales. The technique is shown to be robust to added uncorrelated noise in the slip. A series of synthetic slip distributions is also examined with the new statistical techniques and are shown to differ from the observed earthquake data, indicating useful constraining information is contained in the observations.

2-126

PLASTIC DEFORMATION AT A PROPAGATING RUPTURE FRONT: ITS COUPLING TO FAULT PORE PRESSURE AND INFLUENCE ON THE SEISMIC MOMENT TENSOR *Viesca RC (Harvard), Rice JR (Harvard), and Dunham EM (Harvard)*

We first emphasize through plots of plastic strain and strain rate, taken from computational elastic-plastic modeling of earthquake ruptures, that active plastic deformation is localized to narrow bands occurring in the immediate vicinity of the rupture front. The bands are rooted at the fault plane and are inclined to it. That feature can already be inferred from close inspection of contour plots of plastic strain in the literature (Andrews, 2005; Ben-Zion and Shi, 2005; Duan, 2008; Templeton and Rice, 2008; Viesca et al., 2008), but seems to have generally not been commented upon. Furthermore, in considering that the fault-perpendicular extent of plastic strain increases with propagation distance, and specifically that its components do not necessarily share the same sense of shear with the fault, we can expect its contribution to the moment tensor (under plane-strain deformation) to be a small rotation of the tensor out of line with the actual fault plane. We will show the evolution of the moment tensor orientation with propagation of the rupture tip.

Where plastic straining actively occurs, adjacent to the fault, has relevance for determining fault surface pore pressure changes, and hence couples through the effective stress concept to the dynamics of rupture propagation. These changes depend in part on near-fault undrained pore pressure changes and on alterations by plastic straining to pore fluid permeability and storage coefficients. More precisely, we have extended to the elastic-plastic case (Viesca and Rice, 2009) the determination of fault pore pressure due to poroelastic response of the surface-adjacent material as in Rudnicki and Rice (2006) and Dunham and Rice (2008). The properties of the surface-adjacent material may differ distinctly in character across the slip surface and differ also from material further off-fault (Chester and Chester, 1998; Chester et al., 2004). In extending the analysis, we identify an elastic-plastic hydraulic diffusivity. We find in our elastic-plastic dynamic rupture simulations done so far, in which permeability changes from plastic straining are neglected, that the rupture directivity is consistent with that predicted for poroelastic off-fault deformation.

2-127

FLASH WEAKENING OF SERPENTINITE AT NEAR-SEISMIC SLIP RATES *Kohli AH (Brown), Goldsby DL (Brown), Hirth G (Brown), and Tullis TE (Brown)*

Flash heating of stress-concentrated asperities is one mechanism thought to promote dynamic weakening of earth materials at seismic slip rates (Rice et al.; 2006, 2009). Previous 1-atm torsion experiments on serpentinite, an abundant fault-surface phase in the shallow lithosphere, indicate weakening is purely velocity-dependent and show a $1/V$ decrease in friction above $V = 0.1$ m/s from 0.6 - 0.2 at $V \sim 0.4$ m/s (Goldsby et al.; 2006). Similar results are reported by Hirose et al. 2007 in experiments (up to 1.1 m/s) with large displacements ($\delta = 5$ m). To further investigate the processes responsible for weakening, we performed bidirectional, single and step velocity experiments ($\delta = .04$ m) and supporting microstructural analyses on antigorite serpentinite, conducted over slip rates from 0.01 m/s to 0.4 m/s. Single velocity experiments reinforce previous results showing approximately $1/V$ dependence above a threshold velocity of $V_w = 0.1$ m/s. Step experiments show successive weakening corresponding to velocity steps above V_w , with full weakening occurring in just several millimeters of slip – much smaller displacements than inferred from the higher displacement experiments of Hirose and Bystricky. We varied sample grip mass and complia

2-128

IS FLASH-WEAKENING CAUSED BY MELT? *Weaver SL (Oregon), Chen J (Caltech), and Rempel AW (Oregon)*

Significant progress has been made toward understanding the frictional evolution that determines fault strength during high-speed slip. High-velocity rock friction experiments consistently show that the friction coefficient μ decreases dramatically from its low-speed value μ_0 at a critical weakening velocity V_w that is exceeded by those slip rates ~ 1 m/s typical of seismic events. Temperature increases at localized asperities are implicated in this {it flash-weakening} process. This leads to the testable hypothesis that melting at asperity contacts is responsible for observed changes in strength. We have proposed an elementary theoretical model that predicts the slip-rate dependent changes in μ as a function of the weakening velocity V_w , and the Stefan number SS , which are both determined by the thermal properties and phase behavior of the materials involved. While many of the controlling properties are well documented at ambient conditions, it is challenging to make appropriate {it a priori} estimates for these parameters at the high normal stresses typical of asperity contacts (1--10 GPa). Consequently, it is appropriate to test our model with experimentally observed rock friction data that enable us to extract appropriate physical parameters and assess our initial assumptions. Rock friction experiments have been used to describe frictional behavior for a variety of mono- and multi-minerallic materials at a range of slip rates. We test our theory against these data in order to find the "best" values of parameters V_w , SS , and μ_0 for our friction model. We present the results of these fits to assess both the limitations of our model and the extent to which it is able to capture key aspects of the dynamic evolution of fault strength during rupture.

2-129

DISTINCT ASYMMETRY IN RUPTURE-INDUCED INELASTIC STRAIN ACROSS DIPPING FAULTS: A PREDICTION BASED ON THE MOHR-COULOMB YIELD CRITERION *Ma S (Stanford)*

Off-fault stresses associated with rupture propagation violate the Mohr-Coulomb yield criterion inducing irrecoverable deformation in fault zone. I investigate the distribution of inelastic strain around dipping faults by simulating 2D dynamic ruptures for a 30° reverse fault and a 60° normal

fault in a depth-dependent stress environment. The inelastic zone off the fault broadens as it nears the surface with decreasing confining pressure, forming a skewed 'flower-like' structure bounded atop by the free surface. The inelastic strain in the hanging wall is significantly larger and broader than the footwall for both reverse and normal faults. The occurrence of inelastic strain, however, reduces significantly ground motion (especially on the hanging wall) and gives rise to a reduced asymmetry in ground motion on the hanging wall and footwall compared to elastic solutions. These results provide theoretical predictions for fault zone structure of dipping faults that can be tested by future observational experiments.

2-130

RHEOLOGY OF ANTIGORITE SERPENTINITE AT HIGH TEMPERATURE AND PRESSURE: IMPLICATIONS FOR ASEISMIC FAULT CREEP AND INTERMEDIATE DEPTH SEISMICITY *Chernak LJ (Brown), and Hirth G (Brown)*

We have conducted axial compression deformation experiments within the antigorite stability field and where dehydration to forsterite and talc is expected to constrain the rheology of antigorite serpentinite at high temperatures and pressures. Samples were deformed in a Griggs-type apparatus at 0.5 - 1.5 GPa, 300 - 700°C and strain rates of 10⁻⁵s⁻¹ and 10⁻⁶s⁻¹. Samples experienced localized deformation at temperatures from 300 to 625°C when deformed to high enough strain. Surprisingly, sample ductility decreases with increasing temperature. Samples deformed at 300°C strain harden until ~20% strain when faulting initiates; there is no evidence for localization at low strain. At 400°C, strain hardening ceases at ~10-15% strain and samples are characterized by a broad zone of deformation surrounding one or more fractures. Samples deformed at 550°C and 625°C strain weaken abruptly at ~5-10% strain and contain one distinct fault.

The ductility of serpentinite is important for understanding the stability of sliding and creep along the SAF. As reported by Moore and Rymer (2007) the frictional strength of serpentine minerals is too high to be consistent with the strength of the fault, however, the positive velocity dependence of serpentine is consistent with stable sliding. Strain rate stepping experiments from our study sh

2-131

STRUCTURAL ANALYSIS OF THE CAJON PASS CORE, AND IMPLICATIONS FOR FAULT STRUCTURE AND PROCESSES *Forand D (Utah State), Evans JP (Utah State), and Janecke SU (Utah State)*

We revisit the crystalline drill core from the Cajon Pass, California drill hole, north of the San Andreas Fault (SAF) and Cleghorn fault, to perform a systematic structural analysis of deformation and alteration in cored rocks. The well is ideally situated to test the shallowly dipping San Andreas Fault hypothesis (Fuis et al., 2008). Previous lithologic descriptions of the core did not provide descriptions of deformation processes at depth. The core and outcrop observations of deformed rocks in the western San Bernardino Mountains to provide a sampling of fault-related rocks over a 4.5 km vertical column northeast of the SAF. Shallow sandstones (0-500 m) in the borehole are above gneissic rocks to a depth of ~1425 m. Faulted migmatite dominates below the gneisses to a depth of a fault at ~2300 m. A heterolithologic mix of crystalline rocks below 2300 m is cut by numerous steep to vertical faults to the total depth of 3500 m. The core preserved 19 fault zones, 11 of which are newly identified in this work, with k-spar, epidote and laumontite alteration common in the fault zones. The few fault striate indicate mixed-mode slip. Microstructures include shear fractures containing angular to sub-angular clasts in a laumontite matrix. There is textural evidence for repeated faulting events. Laumontite signatures on XRD analysis of structures from the core, and the marked absence of clay minerals indicate moderate temperature hydrothermal alteration, above those expected at the current depth of the core. Uplift of at least one km is required to

explain these relationships. A fully intact fault zone was cored at 3402 m depth and dips 70°. This fault and an increase in the frequency of faults in the crystalline rocks total depth suggests that Cajon Pass well crossed a major fault zone 100 m above TD. This fault projects at a steep dip to the surface trace of the Cleghorn fault, an active left-lateral fault that reactivated older reverse faults. We rejected a correlation with the SAF because of the steep fault dip, and all crystalline rock types in the core appear to be of San Bernardino basement, not San Gabriel basement. This constrains SAF dip at this location to >45°. The suite of deformed rocks from the surface expression of the Cleghorn fault to the bottom of the borehole indicate that the rocks experienced deformation at $T > 120^{\circ}\text{C}$, with no clay gouge, and in an environment where slip and healing cycled over the history of the deformation.

2-132

COLLATERAL DAMAGE: HOW DAMAGE ZONE FRACTURE DENSITY PROFILES REFLECT THE SLIP DISTRIBUTION *Savage HM (Penn State), and Brodsky EE (UCSC)*

Fault zones contain a distribution of damage. The progression of damage as a function of distance from the fault contains information about the fault evolution and stress field. In this study, we aim to 1) measure the distribution of damage around small, isolated faults and 2) compare the damage distribution over a wide range of faults with varying displacements.

We measure multiple linear fracture density transects along small normal faults located in Santa Cruz, California. Both macroscopic joints and shear fractures are included in our measurements. These small faults have fracture densities that decay rapidly in space and are well-fit by a power law with a decay exponent of $n = \sim -1$. To investigate the damage distribution as a function of displacement, we compare fracture profiles collected from previously published studies to our own field study. The decay exponent from small faults remains ~ -1 , until 100 m of displacement has been achieved. Fracture decay from larger faults is less continuous, due to the superposition of damage peaks associated with secondary fault strands within the damage zone (e.g. Chester and Logan, 1986). Additionally, we find that total fault zone width (as determined by where the fracture density falls to background levels) grows linearly with displacement until 100 m of displacement has been achieved, then the correlation of fault zone width with displacement is much less apparent.

We interpret the change in fracture decay after ~ 100 m of displacement as a manifestation of increasing slip distribution onto secondary fault strands within the damage zone. Although the fracture decay from large faults is not as well fit by a power law, the decrease in the decay exponent reflects the increasing number of secondary fault strands in the damage zone. A simple stochastic model demonstrates that strand formation may be related to the number of fractures within the damage zone available to become fault strands, due to the coalescence of nearest neighbors. These results imply that the presence of a damage zone acts to distribute slip onto multiple surfaces as cracks coalesce into shear planes. Furthermore, small faults produce more off-fault damage than large faults per unit of slip.

References

Chester, F. M. and J. M. Logan, 1986. Implications for mechanical properties of brittle faults from observations of the Punchbowl Fault Zone, California. *Pure and Applied Geophysics* 124: 79-106.

2-133

QUANTIFYING FOCAL MECHANISM HETEROGENEITY FOR FAULT ZONES IN CENTRAL AND SOUTHERN CALIFORNIA *Bailey IW (USC), Ben-Zion Y (USC), Becker TW (USC), and Holschneider M (Potsdam)*

We present a statistical analysis of focal mechanism orientations for nine California fault zones with the goal of quantifying variations of fault zone heterogeneity at seismogenic depths. The focal mechanism data are generated from first motion polarities for earthquakes in the time period 1983–2004, magnitude range 0–5, and depth range 0–15 km. Only mechanisms with good quality solutions are used. We define fault zones based on a 15 km zone around the fault traces according to the USGS Quaternary fault map, and use summations of normalized potency tensors to extract information about the focal mechanism heterogeneity for each fault zone. This is quantified using two measures that are roughly analogous to the standard deviation and skewness of the double-couple orientation distributions. We find a decreasing trend in relative focal mechanism variation as a function of geologically mapped fault trace complexity, indicating a link between the long term evolution of a fault and its seismic behavior over a 20 year time period. The nature of heterogeneity and partitioning of faulting styles are affected by the dominant orientation of the fault zone. This indicates that the heterogeneity of earthquake orientations in a fault zone is correlated with geometrical properties of the main fault and the efficiency of that fault at releasing plate motion. These correlations are observed despite clustering of small earthquakes in zones of complexity along the main faults.

2-134

IMPACTS OF FAULT GEOMETRY ON FAULT SYSTEM BEHAVIORS *Coon ET (Columbia), Shaw BE (LDEO), and Spiegelman M (LDEO)*

Complexity in earthquake populations arises primarily due to two components: friction and fault geometry. We present preliminary investigations into contributions to event population complexity due to fault geometry variation. In one key application, we investigate probabilities of events continuing along multiple, en echelon fault segments in both compressional and extensional regimes as a function of distance between the segments and segment overlap.

These and other results are produced in the course of developing the extended finite element method, XFEM (e.g. [Dolbow, Moes, and Belytschko, 2001]), for static, quasistatic, and dynamic rupture problems on complicated fault networks. This method, part of a

broader class of mesh-free methods, allow faults to be included nearly arbitrarily in a simulation, enabling many simulations with varying fault geometries to be conducted with minimal remeshing.

We introduce the enforcement of failure criteria in dynamic rupture problems under this method, and test the method through a series of two-dimensional static and dynamic benchmarks. We also introduce a novel, "two and a half-dimensional" formulation, where

two-dimensional plates intersect at faults with a constant down-dip while varying along-strike. This enables us to model fault systems with strike-slip, thrust, normal, and mixed-mode faults. These results demonstrate the feasibility of the XFEM for both static and dynamic rupture problems, and enable new studies of fault system behaviors due to fault geometry.

2-135

HIGH-SPEED FRICTION OF PUNCHBOWL FAULT ULTRACATACLASITE IN ROTARY SHEAR: CHARACTERIZATION OF FRICTIONAL HEATING, MECHANICAL BEHAVIOR, AND MICROSTRUCTURE EVOLUTION *Kitajima H (Texas A&M), Chester JS (Texas A&M), Chester FM (Texas A&M), and Shimamoto T (Hiroshima)*

To investigate the frictional behavior of natural faults at seismic slip rates, high-speed rotary shear experiments have been conducted on disaggregated ultracataclasite from the Punchbowl fault. One-mm-thick gouge layers were sheared between 25 mm diameter cylindrical blocks at 0.2-1.5 MPa normal-stress and 0.1-1.3 m/s to total displacements of 1.5-84 m. At the greater velocities and normal stresses the coefficient of sliding friction is significantly reduced as a consequence of frictional heating. In the rotary shear configuration the slip rate, shear displacement and frictional heating of the sheared layer vary with radius. Microstructural observations made from radial sections are combined with the results of thermomechanical models of the samples to understand the frictional deformation mechanisms and mechanical behavior. Four distinct microstructural units are identified in the sheared layers on the basis of particle size distributions, particle shape, development of clay foliation, and degree of localization of shear. All four units are produced within a single experiment at many of the high slip-rate conditions tested. Two of the units, the compacted, slightly sheared and modified starting material and the well-foliated and sheared gouge, display characteristics consistent with shearing at standard laboratory rates where frictional heating is insignificant and the coefficient of friction is in the range of 0.4 to 0.6. The third unit, which displays microstructures consistent with fluidization, is developed only at normal stresses and slip rates that generate temperatures greater than 150 C. The remaining unit represents localized shearing with extreme particle size reduction and, under conditions favoring frictional heating, likely accounts for the dynamic weakening to friction coefficients of approximately 0.2. The temporal development and spatial distribution of the four units are a consequence of the variable conditions imposed by the rotary shear configuration. All of the units have counterparts in natural earthquake slip zones. Microstructural observations and thermomechanical models of the experiments indicate that the normal stress, temperature and mechanisms of deformation in the sheared layers vary with radius, and that the heterogeneous conditions of the gouge layer must be considered in order to accurately infer friction constitutive properties from the experimental data. Work to date has used the thermomechanical model to determine the radial variation in normal stress due to frictional heating and thermal expansion. Current work is focused on extending the model to determine explicitly the velocity and temperature dependence of friction.

2-136

SEISMIC DOCUMENTATION OF ROCK DAMAGE AND HEAL ON THE PARKFIELD SAN ANDREAS AND PRELIMINARY OBSERVATIONS AT THE LONGMAN-SHAN FAULT OF THE M8 WENCHUAN EARTHQUAKE *Li Y (USC), Malin PE (Duke), Vidale JE (Washington), Cochran ES (UCLA), and Chen P (LDEO)*

We used fault-zone trapped waves (FZTWs) recorded at the SAFOD mainhole seismograph installed in the fault zone at a depth of ~3 km and a dense linear surface array across the San Andreas Fault (SAF) to document fault zone rock damage with high-resolution. Observed FZTWs are simulated using 3-D finite-difference methods in terms of a downward tapering 100-200-m-wide LVZ along the SAF at seismogenic depths, within which shear velocities are reduced by 25-50% from wall-rock velocities with the larger velocity reduction at the shallower depth. The maximum velocity reduction is up to ~50% in a 30-40-m-wide fault core, showing the localization of severe rock damage on the SAF. The width and velocities of the damage zone on the SAF at ~3-km depth delineated by FZTWs are verified by the SAFOD drilling and logging studies [Hickman et al., 2005]. The depth distribution of earthquakes generating fault-zone trapped waves indicates

that the LVZ on the SAF extends to depths of at least ~7-8 km. The damage zone is not symmetric but extends farther on the SW side of the main fault trace, implying a possible moving damage zone on the SAF that has accumulated fracturing during historical earthquakes. It could also be due to greater damage in the extensional quadrant near the propagating crack tip of Parkfield earthquakes. We interpret the low-velocity waveguide as being a zone of accumulated damage from recurrent major earthquakes, including the 2004 M6 earthquake. Waveform cross-correlation measurements from repeated explosions and microearthquakes recorded before and after the 2004 M6 Parkfield earthquake illuminate the co-seismic velocity decrease of ~2.5% and post-mainshock increase of ~1.2% within the fault zone in the first 3-4 months, with an approximately logarithmic healing rate and the largest rate in the earliest stage after the mainshock. The ratio between the P and S traveltime changes suggest the opening of new fluid filled cracks during the mainshock. The magnitude of rock damage and heal observed at the SAF Parkfield is most prominent above ~7 km with variations along the fault strike, and also smaller than those observed on the Landers and Hector Mine rupture zones. This difference is probably related to the smaller magnitude mainshock and smaller slip and, possibly, by differences in stress drop, pore-pressure, and rock type.

Recently, we start to study the rock damage and healing on the Longmen-Shan Fault (LSF) that ruptured in the M8 Wenchuan earthquake on May 12, 2008 using the data recorded at Sichuan Seismic Network (SSN) and portable stations. Chen et al. [2008] show that the Wenchuan mainshock included multiple events with the reverse thrusting at the first stage and then becoming to strike-slip gradually, indicating the complexity in faulting mechanism and stress heterogeneity along the LSF. In our preliminary examination of the data from SSN, we identify ~100 clusters of repeated aftershocks among >10,000 aftershocks and pre-shocks. Waveform cross-correlations of repeated events show temporal changes in seismic velocity of P, S and trapped waves associated with the co-seismic damage and post-mainshock healing of fault-zone rock on the LSF caused by the M8 Wenchuan earthquake. We recorded prominent fault-zone trapped waves at stations located within and close to ruptures of the Wenchuan earthquake. Our numerical tests for the trapping efficiency of a low-velocity thrusting fault zone with various geometries at depth using 3-D FD codes provide us a guideline to interpret the FZTWs observed at the thrust-faulting LSF. Preliminary results from modeling of FZTWS show a distinct LVZ on the dipping LSF at varying angles at depth, consistent with the geological structure and drilling results near the rupture. We further examine if the different faulting mechanisms on the LSF and SAF exert different effects on the magnitude of fault damage and heal in the earthquake cycle.

2-137

SLIP MAXIMA AT FAULT JUNCTIONS AND RUPTURING OF BARRIERS DURING THE 2008 WENCHUAN EARTHQUAKE *Shen Z, Sun J, Zhang P, Wan Y, Wang M (UCLA), Bürgmann R (Berkeley), Zeng Y, Gan W, Liao H, and Wang Q*

The disastrous 12 May 2008 Wenchuan, China earthquake took the local population and scientists by surprise. While the Longmen Shan fault zone was well known, geologic and geodetic data indicate < 3 mm/yr deformation rates across the thrust belt. Here we use GPS and InSAR data to invert for fault geometry and slip distribution of the earthquake. From southwest to northeast the fault geometry changes from moderately northwest dipping to near vertical, and the rupture changes from predominantly thrust to dextral faulting. The fault offsets peak near fault junctions near Yingxiu, Beichuan, and Nanba, causing concentrations of fatalities and damage. These fault junctions represent barriers, whose failures in a single event allowed the rupture to cascade through several fault segments, resulting in a major Mw 7.9 earthquake. Earthquake recurrence

intervals across fault segments are estimated at ~4000 years using the coseismic slip distribution and geodetic and geological slip rates.

2-138

OCTOBER 16, 1999 HECTOR MINE EARTHQUAKE REVISITED: INVESTIGATION OF SURFACE RUPTURE WITH AIRBORNE LIDAR *Zhang D (Caltech), Stock JM (Caltech), and Hudnut KW (USGS)*

We reexamine details of the fault slip distribution for the October 16, 1999 Hector Mine earthquake (Mw 7.1) to explore differences in observations as a function of wavelength. Seismology, geodesy (GPS and InSAR), and geology have given similar results on most of the long-wavelength slip features. On the shorter-wavelength variations in fault slip, however, not all methods give the same results. Light Detection and Ranging (LiDAR) is a precise method for monitoring changes to the surface topography. Here we use post-event airborne LiDAR to map the surface rupture distribution; no pre-earthquake LiDAR was available. Within six months after the Hector Mine earthquake, a high-resolution airborne LiDAR survey collected over 70 million data points to observe and document the surface rupture. Due to the limitations of computers at the time, this data set was never thoroughly analyzed, but is now tractable with modern technology. We reformatted, calibrated, analyzed and visualized the data with self-developed scripts and the GEON Points2Grid software package. Throughout the duration of the flights, error in the absolute elevation of the helicopter was usually less than 10 cm. The raw data were processed into different formats, including point clouds, DEMs with 3 m, 2 m and 1 m resolution, and corresponding hillshade models with different light projection directions. We compared the resolution of these products for segments of the fault with clearly visible rupture. We explored the surface topography and rupture distribution along the fault with these surface models using QuickTerrain Modeler and other GIS software packages. We looked in areas beyond the extreme (SE and NW) endpoints of the rupture (as mapped by Treiman et al., 2002). In the northern (0-5 km) and southern (39-45 km) sections along the fault, no surface rupture was obvious along the survey lines, which is consistent with previous field geological surveys. This remains discrepant, however, with the inverse models from seismology, InSAR, and GPS, possibly due to the limited areal coverage of these LiDAR data.

Meeting Participants

AAGAARD Brad, *USGS*
AGNEW Duncan, *UCSD*
AGUIAR Ana, *Stanford*
AGUILAR Victor, *UCLA*
AKCIZ Sinan, *UCI*
ALLAM Amir, *USC*
ALSBURY Sara, *Oregon State*
ALVAREZ Melva, *PCC*
ALVIZURI Celso, *UCSB*
ALWARD William, *Missouri*
AMPUERO Jean Paul, *Caltech*
ANDERSON Greg, *NSF*
ANDERSON Katie, *SDSU*
ANDERSON John, *UNR*
ANDREWS Dudley Joe, *USGS*
ANOOSHEHPOOR Rasool, *UNR*
ARCHULETA Ralph, *UCSB*
ARMSTRONG Jason, *ASU*
ARROWSMITH Ramon, *ASU*
ASIMAKI Domniki, *Georgia Tech*
ASPIOTES Aris, *USGS*
ATKINSON Gail, *Western Ontario*
AVILA Julia, *UCSC*
AVRAHAM Dafna, *UCLA*
BAILEY Iain, *USC*
BALLEW Natalie, *USC*
BALTAY Annemarie, *Stanford*
BARBA Magali, *Berkeley*
BARBOT Sylvain, *UCSD*
BARBOUR Andrew, *IGPP at SIO*
BARNHART William, *Cornell*
BAXTER Sean, *JPL*
BAZARGANI Farhad, *UCLA*
BECKER Thorsten, *USC*
BEELER N. M., *USGS*
BEHR Whitney, *USC*
BEN-ZION Yehuda, *USC*
BENNETT Richard, *Arizona*
BENNETT Scott, *UC Davis*
BENTHIEN Mark, *SCEC / USC*
BEROZA Greg, *Stanford*
BERTI Ryan, *USC*
BHAT Harsha, *USC / Caltech*
BIASI Glenn, *UNR*
BIELAK Jacobo, *CMU*
BIRD Peter, *UCLA*
BLANPIED Michael, *USGS*
BLUME Frederick, *UNAVCO*
BOCK Yehuda, *UCSD*
BOESE Maren, *Caltech*
BOHON Wendy, *ASU*
BOORE David, *USGS*
BORYTA Mark, *Mt. San Antonio College & NAGT*
BOUTWELL Christiann, *SCEC / USC*
BOWLES Christopher,
BOWMAN David, *CSU Fullerton*
BOYD Elena, *UT Austin*
BROCHER Thomas, *USGS*
BRODSKY Emily, *UCSC*
BROTHERS Daniel, *UCSD*
BROWN Justin, *Stanford*
BROWN Kevin, *UCSD*
BROWN Jordan, *USC*
BRUNE James, *UNR*
BÜRGMANN Roland, *Berkeley*
CALLAGHAN Scott, *USC*
CAMPBELL Brian, *Missouri at Columbia*
CAMPBELL Kenneth, *UC Davis*
CELEBI Mehmet, *USGS*
CHANG Jefferson, *Oklahoma*
CHEN Shang-Lin, *Caltech*
CHEN Ting, *Caltech*
CHEN Rui, *CGS*
CHEN Kate, *National Taiwan Normal Univ*
CHEN Jiangzhi, *Oregon*
CHEN Xiaowei, *UCSD*
CHEN Po, *Wyoming*
CHERNAK Linda, *Brown*
CHÉRY Jean, *CNRS*
CHESTER Judith, *Texas A&M*
CHING Kuo-En, *Indiana*
CHOURASIA Amit, *SDSC*
CHU Risheng, *Caltech*
CHUANG Yun-Ruei, *Indiana*
CHUNG Angela, *Stanford*
CLAYTON Robert, *Caltech*
COCHRAN Elizabeth, *UCR*
COLELLA Harmony, *UCR*
COON Ethan, *Columbia*
CROSBY Christopher, *SDSC / UCSD*
CROWELL Brendan, *UCSD*
CRUZ-GUANDIQUE Emerzon, *CSU*
CUI Yifeng, *SDSC*
DAHMEN Karin, *Illinois*
DAUB Eric, *Los Alamos National Lab*
DAVIS Paul, *UCLA*
DAWSON Timothy, *CGS*
DAY Steven, *SDSU*
DE GROOT Robert, *SCEC / USC*
DE HOOGH Greg, *CSULB*
DEDONTNEY Nora, *Harvard*
DEL PARDO Cecilia, *UTEP*
DENOLLE Marine, *Stanford*
DHAR Mahesh, *UNR*
DI TORO Giulio, *INGV*
DIETERICH James, *UCR*
DISCHLER Jennifer, *ASU*
DMOWSKA Renata, *Harvard*
DOLAN James, *USC*
DOMINGUEZ RAMIREZ Luis, *UCLA*
DONG Danan, *JPL*
DONOVAN Jessica, *USC*
DUAN Benchun, *Texas A&M*
DUNHAM Eric, *Stanford*
ELBANNA Ahmed, *Caltech*
ELLIOTT Austin, *UC Davis*
ELLSWORTH William, *USGS*
ELY Geoffrey, *USC*
ERICKSON Brittany, *UCSB*
EUCHNER Fabian, *ETH Zurich*
EVANS James, *Utah State*
FABIAN Amanda, *South Carolina*
FANG Zijun, *UCR*
FEI Yongxin, *UCLA*
FEIGL Kurt, *UW-Madison*
FIALKO Yuri, *SIO / UCSD*
FIELD Edward, *USGS*
FILSON John, *USGS*
FLOYD Michael, *UCR*
FRANKEL Kurt, *Georgia Tech*
FROST Erik, *USC*
FU Jingqiao, *USC*
FUIS Gary, *USGS*
FUNNING Gareth, *UCR*
GABRIEL Alice-Agnes, *ETH Zürich*
GABUCHIAN Vahe, *Caltech*
GANEV Plamen, *USC*
GARCIA Saul, *ELAC*
GAYDALENOK Olga, *Moscow State University*
GERSTENBERGER Matthew, *GNS Science*
GILCHRIST Jacquelyn, *UCR*
GOEBEL Thomas, *USC*
GOLDSBY David, *Brown*
GOLTZ James, *CalEMA*
GONZÁLEZ-GARCÍA Jose Javier, *CICESE*
GORMLEY Deborah, *SCEC*
GOULET Christine, *URS*
GRANT LUDWIG Lisa, *UCI*
GRAVES Robert, *URS*
GUATTERI Mariagiovanna, *Swiss Re*
HADDAD David, *ASU*
HADDADI Hamid, *CGS*
HALLER Kathleen, *USGS*
HANKS Tom, *USGS*
HANNA Alexander, *CSUN*
HARAVITCH Ben, *USC*

Meeting Participants

HARDEBECK Jeanne, *USGS*
HARDING Alistair, *UCSD*
HARDY Jill, *USC*
HARRIS Ruth, *USGS*
HASELTON Curt, *CSU Chico*
HAUKSSON Egill, *Caltech*
HEATON Thomas, *Caltech*
HEERMANCE Richard, *CSUN*
HELMBERGER Donald, *Caltech*
HERMUNDSTAD Ann, *UCSB*
HERRING Thomas, *MIT*
HILLERS Gregor, *Caltech*
HIRTH Greg, *Brown*
HOGAN Phillip, *Fugro West*
HOLLAND Austin, *Arizona*
HOLLIDAY James, *UCD*
HOLT William, *SUNY-Stony Brook*
HOWARD D'Nita, *Wilberforce*
HU Jyr-Ching, *National Taiwan Univ*
HUDNUT Kenneth, *USGS*
HUMPHREYS Eugene, *Oregon*
HUYNH Tran, *SCEC*
IHRIG Michael, *PCC*
IMPERATORI Walter, *ETH Zurich*
JACKSON David, *UCLA*
JAKKA Ravi, *UCR*
JAMASON Paul, *UCSD*
JANECKE Susanne, *Utah State*
JI Kang, *MIT*
JI Chen, *UCSB*
JIN Lizhen, *UCR*
JOHNSON Kaj, *Indiana*
JOHNSON Leonard, *NSF*
JOHNSON Marilyn, *USC*
JONES Lucile, *USGS*
JORDAN Thomas, *USC*
JORDAN, JR. Frank, *John R. Byerly, Inc*
KAGAN Yan, *UCLA*
KALKAN Erol, *USGS*
KANAYA Taka, *Hess Corporation*
KANE Deborah, *SIO / UCSD*
KANEKO Yoshihiro, *Caltech*
KANG Jingqian, *Texas A&M*
KANO Yasuyuki, *Kyoto University*
KANU Chinaemerem, *Indiana*
KARAOGLU Haydar, *CMU*
KAWASAKI Ichiro, *Kyoto University*
KEDAR Sharon, *JPL*
KELL-HILLS Annie, *UNR*
KELLOGG Louise, *UC Davis*
KENDRICK Katherine, *USGS*
KENT Graham, *UNR*
KHAN Mehdi,
KILB Debi, *UCSD*
KIM Caroline, *PCC*
KING Nancy, *USGS*
KITAJIMA Hiroko, *Texas A&M*
KOHLER Monica, *UCLA*
KOHLI Arjun, *Brown*
KONCA Ali Ozgun, *Caltech*
KOZDON Jeremy, *Stanford*
KREYLOS Oliver, *UC Davis*
KRISHNAN Swaminathan, *Caltech*
LANGBEIN John, *USGS*
LANGENHEIM Victoria, *USGS*
LAPUSTA Nadia, *Caltech*
LAVALLEE Daniel, *UCSB*
LE Kimberly, *UC Davis*
LEE Kwangyoon, *UCSD*
LEE En-Jui, *Wyoming*
LEGG Mark, *Legg Geophysical*
LEMERSAL Elizabeth, *USGS*
LEWIS Michael, *USC*
LI Wei, *Georgia Tech*
LI Xiangyu, *UCSB*
LI Yong-Gang, *USC*
LIEL Abbie, *Colorado*
LIPOVSKY Brad, *UCR*
LIU Zaifeng, *Texas A&M*
LIU Qinya, *Toronto*
LIU Qiming, *UCSB*
LIUKIS Maria, *USC*
LLENOS Andrea, *MIT / WHOI*
LOCKNER David, *USGS*
LOGAN John, *Oregon*
LOHMAN Rowena, *Cornell*
LOPEZ Hellen, *PCC*
LOUIE John, *UNR*
LOVELESS Jack, *Harvard*
LOZOS Julian, *UCR*
LU Jiangning, *MIT*
LUO Yan, *Caltech*
LYDEEN Scott, *USGS*
LYNCH David, *Caltech*
MA Shuo, *SDSU*
MADDEN Elizabeth, *Stanford*
MAECHLING Philip, *USC*
MAI Paul, *KAUST*
MARLIYANI Gayatri, *SDSU*
MARQUIS John, *SCEC*
MARSHALL Scott, *Appalachian State*
MARZOCCHI Warner, *INGV*
MASANA Eulalia, *SDSU*
MAYHEW John, *SDSU*
MCAULIFFE Lee, *USC*
MCBURNETT Paul, *CSUN*
MCCARTHY Jill, *USGS*
MCGILL Sally, *CSUSB*
MCGUIRE Kathleen, *CSUN*
MCGUIRE Jeff, *WHOI*
MCKAY Hannah, *CSUN*
MCQUINN Emmett, *UCSD*
MCRANEY John, *SCEC / USC*
MEADE Brendan, *Harvard*
MEDINA LUNA Lorena, *CSUN*
MEHTA Gaurang, *USC / ISI*
MELBOURNE Tim, *CWU*
MELLO Michael, *Caltech*
MELTZNER Aron, *Caltech*
MENGENS Christopher, *USGS*
MILETI Dennis,
MILLER Kate, *Texas A&M*
MILLER Meghan, *USC*
MILNER Kevin, *SCEC*
MINSON Sarah, *Caltech*
MINSTER Bernard, *UCSD*
MITCHELL Erica, *UCSD*
MONELLI Damiano, *ETH Zurich*
MONTES DE OCA John, *USC*
MORELAND Sarah, *CSUSB*
MORTON Nissa, *SDSU*
MUIRHEAD Alicia, *UCSC*
MURPHY Janice, *USGS*
MURRAY-MORALEDA Jessica, *USGS*
MUTO Manami, *Ohsaki Research Institute*
NAEIM Farzad, *John A. Martin & Assoc*
NANJO Kazuyoshi, *Tokyo*
NEE Philip, *UCR*
NEIGHBORS Corrie, *UCR*
NGUYEN Hieu, *UCSD*
NI Sidao, *URS*
NICHOLSON Craig, *UCSB*
NODA Hiroyuki, *Caltech*
NORIEGA Gabriela, *UCI*
OGLESBY David, *UCR*
OHLENDORF Summer, *UW-Madison*
OHYA Fumio, *Kyoto University*
OJHA Lujendra, *Georgia Tech*
OLIVER Brian, *Cal Poly Pomona*
OLSEN Kim, *SDSU*
ONDERDONK Nate, *LBSU*
ORTEGA Gustavo, *CALTRANS-LA*
OSKIN Michael, *UC Davis*
OWEN Susan, *JPL*
OZAKIN Yaman, *USC*
PACE Alan,
PAGE Morgan, *USGS*
PARKER Jay, *JPL*
PATINO Alec, *USC*
PECHPRASARN Thanakij, *USC*
PENG Zhigang, *Georgia Tech*
PHILLIPS David, *UNAVCO*
PLATT John, *USC*
PLESCH Andreas, *Harvard*
POLLITZ Fred, *USGS*
PONTI Daniel, *USGS*
PORTER Ryan, *Arizona*
POUNDERS Erik, *USGS*
POWELL Robert, *USGS*
POWERS Peter, *USGS*
PRAKASH Vikas, *CWRU*
PRESIADO Rhea, *PCC*
PRUITT Aaron, *Appalachian State*
PURASINGHE Rupa, *CSULA*

Meeting Participants

PURASINGHE Ruwanka, *UC Davis*
PURVANCE Matthew, *UNR*
QUIROZ Roque,
RAMIREZ-GUZMAN Leonardo, *USGS*
RAMZAN Shahid, *CSUN*
RECHES Ze'ev, *Oklahoma*
REDDALE Jolene, *San Bernardino County Museum*
REMPEL Alan, *Oregon*
REYNOLDS Evan, *UNC, Chapel Hill*
RICE James, *Harvard*
RICHARDS-DINGER Keith, *UCR*
RIVERA Armando, *ELAC*
ROBINSON Sarah, *ASU*
ROCKWELL Thomas, *SDSU*
RODRIGUEZ Vanessa, *LMU*
ROJAS Otilio, *SDSU*
ROLLINS John, *USC*
ROOD Dylan, *LLNL*
ROTEN Daniel, *SDSU*
ROUSSEAU Nick, *CSUN*
RUBINSTEIN Justin, *USGS*
RUDNICKI John, *Northwestern*
RUNDLE John, *UCD*
RYAN Kenny, *UCR*
RYMER Michael, *USGS*
SALAZAR Joseph, *CSUSB*
SALISBURY James, *SDSU*
SAMMIS Charles, *USC*
SANDWELL David, *UCSD*
SAVAGE Heather, *UCSC*
SCHARER Katherine, *Appalachian State*
SCHLOM Tyanna, *UCI*
SCHMANDT Brandon, *Oregon*
SCHMEDES Jan, *UCSB*
SCHMITT Stuart, *Stanford*
SCHORLEMMER Danijel, *USC*
SCHWARTZ David, *USGS*
SCOTT Eric, *San Bernardino County Museum*
SEGALL Paul, *Stanford*
SELIGSON Hope, *MMI Engineering*
SHAO Guangfu, *UCSB*
SHARP Warren, *Berkeley Geochron Center*
SHAW John, *Harvard*
SHAW Bruce, *LDEO*
SHELLY David, *USGS*
SHI Zheqiang, *SDSU*
SHINTAKU Natsumi, *CSUN*
SIMILA Gerry, *CSUN*
SIMONS Mark, *Caltech*
SLEEP Norman, *Stanford*
SMALL Patrick, *SCEC*
SMITH Deborah, *UCR*
SMITH-KONTER Bridget, *Texas at El Paso*
SOLIS Teira, *UTEP*
SOMALA Surendra, *Caltech*
SOMERVILLE Paul, *URS*
SONG Seok Goo, *URS*
SORLIEN Christopher, *UCSB*
SPRINGER Kathleen, *San Bernardino County Museum*
SPUDICH Paul, *USGS*
STARK Keith, *USGS*
STEIDL Jamison, *UCSB*
STEIN Ross, *USGS*
STEWART Jonathan, *UCLA*
STIRLING Mark, *GNS Science*
STOCK Joann, *Caltech*
STUBAILO Igor, *UCLA*
TABORDA Ricardo, *CMU*
TANIMOTO Toshiro, *UCSB*
TAPE Carl, *Harvard*
THATCHER Wayne, *USGS*
THOMPSON Mayo, *UNR*
THURBER Clifford, *UW-Madison*
TINSLEY John, *USGS*
TOKE Nathan, *ASU*
TORITA Haruhiko, *Ohsaki Research Institute*
TOTTEN Matthew, *Oklahoma*
TRATT David, *Aerospace Corporation*
TREIMAN Jerry, *CGS*
TSANG Rebecca, *SDSU*
TSUDA Kenichi, *Ohsaki Research Institute*
TULLIS Terry, *Brown*
TURCOTTE Donald, *UC Davis*
UCHIDE Takahiko, *UCSD*
VAN DER ELST Nicholas, *UCSC*
VELASQUEZ Christina, *CSUSB*
VIESCA Robert,
WALLS Christian, *UNAVCO*
WANG Qi, *UCLA*
WANG Tien-Huei, *UCR*
WANG Feng, *USC*
WARD Steven, *UCSC*
WDOWINSKI Shimon, *Miami*
WEAVER Stephanie, *Oregon*
WECHSLER Neta, *USC*
WEERARATNE Dayanthie, *CSUN*
WEI Meng, *UCSD*
WEISER Debbie, *USGS and UCLA*
WELCH Kaitlin, *Cincinnati*
WELDON Ray, *Oregon*
WERNER Maximilian, *ETH Zurich*
WESSON Rob, *USGS*
WHITCOMB James, *NSF*
WHITESIDES Andrew, *USC*
WILLIAMS Charles, *GNS Science*
WILLIAMS Patrick, *SDSU*
WILLS Chris, *CGS*
WU Chunquan, *Georgia Tech*
WYATT Frank, *UCSD*
XU Guanshui, *UCR*
XU Shiqing, *USC*
YAMASHITA Warren, *USC*
YANG Wenzheng, *USC*
YANO Tomoko, *UCSB*
YIKILMAZ Mehmet, *UC Davis*
YODER Mark, *UC Davis*
YONG Alan, *USGS*
YOUNG Karen, *USC*
YU Ellen, *Caltech*
YU John, *USC*
YULE Doug, *CSUN*
ZALIAPIN Ilya, *UNR*
ZANDT George, *Arizona*
ZANZERKIA Eva, *NSF*
ZAREIAN Farzin, *UCI*
ZECHAR Jeremy, *Columbia*
ZENG Yuehua, *USGS*
ZHAN Zhongwen, *Caltech*
ZHANG Dongzhou, *Caltech*
ZHANG Wenbo, *Grad Univ of Chinese Acad of Sci*
ZHANG Ziran, *PCC*
ZHAO Peng, *Georgia Tech*
ZHONG Jinqian, *Texas A&M*
ZHOU Jun, *UCSD*
ZIELKE Olaf, *ASU*
ZOBACK Mary Lou, *RMS*

2009 SCEC Annual Meeting (Group 1 Posters)

SUNDAY (September 13, 2009)

16:30-18:30 poster set-up
20:00-22:30 viewing

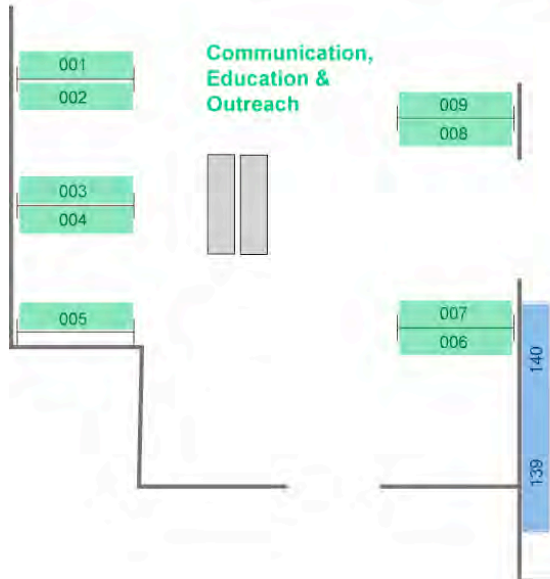
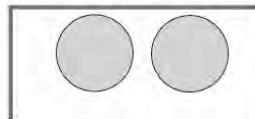
MONDAY (September 14, 2009)

14:30-16:00 viewing
20:30-22:30 viewing

TUESDAY (September 15, 2009)

07:00-08:00 poster removal

Poster Size:
120 cm high x 180cm wide
4 ft high x 6 ft wide



2009 SCEC Annual Meeting (Group 2 Posters)

TUESDAY (September 15, 2009)

07:00-08:00 poster set-up
 14:00-15:30 viewing
 20:00-22:30 viewing

WEDNESDAY (September 16, 2009)

07:00-08:00 poster removal

Poster Size:
 120 cm high x 180cm wide
 4 ft high x 6 ft wide

